The use of Olive Mills Wastewater as a water replacement in concrete mixes

By

Marwan Shuaibi 1205115

Master's Thesis

Submitted in partial fulfillment of the requirements

for the degree of Master of Science in Civil Engineering

in the Department of Civil and Environmental Engineering,

Birzeit University, 2023

Birzeit, Palestine

Advisor:

Dr. Khalil Qatu

جامعة بيرزيت
BIRZEIT UNIVERSITY

تقرير لجنة مناقشة رسالة الماجستير

اسم الطالب/ة مروان منصور شعيبي الرقم الجامعي : 1205115

البرنامج : ماجستير الهندسة المدنية

عنوان رسالة الماجستير (باللغة العربية) :

استخدام مخلفات عصير الزيتون السائلة في الخلطات الخرسانية

عنوان رسالة الماجستير (باللغة الانجليزية):

The use of olivemill wastewater in concrete mixes

قرار اللجنة :

لقد ناقش الطالب/ة المذكور أعلاه رسالته بتاريخ ١٨/٩/٢٠٢٣ ، وقد كان تقدير الرسالة على النحو التالي :

- [x] ناجح
- [ ] ناجح بشرط التعديل
- [ ] راسب

وقد طلبت لجنة المناقشة التعديلات التالية:

1. _____
2. _____

رئيس اللجنة (المشرف): خليل القطو التوقيع: [signature] التاريخ: ١٨/٩/٢٠٢٣

عضو اللجنة: جمال زلاطيمو التوقيع: [signature] التاريخ : 18/9/2023

عضو اللجنة: نزار عامي التوقيع: [signature] التاريخ 18/9/2023

نسخ/ دائرة التسجيل و القبول، العميد، البرنامج، المشرف، أعضاء اللجنة، الطالب/ة

AUTHOR DECLARATION

I declare that this Master's Thesis is my original work and does not comprise any formerly published material or written by another person except where due references have been made in the text and documented in the references list.

Signed:	Date:
Marwan Shuaibi	9/09/2023

ACKNOWLEDGMENT

I would like to express my gratitude to Dr. Khalil Qatu, my advisor, for all the guidance, support, and instruction he provided me through my master's studies, whose invaluable feedback and encouragement greatly influenced how I conducted my experiments and interpreted my findings.

I would further like to thank all Department of Civil and Environmental Engineering teachers for their support and teachings through my journey toward a master's degree.

I also would like to thank the Faculty of Graduate Studies for their financial support for this research.

DEDICATION

To my beloved mother, and my dead father, to my newborn son, Hamzeh, to my wife and the rest of my family that I am blessed with, and to my friends who supported me. To my country Palestine and all Palestinians everywhere, I dedicate this work ….

ABSTRACT

Environmental sustainability considered an important aspect facing the modern world. Different types of wastes are produced all over the world, therefore, enormous efforts are made to minimize the effect of those wastes on the environment, and so this became an active field of study for researchers. The use of wastes in concrete mixes is considered one of the methods that can be utilized to dispose of these wastes, especially since some researchers succeeded in using different types of wastes in concrete mixes while at the same time enhancing concrete characteristics.

In this research, the use of olive mill wastewater (OMWW) in concrete mixes is studied, testing if it can enhance concrete properties, and at the same time dispose of the OMWW which poses a threat to the environment due to its polluting effects.

Firstly, each component of the concrete mix (coarse aggregate, fine aggregate, water, and OMWW) is characterized. After that, different Concrete mixes are prepared by changing w/c ratio, water content, and OMWW replacement levels. The fresh and hardened concrete properties are then tested in the laboratory in accordance with (ASTM C109). X-ray diffraction and SEM images were also used in this research to evaluate the structure of the hardened concrete.

Results show that the addition of OMWW to a concrete mix can increase its slump by (140% on average). And for a certain range of replacement (10% - 20%) and certain level of water content (8% - 10%), it enhances the compressive strength of concrete by an average of (5%). It is found that for around (20%) replacement level and water content higher than (10%), good results can be achieved by adding OMWW to a concrete mix, increasing the slump on a range between (90% - 200%) while approximately maintain strength results unchanged. concrete samples are also tested after (160 days) and an increase in the concrete is observed even for samples that contained up to (100%) OMWW replacement.

Finally, an ANN model was developed to predict the slump and compressive strength of the concrete mix for any selected W/C ratio, water content, and OMWW replacement percentage. Two additional mixes are prepared using the developed model. Results show that ANN was able to predict the properties (both slump and compressive strength) of the concrete mix for the range of w/c between (0.35 – 0.65) with excellent accuracy.

Keywords: OMWW, concrete mixes, SEM, X-ray diffraction, environmental sustainability, compressive strength.

List of Abbreviations

OMWW: Olive Mill Waste Water.

ANN: Artificial Neural Network.

ASTM: American Society for Testing and Materials.

SEM: Scanning Electron Microscopes.

W/C: Water / Cement

W%: Water Content as percentage of weight.

AI: Artificial Inelegance.

BP: Back Propagation.

C.A: Coarse Aggregates

F.A: Fine Aggregates

TABLE OF CONTENTS

CHAPTER TITLE PAGE

CHAPTER ONE: INTRODUCTION 1

1.1. Background 1

1.2. Literature review: 2

1.2.1. OMWW Production: 2

1.2.2. OMWW Composition: 3

1.2.3. OMWW Management: 6

1.2.4. Artificial Neural Network (ANN): 8

1.3. Problem statement: 9

1.4. Objectives: 9

CHAPTER TWO: METHODOLOGY 10

CHAPTER THREE: RESULTS AND DISCUSSION 13

3.1. Raw material characterization: 13

3.2. Concrete mixes preparation: 18

3.3. Fresh concrete: 19

3.4. Hardened concrete: 24

3.5. Time effect on strength: 30

3.6. Cementitious cubes: 30

3.7. Scanning electron microscope (SEM) and X-ray diffraction: 32

3.8. Artificial Neural Network (ANN): 42

CHAPTER FOUR: CONCLUSIONS AND RECOMMENDATIONS 50

REFERENCES 52

Table of Figures

Figure 1: Olive oil extracting methods: a) traditional method, b) three-phase centrifugal extraction, c) two-phase centrifugal extraction. (Cassano et al., 2016) 2
Figure 2: Three-phase centrifugal extraction processes. 3
Figure 3: Typical ANN Model Structure. 9
Figure 4: Concrete cubes crushing machine 11
Figure 5: sand and gravel used in the concrete mixes. 13
Figure 6: Grain Size Distribution for Coarse Aggregates 13
Figure 7: Grain Size Distribution for fine Aggregates 14
Figure 8: Preparation of sand and gravel samples for absorption testing 15
Figure 9: Obtaining process of raw OMWW 16
Figure 10: OMWW replacement ratio vs. chloride level in different selected mixes 17
Figure 11: Concrete mix material preparation for mixing. 18
Figure 12: OMWW (as a percentage of total water content) VS. Slump. 20
Figure 13: Concrete mix A, with 8% water content, and zero slump. 21
Figure 14: Concrete mix B, 12% water content, 0% OMWW, and 11.0cm slump. 21
Figure 15: Concrete mix B, 40% OMWW, and 24.5cm slump 22
Figure 16: Concrete mix C, 10% water content, 0% OMWW, and 4.5cm slump. 22
Figure 17: Concrete mix C, 10% OMWW, and 11.5cm slump 23
Figure 18: Concrete mix C, 80% OMWW, and 24cm slump. 23
Figure 19: Cubes preparation and filling 24
Figure 20: w/c vs. concrete strength at 28 days age for control concrete mixes (0% OMWW) 25
Figure 21: Concrete crushing machine and crushed cube. 25
Figure 22: Relationship between OMWW% as a replacement of total water and concrete strength for Mix A at different ages 26
Figure 23: Crushed cube with a high level of OMWW% 26
Figure 24: Relationship between OMWW% as a replacement of total water and concrete strength for Mix B at different ages 27
Figure 25: Relationship between OMWW% as a replacement of total water and concrete strength for Mix C at different ages 28
Figure 26: Relationship between OMWW% as a replacement of total water and concrete strength for Mix D at different ages 28

Figure 27: Relationship between OMWW% as a replacement of total water and concrete strength for the same water content 29
Figure 28: Relationship between OMWW% as a replacement of total water and concrete strength for the same w/c at a different water content 30
Figure 29: Relationship between OMWW% as a replacement of total water and concrete strength for cement and OMWW cubes at 28 days age 31
Figure 30: Relationship between OMWW% as a replacement of total water and density 31
Figure 31: X-ray diffraction for all samples 33
Figure 32: X-ray diffraction and SEM for sample No.1 (0% OMWW replacement) 34
Figure 33: X-ray diffraction and SEM for sample No.3 (20% OMWW replacement) 34
Figure 34: X-ray diffraction and SEM for sample No.7 (100% OMWW replacement) 35
Figure 35: X-ray diffraction and SEM for sample No.B (0% OMWW replacement) 35
Figure 36: X-ray diffraction and SEM for sample No.U (20% OMWW replacement) 36
Figure 37: X-ray diffraction and SEM for sample No.G (100% OMWW replacement) 36
Figure 38: X-ray diffraction and SEM for sample No.H (0% OMWW replacement) 37
Figure 39: X-ray diffraction and SEM for sample No.J (20% OMWW replacement) 37
Figure 40: X-ray diffraction and SEM for sample No.N (100% OMWW replacement) 38
Figure 41: X-ray diffraction and SEM for sample No.O (0% OMWW replacement) 38
Figure 42: X-ray diffraction and SEM for sample No.R (20% OMWW replacement) 39
Figure 43: X-ray diffraction and SEM for sample No.X (100% OMWW replacement) 39
Figure 44: Amounts of phases and elements (weight %) for sample no. H 40
Figure 45: Amounts of phases and elements (weight %) for sample no. J 40
Figure 46: Amounts of phases and elements (weight %) for sample no. N 41
Figure 47: Plot between actual slump and slump predicted by the ANN model with OMWW replacement. 43
Figure 48: Plot between actual strength and strength predicted by the ANN model with OMWW replacement. 43
Figure 49: Relationship between OMWW% and strength predicted by ANN and from lab testing for w/c =0.35 and 8% water content. 45
Figure 50: Relationship between OMWW% and strength predicted by ANN and from lab testing for w/c =0.5 and 10% water content. 46

Figure 51: Relationship between OMWW% and strength predicted by ANN and from lab testing for w/c =0.65 and 10% and 12% water content..... 46
Figure 52: Relationship between OMWW% and strength predicted by ANN for w/c =0.35 with different water contents 47
Figure 53: Relationship between OMWW% and strength predicted by ANN for w/c =0.5 with different water contents 47
Figure 54: Relationship between OMWW% and strength predicted by ANN for w/c =0.65 with different water contents 48
Figure 55: OMWW replacement level vs. water content level for w/c = 0.50, A) shows the relationship for strength, B) shows the relationship for the slump, and C) shows the relationship for both. 49

Table of Tables

Table 1: a) Chemical characteristics of OMWW and fresh water, b) Chemical characteristics of OMWW from different sources in Palestine..... 4
Table 2: Summary of different components and their effect on concrete mixes 5
Table 3: Proposed Mixes 11
Table 4: Aggregates properties and characteristics..... 14
Table 5: Chemical characteristics of Fresh OMWW, Old (Sedimented) OMWW, and fresh water. 16
Table 6: Mixes Contents and Ratios 18
Table 7: Water content and slump for different W/C ratios..... 19
Table 8: Selected mixes for SEM images and X-ray diffraction 32
Table 9: ANN model mixes expected slump and strength..... 44
Table 10: ANN mixes testing results 44

CHAPTER ONE: INTRODUCTION

1.1. Background

Preservation of environment considered one of the main and difficult challenges facing the world in the past few decades. Most countries allocate a substantial portion of their budgets and enforce laws to minimize environmental hazards and threats. Untreated wastes poses a serious threat to the environment due to their negative impact on the environment and human lives (Ekins & Zenghelis, 2021), moreover, and due to rapid population growth in the modern world, which led to an increase in the amounts and types of produced wastes. The lack of proper methods and strict regulations to properly get rid of these wastes will have a catastrophic impact on the environment (Batayneh et al., 2007).

Third World countries suffer the most from the negative impact of produced wastes. This is due to the lack of strict laws and their poor financial capabilities that can help to nullify the negative effects of these wastes on the environment and human. However, studying waste types and composition can lead to new or more economically feasible methods to treat or reduce the negative effects of these wastes.

Many researchers studied the possibility of using different types of waste in concrete mixes, such as construction wastes (glass, plastic, and demolished concrete), which have been added successfully to concrete mixes to replace up to (20%) of the aggregates used in these mixes (Batayneh et al., 2007). Fly ash has also been successfully added to fresh concrete, replacing (15-35 %) of cement, increasing strength, and sulfate resistance, decreasing permeability, and improving workability (Badur& Chaudhary, 2008). Said A. and Quiroz O. (2018) have shown that using recycled latex paint in concrete mixes can produce superior concrete in terms of strength, while at the same time safely disposing of this harmful and hazardous waste.

In this study, Olive Mills Wastewater (OMWW) is studied. OMWW is one of the byproducts of olive oil production during the harvesting season between October and December each year. Currently, there are several efforts to effectively dispose of that waste using evaporation ponds for example, which despite its low cost and easy implementation aspects, this method reduces the amount of water and maintains the toxicity level of (OMWW), it also

has some drawbacks such as attracting insects or producing unpleasant odors (Slama et al., 2021).

There can be two significant benefits of conducting such a study on using (OMWW):

a) Environmental sustainability benefits: getting rid of such waste relieves nature from receiving it.
b) Economic benefits: results of the study will refer to the optimal mixing ratios and resulting properties enhancements on the fresh concrete, though replacing the quantity of the superplasticizers added to the concrete mix might result in reducing the overall cost of the fresh concrete.

1.2. Literature review:

1.2.1. OMWW Production:

Currently, there are three methods of excavating olive oil, named: traditional; carried out through olive pulp pressing and filtrate centrifugation, and continuous; carried out through direct centrifugation (two-phase or three-phase centrifugal extraction)", as summarized in Figure 1.

Figure 2 depicts three-phase centrifugal extraction processes. This olive oil extraction method is used in many countries in the Mediterranean area (Zbakh & El Abbassi, 2012). Their study found that the oil extraction process yields more than (50%) of (OMWW) around (20%) of oil, and (30%) of solid wastes.

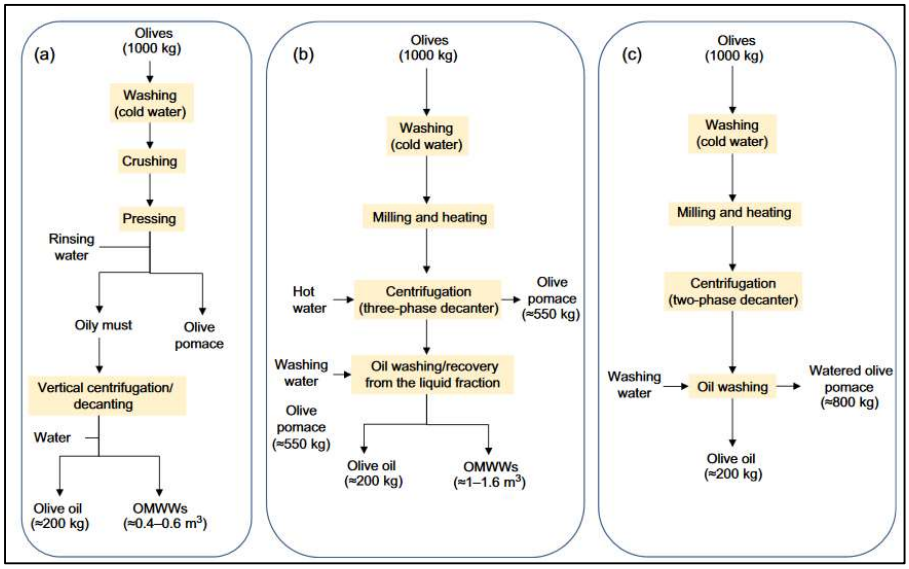

Figure 1: Olive oil extracting methods: a) traditional method, b) three-phase centrifugal extraction, c) two-phase centrifugal extraction. (Cassano et al., 2016)

In Palestine, according to The Palestinian Central Bureau of Statistics (2019), there were around (285) working olive oil mills, which received around (177611 tons) of olive beans in that year, producing (39610 tons) of olive oil (yielding around (22.3%) oil from collected beans), and according to Figure 1, the amount of wastewater produced during the process can be estimated to be around (180,000 to 200,000 m^3).

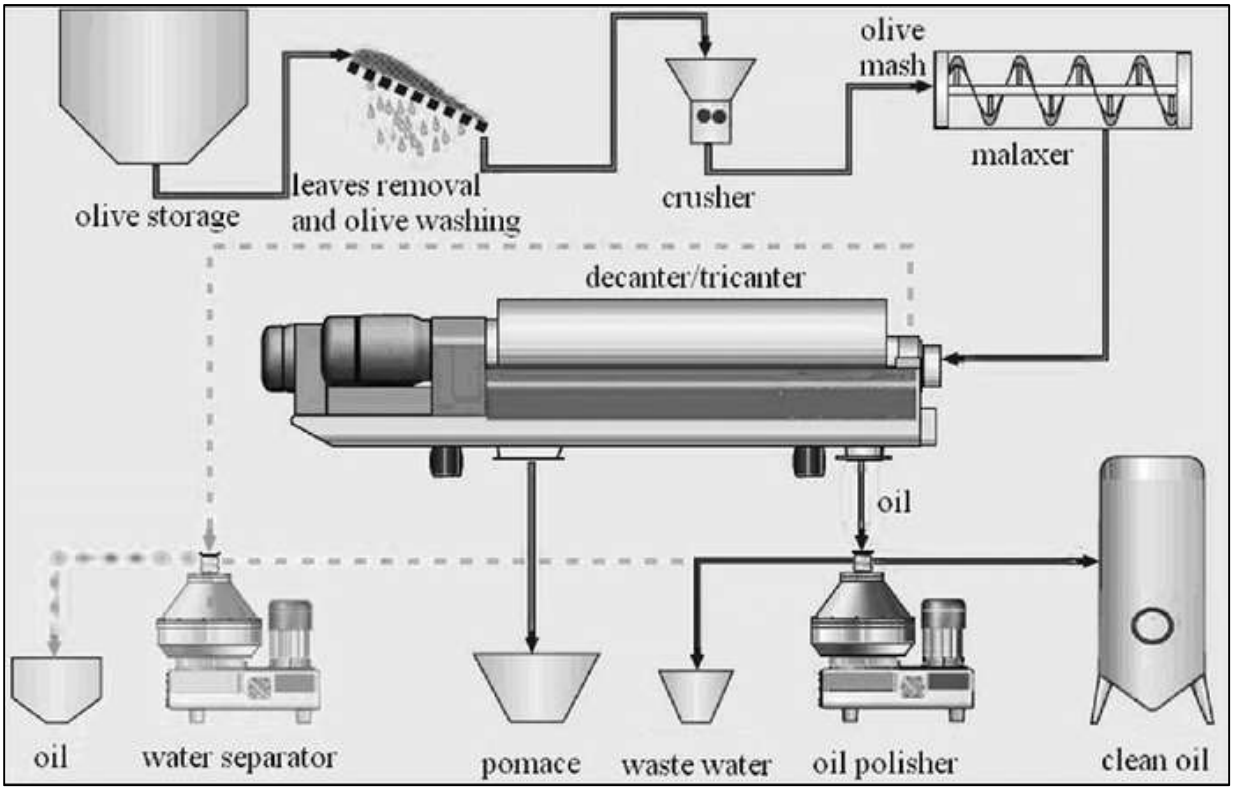

Figure 2: Three-phase centrifugal extraction processes.

1.2.2. OMWW Composition:

The characteristics and properties of the produced (OMWW) depend on the method used to produce olive oil, olive bean storing time, the season of harvesting, type and location of the olive trees, method of harvesting and storing olive beans, and used agricultural or caring techniques. Chemical characteristics were found in Lennartz et al. (2013) and Tamimi studies are shown in Table 1.

Table 1: Chemical characteristics of OMWW and fresh water from different sources

Parameter	OMWW – Jordan	OMWW – Bait Reema	OMWW - Revivim	Fresh Water
PH	5.07	4.6	4.6	7.60
Conductivity (MicroS/cm)	9750	10800	9900	1010
Dry matter (g l^{-1})	33.25	53	88	------
***Organic content (g l^{-1})**	30.57	26	32	------
***Potassium (K) (ppm)**	1050.9	5290	3700	6.75
***Chloride (ppm)**	763.8	1278	1200	82
***Sulfates (SO4) (ppm)**	174.48	158	130	54.90
***Nitrates (NO3) (ppm)**	1.19	Not stated	Not stated	1.11
Sodium (Na) (ppm)	128.8	105	440	50.70
***Calcium (Ca) (ppm)**	137.5	252	203	51.80
Specific Weight	1.03	Not stated	Not stated	--------

Generally, studies show that as the cement pastes contain less alkalies, more shrinkage will occur, and the more the acidity level of the mix, the concrete will show disintegration and surface damage (Smaoui et al., 2005). Knowing that Portland cement pH level is 12, the pH level of the water is part of the total pH level of the mix, however, the final pH level of the mix will be alternated by the chemical reactions between the cement and water. (Smaoui et al., 2005), have shown that adding alkaline water to the mix increases the porosity of the mix and tend to reduce its final strength. Several experimental studies showed that the higher the alkali content in the cement itself, the lower the ultimate strength when tested in the lab. Moreover, higher alkali content in cement is directly responsible for accelerating the strength development in the short term (early strength) but decreases the ultimate (final, long term) strength. Kucche et al. (2015) have shown that the rate of corrosion is higher for water with a pH lower than 3.0, and there was a reduction in the compressive strength and split tensile strength of concrete with the reduction in the value of the pH level of water.

Organic matter in the OMWW is one of the most noticeable elements found in OMWW, this has referred to by other studies, tends to delay hydration, extend setting time, and decrease

compressive strength increase shrinkage strain. Beddaa et al. (2019) stated that organic matter tends to delay the hydration process of the cement paste, and negatively affects strength development, especially at early ages, it also increases the setting times. Yang et al. (2018) also found that the increase of organic materials in the concrete mixes increases the porosity and decreases the compressive strength.

High chloride levels in concrete mixes can increase steel corrosion levels, this is related to the high alkali environment creating a protective film around the reinforcing steel bars, and the attack of chloride ions weakens or destroys that protecting film (Salih, 2012). Wang et. al. (2013) found that the passive coat protecting the steel was destroyed after a certain level of chloride (0.5 M), and localized corrosion was noticed at steel bars surface. ASTM C1602 limits the chloride levels between (500 ppm-1000 ppm), however, it sets no limits for concrete not containing reinforcing steel.

Potassium and Calcium are related to early strength development in concrete mixes that is due to that these two components react with the calcium hydroxide existing on the cement paste, increasing the solid ratio in the solution, and thus improving the early strength of the mix. Nitrates also tend to accelerate the hydration process of the cement thus increasing early strength development and preventing initial frost damage (Yoneyama et al., 2021).

Sulfates tend to reduce the cohesion of the cement paste, thus reducing the final strength of the concrete mix (Sabri Saleh, 2017). ASTM C1602 limits sulfate levels up to (3000 ppm). While sodium with certain ratios (between 2-6%) can increase the strength of the concrete and the early strength development (Oladapo and Ekanem, 2014), however, after that ratio, the strength tends to decrease compared to that between these recommended levels.

Table 2 summarizes the effect of each component on the concrete mix.

Table 2: Summary of different components and their effect on concrete mixes

Component	Effect
pH level	With less alkalies, more surface shrinkage will occur. Adding alkaline water to the mix increases the porosity of the mix and decreases its strength.

	The rate of corrosion is higher for water with a pH lower than 3.0, a reduction in the compressive strength and split tensile strength of concrete.
Organic matter	Tends to delay hydration, extend setting time, and decrease compressive strength increase shrinkage strain. Increases the porosity.
Chloride	Increase steel corrosion levels.
Potassium and Calcium	Improves early strength development.
Nitrates	Accelerate the hydration process of the cement. Increasing early strength development and preventing initial frost damage.
Sulfates	Reduce the cohesion of the cement paste. Reducing the final strength of the concrete mix.
Sodium	Can increase the strength of the concrete and the early strength development.

From the above table, it is expected that the compressive strength of the concrete mixes to be reduced as OMWW% increases in the concrete mix due to the presence of material that tends to decrease the overall strength of the mix.

1.2.3.OMWW Management:

OMWW management is considered a complex problem, and due to that, no single solution can be given to safely treat and dispose of that wastewater. However, current OMWW management methods can be generally categorized into four main categories (Cassano et al., 2016; Zagklis et al., 2013).

1. Disposal; examples such as a direct application on soil, evaporation using evaporation pools, and solar distillation.
2. Physicochemical; examples such as Membrane filtration include technology such as microfiltration, ultrafiltration, nano-filtration, and reverse osmosis for the fractionation of compounds from liquid solutions.
3. Biological; examples such as anaerobic digestion, aerobic treatments, bio treatments,

4. Advanced oxidation methods; examples such as oxidation and advanced oxidation processes, ozonation, and electrocoagulation.

A combined physicochemical and biological system can guarantee high efficiency in terms of pollution control, also, and as the method of treatment changes, so does the cost of the treatment. In general, the cost of treating one cubic meter of OMWW equals the treatment of (200 m^3) of domestic sewage (Tsagaraki et al., 2007).

In Palestine, (OMWW) current management method is the disposal method, by simply collecting that waste in underground tanks inside olive mills and later discharging it to streams (Wadi) so that it is absorbed by the soils. This disposable method is forbidden in some Mediterranean countries (Hadrami H., 2009), as it poses a threat to the local environment due to its polluting effect on the soil and groundwater at the same time, however, this disposable method has the lowest direct cost. Conidi C. et al. (2016) and Hassani et al. (2020) state that (OMWW) imposes a great impact on the environment due to their high phytotoxic level due to the activity of phenolic compounds exist in the olive fruit (olive fruit is very rich in phenolic compounds, around 53% of the fruit content of phenolic compounds passes to the wastewater, (Hanaa and Abdelilah,2012), along with the high concentration of organic matter.

Due to composition, the OMWW contains a high level of organic content, caused by phenolic compounds responsible for the antimicrobial and antioxidant activity of olive oil, it makes biodegradation of the waste difficult for conventional wastewater treatment plants, OMWW components inhibit the growth of microorganisms that are used in the biodegradation process in treatment facilities (ex. anaerobic digestion processes).

In Palestine, sewage treatment plants do not allow discharge of OMWW into the sewage network, illegal discharge leads to sealed pipes, collapsed pumping stations, and treatment plants.

The use of (OMWW) in concrete mixes has not been thoroughly studied, and the effect of adding wastewater to the concrete and steel is still ambiguous. However, a local study conducted by Eng. Habeeb Emseeh (1997) studied the effect of adding the (OMWW) also known locally as (ZEBAR) on the concrete as a replacement for superplasticizers, the study shows that for the short term (cubes crushing on 7, 14, and 28 days) and W/C ratios range from 0.4 to 0.5) with different OMWW/water replacement ratios up to 30%, concrete

workability have increased between 6% up to 400%, and the strength also have increased by 1% to 38%. Along with that study, some local efforts were reported to use (OMWW) on concrete mixes, although the quantities used were humble due to the lack of solid theories or studies to support their use.

It is also worth mentioning that the cost of the using (OMWW) in concrete mixes is only the cost of transporting the material form the olive mills to ready-concrete factories.

1.2.4. Artificial Neural Network (ANN):

The use of artificial inelegance (AI) has become a major part of almost all industrial sectors, with different shapes and forms. ANN has been used in concrete mix design for a while (Qatu, 2019). ANN have been used in many fields of research to predict certain outputs using field measurements and notes (Najjar Y et al., 2005; Najjar Y. et al., 2019). ANN refers to the use of artificial neurons and certain codes, functions, and algorithms to emulate the structure of the human brain. It mainly consists of input layers, hidden layers, and output layers. Each layer contains several nodes (i.e. neurons). Input nodes are connected to the output nodes through the hidden layers with links, see Figure *3*. Each link has a connection weight that represents its significance in the whole network which is optimized in the training stage. Supervised training is called back-propagation (BP), and it mainly consists of two stages: the feedforward stage and the feedback stage (Afandi et al., 2022). This training stage will enable the ANN to solve complex problems using appropriate values (weights) between neurons in different layers (e.g. between inputs and hidden nodes, between hidden nodes and outputs, and between the nodes of the hidden layers). Several activation functions normally are used to complete the linking (mapping) process, with the most famous one being the sigmoidal function (Yousif et al, 2010).

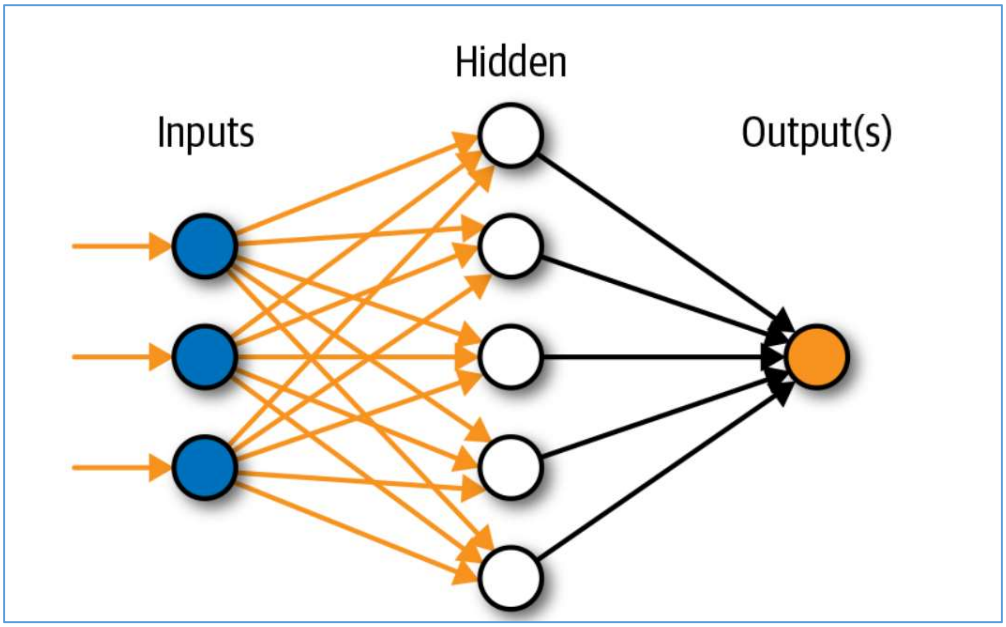

Figure 3: Typical ANN Model Structure.

1.3. Problem statement:

Due to the high cost of treatment of OMWW and the almost absence of law enforcement in the olive production sector, the current disposal methods in many developed countries are considered inefficient. No serious attempts were made to use OMWW in concrete mixes as a disposal method, and the effects of adding OMWW to concrete and how it changes mixes different properties are still unclear.

1.4. Objectives:

The main objective of this research is to determine the effect of using OMWW in concrete mixes as a disposable method for OMWW. Along with studying the effect of adding OMWW to concrete mixes and how this material alters/changes the different properties of the concrete mixes.

Another objective is to develop an ANN model to predict the fresh and hardened concrete properties for a given mixing ratio.

CHAPTER TWO: METHODOLOGY

In this research, the effect of OMWW is studied, properties of fresh and hardened concrete after adding OMWW to concrete mixes will be thoroughly studies.

Firstly, the different components of the concrete mix are characterized. namely; cement, OMWW, fine aggregates, coarse aggregates, and fresh water and OMWW. These tests will be sieve analysis for coarse and fine aggregates, specific gravity, absorption, abrasion, OMWW and normal water composition, and cement strength.

The OMWW used in this research was taken from Dier Ghassaneh village, see Figure 9. Tests have been made on this OMWW to obtain its composition. These tests were performed by Testing Labs Center, at Birzeit University. These tests will cover the following aspects:

- PH level
- Conductivity
- Dry matter
- Organic content
- Mineral matter
- Calcium, Sodium, Potassium, Magnesium Phosphate.
- Chloride, Sulfate, Bromide, Nitrate.
- Specific weight.

The fresh and hardened concrete properties for each mix as will be measured including slump and compressive strength. Slump test importance comes from its ability to measure the ease of fresh concrete to be molded and worked with, the slump test is performed according to ASTM standard C109. with pictures. Additionally, the compressive strength of the hardened concrete is measured according to ASTM C109 and its parameters, cube dimensions, loading rate, machine model etc.

To study the effect of adding OMWW to concrete, several mixes will be designed with different w/c ratios, 0.35, 0.5, and 0.65. Different OMWW replacement ratios will be used for each mix ranging from 0%, 10%, 20%, 40%, 60%, 80%, and 100%. Three cubes to will be tested

at each testing age, 7 days, 14 days, 28 days, and 100 days or more. Table *3* summarizes the proposed mixes with different water content and OMWW ratios.

Table 3: Proposed Mixes

Mix	W/C	Water Content	OMWW%						
A	0.35	8%	0%	10%	20%	40%	60%	80%	100%
B	0.5	12%	0%	10%	20%	40%	60%	80%	100%
C	0.65	10%	0%	10%	20%	40%	60%	80%	100%
D	0.65	12%	0%	10%	20%	40%	60%	80%	100%

Cement cubes will also be prepared using only water and cement to investigate how adding OMWW would affect the chemical reaction between the cement and the water. These cubes will be made with ratios of 0%, 10%, 20%, 40%, 70%, and 100% of replacement between OMWW and normal water. Cubes will be crushed in Birzeit University materials laboratory using the crushing machine shown in Figure *4*.

Figure 4: Concrete cubes crushing machine

SEM and x-ray diffraction pictures will be taken for several hardened concrete samples with different OMWW ratios to investigate any changes when adding OMWW to a concrete mix.

Finally, ANN will be utilized aid in the concrete mix design with OMWW to create a design tool, which will enable the user to insert the desired outcomes in terms of strength and slump, and then receives the results showing the level of OMWW replacement required and the predicted strength and slump for the proposed mix.

ANN structure, training algorithm, program used for training (tr-seq1 from Najjar paper), creating links between different nodes and giving these links proper weights after training.

The criteria for choosing the optimum structure (maximum number of hidden nodes, statistical parameters used to measure the accuracy of ANN model, then start from 1 to max then 2 to max etc.) is based on minimizing the error difference between the predictions of the ANN model and the actual/tested data points.

The data points will be divided into training points, testing points, and validation points. The ANN model will be created to develop logical relationships between the different inputs (e.g. w/c, water content, replacement level, etc.) and the required outputs (e.g. Expected strength and slump). After that, ANN outputs will be utilized to determine the optimized mixes for certain selection criteria, and will then will be tested in the laboratory to validate the outputs of the created ANN model.

CHAPTER THREE: RESULTS AND DISCUSSION

3.1. Raw material characterization:

The first step is to test the input materials used in the concrete mixes, this includes the cement, fine and coarse aggregates, normal (potable) water, and OMWW. The following will show the results for each material.

1- Coarse and Fine Aggregates: Figure *5* shows sand and gravel used in this research, Figure *6* shows sieve analysis results for coarse aggregates, and Figure *7* shows sieve analysis results for fine aggregates. Table *4* shows fine and coarse aggregate properties and characteristics.

Figure 5: sand and gravel used in the concrete mixes.

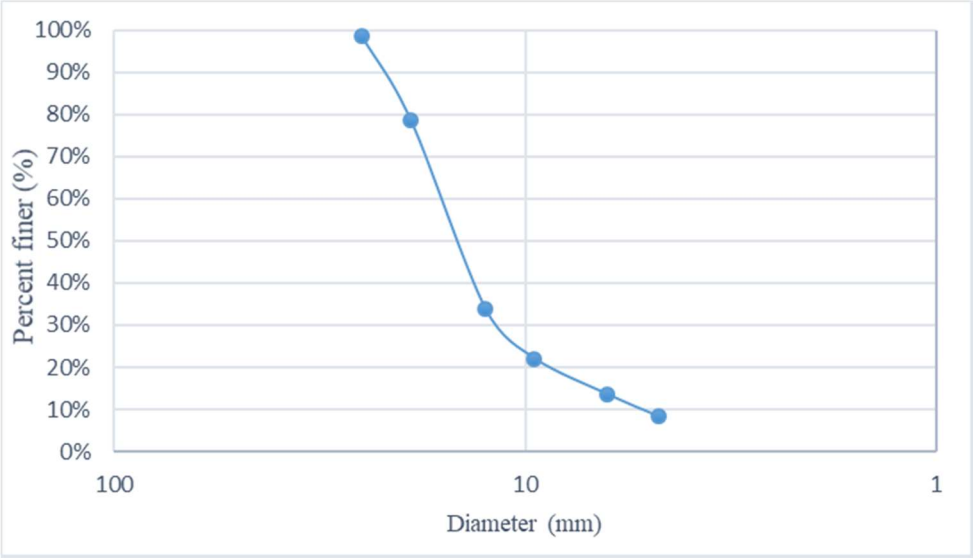

Figure 6: Grain Size Distribution for Coarse Aggregates

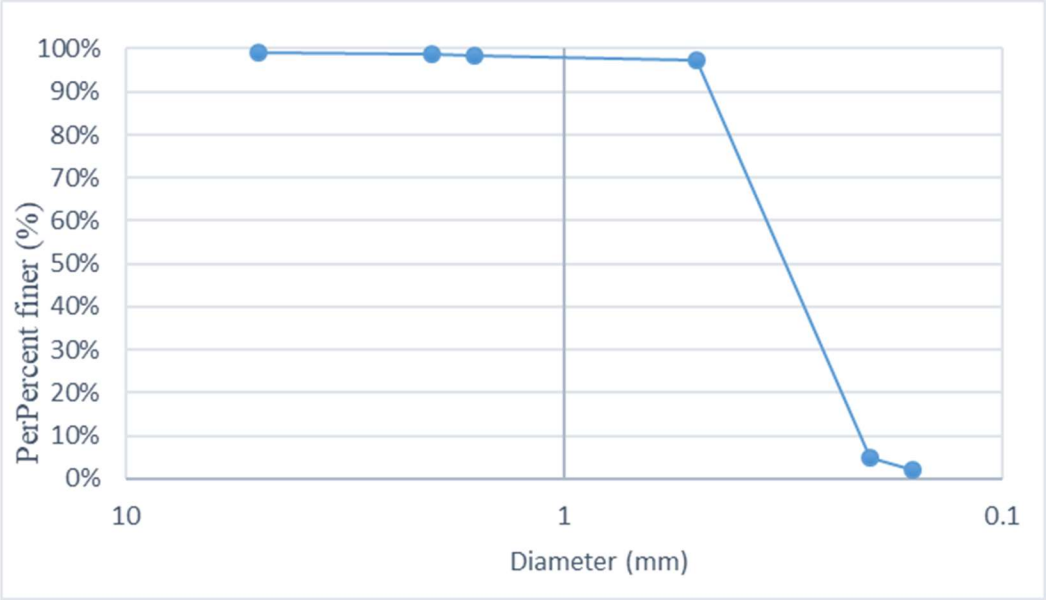

Figure 7: Grain Size Distribution for fine Aggregates

Table 4: Aggregates properties and characteristics.

Material	Absorption %	S.G. dry basis	S.G. S.S.D	Apparent S.G.	LA. Abrasion
Fine Aggregate	1.67	2.47	2.62	2.78	------
Coarse Aggregate	2.53	2.502	2.56	2.67	25-28 %

Figure *8* shows sample preparation for fine and coarse aggregates for absorption test. Compared to ASTM C33, fine aggregates fall in shortage in some categories between No.16 and No.30 sieves in which the used fine aggregates have higher ratios than that stated in ASTM C33. However, for the coarse aggregates used in this research, and as per ASTM C33, the aggregates comply with the ASTM standard to be used in the concrete mixes in both sieve grading and the abrasion ratio which the ASTM states that it shall be less than 50%, and in this research case it was between 25-28%.

Figure 8: Preparation of sand and gravel samples for absorption testing

2- Potable Water: The properties of water are shown in Table *5* which shows the chemical characteristics of water. These tests were performed at the Testing Laboratories Center at Birzeit University.

3- OMWW: properties of OMWW are shown in Table *5* which shows the chemical characteristics of OMWW. These tests were performed at the Testing Laboratories Center at Birzeit University. Figure *9* shows the process of obtaining OMWW.

   OMWW was obtained in two different years, the OMWW used in this research sample was the fresh one obtained during the year (2022). The other samples were obtained one year before (the year 2021), and this was to test the effect of time on the levels of its contents during a year of resting and the effect of sedimentation on the OMWW contents.

Figure 9: Obtaining process of raw OMWW

Table 5: Chemical characteristics of Fresh OMWW, Old (Sedimented) OMWW, and fresh water.

Parameter	Fresh OMWW	Old (sedimented) OMWW	Fresh Water
PH	4.66	4.35	7.62
Conductivity (MicroS/cm)	11255	11436	460
Dry matter	5.13%	4.44%	------
Organic content	4.0%	3.36%	------
Potassium (K) (ppm)	3996	4474	1.71
Chloride (ppm)	1152.29	1046.02	40.43
Sulfates (SO4) (ppm)	347.96	340.62	17.54
Nitrates (NO3) (ppm)	141.09	156.92	5.52
Sodium (Na) (ppm)	244.4	208	28
Calcium (Ca) (ppm)	192.2	194.0	46.1
Specific Weight	9.95	9.98	------

Results show that time does not significantly affect the contents of the OMWW, as seen in Table 5, values of tested elements do not vary that much for a period of one year separating the fresh and old OMWW intakes.

A noticeably high level compared to freshwater are organic content, potassium, chloride, Sulfates, Nitrates, and Sodium levels.

Figure 10 shows the OMWW replacement ratio vs. chloride level in different selected mixes, and as the level of replacement increases, so does the chloride level. As per ASTM, lower and upper limit lines represent the range for chloride in the concrete to pose a threat to the reinforcing steel. However, ASTM does not set a limit for non-reinforced concrete. Note that chloride content depends on water content level, and for higher levels of water content (ex. 12%), allowable replacement levels decrease.

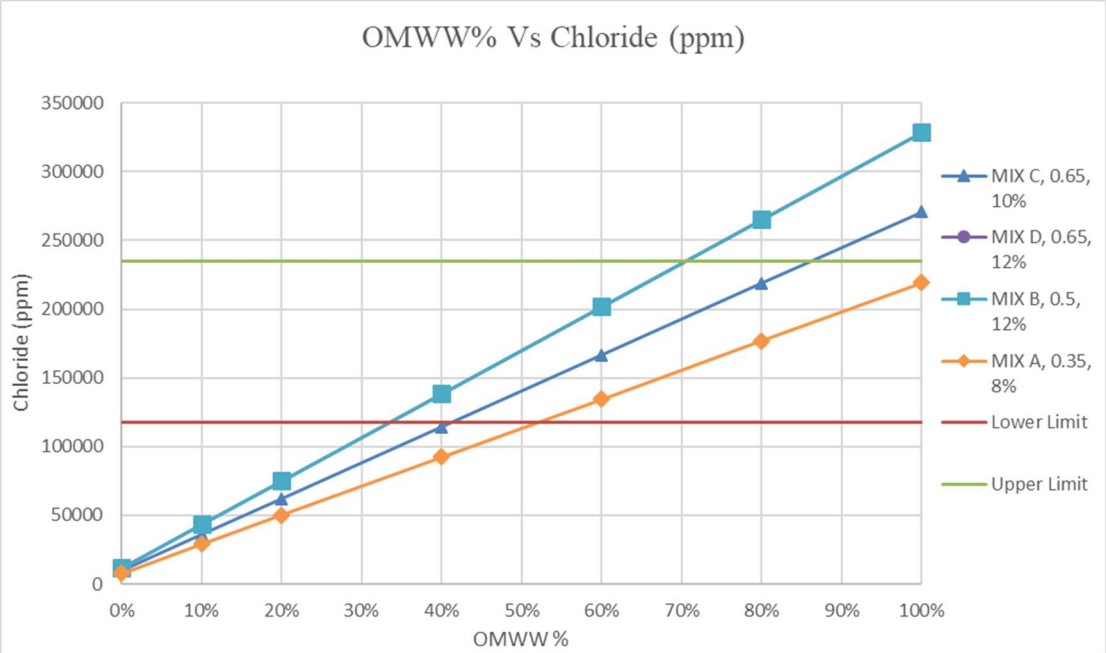

Figure 10: OMWW replacement ratio vs. chloride level in different selected mixes

4- Cement: The used cement was type 42.5 brought from a local ready concrete factory Al-Nabali and Al-Sheik, the strength of the cement when tested alone to give an average compressive strength of (42.5 MPa).

3.2. Concrete mixes preparation:

Laboratory testing for selected W/C ratios and replacement ratios started on 24 November 2022. Different concrete mixes were prepared to be tested in the laboratory, designed mixes differing in the following:

- Water to cement ratio (W/C); which is considered the main factor affecting the strength of the mix. Three W/C ratios were considered; 0.35, 0.5, and 0.65
- Water content level; which is the main factor affecting the slump of the mix. Mix 0.35 was made with low water content thus low slump, mix 0.5 was made with the highest water content, and mix 0.65 was made with a medium water content.

Table 6 shows the quantities and ratios for each selected mix.

Table 6: Mixes Contents and Ratios

Mix	W/C	Water Content (Kg)	Water Content (%)	Cement Content (Kg)	Coarse Aggregate (Kg)	Fine Aggregate (Kg)	Max Aggregate Size (mm)
A	0.35	190	8%	543	960	652	20
B	0.5	285	12%	570	960	530	20
C	0.65	235	10%	361.5	960	788.5	20
D	0.65	285	12%	438.5	960	661.5	20

Figure *11* shows the preparation process for the raw materials to be mixed and tested.

Figure 11: Concrete mix material preparation for mixing.

3.3. Fresh concrete:

1- Control mixes:

Control mixes represent the 0% replacement using only normal water in the mix to set a datum for the after-replacement mix results.

A slump test was used to determine the workability level for the control mixes. As shown in Table *7*, the level of the water is a percentage of the total weight of the mix.

It is noticeable that as the water content increased, despite the ratio of w/c, the slump increased.

Table 7: Water content and slump for different W/C ratios

Mix	W/C	Water content (%) of total mix weight	Slump (cm)
A	0.35	8%	0
C	0.65	10%	4.5
B	0.5	12%	11
D	0.65	12%	18

2- OMWW mixes:

The relationship between OMWW level as a percentage of total water content in the mix and workability was plotted, and it shows that workability increased as the level of replacement increased, see Figure 12.

For the mixes with 8% water content which is considered a low level of water content, adding OMWW shows no effect on workability. However, for the 10% of water content, the slump increased up until the 60% replacement of OMWW, then the slump stabilized at the full collapse level of a slump from that point (60%) up until the 100% replacement level, which means that the effect of OMWW on the slump has faded. At the 12% water content, the increase of slump was at a higher rate compared to the 10% water level, and as the same as the 10% water level mixes, the slump stabilized at the collapse state at

almost 20% of replacement, after that point (20%), adding OMWW to the mix shows no effect on the slump.

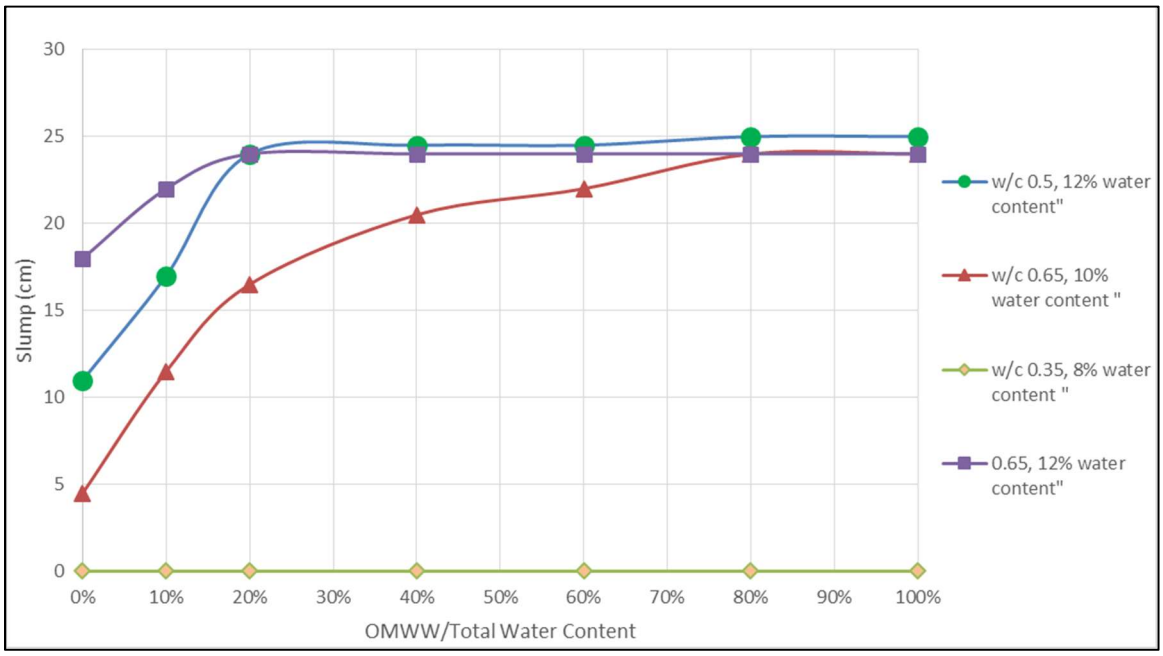

Figure 12: OMWW (as a percentage of total water content) VS. Slump.

The following pictures show the slump of different mixes. Figure 13 shows the slump test for Mix A, and it was zero for all replacement ratios.

Figure 14 and Figure 15 show the slump test for Mix B, which shows a rapid rate to reach total collapse starting with a 20% replacement ratio.

Figure 16 and Figure 17 and Figure 18 show slump test results for Mix C, and results show a lower rate till collapse is reached. Figure 19 shows the process of cube preparation.

Figure 13: Concrete mix A, with 8% water content, and zero slump.

Figure 14: Concrete mix B, 12% water content, 0% OMWW, and 11.0cm slump.

Figure 15: Concrete mix B, 40% OMWW, and 24.5cm slump

Figure 16: Concrete mix C, 10% water content, 0% OMWW, and 4.5cm slump.

Figure 17: Concrete mix C, 10% OMWW, and 11.5cm slump

Figure 18: Concrete mix C, 80% OMWW, and 24cm slump.

Figure 19: Cubes preparation and filling

3.4. Hardened concrete:

1- Control mixes

As mentioned before, concrete cubes of dimensions (10X10X10 cm) were prepared to be tested in the lab, see Figure 21. Three cubes were tested each time, and at testing ages of 7, 14, and 28 days were considered in this report, and later, for more aged cubes.

The first relationship to be drawn is the one between w/c ratio and strength during different testing times. Figure 20 shows that the strength of concrete decreased as the w/c ratio increased.

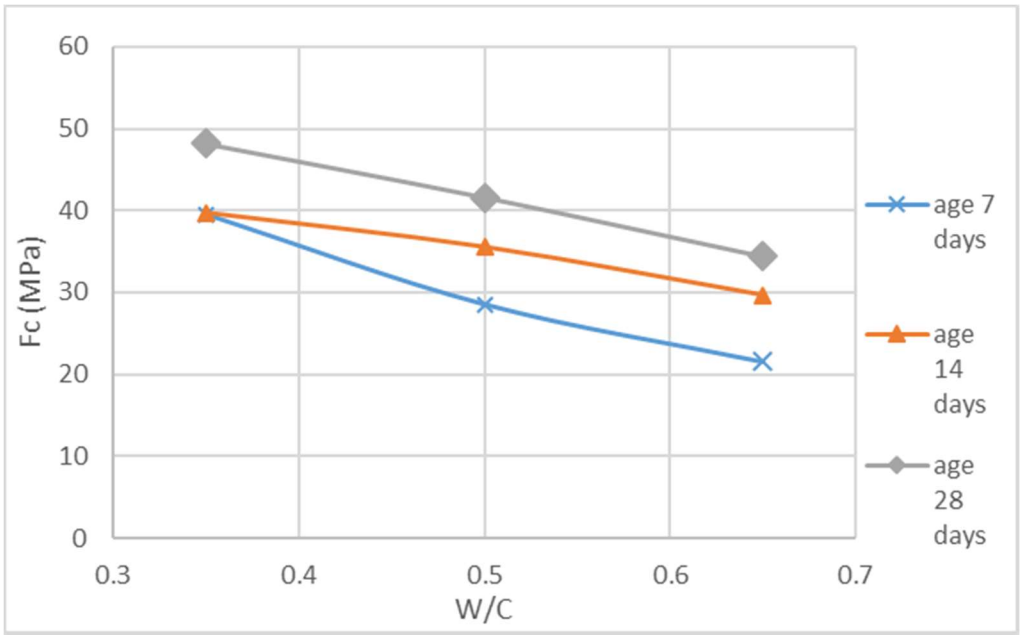

Figure 20: w/c vs. concrete strength at 28 days age for control concrete mixes (0% OMWW)

Figure 21: Concrete crushing machine and crushed cube.

2- OMWW mixes:

- Mix A: w/c = 0.35, 8% water content;

  Figure *22* shows the shape of the relationship between OMWW as a percentage of the total water used in the mix and concrete strength at different ages. The relationship almost stays the same for different testing ages, however, the strength of the concrete greatly decreases as the replacement ratio reaches 80%, and it falls to

very low strength the concrete cubes show a failure mode far from a brittle failure, it almost crumbles by any small force and looks like concrete does not even react or hardened, see Figure 23.

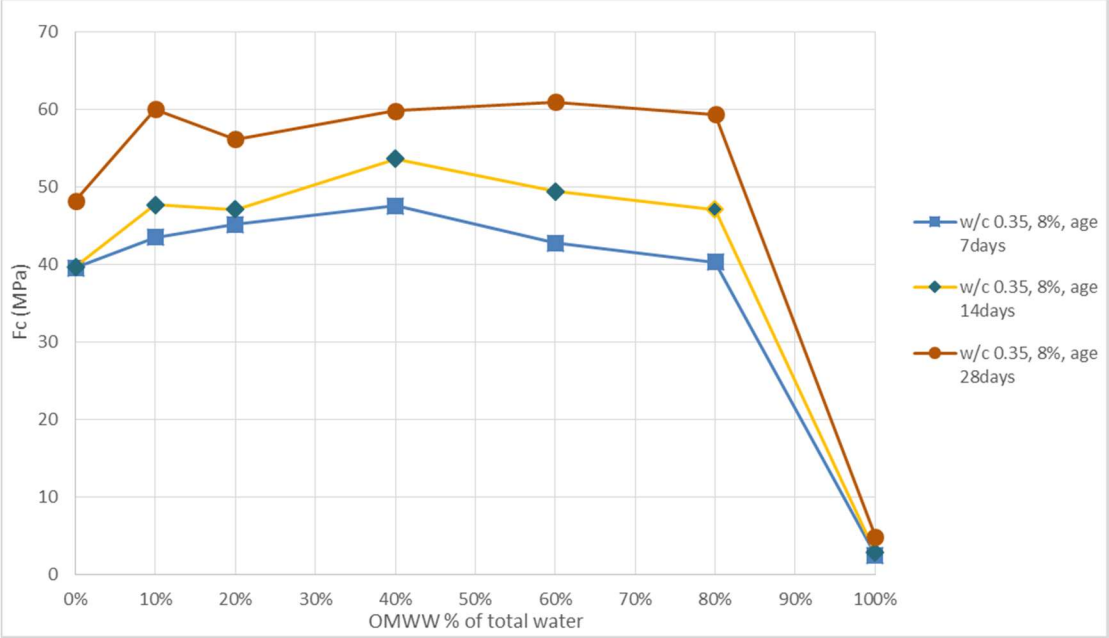

Figure 22: Relationship between OMWW% as a replacement of total water and concrete strength for Mix A at different ages

Figure 23: Crushed cube with a high level of OMWW%

Note that Mix A is the one with the lowest water content (8%), this is reflected in the range it managed to reach before reaching the strength falling area, which is the highest among the other water content levels. However, this range differs between

the mixes as the water content differs thus the amount of OMWW in the mixes differs.

- Mix B: w/c = 0.5, 12% water content

  Figure *24* shows the relationship between OMWW as a percentage of the total water used in this mix and concrete strength at different ages. This is different from the previous relationship as the water content is the highest between all the mixes, which was reflected as the range required till the strength starts to degrade is less than that with 8% water content thus lower OMWW content in total. However, the common thing between these relationships is the increase in OMWW% decreases the strength of the concrete to a very low value.

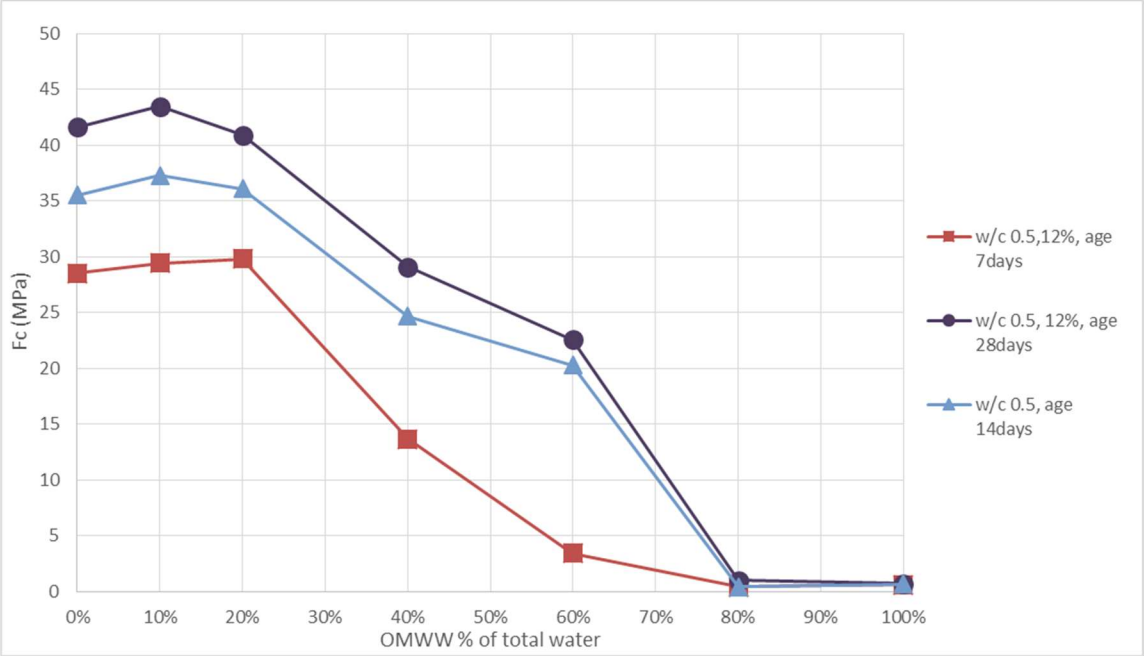

Figure 24: Relationship between OMWW% as a replacement of total water and concrete strength for Mix B at different ages

- Mix C: w/c = 0.65, 10% water content:

  Figure 25 shows the relationship between OMWW as a percentage of the total water used in this mix and concrete strength at different ages. This is also different from the previous relationships as the water content is the medium between all the mixes, which was reflected as the strength degradation started to fall in the middle area between the other two mixes (Mix A & Mix B).

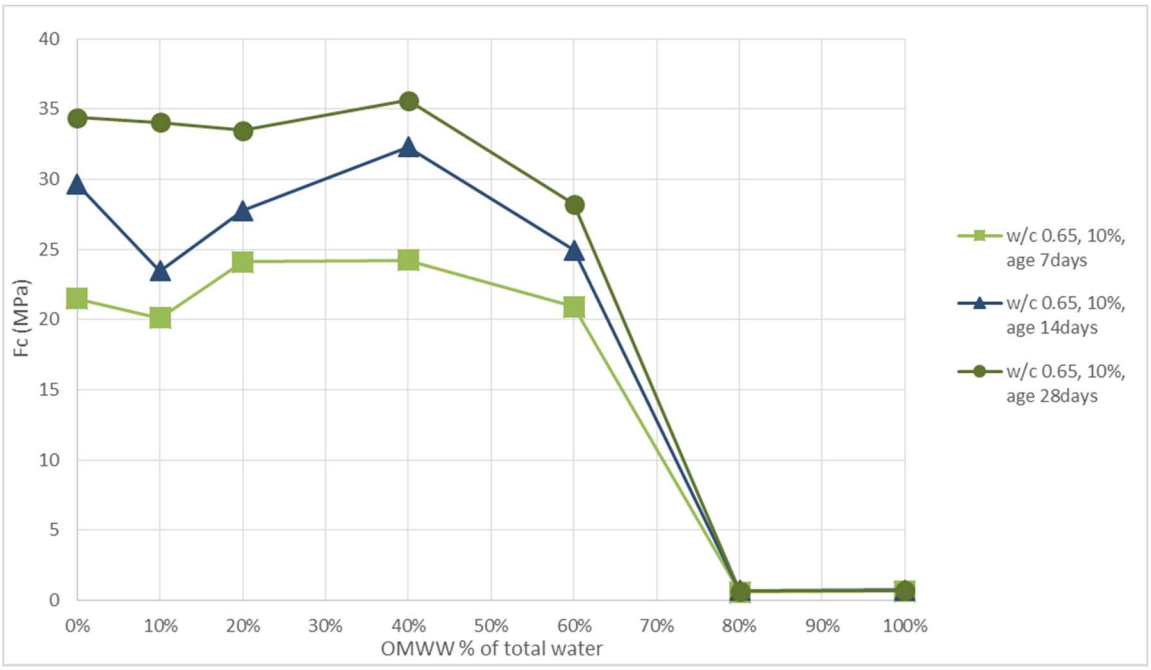

Figure 25: Relationship between OMWW% as a replacement of total water and concrete strength for Mix C at different ages

- Mix D: w/c = 0.65, 12% water content:

  Figure *26* shows the relationship between OMWW as a percentage of the total water used in this mix and concrete strength at different ages. This mix is different from Mix C in water content, which was 12% in this mix instead of 10% in Mix C.

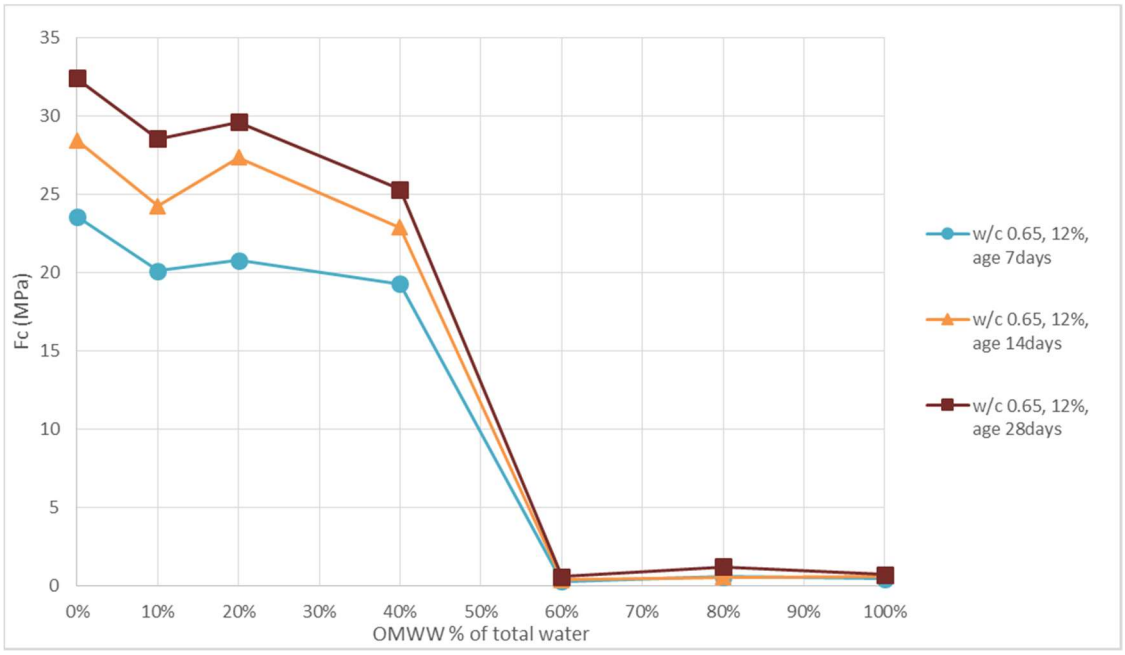

Figure 26: Relationship between OMWW% as a replacement of total water and concrete strength for Mix D at different ages

- Comparison: four mixes should be included (w/c 0.35 WC 8%, and w/c 0.5 WC 12%, w/c 0.65 WC 10%, and w/c 0.65 WC 12%)

  Comparing the different mixes with different OMWW ratios along with the control mixes shows that Mix A with 8% water content has the highest overall strength, and the most mix to resist the degradation in strength when OMWW is added to the mix. Mixes B and C with 12% and 10% water content respectively, show a degradation in the strength but at a higher rate since the water content and thus OMWW content is larger in these mixes.

  Figure *27* shows the relationship between OMWW% as a replacement of total water and concrete strength for the same water content with a different w/c ratio. and Figure *28* shows the relationship between OMWW% as a replacement of total water and concrete strength for the same w/c ratio with different water content.

  It was seen that for the mixes with the same w/c with a different water content, the compressive strength is less in case of higher water content, this can be related to the higher content of organic matter as the OMWW content increases when water content increases. At the same time, and while water content remains the same, the w/c ratio differentiates the curves rather than the water content.

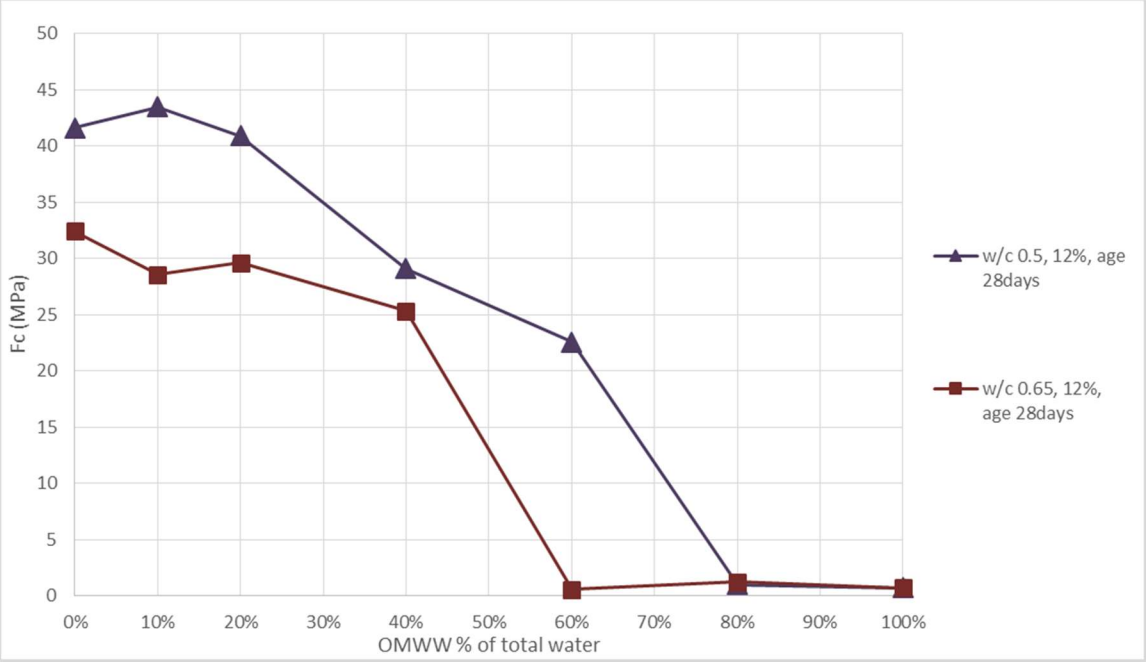

Figure 27: Relationship between OMWW% as a replacement of total water and concrete strength for the same water content

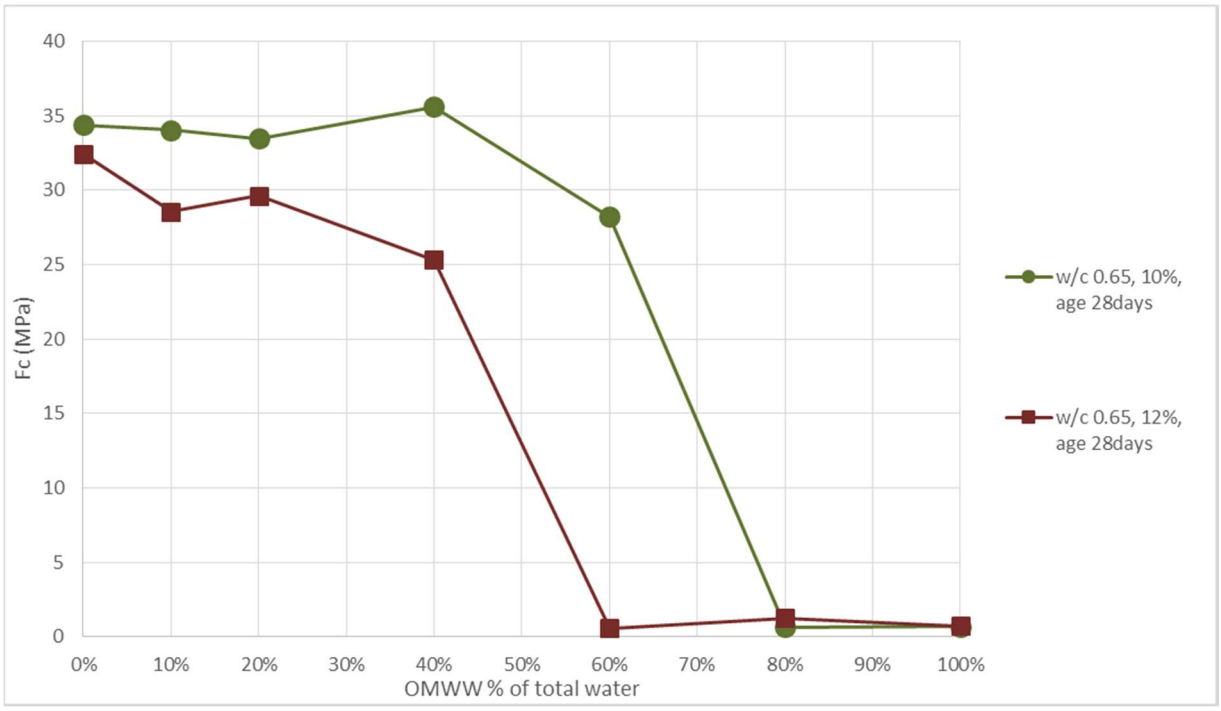

Figure 28: Relationship between OMWW% as a replacement of total water and concrete strength for the same w/c at a different water content

3.5. Time effect on strength:

Mixes were tested at an age of (160 days), to check the effect of time on the strength of the concrete cubes. Results show that cube strength did not decrease and, in most cases, it did increase in the range between 2% and 45%. However, this increase does not seem to have a pattern correlated to the w/c ratio or the water content.

3.6. Cementitious cubes:

As mentioned earlier, different cementitious cubes (7cm X 7cm X 7cm) were prepared with different OMWW replacement ratios. Cubes were crushed at 28 days of age. Figure 29 shows the relationship between the OMWW% in the mixes of cement and water only. It was clear that as OMWW content increases, the strength of the cementitious cubes decreases. This can be related to the higher content of organic matter, and lower alkali levels due to the acidity nature of the OMWW.

It was also noted that the density of the cubes decreased as the OMWW content increased, see Figure 30. This can be related to the higher porosity due to higher organic content as OMWW replacement levels increase

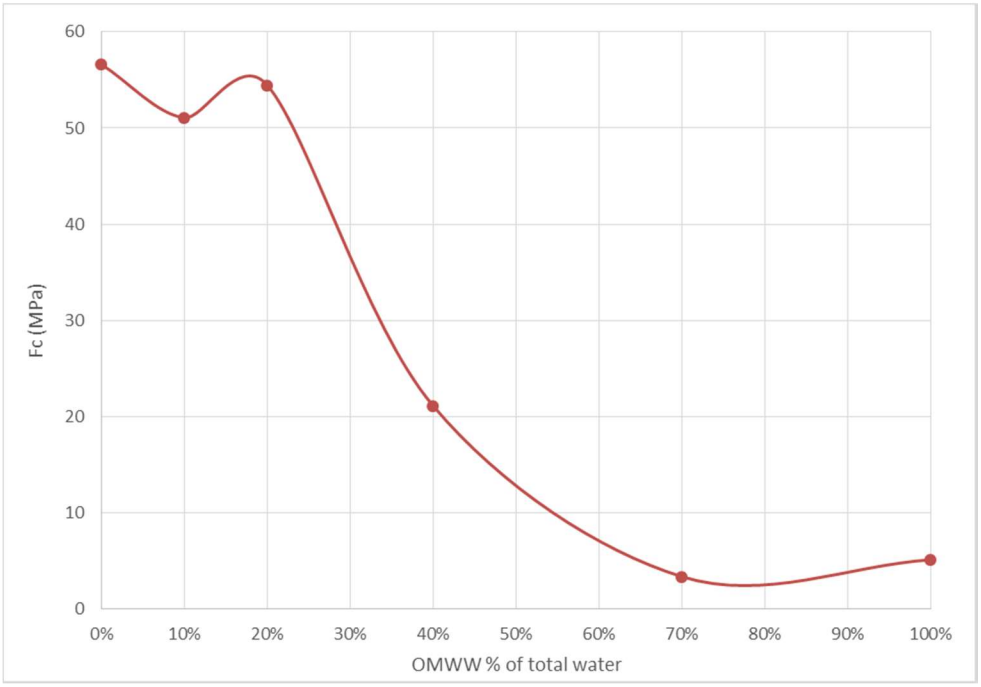

Figure 29: Relationship between OMWW% as a replacement of total water and concrete strength for cement and OMWW cubes at 28 days age

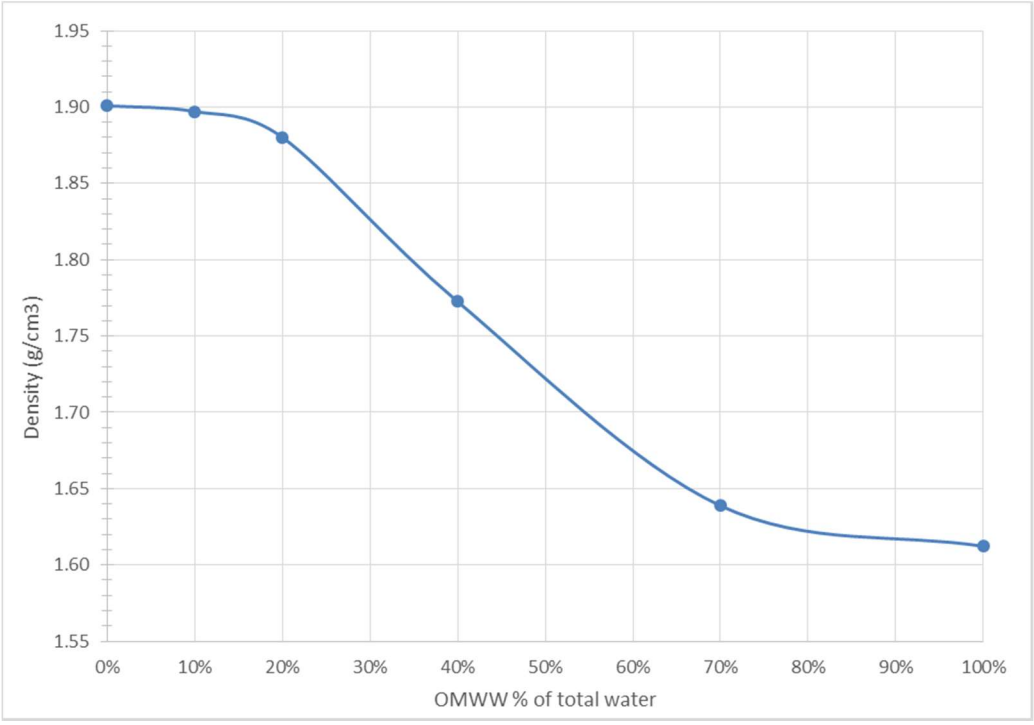

Figure 30: Relationship between OMWW% as a replacement of total water and density

3.7. Scanning electron microscope (SEM) and X-ray diffraction:

To study the effect of adding OMWW to the mix at a micro level, scanning electron microscope (SEM) images were taken for selected samples shown in Table 8.
X-ray diffraction test was also performed on the same samples as per Table 8.
Published papers for Stutzman, et al. (2001) and Uzbaş & Aydın, (2019) were used to understand the content of the taken images.

Table 8: Selected mixes for SEM images and X-ray diffraction

Sample No.	w/c	Water Content	OMWW%	Actual tested strength (MPa)
1	0.65	12%	0%	32.43
3	0.65	12%	20%	29.63
7	0.65	12%	100%	0.73
B	0.35	8%	0%	48.16
U	0.35	8%	20%	56.12
G	0.35	8%	100%	4.86
H	0.50	12%	0%	41.62
J	0.50	12%	20%	40.90
N	0.50	12%	100%	0.74
O	0.65	10%	0%	34.41
R	0.65	10%	20%	33.47
X	0.65	10%	100%	0.71

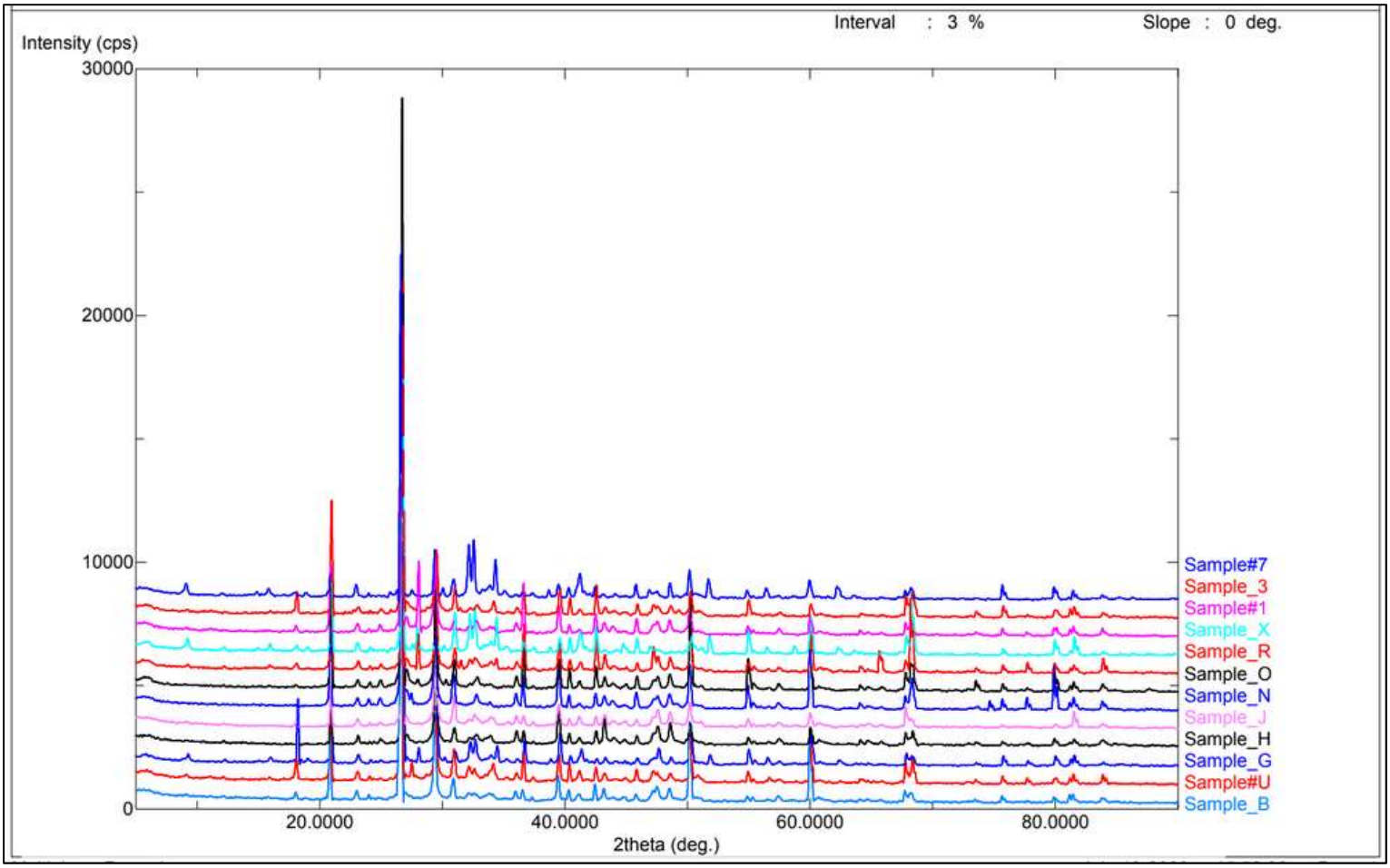

Figure 31: X-ray diffraction for all samples

Figure 31 shows the results of the X-ray for all samples. Results of SEM and X-ray are shown in Figure *32* and Figure *33* and Figure *34* for mix D, Figure *35* and Figure *36* and Figure *37* for mix A, Figure *38* and Figure *39* and Figure *40* for mix B, Figure *41* and Figure *42* and Figure *43* for mix C.

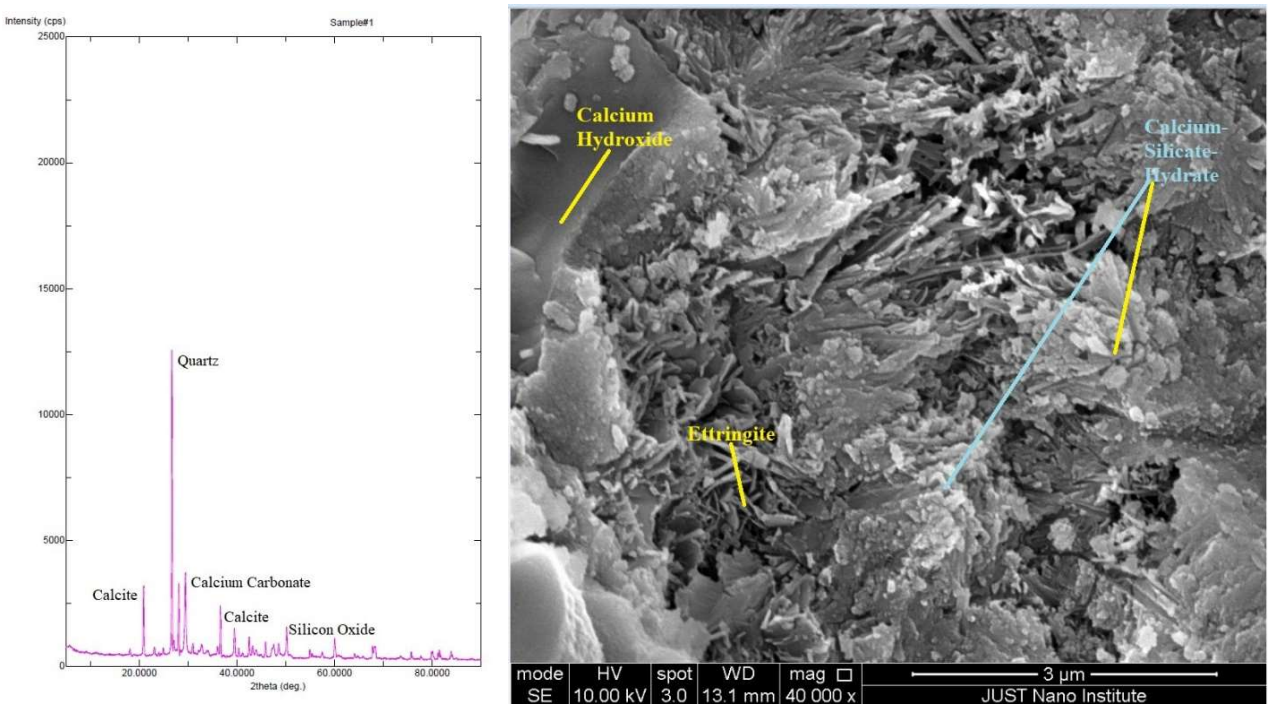

Figure 32: X-ray diffraction and SEM for sample No.1 (0% OMWW replacement)

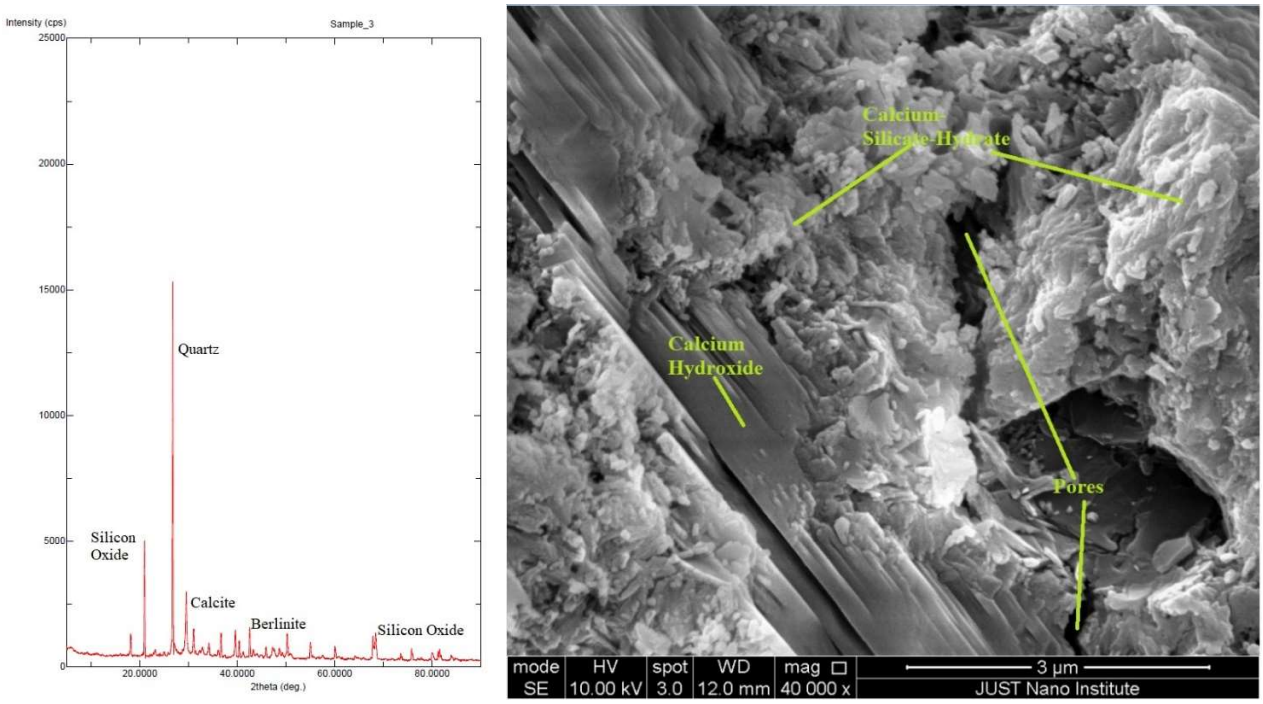

Figure 33: X-ray diffraction and SEM for sample No.3 (20% OMWW replacement)

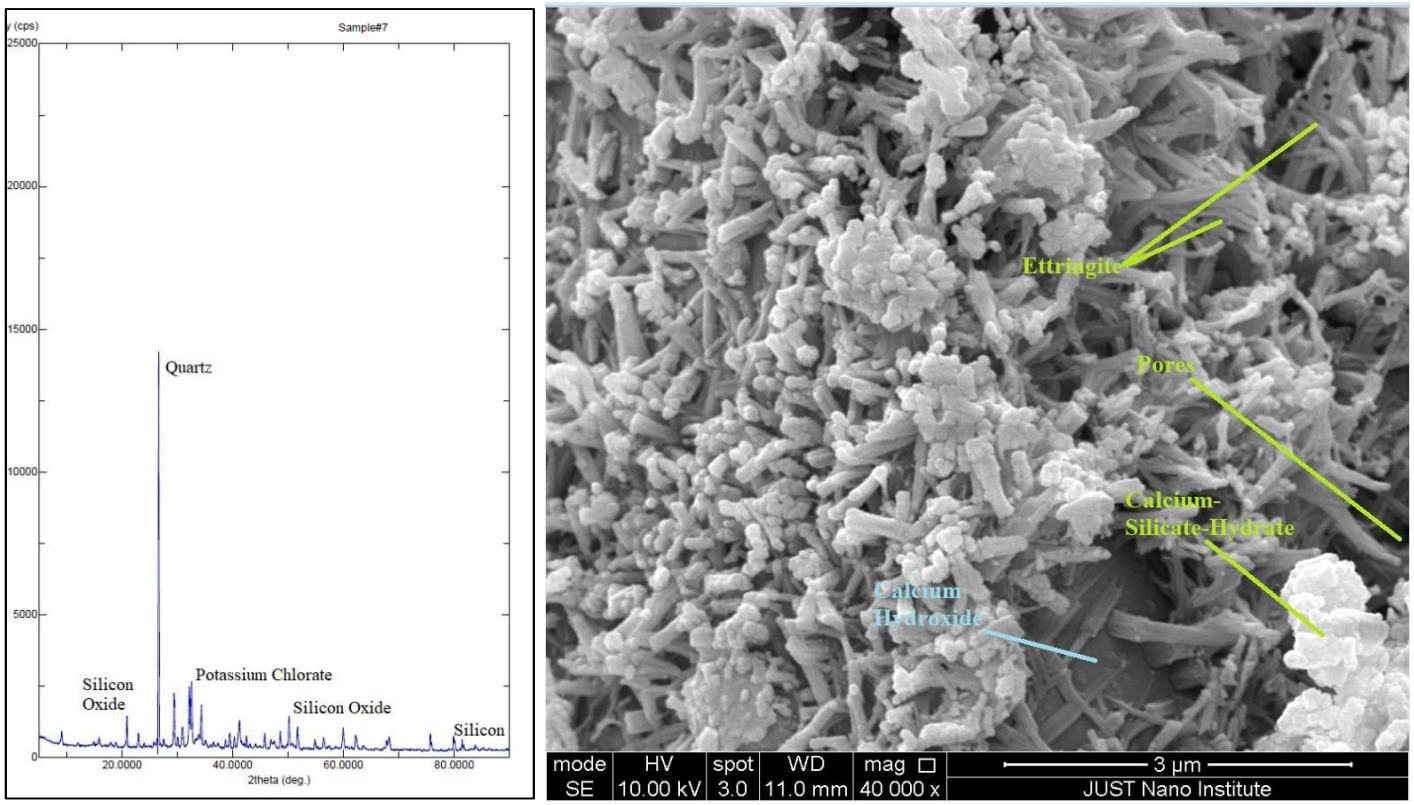

Figure 34: X-ray diffraction and SEM for sample No.7 (100% OMWW replacement)

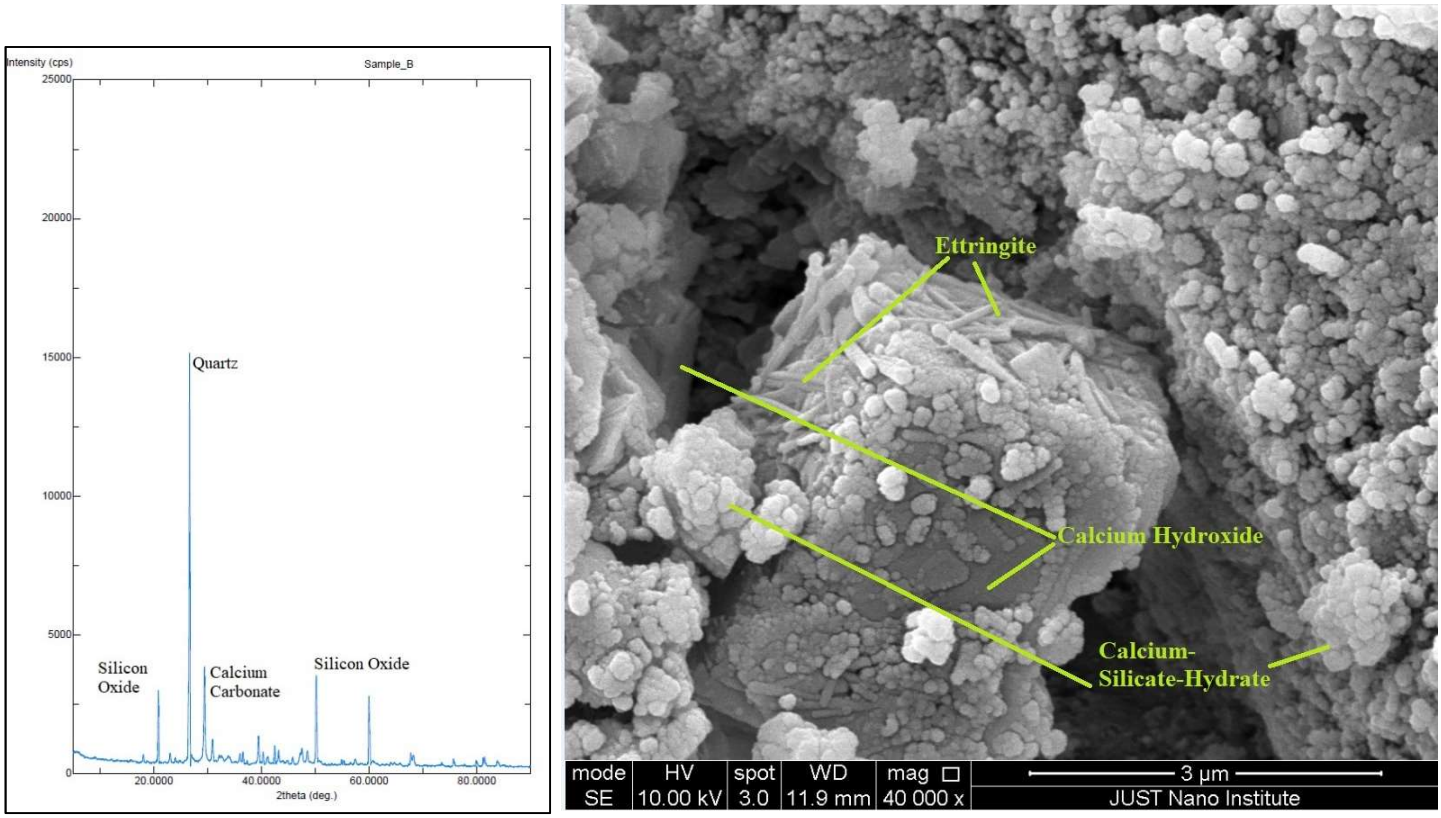

Figure 35: X-ray diffraction and SEM for sample No.B (0% OMWW replacement)

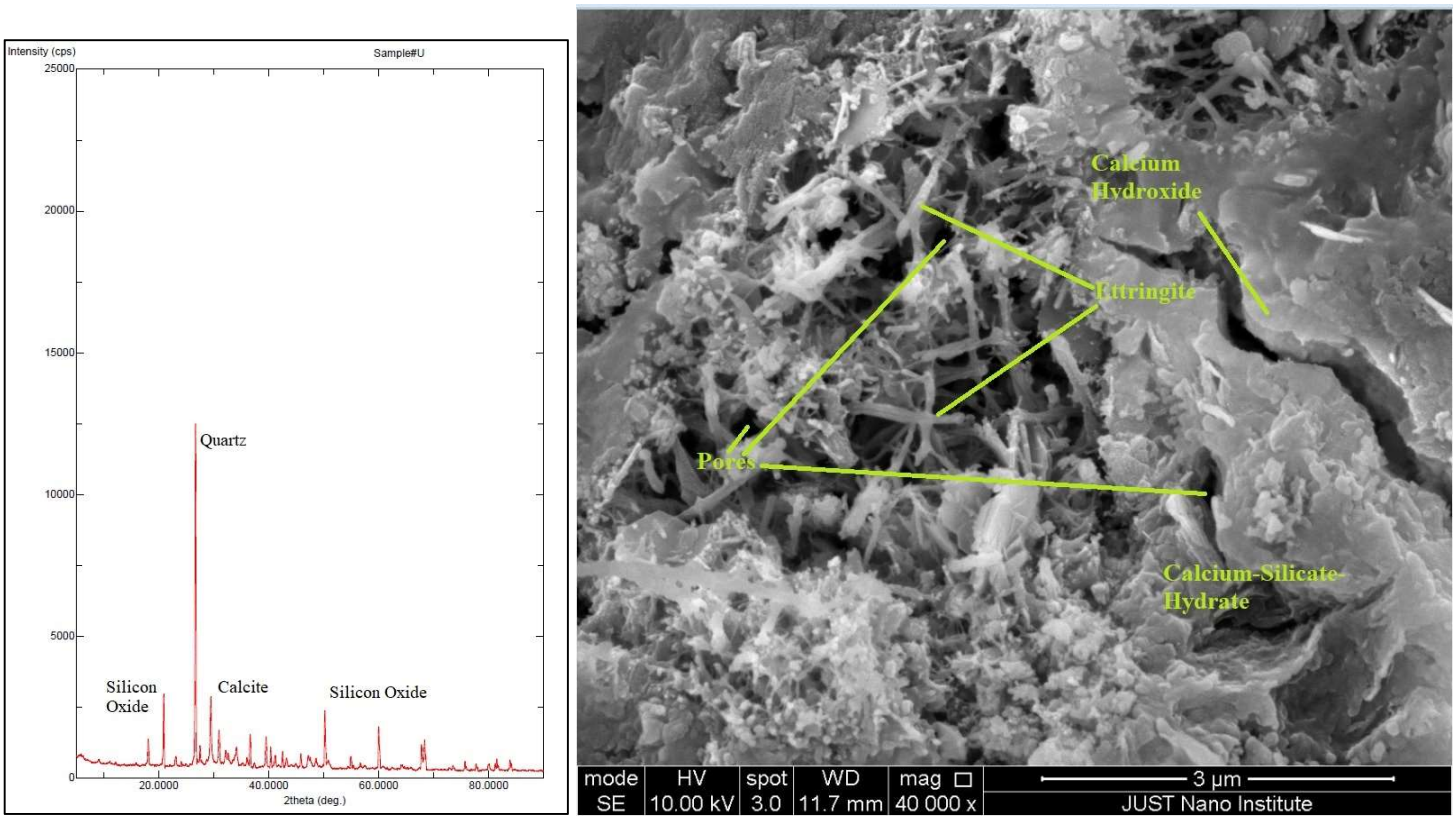

Figure 36: X-ray diffraction and SEM for sample No.U (20% OMWW replacement)

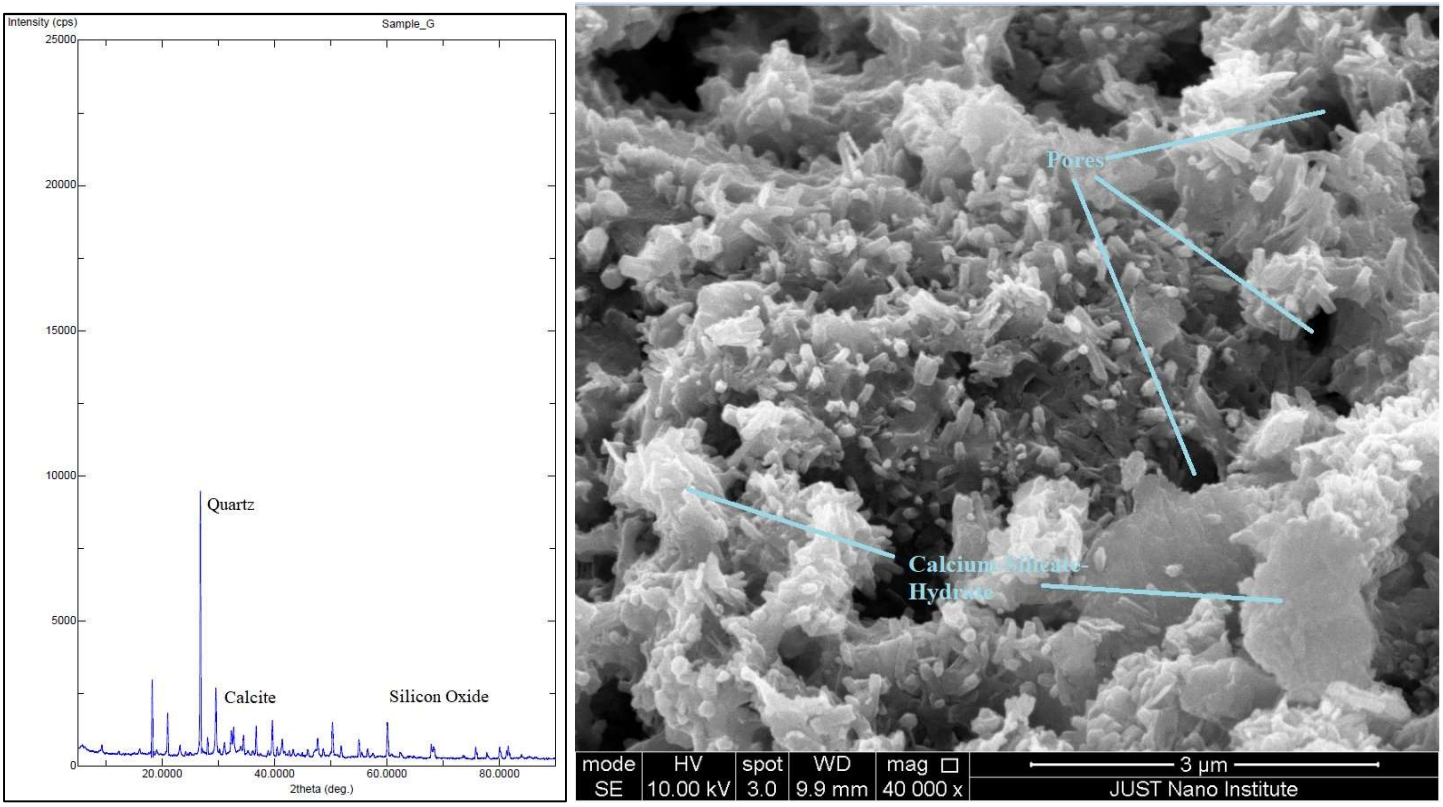

Figure 37: X-ray diffraction and SEM for sample No.G (100% OMWW replacement)

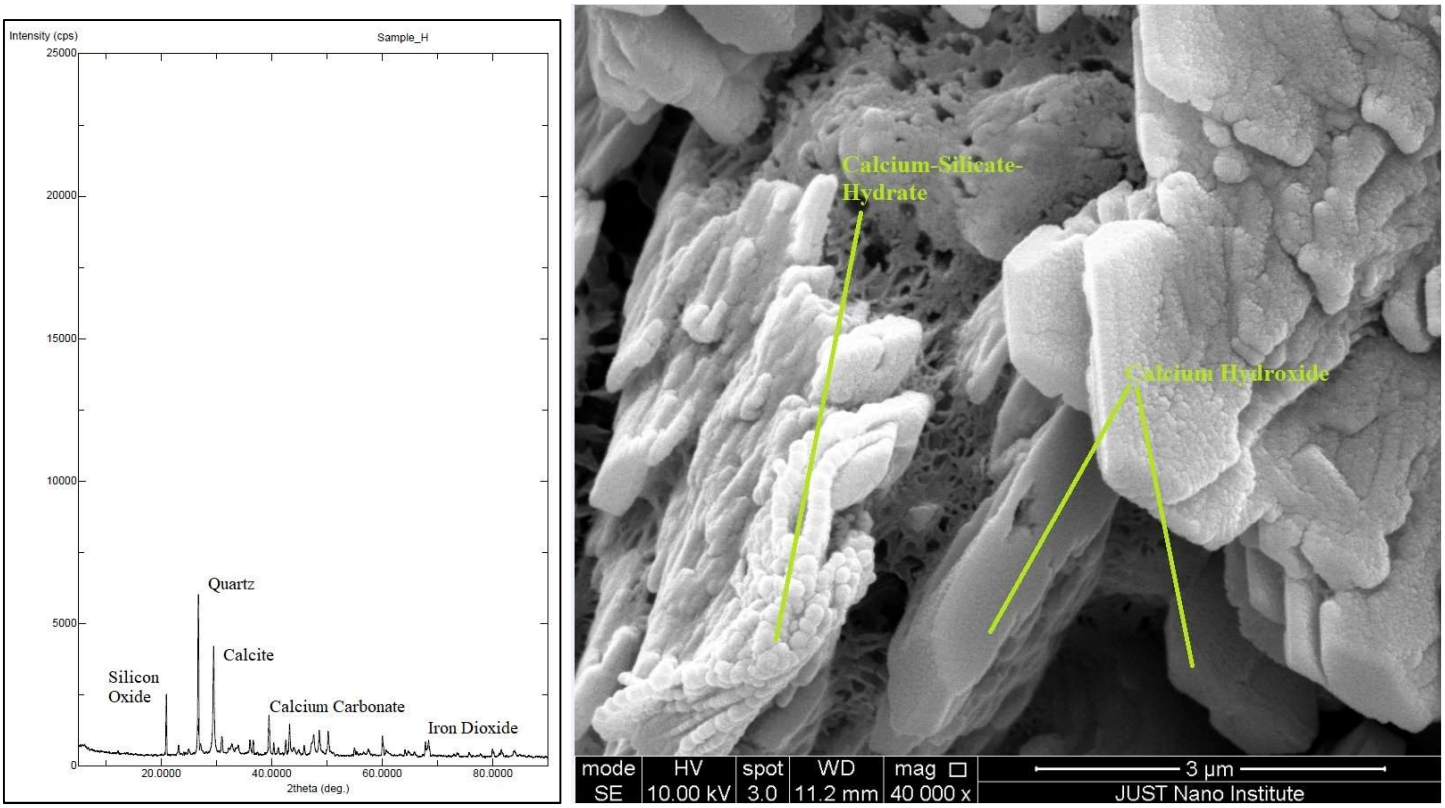

Figure 38: X-ray diffraction and SEM for sample No.H (0% OMWW replacement)

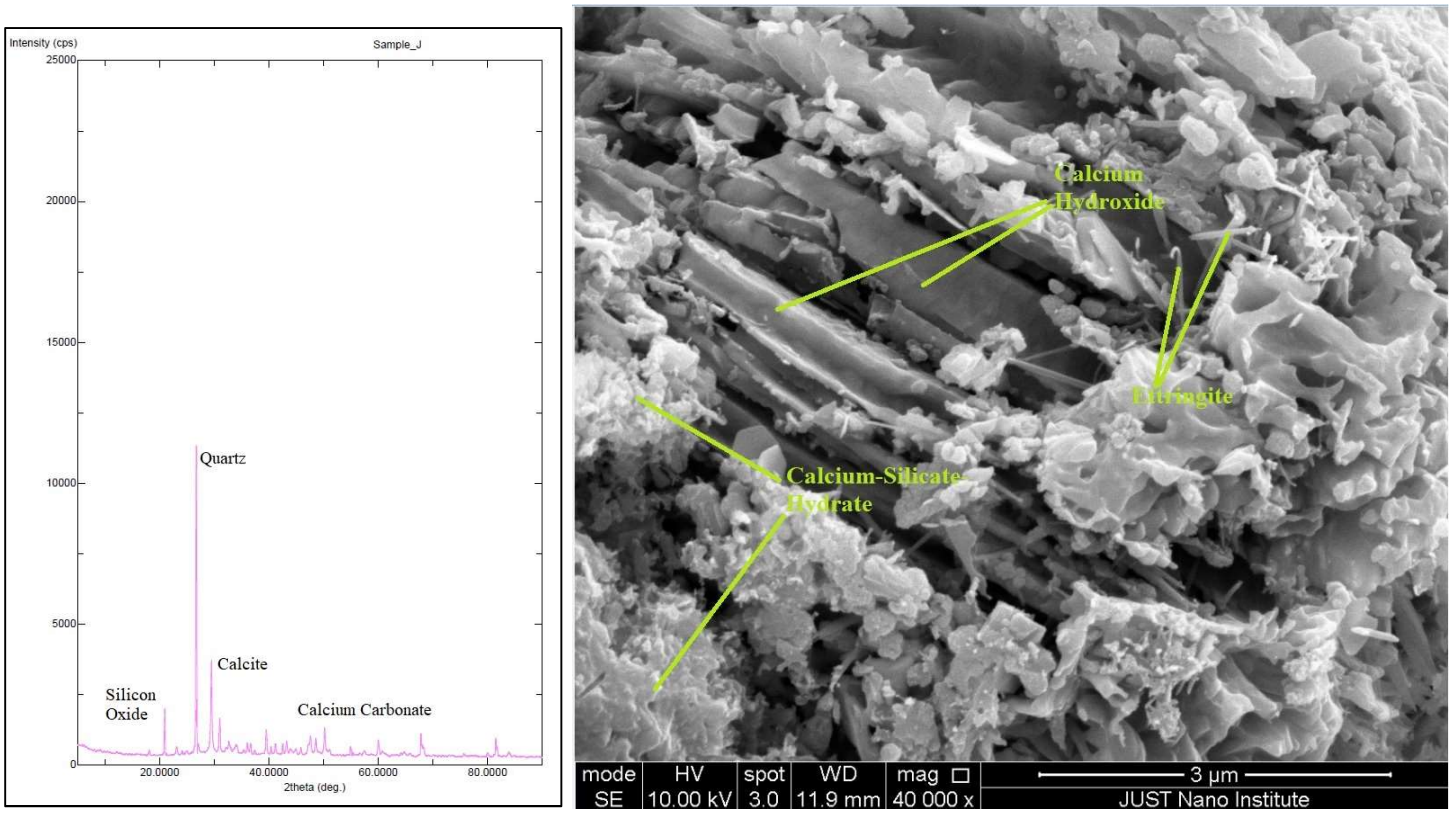

Figure 39: X-ray diffraction and SEM for sample No.J (20% OMWW replacement)

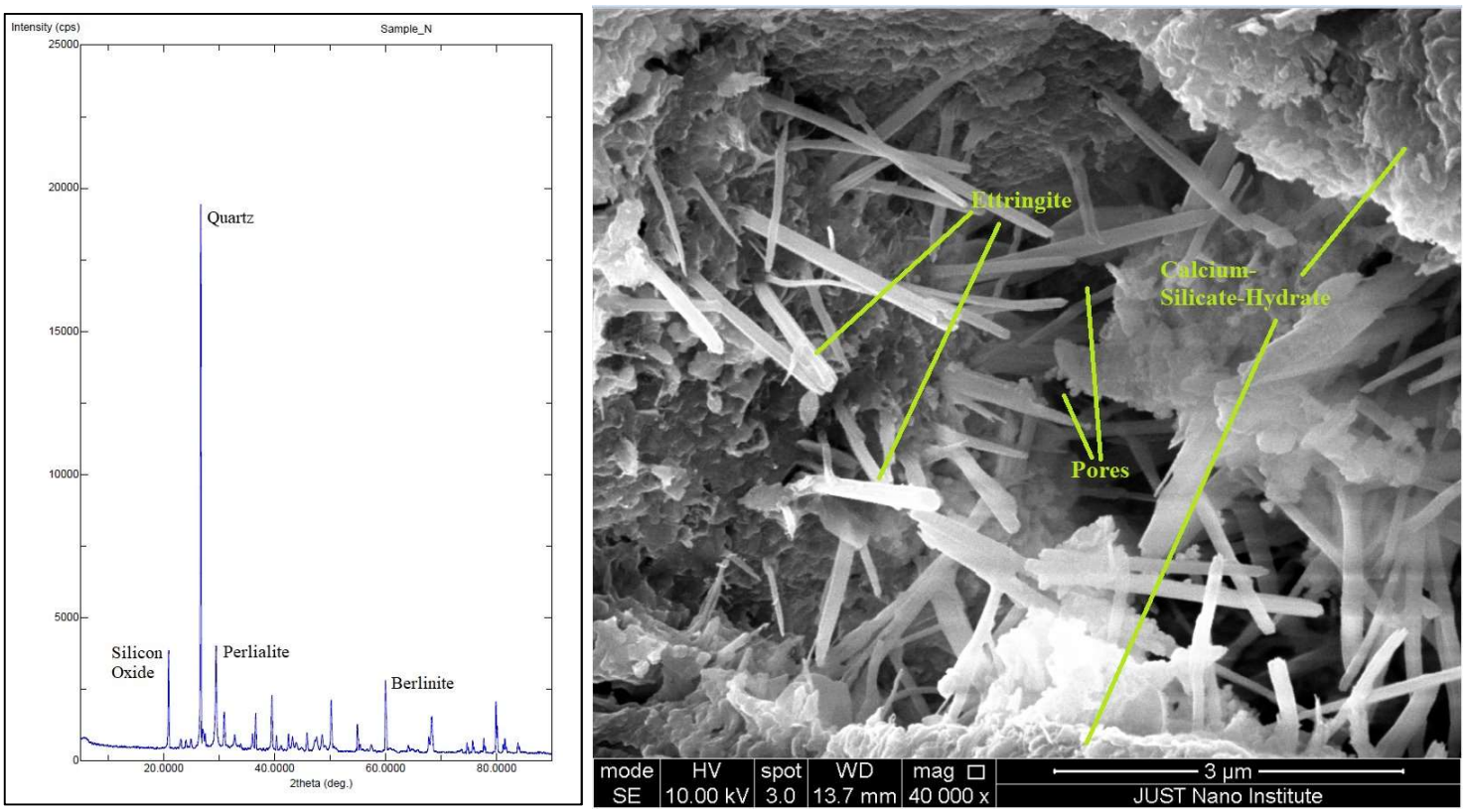

Figure 40: X-ray diffraction and SEM for sample No.N (100% OMWW replacement)

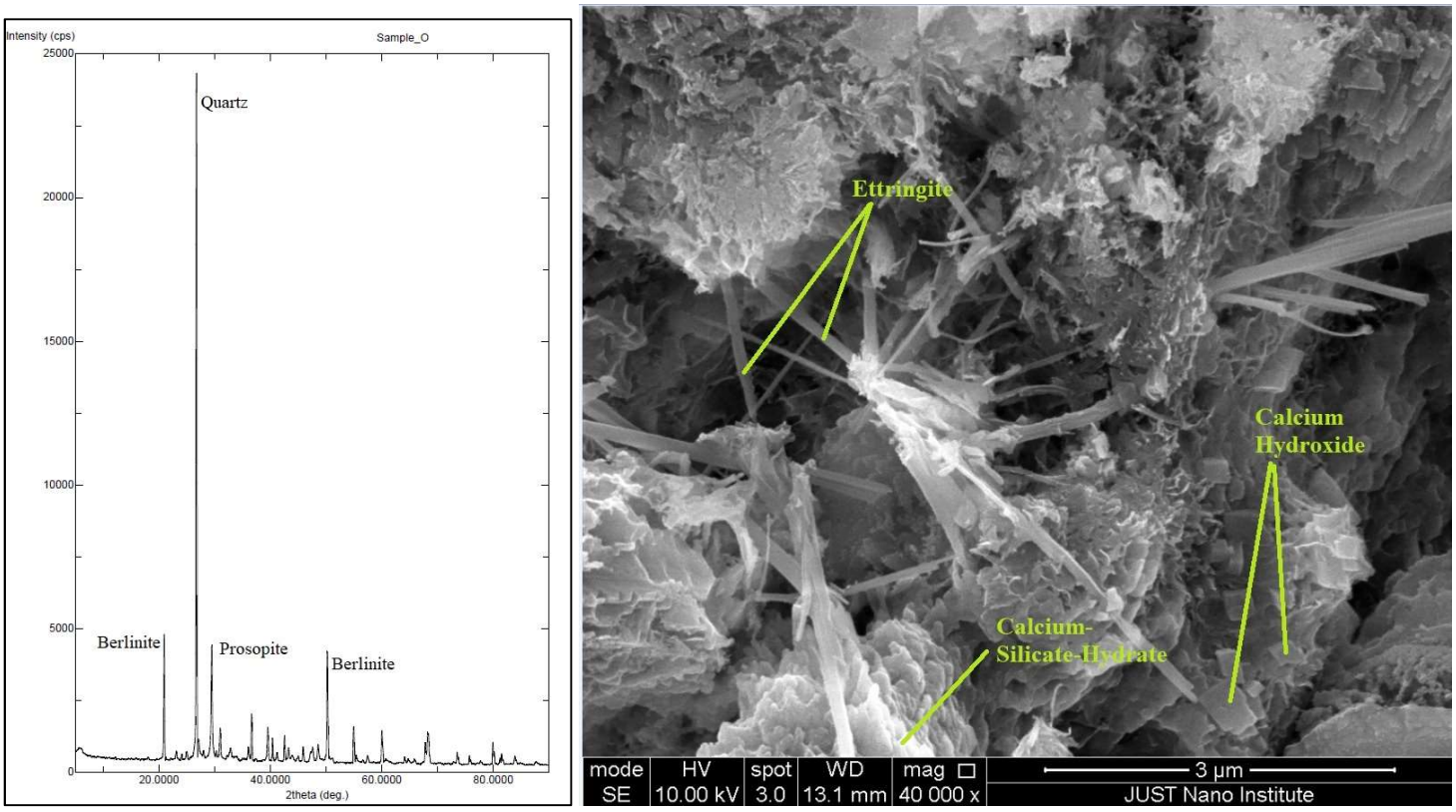

Figure 41: X-ray diffraction and SEM for sample No.O (0% OMWW replacement)

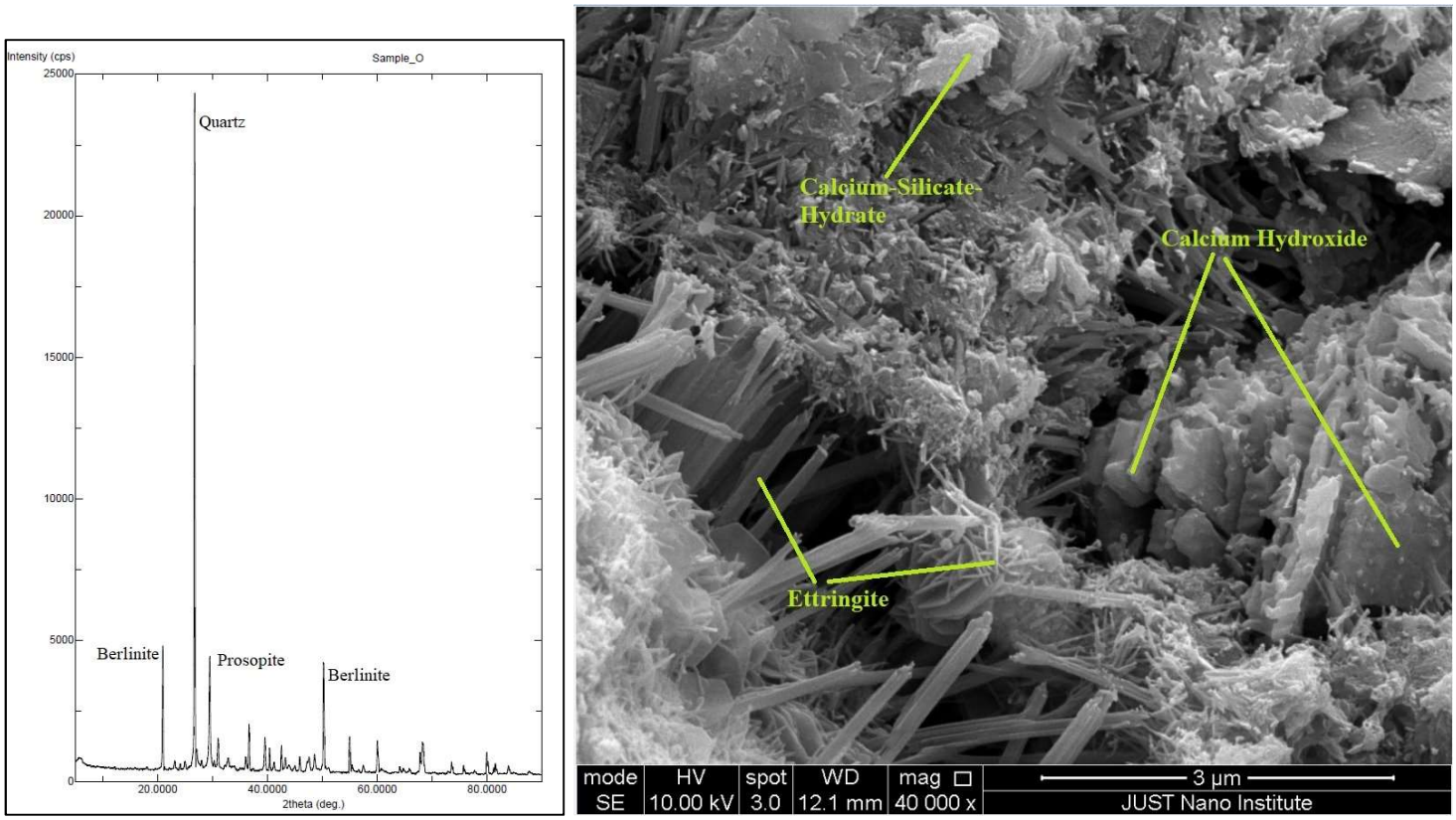

Figure 42: X-ray diffraction and SEM for sample No.R (20% OMWW replacement)

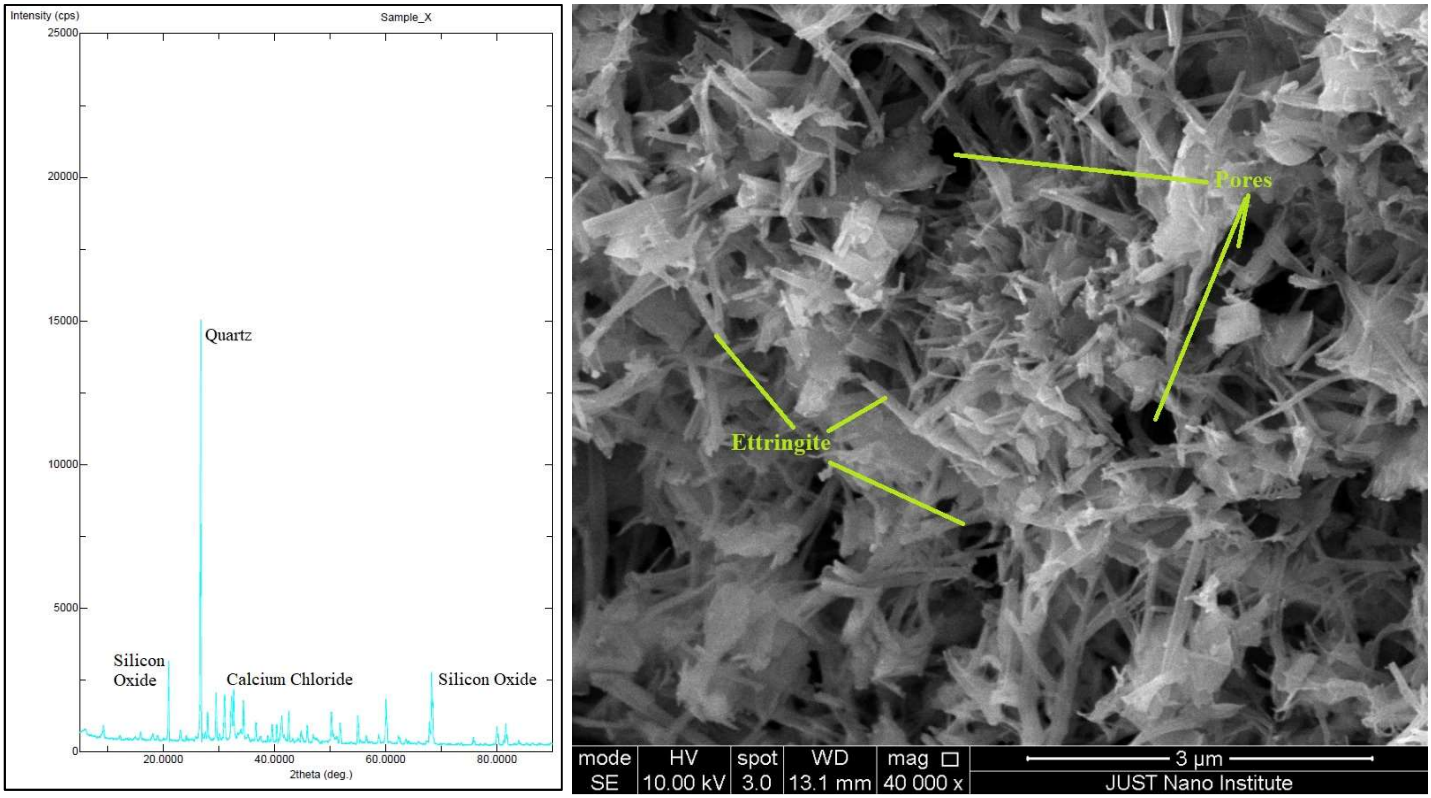

Figure 43: X-ray diffraction and SEM for sample No.X (100% OMWW replacement)

Based on SEM and x-ray images, small traces of organic matter were noticed as small white dotes. However, no noticeable traces of abnormal substances were noticed.

Figure 44 and Figure 45 and Figure 46 show the result of the x-ray diffraction test or samples H, J and N, as they show the amount of phases and elements (weight %).

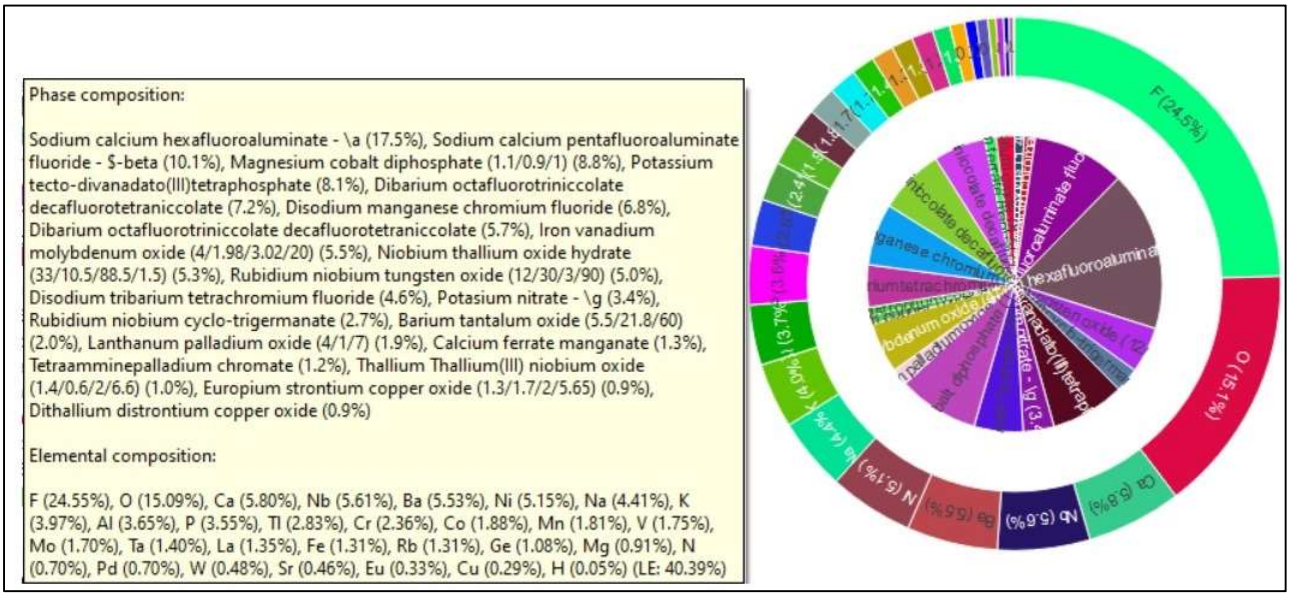

Figure 44: Amounts of phases and elements (weight %) for sample no. H

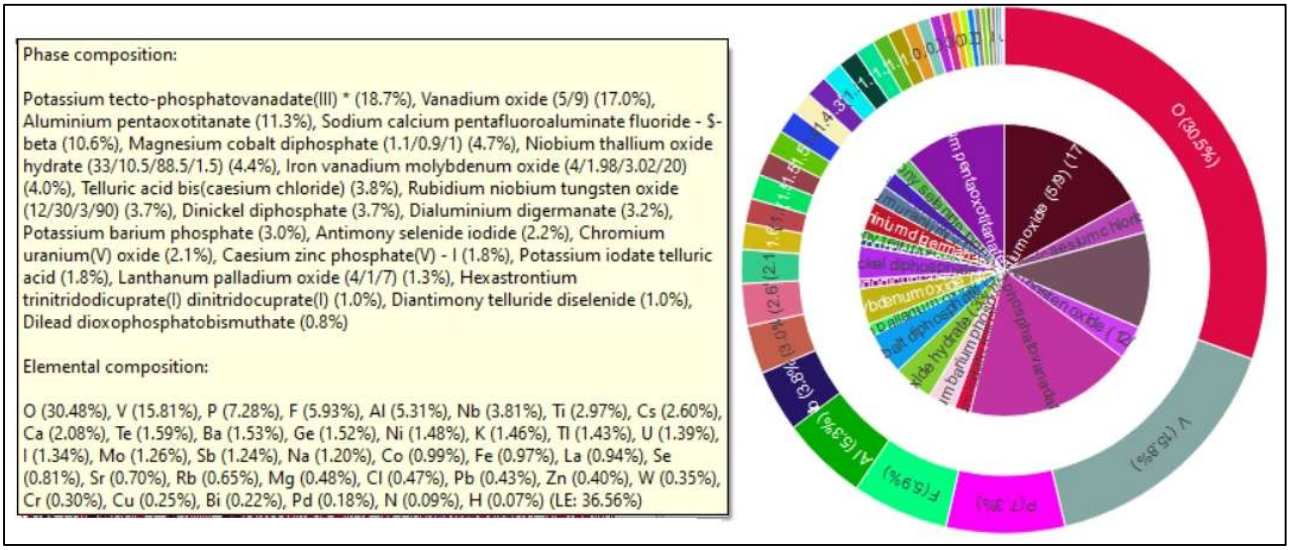

Figure 45: Amounts of phases and elements (weight %) for sample no. J

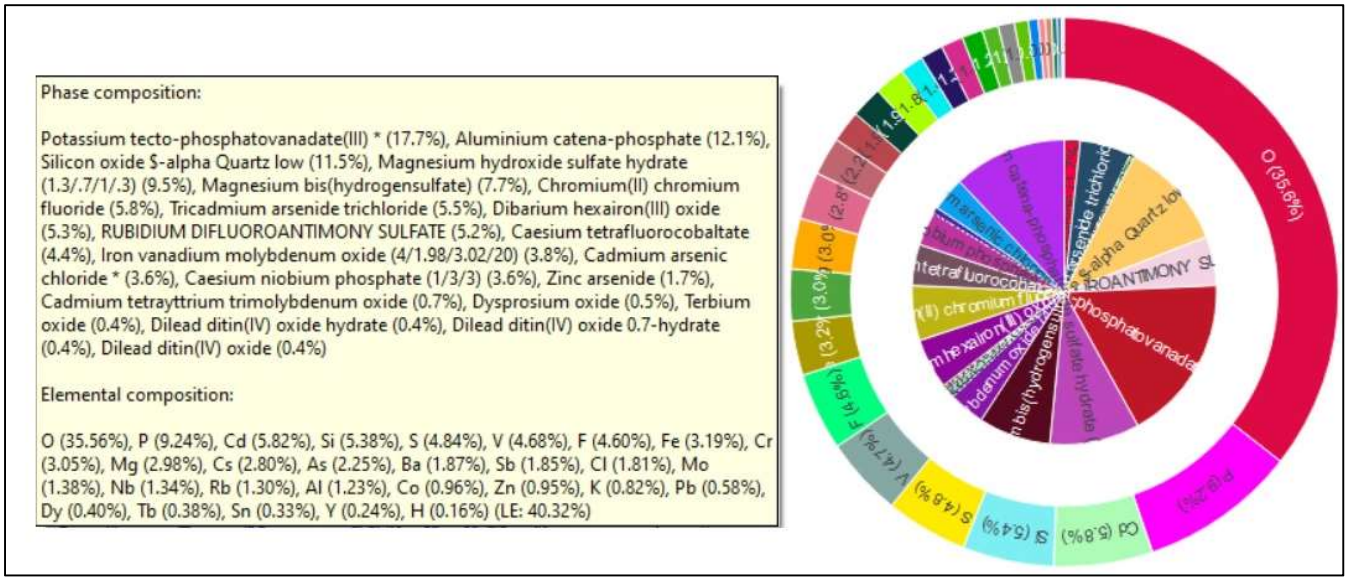

Figure 46: Amounts of phases and elements (weight %) for sample no. N

It was noticed from Figure *44*, Figure *45*, and Figure *46* that the more OMWW in the sample, the more Oxygen content there is, Also Chloride content did increase with the increase of OMWW level in the sample.

Reports for other sample's content by weight (%) are shown in the attached appendices.

3.8. Artificial Neural Network (ANN):

ANN was employed to be a design tool to determine using required outputs, the required levels of inputs to achieve the desired goals.

The first step in the ANN is to determine the number of inputs and the number of required outputs, followed by determining the number of hidden layers and hidden nodes in each hidden layer. The number of hidden nodes will be determined using the following equation:

$$HN = \frac{N\text{-}NO}{C \cdot (IN+NO+1)} \quad (1)$$

Where: N: The number of training data sets.

HN: The number of hidden nodes.

NO: The number of outputs.

IN: The number of inputs

C: The number of data points allocated to each connection weight (constant).

Inputs for the ANN were:

- Water to cement ratio, w/c
- Water Content level (%)
- Replacement level, OMWW (%)

Outputs of the ANN were:

- Control mix strength (with no replacement)
- Control mix slump (with no replacement)
- Mix strength (with replacement)
- Mix slump (with replacement)

Thus, the number of hidden layers was set to 1, and the hidden nodes were set to 6 hidden nodes.

Next, data points (a total of 84 data points) were divided into three different main groups, a) training data group which consists of 56 data points, b) testing data ground which consists of 14 data points, and c) validation data ground which consists from 14 data point too (different

from the training ones). The selection of each group's data points has been considered to include maximum and minimum values for inputs and outputs.

Results of the ANN model after training show that the validation points have reached around 98% level of confidence. Figure 47 and Figure 48 show a plot of the actual results and the predicted results by the ANN model for strength and slump with OMWW replacement.

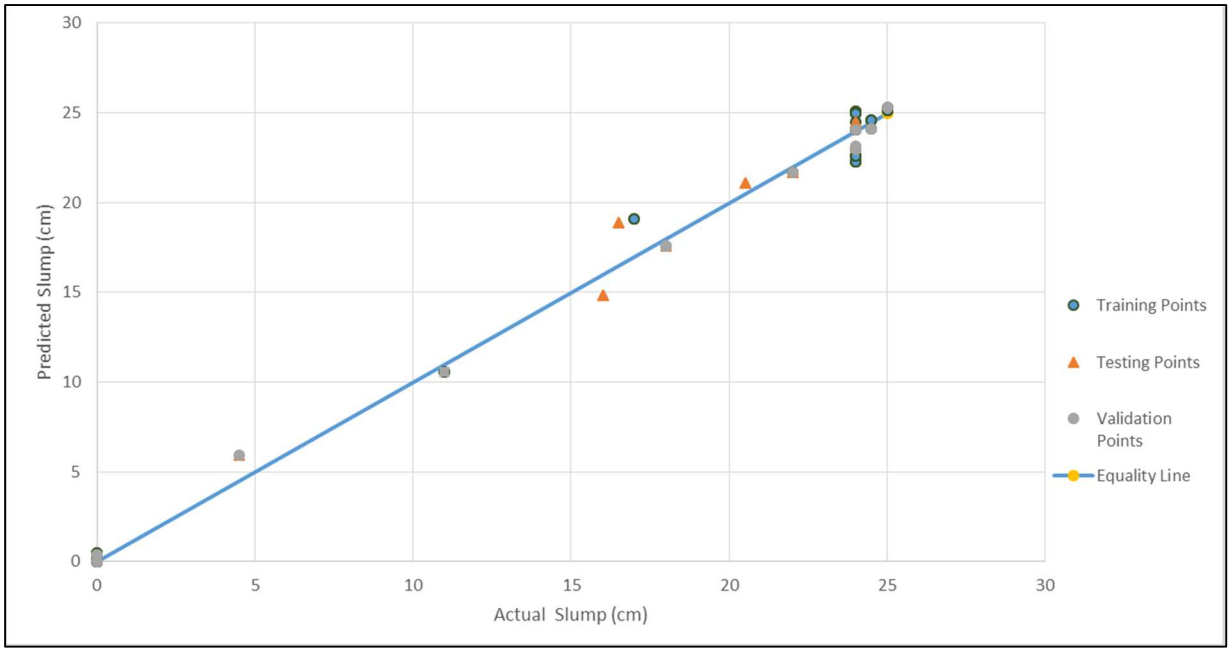

Figure 47: Plot between actual slump and slump predicted by the ANN model with OMWW replacement.

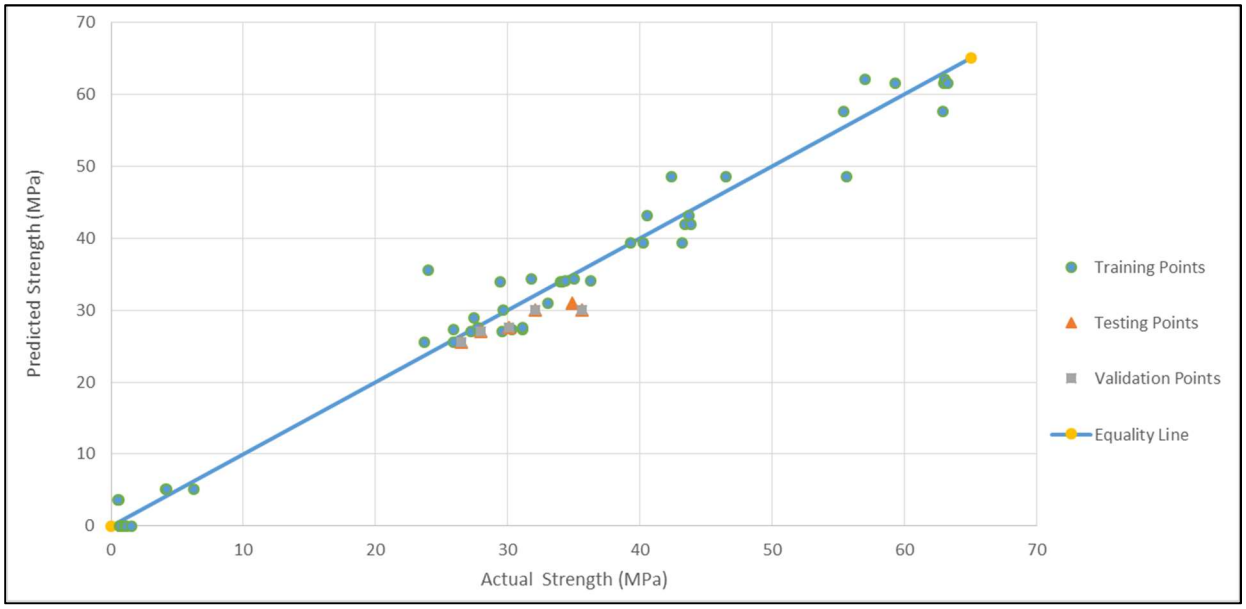

Figure 48: Plot between actual strength and strength predicted by the ANN model with OMWW replacement.

To test the ANN model's ability to predict strength and slump results, two different mixes were prepared using the created ANN model and then tested in the lab to test the actual mix strength and slump results and compare them to those predicted by the ANN model. A total of 4 mixes were prepared and tested at the lab, two with replacement and two without replacement. Table *9* shows the selected mixes and the expected results as the ANN model predicted.

Table 9: ANN model mixes expected slump and strength

Mix No.	w/c	Water content	OMWW%	Expected slump after replacement (cm)	Expected strength after replacement (MPa)	Expected original slump* (cm)	Expected original strength* (MPa)
A	0.45	11.5%	15%	17	48	3	46
B	0.7	9%	50%	18	39	1	37

*Notes: original slump and strength refer to the same w/c ratio and water content, with zero OMWW replacement.

Table 10: ANN mixes testing results

Mix No.	w/c	Water Content	OMWW%	Expected Slump (cm)	Actual tested slump (cm)	Expected Strength (Mpa)	Actual tested strength (Mpa)
1	0.45	11.5%	15%	17	19.5	48	45.83
							49.29
							44.17
2	0.45	11.5%	0%	2.5	3	46	44.94
							45.91
							45.06
3	0.70	9%	50%	18	16	39	18.04
							20.09
							18.24
4	0.70	9%	0%	1	2.5	37	20.15
							20.56
							22.88

As per Table 10, laboratory testing results show that:

- For both tested mixes, the ANN model expected the slump results to a good degree.

- For Mixes 1 and 2 (w/c = 0.45), the ANN model expected the strength for both the control mix (zero replacement) and the mix with replacement with a good degree.
- For Mixes 3 and 4 (w/c = 0.70), testing results show that the strength for zero replacement is close to the mix with 50% OMWW replacement. However, ANN did not expect the strength for both the control (zero replacement) and the replaced mix, this can be related to the fact that the ratio of w/c (0.7) is out of this research laboratory experimental work range since w/c ratios for the tested mixes ranges from (0.35) up to (0.65), so this causes the ANN model to extrapolate the results for higher range of w/c ratios.

After validating the results of the ANN model using lab testing, and knowing that the results of the model are valid for w/c ratios within the testing range (between 0.35 to 0.65), the ANN model was used to predict the strength of the tested mixes to plot and compare strength results between the lab testing results and the ANN model.

Figure 49 and Figure 50 and Figure 51 show the relationship between OMWW% and strength predicted by ANN and from laboratory testing different w/c ratios and different water contents. Results show a good match between ANN simulation and the lab testing results.

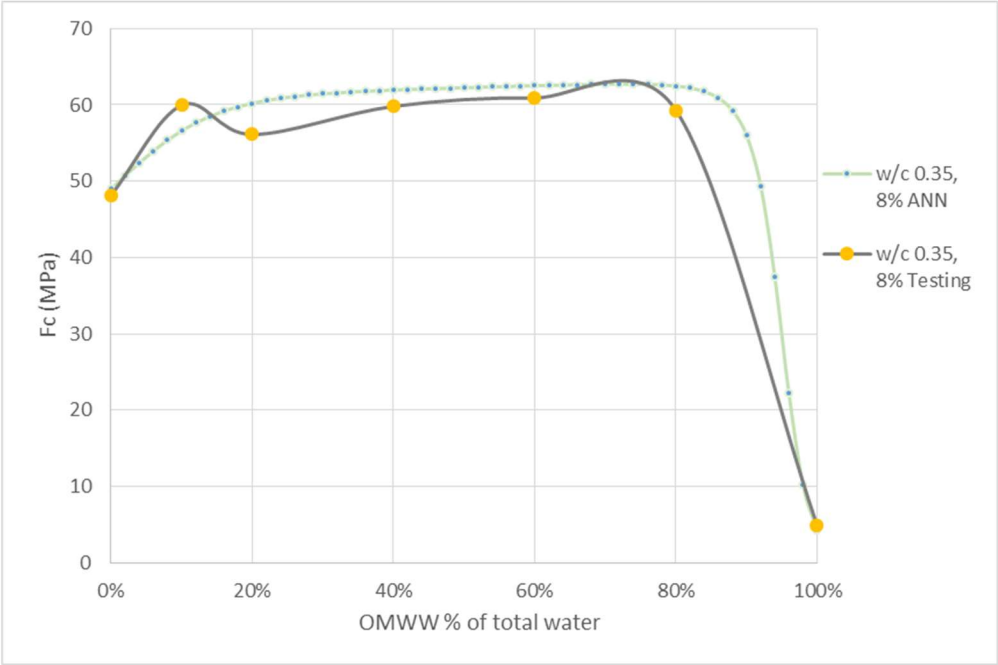

Figure 49: Relationship between OMWW% and strength predicted by ANN and from lab testing for w/c =0.35 and 8% water content.

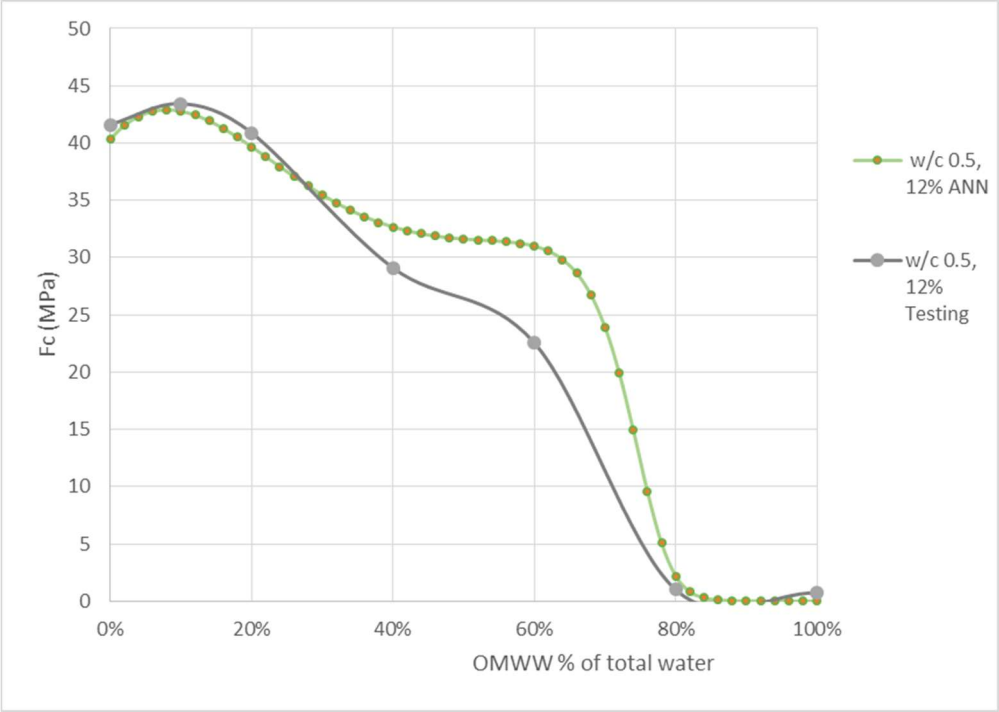

Figure 50: Relationship between OMWW% and strength predicted by ANN and from lab testing for w/c =0.5 and 10% water content.

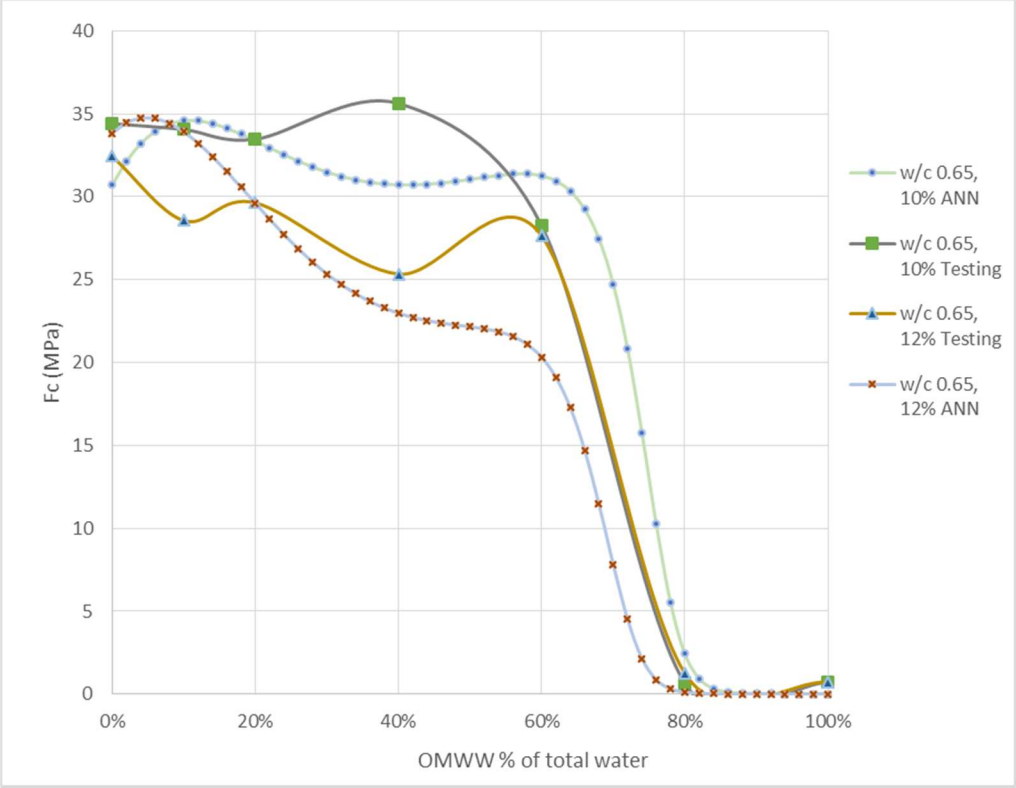

Figure 51: Relationship between OMWW% and strength predicted by ANN and from lab testing for w/c =0.65 and 10% and 12% water content.

This was extended to cover different water contents that were not tested in the lab, see Figure 52, Figure 53, and Figure 54.

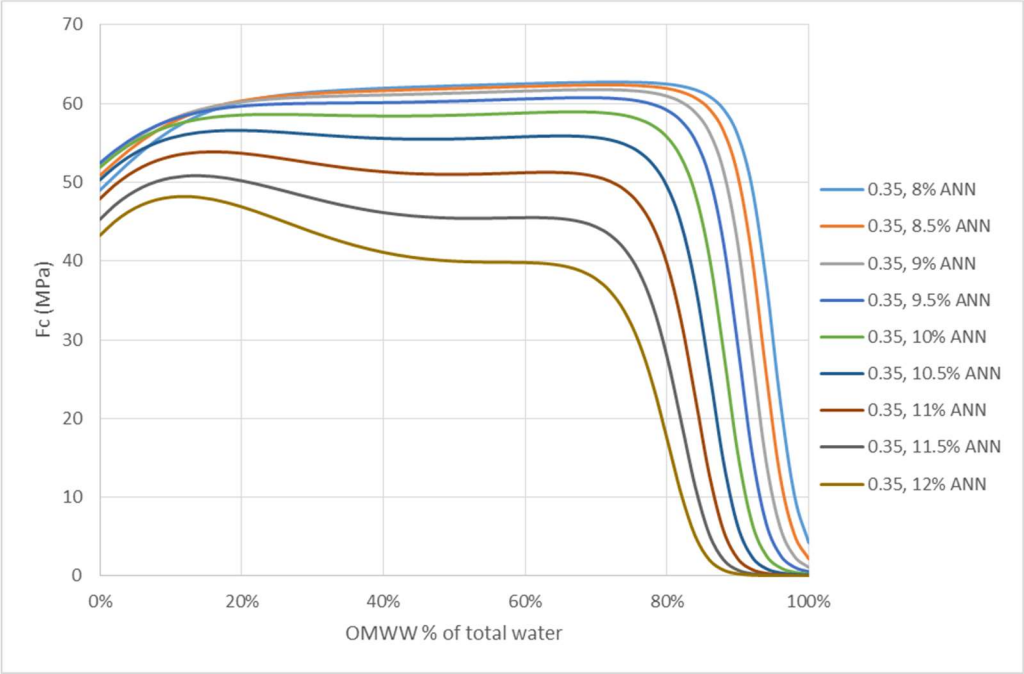

Figure 52: Relationship between OMWW% and strength predicted by ANN for w/c =0.35 with different water contents

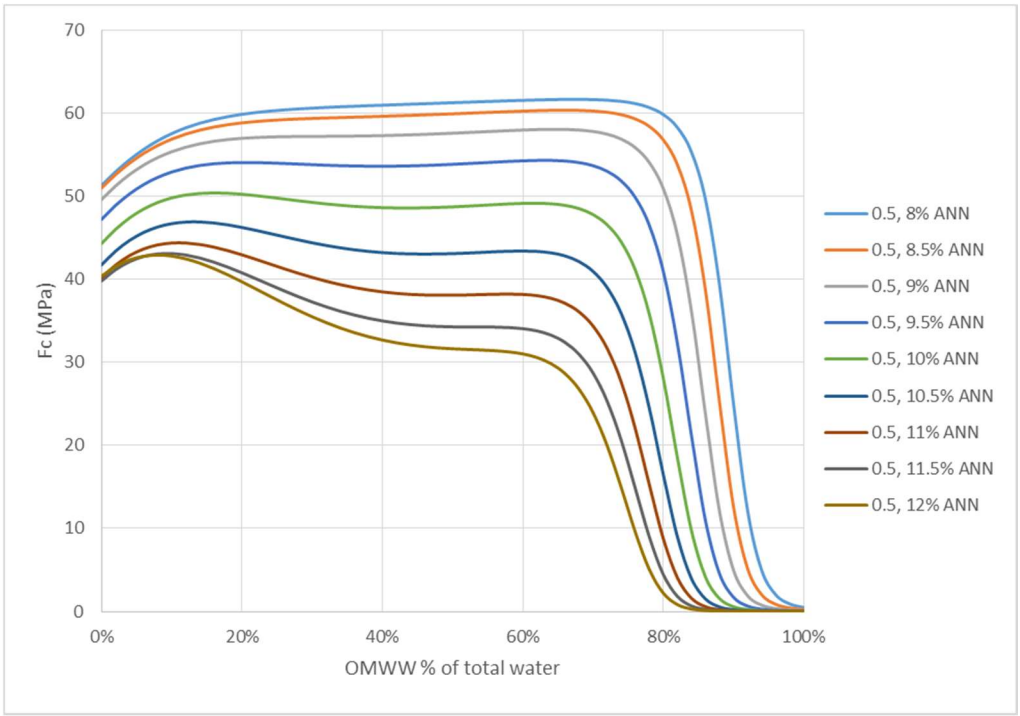

Figure 53: Relationship between OMWW% and strength predicted by ANN for w/c =0.5 with different water contents

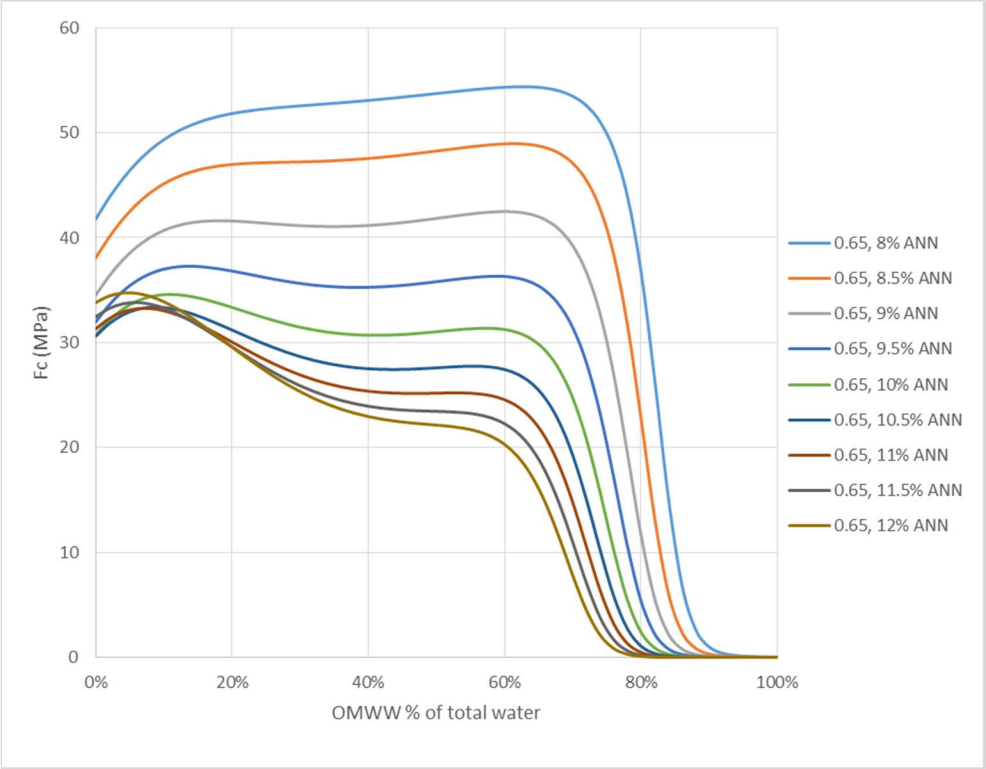

Figure 54: Relationship between OMWW% and strength predicted by ANN for w/c =0.65 with different water contents

MATLAB was used to plot the relationship between the OMWW replacement ratio and the water content for slump and strength, as a sample, results for w/c 0.5, as shown in Figure *55*, show that for a replacement to be effective for the slump, it shall be in a certain range as shown by the curved line, and for strength, an opposite curve is drawn, a third curve is drawn from combining the two curves of strength and slump, this curve shows the area of replacement and water content levels that is optimum for w/c of 0.50. Similar curves can be created for different w/c ratios.

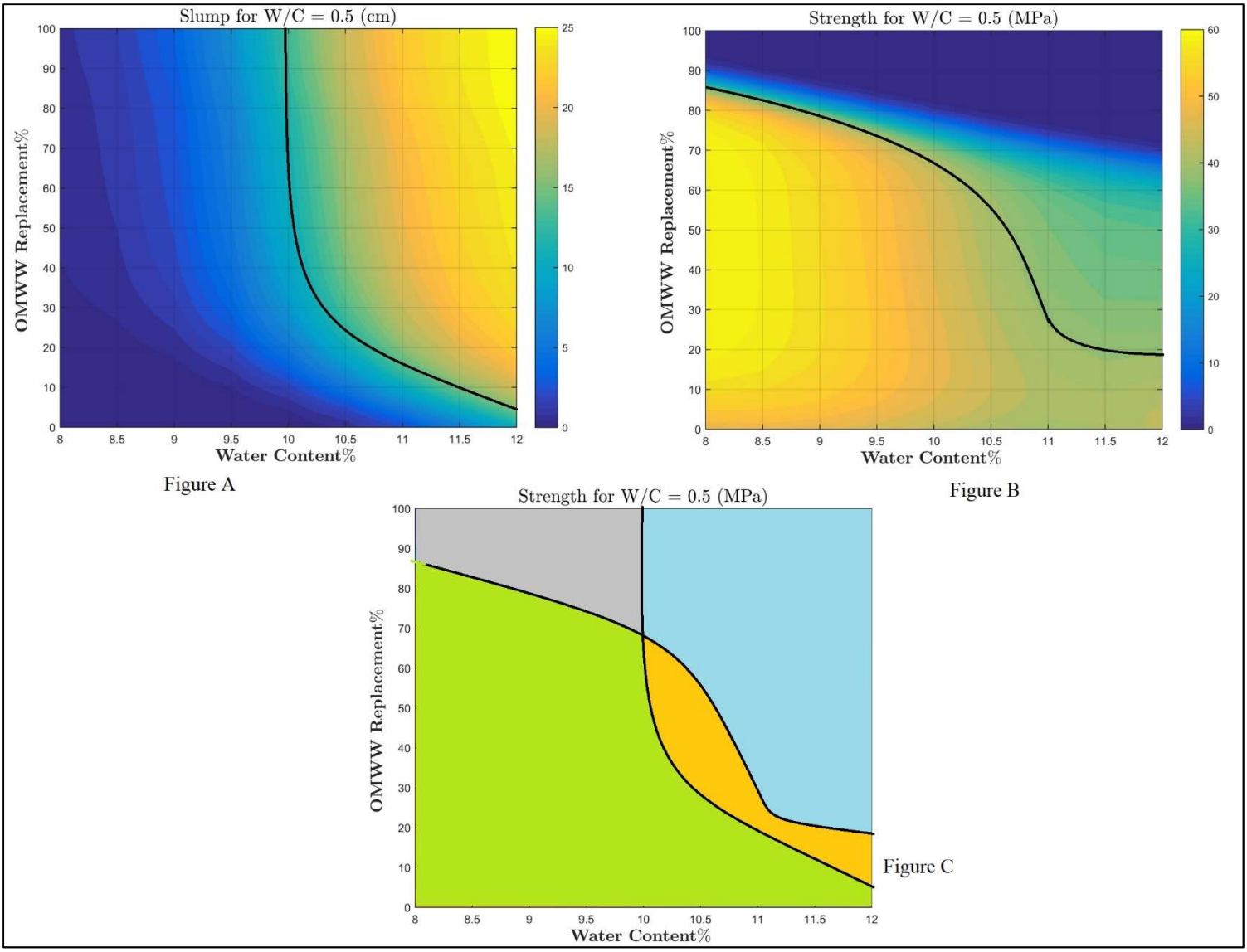

Figure 55: OMWW replacement level vs. water content level for w/c = 0.50, A) shows the relationship for strength, B) shows the relationship for the slump, and C) shows the relationship for both.

CHAPTER FOUR: CONCLUSIONS AND RECOMMENDATIONS

Based on the obtained results it was concluded that OMWW has a significant effect on concrete when added to a concrete mix. The effect of OMWW depends on water content and w/c. It was clear that as water content increased, the effect of OMWW increased too. It was noted that adding OMWW to a concrete mix has increased its slump, this increase depends on the water content of the mix and w/c ratio. Adding OMWW to the concrete mixes increased the slump of Mix B, Mix C, and Mix D to a point of total collapse at certain replacement ratios, depending on water content and replacement level.

Replacing normal water with OMWW (100% replacement level) in a concrete mix greatly decreased concrete compressive strength, this might be related to the composition of the OMWW and the existence of organic matters and other compositions previously mentioned, as crushing of concrete cubes of mixes with high OMWW replacement ratios (80% and 100%) shows a non-hardened concrete inside these cubes.

For low replacement levels (up to 20%), the compressive strength of concrete shows a small deviation from the original strength (original strength with zero OMWW replacement level), and for higher replacement levels, the strength started to decrease until it reaches the point of almost no strength for the full replacement level (100% OMWW instead of normal water). The decrease in the mix strength after adding OMWW to the mix is not a sudden decrease, it started (at low replacement ratios) to show an increase or have no effect on the concrete strength, however, as the replacement ratio increased, the strength started to decrease until it reached almost no strength at the full replacement of OMWW instead of normal water. Also, as the water content increased in the concrete mix, the speed of strength degradation increased.

For the same w/c ratio, increasing water content decreased the strength by (10-20%) for water content changing from 10% to 12%. For the same water content with different w/c ratios, the mix with a lower w/c ratio shows more overall strength compared to a higher w/c ratio for all OMWW replacement levels.

For approximately up to 20% OMWW replacement of total water content, the effect of OMWW shows an increase in a slump without any significant change in the strength.

From testing ages more than 28 days, it was found that strength does not decrease with time, in contrast, it did increase even for mixes with high replacement levels.

ANN model shows a good ability to predict the results of slump and compressive strength for w/c ratio within the research testing range (0.35-0.65), this was validated using laboratory testing for mixes created by the ANN model.

ANN model was used to create figures for different w/c rather than tested ones, and MATLAB was used using points obtained from the ANN model to plot relationships between replacement and expected slump and strength to show optimum ranges for different w/c ratios. These figures can be used as a design tool to optimize the required mix.

It was noted that during the curing period, the oily substance inside OMWW leaked from the concrete to the surrounding water, and it was visible at the surface of the curing water.

Mixes with an OMWW level of less than 30% will not impose any harm on the reinforcing steel as the level of chloride will not reach the limit recommended by the ASTM. It is recommended to use the concrete in a non-reinforced element if higher levels of OMWW are used.

X-ray diffraction results show a trace of oily substance in the concrete, this does increase as the OMWW replacement increases, in addition, and it shows higher oxygen content as the OMWW replacement increases.

Future work:

The work made in this research can be extended to include:

- Different w/c ratios and different water contents.
- Extend the ranges of w/c and water contents beyond and above selected ratios.
- The effect of adding other additives while adding OMWW to the concrete.
- Using different types of cement.
- Use a treatment method for the OMWW and use it in the concrete after treatment.
- ANN model needs more training points in order to be able to design mixes outside the range specified in this research.

Appendices:

Attached to this report are the following appendices:

1- Appendix A: Water samples test results.
2- Appendix B: X-ray reports and SEM images.
3- Appendix C: MATLAB output images.

REFERENCES

Afandi, A., Lusi, N., Catrawedarma, I. G. N. B., Subono, S., & Rudiyanto, B. (2022). Prediction of temperature in 2 meters temperature probe survey in Blawan geothermal field using artificial neural network (ANN) method. *Case Studies in Thermal Engineering*, *38*. https://doi.org/10.1016/j.csite.2022.102309

A, O. S., & B, E. E. (n.d.). *Effect of Sodium Chloride (Nacl) on Concrete Compressive strength; Effect of Sodium Chloride (Nacl) on Concrete Compressive strength*. www.askthebuilder.com/B251

ASTM C1602. (n.d.).

Badur, S., & Chaudhary, R. (2008). UTILIZATION OF HAZARDOUS WASTES AND BY-PRODUCTS AS A GREEN CONCRETE MATERIAL THROUGH S/S PROCESS: A REVIEW. In *Rev.Adv.Mater.Sci* (Vol. 17).

Batayneh, M., Marie, I., & Asi, I. (2007). Use of selected waste materials in concrete mixes. *Waste Management*, *27*(12), 1870–1876. https://doi.org/10.1016/j.wasman.2006.07.026

Beddaa, H., Fraj, A. Ben, Lavergne, F., & Torrenti, J.-M. (2019). *Effect of potassium humate as humic substances from river sediments on the rheology, the hydration and the strength development of a cement paste*. https://www.elsevier.com/open-access/userlicense/1.0/

Cassano, A., Conidi, C., Galanakis, C. M., & Castro-Muñoz, R. (2016). Recovery of polyphenols from olive mill wastewaters by membrane operations. In *Membrane Technologies for Biorefining* (pp. 163–187). Elsevier Inc. https://doi.org/10.1016/B978-0-08-100451-7.00007-4

Ekins, P., & Zenghelis, D. (2021). The costs and benefits of environmental sustainability. *Sustainability Science*, *16*(3), 949–965. https://doi.org/10.1007/s11625-021-00910-5

El Hassani, F. Z., Fadile, A., Faouzi, M., Zinedine, A., Merzouki, M., & Benlemlih, M. (2020). The long term effect of Olive Mill Wastewater (OMW) on organic matter humification in a semi-arid soil. *Heliyon*, *6*(1). https://doi.org/10.1016/j.heliyon.2020.e03181

Guo, Y., Wang, X.-P., Zhu, Y.-F., Zhang, J., Gao, Y.-B., Yang, Z.-Y., Du, R.-G., & Lin, C.-J. (2013). Electrochemical and XPS Study on Effect of Cl-on Corrosion Behavior of Reinforcing Steel in Simulated Concrete Pore Solutions. In *Int. J. Electrochem. Sci* (Vol. 8). www.electrochemsci.org

Kucche, M. K. J., Jamkar, S. S., & Sadgir, P. A. (2015). Quality of Water for Making Concrete: A Review of Literature. *International Journal of Scientific and Research Publications*, *5*(1).

Lallahem, S., Mania, J., Hani, A., & Najjar, Y. (2005). On the use of neural networks to evaluate groundwater levels in fractured media. *Journal of Hydrology*, *307*(1–4), 92–111. https://doi.org/10.1016/j.jhydrol.2004.10.005

Liu, D., Zhang, B., Yang, Y., Xu, W., Ding, Y., & Xia, Z. (2018). Effect of Organic Material Type and Proportion on the Physical and Mechanical Properties of Vegetation-Concrete. *Advances in Materials Science and Engineering*, *2018*. https://doi.org/10.1155/2018/3608750

Mohawesh, O., Mahmoud, M., Janssen, M., & Lennartz, B. (2014). Effect of irrigation with olive mill wastewater on soil hydraulic and solute transport properties. *International Journal of Environmental Science and Technology*, *11*(4), 927–934. https://doi.org/10.1007/s13762-013-0285-1

Qatu, K. (2019). *Optimizing the performance of complex engineering systems aided by artificial neural networks*. https://egrove.olemiss.edu/etd/1962

Sabri Saleh, I. (2017). Effect of External and Internal Sulphate on Compressive Strength of Concrete. In *International Journal of Applied Engineering Research* (Vol. 12). http://www.ripublication.com

Salih Al-Attar, T., Tareq Salih AL-ATTAR, A., & Mustafa Sameer ABDUL-KAREEM, L. (n.d.). *Effect of Chloride Ions Source on Corrosion of Reinforced Normal and High Performance Concrete. Utilization of mineral-sequestration for CO2 in car parks and tunnels View project Performance of Super-Absorbent Polymer (SAP) as an Internal Curing Agent for Self-Compacting Concrete View project EFFECT OF CHLORIDE IONS SOURCE ON CORROSION OF REINFORCED CONCRETE EFFECT OF CHLORIDE IONS SOURCE ON CORROSION OF REINFORCED NORMAL AND HIGH PERFORMANCE CONCRETE*. https://www.researchgate.net/publication/280295710

Sinshaw, T. A., Surbeck, C. Q., Yasarer, H., & Najjar, Y. (2019). Artificial Neural Network for Prediction of Total Nitrogen and Phosphorus in US Lakes. *Journal of Environmental Engineering*, *145*(6). https://doi.org/10.1061/(asce)ee.1943-7870.0001528

Slama, H. Ben, Chenari Bouket, A., Alenezi, F. N., Khardani, A., Luptakova, L., Vallat, A., Oszako, T., Rateb, M. E., & Belbahri, L. (2021). Olive Mill and Olive Pomace Evaporation Pond's By-Products: Toxic Level Determination and Role of Indigenous Microbiota in Toxicity Alleviation. *Applied Sciences*, *11*(11), 5131. https://doi.org/10.3390/app11115131

Smaoui, N., Bérubé, M. A., Fournier, B., Bissonnette, B., & Durand, B. (2005). Effects of alkali addition on the mechanical properties and durability of concrete. *Cement and Concrete Research*, *35*(2), 203–212. https://doi.org/10.1016/j.cemconres.2004.05.007

Stutzman, P. E. (n.d.). Workshop on the Role of Calcium Hydroxide in Concrete). In *Proceedings. J. Skalny*.

Uzbaş, B., & Aydın, A. C. (2019). Analysis of Fly Ash Concrete With Scanning Electron Microscopy and X-Ray Diffraction. *Advances in Science and Technology Research Journal*, *13*(4), 100–110. https://doi.org/10.12913/22998624/114178

Yoneyama, A., Choi, H., Inoue, M., Kim, J., Lim, M., & Sudoh, Y. (2021). Effect of a nitrite/nitrate-based accelerator on the strength development and hydrate formation in cold-weather cementitious materials. *Materials*, *14*(4), 1–14. https://doi.org/10.3390/ma14041006

Zagklis, D. P., Arvaniti, E. C., Papadakis, V. P., & Paraskeva, C. A. (2013). Sustainability analysis and benchmarking of olive mill wastewater treatment methods. In *Journal of Chemical Technology and Biotechnology* (Vol. 88, Issue 5, pp. 742–750). https://doi.org/10.1002/jctb.4036

Zbakh, H., & El Abbassi, A. (2012). Potential use of olive mill wastewater in the preparation of functional beverages: A review. In *Journal of Functional Foods* (Vol. 4, Issue 1, pp. 53–65). https://doi.org/10.1016/j.jff.2012.01.002

♣ *The Palestinian Central Bureau of Statistics (PCBS). "Main Economic Indicators for Olive Presses Activity in Palestine by Governorate / Automation Level, 2019". August 18, 2021. https://www.pcbs.gov.ps/statisticsIndicatorsTables.aspx?lang=en&table_id=908 (Access date: 30/11/2021)*. (n.d.).

Dimitris P., Eleni C., Vagelis G., Christakis A., "Sustainability analysis and benchmarking of olive mill wastewater treatment methods", J Chem Technol Biotechnol (2013): 88: 742–750. DOI 10.1002/jctb.4036

A. Cassano, C. Conid, C.M. Galanakis, R. Castro-Mu~noz, "Recovery of polyphenols from olive mill wastewaters by membrane operations" Membrane Technologies for Biorefining. (2016) http://dx.doi.org/10.1016/B978-0-08-100451-7.00007-4.

Malek Batayneh, Iqbal Marie, Ibrahim Asi, "Use of selected waste materials in concrete mixes", Waste Management, 27, (2007): 1870–1876.

Hanaa Zbakha, Abdelilah El Abbassib, "Potential use of olive mill wastewater in the preparation of functional beverages: A review", JOURNAL OF FUNCTIONAL FOOD, S4, (2012): P 53– 65.

Cengiz Karaca, and H. Huseyin ozturK, "An economical, energetical and environmental management of olive oil production wastes". NEW MEDIT N. 1. (2018).

Houda Ben Slama, Ali Chenari Bouket, Faizah N. Alenezi, Ameur Khardani, Lenka Luptakova, Armelle Vallat, Tomasz Oszako, Mostafa E. Rateb, and Lassaad Belbahri, "Olive Mill and Olive Pomace Evaporation Pond's By-Products: Toxic Level Determination and Role of Indigenous Microbiota in Toxicity Alleviation". Appl. Sci. (2021), 11, 5131. https://doi.org/10.3390/app11115131

Fatima Zahra El Hassani*, Abdelali Fadile, Mouna Faouzi, Abdelah Zinedine,Mohamed Merzouki, Mohamed Benlemlih. "The long-term effect of Olive Mill Wastewater (OMW) on organic matter humification in a semi-arid soil", Heliyon 6, (2020). doi.org/10.1016/j.heliyon.2020.e03181

The Palestinian Central Bureau of Statistics (PCBS). "Main Economic Indicators for Olive Presses Activity in Palestine by Governorate / Automation Level, 2019". August 18, 2021. https://www.pcbs.gov.ps/statisticsIndicatorsTables.aspx?lang=en&table_id=908 (Access date: 30/11/2021)

Paul Ekins, Dimitri Zenghelis. "The costs and benefits of environmental sustainability". Sustainability Science. (2021). 16:949–965. https://doi.org/10.1007/s11625-021-00910-5

Smita Badur, Rubina Chaudhary. "UTILIZATION OF HAZARDOUS WASTES AND BY-PRODUCTS AS A GREEN CONCRETE MATERIAL THROUGH S/S PROCESS: A REVIEW". Rev.Adv.Mater.Sci. 17, (2008), 42-61.

Aly Said, Oscar Quiroz. "Recycling of waste latex paint in concrete: a review". MOJ Polymer Science. (2018). Volume 2 Issue 2. 52–54. DOI: 10.15406/mojps.2018.02.00047

O. Mohawesh, M. Mahmoud, M. Janssen, B. Lennartz. “Effect of irrigation with olive mill wastewater on soil hydraulic and solute transport properties”. International Journal of Environmental Science and Technology. (2013). ISSN 1735-1472. DOI 10.1007/s13762-013-0285-1

A. Akhmad, L. Nuraini, R. Bayu, Subono, Catrawedarma. “Prediction of temperature in 2 meters temperature probe survey in Blawan geothermal field using artificial neural network (ANN) method”. Case Studies in Thermal Engineering 38, (2022), 102309. https://doi.org/10.1016/j.csite.2022.102309

Utepov, Y.; Tulebekova, A.; Aldungarova, A.; Mkilima, T.; Zharassov, S.; Shakhmov, Z.; Bazarbayev, D.; Tolkynbayev, T.; Kaliyeva, Z. Investigating the Influence of Initial Water pH on Concrete Strength Gain Using a Sensors and Sclerometric Test Combination. Infrastructures 2022, 7, 159. https://doi.org/10.3390/infrastructures7120159.

Kucche, M. K. J., Jamkar, D. S. S., & Sadgir, D. P. A. Quality of Water for Making Concrete: A Review of Literature. International Journal of Scientific and Research Publications, Volume 5, Issue 1, January 2015, ISSN 2250-3153 5(1), 10.

Chinmoy Dutta, Md. Abdur Rakib, Md. Akhtar Hossain, Muhammad Harunur Rashid. EFFECT OF MIXING WATER pH ON CONCRETE. 2020. 5th International Conference on Civil Engineering for Sustainable Development (ICCESD 2020), 7~9 February 2020, KUET, Khulna, Bangladesh (ISBN-978-984-34-8764-3).

H. Beddaaa,, Ben Fraja, F. Lavergnea, J-M Torrentic. Effect of potassium humate as humic substances from river sediments on the rheology, the hydration, and the strength development of a cement paste. Cement and concrete composites. (2019). Manuscript_d0412d6b6562b8c6cfbaa25fe8df9852.

Daxiang Liu,1Baohua Zhang,1Yueshu Yang,1Wennian Xu,2Yu Ding,3and Zhenyao Xia

Al-Attar, Tareq. (2011). Effect of Chloride Ions Source on Corrosion of Reinforced Normal and High-Performance Concrete. AGIR Bulletin. 107-112.

Yoneyama A, Choi H, Inoue M, Kim J, Lim M, Sudoh Y. Effect of a Nitrite/Nitrate-Based Accelerator on the Strength Development and Hydrate Formation in Cold-Weather Cementitious Materials. Materials (Basel). 2021 Feb 20;14(4):1006. doi: 10.3390/ma14041006. PMID: 33672722; PMCID: PMC7924375.

Yousif, Salim & Al-gburi, Majid & Abdulkareem, Omar. (2010). DESIGN OF CONCRETE MIXES USING ARTIFICIAL NEURAL NETWORKS. The 2nd Regional. Conf. for Eng. Sci. 1-2/12/2010.

Appendix A: Water samples test results

ISO/IEC 17025:2017

BIRZEIT UNIVERSITY

Testing Laboratories Center

Analytical Report

Report Date : 05 June 2023

Customer : مروان منصور شعيبي

Sample Code	ES-20238666
Source Sample Code	
Sample Name	زيار حديث
Sample Receiving Date	20 May 2023
Sampling date	
Category	Waste Water
Batch No.	
Sample Size	500 ml
Origin	
Prod.Date	Exp.Date
Container Type	Plastic
Sample Condition	ok
Sampled By	مروان منصور شعيبي

Test	Result	Method	Comments
Conductivity	11255 MicroS/cm	StMe	
[A] Potassium (K)	3996.0 ppm	ICP	
Dry matter	5.13 %	StMe	
Organic Content	4.0 %	StMe	
Ash	1.14 %	StMe	
pH	4.66	StMe	
Chloride	1152.29 ppm	HPIC	
Sulfates (SO4)	347.96 ppm	HPIC	
Bromide	Not Detected	HPIC	
Nitrates (NO3)	141.09 ppm	HPIC	
[A] Sodium (Na)	244.4 ppm	ICP	
[NA] Specific Weight	9.95	StMe	
[A] Calcium (Ca)	192.2 ppm	ICP	

BIRZEIT UNIVERSITY

Notes: The Center is only responsible for the results of the sample tested.
This report must not be reissued without the written approval of the Center's director

Adi Qamhieh
Director

1083411

Senior Analyst,
Environmental Analysis Unit

P.O.Box: 14 BIRZEIT, PALESTINE . PHONE: 972-2-2982010 . FAX: 972-2-2982166
e-mail: bzutl@birzeit.edu

[NA] Not accredited [S] Subcontractor *IC Informed by client [A] Accredited

Analytical Report

Report Date : 05 June 2023

Customer : مروان منصور شعيبي

Sample Code	ES-20238666
Source Sample Code	
Sample Name	زيتار حديث
Sample Receiving Date	20 May 2023
Category	Waste Water
Batch No.	
Sample Size	500 ml
Origin	
Prod.Date	Exp.Date
Container Type	Plastic
Sample Condition	ok
Sampled By	مروان منصور شعيبي

Test	Result	Method	Comments
[A] Magnesium (Mg)	146.3 ppm	ICP	
Phosphate (PO4)	747.4 ppm	StMe	

Notes: The Center is only responsible for the results of the sample tested.
This report must not be reissued without the written approval of the Center's director

Adi Qamhieh
Director

1083411

Senior Analyst,
Environmental Analysis Unit

[NA] Not accredited [S] Subcontractor *IC informed by client [A] Accredited

ISO/IEC 17025:2017

BIRZEIT UNIVERSITY

Testing Laboratories Center

Analytical Report

Report Date : 05 June 2023

* Customer : مروان منصور شعيبي

	Sample Code	ES-20236665
*	Source Sample Code	
*	Sample Name	زيبر قديم
	Sample Receiving Date	20 May 2023
	Sampling date	
	Category	Waste Water
	Batch No.	
	Sample Size	500 ml
	Origin	
	Prod.Date	Exp.Date
	Container Type	Plastic
	Sample Condition	ok
*	Sampled By	مروان منصور شعيبي

Test	Result	Method	Comments
Conductivity	11436 MicroS/cm	StMe	
[A] Potassium (K)	4474.0 ppm	ICP	
Dry matter	4.44 %	StMe	
Organic Content	3.36 %	StMe	
Ash	1.08 %	StMe	
pH	4.35	StMe	
Chloride	1046.02 ppm	HPIC	
Sulfates (SO4)	340.62 ppm	HPIC	
Bromide	Not Detected	HPIC	
Nitrates (NO3)	156.92 ppm	HPIC	
[A] Sodium (Na)	208.0 ppm	ICP	
[NA] Specific Weight	9.98	StMe	
[A] Calcium (Ca)	194.0 ppm	ICP	

Notes: The Center is only responsible for the results of the sample tested.
This report must not be reissued without the written approval of the Center's director

Adi Qamhieh
Director

1083410

Senior Analyst,
Environmental Analysis Unit

P.O.Box: 14 BIRZEIT, PALESTINE . PHONE: 972-2-2982010 . FAX: 972-2-2982166
e-mail: bzutl@birzeit.edu

[NA] Not accredited [S] Subcontractor *IC Informed by client [A] Acredited

ISO/IEC 17025:2017

BIRZEIT UNIVERSITY

Testing Laboratories Center

Analytical Report

Report Date : 05 June 2023

Customer : مروان منصور شعيبي

Sample Code	ES-20238665
Source Sample Code	
Sample Name	زيبار قنبم
Sample Receiving Date	20 May 2023
Category	Waste Water
Batch No.	
Sample Size	500 ml
Origin	
Prod.Date	Exp.Date
Container Type	Plastic
Sample Condition	ok
Sampled By	مروان منصور شعيبي

Test	Result	Method	Comments
[A] Magnesium (Mg)	158.1 ppm	ICP	
Phosphate (PO4)	942.2 ppm	SMe	

Notes: The Center is only responsible for the results of the sample tested.
This report must not be reissued without the written approval of the Center's director

Adi Qamhieh
Director

1083410

Senior Analyst,
Environmental Analysis Unit

[NA] Not accredited [S] Subcontractor [C] Informed by client [A] Accredited

ISO/IEC 17025:2017

جامعة بيرزيت
BIRZEIT UNIVERSITY

Testing Laboratories Center

Analytical Report

Report Date : 05 June 2023

- Customer : مروان منصور شعيبي

Sample Code	ES-20238672
- Source Sample Code	
- Sample Name	water
Sample Receiving Date	20 May 2023
Sampling date	
Category	Water
Batch No.	
Sample Size	500 ml
Origin	
Prod.Date	Exp.Date
Container Type	Plastic
Sample Condition	ok
- Sampled By	مروان منصور شعيبي

Test	Result	Method	Comments
Conductivity	460 MicroS/cm	StMe	
[A] Potassium (K)	1.71 ppm	ICP	
pH	7.62	StMe	
Chloride	40.43 ppm	HPIC	
Sulfates (SO4)	17.54 ppm	HPIC	
Bromide	Not Detected	HPIC	
Nitrates (NO3)	5.52 ppm	HPIC	
[A] Sodium (Na)	28.0 ppm	ICP	
[A] Calcium (Ca)	46.1 ppm	ICP	
[A] Magnesium (Mg)	11.9 ppm	ICP	
Phosphate (PO4)	0.21 ppm	StMe	

BIRZEIT UNIVERSITY

Notes: The Center is only responsible for the results of the sample tested.
This report must not be reissued without the written approval of the Center's director

Adi Qamhieh
Director

1083470

Senior Analyst,
Environmental Analysis Unit

P.O.Box: 14 BIRZEIT, PALESTINE . PHONE: 972-2-2982010 . FAX: 972-2-2982166
e-mail: bzutl@birzeit.edu

[NA] Not accredited [S] Subcontractor *IC Informed by client [A] Accredited

Appendix B: X-ray reports and SEM images

Birzeit_12 samples

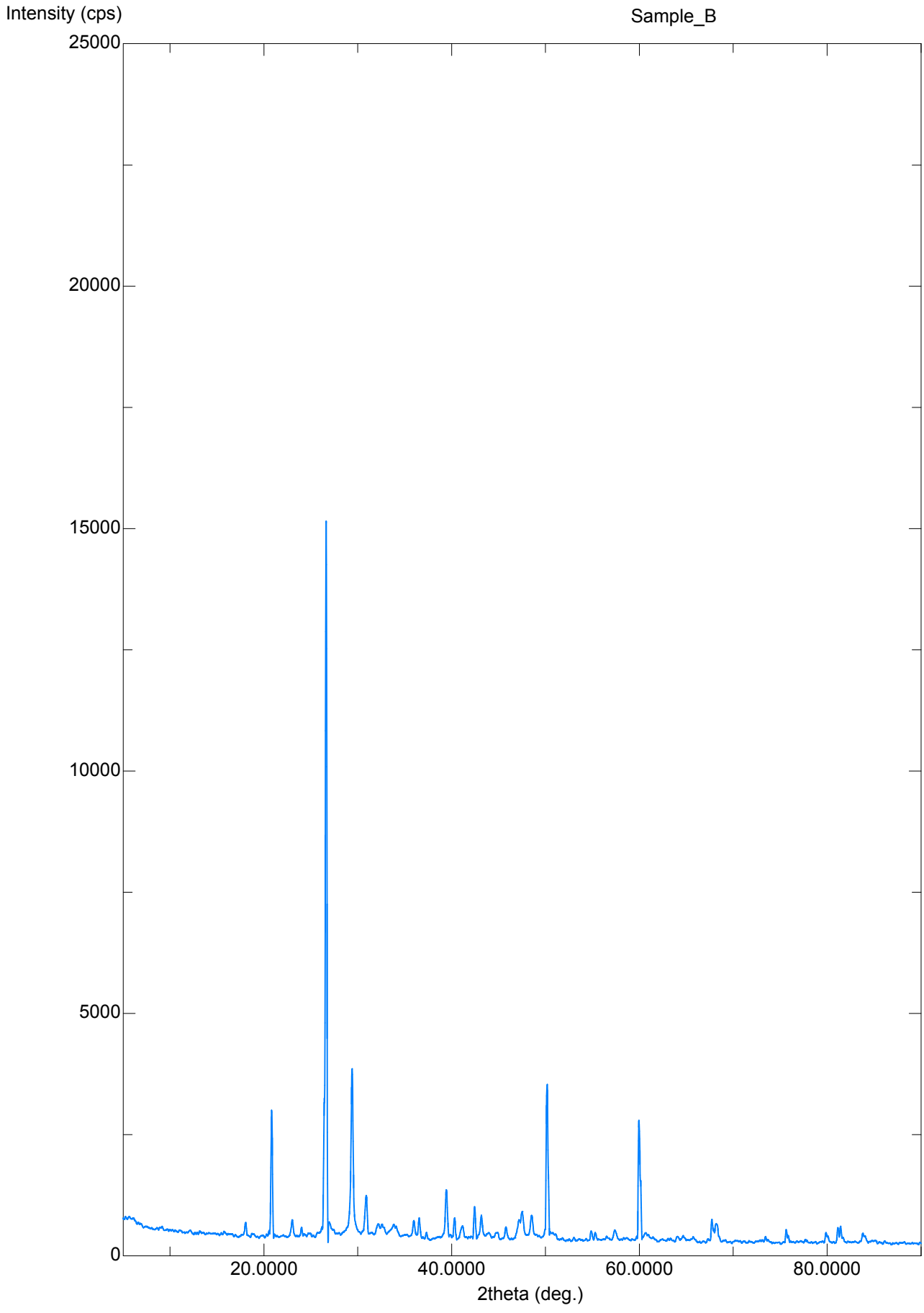

Birzeit_12 samples

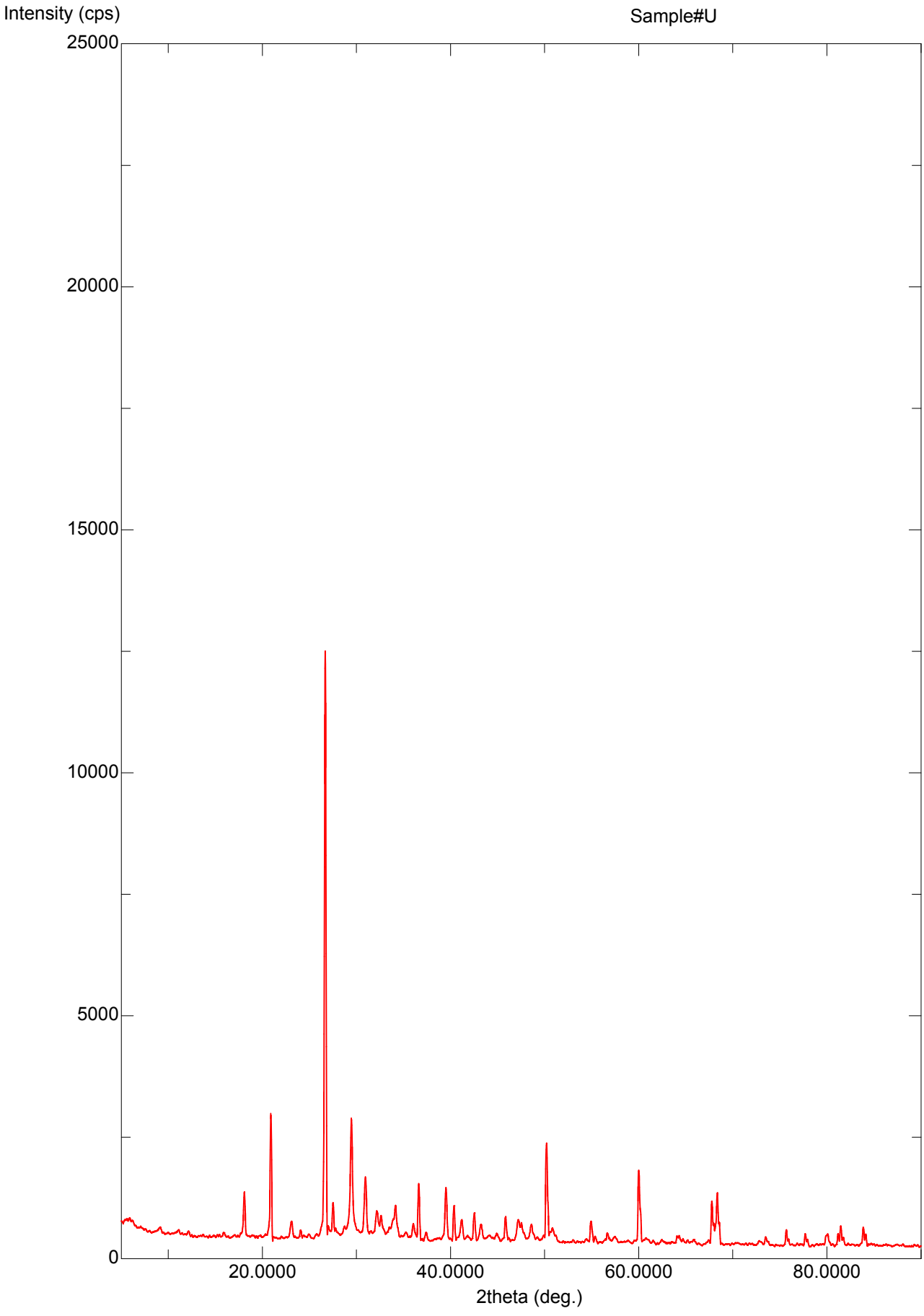

Birzeit_12 samples

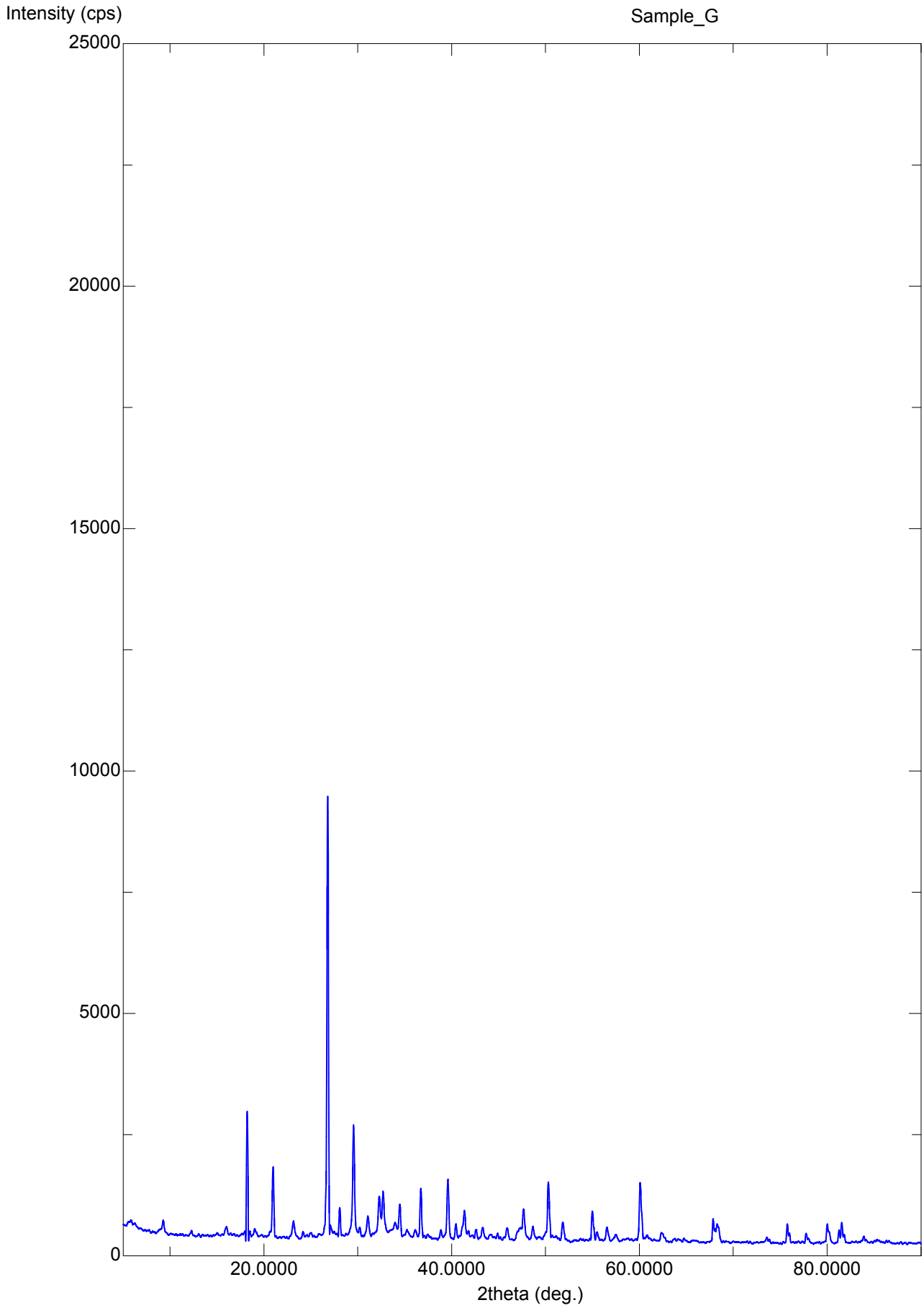

Birzeit_12 samples

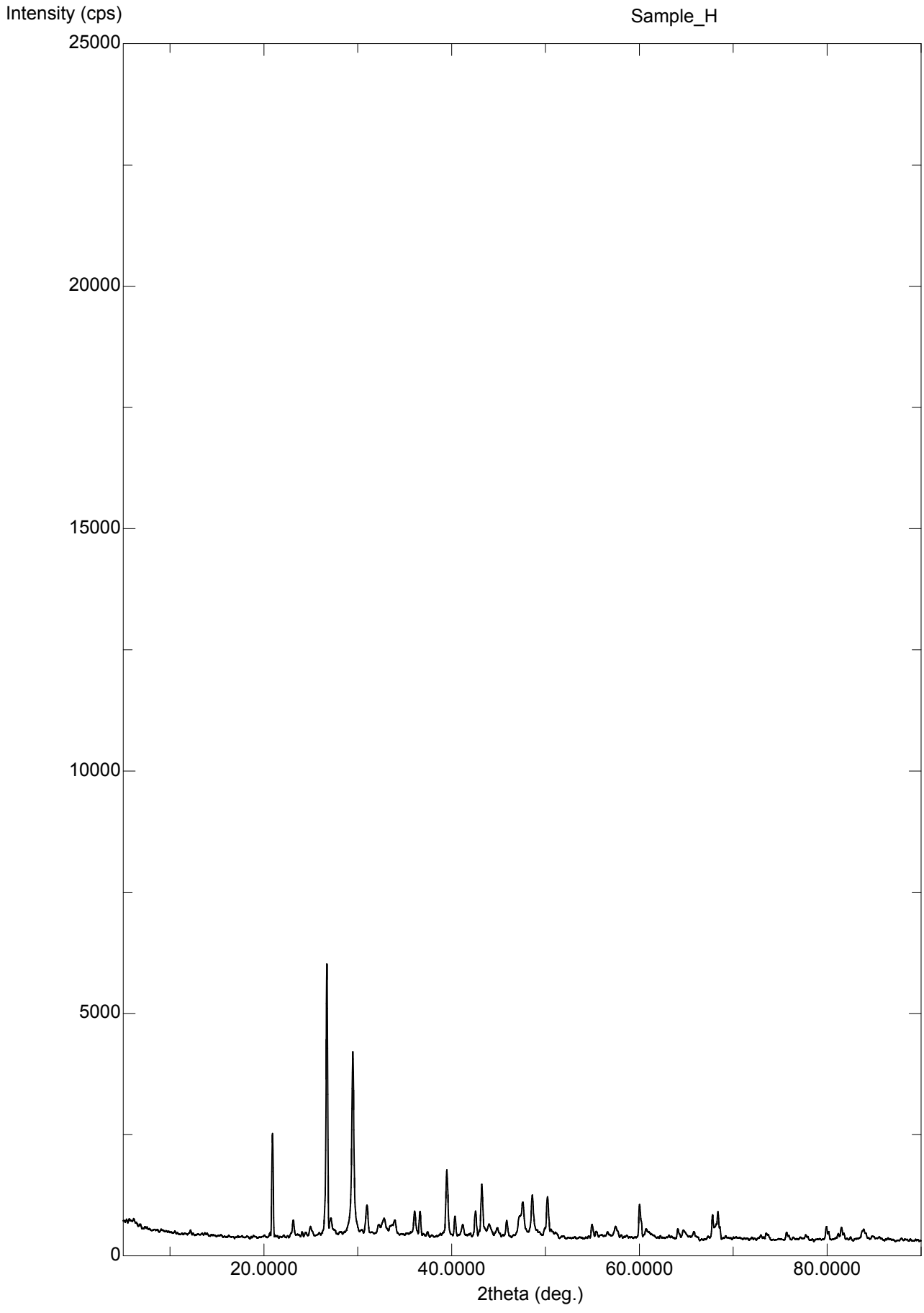

Birzeit_12 samples

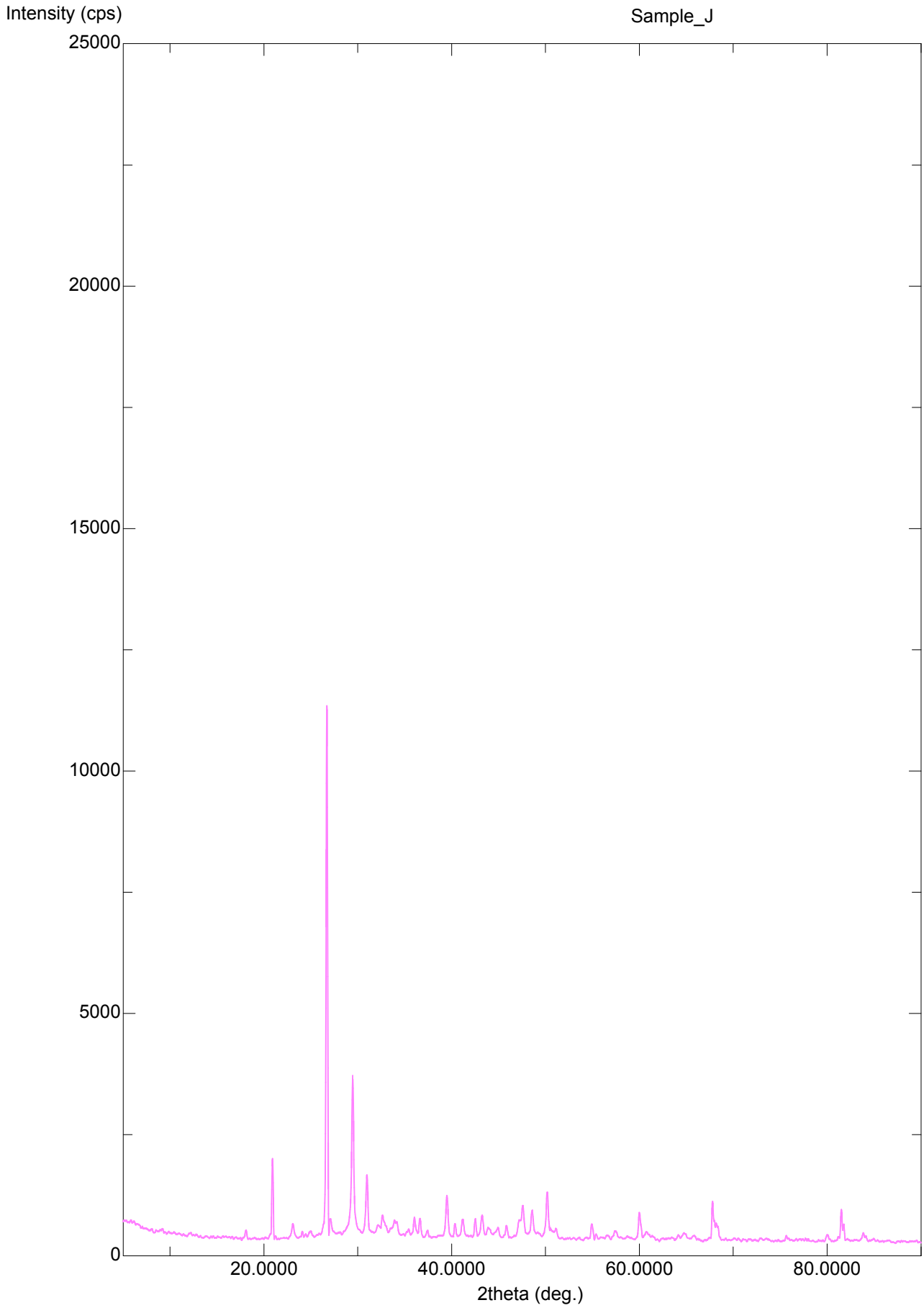

Birzeit_12 samples

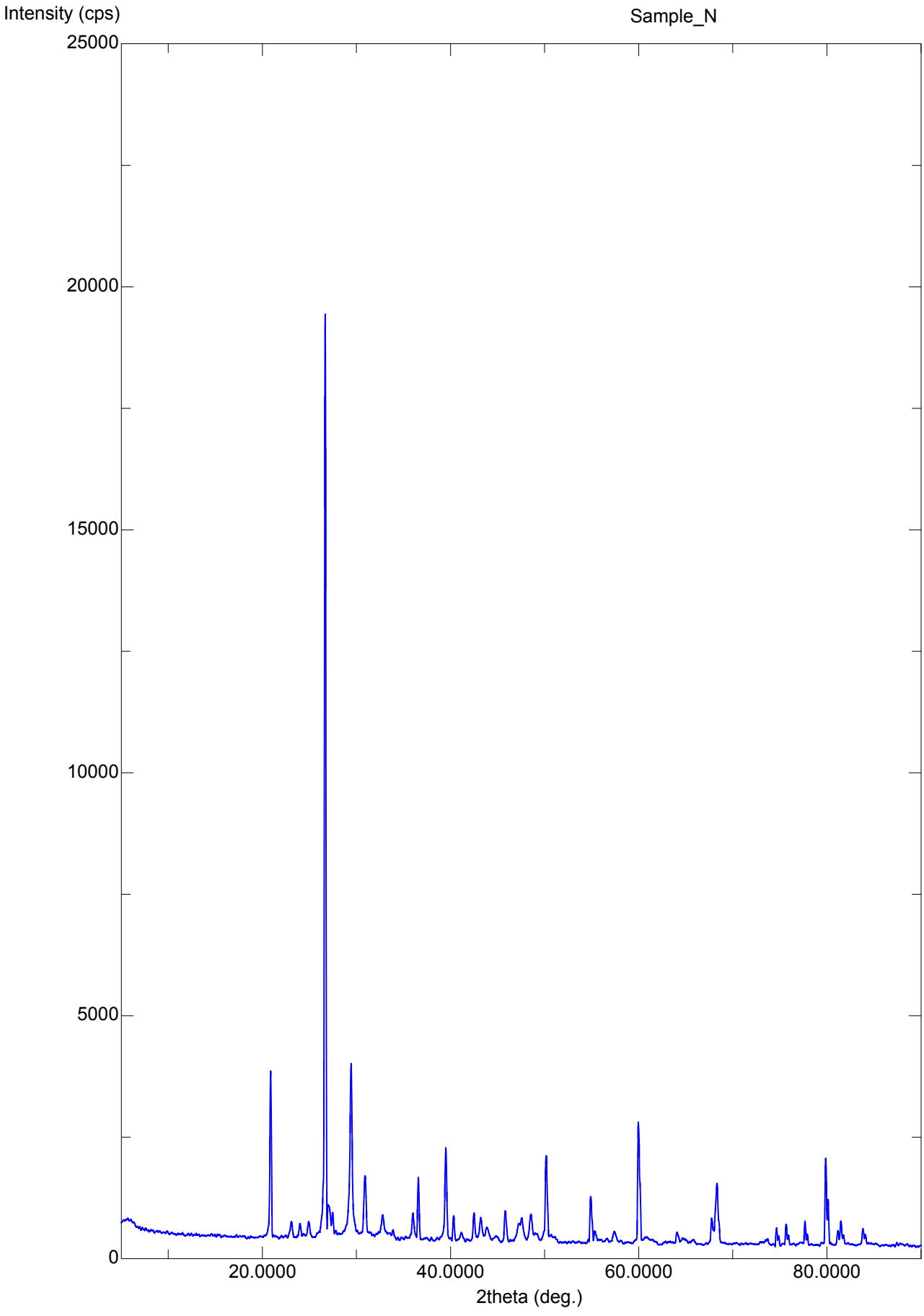

Birzeit_12 samples

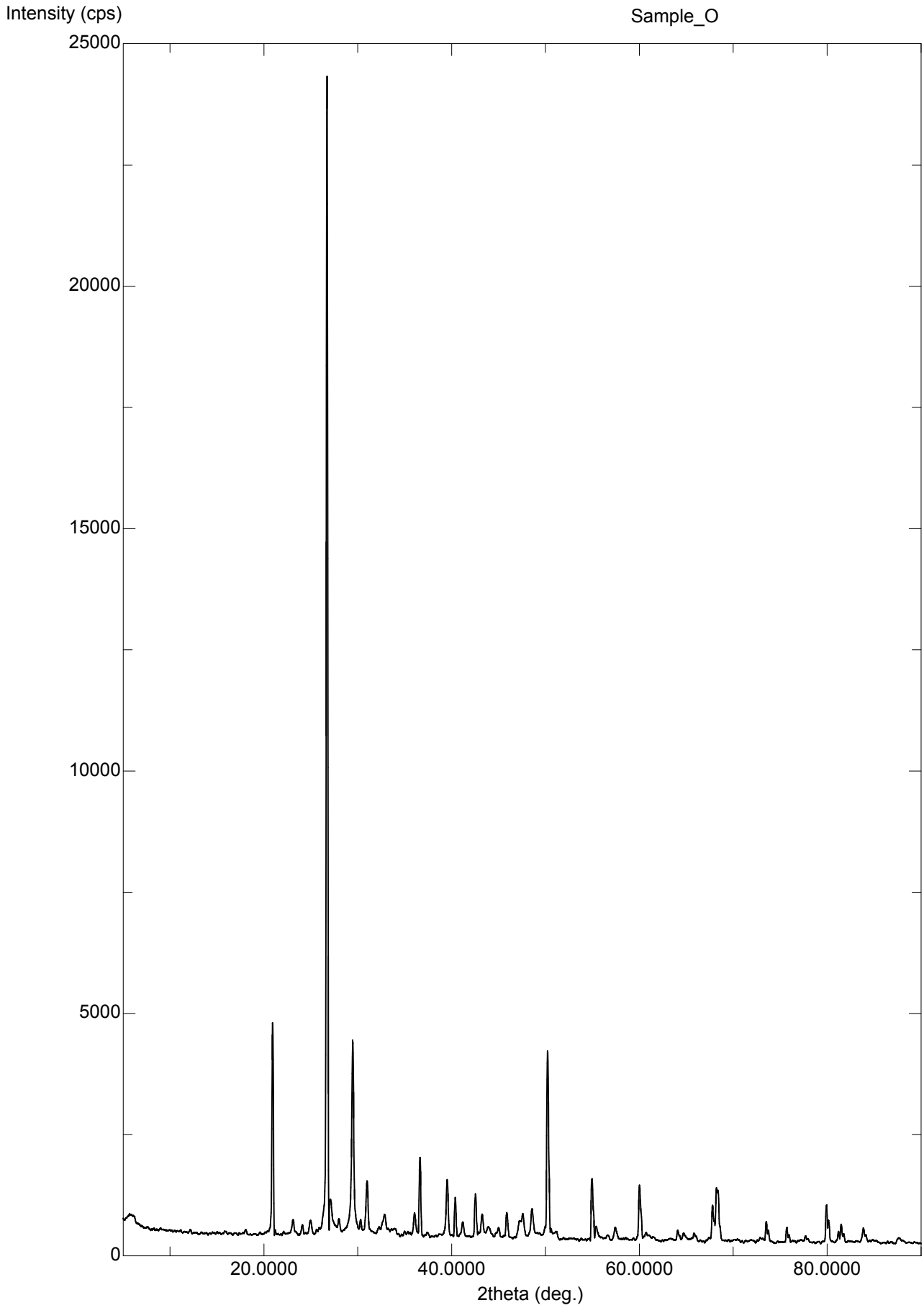

Birzeit_12 samples

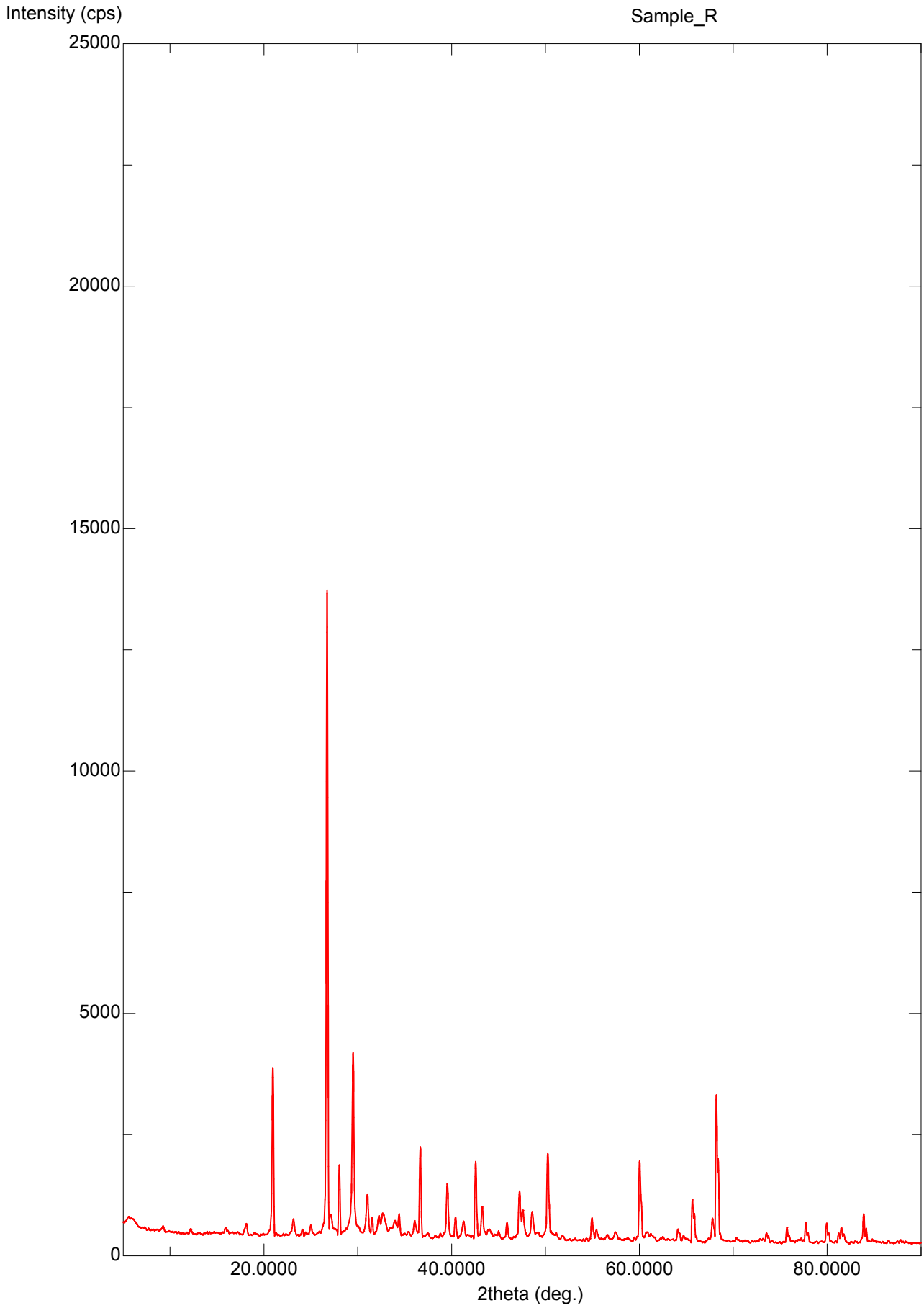

Birzeit_12 samples

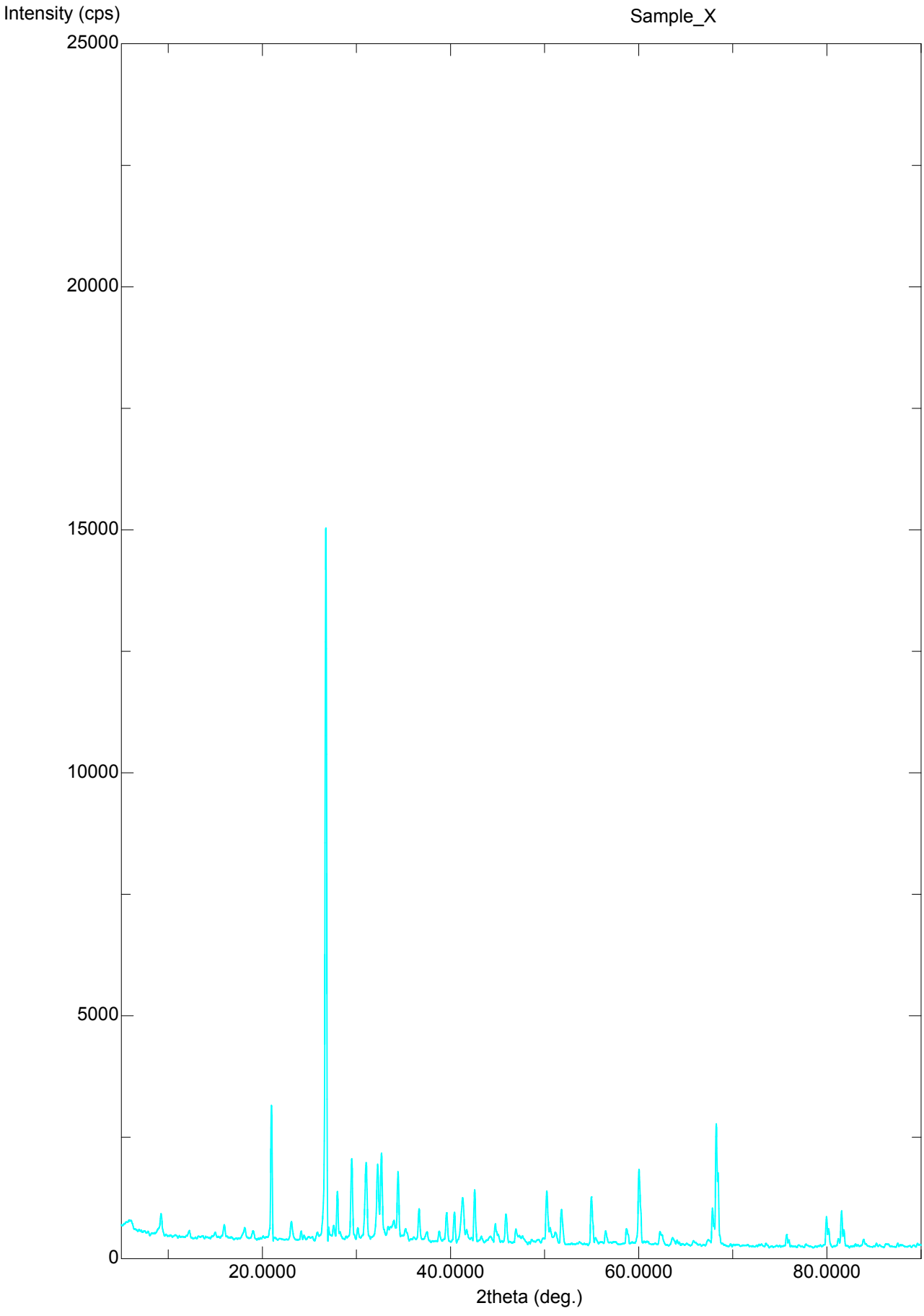

Birzeit_12 samples

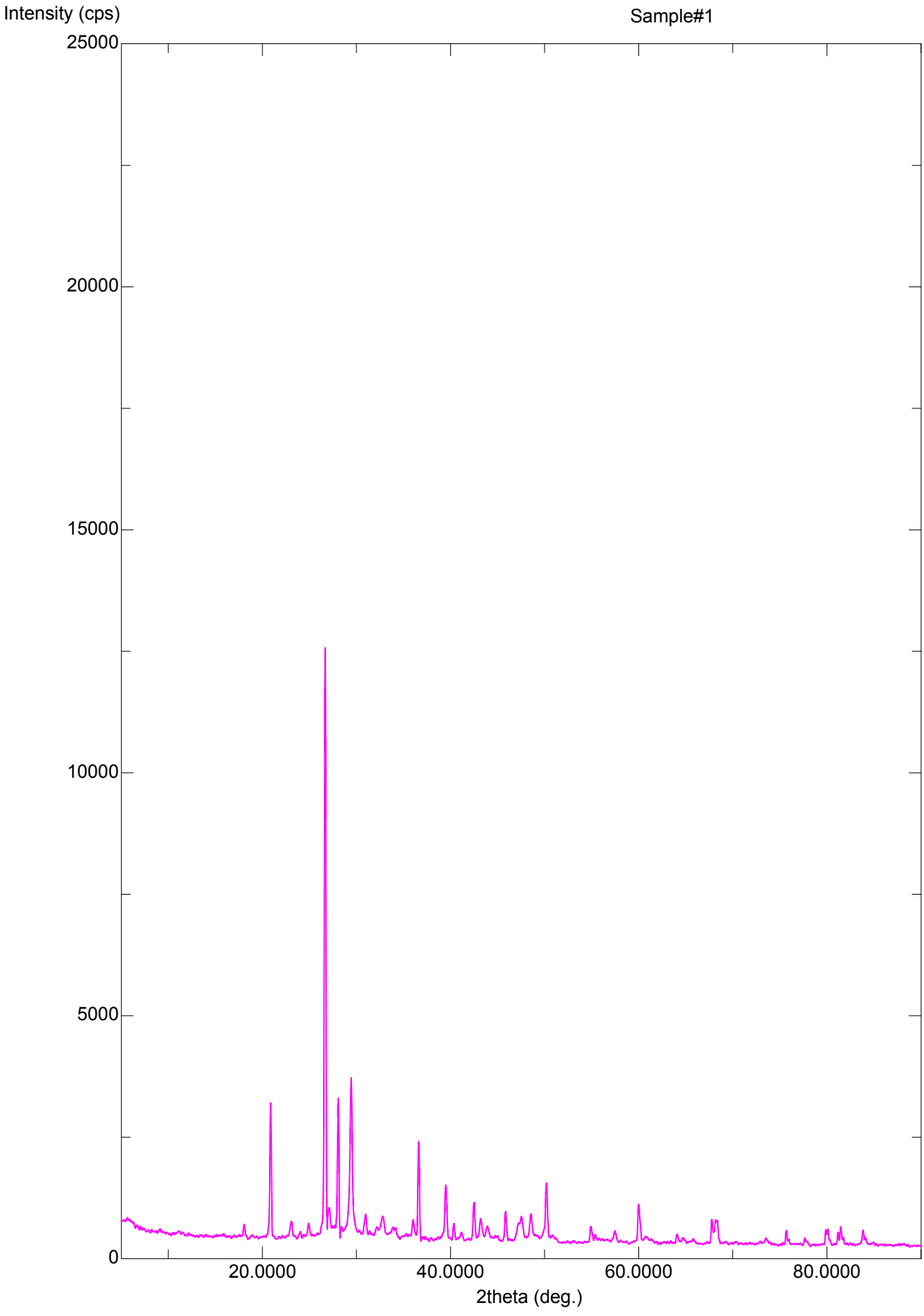

Birzeit_12 samples

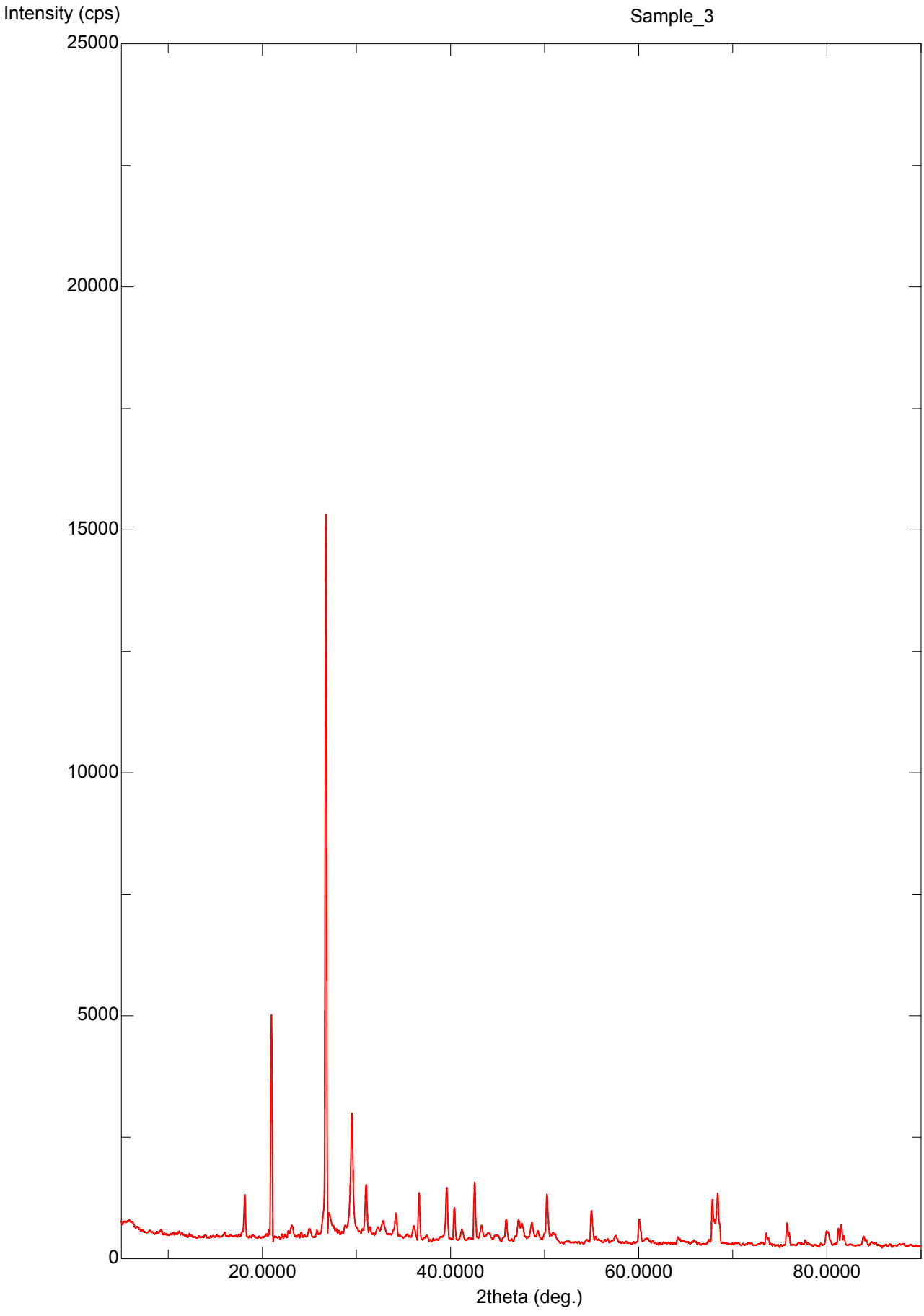

Birzeit_12 samples

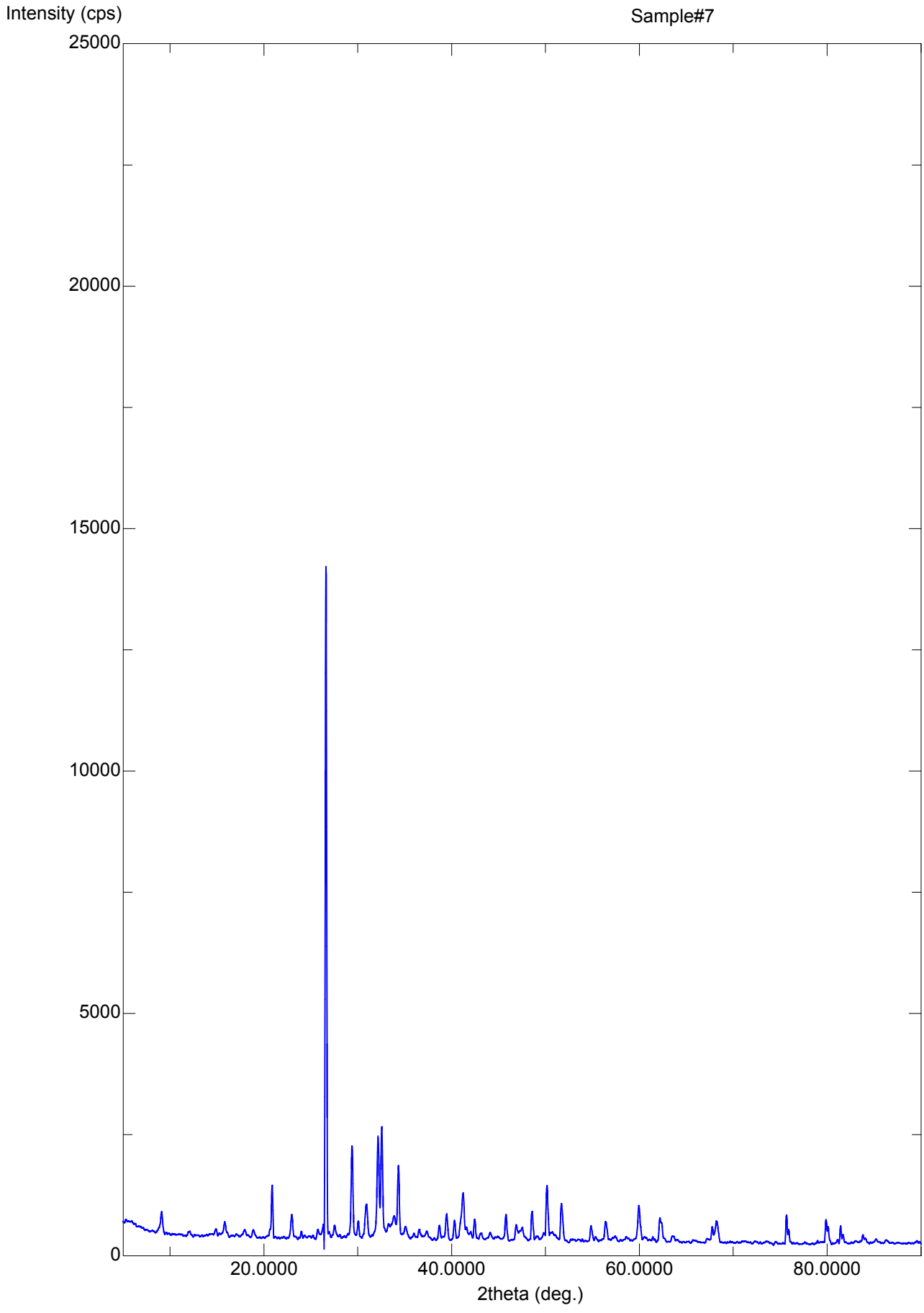

Match! Phase Analysis Report

Sample: Sample#1

Sample Data

File name	Sample#1.raw
File path	G:/.shortcut-targets-by-id/16KlMvpSIqVAUHFFggq9IVgYQzQybBTIu/Marwan - research/Concrete Mix Master Thesis/X-Ray/Birzeit University_XRD_Raw data
Data collected	Jul 13, 2023 07:39:20
Data range	4.980° - 89.980°
Original data range	5.000° - 90.000°
Number of points	4251
Step size	0.020
Rietveld refinement converged	No
Alpha2 subtracted	No
Background subtr.	No
Data smoothed	No
2theta correction	-0.02°
Radiation	X-rays
Wavelength	1.540598 Å

Analysis Results

Phase composition (Weight %)

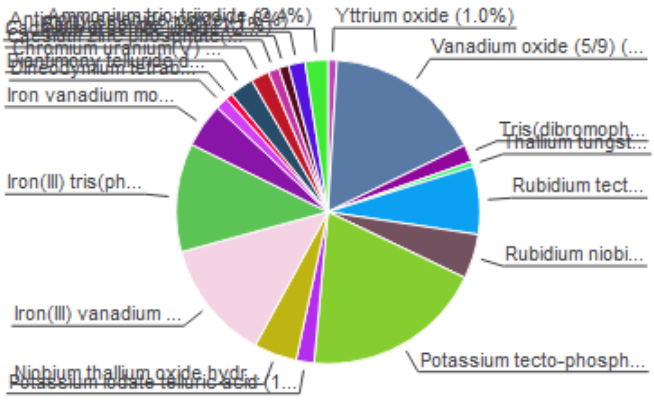

Elemental composition (Weight %)

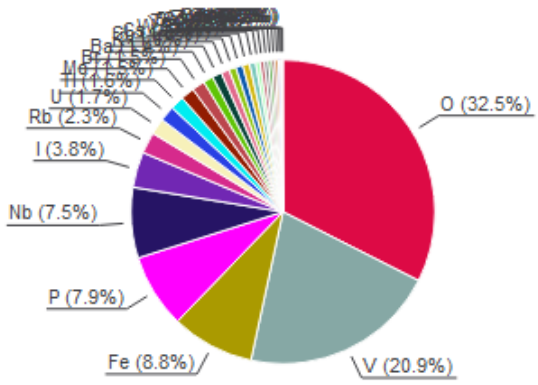

Index	*Amount (%)*	*Name*	*Formula sum*
A	1.0	Yttrium oxide	O3 Y2
B	16.8	Vanadium oxide (5/9)	O9 V5
C	1.9	Tris(dibromophosphazene)	Br6 N3 P3
D	0.5	Thallium tungsten oxide (2/4/13)	O13 Tl2 W4
E	7.2	Rubidium tecto-phosphatodiniobate	Nb2 O8 P Rb
F	4.8	Rubidium niobium tungsten oxide (12/30/3/90)	Nb30 O90 Rb12 W3
G	19.3	Potassium tecto-phosphatovanadate(III) *	K O24 P7 V4
H	1.9	Potassium iodate telluric acid	H6 I K O9 Te
I	4.6	Niobium thallium oxide hydrate (33/10.5/88.5/1.5)	H3 Nb33 O90 Tl10.5
J	12.8	Iron(III) vanadium oxide (6.5/11.5/35)	Fe6.5 O35 V11.5
K	11.5	Iron(III) tris(phosphate) trihydroxide	Fe4 H3 O15 P3
L	4.7	Iron vanadium molybdenum oxide (4/1.98/3.02/20)	Fe4 Mo3.02 O20 V1.98
M	1.3	Dineodymium tetrabarium dicopper oxide	Ba4 Cu2 Nd2 O9
N	0.7	Diantimony telluride diselenide	Sb2 Se2 Te
O	2.6	Chromium uranium(V) oxide	Cr O4 U
P	1.9	Caesium zinc phosphate(V) - I	Cs O4 P Zn
Q	1.2	Cadmium arsenide iodide (2/3/1)	As3 Cd2 I
R	1.1	Barium boride (1/6)	B6 Ba
S	1.8	Antimony selenide iodide	I Sb Se
T	2.4	Ammonium trio-triiodide	H4 I3 N
	0.5	*Unidentified peak area*	

Amounts calculated by RIR (Reference Intensity Ratio) method

Element	*Amount (weight %)*
O	*32.5%(*)*
V	20.9%
Fe	8.8%
P	7.9%
Nb	7.5%
I	3.8%
Rb	2.3%
U	1.7%
Tl	1.6%
Mo	1.5%
Br	1.5%
Ba	1.4%
K	1.1%
Sb	1.0%
Cs	0.9%
W	0.8%
Y	0.7%
Te	0.7%
Se	0.7%
Cd	0.5%
As	0.5%
Zn	0.4%
Cr	0.4%
Nd	0.3%
B	*0.3%(*)*
N	*0.2%(*)*
Cu	0.2%
H	*0.1%(*)*
**LE (sum)*	*33.1%*

Details of identified phases

A: Yttrium oxide (1.0 %)*

Match! Phase Analysis Report

Sample: Sample_3

Sample Data

File name	Sample#3.raw
File path	G:/.shortcut-targets-by-id/16KlMvpSIqVAUHFFggq9lVgYQzQybBTlu/Marwan - research/Concrete Mix Master Thesis/X-Ray/Birzeit University_XRD_Raw data
Data collected	Jul 13, 2023 13:02:42
Data range	4.880° - 89.880°
Original data range	5.000° - 90.000°
Number of points	4251
Step size	0.020
Rietveld refinement converged	No
Alpha2 subtracted	No
Background subtr.	No
Data smoothed	No
2theta correction	-0.12°
Radiation	X-rays
Wavelength	1.540598 Å

Analysis Results

Phase composition (Weight %)

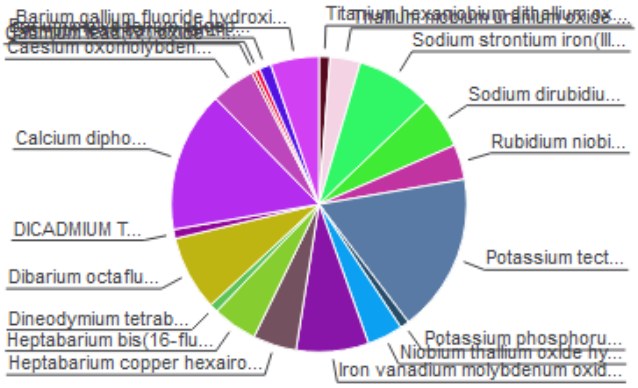

Elemental composition (Weight %)

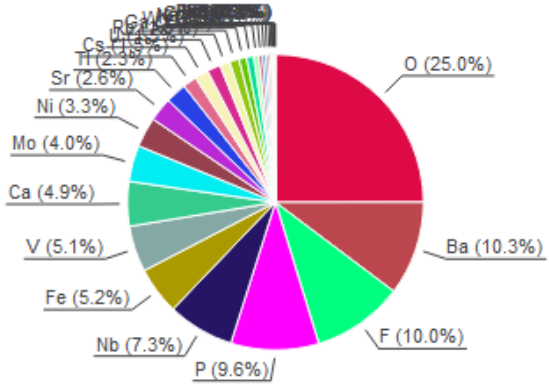

Index	*Amount (%)*	*Name*	*Formula sum*
A	1.2	Titanium hexaniobium dithallium oxide	Nb6 O18 Ti Tl2
B	3.3	Thallium niobium uranium oxide (1/2/2/11.5)	Nb2 O11.5 Tl U2
C	8.4	Sodium strontium iron(III) hexafluoride	F6 Fe Na Sr
D	5.6	Sodium dirubidium tecto-hexaniobotriphosphate(V)	Na Nb6 O24 P3 Rb2
E	3.8	Rubidium niobium tungsten oxide (12/30/3/90)	Nb30 O90 Rb12 W3
F	17.4	Potassium tecto-phosphatovanadate(III) *	K O24 P7 V4
G	1.0	Potassium phosphorus tungsten oxide (.4/2/4/16)	K0.4 O16 P2 W4
H	3.9	Niobium thallium oxide hydrate (33/10.5/88.5/1.5)	H3 Nb33 O90 Tl10.5
I	7.9	Iron vanadium molybdenum oxide (4/1.98/3.02/20)	Fe4 Mo3.02 O20 V1.98
J	4.8	Heptabarium copper hexairon(III) fluoride	Ba7 Cu F34 Fe6
K	4.9	Heptabarium bis(16-fluorotriferrate(III)) dihydrate	Ba7 F32 Fe6 H4 O2
L	0.9	Dineodymium tetrabarium dicopper oxide	Ba4 Cu2 Nd2 O9
M	8.2	Dibarium octafluorotriniccolate decafluorotetraniccolate	Ba2 F18 Ni7
N	1.0	DICADMIUM TRIARSENIDE BROMIDE	As3 Br Cd2
O	15.4	Calcium diphosphate - \b	Ca2 O7 P2
P	4.8	Caesium oxomolybdenum(V) diphosphate	Cs Mo O8 P2
Q	0.4	Cadmium lead(IV) oxide - I	Cd O3 Pb
R	0.5	Bismuth lead barium lanthanum copper oxide	Ba Bi Cu La O6 Pb
S	1.3	Barium molybdenum phosphate (1/2/3)	Ba Mo2 O12 P3
T	5.3	Barium gallium fluoride hydroxide hydrate (7/6/16/16/2)	Ba7 F16 Ga6 H20 O18
	0.6	*Unidentified peak area*	

Amounts calculated by RIR (Reference Intensity Ratio) method

Element	*Amount (weight %)*
O	*25.0%(*)*
Ba	10.3%
F	*10.0%(*)*
P	9.6%
Nb	7.3%
Fe	5.2%
V	5.1%
Ca	4.9%
Mo	4.0%
Ni	3.3%
Sr	2.6%
Tl	2.3%
Cs	1.5%
U	1.5%
Rb	1.5%
Ga	1.1%
W	1.0%
K	0.8%
Na	0.8%
Cd	0.5%
As	0.4%
Pb	0.3%
Cu	0.3%
Nd	0.2%
Br	0.2%
Bi	0.1%
La	0.1%
H	*0.1%(*)*
Ti	0.0%
**LE (sum)*	*35.1%*

Details of identified phases

A: Titanium hexaniobium dithallium oxide (1.2 %)*

Match! Phase Analysis Report

Sample: Sample#7

Sample Data

File name	Sample#7.raw
File path	G:/.shortcut-targets-by-id/16KlMvpSIqVAUHFFggq9IVgYQzQybBTIu/Marwan - research/Concrete Mix Master Thesis/X-Ray/Birzeit University_XRD_Raw data
Data collected	Jul 13, 2023 07:16:32
Data range	5.030° - 90.030°
Original data range	5.000° - 90.000°
Number of points	4251
Step size	0.020
Rietveld refinement converged	No
Alpha2 subtracted	No
Background subtr.	No
Data smoothed	No
2theta correction	0.03°
Radiation	X-rays
Wavelength	1.540598 Å

Analysis Results

Phase composition (Weight %)

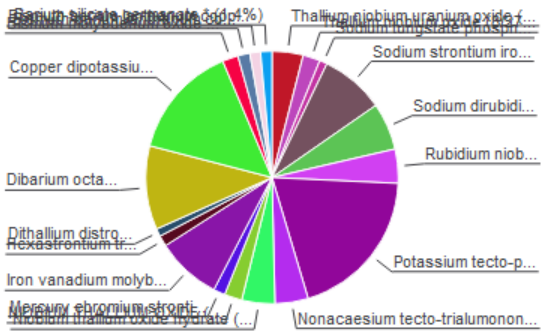

Elemental composition (Weight %)

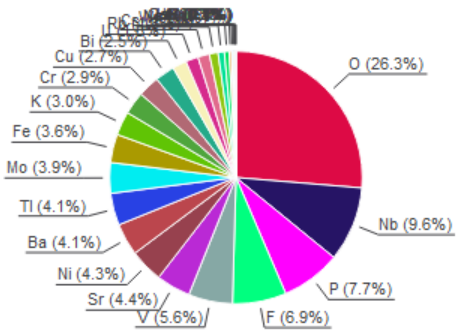

Index	*Amount (%)*	*Name*	*Formula sum*
A	4.0	Thallium niobium uranium oxide (1/2/2/11.5)	Nb2 O11.5 Tl U2
B	2.2	Thallium niobium oxide (8/27.2/72)	Nb27.2 O72 Tl8
C	1.0	Sodium tungstate phosphate *	Na1.7 O44 P4 W12
D	8.2	Sodium strontium iron(III) hexafluoride	F6 Fe Na Sr
E	6.0	Sodium dirubidium tecto-hexaniobotriphosphate(V)	Na Nb6 O24 P3 Rb2
F	4.4	Rubidium niobium tungsten oxide (12/30/3/90)	Nb30 O90 Rb12 W3
G	19.6	Potassium tecto-phosphatovanadate(III) *	K O24 P7 V4
H	4.2	Nonacaesium tecto-trialumononamolybdo(V)undecaphosphate(V)	Al3 Cs9 Mo9 O59 P11
I	4.2	Niobium thallium oxide hydrate (33/10.5/88.5/1.5)	H3 Nb33 O90 Tl10.5
J	2.3	NIOBIUM THALLIUM OXIDE (3.1/1/8.2)	Nb3.09 O8.22 Tl
K	1.5	Mercury chromium strontium copper carbonate oxide (0.46/0.54/4/2/1/6.88)	C Cr0.54 Cu2 Hg0.46 O9.88 Sr4
L	8.3	Iron vanadium molybdenum oxide (4/1.98/3.02/20)	Fe4 Mo3.02 O20 V1.98
M	1.4	Hexastrontium trinitridodicuprate(I) dinitridocuprate(I)	Cu3 N5 Sr6
N	1.0	Dithallium distrontium copper oxide	Cu O6 Sr2 Tl2
O	10.7	Dibarium octafluorotriniccolate decafluorotetraniccolate	Ba2 F18 Ni7
P	14.6	Copper dipotassium dihydrogen phosphatochromate	Cr2 Cu H2 K2 O14 P2
Q	2.0	Bismuth molybdenum oxide (26.4/9.6/68.4)	Bi26.4 Mo9.6 O68.4
R	1.5	Bismuth barium lanthanum copper oxide (2/2.3/0.7/2/8)	Ba2.3 Bi2 Cu2 La0.7 O8
S	1.4	Bismuth barium lanthanum copper oxide (1.6/2.5/0.9/2/8.3)	Ba2.5 Bi1.59 Cu2 La0.91 O8.25
T	1.4	Barium silicate germanate *	Ba Ge3.125 O9 Si0.875
	0.1	*Unidentified peak area*	

Amounts calculated by RIR (Reference Intensity Ratio) method

Element	*Amount (weight %)*
O	*26.3%(*)*
Nb	9.6%
P	7.7%
F	*6.9%(*)*
V	5.6%
Sr	4.4%
Ni	4.3%
Ba	4.1%
Tl	4.1%
Mo	3.9%
Fe	3.6%
K	3.0%
Cr	2.9%
Cu	2.7%
Bi	2.5%
U	1.8%
Rb	1.6%
Cs	1.5%
W	1.1%
Na	0.8%
Ge	0.6%
La	0.3%
Hg	0.2%
N	*0.1%(*)*
Al	0.1%
Si	0.1%
H	*0.1%(*)*
C	*0.0%(*)*
**LE (sum)*	*33.4%*

Details of identified phases

A: Thallium niobium uranium oxide (1/2/2/11.5) (4.0 %)*

Formula sum	Nb2 O11.5 Tl U2
Entry number	96-100-1356
Figure-of-Merit (FoM)	0.612747*
Total number of peaks	497
Peaks in range	497
Peaks matched	128
Intensity scale factor	0.47*
Space group	P m n b
Crystal system	orthorhombic
Unit cell	a= 7.7130 Å b= 10.3290 Å c= 13.9470 Å
I/Ic	4.52
Calc. density	6.278 g/cm³
Reference	Gasperin M, "Synthese et structure de trois niobouranates d'ions monovalents: TlNb~2~ U~2~ O~11.5~, K Nb U O~6~, et Rb Nb U O~6~", Journal of Solid State Chemistry **67**, 219-224 (1987)

B: Thallium niobium oxide (8/27.2/72) (2.2 %)*

Match! Phase Analysis Report

Sample: Sample_B

Sample Data

File name	Sample#B.raw
File path	G:/.shortcut-targets-by-id/16KlMvpSIqVAUHFFggq9lVgYQzQybBTlu/Marwan - research/Concrete Mix Master Thesis/X-Ray/Birzeit University_XRD_Raw data
Data collected	Jul 13, 2023 08:02:51
Data range	4.950° - 89.950°
Original data range	5.000° - 90.000°
Number of points	4251
Step size	0.020
Rietveld refinement converged	No
Alpha2 subtracted	No
Background subtr.	No
Data smoothed	No
2theta correction	-0.05°
Radiation	X-rays
Wavelength	1.540598 Å

Analysis Results

Phase composition (Weight %)

Elemental composition (Weight %)

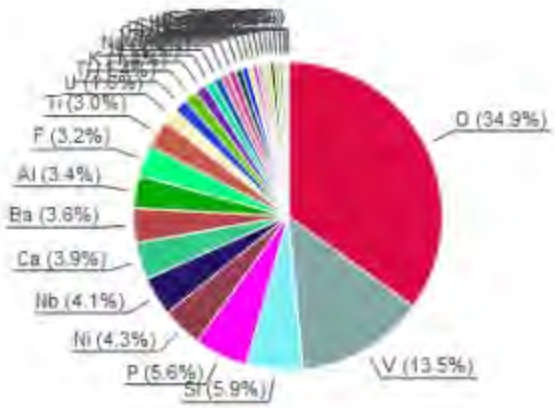

Index	*Amount (%)*	*Name*	*Formula sum*
A	1.1	Yttrium oxide	O3 Y2
B	14.6	Vanadium oxide (5/9)	O9 V5
C	3.4	Sodium nitrate Nitratine	N Na O3
D	10.9	Silicon oxide $-alpha Quartz low	O2 Si
E	4.4	Rubidium niobium tungsten oxide (12/[illegible]/90)	Nb30 O90 Rb13 W3
F	17.4	Potassium tecto-phosphatovanadate(K) /	K O24 P7 [illegible]
G	[illegible]	[illegible]	[illegible]
H	2.9	Potassium barium phosphate	Ba K O4 P
I	4.3	Niobium thallium oxide hydrate (33/10.5/88.5/1.5)	H3 Nb33 O90 Tl10.5
J	0.6	Holmium oxide	Ho2 O3
K	0.7	Hexastrontium trinitridodicuprate(I) dinitridocuprate(I)	Cu3 N5 Sr6
L	0.5	Dysprosium oxide	Dy2 O3
M	2.7	Dinickel diphosphate	Ni2 O7 P2
N	7.5	Dibarium octafluorotrinioccolate decafluoroaluminoccolate	Ba2 F18 Ni7
O	2.3	Chromium uranium(V) oxide	Cr O4 U
P	3.6	Calcium carbonate Calcite	C Ca O3
Q	1.9	Caesium zinc phosphate(V) - I	Cs O4 P Zn
R	1.9	Antimony selenide iodide	I Sb Se
S	11.5	Aluminium pentaoxotitanate	Al2 O5 Ti
T	5.5		Ca4 F2 O7 Si2
	1.7	*Unidentified peak area*	

Amounts calculated by RIR (Reference Intensity Ratio) method

Element	*Amount (weight %)*
O	*34.9%(*)*
V	13.5%
[illegible]	[illegible]
P	5.6%
Ni	4.3%
Nb	4.1%
Ca	3.9%
Ba	3.6%
Al	3.4%
F	3.2%(*)
Ti	3.0%
Tl	1.4%
h	1.4%
I	1.2%
Na	0.9%
Y	0.9%
Cs	0.8%
Rb	0.8%
Sb	0.7%
N	*0.6%(*)*
[illegible]	[illegible]
Sr	0.5%
Dy	0.5%
[illegible]	[illegible]
[illegible]	[illegible]

Match! Phase Analysis Report

Sample: Sample_G

Sample Data

File name	Sample_G.raw
File path	G:/.shortcut-targets-by-id/16KlMvpSIqVAUHFFggq9lVgYQzQybBTIu/Marwan - research/Concrete Mix Master Thesis/X-Ray/Birzeit University_XRD_Raw data
Data collected	Jul 13, 2023 09:18:14
Data range	4.800° - 89.800°
Original data range	5.000° - 90.000°
Number of points	4251
Step size	0.020
Rietveld refinement converged	No
Alpha2 subtracted	No
Background subtr.	No
Data smoothed	No
2theta correction	-0.2°
Radiation	X-rays
Wavelength	1.540598 Å

Analysis Results

Phase composition (Weight %)

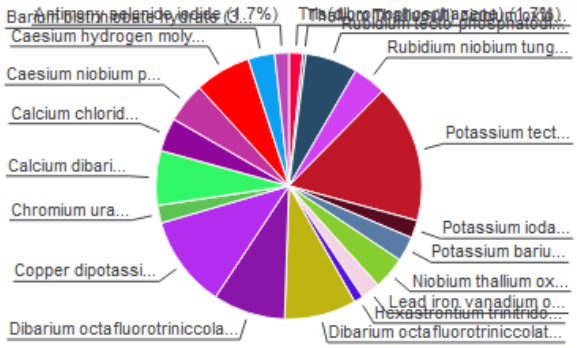

Elemental composition (Weight %)

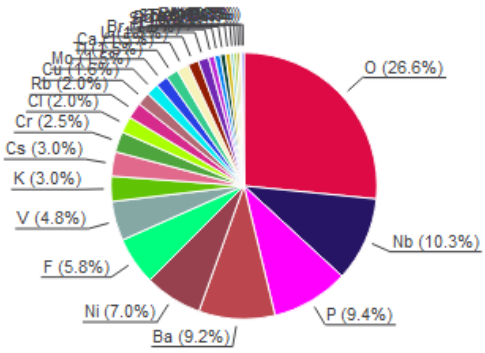

Index	*Amount (%)*	*Name*	*Formula sum*
A	1.7	Tris(dibromophosphazene)	Br6 N3 P3
B	0.4	Thallium Thallium(III) niobium oxide (1.7/0.3/2/6.3)	Nb2 O6.271 Tl2
C	6.3	Rubidium tecto-phosphatodiniobate	Nb2 O8 P Rb
D	4.0	Rubidium niobium tungsten oxide (12/30/3/90)	Nb30 O90 Rb12 W3
E	16.8	Potassium tecto-phosphatovanadate(III) *	K O24 P7 V4
F	2.2	Potassium iodate telluric acid	H6 I K O9 Te
G	3.0	Potassium barium phosphate	Ba K O4 P
H	4.0	Niobium thallium oxide hydrate (33/10.5/88.5/1.5)	H3 Nb33 O90 Tl10.5
I	2.3	Lead iron vanadium oxide (1/1.75/4.25/11)	Fe1.75 O11 Pb V4.25
J	1.1	Hexastrontium trinitridodicuprate(I) dinitridocuprate(I)	Cu3 N5 Sr6
K	8.7	Dibarium octafluorotriniccolate decafluorotetraniccolate	Ba2 F18 Ni7
L	8.8	Dibarium octafluorotriniccolate decafluorotetraniccolate	Ba2 F18 Ni7
M	11.2	Copper dipotassium dihydrogen phosphatochromate	Cr2 Cu H2 K2 O14 P2
N	2.2	Chromium uranium(V) oxide	Cr O4 U
O	6.6	Calcium dibarium bis(hydrogenphosphate(V)) bis(dihydrogenphosphate(V))	Ba2 Ca H6 O16 P4
P	4.1	Calcium chloride dihydrate Sinjarite	Ca Cl2 H4 O2
Q	4.9	Caesium niobium phosphate (1/3/3)	Cs Nb3 O15 P3
R	6.8	Caesium hydrogen molybdatodiphosphate	Cs H Mo O9 P2
S	3.2	Barium bistriniobate hydrate	Ba H2 Nb6 O17
T	1.7	Antimony selenide iodide	I Sb Se
	0.8	*Unidentified peak area*	

Amounts calculated by RIR (Reference Intensity Ratio) method

Element	*Amount (weight %)*
O	*26.6%(*)*
Nb	10.3%
P	9.4%
Ba	9.2%
Ni	7.0%
F	*5.8%(*)*
V	4.8%
K	3.0%
Cs	3.0%
Cr	2.5%
Cl	2.0%
Rb	2.0%
Cu	1.6%
Mo	1.5%
Tl	1.5%
Ca	1.5%
U	1.5%
Br	1.3%
I	1.3%
Sr	0.8%
Pb	0.7%
Sb	0.6%
Te	0.6%
Se	0.4%
W	0.4%
Fe	0.3%
H	*0.3%(*)*
N	*0.2%(*)*
**LE (sum)*	*32.9%*

Details of identified phases

A:

Tris(dibromophosphazene) (1.7 %)*

Formula sum	Br6 N3 P3
Entry number	96-100-8091
Figure-of-Merit (FoM)	0.628316*
Total number of peaks	500
Peaks in range	500
Peaks matched	156
Intensity scale factor	0.19*
Space group	P n m a
Crystal system	orthorhombic
Unit cell	a= 6.6300 Å b= 13.3600 Å c= 14.4300 Å
I/Ic	3.55

Match! Phase Analysis Report

Sample: Sample_H

Sample Data

File name	Sample_H.raw
File path	G:/.shortcut-targets-by-id/16KlMvpSlqVAUHFFggq9lVgYQzQybBTlu/Marwan - research/Concrete Mix Master Thesis/X-Ray/Birzeit University_XRD_Raw data
Data collected	Jul 13, 2023 12:11:51
Data range	4.900° - 89.900°
Original data range	5.000° - 90.000°
Number of points	4251
Step size	0.020
Rietveld refinement converged	No
Alpha2 subtracted	No
Background subtr.	No
Data smoothed	No
2theta correction	-0.1°
Radiation	X-rays
Wavelength	1.540598 Å

Analysis Results

Phase composition (Weight %)

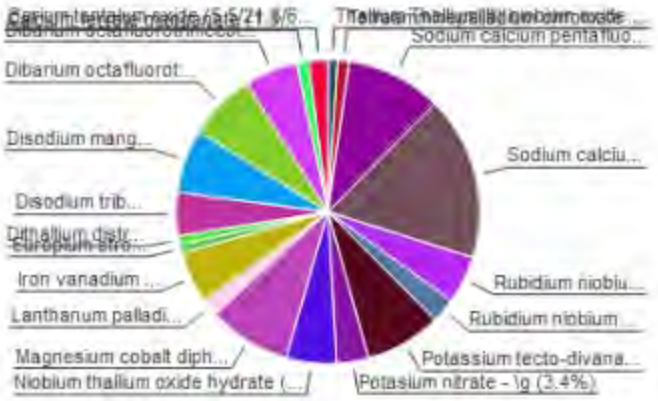

Elemental composition (Weight %)

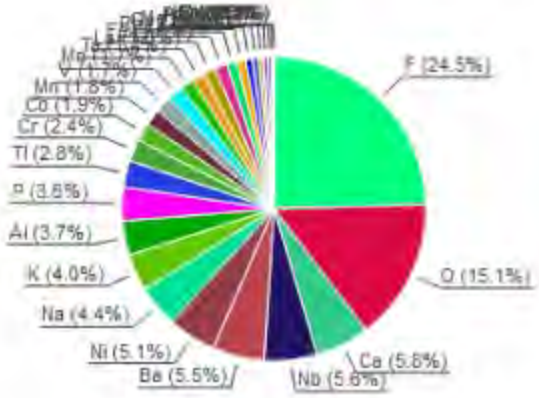

Index	*Amount (%)*	*Name*	*Formula sum*
A	1.0	Thallium Thallium(III) niobium oxide (1.4/0.6/2/6.6)	Nb2 O6.648 Tl2
B	1.2	Tetraamminepalladium chromate	Cr H12 N4 O4 Pd
C	10.1	Sodium calcium pentafluoroaluminate fluoride - $-beta	Al Ca F6 Na
D	17.5	Sodium calcium hexafluoroaluminate - \a	Al Ca F6 Na
E	5.0	Rubidium niobium tungsten oxide (12/30/3/90)	Nb30 O90 Rb12 W3
F	2.7	Rubidium niobium cyclo-trigermanate	Ge3 Nb O9 Rb
G	8.1	Potassium tecto-divanadato(III)tetraphosphate	K6 O16 P4 V2
H	3.4	Potasium nitrate - \g	K N O3
I	5.3	Niobium thallium oxide hydrate (33/10.5/88.5/1.5)	H3 Nb33 O90 Tl10.5
J	8.8	Magnesium cobalt diphosphate (1.1/0.9/1)	Co0.92 Mg1.08 O7 P2
L	3.3	Iron vanadium molybdenum oxide (4/1.98/3.02/20)	Fe4 Mo3 O2 O20 V1.98
M	0.9	Europium strontium copper oxide (1.3/1.7/2/5.65)	Cu2 Eu1.3 O5.65 Sr1.7
N	0.9	Dithallium dobalteum copper oxide	Cu O6 Sr2 Tl2
O	4.6	Disodium tribarium tetrachromium fluoride	Ba3 Cr4 F20 Na2
P	6.8	Disodium manganese chromium fluoride	Cr F7 Mn Na2
Q	1.2	Dibarium octafluorotrinicolate decafluorotetranicolate	Ba2 F18 Ni7
R	5.7	Dibarium octafluorotrinicolate decafluorotetranicolate	Ba2 F18 Ni7
S	1.3	Calcium ferrate manganate	Ca2 Fe2 O5
T	2.0	Barium tantalum oxide (5.5/21.8/60)	Ba5.5 O60 Ta21.8
	0.9	*Unidentified peak area*	

Amounts calculated by RIR (Reference Intensity Ratio) method

Element	*Amount (weight %)*
F	24.5%(*)
O	*15.1%(*)*
Ca	5.8%
Nb	5.6%
Ba	5.5%
Ni	5.1%
Na	4.4%
K	4.0%
Al	3.7%
P	3.6%
Tl	2.8%
Cr	2.4%
Co	1.9%
Mn	1.8%
V	1.7%
Mo	1.7%
Ta	1.4%
La	1.3%
Fe	1.3%
Rb	1.3%
Ge	1.1%
Mg	0.9%
N	*0.7%(*)*
Pd	0.7%
W	0.6%
Sr	0.5%
Eu	0.3%

Match! Phase Analysis Report

Sample: Sample_J

Sample Data

File name	Sample_J.raw
File path	G:/.shortcut-targets-by-id/16KlMvpSIqVAUHFFggq9IVgYQzQybBTlu/Marwan - research/Concrete Mix Master Thesis/X-Ray/Birzeit University_XRD_Raw data
Data collected	Jul 13, 2023 08:55:21
Data range	4.920° - 89.920°
Original data range	5.000° - 90.000°
Number of points	4251
Step size	0.020
Rietveld refinement converged	No
Alpha2 subtracted	No
Background subtr.	No
Data smoothed	No
2theta correction	-0.08°
Radiation	X-rays
Wavelength	1.540598 Å

Analysis Results

Phase composition (Weight %)

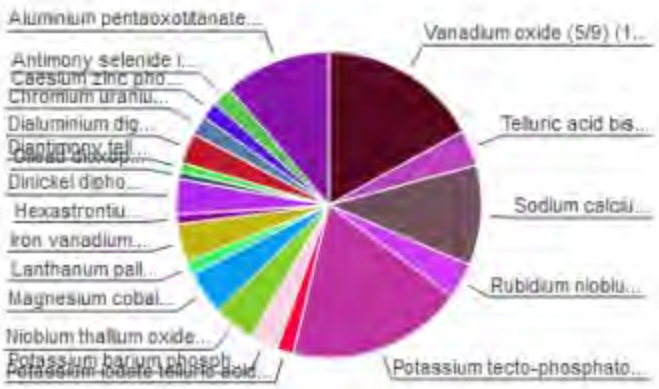

Elemental composition (Weight %)

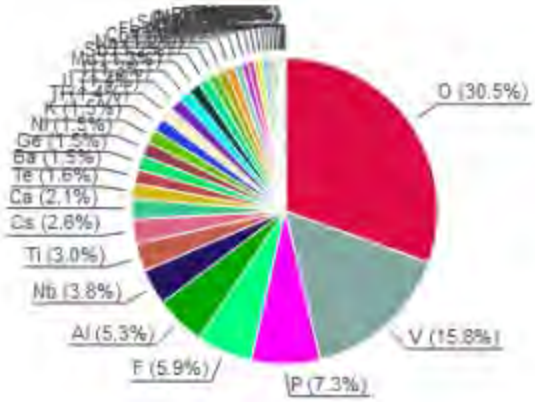

Index	*Amount (%)*	*Name*	*Formula sum*
A	17.0	Vanadium oxide (5/9)	O9 V5
B	3.8	Telluric acid bis(caesium chloride)	Cl2 Cs2 H6 O6 Te
C	10.6	Sodium calcium pentafluoroaluminate fluoride - $-beta	Al Ca F6 Na
D	3.7	Rubidium niobium tungsten oxide (12/30/3/90)	Nb30 O90 Rb12 W3
E	18.7	Potassium tecto-phosphatovanadate(III) *	K O24 P7 V4
F	1.8	Potassium iodate telluric acid	H6 I K O9 Te
G	[illegible]	[illegible]	[illegible]
H	4.4	Niobium thallium oxide hydrate (23/10.5/59.5/1.5)	H4 Nb33 O90 Tl10.5
I	4.7	Magnesium cobalt diphosphate (1.1/0.9/1)	Co0.92 Mg1.08 O7 P2
J	1.3	Lanthanum palladium oxide (4/1/7)	La4 O7 Pd
K	4.0	Iron vanadium molybdenum oxide (4/1.98/3.02/20)	Fe4 Mo3.02 O20 V1.98
L	1.0	Hexastrontium trinitridodicuprate(I) dinitridocuprate(I)	Cu3 N5 Sr6
M	3.7	Dinickel diphosphate	Ni2 O7 P2
N	0.8	Dilead dioxophosphatobismuthate	Bi O6 P Pb2
O	1.0	Diantimony telluride divelenide	Sb2 Se2 Te
P	3.2	Dialuminium digermanate	Al2 Ge2 O7
Q	2.1	Chromium uranium(V) oxide	Cr O4 U
R	1.8	Caesium zinc phosphate(V) - I	Cs O4 P Zn
S	2.2	Antimony selenide iodide	I Sb Se
T	11.3	Aluminium pentaoxotitanate	Al2 O5 Ti
	1.4	*Unidentified peak area*	

Amounts calculated by RIR (Reference Intensity Ratio) method

Element	*Amount (weight %)*
O	30.5%(*)
V	15.8%
P	7.3%
F	5.9%(*)
Al	5.3%
Nb	3.8%
Ti	3.0%
Cs	2.6%
Ca	2.1%
Te	1.6%
Ba	1.5%
Ge	1.5%
Ni	1.5%
K	1.5%
Tl	1.4%
[illegible]	[illegible]
I	1.3%
Mo	1.3%
Sb	1.2%
Na	1.2%
Co	1.0%
Fe	1.0%
La	0.9%
Se	0.9%
Sr	0.7%
Rb	0.7%
Mg	[illegible]

Match! Phase Analysis Report

Sample: Sample_N

Sample Data

File name	Sample_N.raw
File path	G:/.shortcut-targets-by-id/16KlMvpSlqVAUHFFggq9lVgYQzQybBTlu/Marwan - research/Concrete Mix Master Thesis/X-Ray/Birzeit University_XRD_Raw data
Data collected	Jul 13, 2023 10:36:48
Data range	4.710° - 89.710°
Original data range	5.000° - 90.000°
Number of points	4251
Step size	0.020
Rietveld refinement converged	No
Alpha2 subtracted	No
Background subtr.	No
Data smoothed	No
2theta correction	-0.29°
Radiation	X-rays
Wavelength	1.540598 Å

Analysis Results

Phase composition (Weight %)

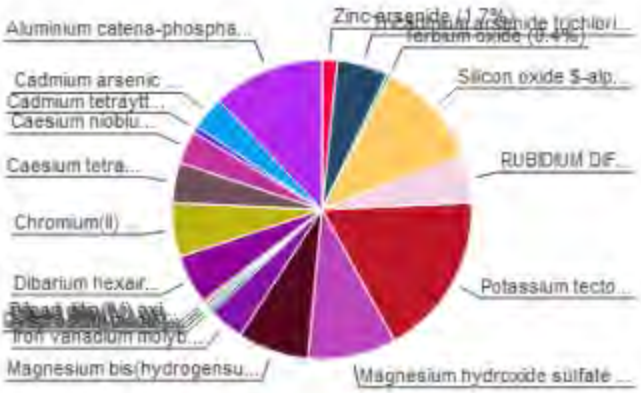

Elemental composition (Weight %)

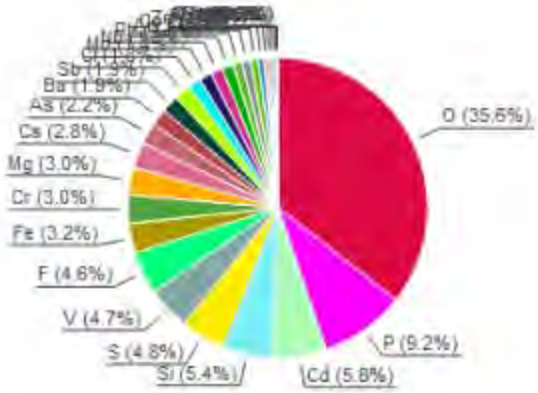

Index	*Amount (%)*	*Name*	*Formula sum*
A	1.7	Zinc arsenide	As2 Zn3
B	5.5	Tricadmium arsenide trichloride	As Cd3 Cl3
C	0.4	Terbium oxide	O3 Tb2
F	17.7	Potassium tecto-phosphatovanadate(III) *	K O24 P7 V4
G	9.5	Magnesium hydroxide sulfate hydrate (1.3/.7/1/.3)	H1.3332 Mg1.3333 O4.9999 S
H	7.7	Magnesium bis(hydrogensulfate)	H2 Mg O8 S2
I	3.8	Iron vanadium molybdenum oxide (4/1.98/3.02/20)	Fe4 Mo3.02 O20 V1.98
J	0.5	Dysprosium oxide	Dy2 O3
L	0.4	Dilead dilin(IV) oxide 0.7-hydrate	H1.4 O6.7 Pb2 Sn2
N	5.3	Dibarium hexairon(III) oxide	Ba2 Fe6 O11
P	4.4	Caesium tetrafluorocobaltate	Co Cs F4
Q	3.6	Caesium niobium phosphate (1/3/3)	Cs Nb3 O15 P3
R	0.7	Cadmium tetrayttrium trimolybdenum oxide	Cd Mo3 O16 Y4
S	3.6	Cadmium arsenic chloride *	As Cd2 Cl2
T	12.1	Aluminium catena-phosphate	Al O9 P3
	2.0	*Unidentified peak area*	

Amounts calculated by RIR (Reference Intensity Ratio) method

Element	*Amount (weight %)*
O	35.6%(*)
P	9.2%
V	4.7%
F	4.6%(*)
Fe	3.2%
Cr	3.0%
Mg	3.0%
Cs	2.8%
As	2.2%
Ba	1.9%
Sb	1.9%
Si	1.8%
Mo	1.4%
Nb	1.3%
Rb	1.3%
Al	1.2%
Co	1.0%
Zn	1.0%
K	0.6%
Pb	0.6%
Dy	0.4%
Tb	0.4%
Sn	0.3%
Y	0.2%
*LE (sum)	40.3%

Match! Phase Analysis Report

Sample: Sample#U

Sample Data

File name	Sample#U.raw
File path	G:/.shortcut-targets-by-id/16KlMvpSIqVAUHFFggq9lVgYQzQybBTIu/Marwan - research/Concrete Mix Master Thesis/X-Ray/Birzeit University_XRD_Raw data
Data collected	Jul 13, 2023 08:25:35
Data range	4.940° - 89.940°
Original data range	5.000° - 90.000°
Number of points	4251
Step size	0.020
Rietveld refinement converged	No
Alpha2 subtracted	No
Background subtr.	No
Data smoothed	No
2theta correction	-0.06°
Radiation	X-rays
Wavelength	1.540598 Å

Analysis Results

Phase composition (Weight %)

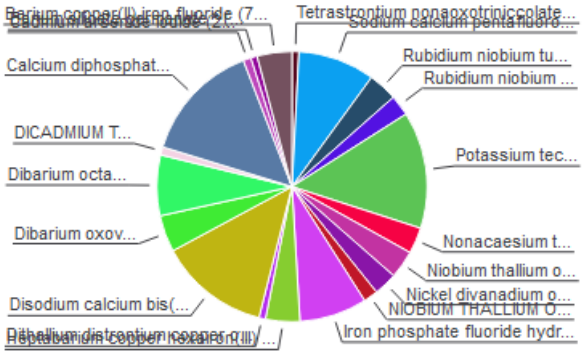

Elemental composition (Weight %)

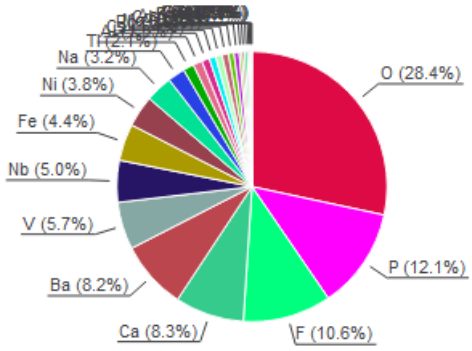

Index	*Amount (%)*	*Name*	*Formula sum*
A	0.8	Tetrastrontium nonaoxotriniccolate	Ni3 O9 Sr4
B	9.2	Sodium calcium pentafluoroaluminate fluoride - $-beta	Al Ca F6 Na
C	3.5	Rubidium niobium tungsten oxide (12/30/3/90)	Nb30 O90 Rb12 W3
D	2.5	Rubidium niobium oxide phosphate (1/3/3/3)	Nb3 O15 P3 Rb
E	14.0	Potassium tecto-phosphatovanadate(III) *	K O24 P7 V4
F	3.1	Nonacaesium tecto-trialumononamolybdo(V)undecaphosphate(V)	Al3 Cs9 Mo9 O59 P11
G	3.3	Niobium thallium oxide hydrate (33/10.5/88.5/1.5)	H3 Nb33 O90 Tl10.5
H	2.8	Nickel divanadium oxide	Ni O6 V2
I	1.7	NIOBIUM THALLIUM OXIDE (3.1/1/8.2)	Nb3.09 O8.22 Tl
J	8.1	Iron phosphate fluoride hydroxide hydrate (1.2/1/0.5/0.2/0.4)	F0.45 Fe1.21 H0.92 O4.55 P
K	4.1	Heptabarium copper hexairon(III) fluoride	Ba7 Cu F34 Fe6
L	0.8	Dithallium distrontium copper oxide	Cu O6 Sr2 Tl2
M	13.2	Disodium calcium bis(hydrogenphosphate(V))	Ca H2 Na2 O8 P2
N	4.4	Dibarium oxovanadium(IV) bis(vanadate(V))	Ba2 O9 V3
O	7.2	Dibarium octafluorotriniccolate decafluorotetraniccolate	Ba2 F18 Ni7
P	1.0	DICADMIUM TRIARSENIDE BROMIDE	As3 Br Cd2
Q	14.4	Calcium diphosphate - \b	Ca2 O7 P2
R	0.9	Cadmium arsenide iodide (2/3/1)	As3 Cd2 I
S	0.8	Barium silicate germanate *	Ba Ge3.125 O9 Si0.875
T	4.1	Barium copper(II) iron fluoride (7/1/6/34)	Ba7 Cu F34 Fe6
	1.7	*Unidentified peak area*	

Amounts calculated by RIR (Reference Intensity Ratio) method

Element	*Amount (weight %)*
O	*28.4%(*)*
P	12.1%
F	*10.6%(*)*
Ca	8.3%
Ba	8.2%
V	5.7%
Nb	5.0%
Fe	4.4%
Ni	3.8%
Na	3.2%
Tl	2.1%
Al	1.3%
Cs	1.1%
Rb	0.9%
Mo	0.8%
Cd	0.8%
As	0.8%
K	0.6%
Sr	0.6%
W	0.3%
Cu	0.3%
Ge	0.3%
I	0.2%
Br	0.1%
H	*0.1%(*)*
Si	0.0%
**LE (sum)*	*39.1%*

Details of identified phases

A: Tetrastrontium nonaoxotriniccolate (0.8 %)*

Formula sum	Ni3 O9 Sr4
Entry number	96-100-4110
Figure-of-Merit (FoM)	0.621800*
Total number of peaks	281
Peaks in range	281
Peaks matched	41
Intensity scale factor	0.15*
Space group	P 3 2 1
Crystal system	trigonal (hexagonal axes)
Unit cell	a= 9.4770 Å c= 7.8250 Å
I/Ic	4.86
Meas. density	5.400 g/cm³

Sample No. 1

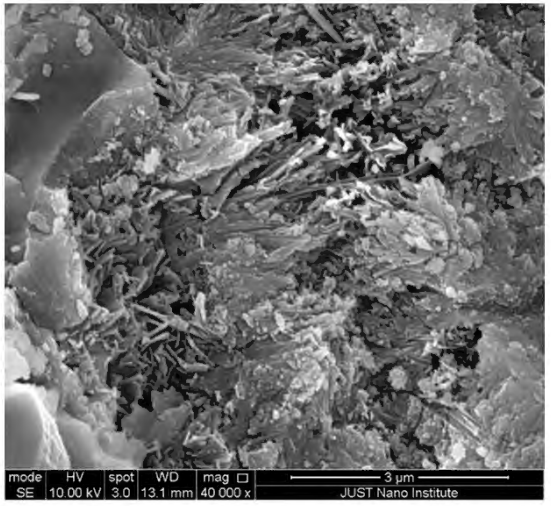
mode HV spot WD mag
SE 10.00 kV 3.0 13.1 mm 40 000 x
3 µm
JUST Nano Institute

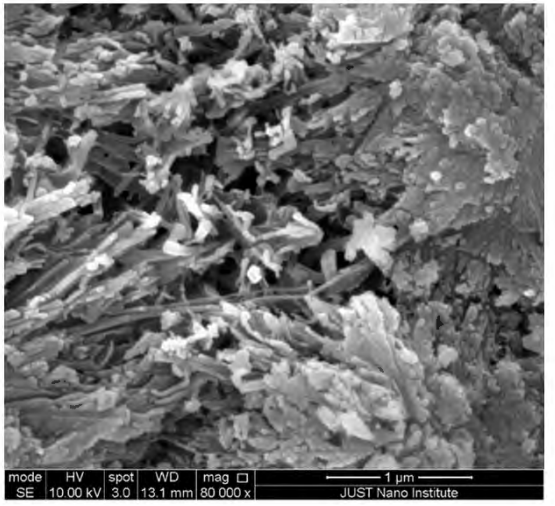
mode HV spot WD mag
SE 10.00 kV 3.0 13.1 mm 80 000 x
1 µm
JUST Nano Institute

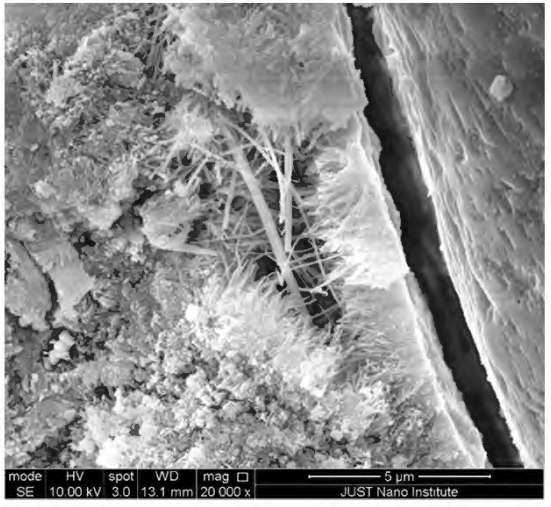
mode HV spot WD mag
SE 10.00 kV 3.0 13.1 mm 20 000 x
5 µm
JUST Nano Institute

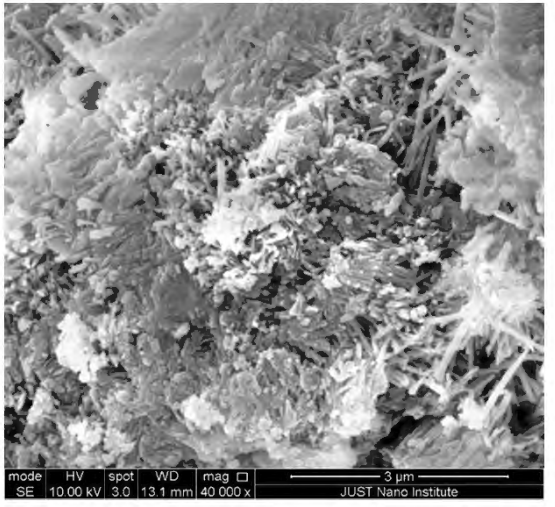
mode HV spot WD mag
SE 10.00 kV 3.0 13.1 mm 40 000 x
3 µm
JUST Nano Institute

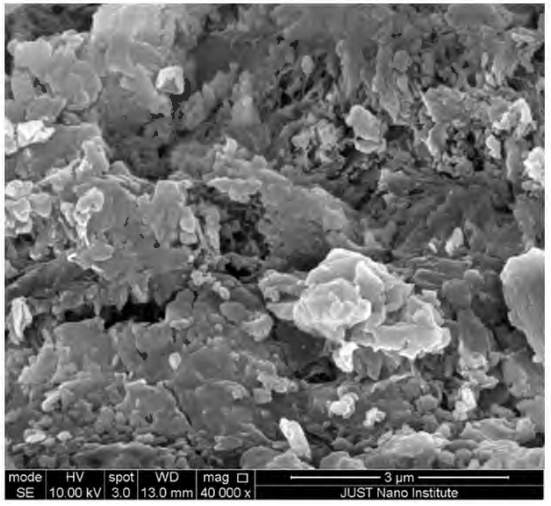
mode HV spot WD mag 3 µm
SE 10.00 kV 3.0 13.0 mm 40 000 x
JUST Nano Institute

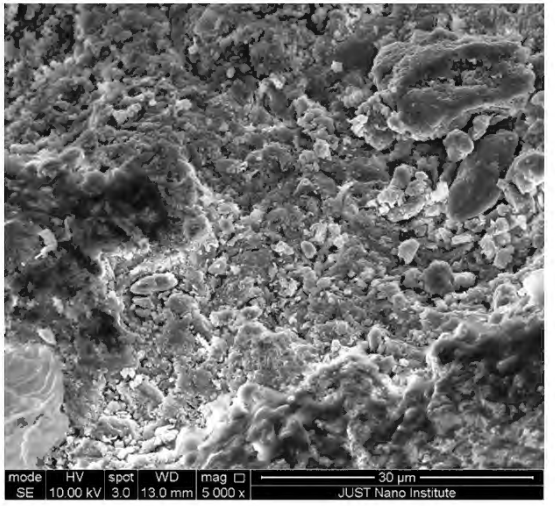
mode HV spot WD mag 30 µm
SE 10.00 kV 3.0 13.0 mm 5 000 x
JUST Nano Institute

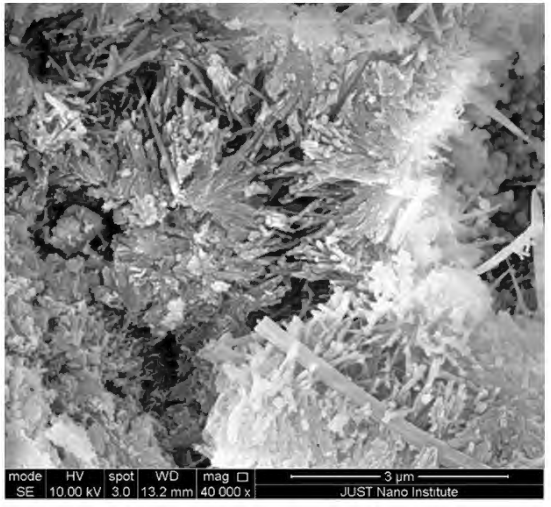
mode HV spot WD mag 3 µm
SE 10.00 kV 3.0 13.2 mm 40 000 x
JUST Nano Institute

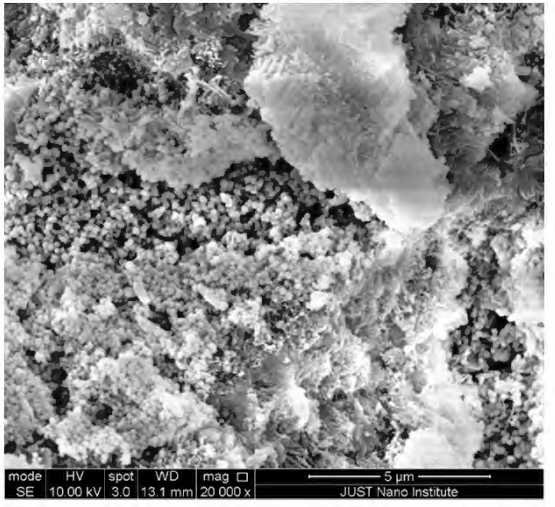
mode HV spot WD mag 5 µm
SE 10.00 kV 3.0 13.1 mm 20 000 x
JUST Nano Institute

Sample No. 3

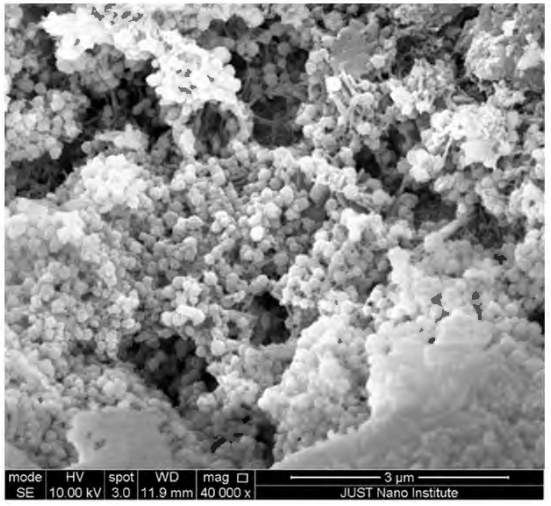
mode
SE
HV
10.00 kV
spot
3.0
WD
11.9 mm
mag
40 000 x
3 µm
JUST Nano Institute

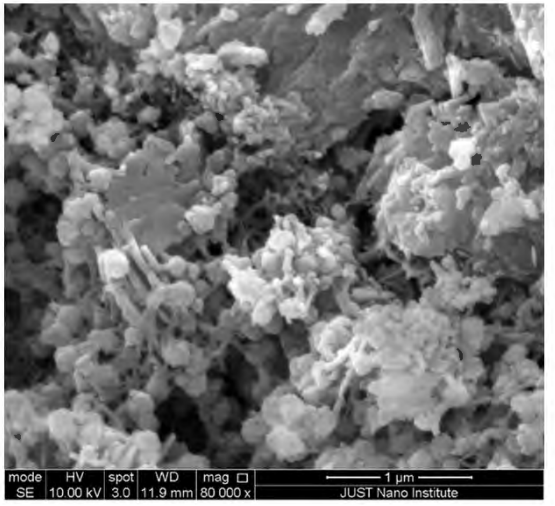
mode
SE
HV
10.00 kV
spot
3.0
WD
11.9 mm
mag
80 000 x
1 µm
JUST Nano Institute

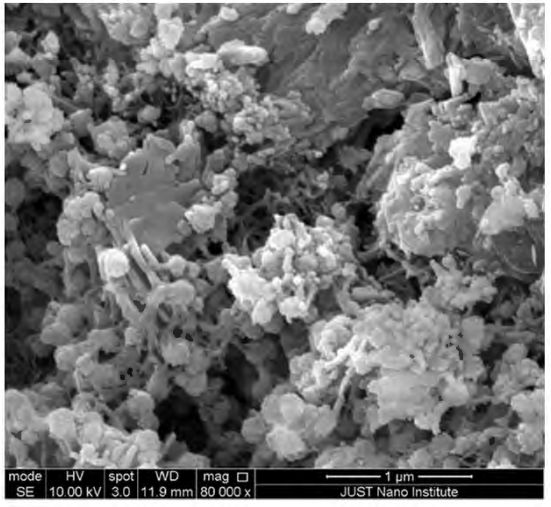
mode
SE
HV
10.00 kV
spot
3.0
WD
11.9 mm
mag
80 000 x
1 µm
JUST Nano Institute

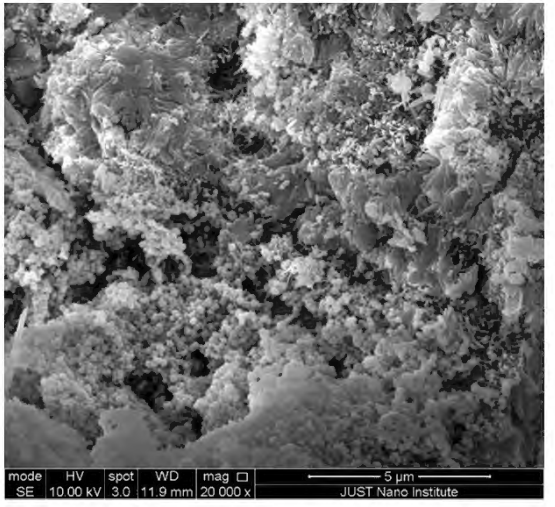
mode
SE
HV
10.00 kV
spot
3.0
WD
11.9 mm
mag
20 000 x
5 µm
JUST Nano Institute

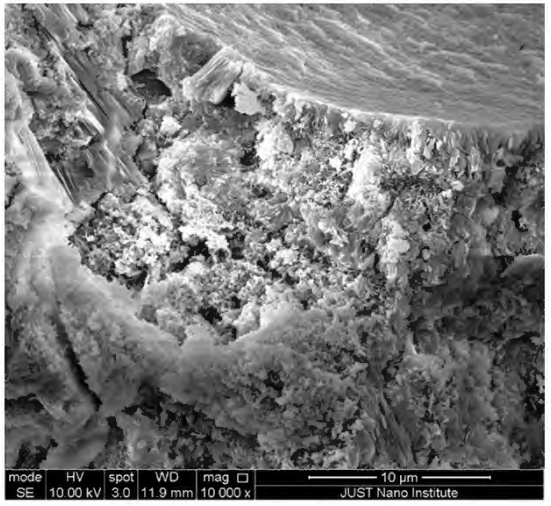
mode SE
HV 10.00 kV
spot 3.0
WD 11.9 mm
mag 10 000 x
10 µm
JUST Nano Institute

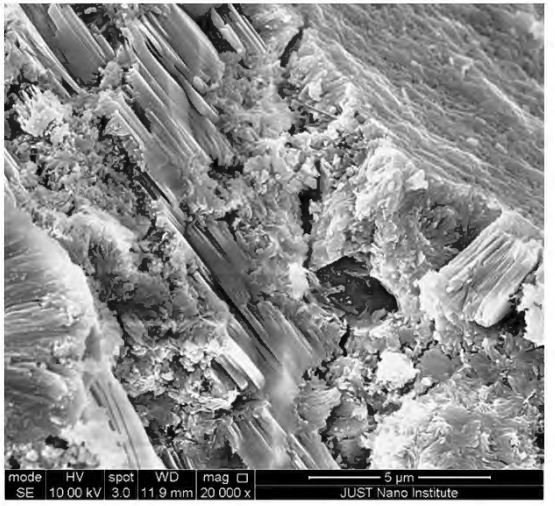
mode SE
HV 10.00 kV
spot 3.0
WD 11.9 mm
mag 20 000 x
5 µm
JUST Nano Institute

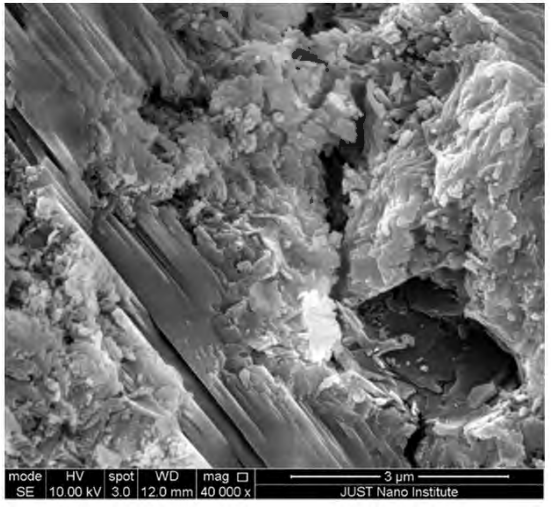
mode SE
HV 10.00 kV
spot 3.0
WD 12.0 mm
mag 40 000 x
3 µm
JUST Nano Institute

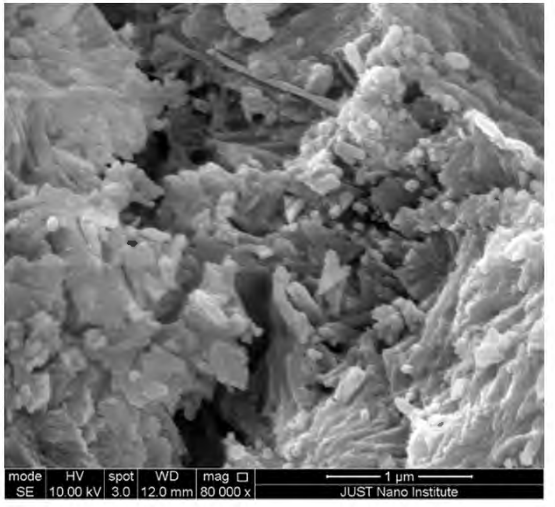
mode SE
HV 10.00 kV
spot 3.0
WD 12.0 mm
mag 80 000 x
1 µm
JUST Nano Institute

Sample No. 7

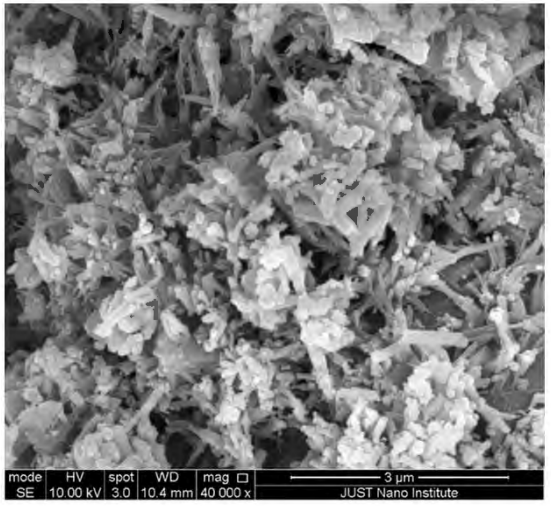
mode SE
HV 10.00 kV
spot 3.0
WD 10.4 mm
mag 40 000 x
3 µm
JUST Nano Institute

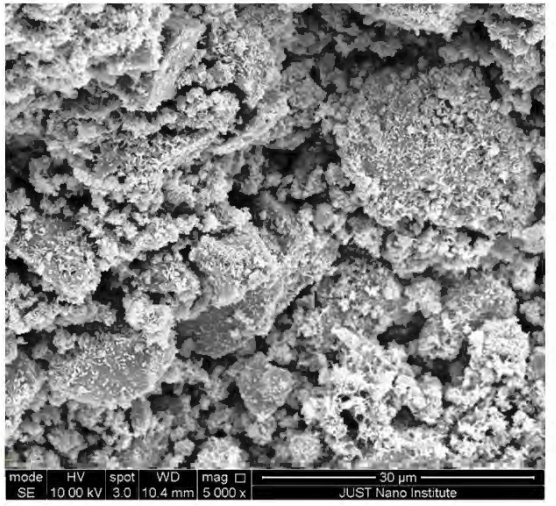
mode SE
HV 10.00 kV
spot 3.0
WD 10.4 mm
mag 5 000 x
30 µm
JUST Nano Institute

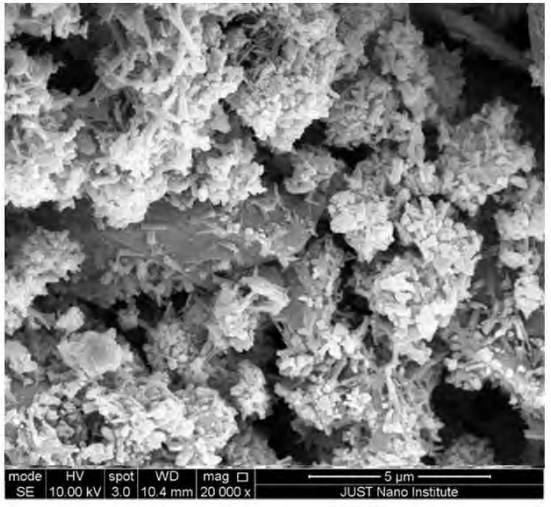
mode SE
HV 10.00 kV
spot 3.0
WD 10.4 mm
mag 20 000 x
5 µm
JUST Nano Institute

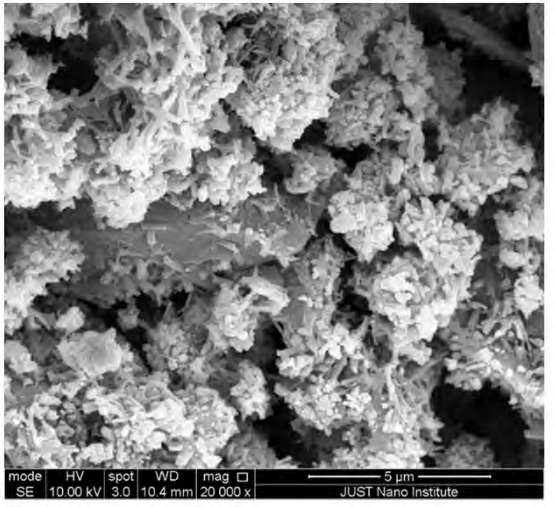
mode SE
HV 10.00 kV
spot 3.0
WD 10.4 mm
mag 20 000 x
5 µm
JUST Nano Institute

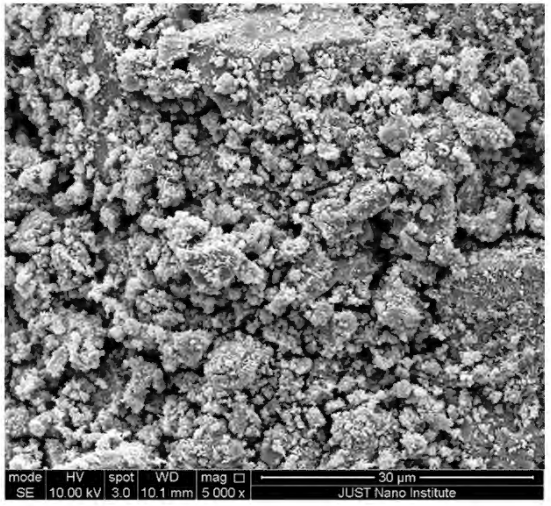
mode
SE
HV
10.00 kV
spot
3.0
WD
10.1 mm
mag
5 000 x
30 µm
JUST Nano Institute

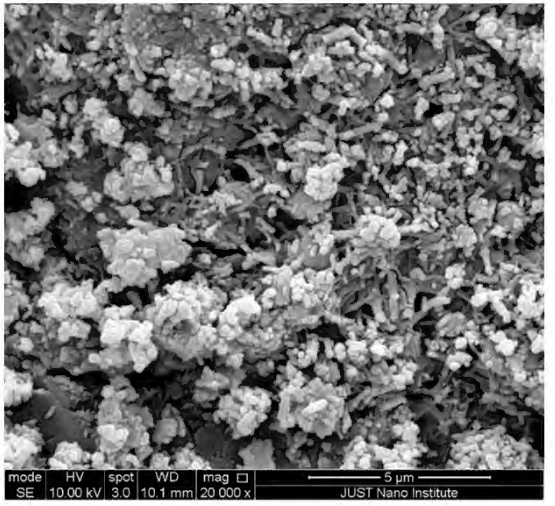
mode
SE
HV
10.00 kV
spot
3.0
WD
10.1 mm
mag
20 000 x
5 µm
JUST Nano Institute

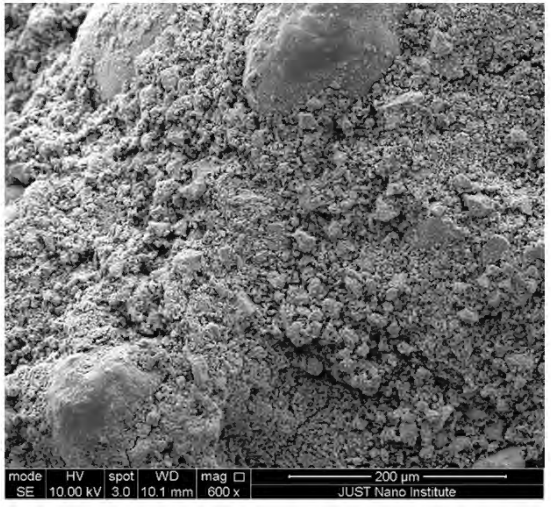
mode
SE
HV
10.00 kV
spot
3.0
WD
10.1 mm
mag
600 x
200 µm
JUST Nano Institute

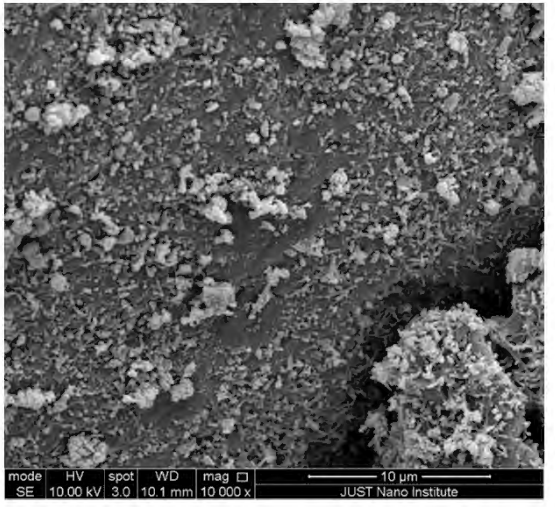
mode
SE
HV
10.00 kV
spot
3.0
WD
10.1 mm
mag
10 000 x
10 µm
JUST Nano Institute

Sample No. B

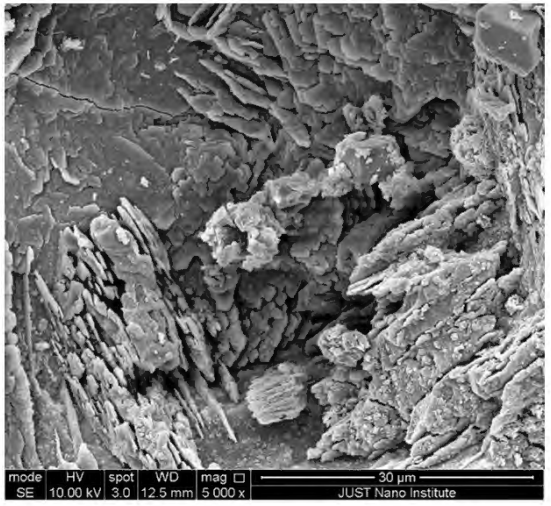
mode
SE
HV
10.00 kV
spot
3.0
WD
12.5 mm
mag
5 000 x
30 µm
JUST Nano Institute

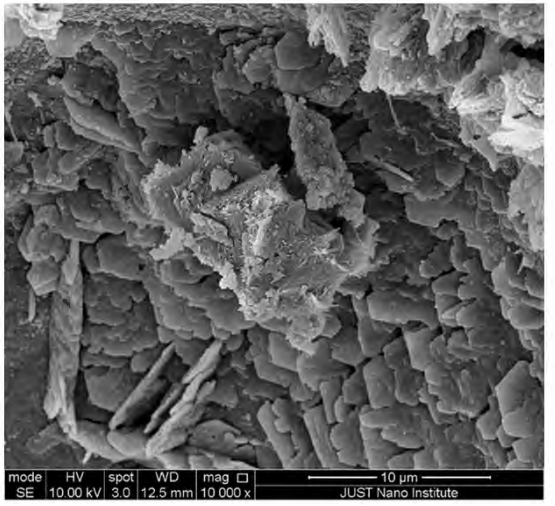
mode
SE
HV
10.00 kV
spot
3.0
WD
12.5 mm
mag
10 000 x
10 µm
JUST Nano Institute

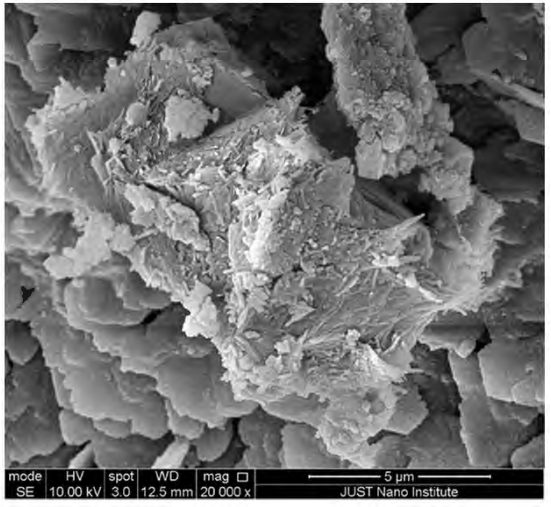
mode
SE
HV
10.00 kV
spot
3.0
WD
12.5 mm
mag
20 000 x
5 µm
JUST Nano Institute

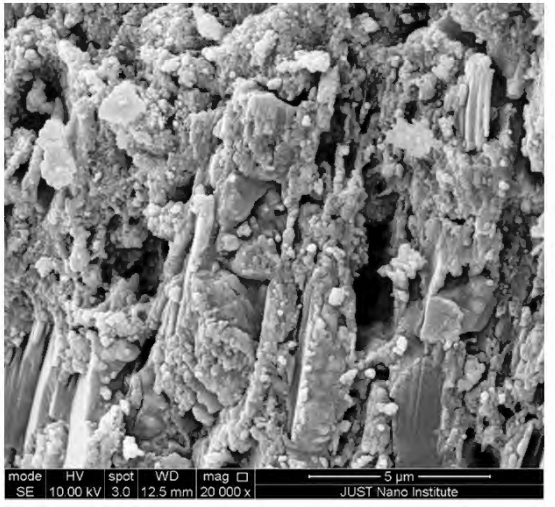
mode
SE
HV
10.00 kV
spot
3.0
WD
12.5 mm
mag
20 000 x
5 µm
JUST Nano Institute

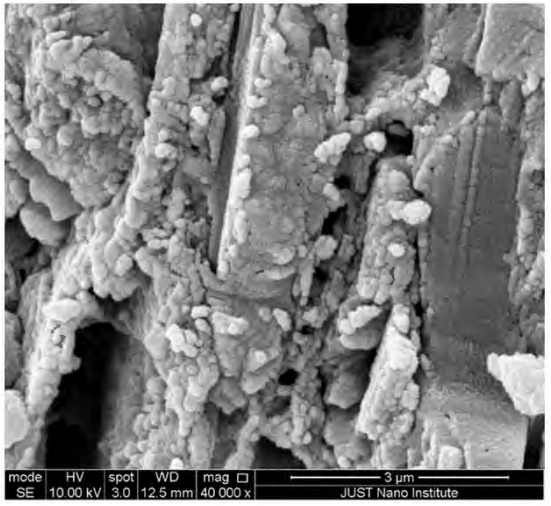
mode HV spot WD mag 3 µm
SE 10.00 kV 3.0 12.5 mm 40 000 x JUST Nano Institute

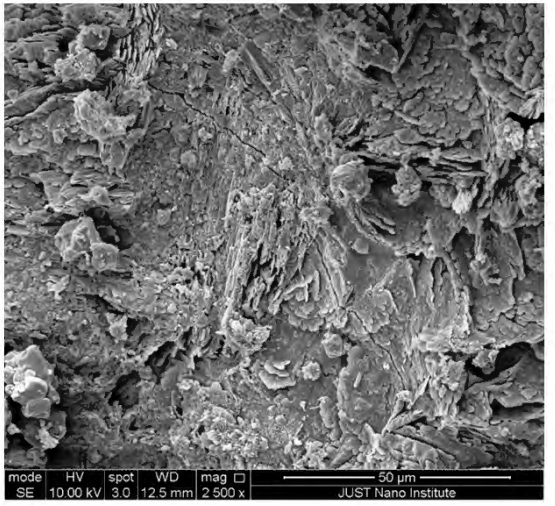
mode HV spot WD mag 50 µm
SE 10.00 kV 3.0 12.5 mm 2 500 x JUST Nano Institute

mode HV spot WD mag 5 µm
SE 10.00 kV 3.0 12.5 mm 20 000 x JUST Nano Institute

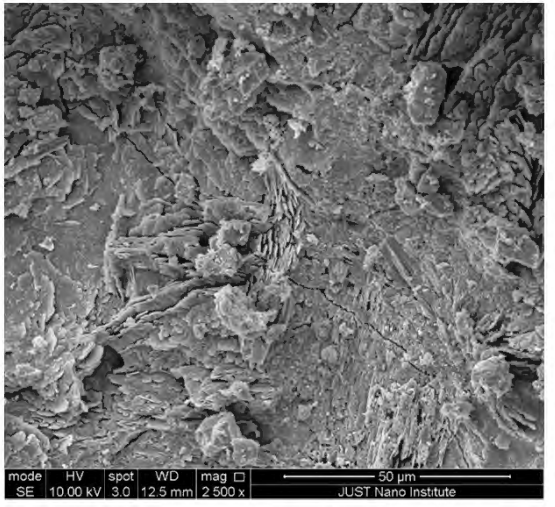
mode HV spot WD mag 50 µm
SE 10.00 kV 3.0 12.5 mm 2 500 x JUST Nano Institute

Sample No. G

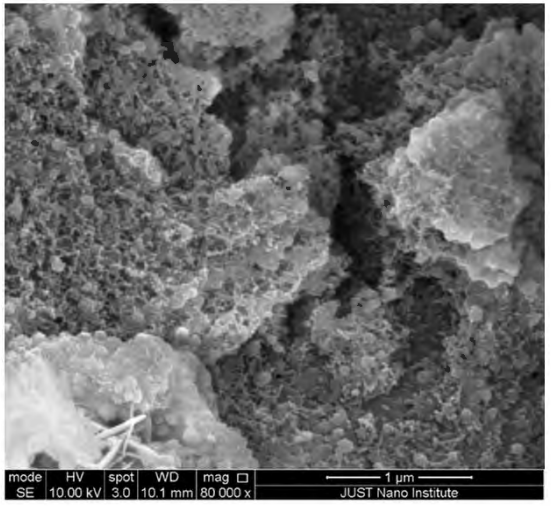
mode HV spot WD mag 1 µm
SE 10.00 kV 3.0 10.1 mm 80 000 x
JUST Nano Institute

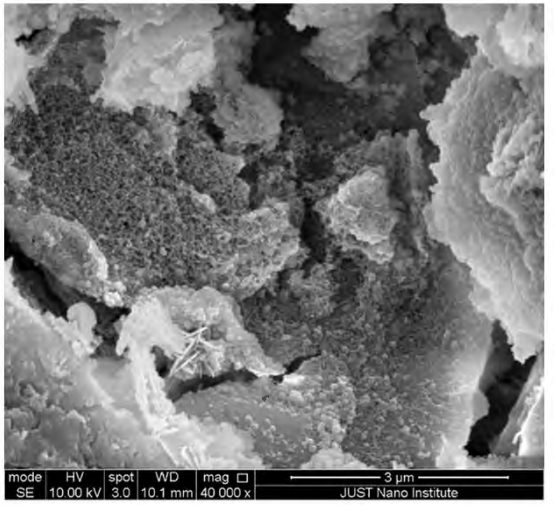
mode HV spot WD mag 3 µm
SE 10.00 kV 3.0 10.1 mm 40 000 x
JUST Nano Institute

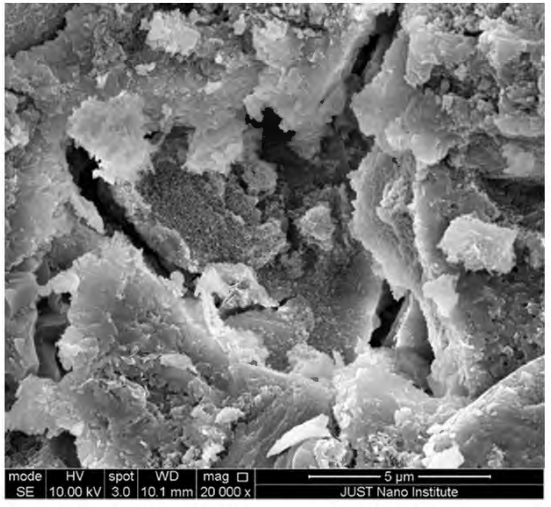
mode HV spot WD mag 5 µm
SE 10.00 kV 3.0 10.1 mm 20 000 x
JUST Nano Institute

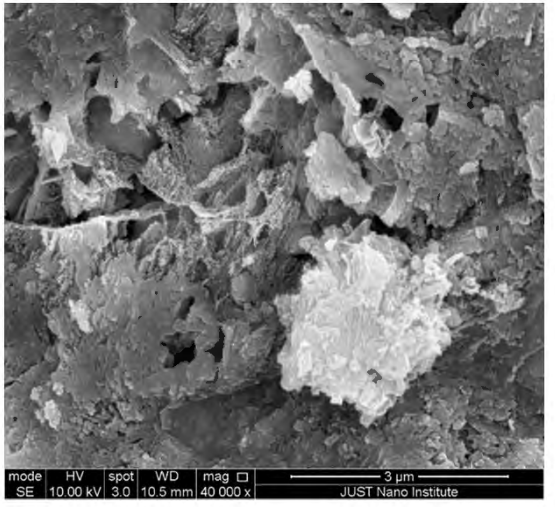
mode HV spot WD mag 3 µm
SE 10.00 kV 3.0 10.5 mm 40 000 x
JUST Nano Institute

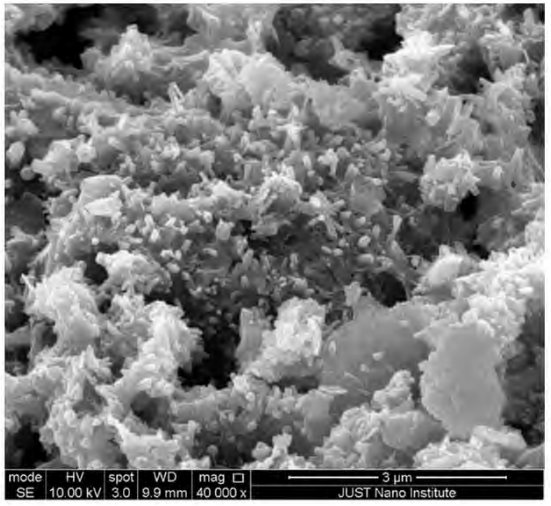
mode HV spot WD mag
SE 10.00 kV 3.0 9.9 mm 40 000 x
3 µm
JUST Nano Institute

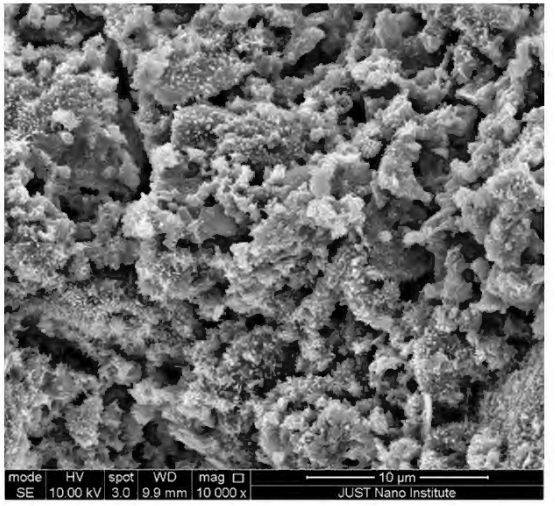
mode HV spot WD mag
SE 10.00 kV 3.0 9.9 mm 10 000 x
10 µm
JUST Nano Institute

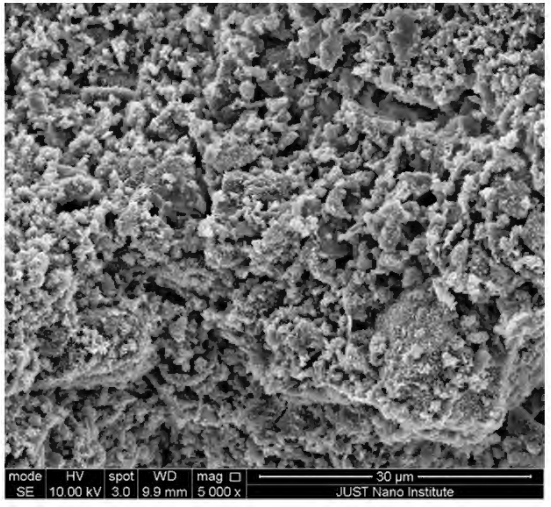
mode HV spot WD mag
SE 10.00 kV 3.0 9.9 mm 5 000 x
30 µm
JUST Nano Institute

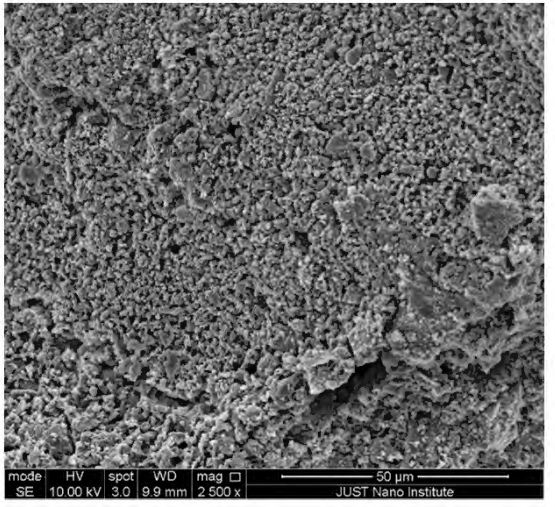
mode HV spot WD mag
SE 10.00 kV 3.0 9.9 mm 2 500 x
50 µm
JUST Nano Institute

Sample No. H

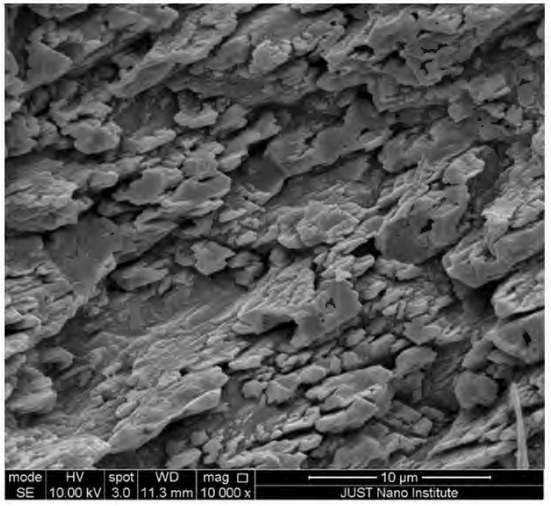
mode
SE
HV
10.00 kV
spot
3.0
WD
11.3 mm
mag
10 000 x
10 µm
JUST Nano Institute

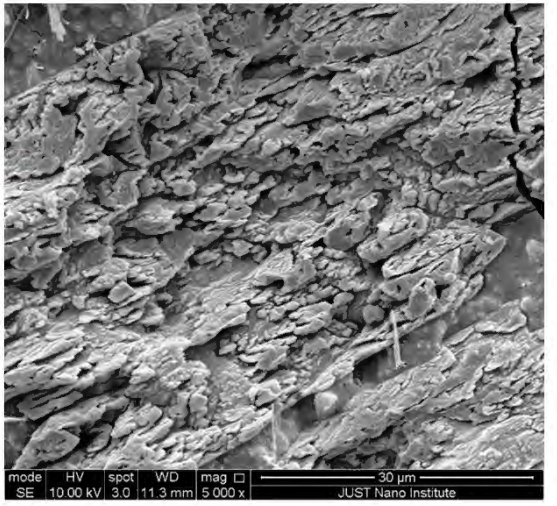
mode
SE
HV
10.00 kV
spot
3.0
WD
11.3 mm
mag
5 000 x
30 µm
JUST Nano Institute

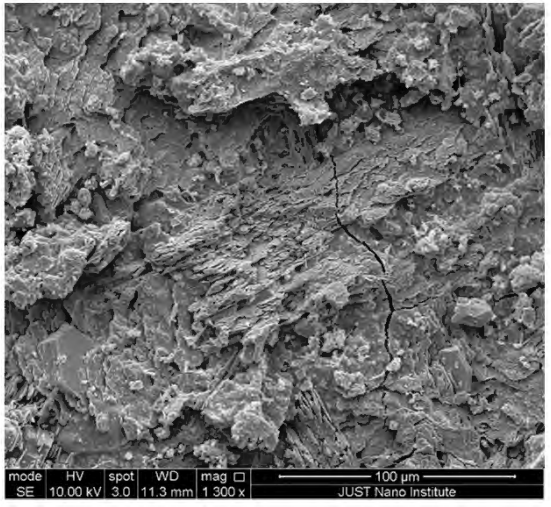
mode
SE
HV
10.00 kV
spot
3.0
WD
11.3 mm
mag
1 300 x
100 µm
JUST Nano Institute

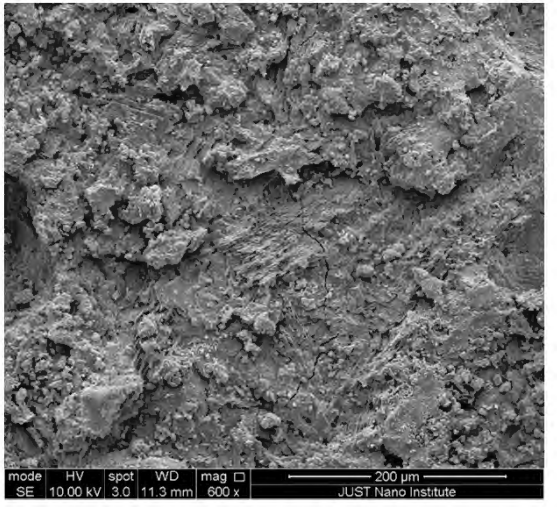
mode
SE
HV
10.00 kV
spot
3.0
WD
11.3 mm
mag
600 x
200 µm
JUST Nano Institute

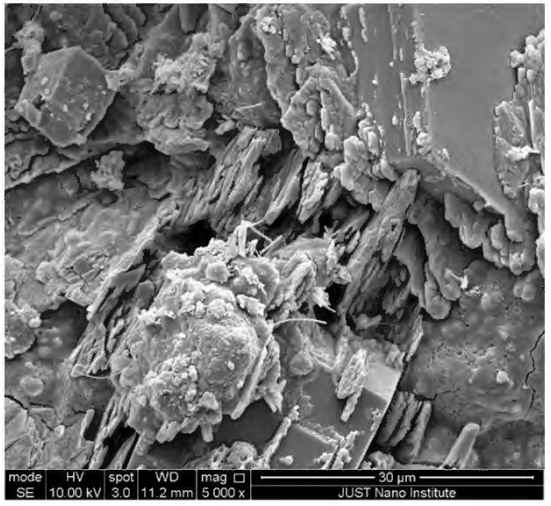
mode
SE
HV
10.00 kV
spot
3.0
WD
11.2 mm
mag
5 000 x
30 µm
JUST Nano Institute

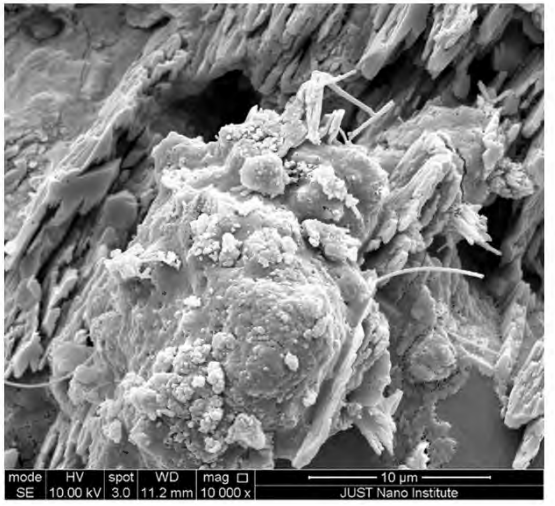
mode
SE
HV
10.00 kV
spot
3.0
WD
11.2 mm
mag
10 000 x
10 µm
JUST Nano Institute

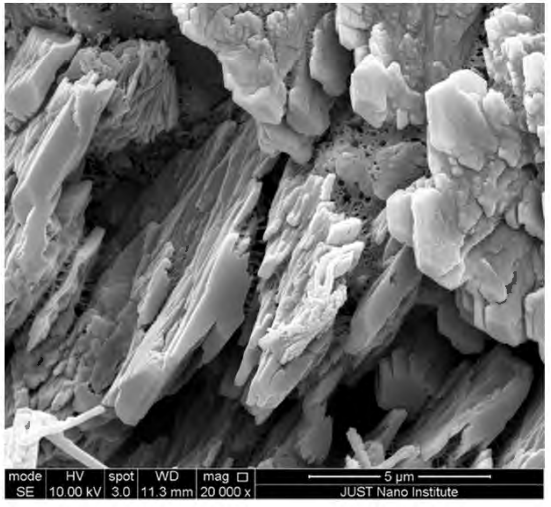
mode
SE
HV
10.00 kV
spot
3.0
WD
11.3 mm
mag
20 000 x
5 µm
JUST Nano Institute

mode
SE
HV
10.00 kV
spot
3.0
WD
11.2 mm
mag
40 000 x
3 µm
JUST Nano Institute

Sample No. J

mode HV spot WD mag 3 µm
SE 10.00 kV 3.0 11.9 mm 40 000 x
JUST Nano Institute

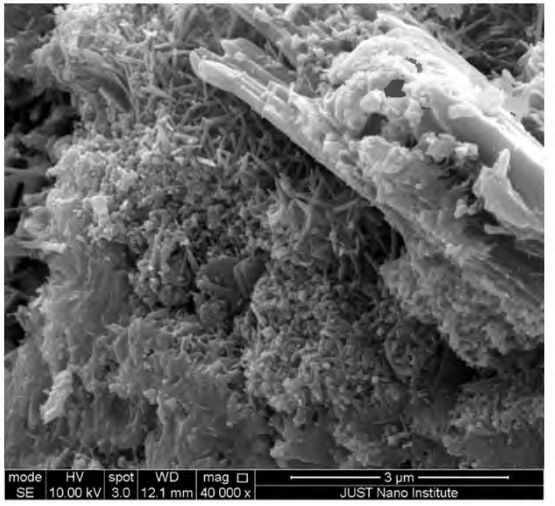
mode HV spot WD mag 3 µm
SE 10.00 kV 3.0 12.1 mm 40 000 x
JUST Nano Institute

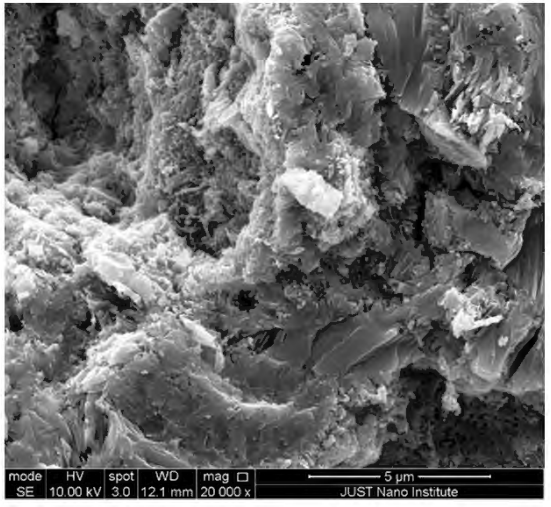
mode HV spot WD mag 5 µm
SE 10.00 kV 3.0 12.1 mm 20 000 x
JUST Nano Institute

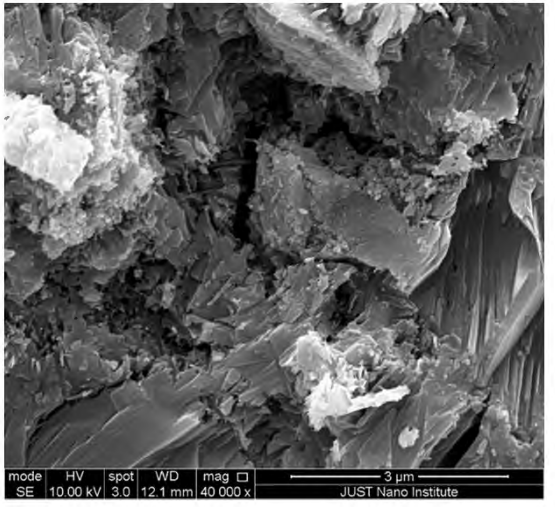
mode HV spot WD mag 3 µm
SE 10.00 kV 3.0 12.1 mm 40 000 x
JUST Nano Institute

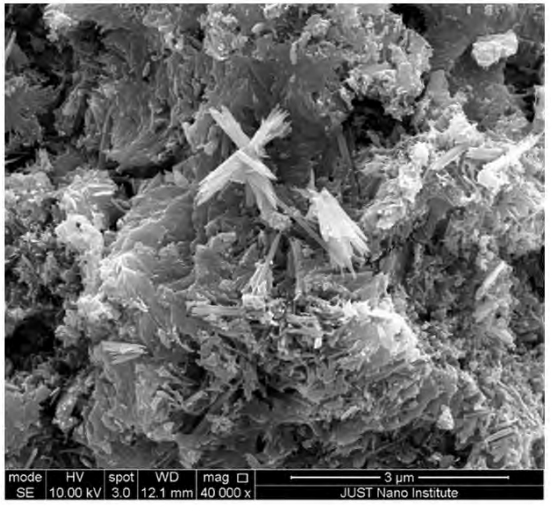
mode
SE
HV
10.00 kV
spot
3.0
WD
12.1 mm
mag
40 000 x
3 µm
JUST Nano Institute

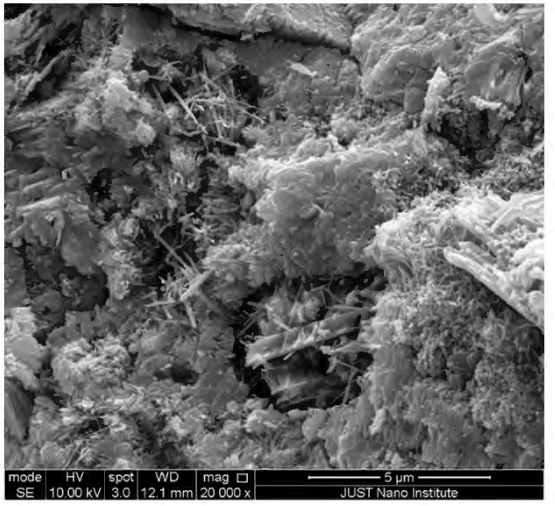
mode
SE
HV
10.00 kV
spot
3.0
WD
12.1 mm
mag
20 000 x
5 µm
JUST Nano Institute

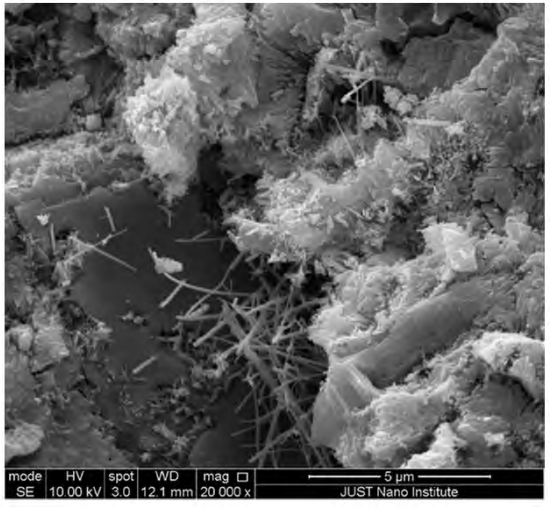
mode
SE
HV
10.00 kV
spot
3.0
WD
12.1 mm
mag
20 000 x
5 µm
JUST Nano Institute

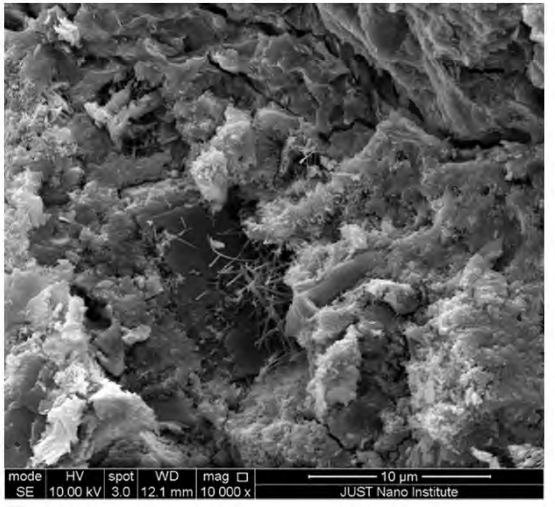
mode
SE
HV
10.00 kV
spot
3.0
WD
12.1 mm
mag
10 000 x
10 µm
JUST Nano Institute

Sample No. N

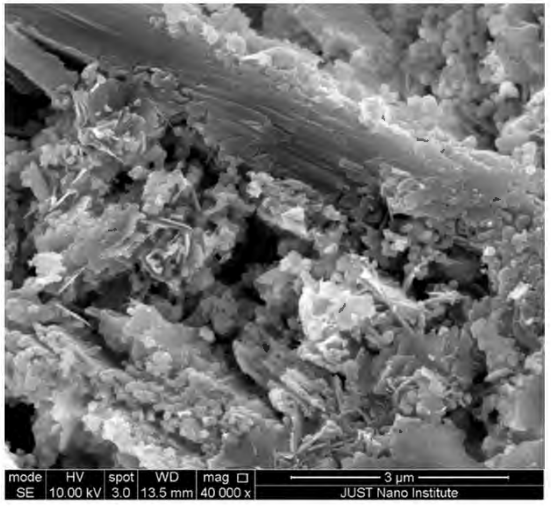
mode HV spot WD mag
SE 10.00 kV 3.0 13.5 mm 40 000 x
3 µm
JUST Nano Institute

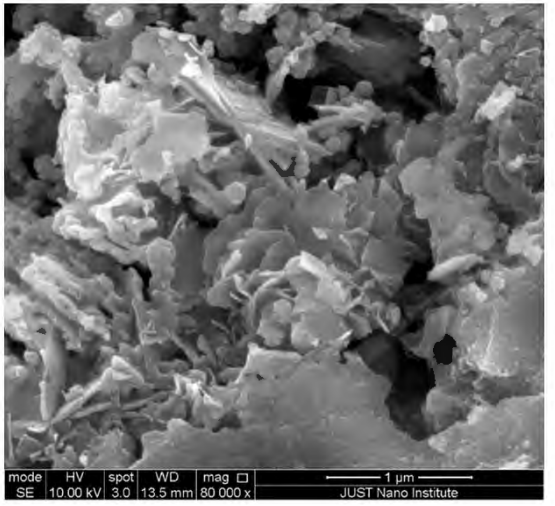
mode HV spot WD mag
SE 10.00 kV 3.0 13.5 mm 80 000 x
1 µm
JUST Nano Institute

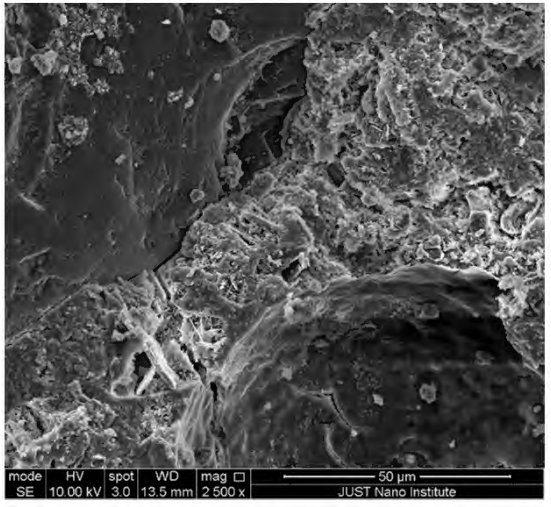
mode HV spot WD mag
SE 10.00 kV 3.0 13.5 mm 2 500 x
50 µm
JUST Nano Institute

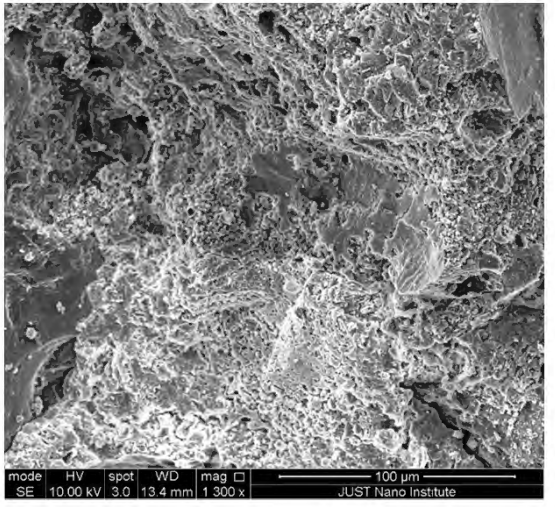
mode HV spot WD mag
SE 10.00 kV 3.0 13.4 mm 1 300 x
100 µm
JUST Nano Institute

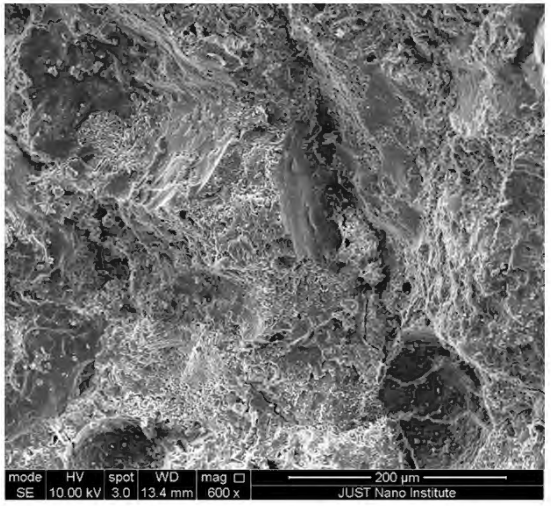
mode HV spot WD mag
SE 10.00 kV 3.0 13.4 mm 600 x
200 µm
JUST Nano Institute

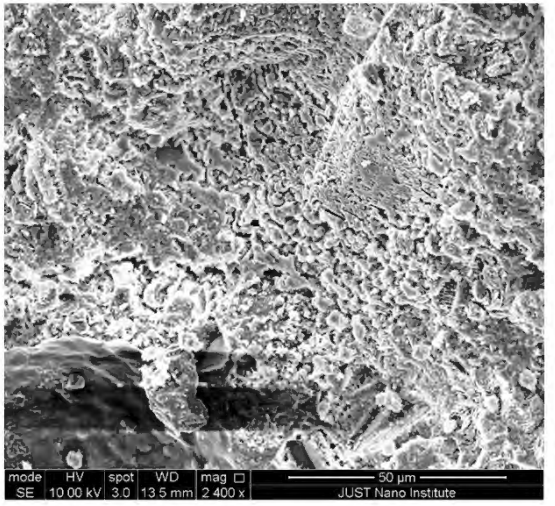
mode HV spot WD mag
SE 10.00 kV 3.0 13.5 mm 2 400 x
50 µm
JUST Nano Institute

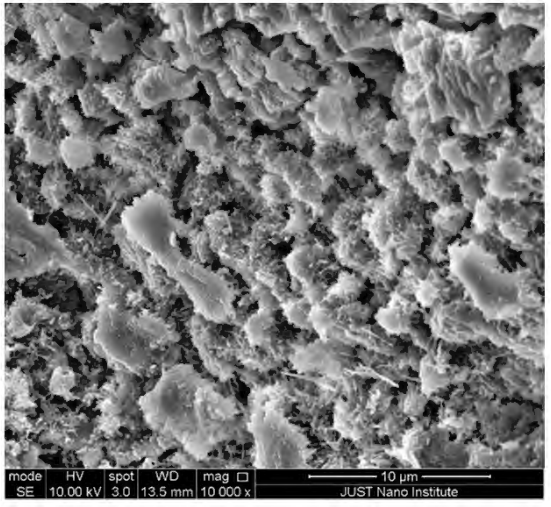
mode HV spot WD mag
SE 10.00 kV 3.0 13.5 mm 10 000 x
10 µm
JUST Nano Institute

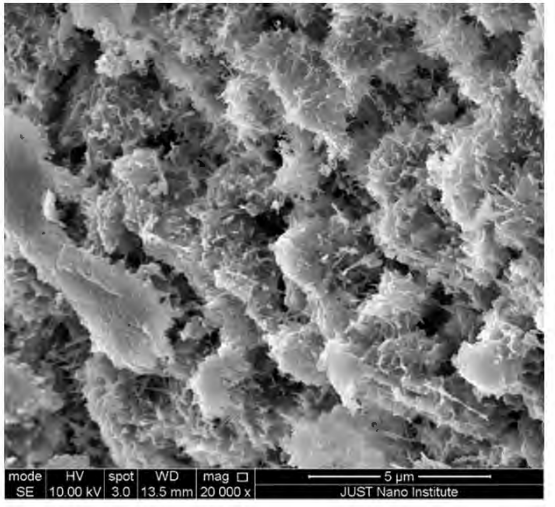
mode HV spot WD mag
SE 10.00 kV 3.0 13.5 mm 20 000 x
5 µm
JUST Nano Institute

Sample No. O

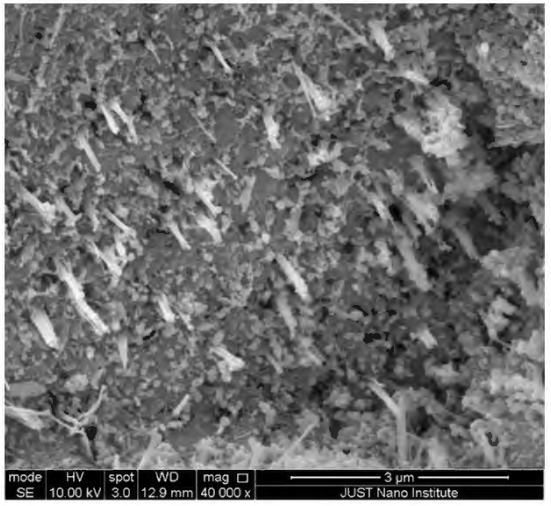
mode
SE
HV
10.00 kV
spot
3.0
WD
12.9 mm
mag
40 000 x
3 µm
JUST Nano Institute

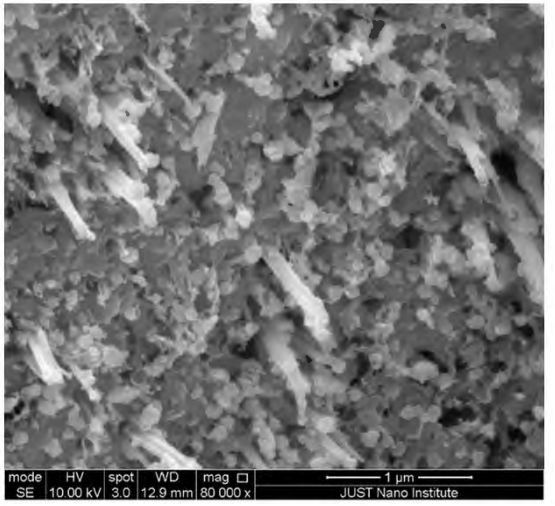
mode
SE
HV
10.00 kV
spot
3.0
WD
12.9 mm
mag
80 000 x
1 µm
JUST Nano Institute

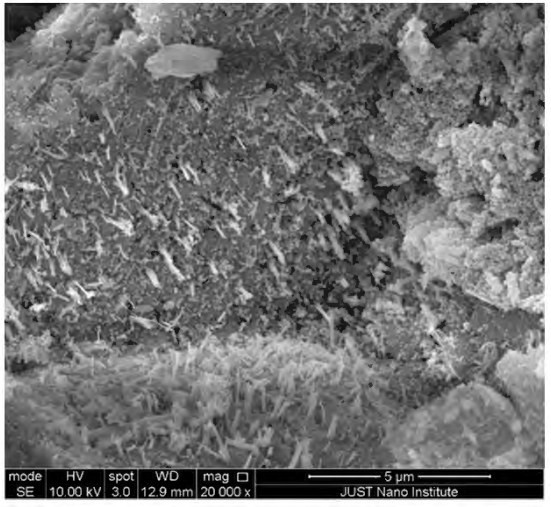
mode
SE
HV
10.00 kV
spot
3.0
WD
12.9 mm
mag
20 000 x
5 µm
JUST Nano Institute

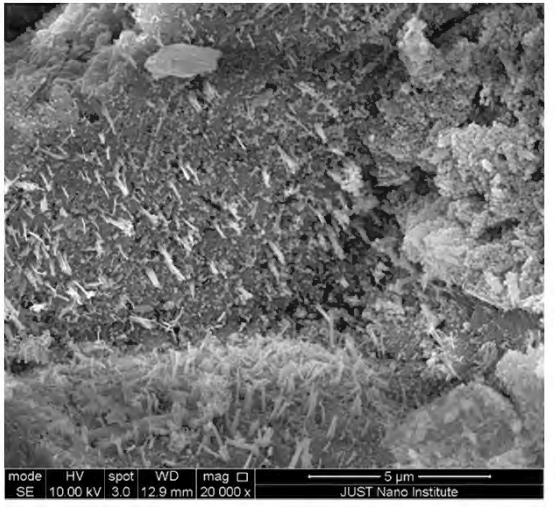
mode
SE
HV
10.00 kV
spot
3.0
WD
12.9 mm
mag
20 000 x
5 µm
JUST Nano Institute

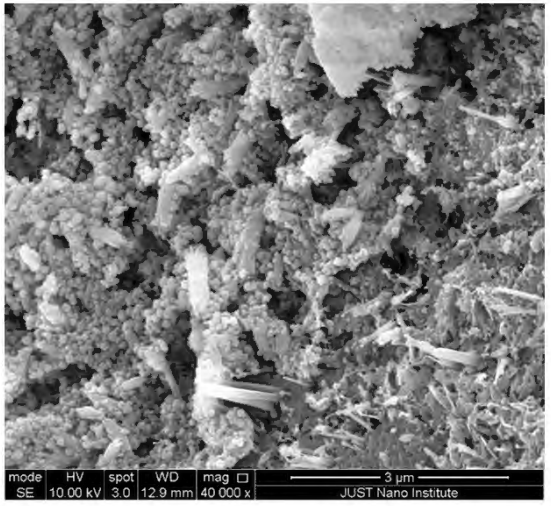
mode
SE
HV
10.00 kV
spot
3.0
WD
12.9 mm
mag
40 000 x
3 µm
JUST Nano Institute

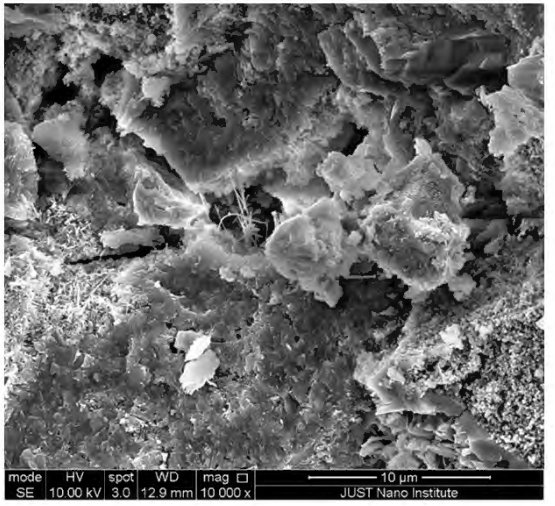
mode
SE
HV
10.00 kV
spot
3.0
WD
12.9 mm
mag
10 000 x
10 µm
JUST Nano Institute

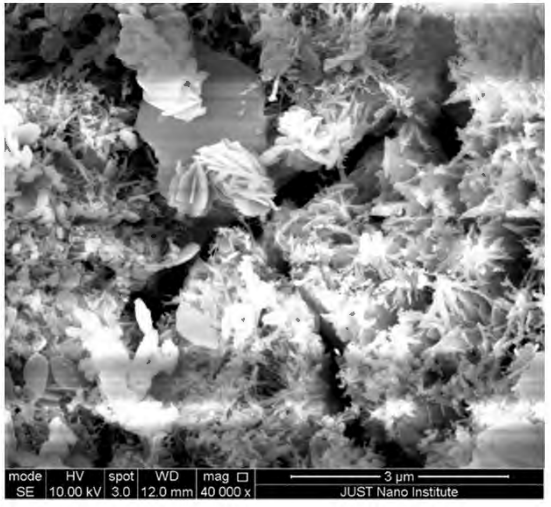
mode
SE
HV
10.00 kV
spot
3.0
WD
12.0 mm
mag
40 000 x
3 µm
JUST Nano Institute

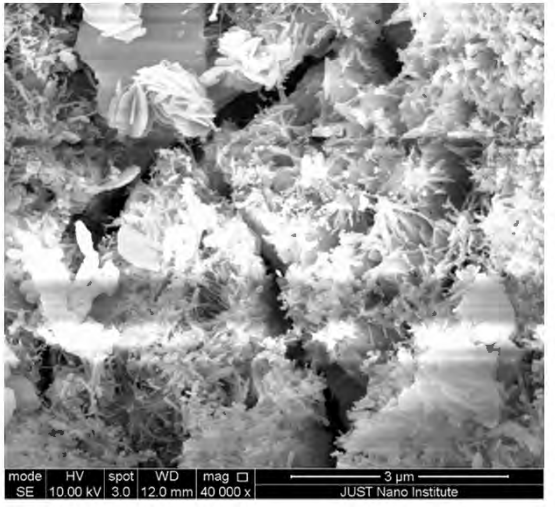
mode
SE
HV
10.00 kV
spot
3.0
WD
12.0 mm
mag
40 000 x
3 µm
JUST Nano Institute

Sample No. R

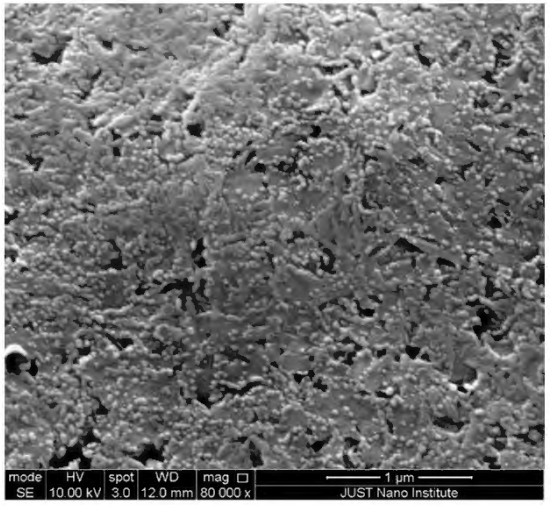
mode HV spot WD mag
SE 10.00 kV 3.0 12.0 mm 80 000 x
1 µm
JUST Nano Institute

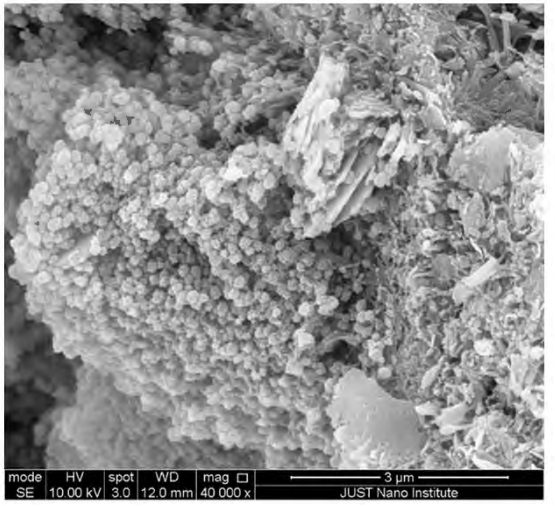
mode HV spot WD mag
SE 10.00 kV 3.0 12.0 mm 40 000 x
3 µm
JUST Nano Institute

mode HV spot WD mag
SE 10.00 kV 3.0 12.0 mm 40 000 x
3 µm
JUST Nano Institute

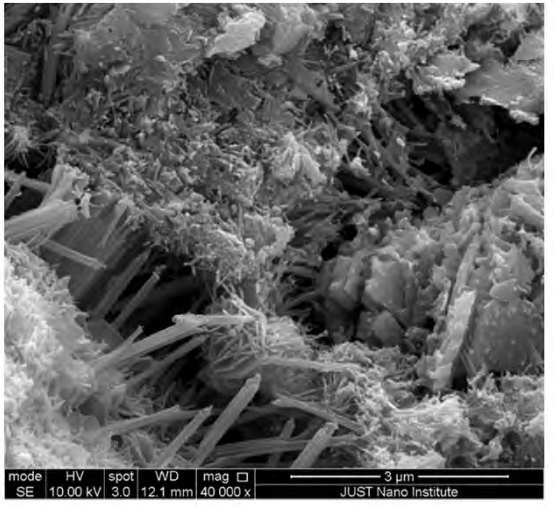
mode HV spot WD mag
SE 10.00 kV 3.0 12.1 mm 40 000 x
3 µm
JUST Nano Institute

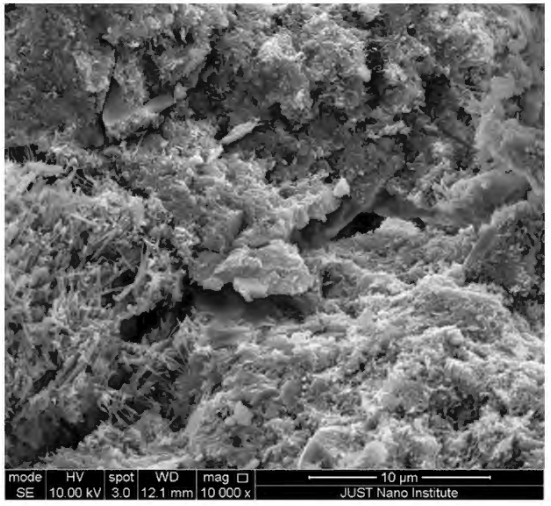
mode HV spot WD mag
SE 10.00 kV 3.0 12.1 mm 10 000 x
10 µm
JUST Nano Institute

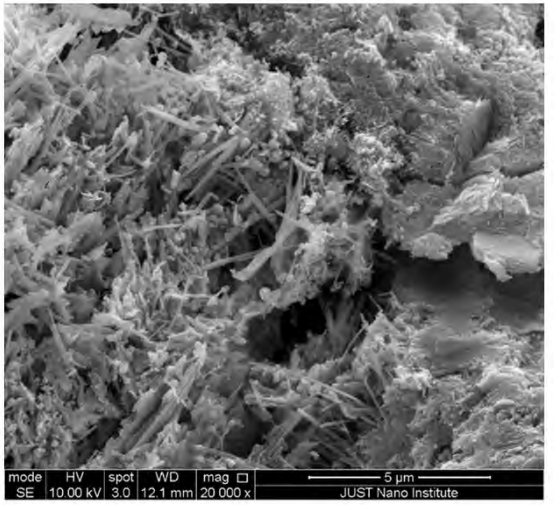
mode HV spot WD mag
SE 10.00 kV 3.0 12.1 mm 20 000 x
5 µm
JUST Nano Institute

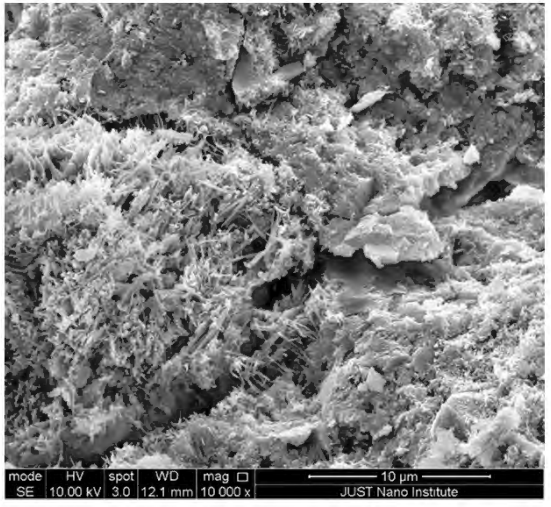
mode HV spot WD mag
SE 10.00 kV 3.0 12.1 mm 10 000 x
10 µm
JUST Nano Institute

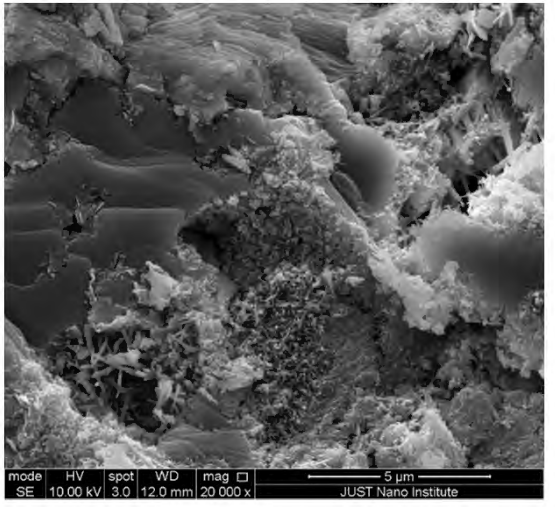
mode HV spot WD mag
SE 10.00 kV 3.0 12.0 mm 20 000 x
5 µm
JUST Nano Institute

Sample No. U

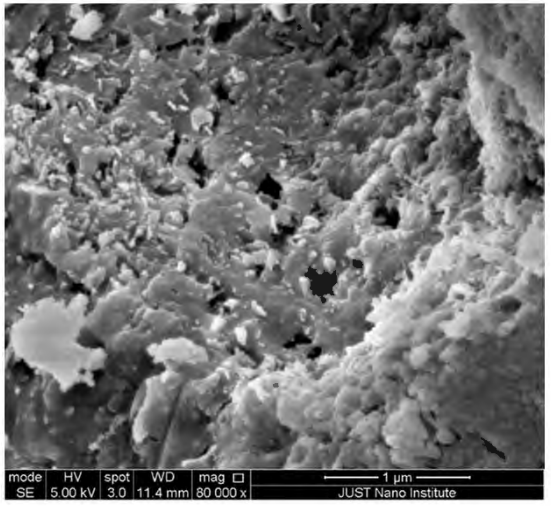
mode HV spot WD mag
SE 5.00 kV 3.0 11.4 mm 80 000 x
1 µm
JUST Nano Institute

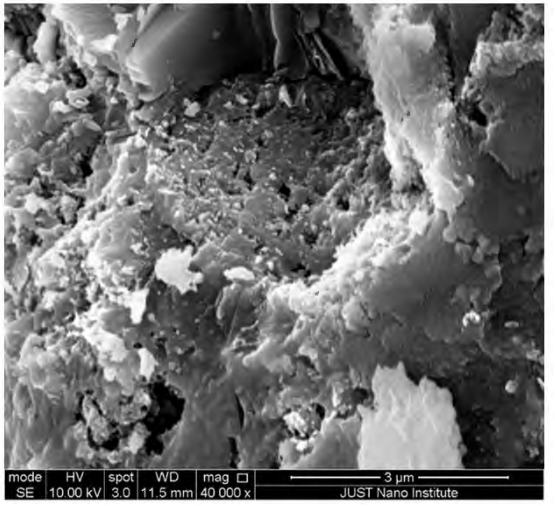
mode HV spot WD mag
SE 10.00 kV 3.0 11.5 mm 40 000 x
3 µm
JUST Nano Institute

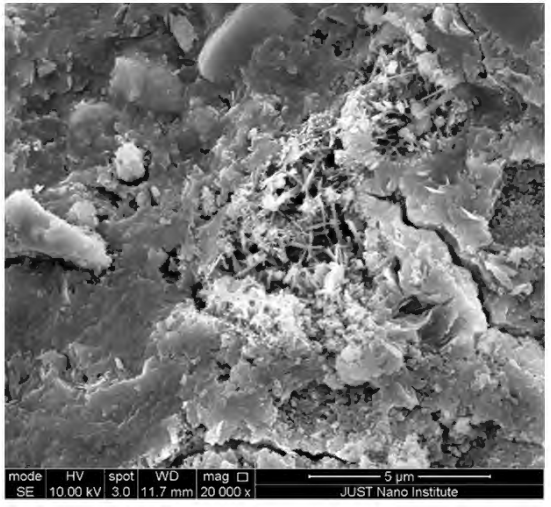
mode HV spot WD mag
SE 10.00 kV 3.0 11.7 mm 20 000 x
5 µm
JUST Nano Institute

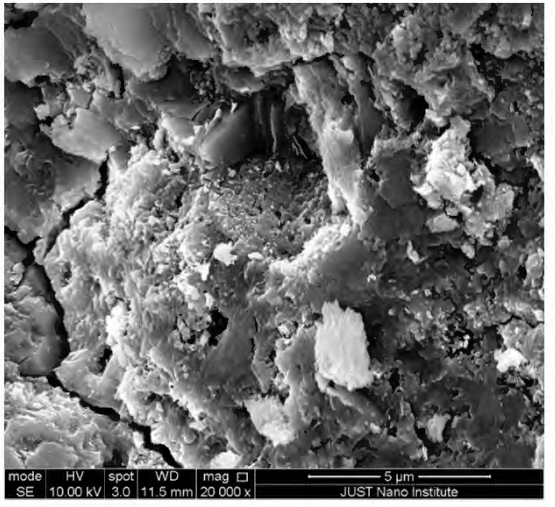
mode HV spot WD mag
SE 10.00 kV 3.0 11.5 mm 20 000 x
5 µm
JUST Nano Institute

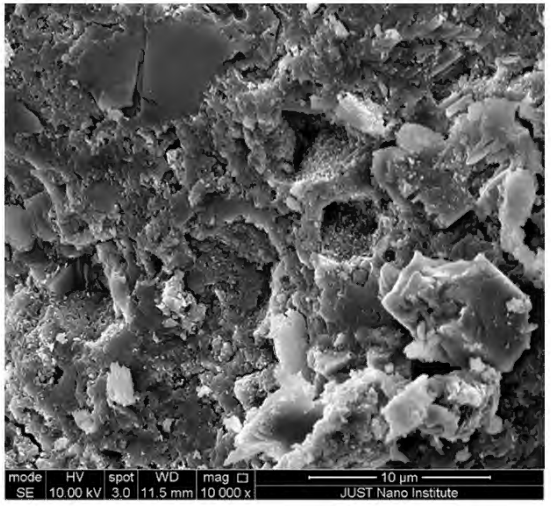
mode HV spot WD mag 10 µm
SE 10.00 kV 3.0 11.5 mm 10 000 x
JUST Nano Institute

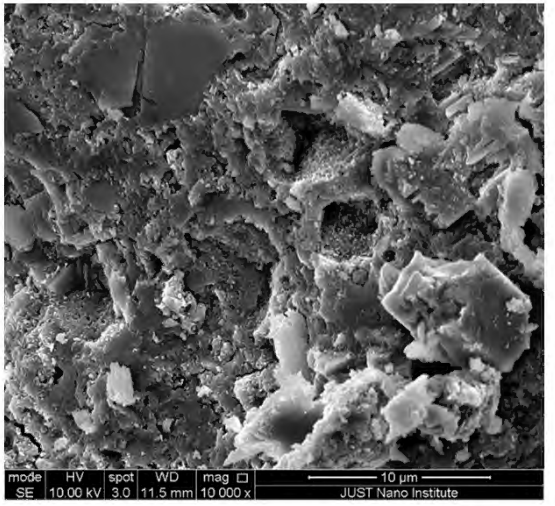
mode HV spot WD mag 10 µm
SE 10.00 kV 3.0 11.5 mm 10 000 x
JUST Nano Institute

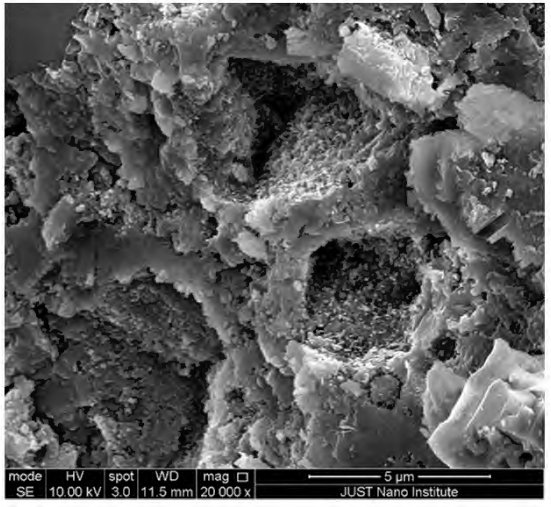
mode HV spot WD mag 5 µm
SE 10.00 kV 3.0 11.5 mm 20 000 x
JUST Nano Institute

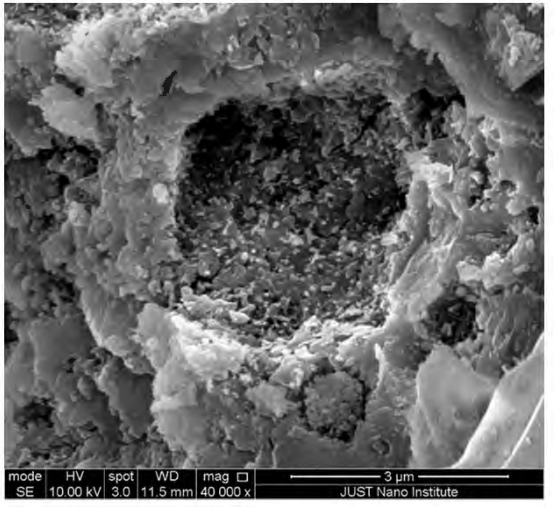
mode HV spot WD mag 3 µm
SE 10.00 kV 3.0 11.5 mm 40 000 x
JUST Nano Institute

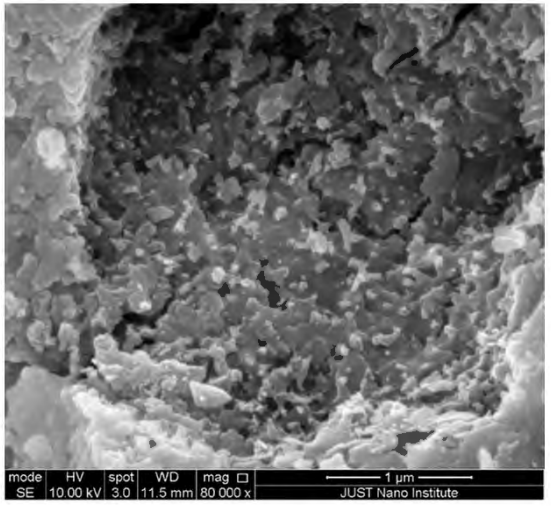
mode SE
HV 10.00 kV
spot 3.0
WD 11.5 mm
mag 80 000 x
1 µm
JUST Nano Institute

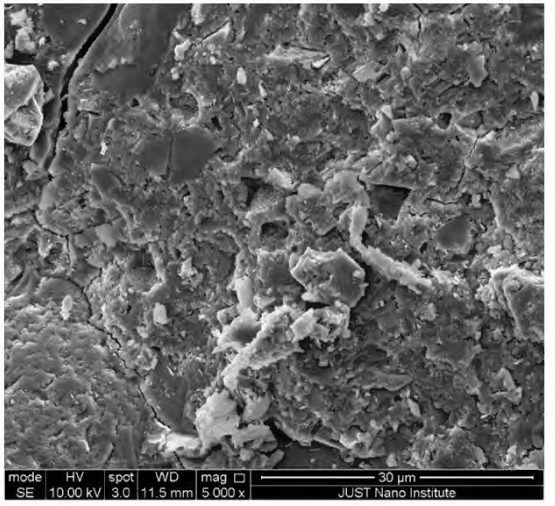
mode SE
HV 10.00 kV
spot 3.0
WD 11.5 mm
mag 5 000 x
30 µm
JUST Nano Institute

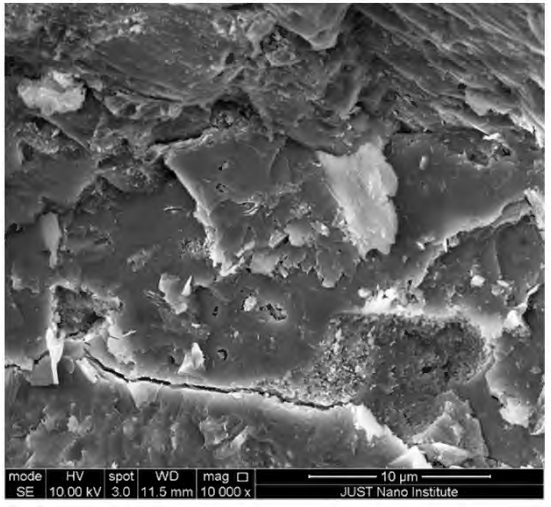
mode SE
HV 10.00 kV
spot 3.0
WD 11.5 mm
mag 10 000 x
10 µm
JUST Nano Institute

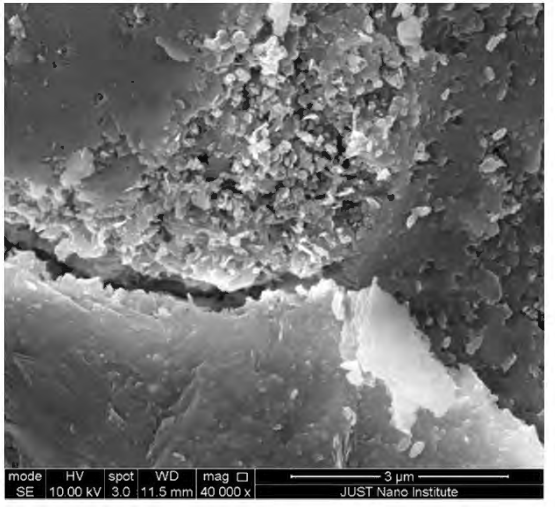
mode SE
HV 10.00 kV
spot 3.0
WD 11.5 mm
mag 40 000 x
3 µm
JUST Nano Institute

Sample No. X

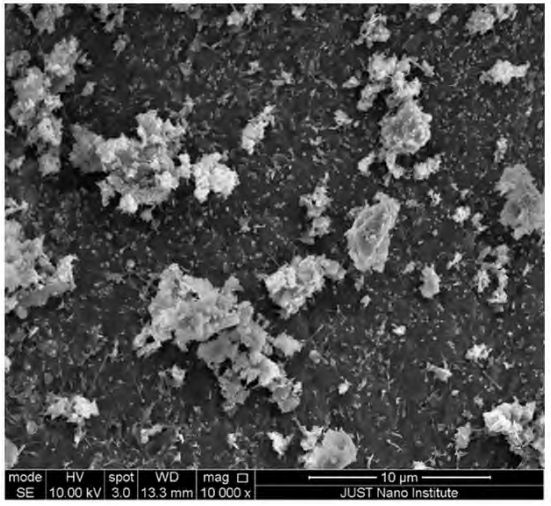
mode SE
HV 10.00 kV
spot 3.0
WD 13.3 mm
mag 10 000 x
10 µm
JUST Nano Institute

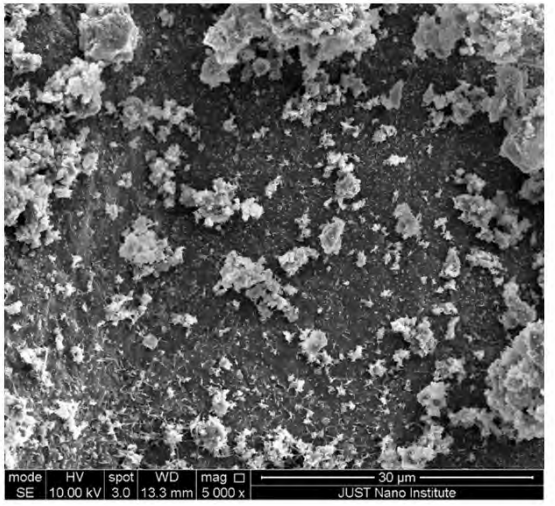
mode SE
HV 10.00 kV
spot 3.0
WD 13.3 mm
mag 5 000 x
30 µm
JUST Nano Institute

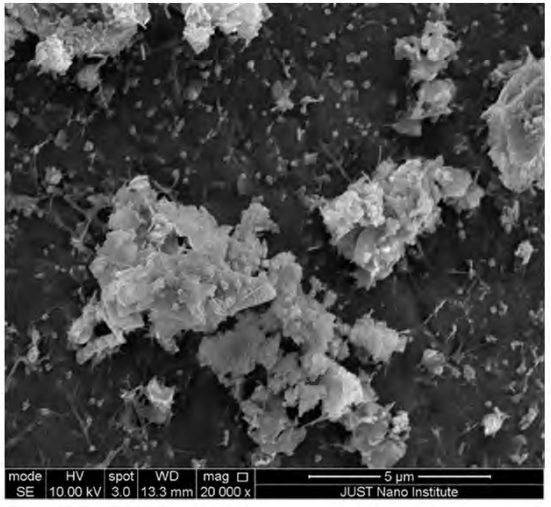
mode SE
HV 10.00 kV
spot 3.0
WD 13.3 mm
mag 20 000 x
5 µm
JUST Nano Institute

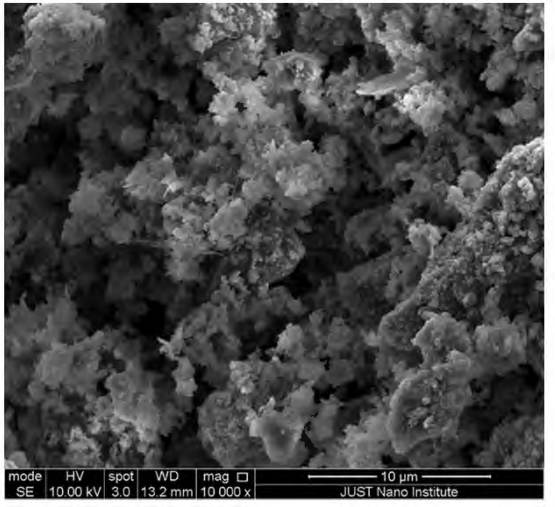
mode SE
HV 10.00 kV
spot 3.0
WD 13.2 mm
mag 10 000 x
10 µm
JUST Nano Institute

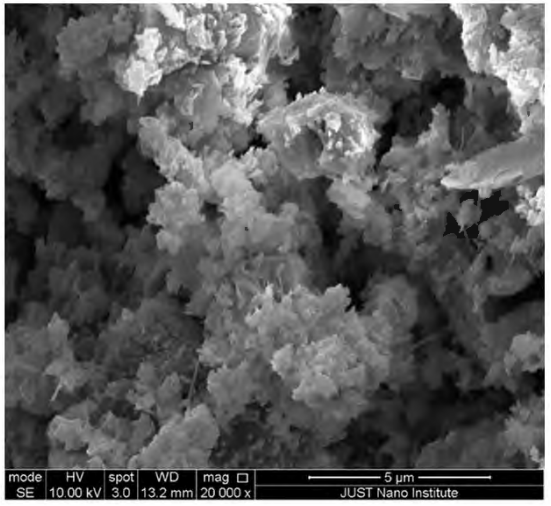
mode SE
HV 10.00 kV
spot 3.0
WD 13.2 mm
mag 20 000 x
5 µm
JUST Nano Institute

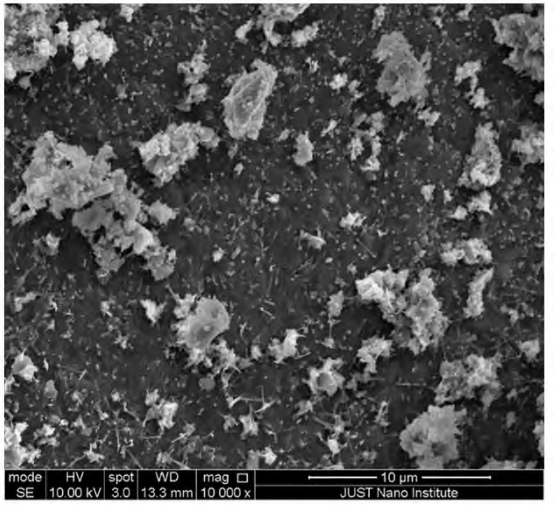
mode SE
HV 10.00 kV
spot 3.0
WD 13.3 mm
mag 10 000 x
10 µm
JUST Nano Institute

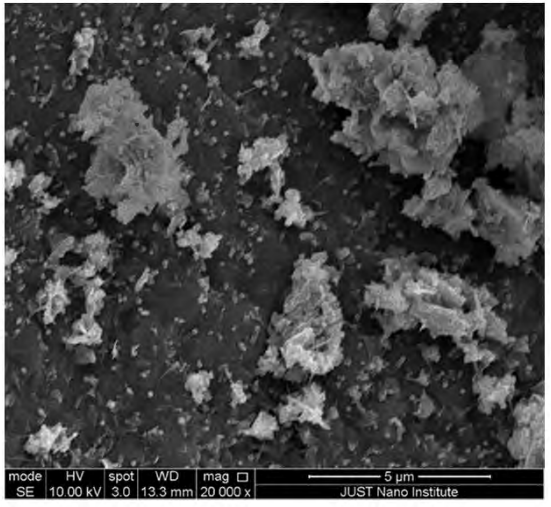
mode SE
HV 10.00 kV
spot 3.0
WD 13.3 mm
mag 20 000 x
5 µm
JUST Nano Institute

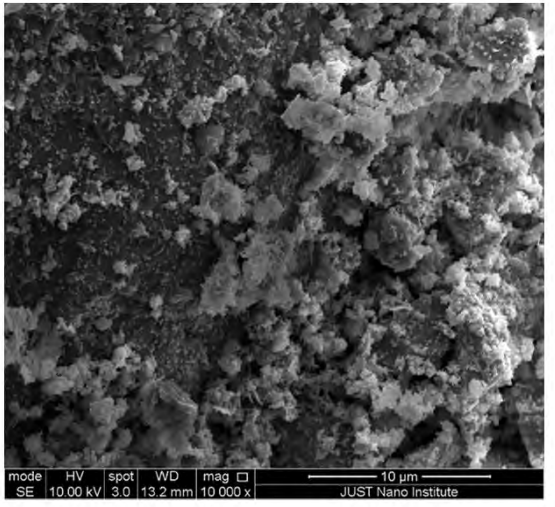
mode SE
HV 10.00 kV
spot 3.0
WD 13.2 mm
mag 10 000 x
10 µm
JUST Nano Institute

Appendix C: MATLAB output images

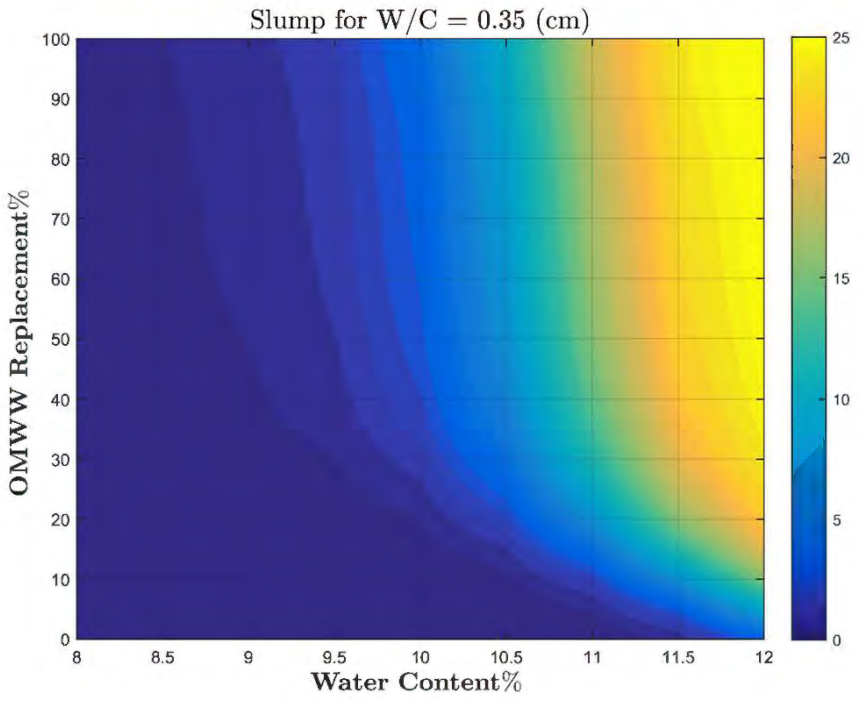
Slump for W/C = 0.35 (cm)
OMWW Replacement%
Water Content%
100
90
80
70
60
50
40
30
20
10
0
8
8.5
9
9.5
10
10.5
11
11.5
12
25
20
15
10
5
0

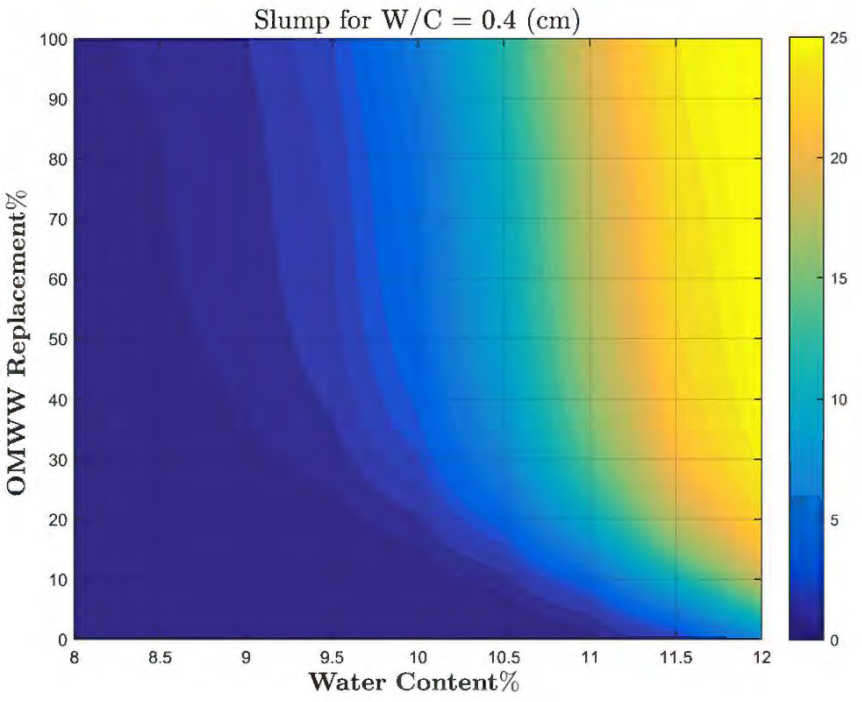
Slump for W/C = 0.4 (cm)
OMWW Replacement%
Water Content%
100
90
80
70
60
50
40
30
20
10
0
8
8.5
9
9.5
10
10.5
11
11.5
12
25
20
15
10
5
0

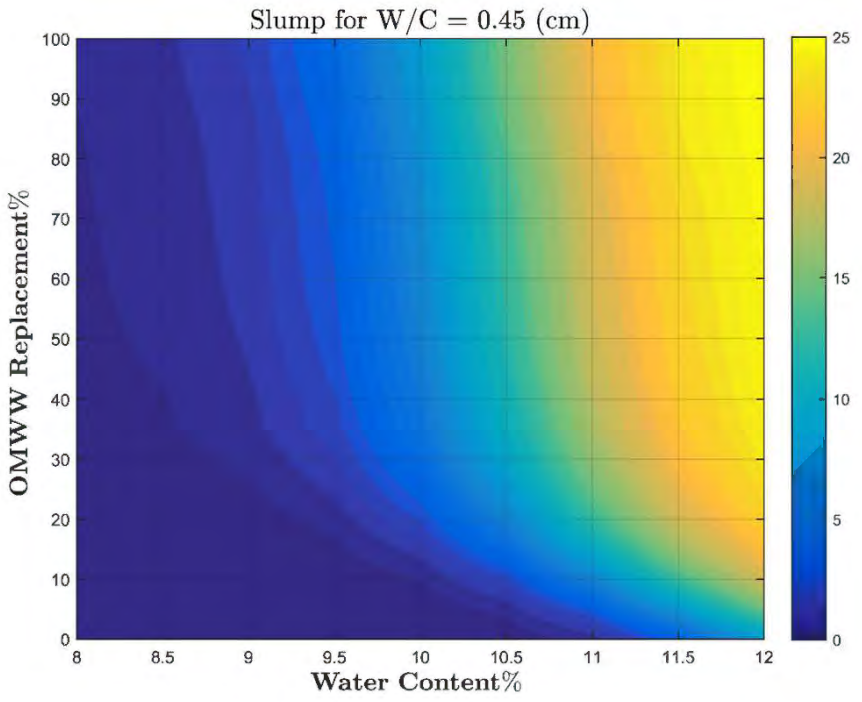
Slump for W/C = 0.45 (cm)
OMWW Replacement%
Water Content%
100
90
80
70
60
50
40
30
20
10
0
8
8.5
9
9.5
10
10.5
11
11.5
12
25
20
15
10
5
0

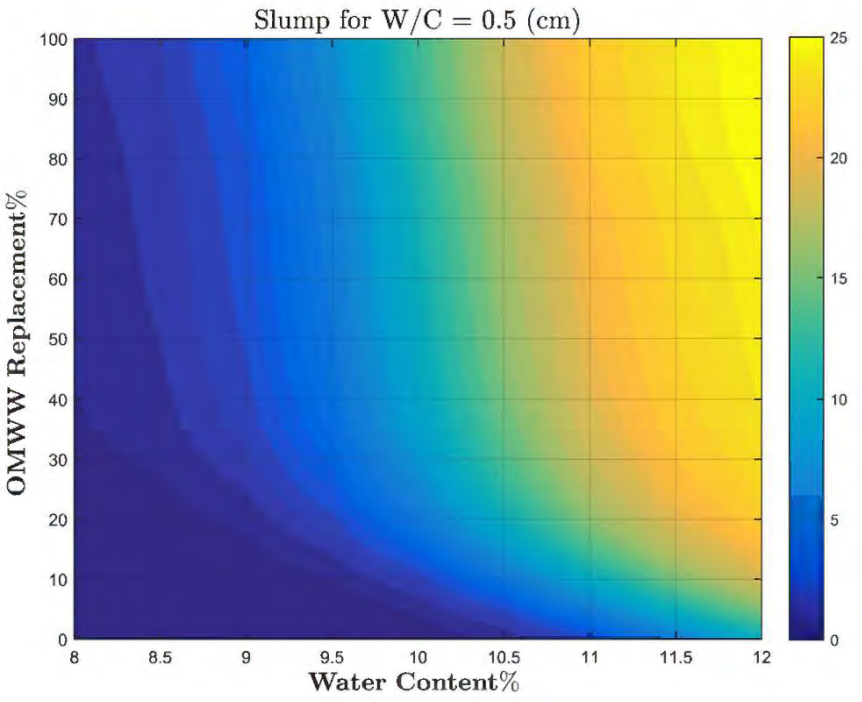
Slump for W/C = 0.5 (cm)
OMWW Replacement%
Water Content%
100
90
80
70
60
50
40
30
20
10
0
8
8.5
9
9.5
10
10.5
11
11.5
12
25
20
15
10
5
0

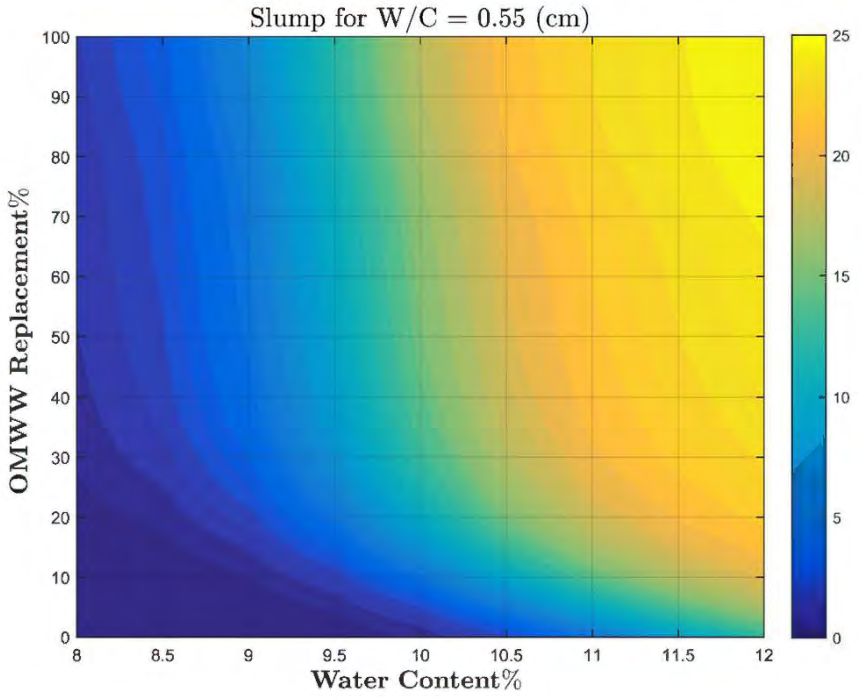
Slump for W/C = 0.55 (cm)
OMWW Replacement%
Water Content%
100
90
80
70
60
50
40
30
20
10
0
8
8.5
9
9.5
10
10.5
11
11.5
12
25
20
15
10
5
0

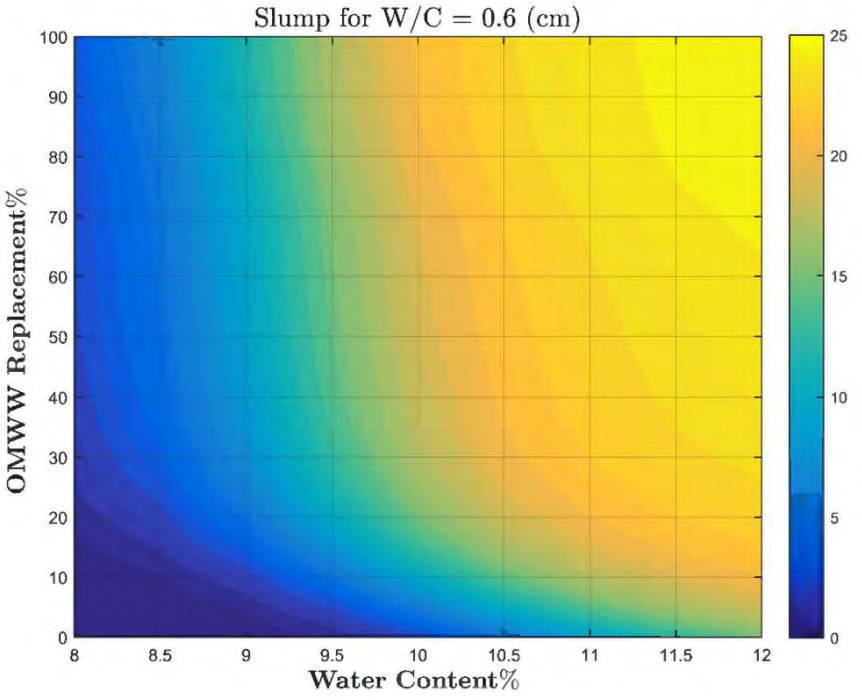
Slump for W/C = 0.6 (cm)
OMWW Replacement%
Water Content%
100
90
80
70
60
50
40
30
20
10
0
8
8.5
9
9.5
10
10.5
11
11.5
12
25
20
15
10
5
0

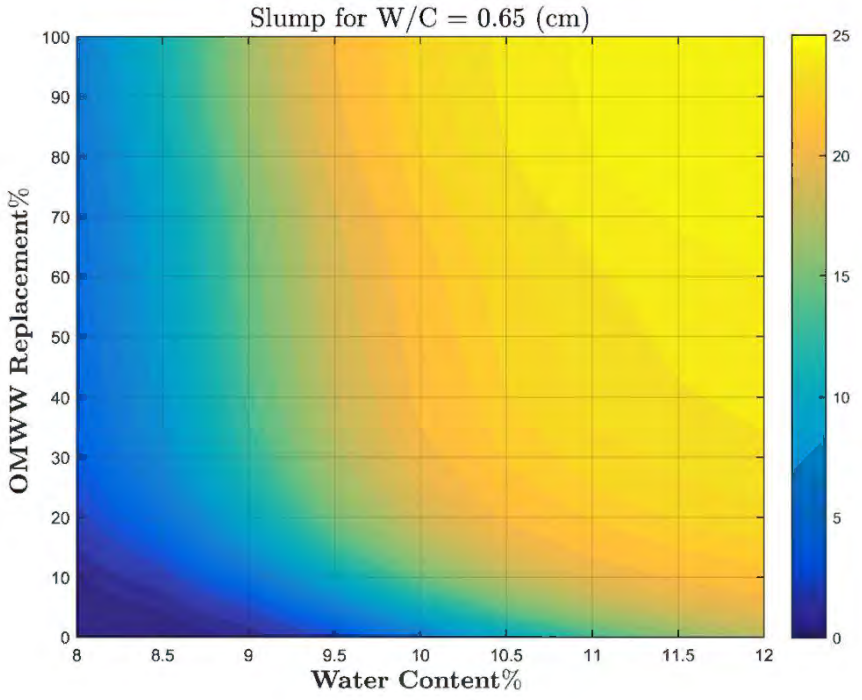
Slump for W/C = 0.65 (cm)
OMWW Replacement%
Water Content%
100
90
80
70
60
50
40
30
20
10
0
8
8.5
9
9.5
10
10.5
11
11.5
12
25
20
15
10
5
0

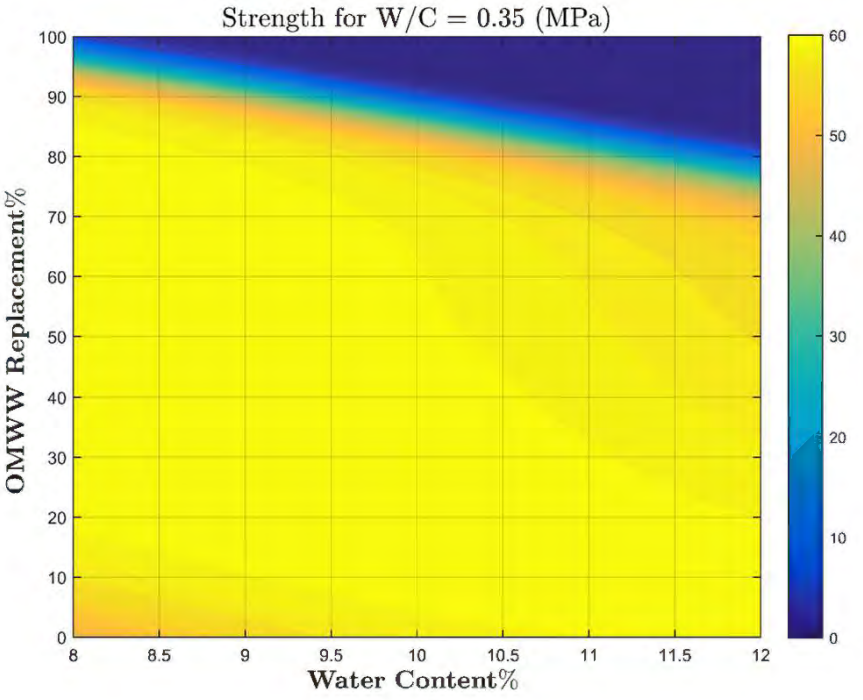
Strength for W/C = 0.35 (MPa)
OMWW Replacement%
Water Content%
100
90
80
70
60
50
40
30
20
10
0
8
8.5
9
9.5
10
10.5
11
11.5
12
60
50
40
30
20
10
0

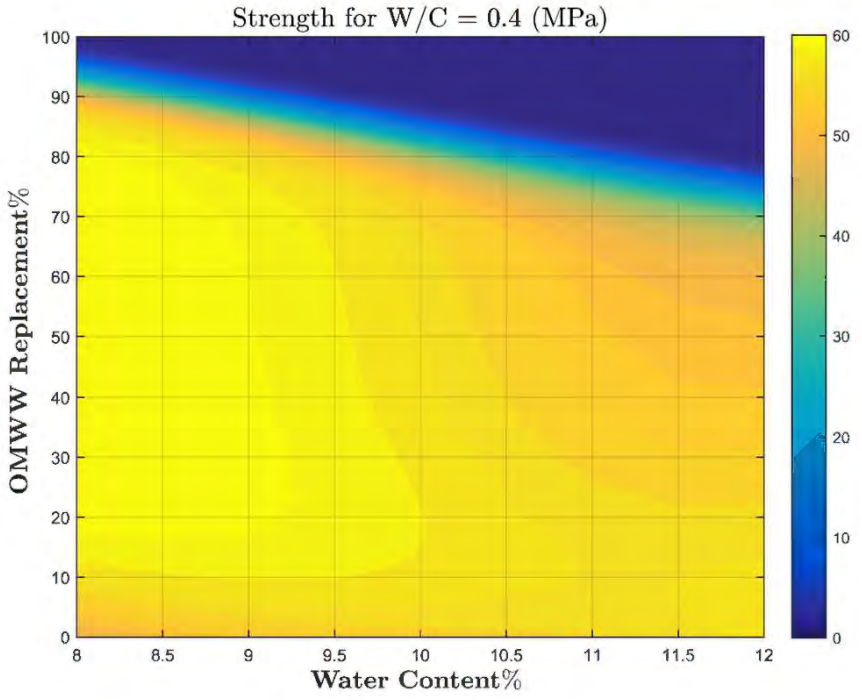
Strength for W/C = 0.4 (MPa)
OMWW Replacement%
Water Content%
100
90
80
70
60
50
40
30
20
10
0
8
8.5
9
9.5
10
10.5
11
11.5
12
60
50
40
30
20
10
0

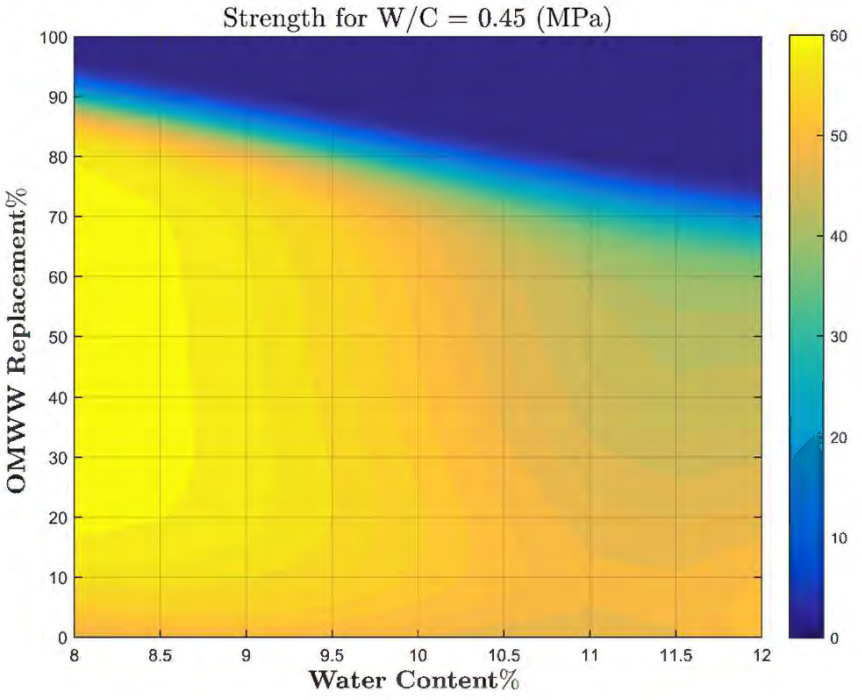
Strength for W/C = 0.45 (MPa)
OMWW Replacement%
Water Content%
100
90
80
70
60
50
40
30
20
10
0
8
8.5
9
9.5
10
10.5
11
11.5
12
60
50
40
30
20
10
0

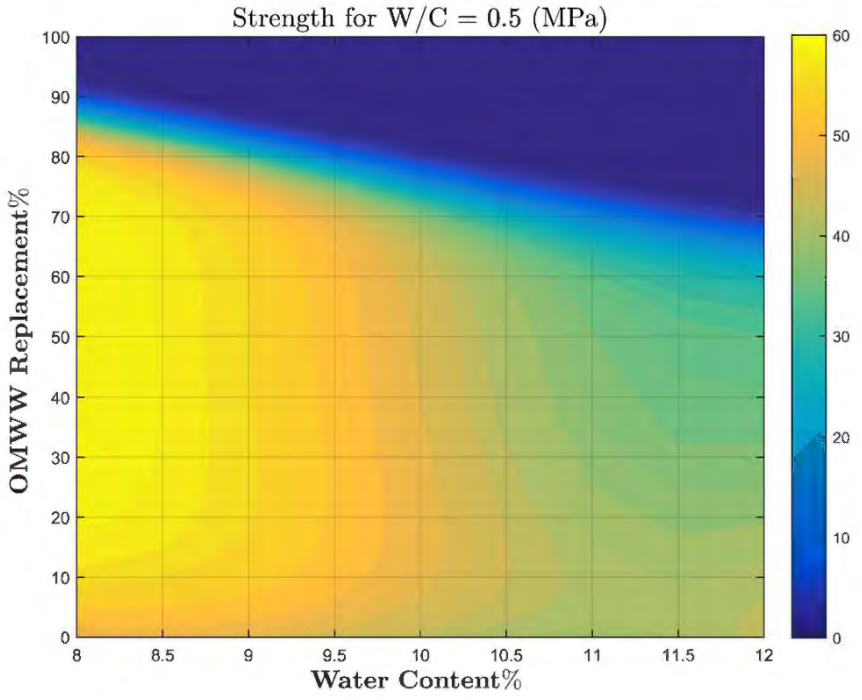
Strength for W/C = 0.5 (MPa)
OMWW Replacement%
Water Content%
100
90
80
70
60
50
40
30
20
10
0
8
8.5
9
9.5
10
10.5
11
11.5
12
60
50
40
30
20
10
0

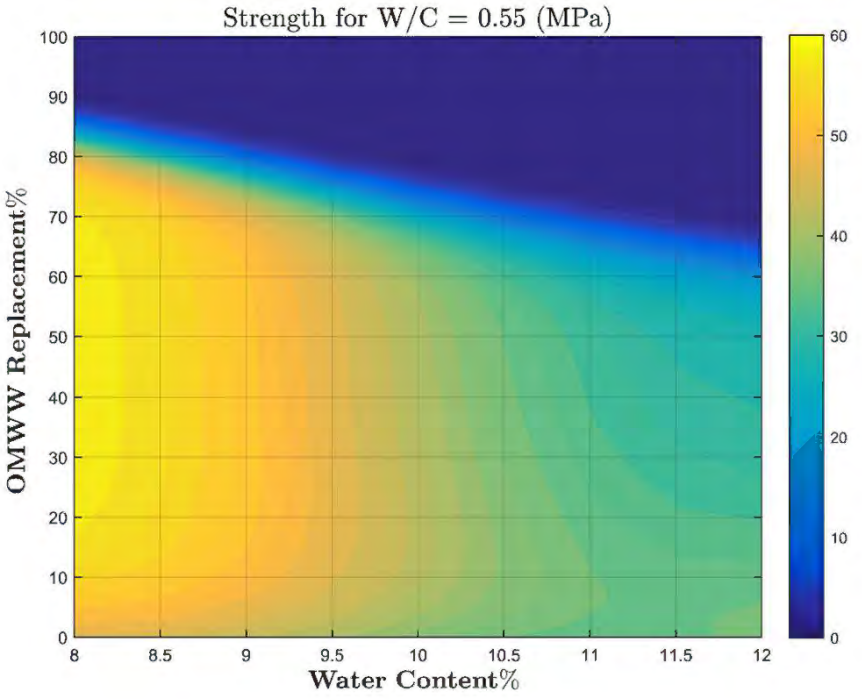
Strength for W/C = 0.55 (MPa)
OMWW Replacement%
Water Content%
100
90
80
70
60
50
40
30
20
10
0
8
8.5
9
9.5
10
10.5
11
11.5
12
60
50
40
30
20
10
0

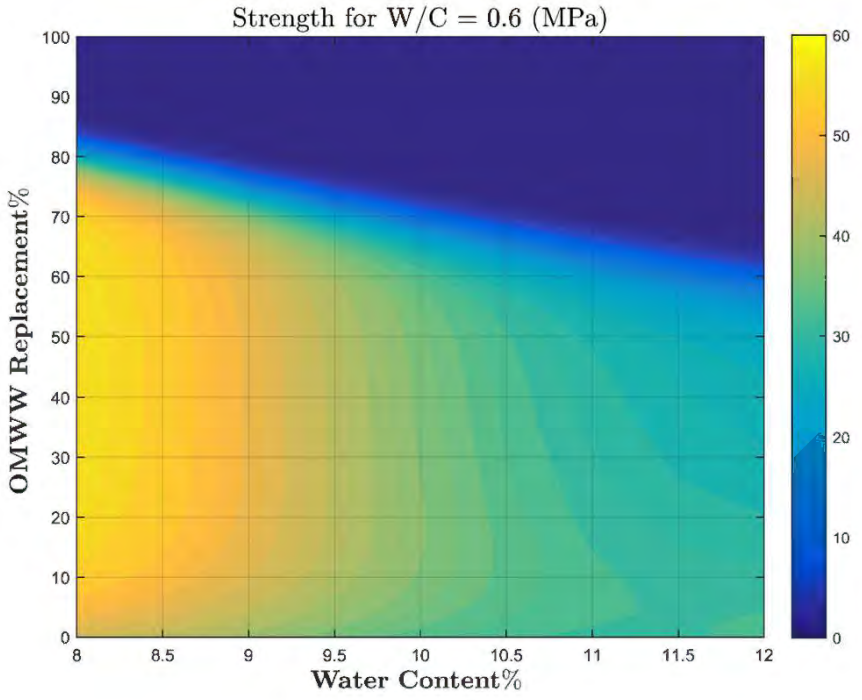
Strength for W/C = 0.6 (MPa)
OMWW Replacement%
Water Content%
100
90
80
70
60
50
40
30
20
10
0
8
8.5
9
9.5
10
10.5
11
11.5
12
60
50
40
30
20
10
0

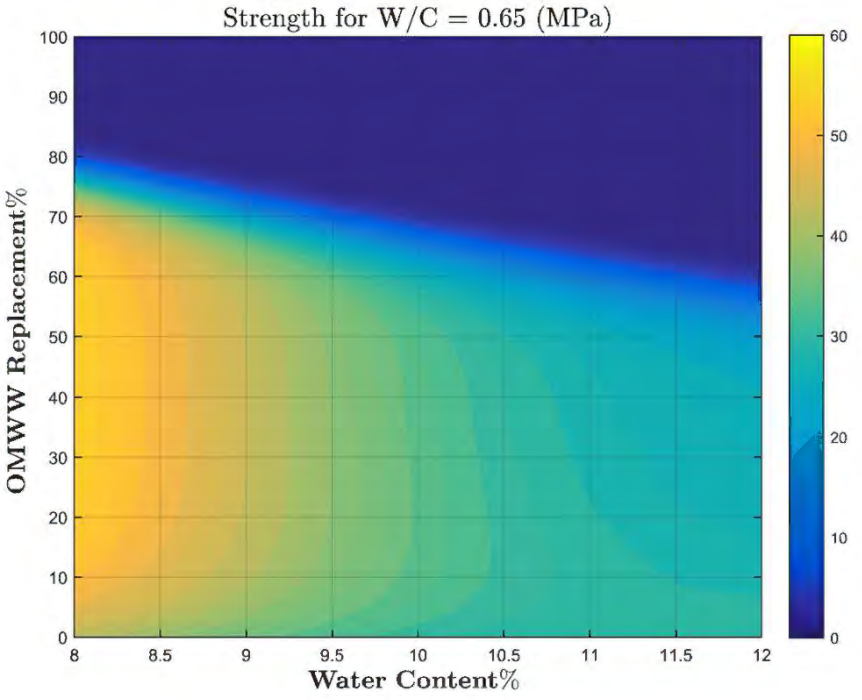
Strength for W/C = 0.65 (MPa)
OMWW Replacement%
Water Content%
100
90
80
70
60
50
40
30
20
10
0
8
8.5
9
9.5
10
10.5
11
11.5
12
60
50
40
30
20
10
0

Appendix A: Water samples test results

Analytical Report

Report Date : 05 June 2023

* Customer : مروان منصور شعيبي

Sample Code	:	ES-20238666
* Source Sample Code	:	
- Sample Name	:	زيبار حديث
Sample Receiving Date	:	20 May 2023
Sampling date	:	
Category	:	Waste Water
Batch No.	:	
Sample Size	:	500 ml
Origin	:	
Prod.Date	:	Exp.Date
Container Type	:	Plastic
Sample Condition	:	ok
* Sampled By	:	مروان منصور شعيبي

Test	Result	Method	Comments
Conductivity	11255 MicroS/cm	StMe	
[A] Potassium (K)	3996.0 ppm	ICP	
Dry matter	5.13 %	StMe	
Organic Content	4.0 %	StMe	
Ash	1.14 %	StMe	
pH	4.66	StMe	
Chloride	1152.29 ppm	HPIC	
Sulfates (SO4)	347.96 ppm	HPIC	
Bromide	Not Detected	HPIC	
Nitrates (NO3)	141.09 ppm	HPIC	
[A] Sodium (Na)	244.4 ppm	ICP	
[NA] Specific Weight	9.95	StMe	
[A] Calcium (Ca)	192.2 ppm	ICP	

Notes: The Center is only responsible for the results of the sample tested.
This report must not be reissued without the written approval of the Center's director

Adi Qamhieh
Director

Senior Analyst,
Environmental Analysis Unit

[NA] Not accredited [S] Subcontractor *IC Informed by clien' [A] Acredited

ISO/IEC 17025:2017

BIRZEIT UNIVERSITY

Testing Laboratories Center

Analytical Report

Report Date : 05 June 2023

Customer : مروان منصور شعيبي

Sample Code	ES-20238666
Source Sample Code	
Sample Name	زيبار حنيث
Sample Receiving Date	20 May 2023
Category	Waste Water
Batch No.	
Sample Size	500 ml
Origin	
Prod.Date	Exp.Date
Container Type	Plastic
Sample Condition	ok
Sampled By	مروان منصور شعيبي

Test	Result	Method	Comments
[A] Magnesium (Mg)	146.3 ppm	ICP	
Phosphate (PO4)	747.4 ppm	StMe	

Notes: The Center is only responsible for the results of the sample tested.
This report must not be reissued without the written approval of the Center's director

Adi Qamhieh
Director

1083411

Senior Analyst,
Environmental Analysis Unit

P.O.Box: 14 BIRZEIT, PALESTINE . PHONE: 972-2-2982010 . FAX: 972-2-2982166
e-mail: bzutl@birzeit.edu

[NA] Not accredited [S] Subcontractor *IC Informed by client [A] Accredited

ISO/IEC 17025:2017

BIRZEIT UNIVERSITY

Testing Laboratories Center

Analytical Report

Report Date : 05 June 2023

* Customer : مروان منصور شعيبي

Sample Code	ES-20238665
* Source Sample Code	
* Sample Name	زيبار قديم
Sample Receiving Date	20 May 2023
Sampling date	
Category	Waste Water
Batch No.	
Sample Size	500 ml
Origin	
Prod.Date	Exp.Date
Container Type	Plastic
Sample Condition	ok
* Sampled By	مروان منصور شعيبي

Test	Result	Method	Comments
Conductivity	11436 MicroS/cm	StMe	
[A] Potassium (K)	4474.0 ppm	ICP	
Dry matter	4.44 %	StMe	
Organic Content	3.36 %	StMe	
Ash	1.08 %	StMe	
pH	4.35	StMe	
Chloride	1046.02 ppm	HPIC	
Sulfates (SO4)	340.62 ppm	HPIC	
Bromide	Not Detected	HPIC	
Nitrates (NO3)	156.92 ppm	HPIC	
[A] Sodium (Na)	208.0 ppm	ICP	
[NA] Specific Weight	9.98	StMe	
[A] Calcium (Ca)	194.0 ppm	ICP	

Notes: The Center is only responsible for the results of the sample tested.
This report must not be reissued without the written approval of the Center's director

Adi Qamhieh
Director

108410

Senior Analyst,
Environmental Analysis Unit

P.O.Box: 14 BIRZEIT, PALESTINE . PHONE: 972-2-2982010 . FAX: 972-2-2982166
e-mail: bzutl@birzeit.edu

[NA] Not accredited [S] Subcontractor *IC Informed by client [A] Acredited

ISO/IEC 17025:2017

BIRZEIT UNIVERSITY

Testing Laboratories Center

Analytical Report

Report Date : 05 June 2023

Customer : مروان منصور شعيبي

Sample Code	ES-20238665
Source Sample Code	
Sample Name	زيبار قديم
Sample Receiving Date	20 May 2023
Category	Waste Water
Batch No.	
Sample Size	500 ml
Origin	
Prod.Date	Exp.Date
Container Type	Plastic
Sample Condition	ok
Sampled By	مروان منصور شعيبي

Test	Result	Method	Comments
[A] Magnesium (Mg)	158.1 ppm	ICP	
Phosphate (PO4)	942.2 ppm	StMe	

Notes: The Center is only responsible for the results of the sample tested.
This report must not be reissued without the written approval of the Center's director

Adi Qamhieh
Director

1083410

Senior Analyst,
Environmental Analysis Unit

P.O.Box: 14 BIRZEIT, PALESTINE . PHONE: 972-2-2982010 . FAX: 972-2-2982166
e-mail: bzutl@birzeit.edu

[NA] Not accredited [S] Subcontractor *IC Informed by client [A] Acredited

ISO/IEC 17025:2017

جامعة بيرزيت
BIRZEIT UNIVERSITY

Testing Laboratories Center

Analytical Report

Report Date : 05 June 2023

- Customer : مروان منصور شعيبي

Sample Code : ES-20238672

- Source Sample Code :
- Sample Name : water

Sample Receiving Date : 20 May 2023

Sampling date :

Category : Water

Batch No. :

Sample Size : 500 ml

Origin :

Exp.Date

Prod.Date :

Container Type : Plastic

Sample Condition : ok

- Sampled By : مروان منصور شعيبي

Test	Result	Method	Comments
Conductivity	460 MicroS/cm	StMe	
[A] Potassium (K)	1.71 ppm	ICP	
pH	7.62	StMe	
Chloride	40.43 ppm	HPIC	
Sulfates (SO4)	17.54 ppm	HPIC	
Bromide	Not Detected	HPIC	
Nitrates (NO3)	5.52 ppm	HPIC	
[A] Sodium (Na)	28.0 ppm	ICP	
[A] Calcium (Ca)	46.1 ppm	ICP	
[A] Magnesium (Mg)	11.9 ppm	ICP	
Phosphate (PO4)	0.21 ppm	StMe	

Testing Laboratories Center BIRZEIT UNIVERSITY

Notes: The Center is only responsible for the results of the sample tested.
This report must not be reissued without the written approval of the Center's director

Adi Qamhieh
Director

1083470

Senior Analyst,
Environmental Analysis Unit

P.O.Box: 14 BIRZEIT, PALESTINE . PHONE: 972-2-2982010 . FAX: 972-2-2982166
e-mail: bzutl@birzeit.edu

[NA] Not accredited [S] Subcontractor *IC Informed by client [A] Acredited

Appendix B: X-ray reports and SEM images

Birzeit_12 samples

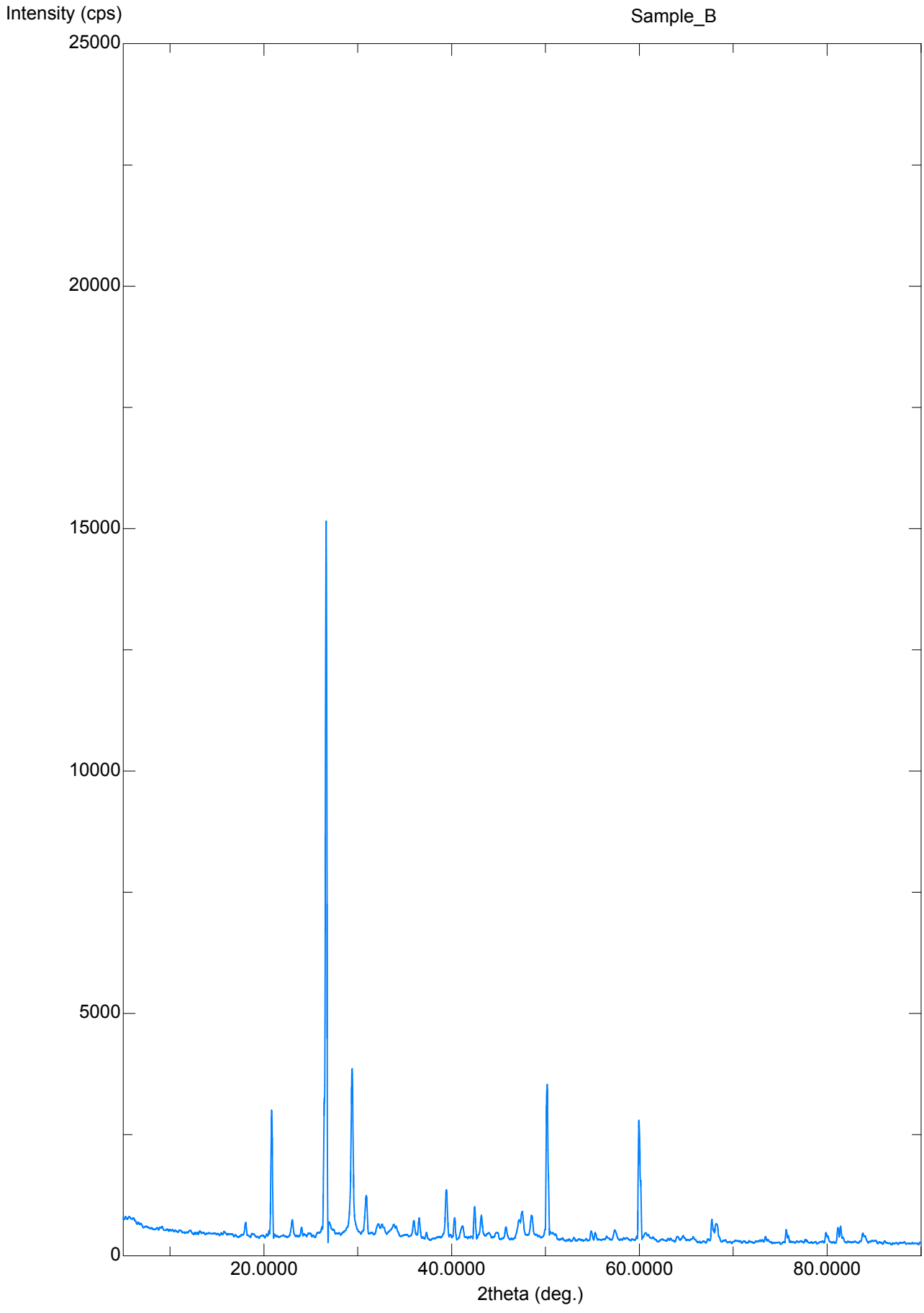

Birzeit_12 samples

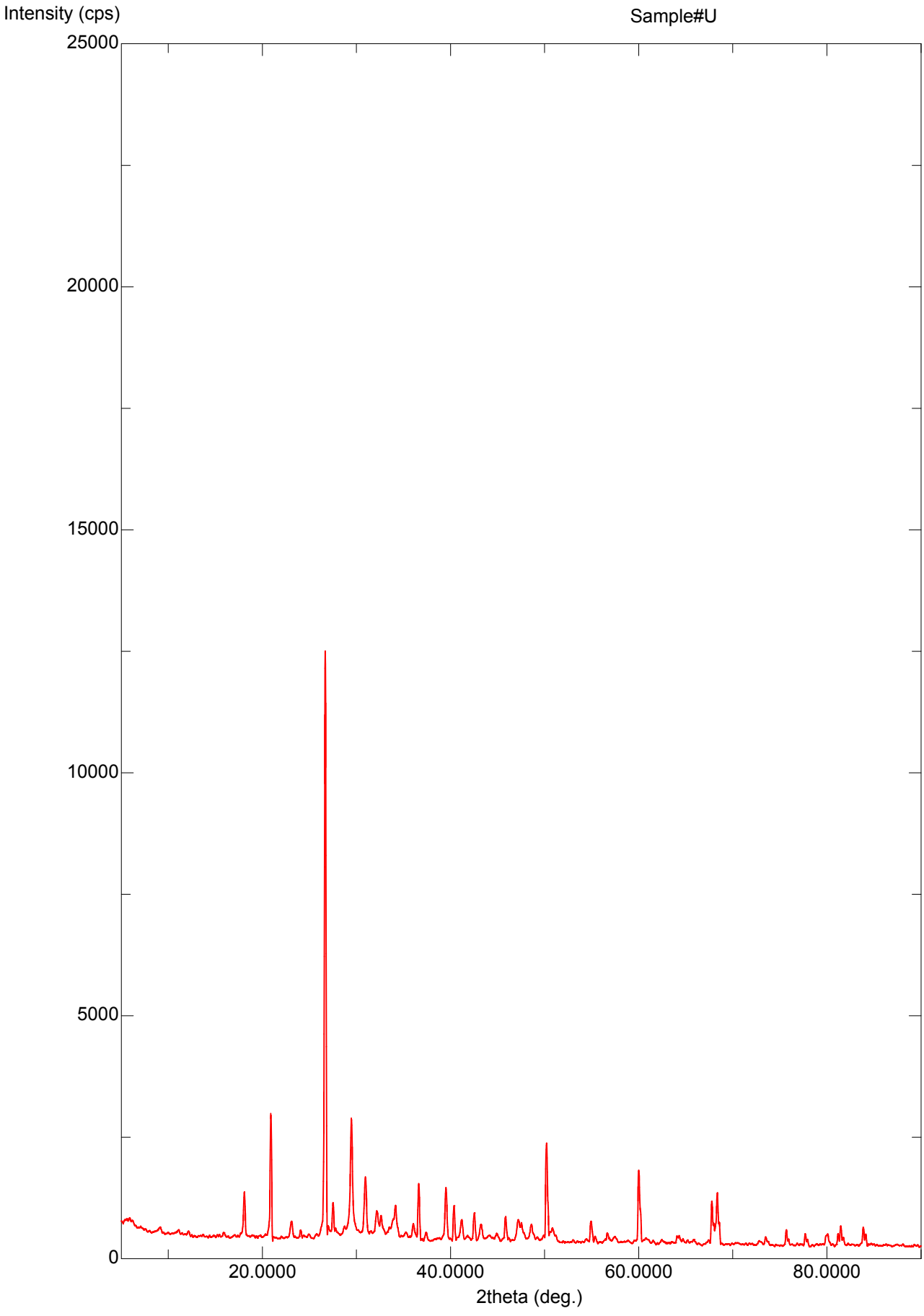

Birzeit_12 samples

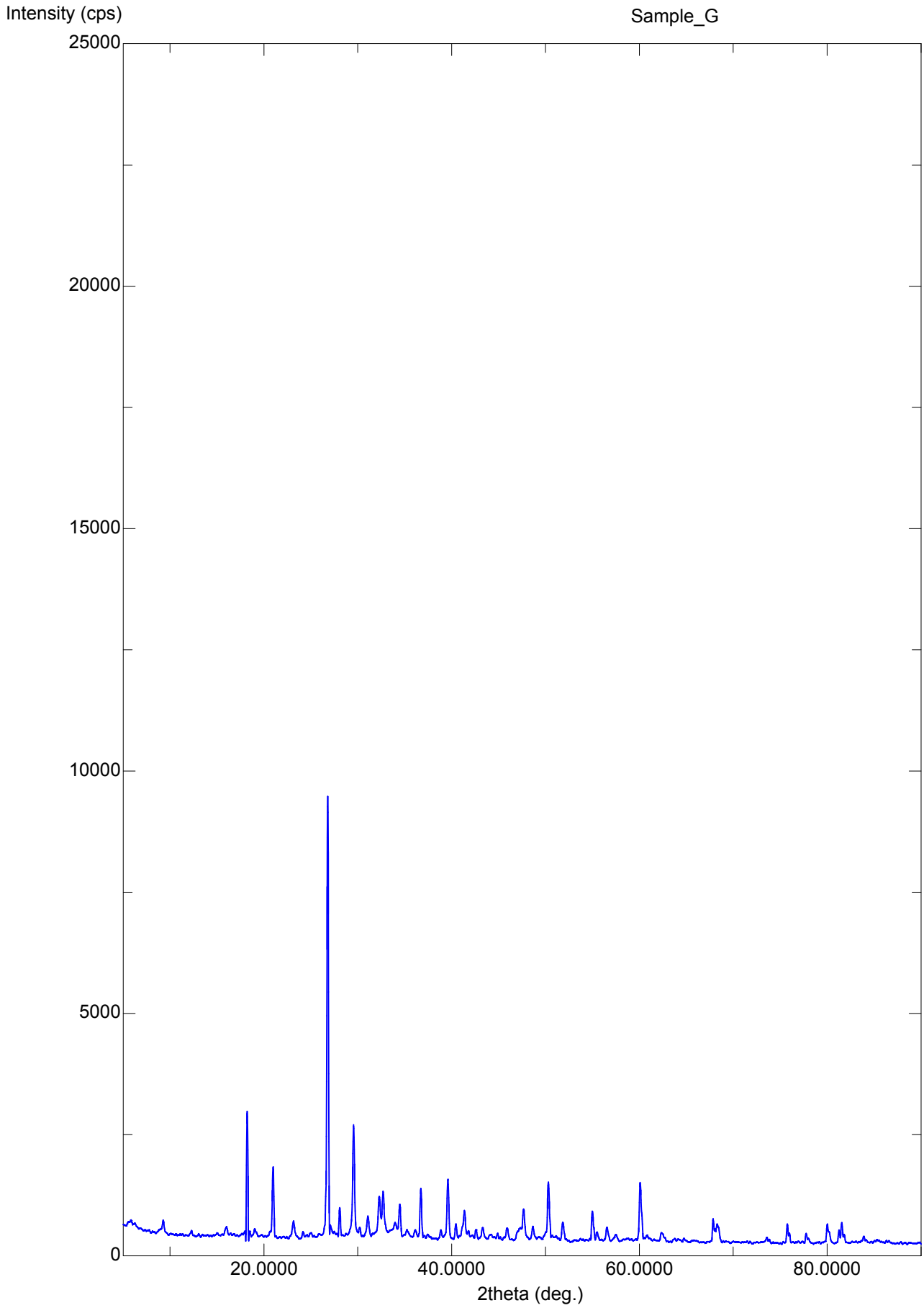

Birzeit_12 samples

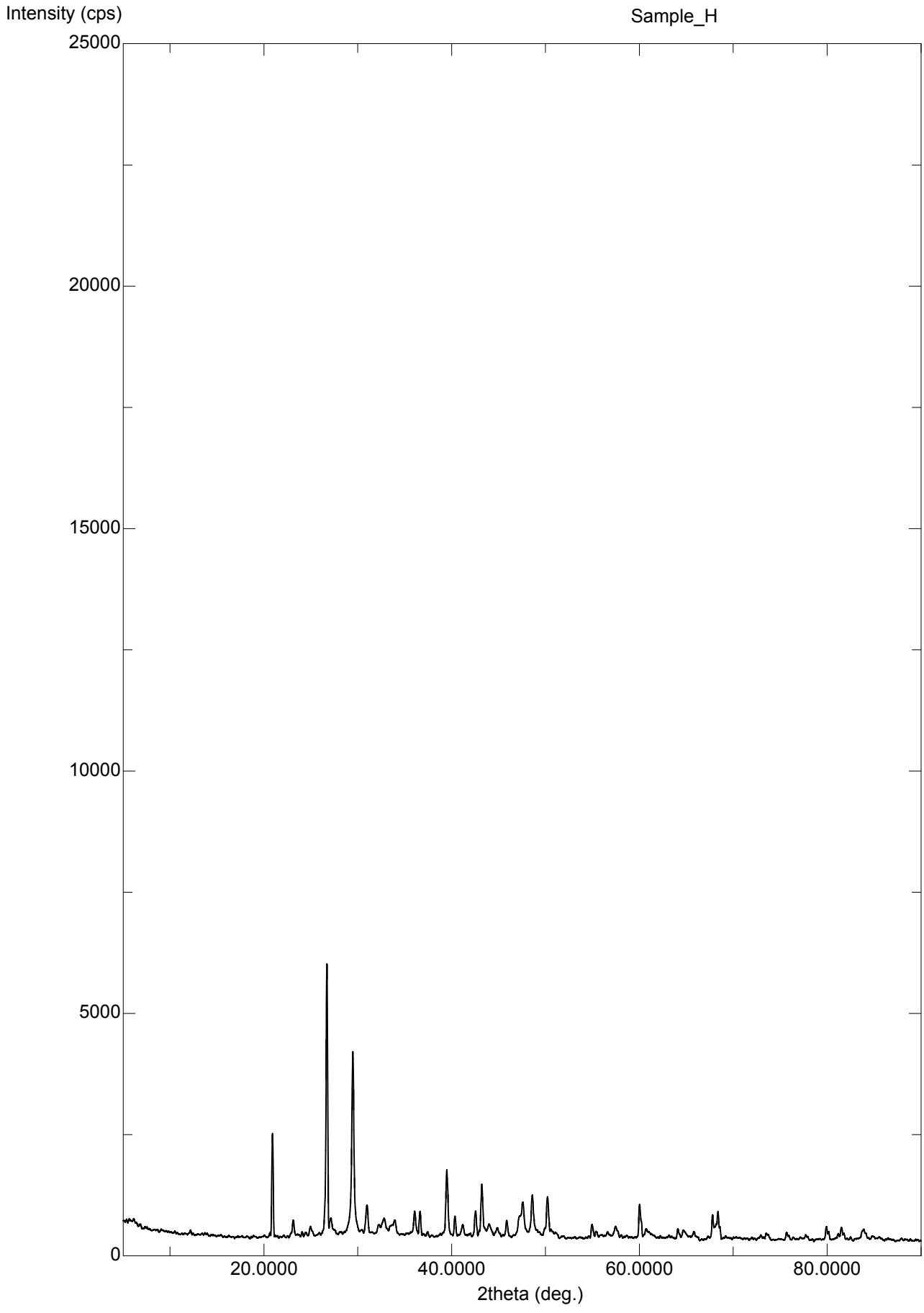

Birzeit_12 samples

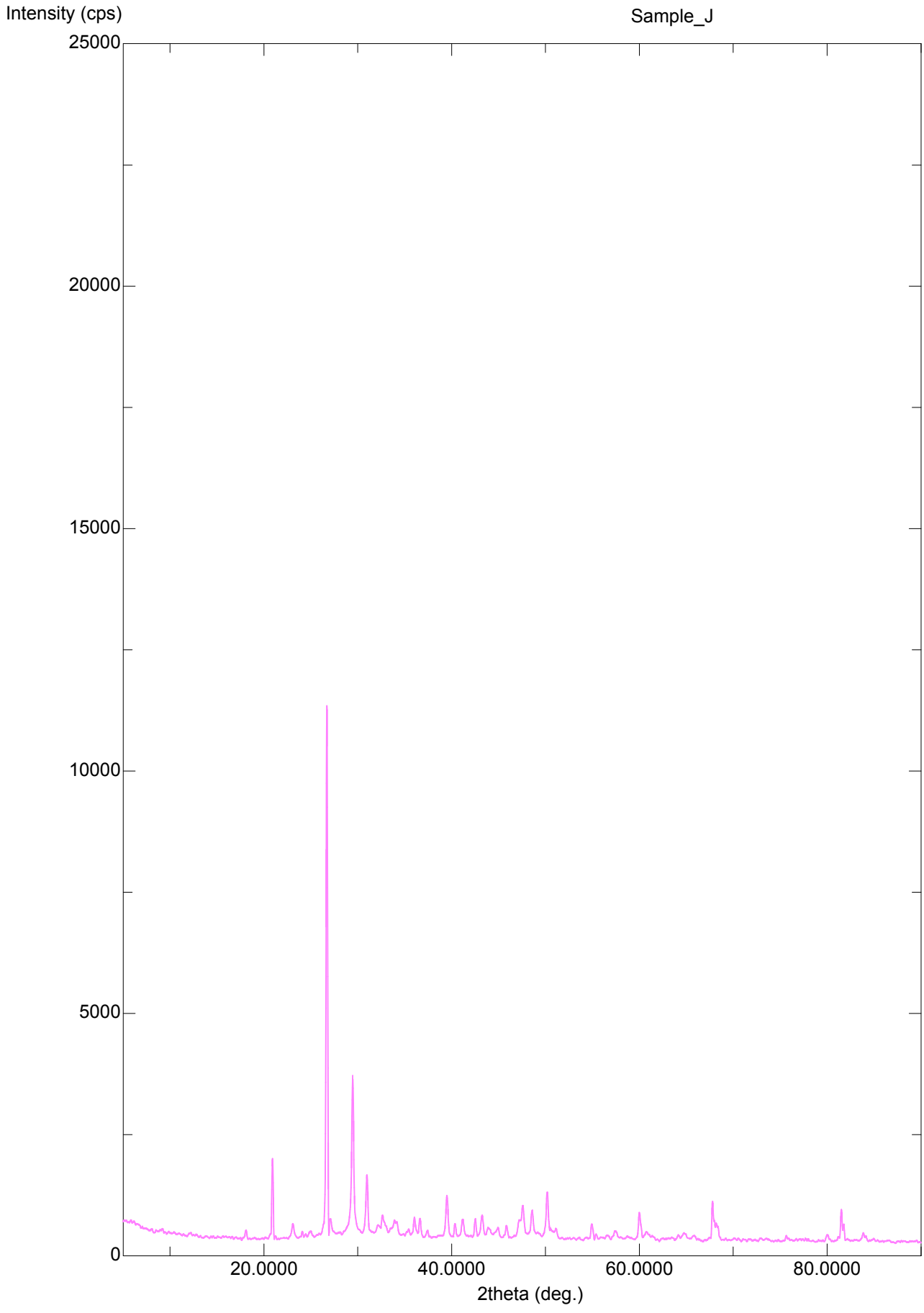

Birzeit_12 samples

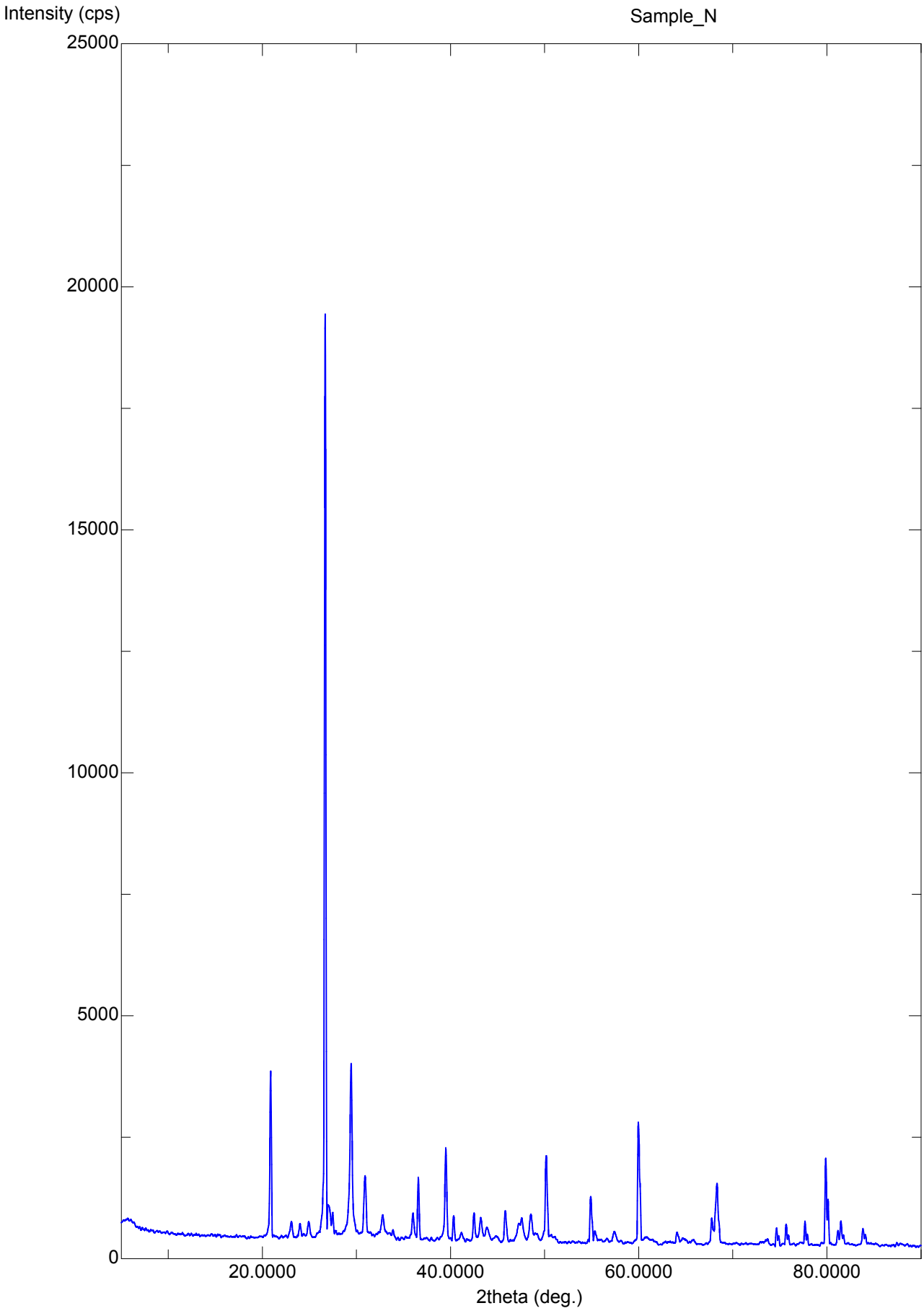

Birzeit_12 samples

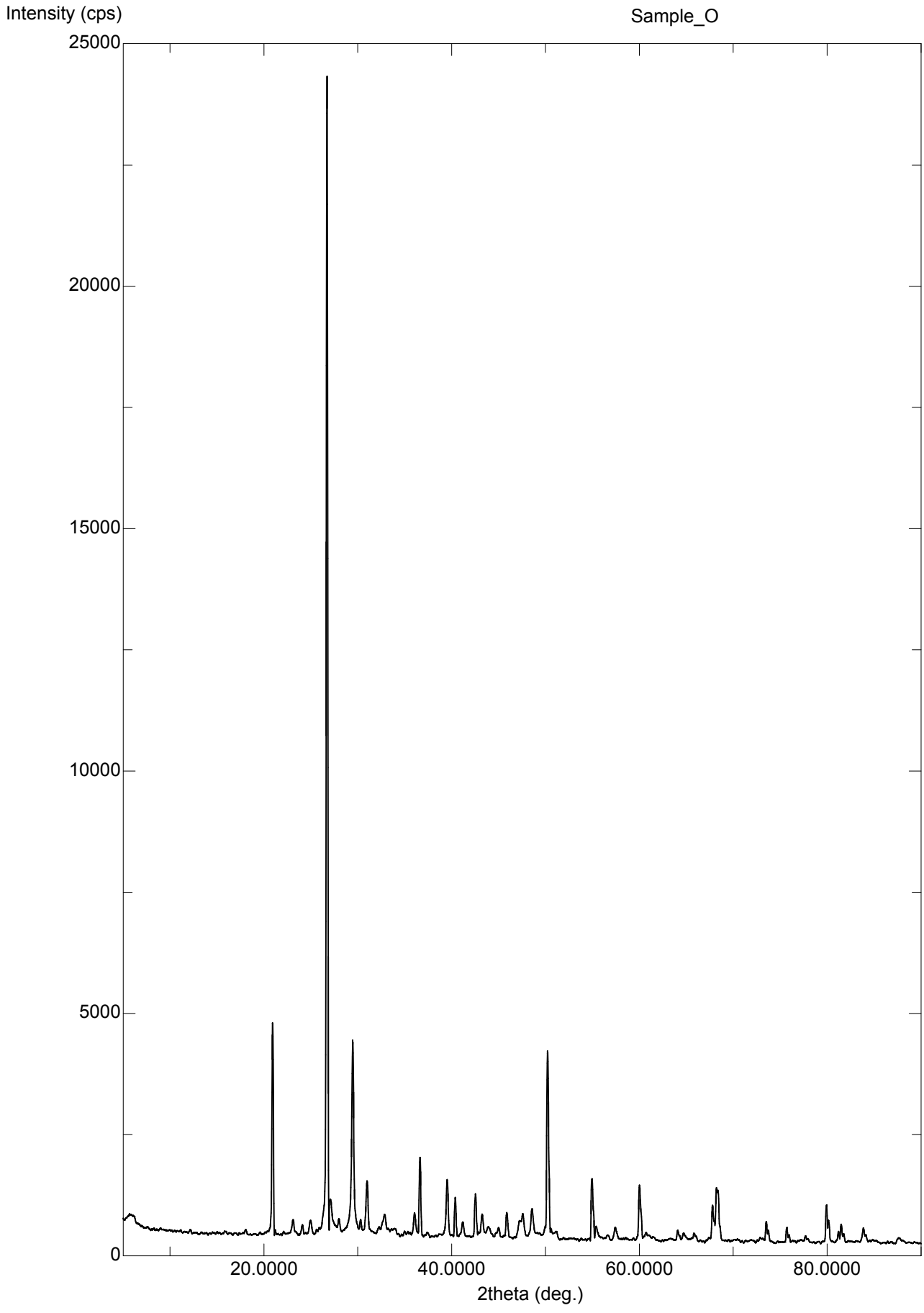

Birzeit_12 samples

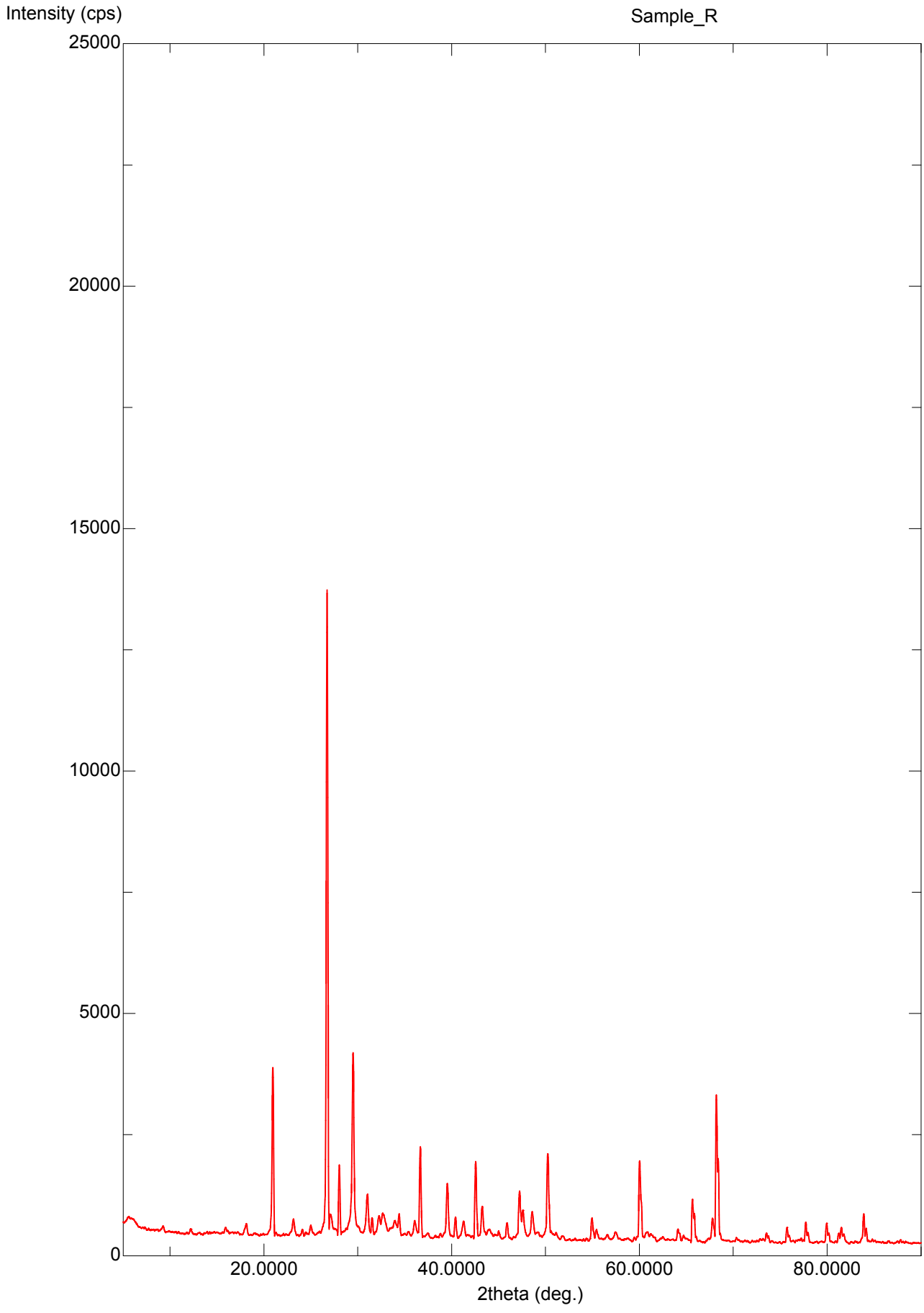

Birzeit_12 samples

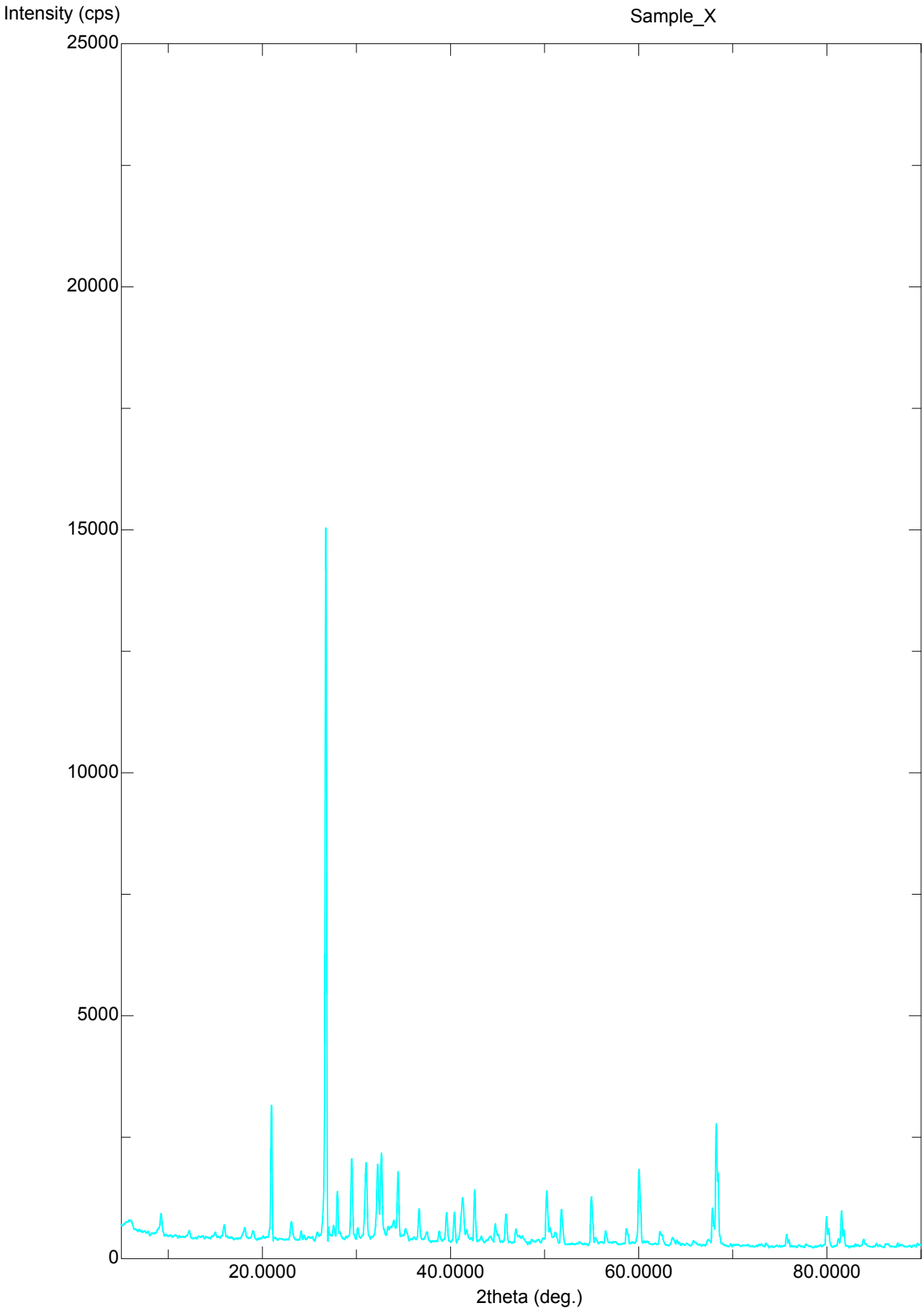

Birzeit_12 samples

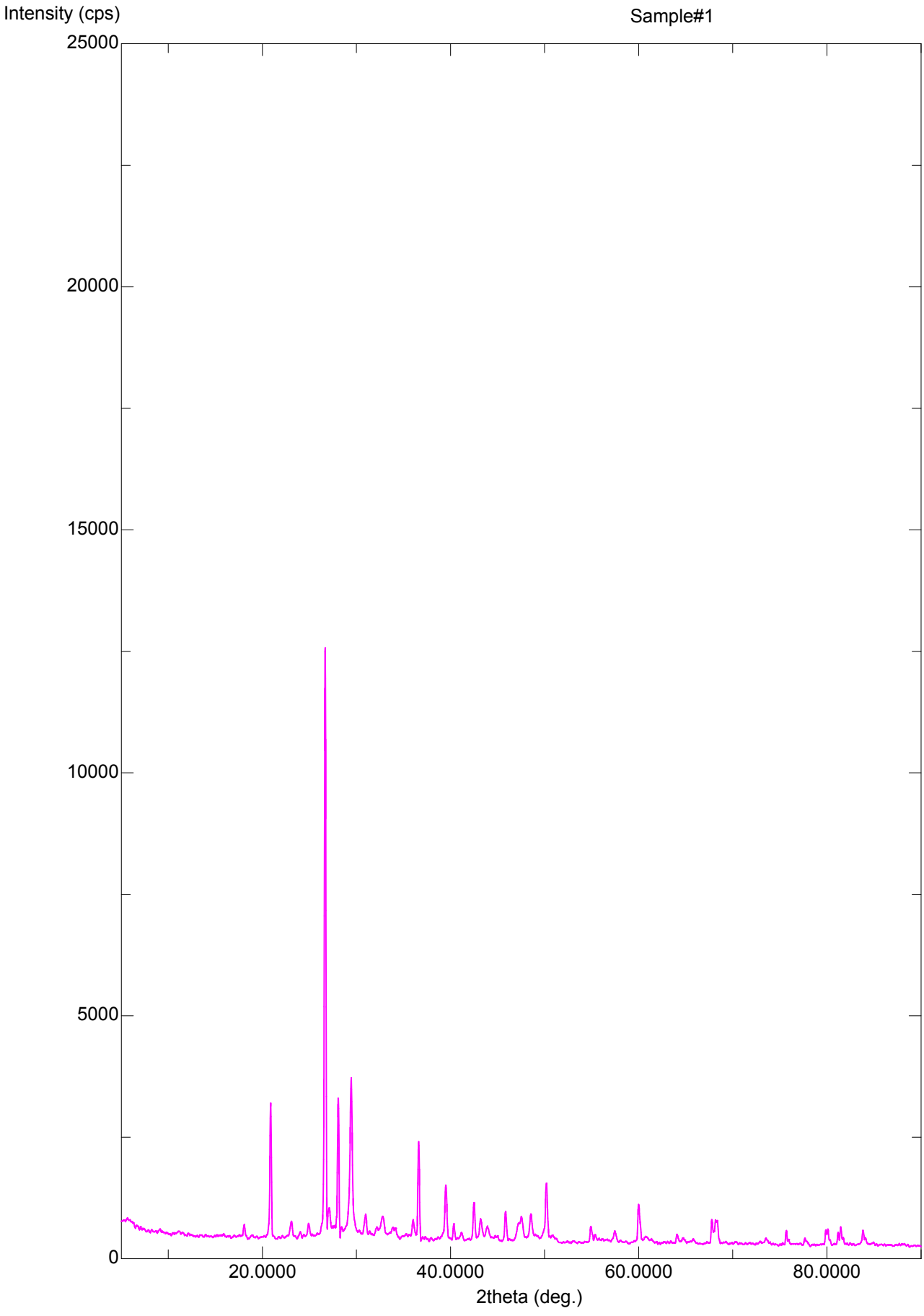

Birzeit_12 samples

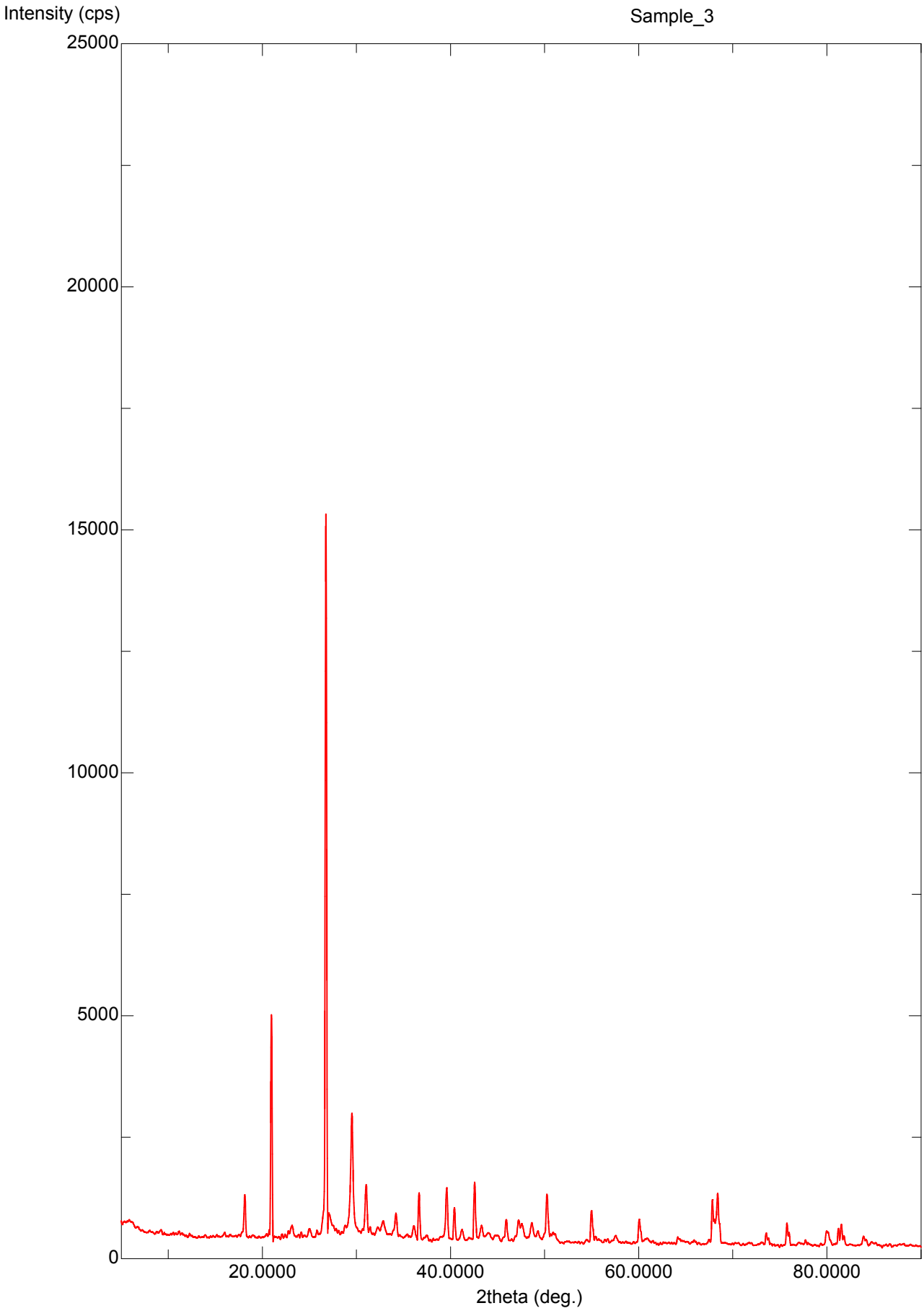

Birzeit_12 samples

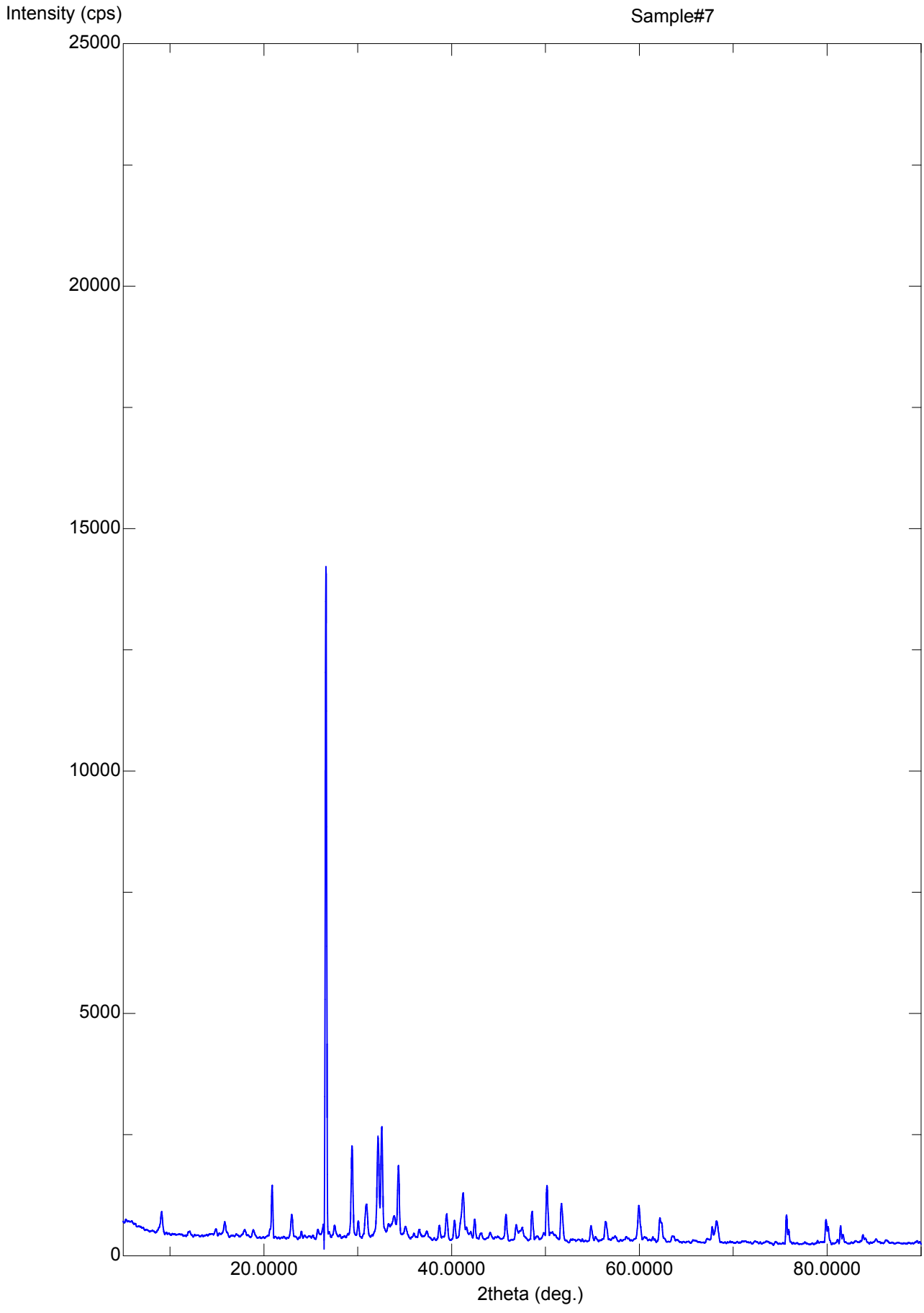

Match! Phase Analysis Report

Sample: Sample#1

Sample Data

File name	Sample#1.raw
File path	G:/.shortcut-targets-by-id/16KlMvpSIqVAUHFFggq9IVgYQzQybBTIu/Marwan - research/Concrete Mix Master Thesis/X-Ray/Birzeit University_XRD_Raw data
Data collected	Jul 13, 2023 07:39:20
Data range	4.980° - 89.980°
Original data range	5.000° - 90.000°
Number of points	4251
Step size	0.020
Rietveld refinement converged	No
Alpha2 subtracted	No
Background subtr.	No
Data smoothed	No
2theta correction	-0.02°
Radiation	X-rays
Wavelength	1.540598 Å

Analysis Results

Phase composition (Weight %)

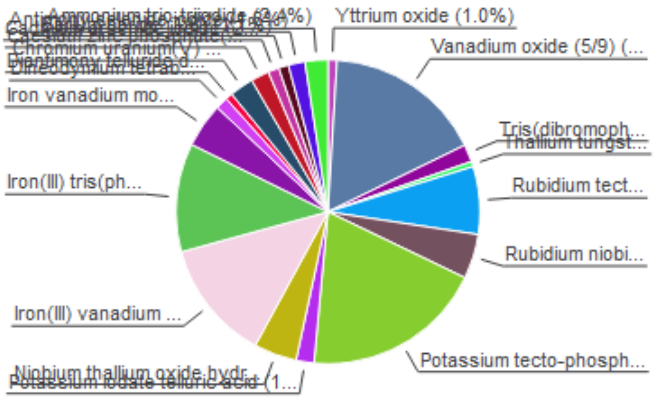

Elemental composition (Weight %)

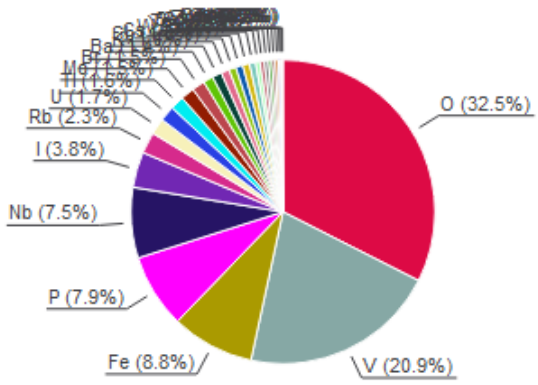

Index	*Amount (%)*	*Name*	*Formula sum*
A	1.0	Yttrium oxide	O3 Y2
B	16.8	Vanadium oxide (5/9)	O9 V5
C	1.9	Tris(dibromophosphazene)	Br6 N3 P3
D	0.5	Thallium tungsten oxide (2/4/13)	O13 Tl2 W4
E	7.2	Rubidium tecto-phosphatodiniobate	Nb2 O8 P Rb
F	4.8	Rubidium niobium tungsten oxide (12/30/3/90)	Nb30 O90 Rb12 W3
G	19.3	Potassium tecto-phosphatovanadate(III) *	K O24 P7 V4
H	1.9	Potassium iodate telluric acid	H6 I K O9 Te
I	4.6	Niobium thallium oxide hydrate (33/10.5/88.5/1.5)	H3 Nb33 O90 Tl10.5
J	12.8	Iron(III) vanadium oxide (6.5/11.5/35)	Fe6.5 O35 V11.5
K	11.5	Iron(III) tris(phosphate) trihydroxide	Fe4 H3 O15 P3
L	4.7	Iron vanadium molybdenum oxide (4/1.98/3.02/20)	Fe4 Mo3.02 O20 V1.98
M	1.3	Dineodymium tetrabarium dicopper oxide	Ba4 Cu2 Nd2 O9
N	0.7	Diantimony telluride diselenide	Sb2 Se2 Te
O	2.6	Chromium uranium(V) oxide	Cr O4 U
P	1.9	Caesium zinc phosphate(V) - I	Cs O4 P Zn
Q	1.2	Cadmium arsenide iodide (2/3/1)	As3 Cd2 I
R	1.1	Barium boride (1/6)	B6 Ba
S	1.8	Antimony selenide iodide	I Sb Se
T	2.4	Ammonium trio-triiodide	H4 I3 N
	0.5	*Unidentified peak area*	

Amounts calculated by RIR (Reference Intensity Ratio) method

Element	*Amount (weight %)*
O	*32.5%(*)*
V	20.9%
Fe	8.8%
P	7.9%
Nb	7.5%
I	3.8%
Rb	2.3%
U	1.7%
Tl	1.6%
Mo	1.5%
Br	1.5%
Ba	1.4%
K	1.1%
Sb	1.0%
Cs	0.9%
W	0.8%
Y	0.7%
Te	0.7%
Se	0.7%
Cd	0.5%
As	0.5%
Zn	0.4%
Cr	0.4%
Nd	0.3%
B	*0.3%(*)*
N	*0.2%(*)*
Cu	0.2%
H	*0.1%(*)*
**LE (sum)*	*33.1%*

Details of identified phases

A: Yttrium oxide (1.0 %)*

Formula sum	O3 Y2
Entry number	96-100-9014
Figure-of-Merit (FoM)	0.601536*
Total number of peaks	80
Peaks in range	80
Peaks matched	11
Intensity scale factor	0.24*
Space group	I a -3
Crystal system	cubic
Unit cell	a= 10.6056 Å
I/Ic	9.22
Calc. density	5.029 g/cm³
Reference	Baldinozzi G., Berar J.-F., Calvarin G., "Rietveld refinement of two-phase Zr-doped Y~2~O~3~", Materials Science Forum **278-281**, 680-685 (1998)

B: Vanadium oxide (5/9) (16.8 %)*

Formula sum	O9 V5
Entry number	96-100-8516
Figure-of-Merit (FoM)	0.607013*
Total number of peaks	497
Peaks in range	497
Peaks matched	142
Intensity scale factor	0.40*
Space group	P -1
Crystal system	triclinic (anorthic)
Unit cell	a= 7.0050 Å b= 8.3629 Å c= 10.9833 Å α= 91.980° β= 108.340 ° γ= 110.390 °
I/Ic	0.88
Calc. density	4.687 g/cm³
Reference	Le Page Y, Bordet P, Marezio M, "Valence ordering in V~5~O~9~ below 120K", Journal of Solid State Chemistry **92**, 380-385 (1991)

C: Tris(dibromophosphazene) (1.9 %)*

Formula sum	Br6 N3 P3
Entry number	96-100-8091
Figure-of-Merit (FoM)	0.607826*
Total number of peaks	500
Peaks in range	500
Peaks matched	136
Intensity scale factor	0.18*
Space group	P n m a
Crystal system	orthorhombic
Unit cell	a= 6.6300 Å b= 13.3600 Å c= 14.4300 Å
I/Ic	3.55
Calc. density	3.192 g/cm³
Reference	de Santis P, Giglio E, Ripamonti A, "The crystal structure of trimeric phosphonitrilic bromide.", Journal of Inorganic and Nuclear Chemistry **24**, 469-474 (1962)

D: Thallium tungsten oxide (2/4/13) (0.5 %)*

Formula sum	O13 Tl2 W4
Entry number	96-100-1081
Figure-of-Merit (FoM)	0.610767*
Total number of peaks	500
Peaks in range	500
Peaks matched	106
Intensity scale factor	0.15*
Space group	P m a b
Crystal system	orthorhombic
Unit cell	a= 7.3270 Å b= 37.8640 Å c= 3.8400 Å
I/Ic	10.10
Calc. density	8.430 g/cm³
Reference	Goreaud M, Labbe P H, Monier J C, Raveau B, "The thallium tungstate Tl~2~ W~4~ O~13~ : A tunnel structure related tothe hexagonal tungsten bronze", Journal of Solid State Chemistry **30**, 311-319 (1979)

E: Rubidium tecto-phosphatodiniobate (7.2 %)*

Formula sum	Nb2 O8 P Rb
Entry number	96-100-1623
Figure-of-Merit (FoM)	0.619709*
Total number of peaks	499
Peaks in range	499
Peaks matched	156
Intensity scale factor	0.43*
Space group	P n m a
Crystal system	orthorhombic
Unit cell	a= 13.8150 Å b= 15.8840 Å c= 12.6750 Å
I/Ic	2.21
Calc. density	4.109 g/cm³
Reference	Leclaire A, Borel M M, Grandin A, Raveau B, "The phosphoniobate RbNb~2~PO~8~: An ordered sbstitution of PO~4~tetrahedra for NbO~6~ octahedra in the HTB structure", Journal of Solid State Chemistry **110**, 256-263 (1994)

F: Rubidium niobium tungsten oxide (12/30/3/90) (4.8 %)*

Formula sum	Nb30 O90 Rb12 W3

Entry number	96-100-1018
Figure-of-Merit (FoM)	0.626444*
Total number of peaks	161
Peaks in range	161
Peaks matched	45
Intensity scale factor	0.56*
Space group	R -3 m
Crystal system	trigonal (hexagonal axes)
Unit cell	a= 7.4860 Å c= 43.1000 Å
I/Ic	4.33
Meas. density	4.570 g/cm³
Calc. density	4.608 g/cm³
Reference	Michel C, Guyomarch A, Raveau B, "Nouveaux echangeurs cationiques avec une structure a tunnelsentrecroises: les oxides A~12~ M~33~ O~90~ et A~12~ M~33~ O~90~(H~2~ O)~12~", Journal of Solid State Chemistry **22**, 393-403 (1977)

G: Potassium tecto-phosphatovanadate(III) * (19.3 %)*

Formula sum	K O24 P7 V4
Entry number	96-100-1565
Figure-of-Merit (FoM)	0.666717*
Total number of peaks	499
Peaks in range	499
Peaks matched	198
Intensity scale factor	0.55*
Space group	P -1
Crystal system	triclinic (anorthic)
Unit cell	a= 10.0846 Å b= 10.2309 Å c= 10.8283 Å α= 112.757° β= 109.226 ° γ= 104.675 °
I/Ic	1.05
Calc. density	3.202 g/cm³
Reference	Benhamada L, Grandin A, Borel M M, Leclaire A, Raveau B, "A vanadium(III) phosphate with V~2~O~10~ octahedral units:KV~4~P~7~O~24~", Journal of Solid State Chemistry **104**, 193-201 (1993)

H: Potassium iodate telluric acid (1.9 %)*

Formula sum	H6 I K O9 Te
Entry number	96-100-8207
Figure-of-Merit (FoM)	0.606531*
Total number of peaks	499
Peaks in range	499
Peaks matched	99
Intensity scale factor	0.25*
Space group	P c 21 n
Crystal system	orthorhombic
Unit cell	a= 14.2200 Å b= 6.6960 Å c= 8.6720 Å
I/Ic	4.76
Calc. density	3.520 g/cm³
Reference	Averbuch-Pouchot M. T., "Crystal Chemistry of Some Addition Compounds of Alkali Iodates withTelluric Acid", Journal of Solid State Chemistry **49**, 368-378 (1983)

I: Niobium thallium oxide hydrate (33/10.5/88.5/1.5) (4.6 %)*

Formula sum	H3 Nb33 O90 Tl10.5
Entry number	96-100-1006
Figure-of-Merit (FoM)	0.663422*
Total number of peaks	161
Peaks in range	161
Peaks matched	50
Intensity scale factor	0.58*
Space group	R -3 m
Crystal system	trigonal (hexagonal axes)
Unit cell	a= 7.5100 Å c= 43.2900 Å
I/Ic	4.67
Calc. density	5.263 g/cm³
Reference	Gasperin M, "Synthese d'une nouvelle famille d'oxydes doubles: A~8~^+^ B~22~^5+^O~59~ structure du compose a thallium et niobium", Acta Crystallographica B (24,1968-38,1982) **33**, 398-402 (1977)

J: Iron(III) vanadium oxide (6.5/11.5/35) (12.8 %)*

Formula sum	Fe6.5 O35 V11.5
Entry number	96-100-8122
Figure-of-Merit (FoM)	0.610922*
Total number of peaks	500
Peaks in range	500
Peaks matched	163
Intensity scale factor	0.40*
Space group	P -1
Crystal system	triclinic (anorthic)
Unit cell	a= 10.2090 Å b= 9.3870 Å c= 6.5640 Å α= 100.520° β= 94.350 ° γ= 98.850 °
I/Ic	1.14
Calc. density	4.123 g/cm³
Reference	Grey I E, Anne M, Collomb A, Muller J, Marezio M, "The Crystal Structure of a New Mixed Oxide of Iron and Vanadium, (FeV)~18~ O~35~", Journal of Solid State Chemistry **37**, 219-227 (1981)

K: Iron(III) tris(phosphate) trihydroxide (11.5 %)*

Formula sum	Fe4 H3 O15 P3
Entry number	96-100-8554
Figure-of-Merit (FoM)	0.617374*
Total number of peaks	291
Peaks in range	291
Peaks matched	74
Intensity scale factor	0.41*
Space group	C 1 2/c 1
Crystal system	monoclinic
Unit cell	a= 19.5800 Å b= 7.3880 Å c= 7.4510 Å β= 102.320 º
I/Ic	1.30
Calc. density	3.528 g/cm³
Reference	Malaman M, Ijjaali M, Venturini G, Gleitzer C, Soubeyroux J L, "Neutron diffraction study of Fe~4~(PO~4~)~3~(OH)~3~: occurrence offerromagnetic Fe~2~O~9~ clusters", European Journal of Solid State Inorganic Chemistry **28**, 519-531 (1991)

L: Iron vanadium molybdenum oxide (4/1.98/3.02/20) (4.7 %)*

Formula sum	Fe4 Mo3.02 O20 V1.98
Entry number	96-100-0124
Figure-of-Merit (FoM)	0.647073*
Total number of peaks	462
Peaks in range	462
Peaks matched	100
Intensity scale factor	0.37*
Space group	P 41 2 2
Crystal system	tetragonal
Unit cell	a= 9.5390 Å c= 17.1411 Å
I/Ic	2.88
Calc. density	3.977 g/cm³
Reference	Laligant Y, Permer L, Le Bail A, "Crystal structure of Fe4 V2 Mo3 O20 determined from conventional X-raypowder diffraction data", European Journal of Solid State Inorganic Chemistry **32**, 325-334 (1995)

M: Dineodymium tetrabarium dicopper oxide (1.3 %)*

Formula sum	Ba4 Cu2 Nd2 O9
Entry number	96-100-1570
Figure-of-Merit (FoM)	0.620548*
Total number of peaks	349
Peaks in range	349
Peaks matched	36
Intensity scale factor	0.32*
Space group	P -4 n 2
Crystal system	tetragonal
Unit cell	a= 12.0717 Å c= 3.8737 Å
I/Ic	8.81
Calc. density	6.523 g/cm³
Reference	Domenges B, Abbattista F, Michel C, Vallino M, Barbey L, Nguyen N, Raveau B, "A one-dimensional cuprate closely related to the "0212"-structure:Nd~2~Ba~4~Cu~2~O~9~", Journal of Solid State Chemistry **106**, 271-281 (1993)

N: Diantimony telluride diselenide (0.7 %)*

Formula sum	Sb2 Se2 Te
Entry number	96-100-8845
Figure-of-Merit (FoM)	0.610288*
Total number of peaks	151
Peaks in range	151
Peaks matched	16
Intensity scale factor	0.27*
Space group	R 3 m
Crystal system	trigonal (hexagonal axes)
Unit cell	a= 4.1120 Å c= 29.4950 Å
I/Ic	13.25
Meas. density	6.100 g/cm³
Calc. density	6.101 g/cm³
Reference	Andriamihaja A, Ibanez A, Jumas J C, Olivier-Fourcade J, Philippot E, "Evolution structurale de la solution solide Sb2 Te(3-x) Se(x) (O < X <2) dans le systeme Sb2 Te3 - Sb2 Se3", Revue de Chimie Minerale **22**, 357-368 (1985)

O: Chromium uranium(V) oxide (2.6 %)*

Formula sum	Cr O4 U
Entry number	96-100-8068
Figure-of-Merit (FoM)	0.612517*
Total number of peaks	338
Peaks in range	338
Peaks matched	28
Intensity scale factor	0.90*
Space group	P b c n
Crystal system	orthorhombic
Unit cell	a= 4.8710 Å b= 11.7870 Å c= 5.0530 Å
I/Ic	12.96
Calc. density	8.105 g/cm³
Reference	Bacmann M, Bertaut E F, "Structure de U Cr O~4~", Bulletin de la Societe Francaise de Mineralogie et de Cristallographie(72,1949-100,1977) **87**, 275-276 (1964)

P: Caesium zinc phosphate(V) -

I (1.9 %) *

Formula sum	Cs O4 P Zn
Entry number	96-100-7239
Figure-of-Merit (FoM)	0.615465 *
Total number of peaks	497
Peaks in range	497
Peaks matched	57
Intensity scale factor	0.27 *
Space group	P n m a
Crystal system	orthorhombic
Unit cell	a= 9.1940 Å b= 5.4900 Å c= 9.3880 Å
I/Ic	5.09
Calc. density	4.110 g/cm³
Reference	Blum D, Durif A, Averbuch-Pouchot M T, "Crystal structures of the three forms of Cs Zn P O4", Ferroelectrics **69**, 283-292 (1986)

Q: Cadmium arsenide iodide (2/3/1) (1.2 %) *

Formula sum	As3 Cd2 I
Entry number	96-100-1838
Figure-of-Merit (FoM)	0.600122 *
Total number of peaks	286
Peaks in range	286
Peaks matched	74
Intensity scale factor	0.21 *
Space group	C 1 c 1
Crystal system	monoclinic
Unit cell	a= 8.4360 Å b= 9.5940 Å c= 7.9520 Å β= 100.650 º
I/Ic	6.49
Calc. density	6.053 g/cm³
Reference	Rebbah A, Leclaire A, Yazbeck J, Deschanvres A, "Structure de l'iodure de cadmium et d'arsenic Cd2 As3 I", Acta Crystallographica B (24,1968-38,1982) **35**, 2197-2199 (1979)

R: Barium boride (1/6) (1.1 %) *

Formula sum	B6 Ba
Entry number	96-100-9053
Figure-of-Merit (FoM)	0.600998 *
Total number of peaks	26
Peaks in range	26
Peaks matched	7
Intensity scale factor	0.28 *
Space group	P m -3 m
Crystal system	cubic
Unit cell	a= 4.2680 Å
I/Ic	9.67
Calc. density	4.318 g/cm³
Reference	Bertaut F, Blum P, "Etude de hexaborures et de la substition alcaline", Comptes Rendus Hebdomadaires des Seances de l'Academie des Sciences(1884 - 1965) **234**, 2621-2623 (1952)

S: Antimony selenide iodide (1.8 %) *

Formula sum	I Sb Se
Entry number	96-100-8205
Figure-of-Merit (FoM)	0.658651 *
Total number of peaks	494
Peaks in range	494
Peaks matched	39
Intensity scale factor	0.37 *
Space group	P n m a
Crystal system	orthorhombic
Unit cell	a= 8.6980 Å b= 4.1270 Å c= 10.4120 Å
I/Ic	7.57
Calc. density	5.822 g/cm³
Reference	Ibanez A, Jumas J C, Olivier-Fourcade J, Philippot E, Maurin M, "Sur les Chalcogeno-iodures d'antimoine SbXI (X=S,Se,Te):Structures etspectroscopie Moessbauer de ^121^Sb", Journal of Solid State Chemistry **48**, 272-283 (1983)

T: Ammonium trio-triiodide (2.4 %) *

Formula sum	H4 I3 N
Entry number	96-101-0244
Figure-of-Merit (FoM)	0.600372 *
Total number of peaks	499
Peaks in range	499
Peaks matched	68
Intensity scale factor	0.36 *
Space group	P m c n
Crystal system	orthorhombic
Unit cell	a= 6.6400 Å b= 9.6600 Å c= 10.8200 Å
I/Ic	5.53
Meas. density	3.750 g/cm³
Calc. density	3.777 g/cm³
Reference	Mooney R C L, "The Configuration of the Triiodide Group in Ammonium Triiodide Crystals.", Zeitschrift fuer Kristallographie, Kristallgeometrie, Kristallphysik,Kristallchemie (-144,1977) **90**, 143-150 (1935)

(*)2theta values have been shifted internally for the calculation of the amounts, the intensity scaling factors as well as the figure-of-merit (FoM), due to the active search-match option 'Automatic zero point adaption'.

Search-Match

Settings

Reference database used	COD-Inorg 2023.06.06
Automatic zeropoint adaptation	Yes
Downgrade entries with low scaling factors	Yes
Minimum figure-of-merit (FoM)	0.60
2theta window for peak corr.	0.30 deg.
Minimum rel. int. for peak corr.	0
Parameter/influence 2theta	0.50
Parameter/influence intensities	0.50
Parameter multiple/single phase(s)	0.50

Peak List

No.	*2theta [°]*	*d [Å]*	*I/I0 (peak height)*	*Counts (peak area)*	*FWHM*	*Matched*
1	18.06	4.9079	19.65	13.70	0.1200	B,C,E,G,H,L,N,T
2	20.86	4.2550	215.25	200.11	0.1600	C,E,G,H,L,M,P,R
3	23.08	3.8505	23.80	22.13	0.1600	B,C,D,E,G,H,J,L,M,O,S,T
4	24.90	3.5730	19.77	22.98	0.2000	B,C,D,E,F,G,H,I,N,Q,T
5	26.66	3.3410	1000.00	929.64	0.1600	B,C,D,E,F,G,H,I,J,K,L,M,O,P,S,T
6	27.08	3.2901	28.38	46.17	0.2800	B,C,D,E,G,H,K,L,N,P
7	28.04	3.1796	224.15	104.19	0.0800	B,C,D,E,F,G,H,J,K,L,N,T
8	28.42	3.1380	14.37	10.02	0.1200	C,D,E,G,I,J,K,L,M,Q
9	29.42	3.0335	232.72	270.43	0.2000	A,B,C,E,F,G,H,I,J,K,L,M,N,O,Q,R,S,T
10	30.96	2.8861	32.61	37.90	0.2000	B,C,D,E,F,G,H,I,J,K,L,M,P,S,T
11	32.14	2.7828	14.00	16.27	0.2000	B,D,E,F,G,I,J,K,L,M,Q,S,T
12	32.78	2.7299	29.84	55.47	0.3200	B,C,E,G,H,J,L,M,N,P,Q,S,T
13	33.84	2.6467	13.77	6.40	0.0800	A,C,D,E,G,H,J,K,L,Q,S,T
14	34.12	2.6257	14.50	10.11	0.1200	B,C,D,E,G,H,K,L,O,P,Q,T
15	35.98	2.4941	24.44	28.40	0.2000	A,B,C,D,E,F,G,H,I,J,S,T
16	36.58	2.4545	149.19	104.02	0.1200	B,C,D,E,F,G,H,I,J,K,L,N,O,Q,R,T
17	39.48	2.2807	78.66	109.69	0.2400	B,C,D,E,F,G,H,I,J,K,L,M,N,P,Q,S
18	40.32	2.2351	19.96	13.92	0.1200	B,C,D,E,F,G,H,I,J,K,L,M,O,P,S,T
19	42.46	2.1272	54.17	50.35	0.1600	B,C,D,E,F,G,H,I,J,L,M,O,P,R,S,T
20	43.18	2.0934	27.21	31.62	0.2000	A,B,C,D,E,G,H,I,J,K,L,O,P,Q,T
21	43.96	2.0581	15.82	11.03	0.1200	B,C,D,E,F,G,H,I,J,K,L,M,N,O,P,Q,S,T
22	45.82	1.9788	42.51	19.76	0.0800	B,C,D,E,F,G,H,I,J,K,L,M,Q,S,T
23	47.52	1.9119	32.02	52.10	0.2800	B,C,D,E,F,G,H,J,K,L,M,N,O,Q,R,S,T
24	48.52	1.8748	36.31	59.07	0.2800	A,B,C,D,E,F,G,I,J,K,L,M,O,P,Q,S
25	50.16	1.8172	88.94	62.01	0.1200	A,B,C,D,E,F,G,H,I,J,K,L,M,N,Q,S,T
26	54.88	1.6716	24.06	11.18	0.0800	A,B,C,D,E,F,G,H,I,J,K,L,M,P,Q,S
27	55.34	1.6588	11.41	7.96	0.1200	B,C,D,E,F,G,H,I,J,K,L,M,P,Q,S,T
28	57.42	1.6035	15.63	18.16	0.2000	A,B,C,D,E,F,G,H,I,J,K,L,M,N,O,P,Q,S,T
29	59.96	1.5415	59.31	41.35	0.1200	B,C,D,E,G,H,I,J,K,L,M,O,P,Q,S,T
30	67.76	1.3818	40.14	27.99	0.1200	B,C,D,F,H,I,J,K,L,M,P,Q,S,T
31	67.94	1.3786	18.97	17.63	0.1600	C,H,I,J,K,L,P,Q
32	68.16	1.3747	36.31	33.76	0.1600	B,C,H,J,K,L,O,P,S
33	68.32	1.3718	31.19	28.99	0.1600	B,C,D,F,H,I,J,K,L,M,O,P,S,T
34	73.50	1.2874	9.11	2.12	0.0400	A,C,D,F,H,I,K,L,M,O,P,Q,R,S,T
35	75.66	1.2559	22.01	10.23	0.0800	C,D,H,I,K,L,M,N,O,P,Q,T
36	80.08	1.1974	24.35	11.32	0.0800	A,C,D,H,L,O,P,Q,S,T
37	81.18	1.1839	19.70	13.73	0.1200	A,C,D,H,L,M,N,P,Q,R,S,T
38	81.46	1.1805	24.83	23.08	0.1600	C,D,H,L,M,N,O,P,Q,S,T
39	83.84	1.1530	21.71	20.18	0.1600	C,D,H,L,M,N,Q,S,T
40	84.06	1.1505	9.00	4.18	0.0800	C,D,H,L,M,O,P,Q,S,T

Integrated Profile Areas

Based on calculated profile

Profile area	***Counts***	***Amount***
Overall diffraction profile	654438	100.00%
Background radiation	459300	70.18%
Diffraction peaks	195138	29.82%
Peak area belonging to selected phases	191615	29.28%
Peak area of phase A (Yttrium oxide)	*1956*	*0.30%*
Peak area of phase B (Vanadium oxide (5/9))	*12278*	*1.88%*
Peak area of phase C (Tris(dibromophosphazene))	*9040*	*1.38%*
Peak area of phase D (Thallium tungsten oxide (2/4/13))	*4210*	*0.64%*
Peak area of phase E (Rubidium tecto-phosphatodiniobate)	*14223*	*2.17%*
Peak area of phase F (Rubidium niobium tungsten oxide (12/30/3/90))	*14431*	*2.21%*
*Peak area of phase G (Potassium tecto-phosphatovanadate(III) *)*	*18760*	*2.87%*
Peak area of phase H (Potassium iodate telluric acid)	*5938*	*0.91%*
Peak area of phase I (Niobium thallium oxide hydrate (33/10.5/88.5/1.5))	*12978*	*1.98%*
Peak area of phase J (Iron(III) vanadium oxide (6.5/11.5/35))	*14780*	*2.26%*
Peak area of phase K (Iron(III) tris(phosphate) trihydroxide)	*16454*	*2.51%*
Peak area of phase L (Iron vanadium molybdenum oxide (4/1.98/3.02/20))	*9866*	*1.51%*
Peak area of phase M (Dineodymium tetrabarium dicopper oxide)	*4329*	*0.66%*
Peak area of phase N (Diantimony telluride diselenide)	*3058*	*0.47%*
Peak area of phase O (Chromium uranium(V) oxide)	*12030*	*1.84%*
Peak area of phase P (Caesium zinc phosphate(V) - I)	*6832*	*1.04%*
Peak area of phase Q (Cadmium arsenide iodide (2/3/1))	*4634*	*0.71%*
Peak area of phase R (Barium boride (1/6))	*6774*	*1.04%*
Peak area of phase S (Antimony selenide iodide)	*6946*	*1.06%*
Peak area of phase T (Ammonium trio-triiodide)	*12097*	*1.85%*
Unidentified peak area	3524	0.54%

Peak Residuals

Peak data	*Counts*	*Amount*
Overall peak intensity	2559	100.00%
Peak intensity belonging to selected phases	2559	99.97%
Unidentified peak intensity	1	0.03%

Diffraction Pattern Graphics

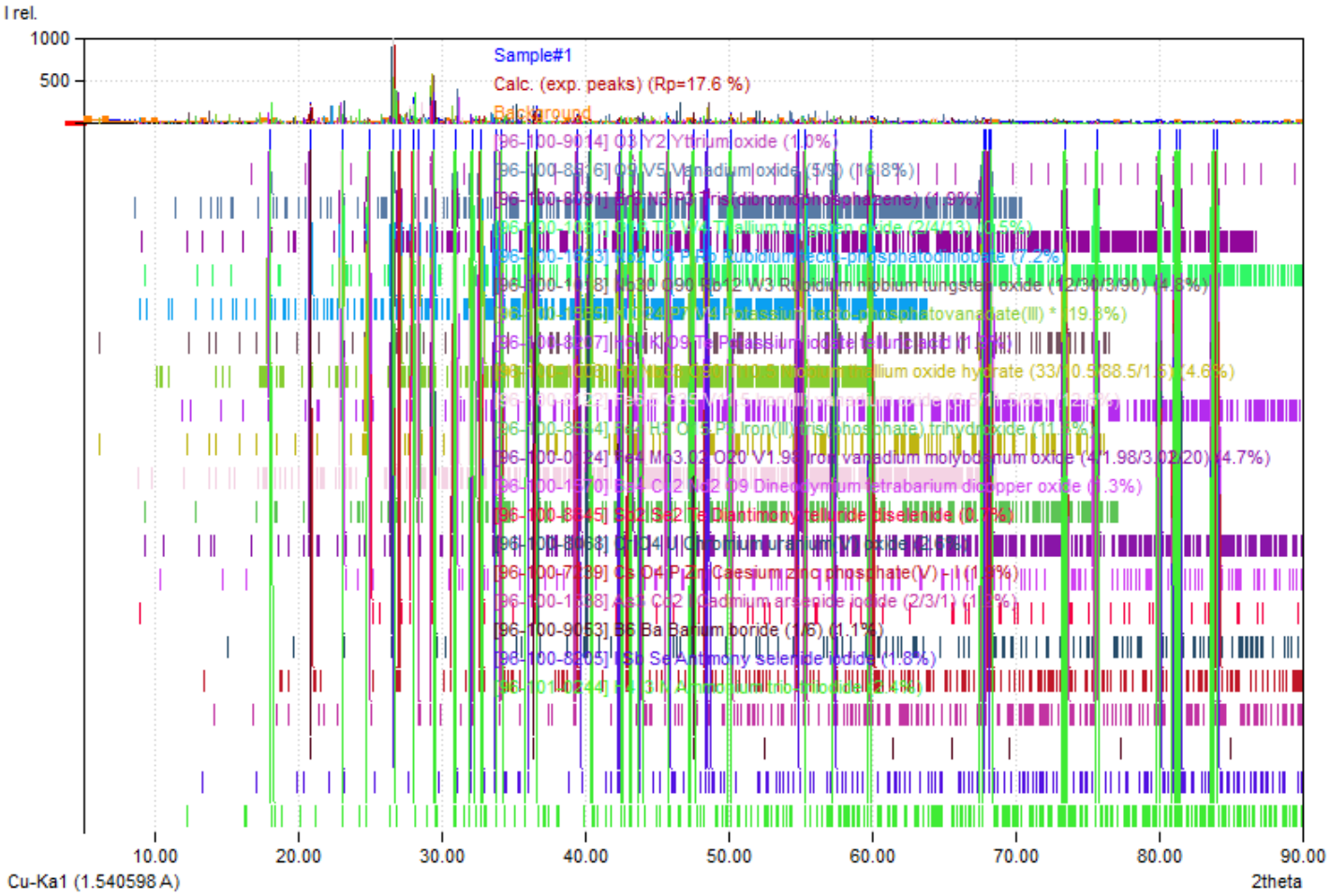

Match! Copyright © 2003-2023 CRYSTAL IMPACT, Bonn, Germany

Amounts of Phases and Elements (Weight %)

Phase composition:

Potassium tecto-phosphatovanadate(III) * (19.3%), Vanadium oxide (5/9) (16.8%), Iron(III) vanadium oxide (6.5/11.5/35) (12.8%), Iron(III) tris(phosphate) trihydroxide (11.5%), Rubidium tecto-phosphatodiniobate (7.2%), Rubidium niobium tungsten oxide (12/30/3/90) (4.8%), Iron vanadium molybdenum oxide (4/1.98/3.02/20) (4.7%), Niobium thallium oxide hydrate (33/10.5/83.5/1.5) (4.6%), Chromium uranium(V) oxide (2.6%), Ammonium trio-triiodide (2.4%), Caesium zinc phosphate(V) - I (1.9%), Potassium iodate telluric acid (1.9%), Tris(dibromophosphazene) (1.9%), Antimony selenide iodide (1.8%), Dineodymium tetrabarium dicopper oxide (1.3%), Cadmium arsenide iodide (2/3/1) (1.2%), Barium boride (1/6) (1.1%), Yttrium oxide (1.0%), Diantimony telluride diselenide (0.7%), Thallium tungsten oxide (2/4/13) (0.5%)

Elemental composition:

O (32.47%), V (20.91%), Fe (8.83%), P (7.89%), Nb (7.49%), I (3.79%), Rb (2.27%), U (1.72%), Tl (1.64%), Mo (1.47%), Br (1.45%), Ba (1.37%), K (1.06%), Sb (1.00%), Cs (0.88%), W (0.75%), Y (0.75%), Te (0.73%), Se (0.65%), Cd (0.46%), As (0.46%), Zn (0.43%), Cr (0.38%), Nd (0.34%), B (0.34%), Ni (0.21%), Cu (0.15%), H (0.11%) (LE: 33.14%)

Match! Phase Analysis Report

Sample: Sample_3

Sample Data

File name	Sample#3.raw
File path	G:/.shortcut-targets-by-id/16KlMvpSIqVAUHFFggq9lVgYQzQybBTlu/Marwan - research/Concrete Mix Master Thesis/X-Ray/Birzeit University_XRD_Raw data
Data collected	Jul 13, 2023 13:02:42
Data range	4.880° - 89.880°
Original data range	5.000° - 90.000°
Number of points	4251
Step size	0.020
Rietveld refinement converged	No
Alpha2 subtracted	No
Background subtr.	No
Data smoothed	No
2theta correction	-0.12°
Radiation	X-rays
Wavelength	1.540598 Å

Analysis Results

Phase composition (Weight %)

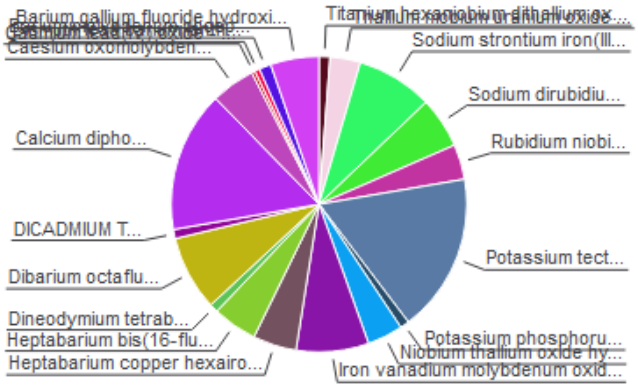

Elemental composition (Weight %)

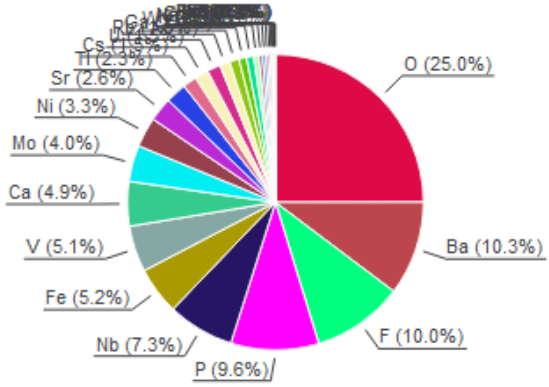

Index	*Amount (%)*	*Name*	*Formula sum*
A	1.2	Titanium hexaniobium dithallium oxide	Nb6 O18 Ti Tl2
B	3.3	Thallium niobium uranium oxide (1/2/2/11.5)	Nb2 O11.5 Tl U2
C	8.4	Sodium strontium iron(III) hexafluoride	F6 Fe Na Sr
D	5.6	Sodium dirubidium tecto-hexaniobotriphosphate(V)	Na Nb6 O24 P3 Rb2
E	3.8	Rubidium niobium tungsten oxide (12/30/3/90)	Nb30 O90 Rb12 W3
F	17.4	Potassium tecto-phosphatovanadate(III) *	K O24 P7 V4
G	1.0	Potassium phosphorus tungsten oxide (.4/2/4/16)	K0.4 O16 P2 W4
H	3.9	Niobium thallium oxide hydrate (33/10.5/88.5/1.5)	H3 Nb33 O90 Tl10.5
I	7.9	Iron vanadium molybdenum oxide (4/1.98/3.02/20)	Fe4 Mo3.02 O20 V1.98
J	4.8	Heptabarium copper hexairon(III) fluoride	Ba7 Cu F34 Fe6
K	4.9	Heptabarium bis(16-fluorotriferrate(III)) dihydrate	Ba7 F32 Fe6 H4 O2
L	0.9	Dineodymium tetrabarium dicopper oxide	Ba4 Cu2 Nd2 O9
M	8.2	Dibarium octafluorotriniccolate decafluorotetraniccolate	Ba2 F18 Ni7
N	1.0	DICADMIUM TRIARSENIDE BROMIDE	As3 Br Cd2
O	15.4	Calcium diphosphate - \b	Ca2 O7 P2
P	4.8	Caesium oxomolybdenum(V) diphosphate	Cs Mo O8 P2
Q	0.4	Cadmium lead(IV) oxide - I	Cd O3 Pb
R	0.5	Bismuth lead barium lanthanum copper oxide	Ba Bi Cu La O6 Pb
S	1.3	Barium molybdenum phosphate (1/2/3)	Ba Mo2 O12 P3
T	5.3	Barium gallium fluoride hydroxide hydrate (7/6/16/16/2)	Ba7 F16 Ga6 H20 O18
	0.6	*Unidentified peak area*	

Amounts calculated by RIR (Reference Intensity Ratio) method

Element	*Amount (weight %)*
O	*25.0%(*)*
Ba	10.3%
F	*10.0%(*)*
P	9.6%
Nb	7.3%
Fe	5.2%
V	5.1%
Ca	4.9%
Mo	4.0%
Ni	3.3%
Sr	2.6%
Tl	2.3%
Cs	1.5%
U	1.5%
Rb	1.5%
Ga	1.1%
W	1.0%
K	0.8%
Na	0.8%
Cd	0.5%
As	0.4%
Pb	0.3%
Cu	0.3%
Nd	0.2%
Br	0.2%
Bi	0.1%
La	0.1%
H	*0.1%(*)*
Ti	0.0%
**LE (sum)*	*35.1%*

Details of identified phases

A: Titanium hexaniobium dithallium oxide (1.2 %)*

Formula sum	Nb6 O18 Ti Tl2
Entry number	96-100-1851
Figure-of-Merit (FoM)	0.601188*
Total number of peaks	221
Peaks in range	221
Peaks matched	26
Intensity scale factor	0.20*
Space group	P -3 m 1
Crystal system	trigonal (hexagonal axes)
Unit cell	a= 7.5370 Å c= 8.2240 Å
I/Ic	5.49
Meas. density	5.420 g/cm³
Calc. density	5.344 g/cm³
Reference	Desgardin G, Robert C, Raveau B, "Etude de comportement du thallium dans de nouvelles structures atunnels entrecroises: Tl2 Nb6 Ti O18 et Tl2 Ta6 Ti O18", Materials Research Bulletin **13**, 621-626 (1978)

B: Thallium niobium uranium oxide (1/2/2/11.5) (3.3 %)*

Formula sum	Nb2 O11.5 Tl U2
Entry number	96-100-1356
Figure-of-Merit (FoM)	0.630699*
Total number of peaks	497
Peaks in range	497
Peaks matched	132
Intensity scale factor	0.46*
Space group	P m n b
Crystal system	orthorhombic
Unit cell	a= 7.7130 Å b= 10.3290 Å c= 13.9470 Å
I/Ic	4.52
Calc. density	6.278 g/cm³
Reference	Gasperin M, "Synthese et structure de trois niobouranates d'ions monovalents: TlNb~2~ U~2~ O~11.5~, K Nb U O~6~, et Rb Nb U O~6~", Journal of Solid State Chemistry **67**, 219-224 (1987)

C: Sodium strontium iron(III) hexafluoride (8.4 %)*

Formula sum	F6 Fe Na Sr
Entry number	96-100-0307
Figure-of-Merit (FoM)	0.608816*
Total number of peaks	499
Peaks in range	499
Peaks matched	79
Intensity scale factor	0.39*
Space group	P 21 21 21
Crystal system	orthorhombic
Unit cell	a= 5.4053 Å b= 9.3103 Å c= 10.3823 Å
I/Ic	1.51
Calc. density	3.565 g/cm³
Reference	Hemon A., Courbion G., "Synthesis and crystal structures of \b-NaSrCrF~6~ and NaSrFeF~6~.Structural correlations with A~2~MF~6~ compounds", European Journal of Solid State and Inorganic Chemistry **29**, 519-531 (1992)

D: Sodium dirubidium tecto-hexaniobotriphosphate(V) (5.6 %)*

Formula sum	Na Nb6 O24 P3 Rb2
Entry number	96-100-1863
Figure-of-Merit (FoM)	0.658809*
Total number of peaks	152
Peaks in range	152
Peaks matched	52
Intensity scale factor	0.76*
Space group	R 32
Crystal system	trigonal (hexagonal axes)
Unit cell	a= 13.3518 Å c= 10.3415 Å
I/Ic	4.43
Calc. density	3.831 g/cm³
Reference	Costentin G, Borel M M, Grandin A, Leclaire A, Raveau B, "A large family of niobium phosphates with the Ca0.5 Cs2 Nb6 P3 O24structure", Materials Research Bulletin **26**, 301-307 (1991)

E: Rubidium niobium tungsten oxide (12/30/3/90) (3.8 %)*

Formula sum	Nb30 O90 Rb12 W3
Entry number	96-100-1018
Figure-of-Merit (FoM)	0.655006*
Total number of peaks	161
Peaks in range	161
Peaks matched	57
Intensity scale factor	0.51*
Space group	R -3 m
Crystal system	trigonal (hexagonal axes)
Unit cell	a= 7.4860 Å c= 43.1000 Å
I/Ic	4.33
Meas. density	4.570 g/cm³
Calc. density	4.608 g/cm³
Reference	Michel C, Guyomarch A, Raveau B, "Nouveaux echangeurs cationiques avec une structure a tunnelsentrecroises: les oxides A~12~ M~33~ O~90~ et A~12~ M~33~ O~90~(H~2~ O)~12~", Journal of Solid State Chemistry **22**, 393-403 (1977)

F: Potassium tecto-phosphatovanadate(III) * (17.4 %)*

Formula sum	K O24 P7 V4
Entry number	96-100-1565
Figure-of-Merit (FoM)	0.667020*
Total number of peaks	499
Peaks in range	499
Peaks matched	231
Intensity scale factor	0.56*
Space group	P -1
Crystal system	triclinic (anorthic)
Unit cell	a= 10.0846 Å b= 10.2309 Å c= 10.8283 Å α= 112.757º β= 109.226 º γ= 104.675 º
I/Ic	1.05
Calc. density	3.202 g/cm³
Reference	Benhamada L, Grandin A, Borel M M, Leclaire A, Raveau B, "A vanadium(III) phosphate with V~2~O~10~ octahedral units:KV~4~P~7~O~24~", Journal of Solid State Chemistry **104**, 193-201 (1993)

G: Potassium phosphorus tungsten oxide (.4/2/4/16) (1.0 %)*

Formula sum	K0.4 O16 P2 W4
Entry number	96-100-1234
Figure-of-Merit (FoM)	0.616789*
Total number of peaks	497
Peaks in range	497
Peaks matched	75
Intensity scale factor	0.30*
Space group	P 1 21/m 1
Crystal system	monoclinic
Unit cell	a= 6.6702 Å b= 5.3228 Å c= 8.9091 Å β= 100.546 º
I/Ic	9.94
Calc. density	5.712 g/cm³
Reference	Giroult J P, Goreaud M, Labbe P, Raveau B, "K~x~ P~2~ W~2~ O~16~: A Bronze with a Tunnel Structure Built up from PO~4~ Tetrahedra and W O~6~ Octahedra", Journal of Solid State Chemistry **44**, 407-414 (1982)

H: Niobium thallium oxide hydrate (33/10.5/88.5/1.5) (3.9 %)*

Formula sum	H3 Nb33 O90 Tl10.5
Entry number	96-100-1006
Figure-of-Merit (FoM)	0.677304*
Total number of peaks	161
Peaks in range	161
Peaks matched	63
Intensity scale factor	0.56*
Space group	R -3 m
Crystal system	trigonal (hexagonal axes)
Unit cell	a= 7.5100 Å c= 43.2900 Å
I/Ic	4.67
Calc. density	5.263 g/cm³
Reference	Gasperin M, "Synthese d'une nouvelle famille d'oxydes doubles: A~8~^+^ B~22~^5+^O~59~ structure du compose a thallium et niobium", Acta Crystallographica B (24,1968-38,1982) **33**, 398-402 (1977)

I: Iron vanadium molybdenum oxide (4/1.98/3.02/20) (7.9 %)*

Formula sum	Fe4 Mo3.02 O20 V1.98
Entry number	96-100-0124
Figure-of-Merit (FoM)	0.693760*
Total number of peaks	462
Peaks in range	462
Peaks matched	114
Intensity scale factor	0.70*
Space group	P 41 2 2
Crystal system	tetragonal
Unit cell	a= 9.5390 Å c= 17.1411 Å
I/Ic	2.88
Calc. density	3.977 g/cm³
Reference	Laligant Y, Permer L, Le Bail A, "Crystal structure of Fe4 V2 Mo3 O20 determined from conventional X-raypowder diffraction data", European Journal of Solid State Inorganic Chemistry **32**, 325-334 (1995)

J: Heptabarium copper hexairon(III) fluoride (4.8 %)*

Formula sum	Ba7 Cu F34 Fe6
Entry number	96-100-0279
Figure-of-Merit (FoM)	0.600232*
Total number of peaks	301
Peaks in range	301
Peaks matched	105
Intensity scale factor	0.28*
Space group	C 1 2/m 1
Crystal system	monoclinic
Unit cell	a= 16.8920 Å b= 11.3310 Å c= 7.6460 Å β= 101.750 º
I/Ic	1.95
Calc. density	4.649 g/cm³
Reference	Renaudin J, Ferey G, Drillon M, De Kozak A, Samouel M, "La structure magnetique du ferrimagnetique monodimensionnel Ba~7~CuFe~6~ F~34~ de type jarlite", Comptes Rendus Hebdomadaires des Seances de l'Academie des Sciences,Serie C, Sciences Chimiques (1966-) **308**, 1217-1222 (1989)

K: Heptabarium bis(16-fluorotriferrate(III)) dihydrate (4.9 %)*

Formula sum	Ba7 F32 Fe6 H4 O2
Entry number	96-100-0376
Figure-of-Merit (FoM)	0.600528*
Total number of peaks	296
Peaks in range	296
Peaks matched	111
Intensity scale factor	0.29*
Space group	C 1 2/m 1
Crystal system	monoclinic
Unit cell	a= 17.0230 Å b= 11.4820 Å c= 7.6240 Å β= 101.130 º
I/Ic	1.94
Calc. density	4.398 g/cm³
Reference	Crosnier-Lopez M P, Calage Y, Duroy H, Fourquet J L, "Ba7 Fe6 F32 . 2(H2 O): original isolated trimers (Fe3 F16)(7-) in a newdefective jarlite-type compound", Zeitschrift fuer Anorganische und Allgemeine Chemie **621**, 1025-1032 (1995)

L: Dineodymium tetrabarium dicopper oxide (0.9 %)*

Formula sum	Ba4 Cu2 Nd2 O9
Entry number	96-100-1570
Figure-of-Merit (FoM)	0.633237*
Total number of peaks	349
Peaks in range	349
Peaks matched	39
Intensity scale factor	0.25*
Space group	P -4 n 2
Crystal system	tetragonal
Unit cell	a= 12.0717 Å c= 3.8737 Å
I/Ic	8.81
Calc. density	6.523 g/cm³
Reference	Domenges B, Abbattista F, Michel C, Vallino M, Barbey L, Nguyen N, Raveau B, "A one-dimensional cuprate closely related to the "0212"-structure:Nd~2~Ba~4~Cu~2~O~9~", Journal of Solid State Chemistry **106**, 271-281 (1993)

M: Dibarium octafluorotriniccolate decafluorotetraniccolate (8.2 %)*

Formula sum	Ba2 F18 Ni7
Entry number	96-100-0250
Figure-of-Merit (FoM)	0.621667*
Total number of peaks	500
Peaks in range	500
Peaks matched	154
Intensity scale factor	0.42*
Space group	P -1
Crystal system	triclinic (anorthic)
Unit cell	a= 6.9240 Å b= 7.2180 Å c= 7.4370 Å α= 94.390º β= 93.200 º γ= 115.820 º
I/Ic	1.67
Calc. density	5.139 g/cm³
Reference	Renaudin J, Ferey G, Kozak A, Samouel M, Lacorre P, "Crystal and magnetic structures of the ferrimagnet Ba~2~ Ni~7~ F~18~", Solid State Communications **65**, 185-188 (1988)

N: DICADMIUM TRIARSENIDE BROMIDE (1.0 %)*

Formula sum	As3 Br Cd2
Entry number	96-100-1295
Figure-of-Merit (FoM)	0.601675*
Total number of peaks	284
Peaks in range	284
Peaks matched	64
Intensity scale factor	0.17*
Space group	C 1 c 1
Crystal system	monoclinic
Unit cell	a= 8.2860 Å b= 9.4080 Å c= 7.9870 Å β= 101.300 º
I/Ic	5.61
Calc. density	5.760 g/cm³
Reference	Rebbah A, Yazbeck J, Lande R, Deschanvres A, "Etudes structurales et optiques des phases du type Cd~2~ A~3~ X (A =As, P", Materials Research Bulletin **16**, 525-533 (1981)

O: Calcium diphosphate - \b (15.4 %)*

Formula sum	Ca2 O7 P2
Entry number	96-100-1557
Figure-of-Merit (FoM)	0.606278*
Total number of peaks	328
Peaks in range	328
Peaks matched	86
Intensity scale factor	0.35*
Space group	P 41
Crystal system	tetragonal
Unit cell	a= 6.6858 Å c= 24.1470 Å
I/Ic	0.74
Calc. density	3.127 g/cm³
Reference	Boudin S., Grandin A., Borel M. M., Leclaire A., Raveau B., "Redetermination of the \b-Ca~2~P~2~O~7~ structure", Acta Crystallographica, Section C: Crystal Structure Communications **49(12)**, 2062-2064 (1993)

P: Caesium oxomolybdenum(V) diphosphate (4.8 %)*

Formula sum	Cs Mo O8 P2
Entry number	96-100-1619

Figure-of-Merit (FoM)	0.605866*
Total number of peaks	498
Peaks in range	498
Peaks matched	156
Intensity scale factor	0.26*
Space group	P 1 21/n 1
Crystal system	monoclinic
Unit cell	a= 5.1340 Å b= 11.7070 Å c= 12.0630 Å β= 91.770 º
I/Ic	1.74
Meas. density	3.900 g/cm³
Calc. density	3.838 g/cm³
Reference	Guesdon A, Borel M M, Leclaire A, Grandin A, Raveau B, "A molybdenum (V) diphosphate closely related to the $-alpha-NaTiP~2~O~7~ structure: Cs(MoO)P~2~O~7~", Journal of Solid State Chemistry **108**, 46-50 (1994)

Q: Cadmium lead(IV) oxide - I (0.4 %)*

Formula sum	Cd O3 Pb
Entry number	96-100-1049
Figure-of-Merit (FoM)	0.620778*
Total number of peaks	80
Peaks in range	80
Peaks matched	18
Intensity scale factor	0.21*
Space group	I a -3
Crystal system	cubic
Unit cell	a= 10.4530 Å
I/Ic	17.91
Calc. density	8.551 g/cm³
Reference	Levy-Clement C, Michel A, "Sur un oxyde double Cd Pb O~3~ de type c des oxydes de lanthanides", Annales de Chimie (Paris) (Vol=Year) **1972**, 275-281 (1972)

R: Bismuth lead barium lanthanum copper oxide (0.5 %)*

Formula sum	Ba Bi Cu La O6 Pb
Entry number	96-100-1571
Figure-of-Merit (FoM)	0.609712*
Total number of peaks	498
Peaks in range	498
Peaks matched	72
Intensity scale factor	0.19*
Space group	P n a n
Crystal system	orthorhombic
Unit cell	a= 5.4071 Å b= 5.4895 Å c= 24.5490 Å
I/Ic	11.56
Calc. density	7.766 g/cm³
Reference	Michel C, Pelloquin D, Hervieu M, Raveau B, Bouree F, "Neutron diffraction study of the modulation free 2201-type structure:BiPbBaLaCuO~6~", European Journal of Solid State Inorganic Chemistry **30**, 991-996 (1993)

S: Barium molybdenum phosphate (1/2/3) (1.3 %)*

Formula sum	Ba Mo2 O12 P3
Entry number	96-100-1430
Figure-of-Merit (FoM)	0.604403*
Total number of peaks	126
Peaks in range	126
Peaks matched	39
Intensity scale factor	0.20*
Space group	R -3 c
Crystal system	trigonal (hexagonal axes)
Unit cell	a= 8.3990 Å c= 23.8950 Å
I/Ic	5.00
Calc. density	4.191 g/cm³
Reference	Leclaire A, Borel M M, Grandin A, Raveau B, "A novel family of mixed valence molybdenum phosphates with a Nasiconstructure, AMo~2~P~3~O~12~ (A= Ca, Sr, Ba)", European Journal of Solid State Inorganic Chemistry **26**, 45-51 (1989)

T: Barium gallium fluoride hydroxide hydrate (7/6/16/16/2) (5.3 %)*

Formula sum	Ba7 F16 Ga6 H20 O18
Entry number	96-100-0400
Figure-of-Merit (FoM)	0.617431*
Total number of peaks	300
Peaks in range	300
Peaks matched	100
Intensity scale factor	0.35*
Space group	C 1 2/m 1
Crystal system	monoclinic
Unit cell	a= 16.9080 Å b= 11.4060 Å c= 7.5420 Å β= 101.280 º
I/Ic	2.15
Calc. density	4.590 g/cm³
Reference	Hemon-Ribaud A, Crosnier-Lopez M P, Fourquet J L, Courbion G, "On new fluorides with the jarlite-type structure: crystal structures ofNa2 Sr7 Al6 F34, Na2 Sr6 Zn Fe6 F34 and Ba7 Ga6 (F, OH)32 . 2H2O", Journal of Fluorine Chemistry **68**, 155-163 (1994)

(*)2theta values have been shifted internally for the calculation of the amounts, the intensity scaling factors as well as the figure-of-merit (FoM), due to the active search-match option 'Automatic zero point adaption'.

Search-Match

Settings

Reference database used	COD-Inorg 2023.06.06
Automatic zeropoint adaptation	Yes
Downgrade entries with low scaling factors	Yes
Minimum figure-of-merit (FoM)	0.60
2theta window for peak corr.	0.30 deg.
Minimum rel. int. for peak corr.	0
Parameter/influence 2theta	0.50
Parameter/influence intensities	0.50
Parameter multiple/single phase(s)	0.50

Peak List

No.	*2theta [°]*	*d [Å]*	*I/I0 (peak height)*	*Counts (peak area)*	*FWHM*	*Matched*
1	10.38	8.5155	7.47	4.35	0.0800	F,G,L
2	10.66	8.2924	7.22	4.20	0.0800	A,B,I,J,K,P,T
3	11.02	8.0223	9.54	19.44	0.2800	F
4	18.02	4.9187	54.94	47.97	0.1200	B,F,G,I,J,M,T
5	20.84	4.2590	312.94	273.27	0.1200	B,C,F,I,K,L,P,Q,S
6	22.98	3.8670	13.36	23.34	0.2400	B,D,F,G,I,J,K,N,O,P,R,T
7	24.00	3.7049	8.56	4.98	0.0800	B,C,E,F,I,J,K,L,M,O,P,Q,R,S,T
8	24.88	3.5758	10.16	20.70	0.2800	E,F,G,H,I,K,M,N,T
9	25.68	3.4662	8.52	2.48	0.0400	A,B,C,D,M,O,R,S
10	26.64	3.3435	1000.00	873.22	0.1200	B,C,D,E,F,G,H,I,J,K,L,M,O,P,T
11	27.40	3.2524	12.34	75.42	0.8400	A,C,E,F,G,H,I,J,K,M,O,P,R,T
12	28.68	3.1101	13.05	22.80	0.2400	B,E,F,H,I,J,K,M,N,O,P,S,T
13	29.40	3.0356	146.91	213.81	0.2000	A,B,D,E,F,H,I,K,L,M,N,O,P,Q,R,T
14	29.98	2.9781	9.30	21.65	0.3200	C,E,H,I,J,M,O,P,R
15	30.90	2.8915	61.64	107.65	0.2400	B,C,F,G,H,I,J,K,O,P,S,T
16	31.30	2.8555	10.68	3.11	0.0400	B,E,F,G,I,J,K,L,M,P,T
17	32.12	2.7844	11.78	17.14	0.2000	A,B,C,D,E,F,G,H,I,J,K,L,M,N,O,P,Q,R,S,T
18	32.70	2.7364	19.56	51.25	0.3600	A,D,F,I,J,K,L,N,O,P,R,S,T
19	34.08	2.6287	28.19	41.03	0.2000	B,C,F,I,J,N,P,Q,R
20	36.50	2.4597	55.77	48.70	0.1200	A,B,C,E,F,G,H,I,J,K,M,P,Q,R,T
21	39.46	2.2818	63.59	55.53	0.1200	B,C,E,F,G,H,I,J,K,L,M,N,O,P,R,S,T
22	40.28	2.2372	39.68	34.65	0.1200	B,D,E,F,H,I,J,K,L,M,N,O,P,Q,R,S,T
23	42.42	2.1291	75.40	65.84	0.1200	A,B,C,D,E,F,G,H,I,J,K,L,M,O,P,Q,R,S,T
24	43.16	2.0943	16.02	27.99	0.2400	A,B,C,F,G,H,I,J,K,M,O,P,R,S,T
25	43.94	2.0590	7.64	15.57	0.2800	A,B,E,F,G,H,I,J,K,L,M,N,P,Q,R,S,T
26	45.78	1.9804	28.37	24.77	0.1200	B,C,E,F,G,H,I,J,K,L,O,P,S,T
27	47.12	1.9271	22.38	39.09	0.2400	A,B,C,D,F,G,H,K,L,M,N,O,P,R,T
28	47.44	1.9149	17.22	60.16	0.4800	B,E,F,I,J,K,L,M,N,P,Q,R,S,T
29	48.50	1.8755	20.11	23.41	0.1600	A,B,C,D,E,F,G,H,I,J,K,L,M,N,O,P,R,T
30	49.14	1.8526	10.97	12.77	0.1600	B,D,E,F,G,H,I,J,K,L,M,N,O,P,Q,S,T
31	50.12	1.8186	60.72	70.69	0.1600	A,B,C,E,F,G,H,I,J,K,L,M,N,P,R,T
32	50.76	1.7972	10.21	5.94	0.0800	A,B,E,F,H,I,J,K,L,M,N,O,P,R,S,T
33	51.02	1.7886	7.29	4.24	0.0800	B,C,D,E,F,G,H,J,K,M,N,O,P,Q,R,T
34	54.84	1.6727	43.24	25.17	0.0800	B,C,E,F,G,H,I,J,K,L,M,N,O,P,R,S,T
35	55.00	1.6682	20.66	18.04	0.1200	B,C,D,E,F,G,H,I,J,K,M,N,O,P,R,S,T
36	57.36	1.6051	6.91	6.03	0.1200	A,B,C,E,F,G,H,I,J,K,L,M,N,O,P,S,T
37	59.92	1.5425	31.62	27.61	0.1200	B,C,D,F,G,I,J,L,M,N,O,P,Q,R,S,T
38	60.10	1.5383	14.36	12.54	0.1200	B,C,D,F,H,I,J,K,L,M,N,O,P,R,S,T
39	64.02	1.4532	7.65	4.46	0.0800	B,C,D,E,G,H,I,J,K,M,N,O,P,Q,R,S,T
40	67.72	1.3825	56.83	49.63	0.1200	B,C,E,G,H,I,L,M,N,O,P,R,S
41	67.90	1.3793	28.64	25.01	0.1200	B,E,G,H,I,M,N,P,S
42	68.28	1.3726	64.34	56.19	0.1200	B,C,E,G,I,M,O,P,R,S
43	68.46	1.3694	20.46	29.78	0.2000	A,B,C,E,H,I,L,M,N,P,R,S
44	73.44	1.2883	13.58	11.86	0.1200	A,B,C,D,E,G,H,I,M,N,O,P,R
45	73.66	1.2850	6.83	1.99	0.0400	B,C,D,E,G,H,I,L,M,N,O,P,Q,R
46	75.64	1.2562	27.53	24.04	0.1200	A,B,C,G,I,L,M,N,P,R,S
47	75.86	1.2531	14.16	8.24	0.0800	B,C,G,H,I,M,N,O,P,Q,R,S
48	79.84	1.2004	17.41	20.27	0.1600	A,B,D,G,I,L,M,N,O,P,R,S
49	80.00	1.1984	12.21	10.67	0.1200	A,B,C,D,G,I,M,N,O,P,Q,R,S
50	81.10	1.1849	21.47	18.75	0.1200	B,C,D,G,I,L,M,N,O,P,Q,R
51	81.42	1.1810	23.48	27.34	0.1600	A,B,D,G,I,L,M,N,O,P,R
52	81.70	1.1777	11.34	6.60	0.0800	A,B,C,G,I,L,M,N,O,P,R,S

Integrated Profile Areas

Based on calculated profile

Profile area	***Counts***	***Amount***
Overall diffraction profile	648957	100.00%
Background radiation	446677	68.83%
Diffraction peaks	202280	31.17%
Peak area belonging to selected phases	198393	30.57%
Peak area of phase A (Iron vanadium molybdenum oxide (4/1.98/3.02/20))	*14371*	*2.21%*
Peak area of phase B (Dibarium octafluorotriniccolate decafluorotetraniccolate)	*15386*	*2.37%*
Peak area of phase C (Heptabarium copper hexairon(III) fluoride)	*10804*	*1.66%*
Peak area of phase D (Sodium strontium iron(III) hexafluoride)	*18230*	*2.81%*
Peak area of phase E (Heptabarium bis(16-fluorotriferrate(III)) dihydrate)	*9672*	*1.49%*
Peak area of phase F (Barium gallium fluoride hydroxide hydrate (7/6/16/16/2))	*10514*	*1.62%*
Peak area of phase G (Niobium thallium oxide hydrate (33/10.5/88.5/1.5))	*12675*	*1.95%*
Peak area of phase H (Rubidium niobium tungsten oxide (12/30/3/90))	*13471*	*2.08%*
Peak area of phase I (Cadmium lead(IV) oxide - I)	*2869*	*0.44%*
Peak area of phase J (Potassium phosphorus tungsten oxide (.4/2/4/16))	*4017*	*0.62%*
Peak area of phase K (DICADMIUM TRIARSENIDE BROMIDE)	*3267*	*0.50%*
Peak area of phase L (Thallium niobium uranium oxide (1/2/2/11.5))	*16534*	*2.55%*
Peak area of phase M (Barium molybdenum phosphate (1/2/3))	*4390*	*0.68%*
Peak area of phase N (Calcium diphosphate - \b)	*11662*	*1.80%*
*Peak area of phase O (Potassium tecto-phosphatovanadate(III) *)*	*15129*	*2.33%*

Peak area of phase P (Dineodymium tetrabarium dicopper oxide)	*2821*	*0.43%*
Peak area of phase Q (Bismuth lead barium lanthanum copper oxide)	*3010*	*0.46%*
Peak area of phase R (Caesium oxomolybdenum(V) diphosphate)	*11641*	*1.79%*
Peak area of phase S (Titanium hexaniobium dithallium oxide)	*2430*	*0.37%*
Peak area of phase T (Sodium dirubidium tecto-hexaniobotriphosphate(V))	*15499*	*2.39%*
Unidentified peak area	3887	0.60%

Diffraction Pattern Graphics

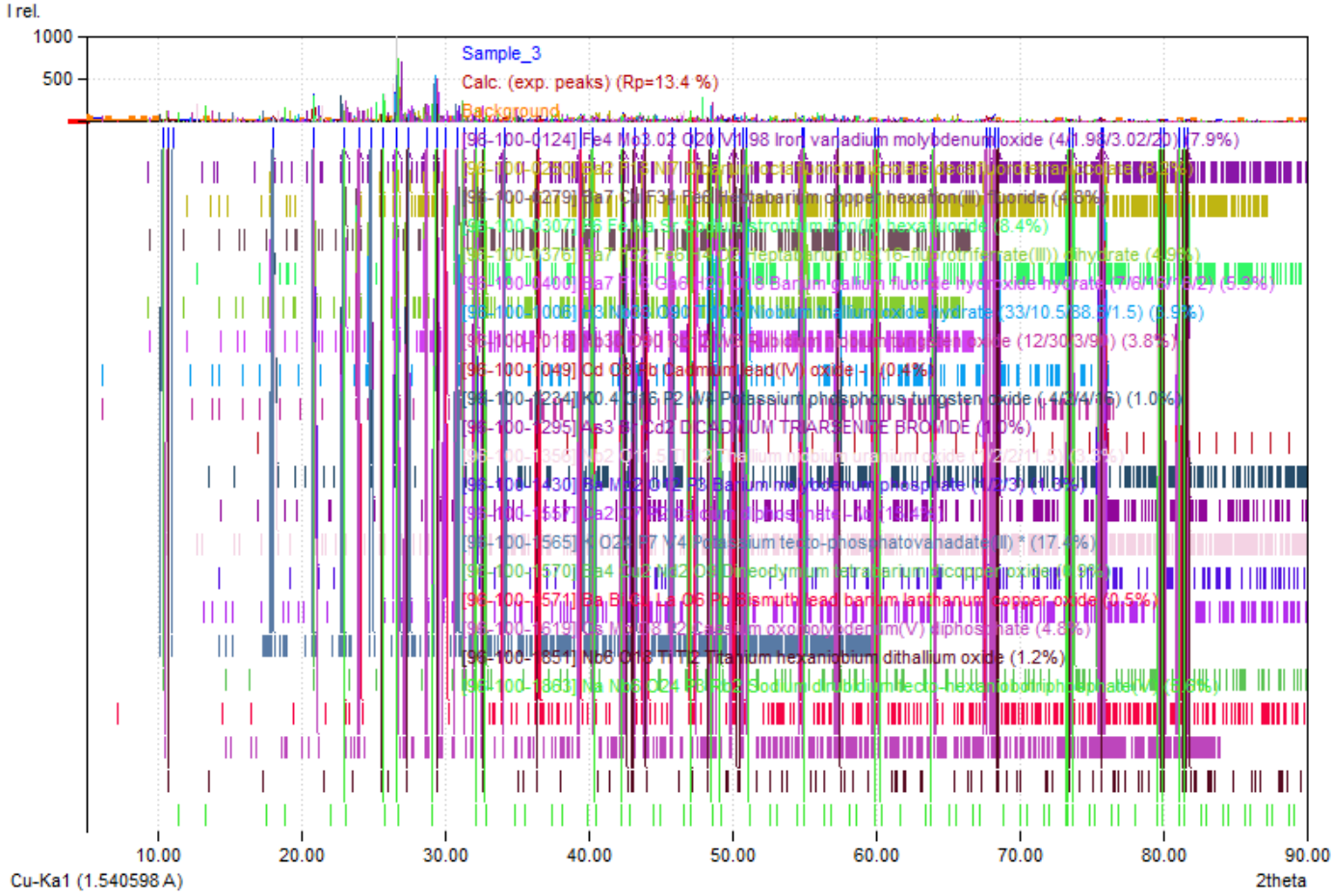

Match! Copyright © 2003-2023 CRYSTAL IMPACT, Bonn, Germany

Amounts of Phases and Elements (Weight %)

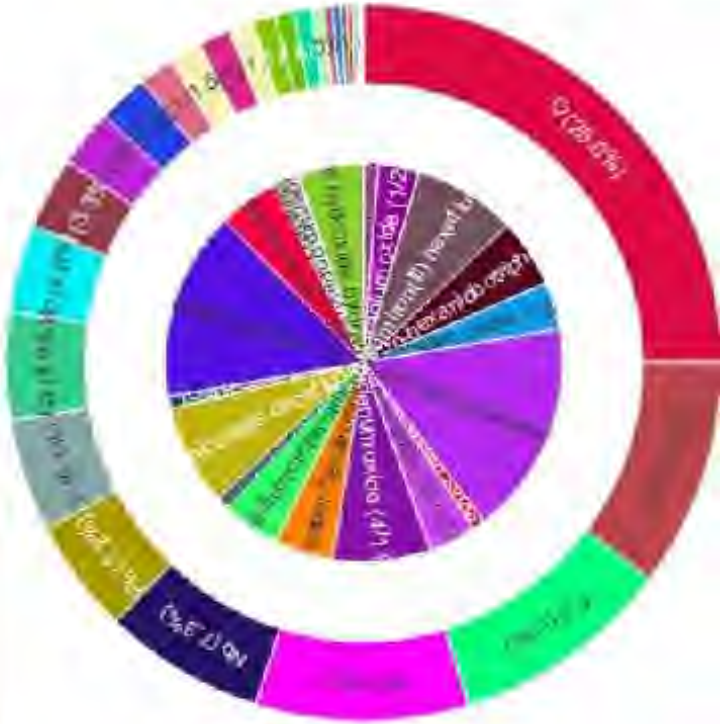

Phase composition:

Potassium tecto-phosphatovanadate(III) * (17.4%), Calcium diphosphate - \b (15.4%), Sodium strontium iron(III) hexafluoride (8.4%), Dibarium octafluorotriniccolate decafluorotetraniccolate (8.2%), Iron vanadium molybdenum oxide (4/1.98/3.02/20) (7.9%), Sodium dirubidium tecto-hexaniobotriphosphate(V) (5.6%), Barium gallium fluoride hydroxide hydrate (7/6/16/16/2) (5.3%), Heptabarium bis(16-fluorotriferrate(III)) dihydrate (4.9%), Caesium oxomolybdenum(V) diphosphate (4.8%), Heptabarium copper hexairon(III) fluoride (4.8%), Niobium thallium oxide hydrate (33/10.5/88.5/1.5) (3.9%), Rubidium niobium tungsten oxide (12/30/3/90) (3.8%), Thallium niobium uranium oxide (1/2/2/11.5) (3.3%), Barium molybdenum phosphate (1/2/3) (1.3%), Titanium hexaniobium dithallium oxide (1.2%), DICADMIUM TRIARSENIDE BROMIDE (1.0%), Potassium phosphorus tungsten oxide (.4/2/4/16) (1.0%), Dineodymium tetrabarium dicopper oxide (0.9%), Bismuth lead barium lanthanum copper oxide (0.5%), Cadmium lead(IV) oxide - I (0.4%)

Elemental composition:

O (24.99%), Ba (10.29%), F (10.00%), P (9.61%), Nb (7.27%), Fe (5.20%), V (5.05%), Ca (4.86%), Mo (3.97%), Ni (3.28%), Sr (2.61%), Ti (2.28%), Cs (1.52%), U (1.50%), Rb (1.45%), Ga (1.11%), W (1.05%), K (0.82%), Na (0.79%), Cd (0.54%), As (0.43%), Pb (0.35%), Cu (0.30%), Nd (0.24%), Br (0.15%), Bi (0.13%), La (0.09%), H (0.07%), Ti (0.04%) (LE: 35.05%)

Match! Phase Analysis Report

Sample: Sample#7

Sample Data

File name	Sample#7.raw
File path	G:/.shortcut-targets-by-id/16KlMvpSIqVAUHFFggq9IVgYQzQybBTIu/Marwan - research/Concrete Mix Master Thesis/X-Ray/Birzeit University_XRD_Raw data
Data collected	Jul 13, 2023 07:16:32
Data range	5.030° - 90.030°
Original data range	5.000° - 90.000°
Number of points	4251
Step size	0.020
Rietveld refinement converged	No
Alpha2 subtracted	No
Background subtr.	No
Data smoothed	No
2theta correction	0.03°
Radiation	X-rays
Wavelength	1.540598 Å

Analysis Results

Phase composition (Weight %)

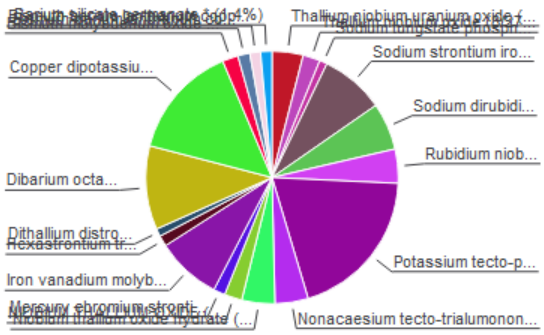

Elemental composition (Weight %)

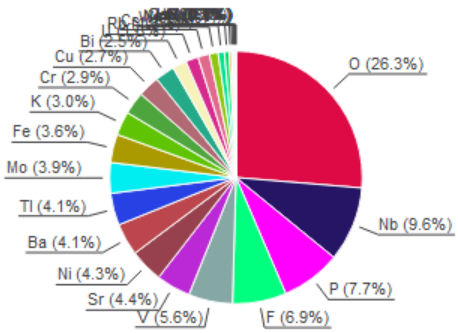

Index	*Amount (%)*	*Name*	*Formula sum*
A	4.0	Thallium niobium uranium oxide (1/2/2/11.5)	Nb2 O11.5 Tl U2
B	2.2	Thallium niobium oxide (8/27.2/72)	Nb27.2 O72 Tl8
C	1.0	Sodium tungstate phosphate *	Na1.7 O44 P4 W12
D	8.2	Sodium strontium iron(III) hexafluoride	F6 Fe Na Sr
E	6.0	Sodium dirubidium tecto-hexaniobotriphosphate(V)	Na Nb6 O24 P3 Rb2
F	4.4	Rubidium niobium tungsten oxide (12/30/3/90)	Nb30 O90 Rb12 W3
G	19.6	Potassium tecto-phosphatovanadate(III) *	K O24 P7 V4
H	4.2	Nonacaesium tecto-trialumononamolybdo(V)undecaphosphate(V)	Al3 Cs9 Mo9 O59 P11
I	4.2	Niobium thallium oxide hydrate (33/10.5/88.5/1.5)	H3 Nb33 O90 Tl10.5
J	2.3	NIOBIUM THALLIUM OXIDE (3.1/1/8.2)	Nb3.09 O8.22 Tl
K	1.5	Mercury chromium strontium copper carbonate oxide (0.46/0.54/4/2/1/6.88)	C Cr0.54 Cu2 Hg0.46 O9.88 Sr4
L	8.3	Iron vanadium molybdenum oxide (4/1.98/3.02/20)	Fe4 Mo3.02 O20 V1.98
M	1.4	Hexastrontium trinitridodicuprate(I) dinitridocuprate(I)	Cu3 N5 Sr6
N	1.0	Dithallium distrontium copper oxide	Cu O6 Sr2 Tl2
O	10.7	Dibarium octafluorotriniccolate decafluorotetraniccolate	Ba2 F18 Ni7
P	14.6	Copper dipotassium dihydrogen phosphatochromate	Cr2 Cu H2 K2 O14 P2
Q	2.0	Bismuth molybdenum oxide (26.4/9.6/68.4)	Bi26.4 Mo9.6 O68.4
R	1.5	Bismuth barium lanthanum copper oxide (2/2.3/0.7/2/8)	Ba2.3 Bi2 Cu2 La0.7 O8
S	1.4	Bismuth barium lanthanum copper oxide (1.6/2.5/0.9/2/8.3)	Ba2.5 Bi1.59 Cu2 La0.91 O8.25
T	1.4	Barium silicate germanate *	Ba Ge3.125 O9 Si0.875
	0.1	*Unidentified peak area*	

Amounts calculated by RIR (Reference Intensity Ratio) method

Element	*Amount (weight %)*
O	*26.3%(*)*
Nb	9.6%
P	7.7%
F	*6.9%(*)*
V	5.6%
Sr	4.4%
Ni	4.3%
Ba	4.1%
Tl	4.1%
Mo	3.9%
Fe	3.6%
K	3.0%
Cr	2.9%
Cu	2.7%
Bi	2.5%
U	1.8%
Rb	1.6%
Cs	1.5%
W	1.1%
Na	0.8%
Ge	0.6%
La	0.3%
Hg	0.2%
N	*0.1%(*)*
Al	0.1%
Si	0.1%
H	*0.1%(*)*
C	*0.0%(*)*
**LE (sum)*	*33.4%*

Details of identified phases

A: Thallium niobium uranium oxide (1/2/2/11.5) (4.0 %)*

Formula sum	Nb2 O11.5 Tl U2
Entry number	96-100-1356
Figure-of-Merit (FoM)	0.612747*
Total number of peaks	497
Peaks in range	497
Peaks matched	128
Intensity scale factor	0.47*
Space group	P m n b
Crystal system	orthorhombic
Unit cell	a= 7.7130 Å b= 10.3290 Å c= 13.9470 Å
I/Ic	4.52
Calc. density	6.278 g/cm³
Reference	Gasperin M, "Synthese et structure de trois niobouranates d'ions monovalents: TlNb~2~ U~2~ O~11.5~, K Nb U O~6~, et Rb Nb U O~6~", Journal of Solid State Chemistry **67**, 219-224 (1987)

B: Thallium niobium oxide (8/27.2/72) (2.2 %)*

Formula sum	Nb27.2 O72 Tl8
Entry number	96-100-4151
Figure-of-Merit (FoM)	0.659411*
Total number of peaks	307
Peaks in range	307
Peaks matched	90
Intensity scale factor	0.28*
Space group	I m 2 m
Crystal system	orthorhombic
Unit cell	a= 7.5340 Å b= 12.9920 Å c= 15.5550 Å
I/Ic	4.82
Calc. density	5.795 g/cm³
Reference	Dupont L, Hervieu M, Pelloquin D, Nowogrocki G, Touboul M, "Synthesis and crystal structure determination of Tl8 Nb27.2 O72 usingTEM and single-crystal x-ray diffraction", Journal of Solid State Chemistry **135**, 282-292 (1998)

C: Sodium tungstate phosphate * (1.0 %)*

Formula sum	Na1.7 O44 P4 W12
Entry number	96-100-1273
Figure-of-Merit (FoM)	0.633607*
Total number of peaks	496
Peaks in range	496
Peaks matched	136
Intensity scale factor	0.27*
Space group	P 1 21/a 1
Crystal system	monoclinic
Unit cell	a= 23.7750 Å b= 5.2910 Å c= 6.5880 Å β= 93.470 º
I/Ic	10.40
Calc. density	6.169 g/cm³
Reference	Benmmoussa A, Groult D, Labbe Ph, Raveau B, "Two New Members of a Series of Monoclinic Sodium Phosphate TungstenBronzes Na~x~ P~4~ O~8~ (W O~3~)~2m~: Na~x~ P~4~ W~8~ O~32~ (m=4) andNa~x~ P~4~ W~12~ O~44~ (m=6)", Acta Crystallographica C (39,1983-) **40**, 573-576 (1984)

D: Sodium strontium iron(III) hexafluoride (8.2 %)*

Formula sum	F6 Fe Na Sr
Entry number	96-100-0307
Figure-of-Merit (FoM)	0.600892*
Total number of peaks	499
Peaks in range	499
Peaks matched	81
Intensity scale factor	0.32*
Space group	P 21 21 21
Crystal system	orthorhombic
Unit cell	a= 5.4053 Å b= 9.3103 Å c= 10.3823 Å
I/Ic	1.51
Calc. density	3.565 g/cm³
Reference	Hemon A., Courbion G., "Synthesis and crystal structures of \b-NaSrCrF~6~ and NaSrFeF~6~.Structural correlations with A~2~MF~6~ compounds", European Journal of Solid State and Inorganic Chemistry **29**, 519-531 (1992)

E: Sodium dirubidium tecto-hexaniobotriphosphate(V) (6.0 %)

Formula sum	Na Nb6 O24 P3 Rb2
Entry number	96-100-1863
Figure-of-Merit (FoM)	0.629717
Total number of peaks	152
Peaks in range	152
Peaks matched	36
Intensity scale factor	0.70
Space group	R 32
Crystal system	trigonal (hexagonal axes)
Unit cell	a= 13.3518 Å c= 10.3415 Å
I/Ic	4.43
Calc. density	3.831 g/cm³
Reference	Costentin G, Borel M M, Grandin A, Leclaire A, Raveau B, "A large family of niobium phosphates with the Ca0.5 Cs2 Nb6 P3 O24structure", Materials Research Bulletin **26**, 301-307 (1991)

F: Rubidium niobium tungsten oxide (12/30/3/90) (4.4 %)*

Formula sum	Nb30 O90 Rb12 W3
Entry number	96-100-1018
Figure-of-Merit (FoM)	0.624619*
Total number of peaks	161
Peaks in range	161
Peaks matched	50
Intensity scale factor	0.49*
Space group	R -3 m
Crystal system	trigonal (hexagonal axes)
Unit cell	a= 7.4860 Å c= 43.1000 Å
I/Ic	4.33
Meas. density	4.570 g/cm³
Calc. density	4.608 g/cm³
Reference	Michel C, Guyomarch A, Raveau B, "Nouveaux echangeurs cationiques avec une structure a tunnelsentrecroises: les oxides A~12~ M~33~ O~90~ et A~12~ M~33~ O~90~(H~2~ O)~12~", Journal of Solid State Chemistry **22**, 393-403 (1977)

G: Potassium tecto-phosphatovanadate(III) * (19.6 %)*

Formula sum	K O24 P7 V4
Entry number	96-100-1565
Figure-of-Merit (FoM)	0.652042*
Total number of peaks	499
Peaks in range	499
Peaks matched	204
Intensity scale factor	0.54*
Space group	P -1
Crystal system	triclinic (anorthic)
Unit cell	a= 10.0846 Å b= 10.2309 Å c= 10.8283 Å α= 112.757º β= 109.226 º γ= 104.675 º
I/Ic	1.05
Calc. density	3.202 g/cm³
Reference	Benhamada L, Grandin A, Borel M M, Leclaire A, Raveau B, "A vanadium(III) phosphate with V~2~O~10~ octahedral units:KV~4~P~7~O~24~", Journal of Solid State Chemistry **104**, 193-201 (1993)

H: Nonacaesium tecto-trialumononamolybdo(V)undecaphosphate(V) (4.2 %)*

Formula sum	Al3 Cs9 Mo9 O59 P11
Entry number	96-100-1642
Figure-of-Merit (FoM)	0.604545*
Total number of peaks	303
Peaks in range	303
Peaks matched	93
Intensity scale factor	0.27*
Space group	P 63/m
Crystal system	hexagonal
Unit cell	a= 16.9890 Å c= 11.8660 Å
I/Ic	2.45
Meas. density	3.880 g/cm³
Calc. density	3.835 g/cm³
Reference	Guesdon A, Borel M M, Leclaire A, Grandin A, Raveau B, "An aluminophosphate of molybdenum(V) with a tunnel structure: Cs9 Mo9Al3 P11 O59", Journal of Solid State Chemistry **114**, 451-458 (1995)

I: Niobium thallium oxide hydrate (33/10.5/88.5/1.5) (4.2 %)*

Formula sum	H3 Nb33 O90 Tl10.5
Entry number	96-100-1006
Figure-of-Merit (FoM)	0.665743*
Total number of peaks	161
Peaks in range	161
Peaks matched	55
Intensity scale factor	0.52*
Space group	R -3 m
Crystal system	trigonal (hexagonal axes)
Unit cell	a= 7.5100 Å c= 43.2900 Å
I/Ic	4.67
Calc. density	5.263 g/cm³
Reference	Gasperin M, "Synthese d'une nouvelle famille d'oxydes doubles: A~8~^+^ B~22~^5+^O~59~ structure du compose a thallium et niobium", Acta Crystallographica B (24,1968-38,1982) **33**, 398-402 (1977)

J: NIOBIUM THALLIUM OXIDE (3.1/1/8.2) (2.3 %)*

Formula sum	Nb3.09 O8.22 Tl
Entry number	96-100-1011
Figure-of-Merit (FoM)	0.616033*
Total number of peaks	308
Peaks in range	308
Peaks matched	48
Intensity scale factor	0.30*
Space group	C 2 2 21
Crystal system	orthorhombic
Unit cell	a= 7.5510 Å b= 13.0050 Å c= 7.7340 Å
I/Ic	5.07
Calc. density	5.448 g/cm³
Reference	Gasperin M, "Un niobate de thallium de type 'bronze hexagonal' excedentaire encations", Acta Crystallographica B (24,1968-38,1982) **33**, 2306-2308 (1977)

K: Mercury chromium strontium copper carbonate oxide (0.46/0.54/4/2/1/6.88) (1.5 %)*

Formula sum	C Cr0.54 Cu2 Hg0.46 O9.88 Sr4
Entry number	96-100-1638
Figure-of-Merit (FoM)	0.613438*
Total number of peaks	218
Peaks in range	218
Peaks matched	29
Intensity scale factor	0.22*
Space group	P 4/m m m
Crystal system	tetragonal
Unit cell	a= 3.8747 Å c= 16.1555 Å
I/Ic	5.59
Calc. density	5.258 g/cm³
Reference	Pelloquin D, Hervieu M, Malo S, Michel C, Maignan A, Raveau B, "Two transition-metal-substituted superconducting mercury-basedoxycarbonates, Hg(1-x) Mx Sr4 Cu2 (C O3) O(6+d) (M=Cr and Mo)", Physica C (Amsterdam) (152,1988-) **246**, 1-10 (1995)

L: Iron vanadium molybdenum oxide (4/1.98/3.02/20) (8.3 %)*

Formula sum	Fe4 Mo3.02 O20 V1.98
Entry number	96-100-0124
Figure-of-Merit (FoM)	0.686811*
Total number of peaks	462
Peaks in range	462
Peaks matched	116
Intensity scale factor	0.63*
Space group	P 41 2 2
Crystal system	tetragonal
Unit cell	a= 9.5390 Å c= 17.1411 Å
I/Ic	2.88
Calc. density	3.977 g/cm³
Reference	Laligant Y, Permer L, Le Bail A, "Crystal structure of Fe4 V2 Mo3 O20 determined from conventional X-raypowder diffraction data", European Journal of Solid State Inorganic Chemistry **32**, 325-334 (1995)

M: Hexastrontium trinitridodicuprate(I) dinitridocuprate(I) (1.4 %)*

Formula sum	Cu3 N5 Sr6
Entry number	96-100-5040
Figure-of-Merit (FoM)	0.629789*
Total number of peaks	354
Peaks in range	354
Peaks matched	41
Intensity scale factor	0.24*
Space group	P 42 m c
Crystal system	tetragonal
Unit cell	a= 8.6570 Å c= 7.3340 Å
I/Ic	6.65
Calc. density	4.751 g/cm³
Reference	DiSalvo F J, Trail S S, Yamane H, Brese N E, "The crystal structure of Sr6 Cu3 N5 with isolated, bent (Cu(I)2 N3)(7-)anions and the single crystal structural determination of Sr Cu N", Journal of Alloys Compd. **255**, 122-129 (1997)

N: Dithallium distrontium copper oxide (1.0 %)*

Formula sum	Cu O6 Sr2 Tl2
Entry number	96-100-1523
Figure-of-Merit (FoM)	0.614989*
Total number of peaks	144
Peaks in range	144
Peaks matched	21
Intensity scale factor	0.34*
Space group	I 4/m m m
Crystal system	tetragonal
Unit cell	a= 3.7464 Å c= 22.3013 Å
I/Ic	13.06
Calc. density	7.889 g/cm³
Reference	Martin C, Maignan A, Huve M, Michel C, Hervieu M, Raveau B, "The influence of alkaline-earth ions on the properties of the"2201"superconductive cuprates: the solid solution Tl~2~Ba~2-x~Sr~x~CuO~6+d~", European Journal of Solid State Inorganic Chemistry **30**, 7-18 (1993)

O: Dibarium octafluorotriniccolate decafluorotetraniccolate (10.7 %)*

Formula sum	Ba2 F18 Ni7
Entry number	96-100-0250
Figure-of-Merit (FoM)	0.624057*
Total number of peaks	500
Peaks in range	500
Peaks matched	146
Intensity scale factor	0.47*
Space group	P -1
Crystal system	triclinic (anorthic)
Unit cell	a= 6.9240 Å b= 7.2180 Å c= 7.4370 Å α= 94.390° β= 93.200 ° γ= 115.820 °
I/Ic	1.67
Calc. density	5.139 g/cm³
Reference	Renaudin J, Ferey G, Kozak A, Samouel M, Lacorre P, "Crystal and magnetic structures of the ferrimagnet Ba~2~ Ni~7~ F~18~", Solid State Communications **65**, 185-188 (1988)

P: Copper dipotassium dihydrogen phosphatochromate (14.6 %)*

Formula sum	Cr2 Cu H2 K2 O14 P2
Entry number	96-100-7043
Figure-of-Merit (FoM)	0.613908*
Total number of peaks	496
Peaks in range	496
Peaks matched	123
Intensity scale factor	0.40*
Space group	P 1 21/c 1
Crystal system	monoclinic
Unit cell	a= 9.5590 Å b= 7.1960 Å c= 8.9830 Å β= 93.730 °
I/Ic	1.05
Calc. density	2.869 g/cm³
Reference	Coing-Boyat J, Durif A, Guitel J C, "Structure cristalline d'un phosphochromate acide de cuivre potassium:Cu K~2~ H~2~ (P Cr O~7~)~2~", Journal of Solid State Chemistry **30**, 329-334 (1979)

Q: Bismuth molybdenum oxide (26.4/9.6/68.4) (2.0 %)*

Formula sum	Bi26.4 Mo9.6 O68.4
Entry number	96-100-4135
Figure-of-Merit (FoM)	0.683536*
Total number of peaks	497
Peaks in range	497
Peaks matched	178
Intensity scale factor	0.46*
Space group	P 1 2/c 1
Crystal system	monoclinic
Unit cell	a= 11.7525 Å b= 5.8005 Å c= 24.8024 Å β= 102.867 °
I/Ic	8.61
Calc. density	7.588 g/cm³
Reference	Vannier R-N, Abraham F, Nowogrocki G, Mairesse G, "New structural and electrical data on Bi-Mo mixed oxides with astructure based on (B12 O14)(infinite) columns", Journal of Solid State Chemistry **142**, 294-304 (1999)

R: Bismuth barium lanthanum copper oxide (2/2.3/0.7/2/8) (1.5 %)*

Formula sum	Ba2.3 Bi2 Cu2 La0.7 O8
Entry number	96-100-1701
Figure-of-Merit (FoM)	0.615640*
Total number of peaks	164
Peaks in range	164
Peaks matched	40
Intensity scale factor	0.36*
Space group	F m m m
Crystal system	orthorhombic
Unit cell	a= 5.5710 Å b= 5.5830 Å c= 31.1040 Å
I/Ic	8.90
Calc. density	7.457 g/cm³
Reference	Pham A Q, Hervieu H, Michel C, Raveau B, "A new member of the 2212-type family: the oxide Bi2 Ba2+x La1-x Cu2 O8+d", Physica C (Amsterdam) (152,1988-) **199**, 321-327 (1992)

S: Bismuth barium lanthanum copper oxide (1.6/2.5/0.9/2/8.3) (1.4 %)*

Formula sum	Ba2.5 Bi1.59 Cu2 La0.91 O8.25
Entry number	96-100-1586
Figure-of-Merit (FoM)	0.602812*
Total number of peaks	213
Peaks in range	213
Peaks matched	30
Intensity scale factor	0.31*
Space group	I 4/m m m
Crystal system	tetragonal
Unit cell	a= 3.9380 Å c= 31.2130 Å
I/Ic	8.73
Calc. density	7.254 g/cm³
Reference	Hervieu M, Pham A Q, Michel C, Raveau B, "A 2212 bismuth cuprate with a non-modulated structure Bi~2-x~La~x~Ba~2.5~La~0.5~Cu~2~O~8.25~", Physica C (Amsterdam) (152,1988-) **209**, 449-455 (1993)

T: Barium silicate germanate
**** (1.4 %)****

Formula sum	Ba Ge3.125 O9 Si0.875
Entry number	96-100-1067
Figure-of-Merit (FoM)	0.601248*
Total number of peaks	275
Peaks in range	275
Peaks matched	54
Intensity scale factor	0.17*
Space group	P 3 1 c
Crystal system	trigonal (hexagonal axes)
Unit cell	a= 11.5950 Å c= 9.7550 Å
I/Ic	4.55
Meas. density	4.660 g/cm³
Calc. density	4.673 g/cm³
Reference	Goreaud M, Choisnet J, Deschanvres A, Raveau B, "Synthese et Evolution Structurale de Nouveaux Silicogermanates Ba Ge(Ge~3-x~ Si~x~) O~9~ de Type Benitoite et de Structure Apparentee", Materials Research Bulletin **8**, 1205-1214 (1973)

(*)2theta values have been shifted internally for the calculation of the amounts, the intensity scaling factors as well as the figure-of-merit (FoM), due to the active search-match option 'Automatic zero point adaption'.

Search-Match

Settings

Reference database used	COD-Inorg 2023.06.06
Automatic zeropoint adaptation	Yes
Downgrade entries with low scaling factors	Yes
Minimum figure-of-merit (FoM)	0.60
2theta window for peak corr.	0.30 deg.
Minimum rel. int. for peak corr.	0
Parameter/influence 2theta	0.50
Parameter/influence intensities	0.50
Parameter multiple/single phase(s)	0.50

Peak List

No.	*2theta [°]*	*d [Å]*	*I/I0 (peak height)*	*Counts (peak area)*	*FWHM*	*Matched*
1	9.13	9.6783	23.81	24.39	0.1600	B,L,P,Q
2	15.87	5.5799	14.69	18.82	0.2000	A,C,F,H,I,M,N,P,Q
3	20.91	4.2449	77.08	39.49	0.0800	A,B,C,D,G,H,L
4	22.99	3.8654	27.96	35.81	0.2000	A,B,C,E,G,H,J,K,L,M,Q,R,S
5	24.03	3.7004	7.67	5.89	0.1200	A,C,D,F,G,H,L,M,N,O,P,Q,R,S,T
6	25.77	3.4543	8.79	11.25	0.2000	A,C,D,E,H,K,L,M,O,P,Q
7	26.63	3.3447	1000.00	768.48	0.1200	A,B,C,D,E,F,G,H,I,J,L,M,N,O,P,Q,R,S,T
8	27.55	3.2351	14.71	18.84	0.2000	A,B,C,D,F,G,H,I,J,K,L,O,Q
9	29.41	3.0346	122.68	94.28	0.1200	A,B,C,E,F,G,I,J,L,M,O,P,Q
10	30.09	2.9675	21.14	16.25	0.1200	B,C,D,F,G,H,I,L,O,Q,R,S,T
11	30.95	2.8870	42.13	75.54	0.2800	A,B,C,F,G,H,I,L,M,N,P,Q,T
12	32.19	2.7785	135.05	172.97	0.2000	A,B,C,D,E,F,G,H,I,K,L,M,N,O,P,Q,R,S,T
13	32.59	2.7454	148.34	152.00	0.1600	C,E,G,H,K,L,M,P,Q,R,S,T
14	33.33	2.6861	15.79	36.41	0.3600	A,B,C,D,G,H,J,K,L,M,P,Q,T
15	33.91	2.6414	25.60	59.03	0.3600	B,C,G,H,L,M,N,O,P,Q,R
16	34.35	2.6086	93.48	95.78	0.1600	A,B,C,D,F,G,H,I,K,L,O,P,Q,R,S
17	35.09	2.5553	12.71	22.79	0.2800	A,B,C,E,G,H,L,M,Q
18	36.53	2.4578	9.00	2.30	0.0400	A,B,C,D,F,G,H,I,J,K,L,O,P,Q,R,S,T
19	38.69	2.3254	15.47	3.96	0.0400	A,B,C,D,F,G,H,I,L,O,P,Q,T
20	39.47	2.2812	29.50	37.78	0.2000	A,C,D,F,G,H,I,K,L,M,O,P,Q,R,S
21	40.31	2.2356	20.76	26.59	0.2000	A,C,E,F,G,H,I,L,N,O,P,Q,R,S,T
22	41.25	2.1868	56.68	87.12	0.2400	A,B,C,G,H,L,M,O,Q,T
23	41.59	2.1697	8.85	9.07	0.1600	A,B,C,F,G,I,J,L,M,N,O,P,Q
24	42.47	2.1268	25.20	12.91	0.0800	A,B,C,D,E,F,G,H,I,J,L,M,O,P,Q,T
25	45.81	1.9792	33.30	17.06	0.0800	A,B,C,D,F,G,H,I,K,L,O,P,Q,R,S,T
26	46.89	1.9361	16.54	12.71	0.1200	A,B,C,D,E,G,H,J,K,L,M,O,Q,R,T
27	47.59	1.9092	11.09	11.36	0.1600	A,C,F,G,H,K,L,N,O,P,Q,R,S,T
28	48.57	1.8730	42.13	21.59	0.0800	A,B,C,D,E,F,G,H,I,J,L,M,N,O,P,Q,T
29	50.15	1.8176	74.34	57.13	0.1200	A,B,C,D,F,G,H,I,J,K,L,M,O,P,Q,T
30	51.71	1.7664	44.69	45.79	0.1600	A,B,C,D,F,G,H,I,J,K,L,N,O,P,Q,R,S,T
31	54.87	1.6719	15.92	20.39	0.2000	A,B,C,D,E,F,G,H,I,J,L,N,O,P,Q,R,S,T
32	56.43	1.6293	22.64	17.40	0.1200	A,B,C,D,E,F,G,H,I,J,K,L,N,O,P,Q,T
33	59.99	1.5408	46.83	23.99	0.0800	A,B,C,D,E,G,H,I,L,M,O,P,Q,T
34	62.21	1.4911	28.82	36.92	0.2000	A,B,C,D,F,H,I,J,K,L,O,P,R,S,T
35	62.39	1.4872	16.93	21.68	0.2000	A,B,C,D,F,H,I,J,K,L,M,N,O,P,T
36	67.79	1.3813	20.36	15.65	0.1200	A,B,C,D,F,H,I,J,K,L,M,N,O,P,R,S,T
37	68.29	1.3724	26.35	33.75	0.2000	A,B,C,D,F,H,I,J,K,L,M,O,P,R,S,T
38	75.71	1.2552	42.92	21.99	0.0800	A,B,C,D,J,K,L,M,O,P,S,T
39	75.93	1.2522	17.88	13.74	0.1200	A,B,C,D,F,I,J,L,M,O,P
40	79.91	1.1995	33.61	25.83	0.1200	A,B,C,D,E,J,K,L,M,N,O,P,R,S
41	80.13	1.1968	17.88	13.74	0.1200	A,B,D,J,K,L,M,N,O,P,R,T
42	81.47	1.1804	23.57	18.11	0.1200	A,B,D,E,J,K,L,M,O,P,R,S,T
43	81.71	1.1776	8.76	6.73	0.1200	A,B,D,J,K,L,M,N,O,P,R,S,T
44	83.85	1.1529	9.58	7.36	0.1200	A,D,J,K,L,M,O,P,R,S,T

Integrated Profile Areas

Based on calculated profile

Profile area	***Counts***	***Amount***
Overall diffraction profile	591073	100.00%
Background radiation	419413	70.96%
Diffraction peaks	171660	29.04%
Peak area belonging to selected phases	170898	28.91%
Peak area of phase A (Iron vanadium molybdenum oxide (4/1.98/3.02/20))	*11379*	*1.93%*
Peak area of phase B (Dibarium octafluorotriniccolate decafluorotetraniccolate)	*14771*	*2.50%*
Peak area of phase C (Sodium strontium iron(III) hexafluoride)	*12203*	*2.06%*
Peak area of phase D (Niobium thallium oxide hydrate (33/10.5/88.5/1.5))	*10152*	*1.72%*
Peak area of phase E (NIOBIUM THALLIUM OXIDE (3.1/1/8.2))	*3064*	*0.52%*
Peak area of phase F (Rubidium niobium tungsten oxide (12/30/3/90))	*11314*	*1.91%*
*Peak area of phase G (Barium silicate germanate *)*	*3580*	*0.61%*
*Peak area of phase H (Sodium tungstate phosphate *)*	*5189*	*0.88%*
Peak area of phase I (Thallium niobium uranium oxide (1/2/2/11.5))	*13637*	*2.31%*
Peak area of phase J (Dithallium distrontium copper oxide)	*5456*	*0.92%*
*Peak area of phase K (Potassium tecto-phosphatovanadate(III) *)*	*15020*	*2.54%*
Peak area of phase L (Bismuth barium lanthanum copper oxide (1.6/2.5/0.9/2/8.3))	*4148*	*0.70%*
Peak area of phase M (Mercury chromium strontium copper carbonate oxide (0.46/0.54/4/2/1/6.88))	*4918*	*0.83%*
Peak area of phase N (Nonacaesium tecto-trialumononamolybdo(V)undecaphosphate(V))	*10746*	*1.82%*

Peak area of phase O (Bismuth barium lanthanum copper oxide (2/2.3/0.7/2/8))	*4423*	*0.75%*
Peak area of phase P (Sodium dirubidium tecto-hexaniobotriphosphate(V))	*10447*	*1.77%*
Peak area of phase Q (Bismuth molybdenum oxide (26.4/9.6/68.4))	*5020*	*0.85%*
Peak area of phase R (Thallium niobium oxide (8/27.2/72))	*4866*	*0.82%*
Peak area of phase S (Hexastrontium trinitridodicuprate(I) dinitridocuprate(I))	*3134*	*0.53%*
Peak area of phase T (Copper dipotassium dihydrogen phosphatochromate)	*17429*	*2.95%*
Unidentified peak area	763	0.13%

Diffraction Pattern Graphics

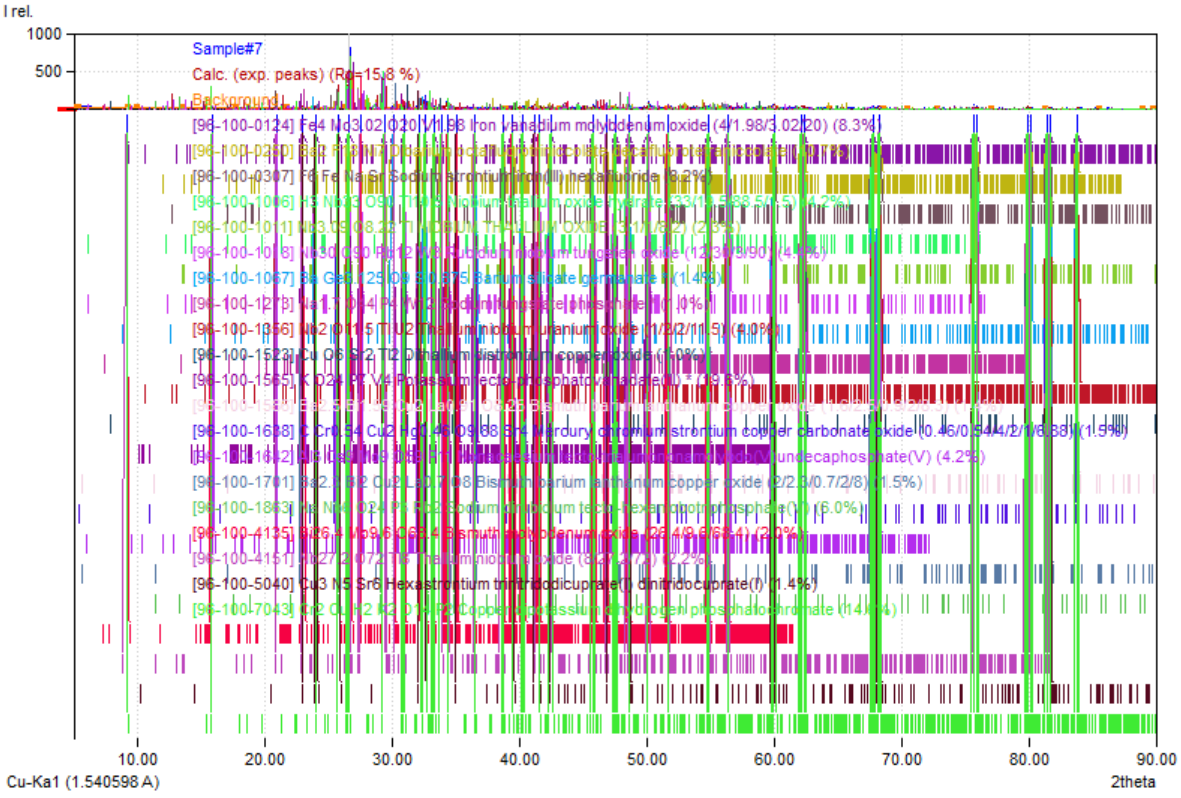

Match! Copyright © 2003-2023 CRYSTAL IMPACT, Bonn, Germany

Amounts of Phases and Elements (Weight %)

Phase composition:

Potassium tecto-phosphatovanadate(III) * (19.6%), Copper dipotassium dihydrogen phosphatochromate (14.6%), Dibarium octafluorotriniccolate decafluorotetraniccolate (10.7%), Iron vanadium molybdenum oxide (4/1.98/3.02/20) (8.3%), Sodium strontium iron(III) hexafluoride (8.2%), Sodium dirubidium tecto-hexaniobotriphosphate(V) (6.0%), Rubidium niobium tungsten oxide (12/30/3/90) (4.4%), Nonacaesium tecto-trialumononamolybdo(V)undecaphosphate(V) (4.2%), Niobium thallium oxide hydrate (33/10.5/88.5/1.5) (4.2%), Thallium niobium uranium oxide (1/2/2/11.5) (4.0%), NIOBIUM THALLIUM OXIDE (3.1/1/8.2) (2.3%), Thallium niobium oxide (8/27.2/72) (2.2%), Bismuth molybdenum oxide (26.4/9.6/68.4) (2.0%), Bismuth barium lanthanum copper oxide (2/2.3/0.7/2/8) (1.5%), Mercury chromium strontium copper carbonate oxide (0.46/0.54/4/2/1/6.88) (1.5%), Barium silicate germanate * (1.4%), Hexastrontium trinitridodicuprate(I) dinitridocuprate(I) (1.4%), Bismuth barium lanthanum copper oxide (1.6/2.5/0.9/2/8.3) (1.4%), Dithallium distrontium copper oxide (1.0%), Sodium tungstate phosphate * (1.0%)

Elemental composition:

O (26.32%), Nb (9.57%), P (7.66%), F (6.89%), V (5.64%), Sr (4.40%), Ni (4.28%), Ba (4.12%), Tl (4.10%), Mo (3.90%), Fe (3.62%), K (3.05%), Cr (2.90%), Cu (2.75%), Bi (2.50%), U (1.81%), Rb (1.61%), Cs (1.48%), W (1.12%), Na (0.80%), Ge (0.61%), La (0.30%), Hg (0.18%), N (0.12%), Al (0.10%), Si (0.07%), H (0.06%), C (0.02%) (LE: 33.41%)

Match! Phase Analysis Report

Sample: Sample_B

Sample Data

File name	Sample#B.raw
File path	G:/.shortcut-targets-by-id/16KlMvpSIqVAUHFFggq9lVgYQzQybBTlu/Marwan - research/Concrete Mix Master Thesis/X-Ray/Birzeit University_XRD_Raw data
Data collected	Jul 13, 2023 08:02:51
Data range	4.950° - 89.950°
Original data range	5.000° - 90.000°
Number of points	4251
Step size	0.020
Rietveld refinement converged	No
Alpha2 subtracted	No
Background subtr.	No
Data smoothed	No
2theta correction	-0.05°
Radiation	X-rays
Wavelength	1.540598 Å

Analysis Results

Phase composition (Weight %)

Elemental composition (Weight %)

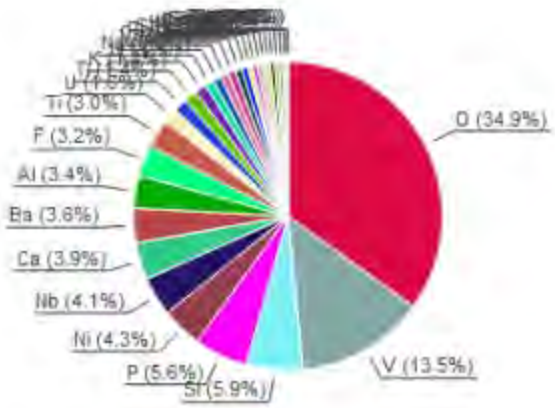

Index	*Amount (%)*	*Name*	*Formula sum*
A	1.1	Yttrium oxide	O3 Y2
B	14.6	Vanadium oxide (5/9)	O9 V5
C	3.4	Sodium nitrate Nitratine	N Na O3
D	10.9	Silicon oxide $-alpha Quartz low	O2 Si
E	4.4	Rubidium niobium tungsten oxide (12/[illegible]/90)	Nb30 O90 Rb13 W3
F	17.4	Potassium tecto-phosphatovanadate(K) /	K O24 P7 [illegible]
G	[illegible]	[illegible]	[illegible]
H	2.9	Potassium barium phosphate	Ba K O4 P
I	4.3	Niobium thallium oxide hydrate (33/10.5/88.5/1.5)	H3 Nb33 O90 Tl10.5
J	0.6	Holmium oxide	Ho2 O3
K	0.7	Hexastrontium trinitridodicuprate(I) dinitridocuprate(I)	Cu3 N5 Sr6
L	0.5	Dysprosium oxide	Dy2 O3
M	2.7	Dinickel diphosphate	Ni2 O7 P2
N	7.5	Dibarium octafluorotrinioccolate decafluoroaluminoccolate	Ba2 F18 Ni7
O	2.3	Chromium uranium(V) oxide	Cr O4 U
P	3.6	Calcium carbonate Calcite	C Ca O3
Q	1.9	Caesium zinc phosphate(V) - I	Cs O4 P Zn
R	1.9	Antimony selenide iodide	I Sb Se
S	11.5	Aluminium pentaoxotitanate	Al2 O5 Ti
T	5.5		Ca4 F2 O7 Si2
	1.7	*Unidentified peak area*	

Amounts calculated by RIR (Reference Intensity Ratio) method

Element	*Amount (weight %)*
O	*34.9%(*)*
V	13.5%
[illegible]	[illegible]
P	5.6%
Ni	4.3%
Nb	4.1%
Ca	3.9%
Ba	3.6%
Al	3.4%
F	3.2%(*)
Ti	3.0%
Tl	1.4%
h	1.4%
I	1.2%
Na	0.9%
Y	0.9%
Cs	0.8%
Rb	0.8%
Sb	0.7%
N	*0.6%(*)*
[illegible]	[illegible]
Sr	0.5%
Dy	0.5%
[illegible]	[illegible]
[illegible]	[illegible]

C	0.49%(*)
[illegible]	[illegible]
[illegible]	[illegible]
[illegible]	[illegible]

Formula sum	Nb30 O90 Rb12 W3
Entry number	96-100-1018
Figure-of-Merit (FoM)	0.637895*
Total number of peaks	161
Peaks in range	161
Peaks matched	52
Intensity scale factor	0.59*
Space group	R -3 m
Crystal system	trigonal (hexagonal axes)
Unit cell	a= 7.4860 Å c= 43.1000 Å
I/Ic	4.33
Meas. density	4.570 g/cm³
Calc. density	4.608 g/cm³
Reference	Michel C, Guyomarch A, Raveau B, "Nouveaux echangeurs cationiques avec une structure a tunnelsentrecroises: les oxydes A~12~ M~33~ O~90~ et A~12~ M~33~ O~90~(H~2~ O)~12~", Journal of Solid State Chemistry **22**, 393-403 (1977)

F: Potassium tecto-phosphatovanadate(III) * (17.4 %)*

Formula sum	K O24 P7 V4
Entry number	96-100-1565
Figure-of-Merit (FoM)	0.643511*
Total number of peaks	499
Peaks in range	499
Peaks matched	207
Intensity scale factor	0.51*
Space group	P -1
Crystal system	triclinic (anorthic)
Unit cell	a= 10.0846 Å b= 10.2309 Å c= 10.8283 Å α= 112.757° β= 109.226 ° γ= 104.875 °
I/Ic	3.05
Calc. density	3.202 g/cm³
Reference	Benhamada L, Grandin A, Borel M M, Leclaire A, Raveau B, "A vanadium(III) phosphate with V~2~O~10~ octahedral units KV~4~P~7~O~24~", Journal of Solid State Chemistry **104**, 193-201 (1993)

G: Potassium iodate telluric acid (1.6 %)*

Formula sum	H6 I K O9 Te
Entry number	96-100-8207
Figure-of-Merit (FoM)	0.640600*
Total number of peaks	499
Peaks in range	499
Peaks matched	115
Intensity scale factor	0.24*
Space group	P c 21 n
Crystal system	orthorhombic
Unit cell	a= 14.2200 Å b= 6.6960 Å c= 8.6720 Å
I/Ic	4.76
Calc. density	3.520 g/cm³
Reference	Averbuch-Pouchot M. T., "Crystal Chemistry of Some Addition Compounds of Alkali Iodates withTelluric Acid", Journal of Solid State Chemistry **49**, 368-378 (1983)

H: Potassium barium phosphate (2.9 %)*

Formula sum	Ba K O4 P
Entry number	96-100-7162
Figure-of-Merit (FoM)	0.615253*
Total number of peaks	500
Peaks in range	500
Peaks matched	66
Intensity scale factor	0.31*
Space group	P n m a
Crystal system	orthorhombic
Unit cell	a= 7.7090 Å b= 5.6630 Å c= 9.9720 Å
I/Ic	3.41
Calc. density	4.140 g/cm³
Reference	Masse R, Durif A, "Chemical preparation and crystal structure refinement of ß Ba P O~4~-monophosphate", Journal of Solid State Chemistry **71**, 574-576 (1987)

I: Niobium thallium oxide hydrate (33/10.5/88.5/1.5) (4.3 %)*

Formula sum	H3 Nb33 O89 Tl10.5
Entry number	96-100-1006
Figure-of-Merit (FoM)	0.676282*
Total number of peaks	161
Peaks in range	161
Peaks matched	59
Intensity scale factor	0.63*
Space group	R -3 m
Crystal system	trigonal (hexagonal axes)

Unit cell	a= 7.5100 Å c= 43.2900 Å
I/Ic	4.67
Calc. density	5.263 g/cm³
Reference	Gasperin M, "Synthese d'une nouvelle famille d'oxydes doubles: A~8~^+^ B~22~^5+^O~69~ structure du compose a thallium et niobium", Acta Crystallographica B (24,1968-38,1982) **33**, 398-402 (1977)

J: Holmium oxide (0.6 %)

Formula sum	Ho2 O3
Entry number	96-101-0336
Figure-of-Merit (FoM)	0.605943
Total number of peaks	84
Peaks in range	84
Peaks matched	15
Intensity scale factor	0.31
Space group	I 21 3
Crystal system	cubic
Unit cell	a= 10.5800 Å
I/Ic	17.87
Calc. density	8.477 g/cm³
Reference	Zachariasen W, "The crystal structure of the modification C of the sesquioxides of therare earth metals, and of indium and thallium.", Norsk Geologisk Tidsskrift **9**, 310-316 (1927)

K: Hexastrontium trinitridodicuprate(I) dinitridocuprate(I) (0.7 %)

Formula sum	Cu3 N5 Sr6
Entry number	96-100-5040
Figure-of-Merit (FoM)	0.639172
Total number of peaks	354
Peaks in range	354
Peaks matched	46
Intensity scale factor	0.15
Space group	P 42 m c
Crystal system	tetragonal
Unit cell	a= 8.6570 Å c= 7.3340 Å
I/Ic	5.65
Calc. density	4.751 g/cm³
Reference	DiSalvo F J, Trail S S, Yamane H, Biese N E, "The crystal structure of Sr6 Cu3 N5 with isolated, bent (Cu(I)2 N3)(7-)anions and the single crystal structural determination of Sr Cu N", Journal of Alloys Compd. **255**, 122-129 (1997)

L: Dysprosium oxide (0.5 %)

Formula sum	Dy2 O3
Entry number	96-101-0337
Figure-of-Merit (FoM)	0.634746
Total number of peaks	84
Peaks in range	84
Peaks matched	14
Intensity scale factor	0.30
Space group	I 21 3
Crystal system	cubic
Unit cell	a= 10.6300 Å
I/Ic	17.80
Calc. density	8.250 g/cm³
Reference	Zachariasen W, "The crystal structure of the modification C of the sesquioxides of therare earth metals, and of indium and thallium.", Norsk Geologisk Tidsskrift **9**, 310-316 (1927)

M: Dinickel diphosphate (2.7 %)

Formula sum	Ni2 O7 P2
Entry number	96-100-7248
Figure-of-Merit (FoM)	0.644435
Total number of peaks	500
Peaks in range	500
Peaks matched	58
Intensity scale factor	0.22
Space group	P 1 21/a 1
Crystal system	monoclinic
Unit cell	a= 5.2120 Å b= 9.9130 Å c= 4.4750 Å β= 97.460 °
I/Ic	2.59
Meas. density	3.080 g/cm³
Calc. density	3.220 g/cm³
Reference	Masse R, Guitel J C, Durif A, "Structure cristalline d'une nouvelle variete de pyrophosphate donickel Ni2 P2 O7", Materials Research Bulletin **14**, 337-341 (1979)

N: Dibarium octafluorotriniccolate decafluorotetraniccolate (7.9 %)

Formula sum	Ba2 F18 Ni7
Entry number	96-100-0249
Figure-of-Merit (FoM)	0.605674

Total number of peaks	498
Peaks in range	498
Peaks matched	161
Intensity scale factor	0.33
Space group	P -1
Crystal system	triclinic (anorthic)
Unit cell	a= 6.9370 Å b= 7.2290 Å c= 7.4560 Å α= 94.370° β= 93.160 ° γ= 115.860 °
I/Ic	1.35
Calc. density	5.110 g/cm³
Reference	Renaudin J, Ferey G, Kozak A, Samouel M, Lacorre P, "Crystal and magnetic structures of the ferrimagnet Ba~2~ Ni~7 F~18~", Solid State Communications **65**, 185-188 (1988)

O: Chromium uranium(V) oxide (2.3 %)

Formula sum	Cr O4 U
Entry number	96-100-8068
Figure-of-Merit (FoM)	0.640274
Total number of peaks	335
Peaks in range	335
Peaks matched	33
Intensity scale factor	0.94
Space group	P b c n
Crystal system	orthorhombic
Unit cell	a= 4.8710 Å b= 11.7870 Å c= 5.0530 Å
I/Ic	12.96
Calc. density	6.105 g/cm³
Reference	Bacmann M, Bertaut E F, "Structure de U Cr O~4~", Bulletin de la Societe Francaise de Mineralogie et de Cristallographie(72,1949-100,1977) **87**, 275-276 (1964)

P: Calcium carbonate Calcite (3.6 %)

Formula sum	C Ca O3
Entry number	96-101-0929
Figure-of-Merit (FoM)	0.701855
Total number of peaks	64
Peaks in range	64
Peaks matched	15
Intensity scale factor	0.34
Space group	R -3 c
Crystal system	rhombohedral
Unit cell	a= 6.3600 Å α= 46.100°
I/Ic	3.62
Calc. density	4.035 g/cm³
Reference	Elliott N, "A Redetermination of the Carbon - Oxygen Distance in Calcite and theNitrogen - Oxygen Distance in Sodium Nitrate", Journal of the American Chemical Society **59**, 1380-1382 (1937)

Q: Caesium zinc phosphate(V) - I (1.9 %)

Formula sum	Cs O4 P Zn
Entry number	96-100-7239
Figure-of-Merit (FoM)	0.615548
Total number of peaks	497
Peaks in range	497
Peaks matched	70
Intensity scale factor	0.29
Space group	P *n* m a
Crystal system	orthorhombic
Unit cell	a= 9.1940 Å b= 5.4900 Å c= 9.3880 Å
I/Ic	5.09
Calc. density	4.110 g/cm³
Reference	Blum D, Durif A, Averbuch-Pouchot M T, "Crystal structures of the three forms of Cs Zn P O4", Ferroelectrics **69**, 283-292 (1986)

R: Antimony selenide iodide (1.9 %)

Formula sum	I Sb Se
Entry number	96-100-8205
Figure-of-Merit (FoM)	0.647549
Total number of peaks	488
Peaks in range	488
Peaks matched	43
Intensity scale factor	0.45
Space group	P *n* m a
Crystal system	orthorhombic
Unit cell	a= 8.6980 Å b= 4.1270 Å c= 10.4120 Å
I/Ic	7.57
Calc. density	5.822 g/cm³
Reference	Ibanez A, Jumas J C, Olivier-Fourcade J, Philippot E, Maurin M, "Sur les Chalcogeno-iodures d'antimoine SbXI

(X=S,Se,Te) Structures et spectroscopie Moessbauer de *121^Sb", Journal of Solid State Chemistry **48**, 272-283 (1983)

S: Aluminium pentaoxotitanate (11.5 %)*

Formula sum	Al2 O5 Ti
Entry number	96-100-0061
Figure-of-Merit (FoM)	0.604941*
Total number of peaks	233
Peaks in range	233
Peaks matched	29
Intensity scale factor	0.55*
Space group	B b m m
Crystal system	orthorhombic
Unit cell	a= 9.4290 Å b= 9.6360 Å c= 3.5910 Å
I/Ic	1.54
Calc. density	3.701 g/cm³
Reference	Morosin B, Lynch R W, "Structure studies on Al~2~ Ti O~5~ at room temperature and at 600C", *Acta Crystallographica B (24,1968-38,1982)* **28**, 1040-1046 (1972)

T: Ca4 F2 O7 Si2 (5.5 %)*

Formula sum	Ca4 F2 O7 Si2
Entry number	96-110-0154
Figure-of-Merit (FoM)	0.661531*
Total number of peaks	500
Peaks in range	500
Peaks matched	163
Intensity scale factor	0.26*
Space group	P 1 21/c 1
Crystal system	monoclinic
Unit cell	a= 7.5397 Å b= 10.5338 Å c= 10.9070 Å β= 109.557 °
I/Ic	1.54
Calc. density	2.982 g/cm³
Reference	Kruger Hannes, Kahlenberg Volker

(*)2theta values have been shifted internally for the calculation of the amounts, the intensity scaling factors as well as the figure-of-merit (FoM), due to the active search-match option 'Automatic zero point adaption'.

Search-Match

Settings

Reference database used	COD-Inorg 2023.06.06
Automatic zeropoint adaptation	Yes
Downgrade entries with low scaling factors	Yes
Minimum figure-of-merit (FoM)	0.60
2theta window for peak corr.	0.30 deg
Minimum rel. int. for peak corr.	0
Parameter/influence 2theta	0.50
Parameter/influence intensities	0.50
Parameter multiple/single phase(s)	0.50

Peak List

No.	2theta [°]	d [Å]	I/I0 (peak height)	Counts (peak area)	FWHM	Matched
1	18.01	4.9214	16.98	10.58	0.0800	B,F,G,H,M
2	20.79	4.2692	141.84	176.77	0.1600	A,B,D,F,G,J,K,Q,S,T
3	22.99	3.8654	20.60	19.25	0.1200	B,C,F,G,H,K,O,P,R
4	25.97	3.7095	13.80	8.60	0.0800	A,B,E,F,G,I,J,K,N,T
5	26.57	3.3521	1000.00	934.72	0.1200	B,D,E,F,G,H,I,J,K,L,M,N,O,Q,R,S,T
6	27.23	3.2723	7.64	28.58	0.4800	B,F,G,I,M,Q,T
7	29.35	3.0406	187.63	350.76	0.2400	A,B,C,E,F,G,H,I,J,K,L,M,N,O,P,R,T
8	30.87	2.8943	44.42	69.21	0.2000	B,E,F,G,I,K,M,Q,R,T
9	32.13	2.7836	13.32	12.45	0.1200	B,C,E,F,I,K,M,N,R
10	32.51	2.7519	13.01	52.72	0.5200	B,F,G,K,Q,S
11	33.81	2.6490	13.24	12.37	0.1200	A,F,G,J,K,L,M,N,R,S,T
12	34.05	2.6309	10.27	6.40	0.0800	B,F,G,O,T
13	35.91	2.4988	16.74	20.86	0.1600	A,B,E,F,G,H,I,J,L,M,N,P,R,T
14	36.49	2.4604	19.91	24.81	0.1600	B,D,E,F,G,H,I,M,N,T
15	39.39	2.2857	52.41	97.98	0.2400	B,D,E,F,G,H,I,K,M,N,P,Q,S,T
16	40.23	2.2399	22.91	14.28	0.0800	B,D,E,F,G,H,I,J,M,N,O,Q,R,T
17	41.13	2.1929	10.50	19.63	0.2400	B,F,G,H,K,N,O,Q,T
18	42.37	2.1315	35.79	22.30	0.0800	B,C,D,E,F,G,H,I,K,M,N,O,Q,R,S,T
19	43.09	2.0976	22.41	27.93	0.1600	B,F,G,H,I,K,L,M,N,O,P,Q,T
20	45.73	1.9824	12.30	15.33	0.1600	B,D,E,F,G,I,N,R,T
21	47.41	1.9160	27.98	34.87	0.1600	B,E,F,G,H,I,M,N,O,P,R,T
22	48.45	1.8773	23.57	58.74	0.3200	A,B,C,E,F,G,H,I,J,K,L,N,O,P,Q,R,T
23	50.09	1.8196	212.73	132.56	0.0800	A,B,D,E,F,G,H,I,J,K,L,M,N,R,T
24	50.75	1.7975	7.21	8.99	0.1600	B,D,E,F,G,H,I,K,M,N,Q,R,S,T
25	54.81	1.6736	12.09	18.83	0.2000	A,B,D,E,F,G,H,I,J,L,M,N,O,Q,R,S,T
26	55.23	1.6618	10.26	8.59	0.1200	B,D,E,F,G,H,I,K,M,N,Q,R,T
27	57.33	1.6058	12.63	23.62	0.2400	A,B,D,E,F,G,H,I,K,L,M,N,O,P,Q,R,S,T
28	59.91	1.5427	171.04	106.58	0.0800	B,C,D,F,G,K,M,N,O,R,T

29	60.07	1.5390	86.69	54.02	0.0800	B,F,G,I,K,L,N,O,Q,T
30	60.65	1.5256	9.21	2.87	0.0400	A,B,E,G,H,I,J,K,M,N,O,Q,R,T
31	60.89	1.5202	8.29	15.43	0.2400	B,C,E,G,H,I,K,M,N,O,P,R,S,T
32	63.95	1.4546	6.43	8.02	0.1600	B,D,E,G,H,I,K,M,N,Q,R,S,T
33	65.73	1.4195	5.66	3.53	0.0800	A,B,D,E,G,H,I,J,K,L,M,N,O,P,Q,T
34	67.67	1.3834	29.06	27.16	0.1200	B,D,E,G,H,I,N,Q,T
35	67.85	1.3802	14.52	13.57	0.1200	B,E,G,H,I,K,N,R,T
36	68.07	1.3763	21.65	20.24	0.1200	B,H,K,N,O,Q,S,T
37	68.23	1.3734	18.98	23.67	0.1600	B,D,E,G,H,I,K,N,O,Q,R,S,T
38	73.39	1.2891	6.86	8.57	0.1600	A,D,E,G,H,I,K,L,M,N,O,Q,R,T
39	75.59	1.2569	17.27	10.76	0.0800	D,E,G,H,K,M,N,O,Q,R,S,T
40	75.81	1.2538	8.66	5.40	0.0800	A,G,H,I,K,L,M,N,O,Q,S,T
41	79.83	1.2005	12.49	7.79	0.0800	A,C,D,G,H,K,L,M,N,T
42	80.01	1.1982	7.16	11.15	0.2000	D,G,H,J,K,M,N,O,Q,R,S,T
43	81.11	1.1848	18.85	17.62	0.1200	A,D,G,H,K,M,N,P,Q,R,S
44	81.37	1.1816	18.37	17.17	0.1200	C,D,G,J,K,M,N,O,Q,R,S
45	81.65	1.1783	5.80	3.61	0.0800	G,K,M,N,O,P,Q,R,S
46	83.75	1.1540	9.79	9.15	0.1200	A,C,D,G,J,K,M,N,O,R,S
47	83.97	1.1515	6.34	13.64	0.2800	G,H,N,P,Q,S

Integrated Profile Areas

Based on calculated profile

Profile area	*Counts*	*Amount*
Overall diffraction profile	625091	100.00%
Background radiation	422104	67.53%
Diffraction peaks	202987	32.47%
Peak area belonging to selected phases	192049	30.72%
Peak area of phase A (Yttrium oxide)	*2618*	*0.42%*
Peak area of phase B (Vanadium oxide (5/9))	*9892*	*1.58%*
Peak area of phase C (Sodium nitrate Nitratine)	*2336*	*0.37%*
Peak area of phase D (Silicon oxide S-alpha Quartz low)	*31334*	*5.01%*
Peak area of phase E (Rubidium niobium tungsten oxide (12/30/3/90))	*15392*	*2.46%*
*Peak area of phase F (Potassium tecto-phosphalovanadate(III) *)*	*20917*	*3.35%*
Peak area of phase G (Potassium iodate telluric acid)	*6738*	*1.08%*
Peak area of phase H (Potassium barium phosphate)	*9088*	*1.45%*
Peak area of phase I (Niobium thallium oxide hydrate (33/10,5/68,5/1,5))	*16315*	*2.61%*
Peak area of phase J (Holmium oxide)	*3141*	*0.50%*
Peak area of phase K (Hexastrontium trinitridodicuprate(I) dinitridocuprate(I))	*2063*	*0.33%*
Peak area of phase L (Dysprosium oxide)	*2272*	*0.36%*
Peak area of phase M (Dinickel diphosphate)	*3611*	*0.58%*
Peak area of phase N (Dibarium octafluorotrinitrocobaltate decafluorotetranitrocobaltate)	*16120*	*2.58%*
Peak area of phase O (Chromium uranium(V) oxide)	*14398*	*2.30%*
Peak area of phase P (Calcium carbonate Calcite)	*3930*	*0.63%*
Peak area of phase Q (Caesium zinc phosphate(V) - (I)	*6466*	*1.03%*
Peak area of phase R (Antimony selenide iodide)	*7884*	*1.26%*
Peak area of phase S (Aluminium pentaoxotitanate)	*11140*	*1.78%*
Peak area of phase T (Ca4 F2 O7 Si2)	*6391*	*1.02%*
Unidentified peak area	10937	1.75%

Diffraction Pattern Graphics

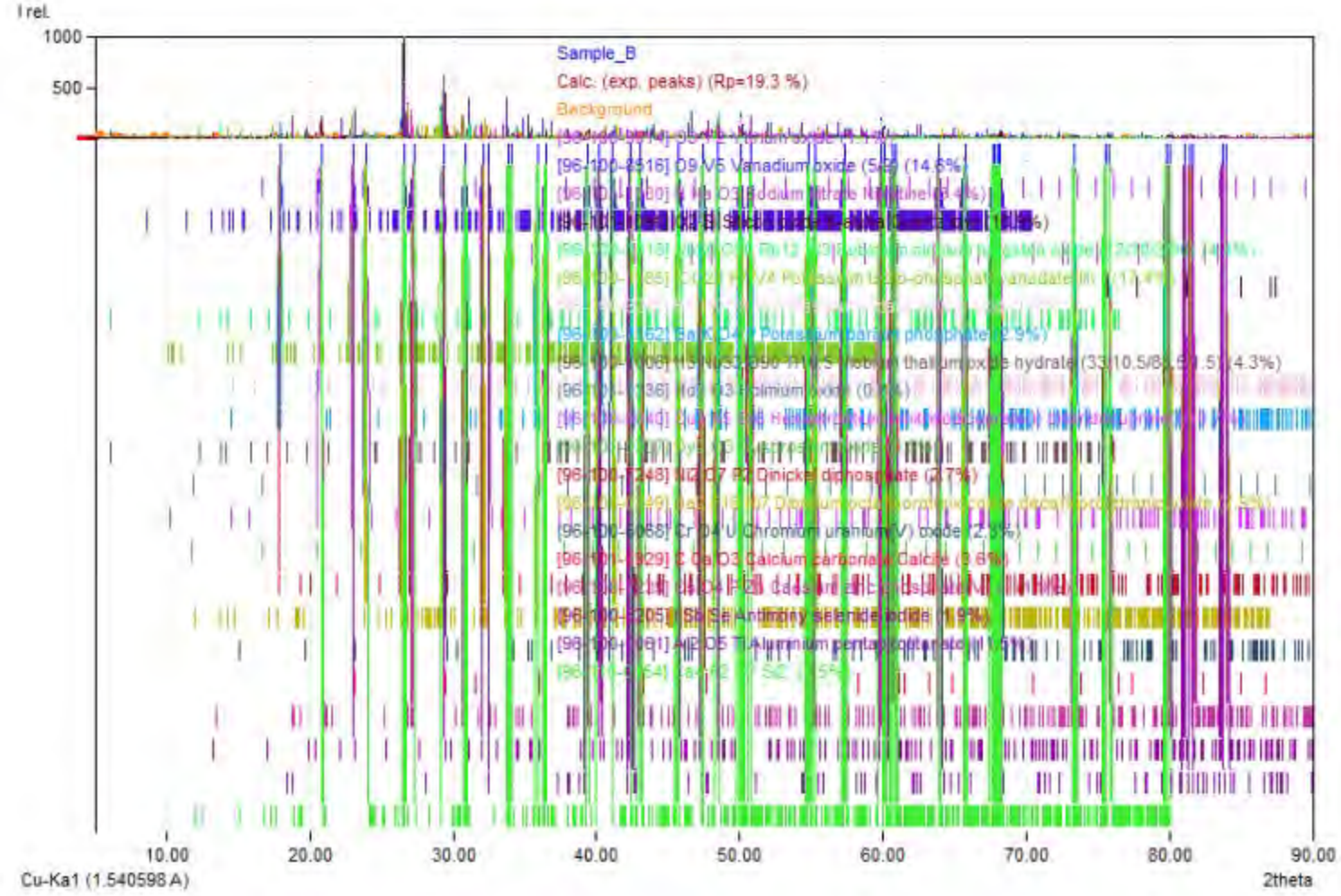

Match! Copyright © 2003-2023 CRYSTAL IMPACT, Bonn, Germany

Amounts of Phases and Elements (Weight %)

Phase composition:

Potassium tecto-phosphatovanadate(III) * (17.4%), Vanadium oxide (5/9) (14.6%), Aluminium pentaoxotitanate (11.5%), Silicon oxide S-alpha Quartz low (10.9%), Dibarium octafluorotriniccolate decafluorotetraniccolate (7.9%), Ca4 F2 O7 Si2 (5.5%), Rubidium niobium tungsten oxide (12/30/3/90) (4.4%), Niobium thallium oxide hydrate (33/10.5/88.5/7.5) (4.3%), Calcium carbonate Calcite (3.6%), Sodium nitrate Nitratine (3.4%), Potassium barium phosphate (2.9%), Dinickel diphosphate (2.7%), Chromium uranium(V) oxide (2.3%), Antimony selenide iodide (1.9%), Caesium zinc phosphate(V) - I (1.9%), Potassium iodate telluric acid (1.6%), Yttrium oxide (1.1%), Hexastrontium trinitridodicuprate(I) dinitridocuprate(I) (0.7%), Holmium oxide (0.6%), Dysprosium oxide (0.5%)

Elemental composition:

O (34.94%), V (13.52%), Si (5.93%), P (5.60%), Ni (4.27%), Nb (4.10%), Ca (3.88%), Ba (3.61%), Al (3.42%), F (3.21%), Ti (3.04%), U (1.57%), Tl (1.39%), K (1.37%), I (1.20%), Na (0.93%), Y (0.87%), Cs (0.84%), Rb (0.78%), Sb (0.71%), N (0.63%), Ho (0.49%), Sr (0.49%), Dy (0.47%), Se (0.46%), Te (0.45%), C (0.44%), W (0.42%), Zn (0.41%), Cr (0.34%), Cu (0.18%), H (0.02%) (LE: 39.24%)

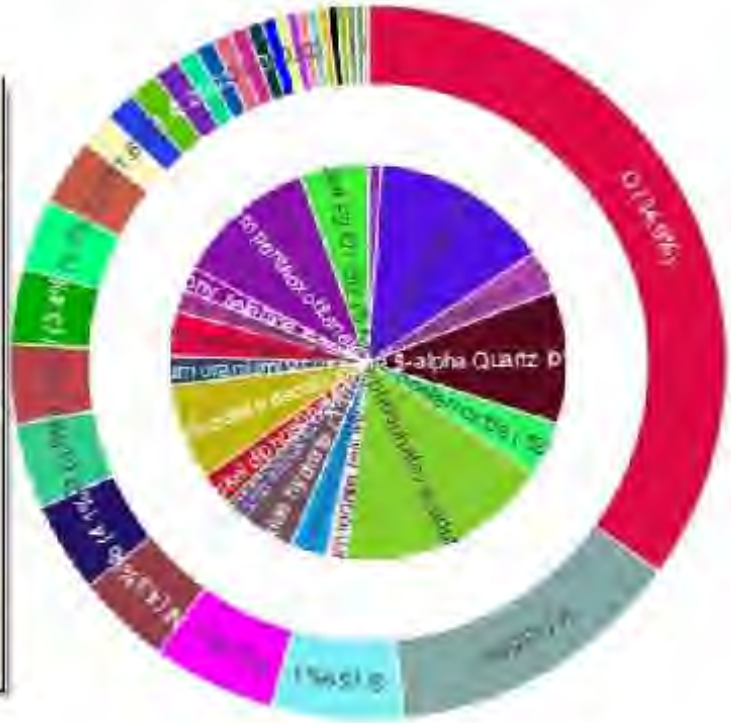

Match! Phase Analysis Report

Sample: Sample_G

Sample Data

File name	Sample_G.raw
File path	G:/.shortcut-targets-by-id/16KlMvpSIqVAUHFFggq9lVgYQzQybBTIu/Marwan - research/Concrete Mix Master Thesis/X-Ray/Birzeit University_XRD_Raw data
Data collected	Jul 13, 2023 09:18:14
Data range	4.800° - 89.800°
Original data range	5.000° - 90.000°
Number of points	4251
Step size	0.020
Rietveld refinement converged	No
Alpha2 subtracted	No
Background subtr.	No
Data smoothed	No
2theta correction	-0.2°
Radiation	X-rays
Wavelength	1.540598 Å

Analysis Results

Phase composition (Weight %)

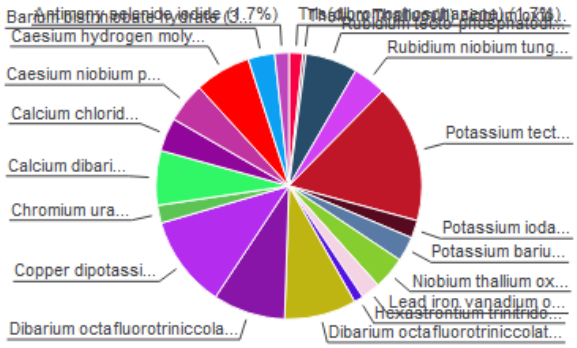

Elemental composition (Weight %)

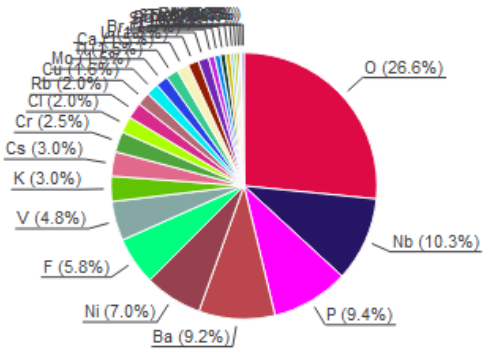

Index	*Amount (%)*	*Name*	*Formula sum*
A	1.7	Tris(dibromophosphazene)	Br6 N3 P3
B	0.4	Thallium Thallium(III) niobium oxide (1.7/0.3/2/6.3)	Nb2 O6.271 Tl2
C	6.3	Rubidium tecto-phosphatodiniobate	Nb2 O8 P Rb
D	4.0	Rubidium niobium tungsten oxide (12/30/3/90)	Nb30 O90 Rb12 W3
E	16.8	Potassium tecto-phosphatovanadate(III) *	K O24 P7 V4
F	2.2	Potassium iodate telluric acid	H6 I K O9 Te
G	3.0	Potassium barium phosphate	Ba K O4 P
H	4.0	Niobium thallium oxide hydrate (33/10.5/88.5/1.5)	H3 Nb33 O90 Tl10.5
I	2.3	Lead iron vanadium oxide (1/1.75/4.25/11)	Fe1.75 O11 Pb V4.25
J	1.1	Hexastrontium trinitridodicuprate(I) dinitridocuprate(I)	Cu3 N5 Sr6
K	8.7	Dibarium octafluorotriniccolate decafluorotetraniccolate	Ba2 F18 Ni7
L	8.8	Dibarium octafluorotriniccolate decafluorotetraniccolate	Ba2 F18 Ni7
M	11.2	Copper dipotassium dihydrogen phosphatochromate	Cr2 Cu H2 K2 O14 P2
N	2.2	Chromium uranium(V) oxide	Cr O4 U
O	6.6	Calcium dibarium bis(hydrogenphosphate(V)) bis(dihydrogenphosphate(V))	Ba2 Ca H6 O16 P4
P	4.1	Calcium chloride dihydrate Sinjarite	Ca Cl2 H4 O2
Q	4.9	Caesium niobium phosphate (1/3/3)	Cs Nb3 O15 P3
R	6.8	Caesium hydrogen molybdatodiphosphate	Cs H Mo O9 P2
S	3.2	Barium bistriniobate hydrate	Ba H2 Nb6 O17
T	1.7	Antimony selenide iodide	I Sb Se
	0.8	*Unidentified peak area*	

Amounts calculated by RIR (Reference Intensity Ratio) method

Element	*Amount (weight %)*
O	*26.6%(*)*
Nb	10.3%
P	9.4%
Ba	9.2%
Ni	7.0%
F	*5.8%(*)*
V	4.8%
K	3.0%
Cs	3.0%
Cr	2.5%
Cl	2.0%
Rb	2.0%
Cu	1.6%
Mo	1.5%
Tl	1.5%
Ca	1.5%
U	1.5%
Br	1.3%
I	1.3%
Sr	0.8%
Pb	0.7%
Sb	0.6%
Te	0.6%
Se	0.4%
W	0.4%
Fe	0.3%
H	*0.3%(*)*
N	*0.2%(*)*
**LE (sum)*	*32.9%*

Details of identified phases

A:

Tris(dibromophosphazene) (1.7 %)*

Formula sum	Br6 N3 P3
Entry number	96-100-8091
Figure-of-Merit (FoM)	0.628316*
Total number of peaks	500
Peaks in range	500
Peaks matched	156
Intensity scale factor	0.19*
Space group	P n m a
Crystal system	orthorhombic
Unit cell	a= 6.6300 Å b= 13.3600 Å c= 14.4300 Å
I/Ic	3.55

Calc. density	3.192 g/cm³
Reference	de Santis P, Giglio E, Ripamonti A, "The crystal structure of trimeric phosphonitrilic bromide.", Journal of Inorganic and Nuclear Chemistry **24**, 469-474 (1962)

B: Thallium Thallium(III) niobium oxide (1.7/0.3/2/6.3) (0.4 %)*

Formula sum	Nb2 O6.271 Tl2
Entry number	96-100-0383
Figure-of-Merit (FoM)	0.611763*
Total number of peaks	59
Peaks in range	59
Peaks matched	13
Intensity scale factor	0.22*
Space group	F d -3 m
Crystal system	cubic
Unit cell	a= 10.6418 Å
I/Ic	17.76
Calc. density	7.660 g/cm³
Reference	Fourquet J L, Duroy H, Lacorre P, "Tl2 Nb2 O6+x (0114, 575-584 (1995)

C: Rubidium tecto-phosphatodiniobate (6.3 %)*

Formula sum	Nb2 O8 P Rb
Entry number	96-100-1623
Figure-of-Merit (FoM)	0.632002*
Total number of peaks	499
Peaks in range	499
Peaks matched	196
Intensity scale factor	0.45*
Space group	P n m a
Crystal system	orthorhombic
Unit cell	a= 13.8150 Å b= 15.8840 Å c= 12.6750 Å
I/Ic	2.21
Calc. density	4.109 g/cm³
Reference	Leclaire A, Borel M M, Grandin A, Raveau B, "The phosphoniobate RbNb~2~PO~8~: An ordered sbstitution of PO~4~tetrahedra for NbO~6~ octahedra in the HTB structure", Journal of Solid State Chemistry **110**, 256-263 (1994)

D: Rubidium niobium tungsten oxide (12/30/3/90) (4.0 %)*

Formula sum	Nb30 O90 Rb12 W3
Entry number	96-100-1018
Figure-of-Merit (FoM)	0.614970*
Total number of peaks	161
Peaks in range	161
Peaks matched	52
Intensity scale factor	0.55*
Space group	R -3 m
Crystal system	trigonal (hexagonal axes)
Unit cell	a= 7.4860 Å c= 43.1000 Å
I/Ic	4.33
Meas. density	4.570 g/cm³
Calc. density	4.608 g/cm³
Reference	Michel C, Guyomarch A, Raveau B, "Nouveaux echangeurs cationiques avec une structure a tunnelsentrecroises: les oxides A~12~ M~33~ O~90~ et A~12~ M~33~ O~90~(H~2~ O)~12~", Journal of Solid State Chemistry **22**, 393-403 (1977)

E: Potassium tecto-phosphatovanadate(III) * (16.8 %)*

Formula sum	K O24 P7 V4
Entry number	96-100-1565
Figure-of-Merit (FoM)	0.648409*
Total number of peaks	499
Peaks in range	499
Peaks matched	218
Intensity scale factor	0.56*
Space group	P -1
Crystal system	triclinic (anorthic)
Unit cell	a= 10.0846 Å b= 10.2309 Å c= 10.8283 Å α= 112.757° β= 109.226 ° γ= 104.675 °
I/Ic	1.05
Calc. density	3.202 g/cm³
Reference	Benhamada L, Grandin A, Borel M M, Leclaire A, Raveau B, "A vanadium(III) phosphate with V~2~O~10~ octahedral units:KV~4~P~7~O~24~", Journal of Solid State Chemistry **104**, 193-201 (1993)

F: Potassium iodate telluric acid (2.2 %)*

Formula sum	H6 I K O9 Te
Entry number	96-100-8207
Figure-of-Merit (FoM)	0.648764*
Total number of peaks	499
Peaks in range	499
Peaks matched	109
Intensity scale factor	0.33*
Space group	P c 21 n
Crystal system	orthorhombic
Unit cell	a= 14.2200 Å b= 6.6960 Å c= 8.6720 Å
I/Ic	4.76
Calc. density	3.520 g/cm³
Reference	Averbuch-Pouchot M. T., "Crystal Chemistry of Some Addition Compounds of Alkali Iodates withTelluric Acid", Journal of Solid State Chemistry **49**, 368-378 (1983)

G: Potassium barium phosphate (3.0 %)*

Formula sum	Ba K O4 P
Entry number	96-100-7162
Figure-of-Merit (FoM)	0.603014*
Total number of peaks	500
Peaks in range	500
Peaks matched	61

Intensity scale factor	0.33*
Space group	P n m a
Crystal system	orthorhombic
Unit cell	a= 7.7090 Å b= 5.6630 Å c= 9.9720 Å
I/Ic	3.41
Calc. density	4.140 g/cm³
Reference	Masse R, Durif A, "Chemical preparation and crystal structure refinement of K Ba P O~4~monophosphate", Journal of Solid State Chemistry **71**, 574-576 (1987)

H: Niobium thallium oxide hydrate (33/10.5/88.5/1.5) (4.0 %)*

Formula sum	H3 Nb33 O90 Tl10.5
Entry number	96-100-1006
Figure-of-Merit (FoM)	0.671087*
Total number of peaks	161
Peaks in range	161
Peaks matched	58
Intensity scale factor	0.59*
Space group	R -3 m
Crystal system	trigonal (hexagonal axes)
Unit cell	a= 7.5100 Å c= 43.2900 Å
I/Ic	4.67
Calc. density	5.263 g/cm³
Reference	Gasperin M, "Synthese d'une nouvelle famille d'oxydes doubles: A~8~^+^ B~22~^5+^O~59~ structure du compose a thallium et niobium", Acta Crystallographica B (24,1968-38,1982) **33**, 398-402 (1977)

I: Lead iron vanadium oxide (1/1.75/4.25/11) (2.3 %)*

Formula sum	Fe1.75 O11 Pb V4.25
Entry number	96-100-4124
Figure-of-Merit (FoM)	0.607531*
Total number of peaks	223
Peaks in range	223
Peaks matched	34
Intensity scale factor	0.30*
Space group	P 63 m c
Crystal system	hexagonal
Unit cell	a= 5.7420 Å c= 13.5070 Å
I/Ic	4.06
Calc. density	6.005 g/cm³
Reference	Mentre O, Dhaussy A-C, Abraham F, Steinfink H, "Effect of iron substitution on the structural, electric, and magneticproperties in R-type Pb Fex V6-x O11, a frustrated system", Journal of Solid State Chemistry **130**, 223-233 (1997)

J: Hexastrontium trinitridodicuprate(I) dinitridocuprate(I) (1.1 %)*

Formula sum	Cu3 N5 Sr6
Entry number	96-100-5040
Figure-of-Merit (FoM)	0.654045*
Total number of peaks	354
Peaks in range	354
Peaks matched	37
Intensity scale factor	0.24*
Space group	P 42 m c
Crystal system	tetragonal
Unit cell	a= 8.6570 Å c= 7.3340 Å
I/Ic	6.65
Calc. density	4.751 g/cm³
Reference	DiSalvo F J, Trail S S, Yamane H, Brese N E, "The crystal structure of Sr6 Cu3 N5 with isolated, bent (Cu(I)2 N3)(7-)anions and the single crystal structural determination of Sr Cu N", Journal of Alloys Compd. **255**, 122-129 (1997)

K: Dibarium octafluorotriniccolate decafluorotetraniccolate (8.7 %)*

Formula sum	Ba2 F18 Ni7
Entry number	96-100-0250
Figure-of-Merit (FoM)	0.634995*
Total number of peaks	500
Peaks in range	500
Peaks matched	163
Intensity scale factor	0.47*
Space group	P -1
Crystal system	triclinic (anorthic)
Unit cell	a= 6.9240 Å b= 7.2180 Å c= 7.4370 Å α= 94.390º β= 93.200 º γ= 115.820 º
I/Ic	1.67
Calc. density	5.139 g/cm³
Reference	Renaudin J, Ferey G, Kozak A, Samouel M, Lacorre P, "Crystal and magnetic structures of the ferrimagnet Ba~2~ Ni~7~ F~18~", Solid State Communications **65**, 185-188 (1988)

L: Dibarium octafluorotriniccolate decafluorotetraniccolate (8.8 %)*

Formula sum	Ba2 F18 Ni7
Entry number	96-100-0249
Figure-of-Merit (FoM)	0.606807*
Total number of peaks	498
Peaks in range	498
Peaks matched	164
Intensity scale factor	0.38*
Space group	P -1
Crystal system	triclinic (anorthic)
Unit cell	a= 6.9370 Å b= 7.2290 Å c= 7.4560 Å α= 94.370º β= 93.160 º γ= 115.860 º
I/Ic	1.35
Calc. density	5.110 g/cm³
Reference	Renaudin J, Ferey G, Kozak A, Samouel M, Lacorre P, "Crystal and magnetic structures of the ferrimagnet Ba~2~ Ni~7~ F~18~", Solid State Communications **65**, 185-188 (1988)

M: Copper dipotassium dihydrogen

phosphatochromate (11.2 %)*

Formula sum	Cr2 Cu H2 K2 O14 P2
Entry number	96-100-7043
Figure-of-Merit (FoM)	0.622859*
Total number of peaks	496
Peaks in range	496
Peaks matched	156
Intensity scale factor	0.37*
Space group	P 1 21/c 1
Crystal system	monoclinic
Unit cell	a= 9.5590 Å b= 7.1960 Å c= 8.9830 Å β= 93.730 º
I/Ic	1.05
Calc. density	2.869 g/cm³
Reference	Coing-Boyat J, Durif A, Guitel J C, "Structure cristalline d'un phosphochromate acide de cuivre potassium:Cu K~2~ H~2~ (P Cr O~7~)~2~", Journal of Solid State Chemistry **30**, 329-334 (1979)

N: Chromium uranium(V) oxide (2.2 %)*

Formula sum	Cr O4 U
Entry number	96-100-8068
Figure-of-Merit (FoM)	0.649451*
Total number of peaks	338
Peaks in range	338
Peaks matched	35
Intensity scale factor	0.89*
Space group	P b c n
Crystal system	orthorhombic
Unit cell	a= 4.8710 Å b= 11.7870 Å c= 5.0530 Å
I/Ic	12.96
Calc. density	8.105 g/cm³
Reference	Bacmann M, Bertaut E F, "Structure de U Cr O~4~", Bulletin de la Societe Francaise de Mineralogie et de Cristallographie(72,1949-100,1977) **87**, 275-276 (1964)

O: Calcium dibarium bis(hydrogenphosphate(V)) bis(dihydrogenphosphate(V)) (6.6 %)*

Formula sum	Ba2 Ca H6 O16 P4
Entry number	96-100-0441
Figure-of-Merit (FoM)	0.601135*
Total number of peaks	499
Peaks in range	499
Peaks matched	167
Intensity scale factor	0.25*
Space group	P 1 21/a 1
Crystal system	monoclinic
Unit cell	a= 12.3872 Å b= 10.2046 Å c= 5.4946 Å β= 100.767 º
I/Ic	1.21
Calc. density	3.395 g/cm³
Reference	Toumi M., Chabchoub S., Smiri-Dogguy L., Laligant Y., "Ab-initio powder structure determination of CaBa~2~(HPO~4~)~2~(H~2~PO~4~)~2~:a new phosphate with a M(T\F~4~)~4~ chain structure", European Journal of Solid State and Inorganic Chemistry **34**, 1249-1257 (1997)

P: Calcium chloride dihydrate Sinjarite (4.1 %)*

Formula sum	Ca Cl2 H4 O2
Entry number	96-100-1836
Figure-of-Merit (FoM)	0.600748*
Total number of peaks	500
Peaks in range	500
Peaks matched	67
Intensity scale factor	0.22*
Space group	P b c n
Crystal system	orthorhombic
Unit cell	a= 5.8930 Å b= 7.4690 Å c= 12.0700 Å
I/Ic	1.72
Meas. density	1.860 g/cm³
Calc. density	1.838 g/cm³
Reference	Leclaire A., Borel M. M., "Le dichlorure de calcium dihydrate", Acta Crystallographica, Section B **33**, 1608-1610 (1977)

Q: Caesium niobium phosphate (1/3/3) (4.9 %)*

Formula sum	Cs Nb3 O15 P3
Entry number	96-100-1451
Figure-of-Merit (FoM)	0.622090*
Total number of peaks	499
Peaks in range	499
Peaks matched	166
Intensity scale factor	0.35*
Space group	P n n m
Crystal system	orthorhombic
Unit cell	a= 13.4454 Å b= 14.8114 Å c= 6.4422 Å
I/Ic	2.27
Calc. density	3.854 g/cm³
Reference	Borel M M, Grandin A, Costentin G, Leclaire A, Raveau B, "A new series of bronzes and bronzoids with KNb~3~P~3~O~15~ structure", Materials Research Bulletin **25**, 1155-1160 (1990)

R: Caesium hydrogen molybdatodiphosphate (6.8 %)*

Formula sum	Cs H Mo O9 P2
Entry number	96-100-8437
Figure-of-Merit (FoM)	0.604266*
Total number of peaks	498
Peaks in range	498
Peaks matched	161
Intensity scale factor	0.44*
Space group	P 1 21/a 1
Crystal system	monoclinic
Unit cell	a= 9.6700 Å b= 14.2310 Å c= 6.2650 Å β= 100.100 º

I/Ic	2.01
Calc. density	3.410 g/cm³
Reference	Averbuch-Pouchot M T, "Synthesis and Crystal Structure of Cs H Mo O~2~ (P~2~ O~7~)", Journal of Solid State Chemistry **79**, 296-299 (1989)

S: Barium bistriniobate hydrate (3.2 %)*

Formula sum	Ba H2 Nb6 O17
Entry number	96-100-1384
Figure-of-Merit (FoM)	0.624916*
Total number of peaks	323
Peaks in range	323
Peaks matched	59
Intensity scale factor	0.39*
Space group	I m m m
Crystal system	orthorhombic
Unit cell	a= 8.6200 Å b= 21.6100 Å c= 3.8110 Å
I/Ic	3.77
Calc. density	4.522 g/cm³
Reference	Nedjar R, Borel M M, Leclaire A, Raveau B, "Ba (Nb~3~ O~8~)~2~ * (H~2~ O): A novel lamellar niobate", Materials Research Bulletin **23**, 495-500 (1988)

T: Antimony selenide iodide (1.7 %)*

Formula sum	I Sb Se
Entry number	96-100-8205
Figure-of-Merit (FoM)	0.645469*
Total number of peaks	494
Peaks in range	494
Peaks matched	49
Intensity scale factor	0.41*
Space group	P n m a
Crystal system	orthorhombic
Unit cell	a= 8.6980 Å b= 4.1270 Å c= 10.4120 Å
I/Ic	7.57
Calc. density	5.822 g/cm³
Reference	Ibanez A, Jumas J C, Olivier-Fourcade J, Philippot E, Maurin M, "Sur les Chalcogeno-iodures d'antimoine SbXI (X=S,Se,Te):Structures etspectroscopie Moessbauer de ^121^Sb", Journal of Solid State Chemistry **48**, 272-283 (1983)

(*)2theta values have been shifted internally for the calculation of the amounts, the intensity scaling factors as well as the figure-of-merit (FoM), due to the active search-match option 'Automatic zero point adaption'.

Search-Match

Settings

Reference database used	COD-Inorg 2023.06.06
Automatic zeropoint adaptation	Yes
Downgrade entries with low scaling factors	Yes
Minimum figure-of-merit (FoM)	0.60
2theta window for peak corr.	0.30 deg.
Minimum rel. int. for peak corr.	0
Parameter/influence 2theta	0.50
Parameter/influence intensities	0.50
Parameter multiple/single phase(s)	0.50

Peak List

No.	2theta [°]	d [Å]	I/I0 (peak height)	Counts (peak area)	FWHM	Matched
1	9.06	9.7530	20.61	14.68	0.1600	A,C,M,Q
2	15.84	5.5904	15.00	5.34	0.0800	A,C,D,F,H,J,M,R,S
3	18.02	4.9187	315.37	112.34	0.0800	A,C,E,F,G,I,K,M,Q
4	18.82	4.7114	12.03	14.99	0.2800	C,E,I,K,L,M,O,R
5	20.78	4.2712	140.30	99.95	0.1600	A,C,E,F,J,O,P,Q,R,S
6	22.96	3.8703	27.18	19.37	0.1600	A,C,E,F,G,J,N,O,Q,S,T
7	26.60	3.3484	1000.00	534.30	0.1200	A,C,D,E,F,G,H,I,J,K,L,M,N,O,Q,R,S,T
8	27.86	3.1998	58.17	20.72	0.0800	A,B,C,D,E,F,G,H,K,L,M,O,P,Q,T
9	29.34	3.0416	217.15	154.69	0.1600	A,B,C,D,E,F,G,H,J,K,L,M,N,O,P,Q,R,T
10	30.00	2.9762	14.84	7.93	0.1200	A,C,D,F,H,K,L,O,Q,R,T
11	30.86	2.8952	35.37	31.49	0.2000	A,C,D,E,F,H,I,J,M,O,Q,R,S,T
12	32.08	2.7878	73.50	78.54	0.2400	C,D,E,H,I,J,K,L,M,O,P,Q,R,T
13	32.50	2.7527	81.83	58.30	0.1600	A,E,F,J,K,L,M,O,P,Q,R,S
14	33.74	2.6544	21.94	7.81	0.0800	A,B,C,E,F,I,J,K,L,M,O,P,Q,R,S,T
15	34.26	2.6153	59.69	42.52	0.1600	A,C,E,F,H,M,N,O,Q,R,T
16	36.50	2.4597	101.11	36.02	0.0800	A,B,C,D,E,F,G,H,I,K,L,M,O,Q,R
17	38.64	2.3283	11.93	6.38	0.1200	A,C,D,E,F,G,H,I,K,L,M,N,O,P,Q,R,S,T
18	39.38	2.2862	103.83	73.97	0.1600	A,C,D,E,F,G,H,J,K,L,M,O,P,Q,R,S
19	40.24	2.2393	23.52	20.95	0.2000	A,C,D,E,F,G,H,I,K,L,M,N,O,P,Q,R,S,T
20	41.16	2.1914	49.63	53.03	0.2400	A,C,E,F,G,I,J,K,L,N,O,P,Q,R
21	42.38	2.1311	14.71	5.24	0.0800	A,C,D,E,F,G,H,J,K,L,M,N,O,P,Q,R,S,T
22	43.08	2.0980	17.30	12.32	0.1600	A,C,E,F,G,H,J,K,L,M,N,O,P,Q,R,S
23	45.70	1.9837	21.15	7.53	0.0800	A,C,E,F,H,K,L,M,O,P,Q,R,T
24	47.44	1.9149	59.30	52.81	0.2000	A,C,D,E,F,G,H,K,L,M,N,O,P,Q,R,S,T
25	48.46	1.8769	22.54	20.07	0.2000	A,B,C,D,E,G,H,I,J,K,L,M,N,O,P,Q,R,S,T
26	50.10	1.8193	121.96	65.16	0.1200	A,C,D,E,F,G,H,I,J,K,L,M,O,P,Q,R,S,T
27	51.62	1.7692	35.89	12.78	0.0800	A,B,C,D,E,F,G,H,I,K,L,M,N,O,P,Q,R
28	54.78	1.6744	70.19	25.00	0.0800	A,B,C,D,E,F,G,H,I,K,L,M,N,O,P,Q,R,S,T
29	55.26	1.6610	20.49	10.95	0.1200	A,C,D,E,F,G,H,I,J,K,L,M,O,P,Q,R,S,T
30	56.34	1.6317	29.94	21.33	0.1600	A,C,D,E,F,G,H,K,L,M,N,O,P,Q,R,S
31	57.30	1.6066	14.59	10.39	0.1600	A,B,C,D,E,F,G,H,I,J,K,L,M,N,O,P,Q,R,S,T
32	59.88	1.5434	131.88	70.46	0.1200	A,C,E,F,I,J,K,L,M,O,P,Q,R,S,T
33	60.06	1.5392	54.05	28.88	0.1200	A,B,C,E,F,H,J,K,L,M,N,O,Q,R
34	60.56	1.5277	10.25	7.30	0.1600	A,C,D,F,G,H,I,J,K,L,M,N,O,P,Q,R,S,T
35	62.12	1.4930	17.02	15.16	0.2000	A,B,C,D,F,H,I,K,L,M,N,O,P,Q,R,S,T
36	67.66	1.3836	50.41	17.95	0.0800	A,B,D,F,G,H,K,L,M,O,P,Q,R,S,T
37	67.84	1.3804	25.39	13.57	0.1200	A,D,F,G,H,I,J,K,L,M,O,P,R,S,T
38	68.06	1.3765	35.65	19.05	0.1200	A,G,J,K,L,M,N,P,Q,R
39	68.24	1.3733	25.63	13.69	0.1200	A,D,F,G,H,I,J,K,L,M,N,O,P,Q,R,T
40	75.56	1.2574	38.89	20.78	0.1200	A,D,F,G,I,J,K,L,M,N,O,P,Q,R,S,T
41	75.78	1.2543	17.01	6.06	0.0800	A,B,F,G,H,J,K,L,M,N,O,Q,R,S
42	77.58	1.2296	16.28	5.80	0.0800	A,B,F,G,I,J,K,L,M,N,O,Q,R,S,T
43	79.80	1.2009	35.04	18.72	0.1200	A,F,G,J,K,L,M,O,P,Q,S,T

44	80.02	1.1981	18.69	13.31	0.1600	A,F,G,I,J,K,L,M,N,O,P,Q,S,T
45	81.08	1.1851	27.36	9.75	0.0800	A,F,G,I,J,K,L,M,O,P,Q,S,T
46	81.36	1.1817	38.18	20.40	0.1200	A,I,J,K,L,M,N,O,P,Q,S,T
47	81.62	1.1786	14.89	10.61	0.1600	A,F,I,J,K,L,M,N,O,P,Q,T
48	83.72	1.1543	11.92	6.37	0.1200	A,F,I,J,K,L,M,N,O,P,Q,S,T

Integrated Profile Areas

Based on calculated profile

Profile area	***Counts***	***Amount***
Overall diffraction profile	580789	100.00%
Background radiation	415256	71.50%
Diffraction peaks	165533	28.50%
Peak area belonging to selected phases	160983	27.72%
Peak area of phase A (Tris(dibromophosphazene))	*5549*	*0.96%*
Peak area of phase B (Thallium Thallium(III) niobium oxide (1.7/0.3/2/6.3))	*1229*	*0.21%*
Peak area of phase C (Rubidium tecto-phosphatodiniobate)	*10972*	*1.89%*
Peak area of phase D (Rubidium niobium tungsten oxide (12/30/3/90))	*10489*	*1.81%*
*Peak area of phase E (Potassium tecto-phosphatovanadate(III) *)*	*10082*	*1.74%*
Peak area of phase F (Potassium iodate telluric acid)	*4681*	*0.81%*
Peak area of phase G (Potassium barium phosphate)	*5431*	*0.94%*
Peak area of phase H (Niobium thallium oxide hydrate (33/10.5/88.5/1.5))	*8878*	*1.53%*
Peak area of phase I (Lead iron vanadium oxide (1/1.75/4.25/11))	*5873*	*1.01%*
Peak area of phase J (Hexastrontium trinitridodicuprate(I) dinitridocuprate(I))	*1894*	*0.33%*
Peak area of phase K (Dibarium octafluorotriniccolate decafluorotetraniccolate)	*13290*	*2.29%*
Peak area of phase L (Dibarium octafluorotriniccolate decafluorotetraniccolate)	*14931*	*2.57%*
Peak area of phase M (Copper dipotassium dihydrogen phosphatochromate)	*12011*	*2.07%*
Peak area of phase N (Chromium uranium(V) oxide)	*7427*	*1.28%*
Peak area of phase O (Calcium dibarium bis(hydrogenphosphate(V)) bis(dihydrogenphosphate(V)))	*10905*	*1.88%*
Peak area of phase P (Calcium chloride dihydrate Sinjarite)	*4014*	*0.69%*
Peak area of phase Q (Caesium niobium phosphate (1/3/3))	*8469*	*1.46%*
Peak area of phase R (Caesium hydrogen molybdatodiphosphate)	*13799*	*2.38%*
Peak area of phase S (Barium bistriniobate hydrate)	*6279*	*1.08%*
Peak area of phase T (Antimony selenide iodide)	*4779*	*0.82%*
Unidentified peak area	4550	0.78%

Diffraction Pattern Graphics

Match! Copyright © 2003-2023 CRYSTAL IMPACT, Bonn, Germany

Amounts of Phases and Elements (Weight %)

Phase composition:

Potassium tecto-phosphatovanadate(III) * (16.8%), Copper dipotassium dihydrogen phosphatochromate (11.2%), Dibarium octafluorotriniccolate decafluorotetraniccolate (8.8%), Dibarium octafluorotriniccolate decafluorotetraniccolate (8.7%), Caesium hydrogen molybdatodiphosphate (6.8%), Calcium dibarium bis(hydrogenphosphate(V)) bis(dihydrogenphosphate(V)) (6.6%), Rubidium tecto-phosphatodiniobate (6.3%), Caesium niobium phosphate (1/3/3) (4.9%), Calcium chloride dihydrate Sinjarite (4.1%), Rubidium niobium tungsten oxide (12/30/3/90) (4.0%), Niobium thallium oxide hydrate (33/10.5/88.5/1.5) (4.0%), Barium bistriniobate hydrate (3.2%), Potassium barium phosphate (3.0%), Lead iron vanadium oxide (1/1.75/4.25/11) (2.3%), Potassium iodate telluric acid (2.2%), Chromium uranium(V) oxide (2.2%), Antimony selenide iodide (1.7%), Tris(dibromophosphazene) (1.7%), Hexastrontium trinitridodicuprate(I) dinitridocuprate(I) (1.1%), Thallium Thallium(III) niobium oxide (1.7/0.3/2/6.3) (0.4%)

Elemental composition:

O (26.57%), Nb (10.26%), P (9.42%), Ba (9.25%), Ni (7.01%), F (5.83%), V (4.79%), K (3.04%), Cs (2.96%), Cr (2.50%), Cl (1.96%), Rb (1.96%), Cu (1.61%), Mo (1.51%), Tl (1.50%), Ca (1.49%), U (1.45%), Br (1.30%), I (1.20%), Sr (0.75%), Pb (0.69%), Sb (0.64%), Te (0.62%), Sc (0.41%), W (0.38%), Fe (0.33%), H (0.26%), N (0.21%) (LE: 32.88%)

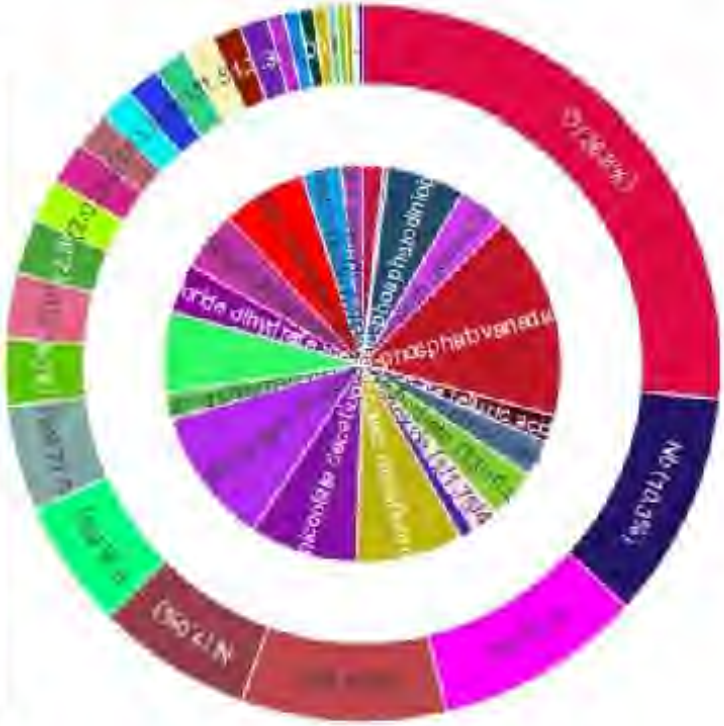

Match! Phase Analysis Report

Sample: Sample_H

Sample Data

File name	Sample_H.raw
File path	G:/.shortcut-targets-by-id/16KlMvpSlqVAUHFFggq9lVgYQzQybBTlu/Marwan - research/Concrete Mix Master Thesis/X-Ray/Birzeit University_XRD_Raw data
Data collected	Jul 13, 2023 12:11:51
Data range	4.900° - 89.900°
Original data range	5.000° - 90.000°
Number of points	4251
Step size	0.020
Rietveld refinement converged	No
Alpha2 subtracted	No
Background subtr.	No
Data smoothed	No
2theta correction	-0.1°
Radiation	X-rays
Wavelength	1.540598 Å

Analysis Results

Phase composition (Weight %)

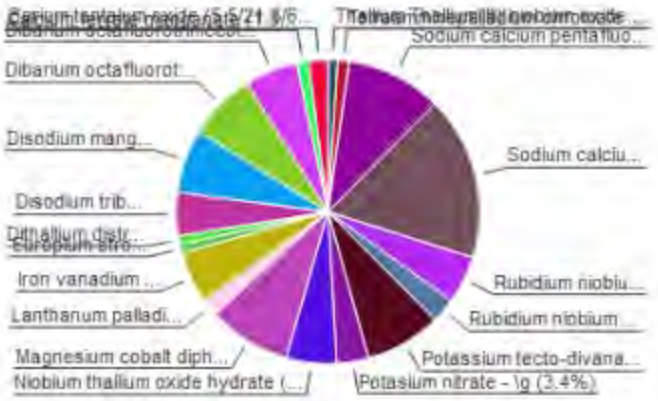

Elemental composition (Weight %)

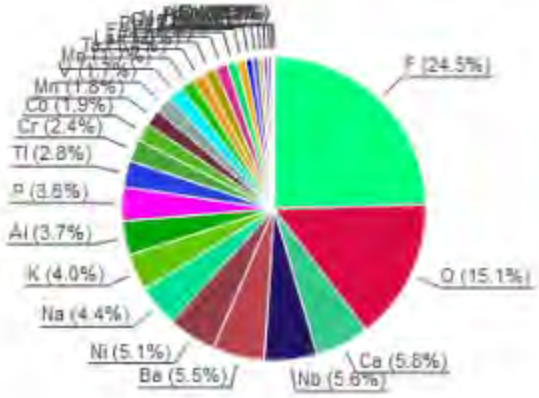

Index	*Amount (%)*	*Name*	*Formula sum*
A	1.0	Thallium Thallium(III) niobium oxide (1.4/0.6/2/6.6)	Nb2 O6.648 Tl2
B	1.2	Tetraamminepalladium chromate	Cr H12 N4 O4 Pd
C	10.1	Sodium calcium pentafluoroaluminate fluoride - $-beta	Al Ca F6 Na
D	17.5	Sodium calcium hexafluoroaluminate - \a	Al Ca F6 Na
E	5.0	Rubidium niobium tungsten oxide (12/30/3/90)	Nb30 O90 Rb12 W3
F	2.7	Rubidium niobium cyclo-trigermanate	Ge3 Nb O9 Rb
G	8.1	Potassium tecto-divanadato(III)tetraphosphate	K6 O16 P4 V2
H	3.4	Potasium nitrate - \g	K N O3
I	5.3	Niobium thallium oxide hydrate (33/10.5/88.5/1.5)	H3 Nb33 O90 Tl10.5
J	8.8	Magnesium cobalt diphosphate (1.1/0.9/1)	Co0.92 Mg1.08 O7 P2
L	3.3	Iron vanadium molybdenum oxide (4/1.98/3.02/20)	Fe4 Mo3 O2 O20 V1.98
M	0.9	Europium strontium copper oxide (1.3/1.7/2/5.65)	Cu2 Eu1.3 O5.65 Sr1.7
N	0.9	Dithallium dobalteum copper oxide	Cu O6 Sr2 Tl2
O	4.6	Disodium tribarium tetrachromium fluoride	Ba3 Cr4 F20 Na2
P	6.8	Disodium manganese chromium fluoride	Cr F7 Mn Na2
Q	1.2	Dibarium octafluorotrinicolate decafluorotetranicolate	Ba2 F18 Ni7
R	5.7	Dibarium octafluorotrinicolate decafluorotetranicolate	Ba2 F18 Ni7
S	1.3	Calcium ferrate manganate	Ca2 Fe2 O5
T	2.0	Barium tantalum oxide (5.5/21.8/60)	Ba5.5 O60 Ta21.8
	0.9	*Unidentified peak area*	

Amounts calculated by RIR (Reference Intensity Ratio) method

Element	*Amount (weight %)*
F	24.5%(*)
O	*15.1%(*)*
Ca	5.8%
Nb	5.6%
Ba	5.5%
Ni	5.1%
Na	4.4%
K	4.0%
Al	3.7%
P	3.6%
Tl	2.8%
Cr	2.4%
Co	1.9%
Mn	1.8%
V	1.7%
Mo	1.7%
Ta	1.4%
La	1.3%
Fe	1.3%
Rb	1.3%
Ge	1.1%
Mg	0.9%
N	*0.7%(*)*
Pd	0.7%
W	0.6%
Sr	0.5%
Eu	0.3%

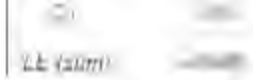

Details of identified phases

A: Thallium Thallium(III) niobium oxide (1.4/0.6/2/5.6) (1.0 %)

Formula sum	Nb2 O6.648 Tl2
Entry number	96-100-0387
Figure-of-Merit (FoM)	0.607904
Total number of peaks	52
Peaks in range	52
Peaks matched	14
Intensity scale factor	0.67
Space group	F d -3 m
Crystal system	cubic
Unit cell	a= 10.6313 Å
I/Ic	16.15
Calc. density	7.749 g/cm³
Reference	Fourquet J.L, Duroy H, Lacorre P. "Tl2 Nb2 O6+x (0114, 575-584 (1995)

B: Tetraamminepalladium chromate (1.2 %)

Formula sum	Cr H12 N4 O4 Pd
Entry number	96-100-0345
Figure-of-Merit (FoM)	0.613547
Total number of peaks	215
Peaks in range	215
Peaks matched	40
Intensity scale factor	0.25
Space group	I 41/a m d
Crystal system	tetragonal
Unit cell	a= 7.3177 Å c= 15.2890 Å
I/Ic	5.88
Calc. density	2.357 g/cm³
Reference	Laligant Y. "On the first palladium chromate: crystal structure of Pd(NH~3~)~4~(CrO~4~)", European Journal of Solid State Inorganic Chemistry **30**, 681-688 (1993)

C: Sodium calcium pentafluoroaluminate fluoride - S-beta (10.1 %)

Formula sum	Al Ca F6 Na
Entry number	96-100-0418
Figure-of-Merit (FoM)	0.620159
Total number of peaks	189
Peaks in range	189
Peaks matched	31
Intensity scale factor	0.54
Space group	P 3 2 1
Crystal system	trigonal (hexagonal axes)
Unit cell	a= 8.9295 Å c= 5.0642 Å
I/Ic	1.50
Meas. density	2.880 g/cm³
Calc. density	2.906 g/cm³
Reference	Hemon A, Courbion G, "The Na F - Ca F2 - Al F3 system: structures of S-beta- Na Ca Al F6 and Na4 Ca4 Al7 F33", Journal of Solid State Chemistry **84**, 153-164 (1990)

D: Sodium calcium hexafluoroaluminate - Ia (17.5 %)

Formula sum	Al Ca F6 Na
Entry number	96-100-0150
Figure-of-Merit (FoM)	0.634281
Total number of peaks	499
Peaks in range	499
Peaks matched	205
Intensity scale factor	0.44
Space group	P 1 21/c 1
Crystal system	monoclinic
Unit cell	a= 5.7423 Å b= 5.1927 Å c= 20.3514 Å β= 91.499 °
I/Ic	0.70
Calc. density	2.934 g/cm³
Reference	Le Bail A., Hemon-Ribaud A., Courbion G., "Structure of Ia-NaCaAlF~6~ determined ab initio from conventional powder diffraction data", European Journal of Solid State and Inorganic Chemistry **35(3)**, 265-272 (1998)

E: Rubidium niobium tungsten oxide (12/30/3/90) (5.0 %)

Formula sum	Nb30 O90 Rb12 W3
Entry number	96-100-1018
Figure-of-Merit (FoM)	0.674643

Total number of peaks	161
Peaks in range	161
Peaks matched	77
Intensity scale factor	0.78*
Space group	R -3 m
Crystal system	trigonal (hexagonal axes)
Unit cell	a= 7.4860 Å c= 43.1000 Å
I/Ic	4.33
Meas. density	4.570 g/cm³
Calc. density	4.608 g/cm³
Reference	Michel C, Guyomarch A, Raveau B, "Nouveaux echangeurs cationiques avec une structure a tunnelsentrecroises: les oxides A~12~ M~33~ O~90~ et A~12~ M~33~ O~90~(H~2~ O)~12~", Journal of Solid State Chemistry **22**, 393-403 (1977)

F: Rubidium niobium cyclo-trigermanate (2.7 %)*

Formula sum	Ge3 Nb O9 Rb
Entry number	96-100-1077
Figure-of-Merit (FoM)	0.620987*
Total number of peaks	202
Peaks in range	202
Peaks matched	31
Intensity scale factor	0.41*
Space group	P -6 c 2
Crystal system	hexagonal
Unit cell	a= 7.0360 Å c= 10.1320 Å
I/Ic	4.31
Calc. density	4.127 g/cm³
Reference	Choisnet J, Deschanvres A, Raveau B, "Sur de nouveaux germanates et silicates de type benitoite", Journal of Solid State Chemistry **4**, 209-218 (1972)

G: Potassium tecto-divanadato(III)tetraphosphate (8.1 %)*

Formula sum	K6 O16 P4 V2
Entry number	96-100-1476
Figure-of-Merit (FoM)	0.600836*
Total number of peaks	500
Peaks in range	500
Peaks matched	211
Intensity scale factor	0.31*
Space group	P 1 21/c 1
Crystal system	monoclinic
Unit cell	a= 9.5780 Å b= 11.0970 Å c= 16.1270 Å β= 121.670 °
I/Ic	1.07
Calc. density	2.901 g/cm³
Reference	Benhamada L, Grandin A, Borel M M, Leclaire A, Raveau B, "A new vanadium III potassium phosphate with a cage structure:K~6~V~2~P~4~O~16~", Journal of Solid State Chemistry **91**, 264-270 (1991)

H: Potassium nitrate - \g (3.4 %)*

Formula sum	K N O3
Entry number	96-100-0052
Figure-of-Merit (FoM)	0.636285*
Total number of peaks	76
Peaks in range	76
Peaks matched	17
Intensity scale factor	0.33*
Space group	R 3 m
Crystal system	trigonal (hexagonal axes)
Unit cell	a= 5.4670 Å c= 9.1560 Å
I/Ic	2.74
Calc. density	2.109 g/cm³
Reference	Nimmo J. K., Lucas B. W., "The crystal structures of \g- and \b-KNO~3~ and the\a \\leftarrow \g \\leftarrow \b phase transformations", Acta Crystallographica B (24,1968-38,1982) **32(7)**, 1968-1971 (1976)

I: Niobium thallium oxide hydrate (33/10.5/88.5/1.5) (5.3 %)*

Formula sum	H3 Nb33 O90 Tl10.5
Entry number	96-100-1006
Figure-of-Merit (FoM)	0.714966*
Total number of peaks	161
Peaks in range	161
Peaks matched	82
Intensity scale factor	0.69*
Space group	R -3 m
Crystal system	trigonal (hexagonal axes)
Unit cell	a= 7.5100 Å c= 43.2900 Å
I/Ic	4.67
Calc. density	5.263 g/cm³
Reference	Gasperin M, "Synthese d'une nouvelle famille d'oxydes doubles: A~8~^+^ B~22~^5+^O~59~ structure du compose a thallium et niobium", Acta Crystallographica B (24,1968-38,1982) **33**, 398-402 (1977)

J: Magnesium cobalt diphosphate (1.1/0.9/1) (8.6 %)*

Formula sum	Co0.92 Mg1.08 O7 P2
Entry number	96-100-1465
Figure-of-Merit (FoM)	0.684858*
Total number of peaks	499
Peaks in range	499
Peaks matched	129
Intensity scale factor	0.45*
Space group	P 1 21/c 1
Crystal system	monoclinic
Unit cell	a= 6.9770 Å b= 8.3300 Å c= 9.0320 Å β= 113.740 °
I/Ic	1.44
Calc. density	3.516 g/cm³
Reference	Riou D, Leclaire A, Raveau B, "Structure of a cobalt magnesium diphosphate: (Mg~x~Co~1-x~)~2~P~2~O~7~", Acta Crystallographica C (39,1983-) **47**, 1583-1585 (1991)

K: Lanthanum palladium oxide (4/1/7) (1.9 %)*

Formula sum	La4 O7 Pd
Entry number	96-100-0485
Figure-of-Merit (FoM)	0.679104*
Total number of peaks	307
Peaks in range	307
Peaks matched	73
Intensity scale factor	0.41*
Space group	C 1 2/m 1
Crystal system	monoclinic
Unit cell	a= 13.4690 Å b= 4.0262 Å c= 9.4460 Å β= 133.420 °
I/Ic	6.05
Calc. density	6.907 g/cm³
Reference	Attfield J P, Perey G, "Structural correlations within the lanthanum palladium oxide family", Journal of Solid State Chemistry **80**, 286-298 (1989)

L: Iron vanadium molybdenum oxide (4/1.98/3.02/20) (5.5 %)*

Formula sum	Fe4 Mo3.02 O20 V1.98
Entry number	96-100-0124
Figure-of-Merit (FoM)	0.703950*
Total number of peaks	462
Peaks in range	462
Peaks matched	156
Intensity scale factor	0.56*
Space group	P 41 2 2
Crystal system	tetragonal
Unit cell	a= 9.5390 Å c= 17.1411 Å
I/Ic	2.68
Calc. density	3.977 g/cm³
Reference	Lalligant Y, Perrel L, Le Ball A, "Crystal structure of Fe4 V2 Mo3 O20 determined from conventional X-raypowder diffraction data", European Journal of Solid State Inorganic Chemistry **32**, 325-334 (1995)

M: Europium strontium copper oxide (1.3/1.7/2/5.65) (0.9 %)*

Formula sum	Cu2 Eu1.3 O5.65 Sr1.7
Entry number	96-100-1158
Figure-of-Merit (FoM)	0.623956*
Total number of peaks	322
Peaks in range	322
Peaks matched	110
Intensity scale factor	0.15*
Space group	I m m m
Crystal system	orthorhombic
Unit cell	a= 3.7440 Å b= 11.3870 Å c= 20.0470 Å
I/Ic	4.63
Calc. density	6.604 g/cm³
Reference	Nguyen N, Choisnet J, Raveau B, "Intercroissances des structures de type Perovskite et Sr O defitairesen oxygene: les oxydes Ln~2-x~ Sr~1+x~ Cu~2~O~6-x/2~ (Ln = Sm, Eu, Gd)", Materials Research Bulletin **17**, 567-573 (1982)

N: Dithallium distrontium copper oxide (0.9 %)*

Formula sum	Cu O6 Sr2 Tl2
Entry number	96-100-1523
Figure-of-Merit (FoM)	0.606477*
Total number of peaks	144
Peaks in range	144
Peaks matched	28
Intensity scale factor	0.43*
Space group	I 4/m m m
Crystal system	tetragonal

Unit cell	a= 3.7464 Å c= 22.3013 Å
I/Ic	13.06
Calc. density	7.889 g/cm³
Reference	Martin C, Maignan A, Huve M, Michel C, Hervieu M, Raveau B, "The influence of alkaline-earth ions on the properties of the"2201"superconductive cuprates: the solid solution Tl~2~Ba~2-x~Sr~x~CuO~6+d~", European Journal of Solid State Inorganic Chemistry **30**, 7-18 (1993)

O: Disodium tribarium tetrachromium fluoride (4.6 %)*

Formula sum	Ba3 Cr4 F20 Na2
Entry number	96-100-0339
Figure-of-Merit (FoM)	0.602497*
Total number of peaks	496
Peaks in range	496
Peaks matched	210
Intensity scale factor	0.24*
Space group	P 1 21/n 1
Crystal system	monoclinic
Unit cell	a= 7.2620 Å b= 20.6680 Å c= 5.4310 Å β= 90.760 °
I/Ic	1.47
Meas. density	4.260 g/cm³
Calc. density	4.261 g/cm³
Reference	Abjean P, Leblanc M, De Pape R, Ferey G, "Structure of Na~2~ Ba~3~ Cr~4~ F~20~", Acta Crystallographica C (39,1983-) **41**, 1696-1698 (1985)

P: Disodium manganese chromium fluoride (6.8 %)*

Formula sum	Cr F7 Mn Na2
Entry number	96-100-0296
Figure-of-Merit (FoM)	0.639615*
Total number of peaks	286
Peaks in range	286
Peaks matched	81
Intensity scale factor	0.53*
Space group	P 31 2 1
Crystal system	trigonal (hexagonal axes)
Unit cell	a= 7.4210 Å c= 18.1660 Å
I/Ic	2.21
Calc. density	3.287 g/cm³
Reference	Courbion G, Ferey G, Holler H, Babel D, "On trigonal weberites: structure refinement of Na~2~MnCrF~7~ andNa~2~MnGaF~7~", European Journal of Solid State Inorganic Chemistry **25**, 435-447 (1988)

Q: Dibarium octafluorotriniccolate decafluorotetraniccolate (7.2 %)*

Formula sum	Ba2 F18 Ni7
Entry number	96-100-0249
Figure-of-Merit (FoM)	0.633072*
Total number of peaks	498
Peaks in range	498
Peaks matched	213
Intensity scale factor	0.35*
Space group	P -1
Crystal system	triclinic (anorthic)
Unit cell	a= 6.9370 Å b= 7.2290 Å c= 7.4560 Å α= 94.370° β= 93.160 ° γ= 115.660 °
I/Ic	1.35
Calc. density	5.110 g/cm³
Reference	Renaudin J, Ferey G, Kozak A, Samouel M, Lacorre P, "Crystal and magnetic structures of the ferrimagnet Ba~2~ Ni~7~ F~18~", Solid State Communications **65**, 185-188 (1988)

R: Dibarium octafluorotriniccolate decafluorotetraniccolate (5.7 %)*

Formula sum	Ba2 F18 Ni7
Entry number	96-100-0250
Figure-of-Merit (FoM)	0.637845*
Total number of peaks	500
Peaks in range	500
Peaks matched	215
Intensity scale factor	0.34*
Space group	P -1
Crystal system	triclinic (anorthic)
Unit cell	a= 6.9240 Å b= 7.2160 Å c= 7.4370 Å α= 94.390° β= 93.200 ° γ= 115.620 °
I/Ic	1.67
Calc. density	5.139 g/cm³
Reference	Renaudin J, Ferey G, Kozak A, Samouel M, Lacorre P, "Crystal and magnetic structures of the ferrimagnet Ba~2~ Ni~7~ F~18~", Solid State Communications **65**, 185-188 (1988)

S: Calcium ferrate manganate (1.3 %)*

Formula sum	Ca3 Mn3 O8.02
Entry number	96-100-0195

Figure-of-Merit (FoM)	0.632109[*]
Total number of peaks	432
Peaks in range	432
Peaks matched	62
Intensity scale factor	0.15[*]
Space group	P m 2 a
Crystal system	orthorhombic
Unit cell	a= 5.3320 Å b= 11.1800 Å c= 5.4560 Å
I/Ic	3.28
Calc. density	4.237 g/cm³
Reference	Nguyen N, Calage Y, Varret F, Ferey G, Calmaert V, Hervieu M, Raveau B, "The oxygen defect Perovskite Ca~3~ Mn~1.35~ Fe~1.65~ O~8.02~, a highlyfrustrated antiferromagnet", Journal of Solid State Chemistry **53**, 398-405 (1984)

T: Barium tantalum oxide (5.5/21.6/60) (2.0 %)[*]

Formula sum	Ba5.5 O60 Ta21.6
Entry number	96-100-1161
Figure-of-Merit (FoM)	0.623363[*]
Total number of peaks	264
Peaks in range	264
Peaks matched	108
Intensity scale factor	0.32[*]
Space group	P 4
Crystal system	tetragonal
Unit cell	a= 17.8000 Å c= 3.9050 Å
I/Ic	4.51
Meas. density	7.550 g/cm³
Calc. density	7.789 g/cm³
Reference	Gasperin M, "Structure cristalline du bronze de tungstene: Ba O (Ta~2~ O~5~)~2~", Bulletin de la Societe Francaise de Mineralogie et de Cristallographie(72,1949-100,1977) **90**, 172-175 (1967)

[*]*2theta values have been shifted internally for the calculation of the amounts, the intensity scaling factors as well as the figure-of-merit (FoM), due to the active search-match option 'Automatic zero point adaption'.*

Search-Match

Settings

Reference database used	COD-Inorg 2023.06.06
Automatic zeropoint adaptation	Yes
Downgrade entries with low scaling factors	Yes
Minimum figure-of-merit (FoM)	0.60
2theta window for peak corr.	0.30 deg.
Minimum rel. int. for peak corr.	0
Parameter/influence 2theta	0.50
Parameter/influence intensities	0.50
Parameter multiple/single phase(s)	0.50

Peak List

No.	2theta [°]	d [Å]	I/I0 (peak height)	Counts (peak area)	FWHM	Matched
1	20.80	4.2671	367.86	113.99	0.1200	B,C,G,H,L,O,T
2	23.02	3.8604	57.93	23.93	0.1600	B,C,F,G,J,L,S,T
3	24.34	3.6539	12.95	2.66	0.0800	B,D,E,G,I,L,M,N,O,P,R
4	24.64	3.5815	30.41	18.84	0.2400	E,G,I,L,M,O,Q,R,S,T
5	26.62	3.3459	1000.00	413.15	0.1600	C,D,E,F,G,I,K,L,M,N,O,Q,R
6	27.04	3.2949	40.99	21.17	0.2000	B,D,E,G,H,L,M,O,Q,R,T
7	29.36	3.0396	623.48	386.36	0.2400	A,D,E,F,G,H,I,J,K,L,P,Q,R,S,T
8	30.38	2.9398	14.57	6.02	0.1600	C,E,G,I,J,K,R,T
9	30.88	2.8934	96.20	59.62	0.2400	D,E,F,G,I,K,L,M,N,O,P,T
10	32.14	2.7828	31.83	9.86	0.1200	D,E,G,I,J,L,M,N,O,Q,R,S,T
11	32.68	2.7380	51.11	58.07	0.4400	B,D,G,H,L,M,O,P,S,T
12	33.82	2.6483	45.53	42.32	0.3600	A,B,D,G,J,L,M,N,O,Q,R,S
13	35.94	2.4968	77.07	31.84	0.1600	D,E,G,I,K,M,O,Q,R,S,T
14	36.52	2.4584	73.88	22.89	0.1200	D,E,G,I,J,K,L,M,O,Q,R,S,T
15	39.40	2.2851	201.52	62.44	0.1200	B,C,D,E,G,H,I,J,K,L,M,O,Q,R
16	40.24	2.2393	63.30	26.15	0.1600	B,C,D,E,F,G,I,J,K,L,M,N,O,P,Q,R,S,T
17	41.08	2.1956	33.48	17.29	0.2000	B,C,D,G,J,K,L,M,O,P,Q,R,S,T
18	42.42	2.1291	82.81	17.11	0.0800	B,C,D,E,G,I,J,K,L,M,O,P,Q,R,T
19	43.08	2.0980	154.76	47.95	0.1200	B,D,F,G,H,I,J,K,L,M,O,P,Q,R,T
20	43.90	2.0607	35.71	25.82	0.2800	D,E,F,G,H,I,J,K,L,M,N,O,Q,R,S,T
21	44.72	2.0248	23.42	12.09	0.2000	D,E,F,G,I,J,K,L,O,P,Q,R,S
22	45.76	1.9812	53.08	10.97	0.0800	B,C,D,E,G,I,J,K,L,M,O,Q,T
23	47.48	1.9134	114.80	94.86	0.3200	B,C,D,E,F,G,I,J,K,L,M,N,O,Q,R,S,T
24	48.48	1.8762	138.88	71.72	0.2000	A,B,D,E,F,G,I,J,L,M,N,O,R,S,T
25	48.98	1.8582	21.01	6.51	0.1200	D,E,G,I,J,K,L,M,N,O,P,Q,R,S,T
26	49.24	1.8490	16.59	5.14	0.1200	D,E,G,J,K,M,N,O,P,Q,R,T
27	50.08	1.8200	139.64	57.69	0.1600	B,D,G,I,L,M,O,P,Q,R,S,T
28	50.48	1.8065	27.32	8.46	0.1200	C,E,G,I,L,M,O,Q,S,T
29	50.68	1.7998	19.53	2.02	0.0400	A,D,E,G,I,L,M,O,R
30	50.94	1.7912	17.27	10.70	0.2400	D,E,G,J,N,O,P,Q,R,S,T
31	54.64	1.6727	50.66	15.70	0.1200	A,B,C,D,E,F,G,H,I,J,K,L,M,N,O,Q,R,S,T
32	55.30	1.6599	21.80	2.25	0.0400	B,D,E,F,G,I,J,K,L,O,P,Q,R,T

33	56.52	1.6269	21.25	4.39	0.0800	A,B,D,E,F,G,I,J,K,L,M,N,O,P,Q,R,S,T
34	57.36	1.6051	39.71	8.20	0.0800	A,B,C,D,E,F,G,I,J,K,L,M,O,P,Q,R,T
35	59.92	1.5425	125.07	25.84	0.0800	C,D,G,J,L,M,O,Q,R,T
36	60.10	1.5383	64.94	20.12	0.1200	A,B,C,D,G,I,J,L,M,O,P,Q,R,S,T
37	60.60	1.5268	33.85	10.49	0.1200	D,E,F,G,H,I,J,K,L,M,O,Q,R,S,T
38	60.96	1.5186	20.93	8.65	0.1600	D,E,F,G,I,J,L,M,N,O,P,Q,R,S,T
39	63.06	1.4730	13.03	1.35	0.0400	B,C,D,E,F,I,J,K,L,M,O,P,Q,R,S,T
40	64.00	1.4536	37.52	7.75	0.0800	B,C,D,E,F,I,J,K,L,M,O,P,Q,T
41	64.18	1.4500	18.55	5.76	0.1200	D,E,H,I,J,K,M,O,Q,R,S,T
42	64.58	1.4420	29.34	9.09	0.1200	D,E,F,I,J,L,M,O,P,Q,R,S,T
43	65.72	1.4197	25.92	8.03	0.1200	A,D,E,I,J,K,L,M,O,P,Q,R,T
44	67.70	1.3829	88.52	36.57	0.1600	A,D,E,F,I,J,K,L,M,N,O,P,Q,R,S,T
45	67.88	1.3797	34.18	10.59	0.1200	B,D,E,I,J,K,L,O,Q,R,T
46	68.28	1.3726	103.50	32.07	0.1200	D,E,H,J,K,L,M,O,Q,R,S,T
47	68.46	1.3694	41.18	12.76	0.1200	B,D,E,I,J,K,L,M,N,O,P,Q,R,S,T
48	73.42	1.2886	21.76	4.49	0.0800	C,D,E,F,I,J,K,L,M,N,O,Q,R,T
49	73.60	1.2859	15.48	11.19	0.2800	C,D,E,F,H,I,J,K,L,M,O,P,Q,R,S,T
50	75.60	1.2568	25.92	5.35	0.0800	D,E,J,K,L,M,O,P,Q,R,T
51	75.80	1.2540	14.86	3.07	0.0800	A,B,D,H,I,J,L,M,O,Q,R,S,T
52	77.62	1.2291	18.24	3.77	0.0800	A,B,C,F,J,K,L,M,N,O,P,Q,R,T
53	79.82	1.2006	80.43	16.63	0.1200	B,C,J,K,L,M,N,O,P,Q,R,S,T
54	80.06	1.1976	30.15	9.34	0.1200	F,J,K,L,M,N,O,Q,R,S,T
55	81.08	1.1851	23.91	7.41	0.1200	A,F,J,K,L,M,N,P,Q,R,S,T
56	81.44	1.1808	44.18	18.25	0.1600	C,J,K,L,M,Q,R,T
57	81.70	1.1777	22.96	4.74	0.0800	F,H,J,K,L,M,N,Q,R,S,T
58	83.60	1.1534	40.56	20.94	0.2000	B,J,K,L,M,P,Q,R,S
59	84.00	1.1512	19.24	1.99	0.0400	C,F,H,J,L,M,P,Q,R
60	84.72	1.1432	18.12	3.74	0.0800	B,F,H,J,K,L,M,P,Q,R,S
61	84.86	1.1417	15.29	3.16	0.0800	B,C,H,J,K,L,M,N,Q,R,S
62	85.46	1.1352	15.28	1.58	0.0400	A,C,J,K,L,M,P,Q,R,S

Integrated Profile Areas

Based on calculated profile

Profile area	*Counts*	*Amount*
Overall diffraction profile	636034	100.00%
Background radiation	481096	75.64%
Diffraction peaks	154938	24.36%
Peak area belonging to selected phases	149327	23.48%
Peak area of phase A (Potasium nitrate - \g)	*2571*	*0.40%*
Peak area of phase B (Iron vanadium molybdenum oxide (4/1.98/3.02/20))	*10003*	*1.57%*
Peak area of phase C (Sodium calcium hexafluoroaluminate - \a)	*11044*	*1.74%*
Peak area of phase D (Calcium ferrate manganate)	*2127*	*0.33%*
Peak area of phase E (Dibarium octafluorotriniccolate decafluorotetraniccolate)	*12864*	*2.02%*
Peak area of phase F (Dibarium octafluorotriniccolate decafluorotetraniccolate)	*9837*	*1.55%*
Peak area of phase G (Disodium manganese chromium fluoride)	*6315*	*0.99%*
Peak area of phase H (Disodium tribarium tetrachromium fluoride)	*11317*	*1.78%*
Peak area of phase I (Tetraamminepalladium chromate)	*2859*	*0.45%*
Peak area of phase J (Thallium Thallium(III) niobium oxide (1.4/0.6/2/6.6))	*3737*	*0.59%*
Peak area of phase K (Sodium calcium pentafluoroaluminate fluoride - \-beta)	*8935*	*1.40%*
Peak area of phase L (Lanthanum palladium oxide (4/1/7))	*5346*	*0.84%*
Peak area of phase M (Niobium thallium oxide hydrate (33/10.5/66.5/1.5))	*13998*	*2.20%*
Peak area of phase N (Rubidium niobium tungsten oxide (12/30/3/90))	*15797*	*2.48%*
Peak area of phase O (Rubidium niobium cyclo-trigermanate)	*5812*	*0.91%*
Peak area of phase P (Europium strontium copper oxide (1.3/1.7/2/5.65))	*4087*	*0.64%*
Peak area of phase Q (Barium tantalum oxide (5.5/21.8/60))	*5184*	*0.82%*
Peak area of phase R (Magnesium cobalt diphosphate (1.1/0.9/1))	*6874*	*1.08%*
Peak area of phase S (Potassium tecto-divanadato(III)tetraphosphate)	*5777*	*0.91%*
Peak area of phase T (Dithallium distrontium copper oxide)	*4845*	*0.76%*
Unidentified peak area	5610	0.88%

Peak Residuals

Peak data	*Counts*	*Amount*
Overall peak intensity	2022	100.00%
Peak intensity belonging to selected phases	2021	99.96%
Unidentified peak intensity	1	0.04%

Diffraction Pattern Graphics

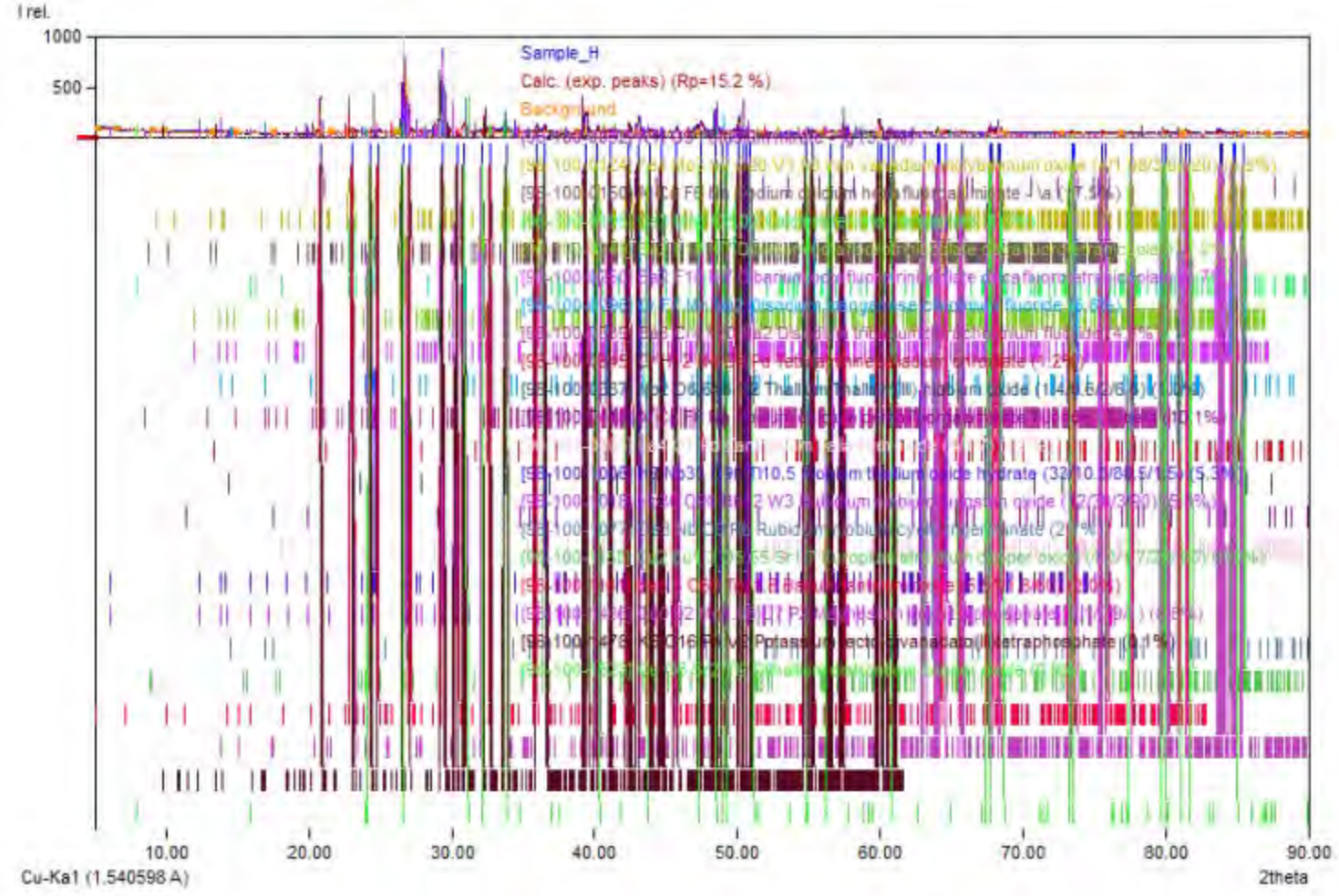

Match! Copyright © 2003-2023 CRYSTAL IMPACT, Bonn, Germany

Amounts of Phases and Elements (Weight %)

Phase composition:

Sodium calcium hexafluoroaluminate - \a (17.5%), Sodium calcium pentafluoroaluminate fluoride - S-beta (10.1%), Magnesium cobalt diphosphate (1.1/0.9/1) (8.8%), Potassium tecto-divanadato(III)tetraphosphate (8.1%), Dibarium octafluorotriniccolate decafluorotetraniccolate (7.2%), Disodium manganese chromium fluoride (6.8%), Dibarium octafluorotriniccolate decafluorotetraniccolate (5.7%), Iron vanadium molybdenum oxide (4/1.98/3.02/20) (5.5%), Niobium thallium oxide hydrate (33/10.5/88.5/1.5) (5.3%), Rubidium niobium tungsten oxide (12/30/3/90) (5.0%), Disodium tribarium tetrachromium fluoride (4.6%), Potesium nitrate - \g (3.4%), Rubidium niobium cyclo-trigermanate (2.7%), Banum tantalum oxide (5.5/21.8/60) (2.0%), Lanthanum palladium oxide (4/1/7) (1.9%), Calcium ferrate manganate (1.3%), Tetraamminepalladium chromate (1.2%), Thallium Thallium(III) niobium oxide (1.4/0.6/2/6.6) (1.0%), Europium strontium copper oxide (1.3/1.7/2/5.65) (0.9%), Dithallium distrontium copper oxide (0.9%)

Elemental composition:

F (24.55%), O (15.09%), Ca (5.80%), Nb (5.61%), Ba (5.53%), Ni (5.15%), Na (4.41%), K (3.97%), Al (3.65%), P (3.55%), Tl (2.83%), Cr (2.36%), Co (1.88%), Mn (1.81%), V (1.75%), Mo (1.70%), Ta (1.40%), La (1.35%), Fe (1.31%), Rb (1.31%), Ge (1.08%), Mg (0.91%), N (0.70%), Pd (0.70%), W (0.48%), Sr (0.46%), Eu (0.33%), Cu (0.29%), H (0.05%) (LE: 40.39%)

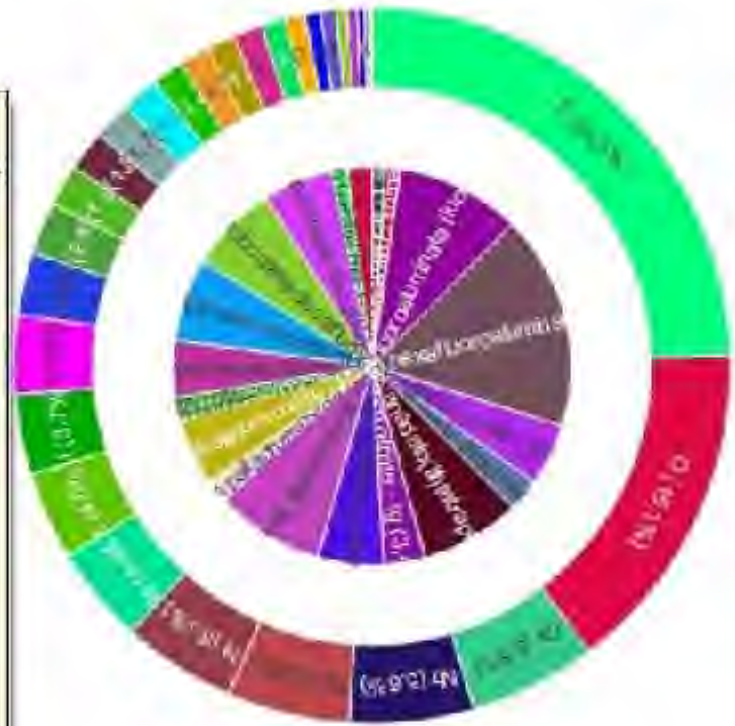

Match! Phase Analysis Report

Sample: Sample_J

Sample Data

File name	Sample_J.raw
File path	G:/.shortcut-targets-by-id/16KlMvpSIqVAUHFFggq9IVgYQzQybBTlu/Marwan - research/Concrete Mix Master Thesis/X-Ray/Birzeit University_XRD_Raw data
Data collected	Jul 13, 2023 08:55:21
Data range	4.920° - 89.920°
Original data range	5.000° - 90.000°
Number of points	4251
Step size	0.020
Rietveld refinement converged	No
Alpha2 subtracted	No
Background subtr.	No
Data smoothed	No
2theta correction	-0.08°
Radiation	X-rays
Wavelength	1.540598 Å

Analysis Results

Phase composition (Weight %)

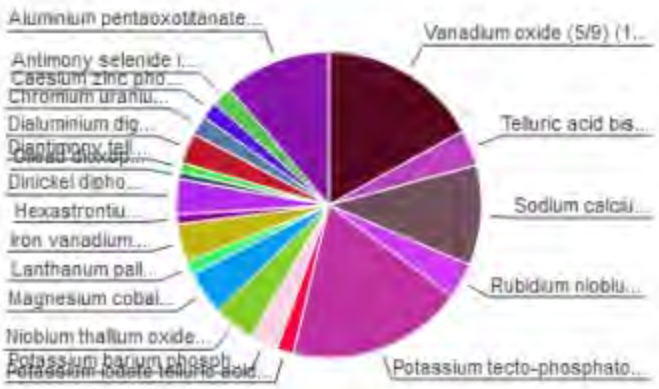

Elemental composition (Weight %)

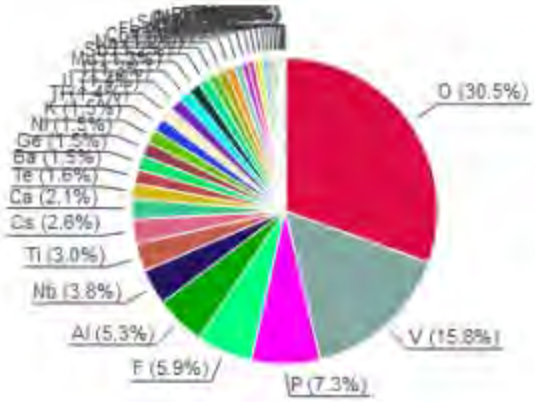

Index	*Amount (%)*	*Name*	*Formula sum*
A	17.0	Vanadium oxide (5/9)	O9 V5
B	3.8	Telluric acid bis(caesium chloride)	Cl2 Cs2 H6 O6 Te
C	10.6	Sodium calcium pentafluoroaluminate fluoride - $-beta	Al Ca F6 Na
D	3.7	Rubidium niobium tungsten oxide (12/30/3/90)	Nb30 O90 Rb12 W3
E	18.7	Potassium tecto-phosphatovanadate(III) *	K O24 P7 V4
F	1.8	Potassium iodate telluric acid	H6 I K O9 Te
G	[illegible]	[illegible]	[illegible]
H	4.4	Niobium thallium oxide hydrate (23/10.5/59.5/1.5)	H4 Nb23 O90 Tl10.5
I	4.7	Magnesium cobalt diphosphate (1.1/0.9/1)	Co0.92 Mg1.08 O7 P2
J	1.3	Lanthanum palladium oxide (4/1/7)	La4 O7 Pd
K	4.0	Iron vanadium molybdenum oxide (4/1.98/3.02/20)	Fe4 Mo3.02 O20 V1.98
L	1.0	Hexastrontium trinitridodicuprate(I) dinitridocuprate(I)	Cu3 N5 Sr6
M	3.7	Dinickel diphosphate	Ni2 O7 P2
N	0.8	Dilead dioxophosphatobismuthate	Bi O6 P Pb2
O	1.0	Diantimony telluride divelenide	Sb2 Se2 Te
P	3.2	Dialuminium digermanate	Al2 Ge2 O7
Q	2.1	Chromium uranium(V) oxide	Cr O4 U
R	1.8	Caesium zinc phosphate(V) - I	Cs O4 P Zn
S	2.2	Antimony selenide iodide	I Sb Se
T	11.3	Aluminium pentaoxotitanate	Al2 O5 Ti
	1.4	*Unidentified peak area*	

Amounts calculated by RIR (Reference Intensity Ratio) method

Element	*Amount (weight %)*
O	30.5%(*)
V	15.8%
P	7.3%
F	5.9%(*)
Al	5.3%
Nb	3.8%
Ti	3.0%
Cs	2.6%
Ca	2.1%
Te	1.6%
Ba	1.5%
Ge	1.5%
Ni	1.5%
K	1.5%
Tl	1.4%
[illegible]	[illegible]
I	1.3%
Mo	1.3%
Sb	1.2%
Na	1.2%
Co	1.0%
Fe	1.0%
La	0.9%
Se	0.9%
Sr	0.7%
Rb	0.7%
Mg	[illegible]

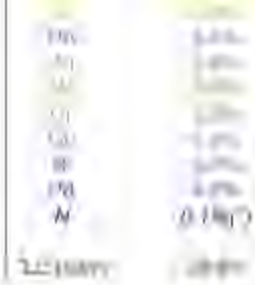

Details of identified phases

A: Vanadium oxide (5/9) (17.0 %)

Formula sum	O9 V5
Entry number	96-100-8516
Figure-of-Merit (FoM)	0.625549
Total number of peaks	497
Peaks in range	497
Peaks matched	184
Intensity scale factor	0.48
Space group	P -1
Crystal system	triclinic (anorthic)
Unit cell	a= 7.0050 Å b= 8.3629 Å c= 10.9833 Å α= 91.980° β= 108.340 ° γ= 110.390 °
I/Ic	0.88
Calc. density	4.687 g/cm³
Reference	Le Page Y, Bordet P, Marezio M, "Valence ordering in V~5~O~9~ below 120K", Journal of Solid State Chemistry **92**, 380-385 (1991)

B: Telluric acid bis(caesium chloride) (3.8 %)

Formula sum	Cl2 Cs2 H6 O6 Te
Entry number	96-100-8452
Figure-of-Merit (FoM)	0.603052
Total number of peaks	500
Peaks in range	500
Peaks matched	127
Intensity scale factor	0.29
Space group	P 1 21/c 1
Crystal system	monoclinic
Unit cell	a= 6.2430 Å b= 11.1540 Å c= 7.8620 Å β= 107.480 °
I/Ic	2.44
Calc. density	3.602 g/cm³
Reference	Averbuch-Pouchot M T, "Crystal structure of a new telluric acid adduct : Te(OH)~6~.2CsCl", Zeitschrift fuer Kristallographie (149,1979-) **182**, 291-295 (1988)

C: Sodium calcium pentafluoroaluminate fluoride - $-beta (10.6 %)

Formula sum	Al Ca F6 Na
Entry number	96-100-0418
Figure-of-Merit (FoM)	0.609237
Total number of peaks	189
Peaks in range	189
Peaks matched	21
Intensity scale factor	0.51
Space group	P 3 2 1
Crystal system	trigonal (hexagonal axes)
Unit cell	a= 8.9295 Å c= 5.0642 Å
I/Ic	1.50
Meas. density	2.880 g/cm³
Calc. density	2.906 g/cm³
Reference	Herron A, Courbion G, "The Na F - Ca F2 - Al F3 system: structures of $-beta- Na Ca Al F6 andNa4 Ca4 Al7 F33", Journal of Solid State Chemistry **84**, 153-164 (1990)

D: Rubidium niobium tungsten oxide (12/30/3/90) (3.7 %)

Formula sum	Nb30 O90 Rb12 W3
Entry number	96-100-1018
Figure-of-Merit (FoM)	0.631205
Total number of peaks	161
Peaks in range	161
Peaks matched	53
Intensity scale factor	0.51
Space group	R -3 m
Crystal system	trigonal (hexagonal axes)
Unit cell	a= 7.4860 Å c= 43.1000 Å
I/Ic	4.33
Meas. density	4.570 g/cm³

Calc. density	4.608 g/cm³
Reference	Michel C, Guyomarch A, Raveau B, "Nouveaux echangeurs cationiques avec une structure a tunnelsentrecroises: les oxides A~12~ M~33~ O~80~ et A~12~ M~33~ O~90~(H~2~ O)~12~", Journal of Solid State Chemistry **22**, 393-403 (1977)

E: Potassium tecto-phosphatovanadate(III) * (18.7 %)*

Formula sum	K O24 P7 V4
Entry number	96-100-1565
Figure-of-Merit (FoM)	0.678667
Total number of peaks	490
Peaks in range	499
Peaks matched	245
Intensity scale factor	0.62
Space group	P -1
Crystal system	triclinic (anorthic)
Unit cell	a= 10.0846 Å b= 10.2309 Å c= 10.8285 Å α= 112.757° β= 109.226 ° γ= 104.675 °
I/Ic	1.05
Calc. density	3.202 g/cm³
Reference	Benhamada L, Grandin A, Borel M M, Leclaire A, Raveau B, "A vanadium(III) phosphate with V~2~O~10~ octahedral units:KV~4~P~7~O~24~", Journal of Solid State Chemistry **104**, 103-201 (1993)

F: Potassium iodate telluric acid (1.8 %)*

Formula sum	H6 I K O9 Te
Entry number	96-100-8207
Figure-of-Merit (FoM)	0.627319
Total number of peaks	490
Peaks in range	499
Peaks matched	101
Intensity scale factor	0.27
Space group	P c 21 n
Crystal system	orthorhombic
Unit cell	a= 14.2200 Å b= 6.6960 Å c= 6.6720 Å
I/Ic	4.76
Calc. density	3.520 g/cm³
Reference	Averbuch-Pouchot M. T., "Crystal Chemistry of Some Addition Compounds of Alkali Iodates WithTelluric Acid", Journal of Solid State Chemistry **49**, 368-376 (1983)

G: Potassium barium phosphate (3.0 %)*

Formula sum	Ba K O4 P
Entry number	96-100-7162
Figure-of-Merit (FoM)	0.613050
Total number of peaks	500
Peaks in range	500
Peaks matched	53
Intensity scale factor	0.33
Space group	P n m a
Crystal system	orthorhombic
Unit cell	a= 7.7090 Å b= 5.6630 Å c= 9.9720 Å
I/Ic	3.41
Calc. density	4.140 g/cm³
Reference	Masse R, Durif A, "Chemical preparation and crystal structure refinement of K Ba P O~4~-monophosphate", Journal of Solid State Chemistry **71**, 574-576 (1987)

H: Niobium thallium oxide hydrate (33/10.5/88.5/1.5) (4.4 %)*

Formula sum	H3 Nb33 O90 Tl10.5
Entry number	96-100-1006
Figure-of-Merit (FoM)	0.674978
Total number of peaks	161
Peaks in range	161
Peaks matched	60
Intensity scale factor	0.66
Space group	R -3 m
Crystal system	trigonal (hexagonal axes)
Unit cell	a= 7.5100 Å c= 43.2900 Å
I/Ic	4.67
Calc. density	5.263 g/cm³
Reference	Gasperin M, "Synthese d'une nouvelle famille d'oxydes doubles: A~6-x~+ B~22-x~5+ O~55~ structure du compose a thallium et niobium", Acta Crystallographica B (24,1968-38,1982) **33**, 398-402 (1977)

I: Magnesium cobalt diphosphate (1.1/0.9/1) (4.7 %)*

Formula sum	Co0.92 Mg1.08 O7 P2
Entry number	96-100-1466
Figure-of-Merit (FoM)	0.617543
Total number of peaks	499
Peaks in range	499

Peaks matched	92
Intensity scale factor	0.21*
Space group	P 1 21/c 1
Crystal system	monoclinic
Unit cell	a= 6.9770 Å b= 8.3300 Å c= 9.0320 Å β= 115.740 °
I/Ic	1.44
Calc. density	3.516 g/cm³
Reference	Riou D, Leclaire A, Raveau B, "Structure of a cobalt magnesium diphosphate: (Mg~x~Co~1-x~)~2~P~2~O~7~", Acta Crystallographica C (39,1983-) **47**, 1583-1585 (1991)

J: Lanthanum palladium oxide (4/1/7) (1.3 %)*

Formula sum	La4 O7 Pd
Entry number	96-100-0485
Figure-of-Merit (FoM)	0.607211*
Total number of peaks	307
Peaks in range	307
Peaks matched	42
Intensity scale factor	0.25*
Space group	C 1 2/m 1
Crystal system	monoclinic
Unit cell	a= 13.4690 Å b= 4.0262 Å c= 9.4480 Å β= 133.420 °
I/Ic	6.05
Calc. density	6.907 g/cm³
Reference	Attfield J P, Ferey G, "Structural correlations within the lanthanum palladium oxide family", Journal of Solid State Chemistry **80**, 286-298 (1989)

K: Iron vanadium molybdenum oxide (4/1.98/3.02/20) (4.0 %)*

Formula sum	Fe4 Mo3.02 O20 V1.98
Entry number	96-100-0124
Figure-of-Merit (FoM)	0.660900*
Total number of peaks	462
Peaks in range	462
Peaks matched	111
Intensity scale factor	0.37*
Space group	P 41 2 2
Crystal system	tetragonal
Unit cell	a= 8.5390 Å c= 17.1411 Å
I/Ic	2.88
Calc. density	3.977 g/cm³
Reference	Laligant Y, Perrner L, Le Bail A, "Crystal structure of Fe4 V2 Mo3 O20 determined from conventional X-raypowder diffraction data", European Journal of Solid State Inorganic Chemistry **32**, 325-334 (1995)

L: Hexastrontium trinitridodicuprate(I) dinitridocuprate(I) (1.0 %)*

Formula sum	Cu3 N5 Sr6
Entry number	96-100-5040
Figure-of-Merit (FoM)	0.629743*
Total number of peaks	354
Peaks in range	354
Peaks matched	41
Intensity scale factor	0.22*
Space group	P 42 m c
Crystal system	tetragonal
Unit cell	a= 8.6570 Å c= 7.3340 Å
I/Ic	6.65
Calc. density	4.751 g/cm³
Reference	DiSalvo F J, Trail S S, Yamane H, Brese N E, "The crystal structure of Sr6 Cu3 N5 with isolated, bent (Cu(I)2 N3)(7-)anions and the single crystal structural determination of Sr Cu N", Journal of Alloys Compd. **255**, 122-123 (1997)

M: Dinickel diphosphate (3.7 %)*

Formula sum	Ni2 O7 P2
Entry number	96-100-7248
Figure-of-Merit (FoM)	0.638861*
Total number of peaks	500
Peaks in range	500
Peaks matched	43
Intensity scale factor	0.30*
Space group	P 1 21/a 1
Crystal system	monoclinic
Unit cell	a= 5.2120 Å b= 8.8130 Å c= 4.4750 Å β= 97.460 °
I/Ic	2.59
Meas. density	3.060 g/cm³
Calc. density	4.220 g/cm³
Reference	Masse R, Guitel J C, Durif A, "Structure cristalline d'une nouvelle variante de pyrophosphate dinickel Ni2 P2 O7", Materials Research Bulletin **14**, 337-341 (1979)

N: Diload dioxophosphatobismuthate (0.8 %)

Formula sum	Bi O6 P Pb2
Entry number	96-100-4126
Figure-of-Merit (FoM)	0.621938
Total number of peaks	499
Peaks in range	499
Peaks matched	78
Intensity scale factor	0.32
Space group	P n m a
Crystal system	orthorhombic
Unit cell	a= 5.9300 Å b= 9.0790 Å c= 11.4730 Å
I/Ic	12.92
Meas. density	7.930 g/cm³
Calc. density	8.068 g/cm³
Reference	Mizrahi A, Wignacourt J-P, Steinfink H, "Pb2 Bi O2 P O4, a new oxyphosphate" Journal of Solid State Chemistry **133**, 516-521 (1997)

O: Diantimony telluride diselenide (1.0 %)*

Formula sum	Sb2 Se2 Te
Entry number	96-100-8845
Figure-of-Merit (FoM)	0.637233*
Total number of peaks	151
Peaks in range	151
Peaks matched	16
Intensity scale factor	0.41*
Space group	R 3 m
Crystal system	trigonal (hexagonal axes)
Unit cell	a= 4.1120 Å c= 29.4950 Å
I/Ic	13.25
Meas. density	6.100 g/cm³
Calc. density	6.101 g/cm³
Reference	Andriamihaja A, Ibanez A, Jumas J C, Olivier-Fourcade J, Philippot E, "Evolution structurale de la solution solide Sb2 Te(3-x) Se(x) (0 < X<2) dans le systeme Sb2 Te3 - Sb2 Se3", Revue de Chimie Minerale **22**, 357-366 (1985)

P: Dialuminium digermanate (3.2 %)*

Formula sum	Al2 Ge2 O7
Entry number	96-100-1677
Figure-of-Merit (FoM)	0.607703*
Total number of peaks	289
Peaks in range	289
Peaks matched	48
Intensity scale factor	0.21*
Space group	C 1 2/c 1
Crystal system	monoclinic
Unit cell	a= 7.1320 Å b= 7.7416 Å c= 9.7020 Å β= 110.620 °
I/Ic	2.03
Meas. density	4.000 g/cm³
Calc. density	4.122 g/cm³
Reference	Agafonov V, Kahn A, Michel D, Perez y Jorba M, "Crystal structure of a new digermanate: Al2 Ge2 O7", Journal of Solid State Chemistry **62**, 402-404 (1986)

Q: Chromium uranium(V) oxide (2.1 %)*

Formula sum	Cr O4 U
Entry number	96-100-8068
Figure-of-Merit (FoM)	0.635558*
Total number of peaks	338
Peaks in range	338
Peaks matched	32
Intensity scale factor	0.65*
Space group	P b c n
Crystal system	orthorhombic
Unit cell	a= 4.8710 Å b= 11.7870 Å c= 5.0530 Å
I/Ic	12.96
Calc. density	8.105 g/cm³
Reference	Bacmann M, Bertaut E F, "Structure de U Cr O~4~", Bulletin de la Societe Francaise de Mineralogie et de Cristallographie(72,1949-100,1977) **87**, 275-276 (1964)

R: Caesium zinc phosphate(V) - I (1.8 %)*

Formula sum	Cs O4 P Zn
Entry number	96-100-7239
Figure-of-Merit (FoM)	0.646173*
Total number of peaks	497
Peaks in range	497
Peaks matched	54
Intensity scale factor	

	0.29
Space group	P n m a
Crystal system	orthorhombic
Unit cell	a= 9.1840 Å b= 5.4900 Å c= 9.3860 Å
I/Ic	5.09
Calc. density	4.110 g/cm³
Reference	Blum D, Durif A, Averbuch-Pouchot M T, "Crystal structures of the three forms of Cs Zn P O4", Ferroelectrics **69**, 283-292 (1986)

S: Antimony selenide iodide (2.2 %)*

Formula sum	I Sb Se
Entry number	96-100-8205
Figure-of-Merit (FoM)	0.670137
Total number of peaks	494
Peaks in range	494
Peaks matched	44
Intensity scale factor	0.62
Space group	P n m a
Crystal system	orthorhombic
Unit cell	a= 8.6980 Å b= 4.1270 Å c= 10.4120 Å
I/Ic	7.57
Calc. density	5.822 g/cm³
Reference	Ibanez A, Jumas J C, Olivier-Fourcade J, Philippot E, Maurin M, "Sur les Chalcogeno-Iodures d'antimoine SbXI (X=S,Se,Te).Structures etspectroscopie Moessbauer de ^121^Sb", Journal of Solid State Chemistry **48**, 272-283 (1983)

T: Aluminium pentaoxotitanate (11.3 %)*

Formula sum	Al2 O5 Ti
Entry number	96-100-0061
Figure-of-Merit (FoM)	0.604606
Total number of peaks	233
Peaks in range	233
Peaks matched	27
Intensity scale factor	0.55
Space group	B b m m
Crystal system	orthorhombic
Unit cell	a= 9.4290 Å b= 9.6360 Å c= 3.5910 Å
I/Ic	1.64
Calc. density	3.701 g/cm³
Reference	Morosin B, Lynch R W, "Structure studies on Al~2~ Ti O~5~ at room temperature and at 600C", Acta Crystallographica B (24,1968-38,1982) **28**, 1040-1046 (1972)

(*) *2theta values have been shifted internally for the calculation of the amounts, the intensity scaling factors as well as the figure-of-merit (FoM), due to the active search-match option 'Automatic zero point adaption'.*

Search-Match

Settings

Reference database used	COD-Inorg 2023.06.06
Automatic zeropoint adaptation	Yes
Downgrade entries with low scaling factors	Yes
Minimum figure-of-merit (FoM)	0.60
2theta window for peak corr.	0.30 deg.
Minimum rel. int. for peak corr.	0
Parameter/influence 2theta	0.50
Parameter/influence intensities	0.50
Parameter multiple/single phase(s)	0.50

Peak List

No.	2theta [°]	d [Å]	I/I0 (peak height)	Counts (peak area)	FWHM	Matched
1	9.12	9.6889	6.93	7.62	0.1600	K,O
2	12.14	7.2846	6.03	10.26	0.2400	D,F,H,N
3	18.02	4.9187	12.05	7.71	0.1200	A,B,E,F,G,J,K,M,O
4	20.84	4.2590	145.23	92.91	0.1200	C,E,F,K,R,T
5	23.02	3.8604	19.75	16.84	0.1600	A,B,C,E,F,G,I,K,L,P,Q,S
6	24.02	3.7019	7.90	1.68	0.0400	A,B,D,E,F,I,J,K,L
7	26.62	3.3459	1000.00	639.79	0.1200	A,B,C,D,E,F,G,H,J,K,L,P,Q,R,S,T
8	26.98	3.3021	15.41	29.56	0.3600	A,B,D,E,F,K,M,O,P,R
9	29.38	3.0376	266.72	284.41	0.2000	A,D,E,F,G,H,I,J,K,L,M,N,O,Q,S
10	29.94	2.9820	8.56	1.83	0.0400	B,I,J,K,P,S
11	30.12	2.9646	9.43	6.04	0.1200	A,D,E,F,H,I,J,K,N,P,Q,R
12	30.90	2.8915	97.49	103.96	0.2000	A,B,D,E,F,G,H,J,K,L,M,N,R,S
13	32.10	2.7861	16.43	35.04	0.4000	A,B,D,E,H,I,K,L,M,S
14	32.52	2.7511	30.98	19.82	0.1200	A,B,E,F,K,L,N,R,T
15	33.00	2.7122	13.15	11.22	0.1600	A,B,E,F,O,R,S
16	33.80	2.6498	23.94	25.62	0.2000	B,E,F,K,L,M,S,T
17	34.06	2.6302	21.01	22.40	0.2000	A,B,E,F,I,K,N,P,Q
18	35.38	2.5350	11.11	9.48	0.1600	A,B,C,E,F,G,I,J,K,N,P,Q,R,S
19	35.94	2.4968	32.17	27.45	0.1600	A,B,D,E,F,G,H,J,M,N,P,S
20	36.54	2.4571	31.57	26.93	0.1600	A,B,D,E,F,G,H,I,J,K,N,O

21	37.34	2.4063	11.97	5.10	0.0800	A,C,D,E,H,I,K,L,N,P,T
22	39.42	2.2840	67.27	86.07	0.2400	A,B,C,D,E,F,G,H,I,J,K,L,M,N,O,P,R,T
23	40.30	2.2361	22.41	9.56	0.0800	A,B,C,D,E,F,G,H,I,J,K,M,N,P,Q,R,S
24	41.10	2.1944	26.30	28.04	0.2000	A,C,E,F,G,I,J,K,L,N,Q,R
25	42.40	2.1301	29.62	12.64	0.0800	A,B,C,D,E,F,G,H,I,J,K,L,M,N,O,P,Q,R,S,T
26	43.14	2.0953	32.62	34.78	0.2000	A,B,E,F,G,H,I,K,L,M,N,Q,R
27	43.84	2.0634	13.00	24.95	0.3600	A,B,D,E,F,G,H,I,K,L,M,N,O,Q,R,S
28	44.90	2.0171	12.97	8.30	0.1200	A,B,D,E,F,H,I,J,L,M,N,O,P,R,S
29	45.74	1.9820	17.99	11.51	0.1200	A,B,C,D,E,F,H,I,J,K,N,P,S
30	47.46	1.9134	50.91	54.29	0.2000	A,B,C,D,E,F,G,H,I,J,K,M,N,O,P,Q,S,T
31	48.46	1.8769	38.74	41.31	0.2000	A,B,D,E,G,H,I,K,L,N,P,Q,R,S
32	50.10	1.8193	77.76	86.33	0.1600	A,B,D,E,F,G,H,K,L,M,N,O,S
33	50.50	1.8058	9.13	7.79	0.1600	A,B,C,D,E,F,G,H,K,M,N,R,S
34	51.06	1.7873	11.23	4.79	0.0800	A,B,D,E,F,G,H,I,K,L,M,N,P,Q,R,T
35	54.82	1.6733	21.75	13.91	0.1200	A,B,C,D,E,F,G,H,I,J,K,M,P,Q,R,T
36	54.98	1.6688	9.90	4.22	0.0800	A,B,D,E,F,G,H,I,J,K,N,P,R,S,T
37	57.32	1.6061	10.41	11.10	0.2000	A,B,C,D,E,F,G,H,I,J,K,L,M,N,O,P,Q,R,S,T
38	59.92	1.5425	43.33	27.72	0.1200	A,B,C,E,F,H,I,K,L,M,N,P,Q,R,S
39	60.68	1.5250	9.03	5.76	0.1200	A,B,D,F,G,H,I,K,L,M,N,O,P,Q,R,T
40	64.64	1.4408	8.71	11.14	0.2400	A,B,D,F,G,H,I,J,K,L,M,N,P,Q,S,T
41	67.72	1.3825	70.93	45.38	0.1200	A,B,D,F,G,H,I,J,K,L,N,R,S
42	67.90	1.3793	31.34	13.37	0.0800	A,D,F,G,H,I,J,K,N
43	68.10	1.3757	29.57	18.92	0.1200	A,B,F,G,K,L,N,Q,R,S,T
44	68.26	1.3726	21.79	18.69	0.1600	A,B,D,F,G,H,I,J,K,L,N,P,Q,R,S,T
45	80.06	1.1984	7.84	1.67	0.0400	B,F,G,I,J,K,L,M,N,P,Q,R,S,T
46	81.44	1.1808	53.73	34.38	0.1200	B,C,F,I,J,K,L,M,N,P,Q,R,S,T
47	81.70	1.1777	26.05	16.67	0.1200	B,F,I,J,K,L,M,N,O,P,Q,R,S,T
48	83.60	1.1554	11.02	9.40	0.1600	B,F,G,I,J,K,L,M,N,O,P,Q,R,S,T

Integrated Profile Areas

Based on calculated profile

Profile area	*Counts*	*Amount*
Overall diffraction profile	611337	100.00%
Background radiation	433402	70.89%
Diffraction peaks	177935	29.11%
Peak area belonging to selected phases	169351	27.70%
Peak area of phase A (Aluminium pentaoxotitanate)	*7915*	*1.29%*
Peak area of phase B (Iron vanadium molybdenum oxide (4/1.98/3.02/20))	*8357*	*1.37%*
Peak area of phase C (Sodium calcium pentafluoroaluminate fluoride - β-bela)	*10204*	*1.67%*
Peak area of phase D (Lanthanum palladium oxide (4/1/7))	*3760*	*0.62%*
Peak area of phase E (Niobium thallium oxide hydrate (33/10.5/88.5/1.5))	*14009*	*2.29%*
Peak area of phase F (Rubidium niobium tungsten oxide (12/30/3/90))	*13088*	*2.14%*
Peak area of phase G (Magnesium cobalt diphosphate (1.1/0.9/1))	*3770*	*0.62%*
*Peak area of phase H (Potassium tecto-phosphatovanadate(III) *)*	*17897*	*2.93%*
Peak area of phase I (Dialuminium digermanate)	*5770*	*0.94%*
Peak area of phase J (Dilead dioxophosphatobismuthate)	*4626*	*0.76%*
Peak area of phase K (Hexastrontium trinitridodicuprate(I) dinitridocuprate(I))	*3180*	*0.52%*
Peak area of phase L (Potassium barium phosphate)	*8764*	*1.43%*
Peak area of phase M (Caesium zinc phosphate(V) - II	*6759*	*1.11%*
Peak area of phase N (Dinickel diphosphate)	*4031*	*0.66%*
Peak area of phase O (Chromium uranium(V) oxide)	*8172*	*1.34%*
Peak area of phase P (Antimony selenide iodide)	*9401*	*1.54%*
Peak area of phase Q (Potassium iodate telluric acid)	*5460*	*0.89%*
Peak area of phase R (Telluric acid bis(caesium chloride))	*15665*	*2.56%*
Peak area of phase S (Vanadium oxide (5/9))	*14410*	*2.36%*
Peak area of phase T (Diantimony telluride diselenide)	*4114*	*0.67%*
Unidentified peak area	8583	1.40%

Peak Residuals

Peak data	*Counts*	*Amount*
Overall peak intensity	2008	100.00%
Peak intensity belonging to selected phases	2008	99.96%
Unidentified peak intensity	1	0.04%

Diffraction Pattern Graphics

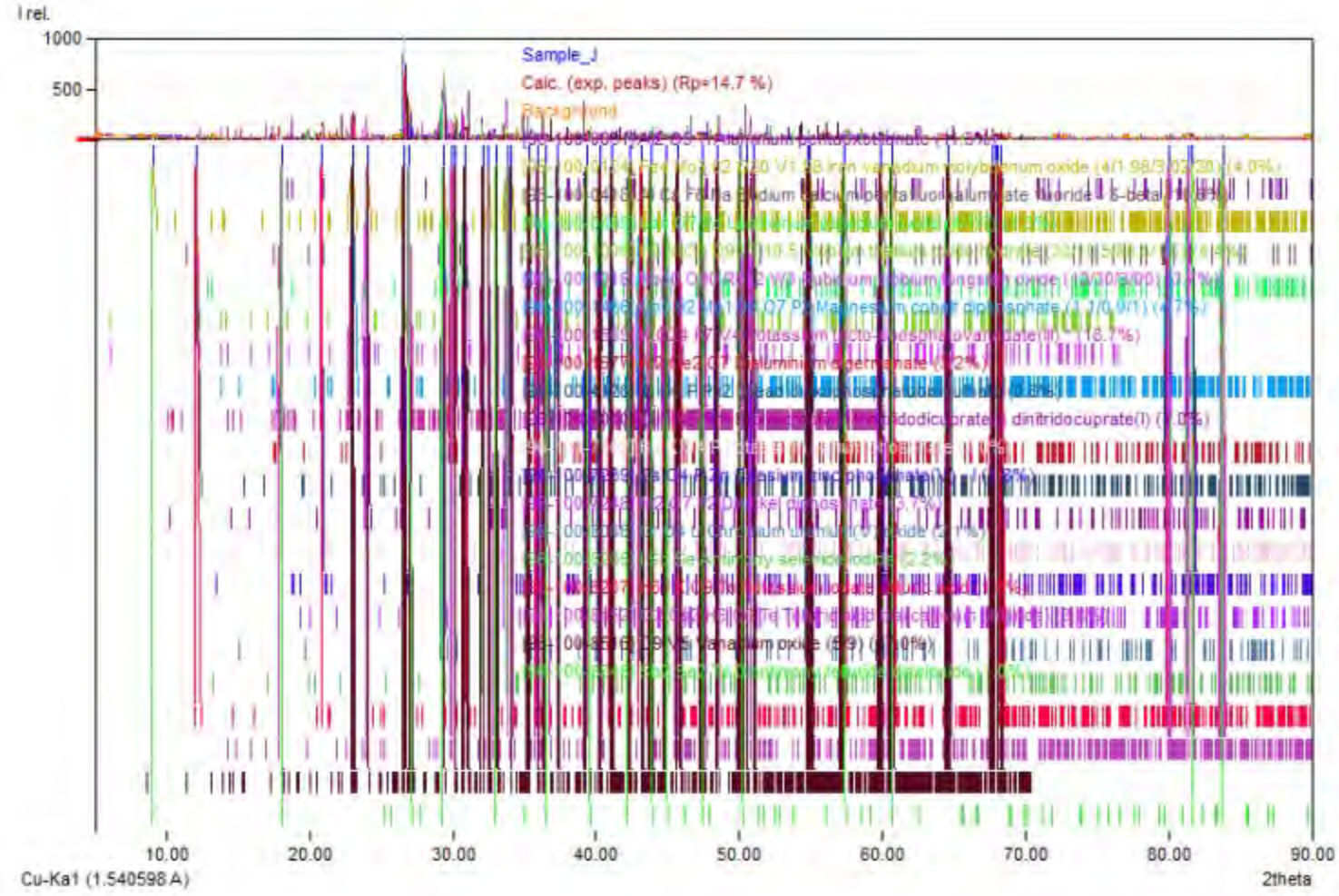

Match! Copyright © 2003-2023 CRYSTAL IMPACT, Bonn, Germany

Amounts of Phases and Elements (Weight %)

Phase composition:

Potassium tecto-phosphatovanadate(III) * (18.7%), Vanadium oxide (5/9) (17.0%), Aluminium penteoxotitanate (11.3%), Sodium calcium pentafluoroaluminate fluoride - S-beta (10.6%), Magnesium cobalt diphosphate (1.1/0.9/1) (4.7%), Niobium thallium oxide hydrate (33/10.5/88.5/7.5) (4.4%), Iron vanadium molybdenum oxide (4/1.98/3.02/20) (4.0%), Telluric acid bis(caesium chloride) (3.8%), Rubidium niobium tungsten oxide (12/30/3/90) (3.7%), Dinickel diphosphate (3.7%), Dialuminium digermanate (3.2%), Potassium barium phosphate (3.0%), Antimony selenide iodide (2.2%), Chromium uranium(V) oxide (2.1%), Caesium zinc phosphate(V) - I (1.8%), Potassium iodate telluric acid (1.8%), Lanthanum palladium oxide (4/1/7) (1.3%), Hexastrontium trinitridodicuprate(I) dinitridocuprate(I) (1.0%), Diantimony telluride diselenide (1.0%), Dilead dioxophosphatobismuthate (0.8%)

Elemental composition:

O (30.48%), V (15.81%), P (7.28%), F (5.93%), Al (5.31%), Nb (3.81%), Ti (2.97%), Cs (2.60%), Ca (2.08%), Te (1.59%), Ba (1.53%), Ge (1.52%), Ni (1.48%), K (1.46%), Tl (1.43%), U (1.39%), I (1.34%), Mo (1.26%), Sb (1.24%), Na (1.20%), Co (0.99%), Fe (0.97%), La (0.94%), Se (0.81%), Sr (0.70%), Rb (0.65%), Mg (0.48%), Cl (0.47%), Pb (0.43%), Zn (0.40%), W (0.35%), Cr (0.30%), Cu (0.25%), Br (0.22%), Pd (0.18%), N (0.09%), H (0.07%) {LE 36.56%}

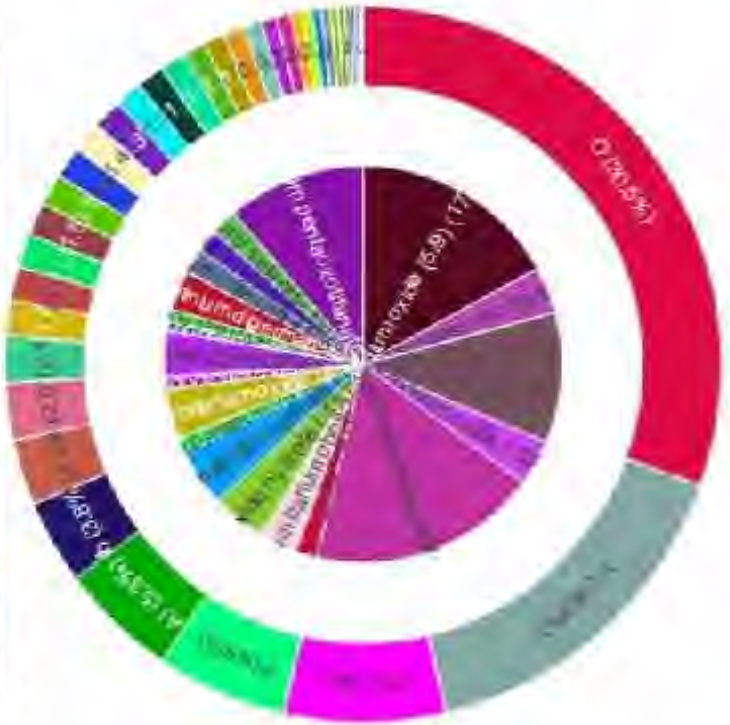

Match! Phase Analysis Report

Sample: Sample_N

Sample Data

File name	Sample_N.raw
File path	G:/.shortcut-targets-by-id/16KlMvpSlqVAUHFFggq9lVgYQzQybBTlu/Marwan - research/Concrete Mix Master Thesis/X-Ray/Birzeit University_XRD_Raw data
Data collected	Jul 13, 2023 10:36:48
Data range	4.710° - 89.710°
Original data range	5.000° - 90.000°
Number of points	4251
Step size	0.020
Rietveld refinement converged	No
Alpha2 subtracted	No
Background subtr.	No
Data smoothed	No
2theta correction	-0.29°
Radiation	X-rays
Wavelength	1.540598 Å

Analysis Results

Phase composition (Weight %)

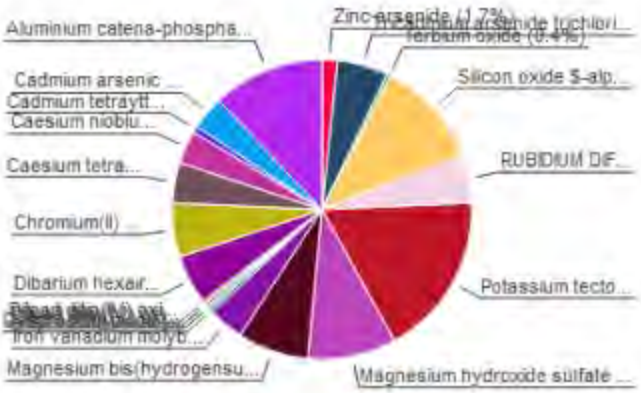

Elemental composition (Weight %)

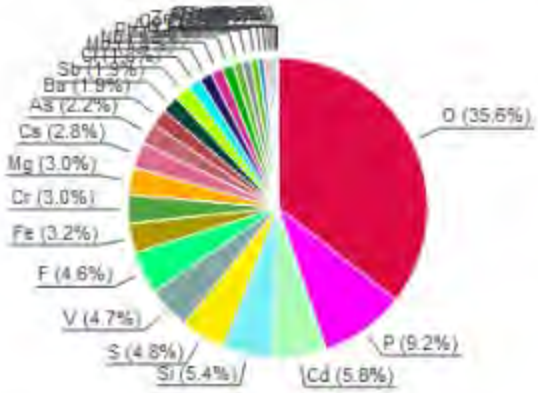

Index	*Amount (%)*	*Name*	*Formula sum*
A	1.7	Zinc arsenide	As2 Zn3
B	5.5	Tricadmium arsenide trichloride	As Cd3 Cl3
C	0.4	Terbium oxide	O3 Tb2
F	17.7	Potassium tecto-phosphatovanadate(III) *	K O24 P7 V4
G	9.5	Magnesium hydroxide sulfate hydrate (1.3/.7/1/.3)	H1.3332 Mg1.3333 O4.9999 S
H	7.7	Magnesium bis(hydrogensulfate)	H2 Mg O8 S2
I	3.8	Iron vanadium molybdenum oxide (4/1.98/3.02/20)	Fe4 Mo3.02 O20 V1.98
J	0.5	Dysprosium oxide	Dy2 O3
L	0.4	Dilead dilin(IV) oxide 0.7-hydrate	H1.4 O6.7 Pb2 Sn2
N	5.3	Dibarium hexairon(III) oxide	Ba2 Fe6 O11
P	4.4	Caesium tetrafluorocobaltate	Co Cs F4
Q	3.6	Caesium niobium phosphate (1/3/3)	Cs Nb3 O15 P3
R	0.7	Cadmium tetrayttrium trimolybdenum oxide	Cd Mo3 O16 Y4
S	3.6	Cadmium arsenic chloride *	As Cd2 Cl2
T	12.1	Aluminium catena-phosphate	Al O9 P3
	2.0	*Unidentified peak area*	

Amounts calculated by RIR (Reference Intensity Ratio) method

Element	*Amount (weight %)*
O	35.6%(*)
P	9.2%
V	4.7%
F	4.6%(*)
Fe	3.2%
Cr	3.0%
Mg	3.0%
Cs	2.8%
As	2.2%
Ba	1.9%
Sb	1.9%
Si	1.8%
Mo	1.4%
Nb	1.3%
Rb	1.3%
Al	1.2%
Co	1.0%
Zn	1.0%
K	0.6%
Pb	0.6%
Dy	0.4%
Tb	0.4%
Sn	0.3%
Y	0.2%
*LE (sum)	40.3%

Details of identified phases

A: Zinc arsenide (1.7 %)*

Formula sum	As2 Zn3
Entry number	96-101-1350
Figure-of-Merit (FoM)	0.627541*
Total number of peaks	412
Peaks in range	412
Peaks matched	54
Intensity scale factor	0.28*
Space group	P 42/n m c
Crystal system	tetragonal
Unit cell	a= 8.3160 Å c= 11.7600 Å
I/Ic	5.69
Meas. density	5.580 g/cm³
Calc. density	5.652 g/cm³
Reference	Stackelberg M von, Paulus R, "Untersuchungen an den Phosphiden und Arseniden des Zinks und Cadmiums.Das Zn3 P2 - Gitter", Zeitschrift fuer Physikalische Chemie, Abteilung B: Chemie derElementarprozesse, Aufbau der Materie **28**, 427-460 (1935)

B: Tricadmium arsenide trichloride (5.5 %)*

Formula sum	As Cd3 Cl3
Entry number	96-100-1626
Figure-of-Merit (FoM)	0.626365*
Total number of peaks	500
Peaks in range	500
Peaks matched	111
Intensity scale factor	0.36*
Space group	P n m a
Crystal system	orthorhombic
Unit cell	a= 13.1440 Å b= 8.1020 Å c= 7.0820 Å
I/Ic	2.25
Meas. density	4.580 g/cm³
Calc. density	4.566 g/cm³
Reference	Rebbah A, Yazbeck J, Deschanvres A, "Structure de Cd3 As Cl3 et Donnees Cristallographiques de Cd3 P Cl3", Acta Crystallographica B (24,1968-38,1982) **36**, 1744-1745 (1980)

C: Terbium oxide (0.4 %)*

Formula sum	O3 Tb2
Entry number	96-101-0338
Figure-of-Merit (FoM)	0.644515*
Total number of peaks	84
Peaks in range	84
Peaks matched	18
Intensity scale factor	0.22*
Space group	I 21 3
Crystal system	cubic
Unit cell	a= 10.7000 Å
I/Ic	17.23
Calc. density	7.934 g/cm³
Reference	Zachariasen W, "The crystal structure of the modification C of the sesquioxides of therare earth metals, and of indium and Thallium.", Norsk Geologisk Tidsskrift **9**, 310-316 (1927)

D: Silicon oxide $-alpha Quartz low (11.5 %)*

Formula sum	O2 Si
Entry number	96-101-1098
Figure-of-Merit (FoM)	0.770398*
Total number of peaks	70
Peaks in range	70
Peaks matched	23
Intensity scale factor	0.97*
Space group	P 31 2 1
Crystal system	trigonal (hexagonal axes)
Unit cell	a= 4.9130 Å c= 5.4040 Å
I/Ic	2.91
Meas. density	2.660 g/cm³
Calc. density	2.649 g/cm³
Reference	Wei P. H., "Die Bindung im Quarz", Zeitschrift fuer Kristallographie, Kristallgeometrie, Kristallphysik,Kristallchemie (-144,1977) **92**, 355-362 (1935)

E: RUBIDIUM DIFLUOROANTIMONY SULFATE (5.2 %)*

Formula sum	F2 O4 Rb S Sb
Entry number	96-100-8188
Figure-of-Merit (FoM)	0.638463*
Total number of peaks	500
Peaks in range	500
Peaks matched	89
Intensity scale factor	0.39*

Space group	P n a 21
Crystal system	orthorhombic
Unit cell	a= 9.6010 Å b= 11.5100 Å c= 5.2020 Å
I/Ic	2.62
Meas. density	3.930 g/cm³
Calc. density	3.943 g/cm³
Reference	Fourcade R, Bourgault M, Bonnet B, Ducourant B, "Synthese et structure du sulfate double M Sb F~2~ S O~4~ (M = Rb,Cs)", Journal of Solid State Chemistry **43**, 61-66 (1982)

F: Potassium tecto-phosphatovanadate(III) * (17.7 %)*

Formula sum	K O24 P7 V4
Entry number	96-100-1565
Figure-of-Merit (FoM)	0.650567*
Total number of peaks	499
Peaks in range	499
Peaks matched	203
Intensity scale factor	0.54*
Space group	P -1
Crystal system	triclinic (anorthic)
Unit cell	a= 10.0846 Å b= 10.2309 Å c= 10.8283 Å α= 112.757° β= 109.226 ° γ= 104.675 °
I/Ic	1.05
Calc. density	3.202 g/cm³
Reference	Benhamada L, Grandin A, Borel M M, Leclaire A, Raveau B, "A vanadium(III) phosphate with V~2~O~10~ octahedral units:KV~4~P~7~O~24~", Journal of Solid State Chemistry **104**, 193-201 (1993)

G: Magnesium hydroxide sulfate hydrate (1.3/.7/1/.3) (9.5 %)*

Formula sum	H1.3332 Mg1.3333 O4.9999 S
Entry number	96-110-0076
Figure-of-Merit (FoM)	0.619373*
Total number of peaks	122
Peaks in range	122
Peaks matched	27
Intensity scale factor	0.50*
Space group	I 41/a m d
Crystal system	tetragonal
Unit cell	a= 5.2420 Å c= 12.0950 Å
I/Ic	1.80
Calc. density	2.711 g/cm³
Reference	Keefer K D, Hocheila M F jr., de Jong B H W S, "The Structure of the Magnesium Hydroxide Sulfate Hydrate Mg S O~4~ (Mg(O H)~2~)~.3333~ (H~2~ O)~.3333~", Acta Crystallographica B (24,1968-38,1982) **37**, 1003-1006 (1981)

H: Magnesium bis(hydrogensulfate) (7.7 %)*

Formula sum	H2 Mg O8 S2
Entry number	96-110-0085
Figure-of-Merit (FoM)	0.648968*
Total number of peaks	500
Peaks in range	500
Peaks matched	77
Intensity scale factor	0.29*
Space group	P 1 21/n 1
Crystal system	monoclinic
Unit cell	a= 7.2990 Å b= 8.2730 Å c= 4.9400 Å β= 99.990 °
I/Ic	1.30
Calc. density	2.468 g/cm³
Reference	Simonov M A, Troyanov S I, Kemnitz E, Haas D, Kammler M, "Crystal structure of Mg (H S O~4~)~2~", Kristallografiya **31**, 1220-1221 (1986)

I: Iron vanadium molybdenum oxide (4/1.98/3.02/20) (3.8 %)*

Formula sum	Fe4 Mo3.02 O20 V1.98
Entry number	96-100-0124
Figure-of-Merit (FoM)	0.672030*
Total number of peaks	462
Peaks in range	462
Peaks matched	131
Intensity scale factor	0.32*
Space group	P 41 2 2
Crystal system	tetragonal
Unit cell	a= 9.5390 Å c= 17.1411 Å
I/Ic	2.86
Calc. density	3.977 g/cm³
Reference	Lalligant Y, Perrier L, Le Bail A, "Crystal structure of Fe4 V2 Mo3 O20 determined from conventional X-raypowder diffraction data", European Journal of Solid State Inorganic Chemistry **32**, 325-334 (1995)

J: Dysprosium oxide (0.5 %)*

Formula sum	Dy2 O3
Entry number	96-101-0337
Figure-of-Merit (FoM)	0.601881*

Total number of peaks	84
Peaks in range	84
Peaks matched	17
Intensity scale factor	0.23
Space group	I 21 3
Crystal system	cubic
Unit cell	a= 10.6300 Å
I/Ic	17.60
Calc. density	9.250 g/cm³
Reference	Zachariasen W. "The crystal structure of the modification C of the sesquioxides of the rare earth metals, and of indium and thallium" Norsk Geologisk Tidsskrift **9**, 310-316 (1927)

K: Dilead ditin(IV) oxide hydrate (0.4 %)

Formula sum	H2 O7 Pb2 Sn2
Entry number	96-100-1093
Figure-of-Merit (FoM)	0.600594
Total number of peaks	53
Peaks in range	53
Peaks matched	12
Intensity scale factor	0.20
Space group	F d -3 m
Crystal system	cubic
Unit cell	a= 10.7186 Å
I/Ic	19.56
Calc. density	8.241 g/cm³
Reference	Morgenstern Badarau I, Michel M A. "Sur un compose de type pyrochlore de formule Pb~2~ Sn~2~ O~6~ (H~2~ O)X", Annales de Chimie (Paris) (Vol=Year) **1971**, 109-124 (1971)

L: Dilead ditin(IV) oxide 0.7-hydrate (0.4 %)

Formula sum	H1.4 O6.7 Pb2 Sn2
Entry number	96-100-1147
Figure-of-Merit (FoM)	0.600620
Total number of peaks	53
Peaks in range	53
Peaks matched	12
Intensity scale factor	0.20
Space group	F d -3 m
Crystal system	cubic
Unit cell	a= 10.7186 Å
I/Ic	19.73
Calc. density	8.195 g/cm³
Reference	Morgenstern Badarau I, Michel A. "Mise en evidence d'une nouvelle phase de type pyrochlore: Pb~2~ Sn~2~O~6~ (H~2~ O)~x~", Comptes Rendus Hebdomadaires des Seances de l'Academie des Sciences,Serie C: Sciences Chimiques (1966-) **271**, 1313-1316 (1970)

M: Dilead ditin(IV) oxide (0.4 %)

Formula sum	O6 Pb2 Sn2
Entry number	96-100-1094
Figure-of-Merit (FoM)	0.600713
Total number of peaks	53
Peaks in range	53
Peaks matched	12
Intensity scale factor	0.20
Space group	F d -3 m
Crystal system	cubic
Unit cell	a= 10.7186 Å
I/Ic	19.97
Calc. density	8.067 g/cm³
Reference	Morgenstern Badarau I, Michel M A, "Sur un compose de type pyrochlore de formule Pb~2~Sn~2~ O~6~ (H~2~ O)X", Annales de Chimie (Paris) (Vol=Year) **1971**, 109-124 (1971)

N: Dibarium hexairon(III) oxide (5.3 %)

Formula sum	Ba2 Fe6 O11
Entry number	96-100-4047
Figure-of-Merit (FoM)	0.607999
Total number of peaks	500
Peaks in range	500
Peaks matched	166
Intensity scale factor	0.26
Space group	P n n m
Crystal system	orthorhombic
Unit cell	a= 23.0240 Å b= 5.1810 Å c= 5.9000 Å
I/Ic	1.67
Meas. density	4.960 g/cm³
Calc. density	4.915 g/cm³
Reference	Bolvin J C, Thomas D, Pouillard G, Perrot F. "Determination de la structure cristalline du ferrite de baryum BaFe~6~ O~11~" Journal of Solid State Chemistry **29**, 101-108 (1979)

O: Chromium(II) chromium fluoride (5.8 %)*

Formula sum	Cr2 F5
Entry number	96-100-0421
Figure-of-Merit (FoM)	0.615477*
Total number of peaks	285
Peaks in range	285
Peaks matched	43
Intensity scale factor	0.34*
Space group	C 1 2/c 1
Crystal system	monoclinic
Unit cell	a= 7.7526 Å b= 7.5228 Å c= 7.4477 Å β= 124.081 °
I/Ic	2.00
Calc. density	3.673 g/cm³
Reference	Lacorre P, Ferey G, Pannetier J, "The magnetic structure of Cr2 F5", Journal of Solid State Chemistry **98**, 227-236 (1992)

P: Caesium tetrafluorocobaltate (4.4 %)*

Formula sum	Co Cs F4
Entry number	96-100-0491
Figure-of-Merit (FoM)	0.644248*
Total number of peaks	218
Peaks in range	218
Peaks matched	70
Intensity scale factor	0.46*
Space group	I -4 c 2
Crystal system	tetragonal
Unit cell	a= 12.4476 Å c= 12.9277 Å
I/Ic	3.67
Calc. density	4.440 g/cm³
Reference	Lacorre P, Pannetier J, Fischer T, Hoppe R, Ferey G, "Ordered magnetic frustration: XVI.Magnetic structure of Cs Co F4 at 1.5K", Journal of Solid State Chemistry **93**, 37-45 (1991)

Q: Caesium niobium phosphate (1/3/3) (3.6 %)*

Formula sum	Cs Nb3 O15 P2
Entry number	96-100-1451
Figure-of-Merit (FoM)	0.614387*
Total number of peaks	499
Peaks in range	499
Peaks matched	180
Intensity scale factor	0.23*
Space group	P n n m
Crystal system	orthorhombic
Unit cell	a= 13.4454 Å b= 14.8114 Å c= 6.4422 Å
I/Ic	2.27
Calc. density	3.854 g/cm³
Reference	Borel M M, Grandin A, Costentin G, Leclaire A, Raveau B, "A new series of bronzes and bronzoids with KNb~3~P~3~O~15~ structure", Materials Research Bulletin **25**, 1155-1160 (1990)

R: Cadmium tetrayttrium trimolybdenum oxide (0.7 %)*

Formula sum	Cd Mo3 O16 Y4
Entry number	96-100-6105
Figure-of-Merit (FoM)	0.649172*
Total number of peaks	137
Peaks in range	137
Peaks matched	23
Intensity scale factor	0.21*
Space group	P n -3 n
Crystal system	cubic
Unit cell	a= 10.6860 Å
I/Ic	10.69
Meas. density	4.870 g/cm³
Calc. density	5.504 g/cm³
Reference	Bourdet J B, Chevalier R, Fournier J P, Kohlmuller R, Omaly J, "A structural study of cadmium yttrium molybdate Cd Y~4~ Mo~3~ O~16~", Acta Crystallographica B (24,1968-38,1982) **38**, 2371-2374 (1982)

S: Cadmium arsenic chloride * (3.6 %)*

Formula sum	As Cd2 Cl2
Entry number	96-100-1162
Figure-of-Merit (FoM)	0.621103*
Total number of peaks	498
Peaks in range	498
Peaks matched	122
Intensity scale factor	0.32*
Space group	P 1 21/b 1
Crystal system	monoclinic
Unit cell	a= 7.6560 Å b= 9.1930 Å c= 8.1890 Å β= 119.950 °
I/Ic	5.04

Meas. density	4.860 g/cm³
Calc. density	4.803 g/cm³
Reference	Rebbah A, Yazbeck J, Leclaire A, Deschanvres A. "Structure du Dichlorure d'Arsenic et de Dicadmium", Acta Crystallographica B (24,1968-38,1982) **36**, 771-773 (1980)

T: Aluminium catena-phosphate (12.1 %)*

Formula sum	Al O9 P3
Entry number	96-101-0267
Figure-of-Merit (FoM)	0.625739*
Total number of peaks	108
Peaks in range	108
Peaks matched	23
Intensity scale factor	0.73*
Space group	I -4 3 d
Crystal system	cubic
Unit cell	a= 13.6809 A
I/Ic	2.08
Calc. density	2.769 g/cm³
Reference	Pauling L, Sherman J. "The Crystal Structure of Aluminum Metaphosphate, Al (P O3~)3~", Zeitschrift fuer Kristallographie, Kristallgeometrie, Kristallphysik,Kristallchemie (-144,1977) **96**, 481-487 (1937)

(*)2theta values have been shifted internally for the calculation of the amounts, the intensity scaling factors as well as the figure-of-merit (FoM), due to the active search-match option 'Automatic zero point adaption'.

Search-Match

Settings

Reference database used:	COD-Inorg 2023.06.08
Automatic zeropoint adaptation	Yes
Downgrade entries with low scaling factors	Yes
Minimum figure-of-merit (FoM)	0.60
2theta window for peak corr.	0.30 deg.
Minimum rel. int. for peak corr.	0
Parameter/influence 2theta	0.50
Parameter/influence intensities	0.50
Parameter multiple/single phase(s)	0.50

Peak List

No.	2theta [°]	d [Å]	I/I0 (peak height)	Counts (peak area)	FWHM	Matched
1	5.37	16.4436	6.13	2.21	0.0400	
2	20.59	4.3102	171.66	185.42	0.1200	C,D,E,F,I,J,N,Q,R,T
3	22.79	3.8988	16.75	36.25	0.2400	A,F,H,I,N,P,Q,S
4	23.75	3.7434	13.22	9.52	0.0800	B,C,F,H,J,K,L,M,O,Q,R,S
5	24.69	3.6029	14.33	15.48	0.1200	E,F,H,I,P,Q,S,T
6	26.39	3.3746	1000.00	1080.19	0.1200	A,B,C,D,E,F,G,H,I,J,N,O,P,Q,R,S,T
7	27.17	3.2794	24.82	17.87	0.0800	B,F,H,I,Q,S
8	27.49	3.2420	6.21	6.71	0.1200	F,G,I,K,L,M,N,O,P,Q,S
9	29.13	3.0631	163.96	295.19	0.2000	B,C,E,F,I,J,K,L,M,N,O,P,Q,R,S,T
10	30.63	2.9164	55.42	99.77	0.2000	A,B,E,F,I,N,P,Q,T
11	32.49	2.7536	19.76	35.57	0.2000	A,B,E,F,H,I,N,Q,S
12	33.59	2.6659	7.04	2.54	0.0400	B,C,E,F,I,J,K,L,M,N,P,Q,R,S,T
13	35.69	2.5137	22.23	40.03	0.2000	A,B,C,F,H,I,J,N,O,P,Q,R,S
14	36.27	2.4748	60.16	65.00	0.1200	B,D,E,F,I,K,L,M,N,P,Q,S,T
15	39.19	2.2969	88.17	63.49	0.0800	A,B,C,D,E,F,G,H,I,N,P,Q,S
16	40.01	2.2517	23.82	25.73	0.1200	A,B,D,E,F,H,I,J,N,P,Q,S
17	42.19	2.1402	26.61	28.74	0.1200	A,B,D,E,F,I,N,O,P,Q
18	42.91	2.1060	19.96	50.37	0.2800	B,C,E,F,H,I,N,P,Q,R,S,T
19	43.51	2.0783	10.79	19.42	0.2000	A,B,E,F,H,I,J,N,O,P,Q
20	43.67	2.0711	6.89	12.40	0.2000	B,F,G,H,I,K,L,M,O,P,Q,S
21	45.51	1.9915	28.48	51.28	0.2000	A,B,D,E,F,H,I,N,O,Q,R,S
22	47.27	1.9214	20.37	44.01	0.2400	B,E,F,H,I,N,P,Q,S,T
23	48.21	1.8861	22.94	66.08	0.3200	C,E,F,I,J,K,L,M,N,O,P,Q,R,T
24	48.73	1.8672	5.57	18.04	0.3600	A,B,E,F,G,H,I,N,Q,S
25	49.85	1.8278	92.96	100.41	0.1200	A,C,F,H,I,P,Q,R
26	50.01	1.8223	39.61	43.01	0.1200	A,B,D,E,F,H,J,N,P,Q,S,T
27	54.59	1.6798	51.10	55.19	0.1200	A,E,F,I,J,N,P,Q,S,T
28	54.79	1.6752	21.48	30.93	0.1600	B,D,F,N,O,S
29	55.03	1.6674	9.87	7.11	0.0800	A,B,E,F,G,I,N,O,P,Q,R,S
30	57.11	1.6115	9.19	23.17	0.2800	A,B,C,D,E,F,G,H,I,K,L,M,N,O,P,Q,R,S,T
31	59.67	1.5483	156.55	98.33	0.0800	B,E,F,H,I,K,L,M,N,P,Q
32	59.83	1.5446	67.33	72.73	0.1200	C,D,E,F,H,I,N,O,P,Q,R,S,T
33	63.77	1.4583	10.72	7.72	0.0800	A,B,E,I,N,O,P,Q,S
34	63.93	1.4550	6.09	4.38	0.0800	B,C,D,G,I,N,P,Q,R,S,T
35	67.47	1.3870	26.44	28.56	0.1200	A,B,E,G,H,I,N,O,P,Q,R,S,T
36	67.65	1.3838	12.86	13.89	0.1200	B,D,E,G,H,I,N,Q,S
37	68.03	1.3770	63.67	68.77	0.1200	A,B,D,E,G,H,I,N,P,Q,S,T
38	73.41	1.2888	5.58	2.01	0.0400	A,B,D,E,G,H,I,J,N,O,P,Q,R,S
39	74.35	1.2748	20.84	15.01	0.0800	B,C,E,H,I,N,O,P,Q,R,S,T
40	74.57	1.2716	10.22	7.36	0.0800	A,B,E,G,I,J,N,O,P,Q,S
41	75.37	1.2601	23.24	16.74	0.0800	B,C,E,H,I,K,L,M,N,O,P,Q,R,S
42	75.61	1.2567	9.82	7.07	0.0800	A,B,D,E,H,I,J,N,O,P,Q,S,T
43	77.38	1.2321	26.42	19.03	0.0800	A,B,E,H,I,J,N,O,P,Q,R,S,T

44	77.63	1.2289	11.39	12.30	0.1200	B,C,D,E,G,H,I,K,L,M,N,O,P,Q,R,S
45	79.59	1.2035	93.49	97.33	0.0800	B,E,H,I,J,N,P,Q,S,T
46	79.83	1.2005	47.79	51.62	0.1200	A,B,D,E,H,I,K,L,M,N,P,Q,S
47	80.89	1.1874	14.72	15.90	0.1200	A,B,E,H,I,J,N,O,P,Q,R,S
48	81.21	1.1835	23.02	24.87	0.1200	B,D,E,H,I,N,O,P,Q,S
49	81.45	1.1807	9.46	13.62	0.1600	A,B,C,D,E,H,I,N,O,P,Q,R,S,T
50	83.55	1.1562	16.76	24.14	0.1600	B,E,H,I,N,O,P,Q,S
51	83.81	1.1533	9.82	10.61	0.1200	A,B,C,D,E,G,H,I,N,O,Q,R,S,T

Integrated Profile Areas

Based on calculated profile

Profile area	*Counts*	*Amount*
Overall diffraction profile	689385	100.00%
Background radiation	443235	64.29%
Diffraction peaks	246150	35.71%
Peak area belonging to selected phases	232070	33.66%
Peak area of phase A (Zinc arsenide)	*4069*	*0.59%*
Peak area of phase B (Tricadmium arsenide trichloride)	*17192*	*2.49%*
Peak area of phase C (Terbium oxide)	*2035*	*0.30%*
Peak area of phase D (Silicon oxide S-alpha Quartz low)	*37268*	*5.41%*
Peak area of phase E (RUBIDIUM DIFLUOROANTIMONY SULFATE)	*18427*	*2.67%*
*Peak area of phase F (Potassium tecto-phosphatovanadate(III) *)*	*28854*	*4.19%*
Peak area of phase G (Magnesium hydroxide sulfate hydrate (1/3/7/1/3))	*14302*	*2.07%*
Peak area of phase H (Magnesium bis(hydrogensulfate))	*7585*	*1.10%*
Peak area of phase I (Iron vanadium molybdenum oxide (4/1.98/3.02/20))	*11249*	*1.63%*
Peak area of phase J (Dysprosium oxide)	*3086*	*0.46%*
Peak area of phase K (Dilead ditin(IV) oxide hydrate)	*1683*	*0.24%*
Peak area of phase L (Dilead ditin(IV) oxide 0.7-hydrate)	*1670*	*0.24%*
Peak area of phase M (Dilead ditin(IV) oxide)	*1631*	*0.24%*
Peak area of phase N (Dibarium hexairon(III) oxide)	*19007*	*2.76%*
Peak area of phase O (Chromium(II) chromium fluoride)	*8076*	*1.17%*
Peak area of phase P (Caesium tetrafluorocobaltate)	*16380*	*2.38%*
Peak area of phase Q (Caesium niobium phosphate (1/3/3))	*12421*	*1.80%*
Peak area of phase R (Cadmium tetrayttrium trimolybdenum oxide)	*1790*	*0.26%*
*Peak area of phase S (Cadmium arsenic chloride *)*	*15826*	*2.30%*
Peak area of phase T (Aluminium catena-phosphate)	*9516*	*1.38%*
Unidentified peak area	14080	2.04%

Peak Residuals

Peak data	*Counts*	*Amount*
Overall peak intensity	3113	100.00%
Peak intensity belonging to selected phases	3111	99.94%
Unidentified peak intensity	2	0.06%

Diffraction Pattern Graphics

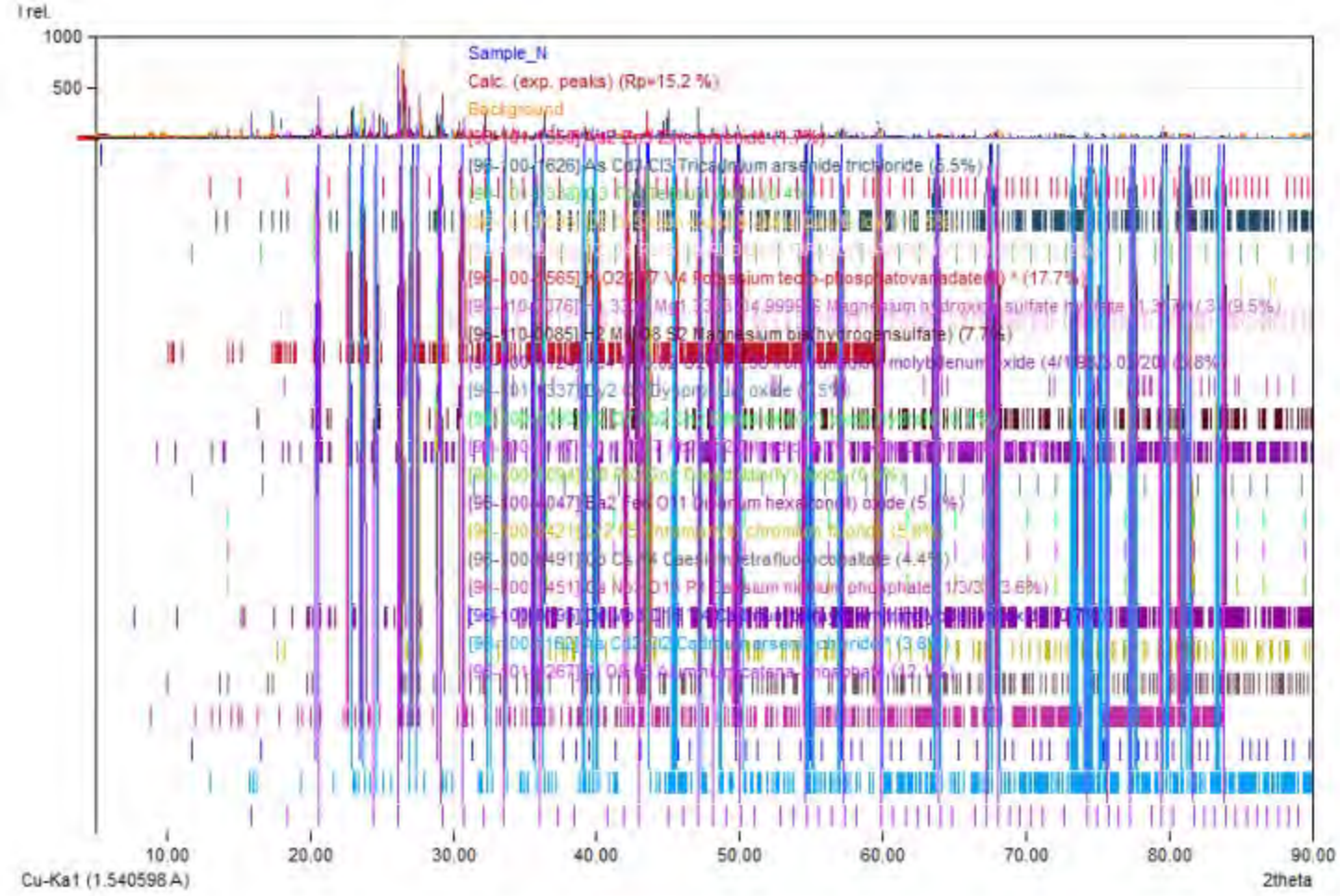

Match! Copyright © 2003-2023 CRYSTAL IMPACT, Bonn, Germany

Amounts of Phases and Elements (Weight %)

Phase composition:

Potassium tecto-phosphatovanadate(III) * (17.7%), Aluminium catena-phosphate (12.1%), Silicon oxide S alpha Quartz low (11.5%), Magnesium hydroxide sulfate hydrate (1.3/.7/1/.3) (9.5%), Magnesium bis(hydrogensulfate) (7.7%), Chromium(II) chromium fluoride (5.8%), Tricadmium arsenide trichloride (5.5%), Dibarium hexairon(III) oxide (5.3%), RUBIDIUM DIFLUORDANTIMONY SULFATE (5.2%), Caesium tetrafluorocobaltate (4.4%), Iron vanadium molybdenum oxide (4/1.98/3.02/20) (3.8%), Cadmium arsenic chloride * (3.6%), Caesium niobium phosphate (1/3/3) (3.6%), Zinc arsenide (1.7%), Cadmium tetrayttrium trimolybdenum oxide (0.7%), Dysprosium oxide (0.5%), Terbium oxide (0.4%), Dilead ditin(IV) oxide hydrate (0.4%), Dilead ditin(IV) oxide 0.7-hydrate (0.4%), Dilead ditin(IV) oxide (0.4%)

Elemental composition:

O (35.56%), P (9.24%), Cd (5.82%), Si (5.38%), S (4.84%), V (4.68%), F (4.60%), Fe (3.19%), Cr (3.05%), Mg (2.98%), Cs (2.80%), As (2.25%), Ba (1.87%), Sb (1.85%), Cl (1.81%), Mo (1.38%), Nb (1.34%), Rb (1.30%), Al (1.23%), Co (0.96%), Zn (0.95%), K (0.82%), Pb (0.58%), Dy (0.40%), Tb (0.38%), Sn (0.33%), Y (0.24%), H (0.16%) (LE: 40.32%)

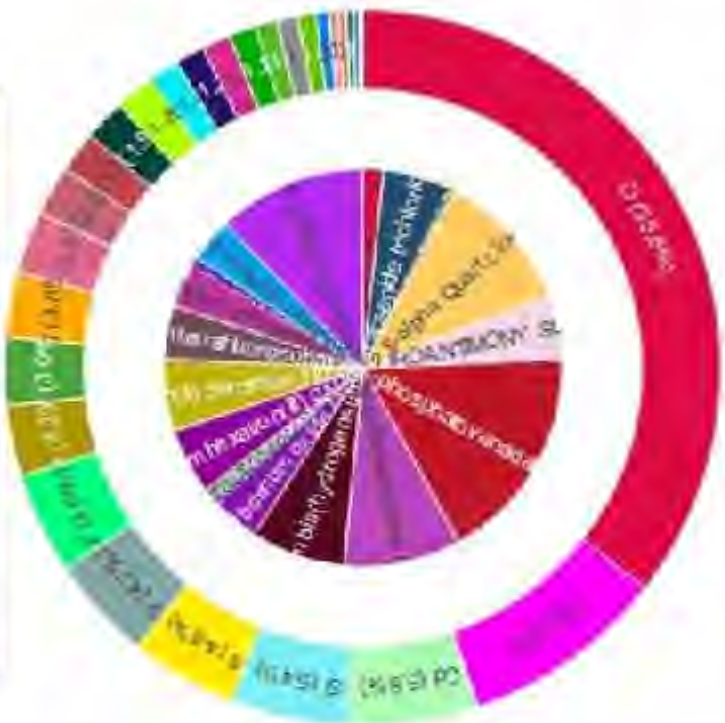

Match! Phase Analysis Report

Sample: Sample#U

Sample Data

File name	Sample#U.raw
File path	G:/.shortcut-targets-by-id/16KlMvpSIqVAUHFFggq9lVgYQzQybBTIu/Marwan - research/Concrete Mix Master Thesis/X-Ray/Birzeit University_XRD_Raw data
Data collected	Jul 13, 2023 08:25:35
Data range	4.940° - 89.940°
Original data range	5.000° - 90.000°
Number of points	4251
Step size	0.020
Rietveld refinement converged	No
Alpha2 subtracted	No
Background subtr.	No
Data smoothed	No
2theta correction	-0.06°
Radiation	X-rays
Wavelength	1.540598 Å

Analysis Results

Phase composition (Weight %)

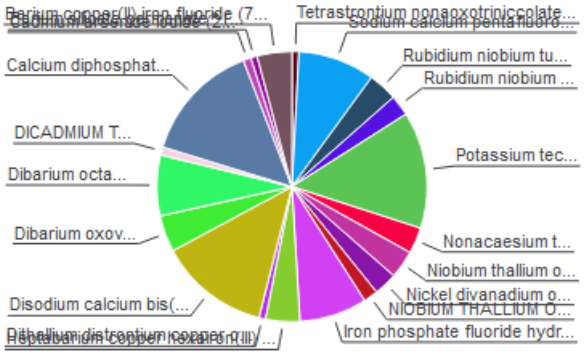

Elemental composition (Weight %)

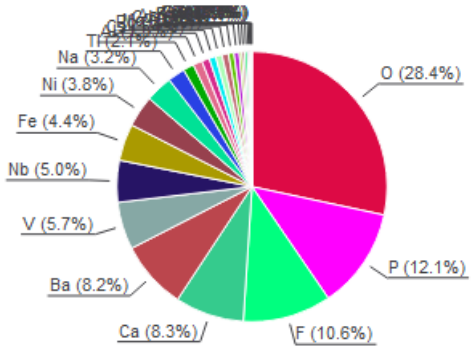

Index	*Amount (%)*	*Name*	*Formula sum*
A	0.8	Tetrastrontium nonaoxotriniccolate	Ni3 O9 Sr4
B	9.2	Sodium calcium pentafluoroaluminate fluoride - $-beta	Al Ca F6 Na
C	3.5	Rubidium niobium tungsten oxide (12/30/3/90)	Nb30 O90 Rb12 W3
D	2.5	Rubidium niobium oxide phosphate (1/3/3/3)	Nb3 O15 P3 Rb
E	14.0	Potassium tecto-phosphatovanadate(III) *	K O24 P7 V4
F	3.1	Nonacaesium tecto-trialumononamolybdo(V)undecaphosphate(V)	Al3 Cs9 Mo9 O59 P11
G	3.3	Niobium thallium oxide hydrate (33/10.5/88.5/1.5)	H3 Nb33 O90 Tl10.5
H	2.8	Nickel divanadium oxide	Ni O6 V2
I	1.7	NIOBIUM THALLIUM OXIDE (3.1/1/8.2)	Nb3.09 O8.22 Tl
J	8.1	Iron phosphate fluoride hydroxide hydrate (1.2/1/0.5/0.2/0.4)	F0.45 Fe1.21 H0.92 O4.55 P
K	4.1	Heptabarium copper hexairon(III) fluoride	Ba7 Cu F34 Fe6
L	0.8	Dithallium distrontium copper oxide	Cu O6 Sr2 Tl2
M	13.2	Disodium calcium bis(hydrogenphosphate(V))	Ca H2 Na2 O8 P2
N	4.4	Dibarium oxovanadium(IV) bis(vanadate(V))	Ba2 O9 V3
O	7.2	Dibarium octafluorotriniccolate decafluorotetraniccolate	Ba2 F18 Ni7
P	1.0	DICADMIUM TRIARSENIDE BROMIDE	As3 Br Cd2
Q	14.4	Calcium diphosphate - \b	Ca2 O7 P2
R	0.9	Cadmium arsenide iodide (2/3/1)	As3 Cd2 I
S	0.8	Barium silicate germanate *	Ba Ge3.125 O9 Si0.875
T	4.1	Barium copper(II) iron fluoride (7/1/6/34)	Ba7 Cu F34 Fe6
	1.7	*Unidentified peak area*	

Amounts calculated by RIR (Reference Intensity Ratio) method

Element	*Amount (weight %)*
O	*28.4%(*)*
P	12.1%
F	*10.6%(*)*
Ca	8.3%
Ba	8.2%
V	5.7%
Nb	5.0%
Fe	4.4%
Ni	3.8%
Na	3.2%
Tl	2.1%
Al	1.3%
Cs	1.1%
Rb	0.9%
Mo	0.8%
Cd	0.8%
As	0.8%
K	0.6%
Sr	0.6%
W	0.3%
Cu	0.3%
Ge	0.3%
I	0.2%
Br	0.1%
H	*0.1%(*)*
Si	0.0%
**LE (sum)*	*39.1%*

Details of identified phases

A: Tetrastrontium nonaoxotriniccolate (0.8 %)*

Formula sum	Ni3 O9 Sr4
Entry number	96-100-4110
Figure-of-Merit (FoM)	0.621800*
Total number of peaks	281
Peaks in range	281
Peaks matched	41
Intensity scale factor	0.15*
Space group	P 3 2 1
Crystal system	trigonal (hexagonal axes)
Unit cell	a= 9.4770 Å c= 7.8250 Å
I/Ic	4.86
Meas. density	5.400 g/cm³

Calc. density	5.488 g/cm³
Reference	Abraham F, Minaud S, Renard C, "Preliminary crystal structure of mixed-valency Sr4 Ni3 O9, the actualformula of the so-called Sr5 Ni4 O11", Journal of Materials Chemistry **4(11)**, 1763-1764 (1994)

B: Sodium calcium pentafluoroaluminate fluoride - $-beta (9.2 %)*

Formula sum	Al Ca F6 Na
Entry number	96-100-0418
Figure-of-Merit (FoM)	0.629933*
Total number of peaks	189
Peaks in range	189
Peaks matched	23
Intensity scale factor	0.52*
Space group	P 3 2 1
Crystal system	trigonal (hexagonal axes)
Unit cell	a= 8.9295 Å c= 5.0642 Å
I/Ic	1.50
Meas. density	2.880 g/cm³
Calc. density	2.906 g/cm³
Reference	Hemon A, Courbion G, "The Na F - Ca F2 - Al F3 system: structures of $-beta- Na Ca Al F6 andNa4 Ca4 Al7 F33", Journal of Solid State Chemistry **84**, 153-164 (1990)

C: Rubidium niobium tungsten oxide (12/30/3/90) (3.5 %)*

Formula sum	Nb30 O90 Rb12 W3
Entry number	96-100-1018
Figure-of-Merit (FoM)	0.667095*
Total number of peaks	161
Peaks in range	161
Peaks matched	63
Intensity scale factor	0.57*
Space group	R -3 m
Crystal system	trigonal (hexagonal axes)
Unit cell	a= 7.4860 Å c= 43.1000 Å
I/Ic	4.33
Meas. density	4.570 g/cm³
Calc. density	4.608 g/cm³
Reference	Michel C, Guyomarch A, Raveau B, "Nouveaux echangeurs cationiques avec une structure a tunnelsentrecroises: les oxides A~12~ M~33~ O~90~ et A~12~ M~33~ O~90~(H~2~ O)~12~", Journal of Solid State Chemistry **22**, 393-403 (1977)

D: Rubidium niobium oxide phosphate (1/3/3/3) (2.5 %)*

Formula sum	Nb3 O15 P3 Rb
Entry number	96-100-1462
Figure-of-Merit (FoM)	0.609247*
Total number of peaks	500
Peaks in range	500
Peaks matched	195
Intensity scale factor	0.19*
Space group	P n n m
Crystal system	orthorhombic
Unit cell	a= 13.3520 Å b= 14.7600 Å c= 6.4570 Å
I/Ic	2.02
Calc. density	3.638 g/cm³
Reference	Borel M M, Benabbas A, Rebbah H, Grandin A, Leclaire A, Raveau B, "A large family of niobium phosphate bronzes and bronzoids withKNb~3~P~3~O~15~ structure", European Journal of Solid State Inorganic Chemistry **27**, 525-535 (1990)

E: Potassium tecto-phosphatovanadate(III) * (14.0 %)*

Formula sum	K O24 P7 V4
Entry number	96-100-1565
Figure-of-Merit (FoM)	0.672962*
Total number of peaks	499
Peaks in range	499
Peaks matched	230
Intensity scale factor	0.56*
Space group	P -1
Crystal system	triclinic (anorthic)
Unit cell	a= 10.0846 Å b= 10.2309 Å c= 10.8283 Å α= 112.757° β= 109.226 ° γ= 104.675 °
I/Ic	1.05
Calc. density	3.202 g/cm³
Reference	Benhamada L, Grandin A, Borel M M, Leclaire A, Raveau B, "A vanadium(III) phosphate with V~2~O~10~ octahedral units:KV~4~P~7~O~24~", Journal of Solid State Chemistry **104**, 193-201 (1993)

F: Nonacaesium tecto-trialumononamolybdo(V)undecaphosphate(V) (3.1 %)*

Formula sum	Al3 Cs9 Mo9 O59 P11
Entry number	96-100-1642
Figure-of-Merit (FoM)	0.615763*
Total number of peaks	303
Peaks in range	303
Peaks matched	116
Intensity scale factor	0.29*
Space group	P 63/m
Crystal system	hexagonal
Unit cell	a= 16.9890 Å c= 11.8660 Å
I/Ic	2.45
Meas. density	3.880 g/cm³
Calc. density	3.835 g/cm³
Reference	Guesdon A, Borel M M, Leclaire A, Grandin A, Raveau B, "An aluminophosphate of molybdenum(V) with a tunnel structure: Cs9 Mo9Al3 P11 O59", Journal of Solid State Chemistry **114**, 451-458 (1995)

G: Niobium thallium oxide hydrate (33/10.5/88.5/1.5) (3.3 %)*

Formula sum	H3 Nb33 O90 Tl10.5
Entry number	96-100-1006
Figure-of-Merit (FoM)	0.708818*
Total number of peaks	161
Peaks in range	161
Peaks matched	70
Intensity scale factor	0.59*
Space group	R -3 m
Crystal system	trigonal (hexagonal axes)
Unit cell	a= 7.5100 Å c= 43.2900 Å
I/Ic	4.67
Calc. density	5.263 g/cm³
Reference	Gasperin M, "Synthese d'une nouvelle famille d'oxydes doubles: A~8~^+^ B~22~^5+^O~59~ structure du compose a thallium et niobium", Acta Crystallographica B (24,1968-38,1982) **33**, 398-402 (1977)

H: Nickel divanadium oxide (2.8 %)*

Formula sum	Ni O6 V2
Entry number	96-100-0095
Figure-of-Merit (FoM)	0.600801*
Total number of peaks	498
Peaks in range	498
Peaks matched	165
Intensity scale factor	0.15*
Space group	P -1
Crystal system	triclinic (anorthic)
Unit cell	a= 7.1300 Å b= 4.7910 Å c= 8.8250 Å α= 90.160º β= 102.130 º γ= 94.190 º
I/Ic	1.43
Calc. density	4.349 g/cm³
Reference	Le Bail A, Lafontaine M A, "Structure determination of NiV~2~O~6~ from X-ray powder diffraction : arutile-ramsdellite intergrowth", European Journal of Solid State Inorganic Chemistry **27**, 671-680 (1990)

I: NIOBIUM THALLIUM OXIDE (3.1/1/8.2) (1.7 %)*

Formula sum	Nb3.09 O8.22 Tl
Entry number	96-100-1011
Figure-of-Merit (FoM)	0.612612*
Total number of peaks	308
Peaks in range	308
Peaks matched	64
Intensity scale factor	0.33*
Space group	C 2 2 21
Crystal system	orthorhombic
Unit cell	a= 7.5510 Å b= 13.0050 Å c= 7.7340 Å
I/Ic	5.07
Calc. density	5.448 g/cm³
Reference	Gasperin M, "Un niobate de thallium de type 'bronze hexagonal' excedentaire encations", Acta Crystallographica B (24,1968-38,1982) **33**, 2306-2308 (1977)

J: Iron phosphate fluoride hydroxide hydrate (1.2/1/0.5/0.2/0.4) (8.1 %)*

Formula sum	F0.45 Fe1.21 H0.92 O4.55 P
Entry number	96-100-0352
Figure-of-Merit (FoM)	0.619690*
Total number of peaks	121
Peaks in range	121
Peaks matched	19
Intensity scale factor	0.75*
Space group	I 41/a m d
Crystal system	tetragonal
Unit cell	a= 5.1840 Å c= 13.0400 Å
I/Ic	2.43
Calc. density	3.416 g/cm³
Reference	Loiseau Th, Lacorre Ph, Calage Y, Greneche J M, Ferey G, "Crystal structure and magnetic study of a new iron(III) phosphate,Fe~1.21~PO~4~X (X=F, OH, H~2~O), isostructural with 3MgSO~4~ .Mg(OH)~2~ . H~2~O", Journal of Solid State Chemistry **105**, 417-427 (1993)

K: Heptabarium copper hexairon(III) fluoride (4.1 %)*

Formula sum	Ba7 Cu F34 Fe6
Entry number	96-100-0279
Figure-of-Merit (FoM)	0.612674*
Total number of peaks	301
Peaks in range	301
Peaks matched	129
Intensity scale factor	0.30*
Space group	C 1 2/m 1
Crystal system	monoclinic
Unit cell	a= 16.8920 Å b= 11.3310 Å c= 7.6460 Å β= 101.750 º
I/Ic	1.95
Calc. density	4.649 g/cm³
Reference	Renaudin J, Ferey G, Drillon M, De Kozak A, Samouel M, "La structure magnetique du ferrimagnetique monodimensionnel Ba~7~ CuFe~6~ F~34~ de type jarlite", Comptes Rendus Hebdomadaires des Seances de l'Academie des Sciences,Serie C, Sciences Chimiques (1966-) **308**, 1217-1222 (1989)

L: Dithallium distrontium copper oxide (0.8 %)*

Formula sum	Cu O6 Sr2 Tl2
Entry number	96-100-1523
Figure-of-Merit (FoM)	0.602648*
Total number of peaks	144
Peaks in range	144
Peaks matched	22
Intensity scale factor	0.39*
Space group	I 4/m m m

Crystal system	tetragonal
Unit cell	a= 3.7464 Å c= 22.3013 Å
I/Ic	13.06
Calc. density	7.889 g/cm³
Reference	Martin C, Maignan A, Huve M, Michel C, Hervieu M, Raveau B, "The influence of alkaline-earth ions on the properties of the"2201"superconductive cuprates: the solid solution Tl~2~Ba~2-x~Sr~x~CuO~6+d~", European Journal of Solid State Inorganic Chemistry **30**, 7-18 (1993)

M: Disodium calcium bis(hydrogenphosphate(V)) (13.2 %)*

Formula sum	Ca H2 Na2 O8 P2
Entry number	96-100-0141
Figure-of-Merit (FoM)	0.602568*
Total number of peaks	497
Peaks in range	497
Peaks matched	118
Intensity scale factor	0.25*
Space group	P 1 21 1
Crystal system	monoclinic
Unit cell	a= 9.0652 Å b= 7.1468 Å c= 5.4700 Å β= 98.782 º
I/Ic	0.49
Calc. density	2.636 g/cm³
Reference	Ben Chaabane T, Smiri-Dogguy L, Laligant Y, Le Bail A, "Structure of Na2 Ca (H P O4)2 determined ab initio from conventionalpowder diffraction data", European Journal of Solid State Inorganic Chemistry **34**, 937-946 (1997)

N: Dibarium oxovanadium(IV) bis(vanadate(V)) (4.4 %)*

Formula sum	Ba2 O9 V3
Entry number	96-100-4117
Figure-of-Merit (FoM)	0.648747*
Total number of peaks	499
Peaks in range	499
Peaks matched	112
Intensity scale factor	0.56*
Space group	P 1 21/m 1
Crystal system	monoclinic
Unit cell	a= 9.3020 Å b= 5.9690 Å c= 8.1180 Å β= 113.960 º
I/Ic	3.34
Meas. density	4.650 g/cm³
Calc. density	4.607 g/cm³
Reference	Dhaussy A-C, Abraham F, Mentre O, Steinfink H, "Crystal structure and characterization of Ba2 V3 O9: a vanadyl(IV)vanadate containing rutile-like chains of V O6 octahedra", Journal of Solid State Chemistry **126**, 328-335 (1996)

O: Dibarium octafluorotriniccolate decafluorotetraniccolate (7.2 %)*

Formula sum	Ba2 F18 Ni7
Entry number	96-100-0250
Figure-of-Merit (FoM)	0.621887*
Total number of peaks	500
Peaks in range	500
Peaks matched	179
Intensity scale factor	0.46*
Space group	P -1
Crystal system	triclinic (anorthic)
Unit cell	a= 6.9240 Å b= 7.2180 Å c= 7.4370 Å α= 94.390º β= 93.200 º γ= 115.820 º
I/Ic	1.67
Calc. density	5.139 g/cm³
Reference	Renaudin J, Ferey G, Kozak A, Samouel M, Lacorre P, "Crystal and magnetic structures of the ferrimagnet Ba~2~ Ni~7~ F~18~", Solid State Communications **65**, 185-188 (1988)

P: DICADMIUM TRIARSENIDE BROMIDE (1.0 %)*

Formula sum	As3 Br Cd2
Entry number	96-100-1295
Figure-of-Merit (FoM)	0.603130*
Total number of peaks	284
Peaks in range	284
Peaks matched	70
Intensity scale factor	0.21*
Space group	C 1 c 1
Crystal system	monoclinic
Unit cell	a= 8.2860 Å b= 9.4080 Å c= 7.9870 Å β= 101.300 º
I/Ic	5.61
Calc. density	5.760 g/cm³
Reference	Rebbah A, Yazbeck J, Lande R, Deschanvres A, "Etudes structurales et optiques des phases du type Cd~2~ A~3~ X (A =As, P", Materials Research Bulletin **16**, 525-533 (1981)

Q: Calcium diphosphate - \b (14.4 %)*

Formula sum	Ca2 O7 P2
Entry number	96-100-1557
Figure-of-Merit (FoM)	0.634388*
Total number of peaks	328
Peaks in range	328
Peaks matched	96
Intensity scale factor	0.41*
Space group	P 41
Crystal system	tetragonal
Unit cell	a= 6.6858 Å c= 24.1470 Å
I/Ic	0.74
Calc. density	3.127 g/cm³
Reference	Boudin S., Grandin A., Borel M. M., Leclaire A., Raveau B., "Redetermination of the \b-Ca~2~P~2~O~7~ structure", Acta Crystallographica, Section C: Crystal Structure Communications **49(12)**, 2062-2064 (1993)

R: Cadmium arsenide iodide

(2/3/1) (0.9 %) *

Formula sum	As3 Cd2 I
Entry number	96-100-1838
Figure-of-Merit (FoM)	0.609625*
Total number of peaks	286
Peaks in range	286
Peaks matched	92
Intensity scale factor	0.23*
Space group	C 1 c 1
Crystal system	monoclinic
Unit cell	a= 8.4360 Å b= 9.5940 Å c= 7.9520 Å β= 100.650 º
I/Ic	6.49
Calc. density	6.053 g/cm³
Reference	Rebbah A, Leclaire A, Yazbeck J, Deschanvres A, "Structure de l'iodure de cadmium et d'arsenic Cd2 As3 I", Acta Crystallographica B (24,1968-38,1982) **35**, 2197-2199 (1979)

S: Barium silicate germanate
**** (0.8 %)*** *

Formula sum	Ba Ge3.125 O9 Si0.875
Entry number	96-100-1067
Figure-of-Merit (FoM)	0.615863*
Total number of peaks	275
Peaks in range	275
Peaks matched	70
Intensity scale factor	0.13*
Space group	P 3 1 c
Crystal system	trigonal (hexagonal axes)
Unit cell	a= 11.5950 Å c= 9.7550 Å
I/Ic	4.55
Meas. density	4.660 g/cm³
Calc. density	4.673 g/cm³
Reference	Goreaud M, Choisnet J, Deschanvres A, Raveau B, "Synthese et Evolution Structurale de Nouveaux Silicogermanates Ba Ge(Ge~3-x~ Si~x~) O~9~ de Type Benitoite et de Structure Apparentee", Materials Research Bulletin **8**, 1205-1214 (1973)

T: Barium copper(II) iron fluoride
(7/1/6/34) (4.1 %) *

Formula sum	Ba7 Cu F34 Fe6
Entry number	96-100-0221
Figure-of-Merit (FoM)	0.607397*
Total number of peaks	301
Peaks in range	301
Peaks matched	137
Intensity scale factor	0.31*
Space group	C 1 2/m 1
Crystal system	monoclinic
Unit cell	a= 16.9820 Å b= 11.3720 Å c= 7.6630 Å β= 101.470 º
I/Ic	1.96
Calc. density	4.593 g/cm³
Reference	Renaudin J, Ferey G, Kozak A de, Samouel M, "Fluorures complexes de cuivre(II). VI. Structure cristalline de Ba~7~Cu Fe~6~ F~34~", Revue de Chimie Minerale **24**, 295-304 (1987)

(*) 2theta values have been shifted internally for the calculation of the amounts, the intensity scaling factors as well as the figure-of-merit (FoM), due to the active search-match option 'Automatic zero point adaption'.

Search-Match

Settings

Reference database used	COD-Inorg 2023.06.06
Automatic zeropoint adaptation	Yes
Downgrade entries with low scaling factors	Yes
Minimum figure-of-merit (FoM)	0.60
2theta window for peak corr.	0.30 deg.
Minimum rel. int. for peak corr.	0
Parameter/influence 2theta	0.50
Parameter/influence intensities	0.50
Parameter multiple/single phase(s)	0.50

Peak List

No.	*2theta [º]*	*d [Å]*	*I/I0 (peak height)*	*Counts (peak area)*	*FWHM*	*Matched*
1	18.04	4.9133	72.16	63.17	0.1600	D,E,F,H,I,K,M,N,S,T
2	20.86	4.2550	219.18	95.94	0.0800	B,D,E,F,H,M,N,T
3	23.06	3.8538	24.50	26.81	0.2000	B,D,E,F,H,I,K,T
4	24.02	3.7019	14.01	9.20	0.1200	C,D,E,F,H,K,L,M,N,O,Q,S,T
5	26.62	3.3459	1000.00	656.58	0.1200	B,C,D,E,F,G,H,I,J,K,L,M,N,O,Q,S,T
6	27.46	3.2455	55.43	36.39	0.1200	C,D,E,F,G,H,I,J,K,T
7	27.72	3.2156	12.46	10.91	0.1600	C,D,E,F,G,J,M,O,Q,T
8	28.64	3.1144	15.63	17.10	0.2000	A,C,D,E,F,G,H,K,N,O,P,Q,R,S,T
9	29.40	3.0356	184.83	202.26	0.2000	A,C,D,E,G,H,I,O,P,Q,R,T
10	30.92	2.8897	91.33	99.95	0.2000	A,C,D,E,F,G,H,K,L,M,N,Q,S,T
11	32.14	2.7828	41.77	73.14	0.3200	C,E,F,G,K,L,M,N,O,P,Q,R,S,T
12	32.54	2.7495	31.43	27.51	0.1600	A,D,E,F,K,M,N,O,Q,S,T
13	32.88	2.7218	9.68	10.59	0.2000	D,E,F,H,I,K,M,P,R,S,T
14	34.08	2.6287	50.04	54.75	0.2000	A,D,E,F,H,K,L,M,P,R
15	36.00	2.4927	21.28	13.97	0.1200	A,C,D,E,F,G,H,I,K,M,N,O,Q,S,T
16	36.54	2.4571	90.39	39.56	0.0800	C,D,E,F,G,H,I,K,M,N,O,R,S,T
17	39.44	2.2829	79.87	87.41	0.2000	A,B,C,D,E,F,G,H,J,K,M,N,O,P,Q,R,T
18	40.28	2.2372	57.99	25.38	0.0800	A,B,C,D,E,F,G,H,K,L,M,N,O,P,Q,S,T
19	41.14	2.1924	28.89	37.94	0.2400	A,B,D,E,F,H,K,M,N,O,Q,S,T
20	42.44	2.1282	44.41	29.16	0.1200	B,C,D,E,F,G,H,I,K,M,N,O,Q,S,T
21	43.14	2.0953	22.47	24.59	0.2000	D,E,F,G,H,I,K,M,N,O,Q,R,S,T
22	44.88	2.0180	10.70	4.68	0.0800	A,C,D,E,F,G,H,I,J,K,M,N,O,P,Q,R,S,T
23	45.78	1.9804	41.11	26.99	0.1200	A,B,C,D,E,F,G,H,K,N,Q,R,S,T
24	47.44	1.9149	24.77	27.11	0.2000	B,C,D,E,F,G,H,K,L,M,N,O,P,R,S,T
25	48.54	1.8740	25.16	33.05	0.2400	A,C,D,E,F,G,H,I,J,K,L,M,N,O,P,Q,R,S,T
26	50.12	1.8186	185.70	81.28	0.0800	A,C,D,E,F,G,H,I,K,M,N,O,P,S,T
27	50.54	1.8045	12.72	61.26	0.8800	A,B,C,D,E,F,G,H,I,K,M,N,O,P,Q,R,S,T
28	54.86	1.6721	36.44	23.92	0.1200	B,C,D,E,F,G,H,K,L,M,N,O,P,Q,R,S,T

29	55.32	1.6593	9.76	8.55	0.1600	A,C,D,E,F,G,H,I,J,K,M,N,O,Q,R,T
30	56.62	1.6243	19.71	8.63	0.0800	A,C,D,E,F,G,H,I,J,K,M,N,O,P,Q,S,T
31	57.42	1.6035	10.09	11.04	0.2000	A,B,C,D,E,F,G,H,I,J,K,M,N,O,P,Q,R,S,T
32	59.94	1.5420	141.28	92.76	0.1200	A,B,D,E,F,H,K,M,N,O,P,Q,R,S,T
33	60.10	1.5383	57.41	25.13	0.0800	A,B,D,E,F,G,H,K,M,N,O,P,Q,R,T
34	60.70	1.5245	10.44	43.40	0.7600	A,C,D,F,G,H,I,K,L,M,N,O,Q,R,S,T
35	62.36	1.4878	9.64	12.66	0.2400	A,B,C,D,F,G,H,I,K,L,M,N,O,P,Q,R,S
36	64.04	1.4528	16.95	11.13	0.1200	A,B,C,D,F,G,H,J,K,M,N,O,P,Q,R,S,T
37	65.78	1.4185	9.90	2.17	0.0400	A,C,D,F,G,H,I,K,M,N,O,P,Q,R,S,T
38	67.72	1.3825	82.41	36.07	0.0800	C,D,F,G,H,L,M,N,O,P,Q,R,S
39	67.90	1.3793	39.56	25.98	0.1200	A,C,D,F,G,H,I,J,M,N,O,P,R,S
40	68.30	1.3722	96.00	63.03	0.1200	C,D,F,H,I,M,N,O,Q
41	68.48	1.3690	37.49	16.41	0.0800	A,C,D,F,G,H,J,L,M,N,O,P,Q,R,S
42	73.44	1.2883	14.21	6.22	0.0800	A,B,C,D,G,H,I,L,M,N,O,P,Q,R,S
43	75.64	1.2562	26.95	11.80	0.0800	A,D,G,H,I,J,M,N,O,P,R,S
44	77.64	1.2288	19.43	8.50	0.0800	A,D,H,I,J,L,M,N,O,P,Q,R,S
45	80.02	1.1981	16.72	14.63	0.1600	A,D,H,I,J,L,M,O,P,Q,R,S
46	81.42	1.1810	31.97	20.99	0.1200	A,D,H,I,M,N,O,P,Q,R
47	81.68	1.1779	11.12	7.30	0.1200	A,B,D,H,I,L,M,N,O,P,Q,R,S
48	83.82	1.1532	30.87	13.51	0.0800	D,H,I,J,M,N,O,P,Q,R,S
49	84.08	1.1503	17.33	7.59	0.0800	B,D,H,I,M,N,O,P,Q,R,S

Integrated Profile Areas

Based on calculated profile

Profile area	***Counts***	***Amount***
Overall diffraction profile	649579	100.00%
Background radiation	447175	68.84%
Diffraction peaks	202404	31.16%
Peak area belonging to selected phases	191644	29.50%
Peak area of phase A (Nickel divanadium oxide)	*4099*	*0.63%*
Peak area of phase B (Disodium calcium bis(hydrogenphosphate(V)))	*10619*	*1.63%*
Peak area of phase C (Barium copper(II) iron fluoride (7/1/6/34))	*10092*	*1.55%*
Peak area of phase D (Dibarium octafluorotriniccolate decafluorotetraniccolate)	*15827*	*2.44%*
Peak area of phase E (Heptabarium copper hexairon(III) fluoride)	*12084*	*1.86%*
Peak area of phase F (Iron phosphate fluoride hydroxide hydrate (1.2/1/0.5/0.2/0.4))	*10714*	*1.65%*
Peak area of phase G (Sodium calcium pentafluoroaluminate fluoride - $-beta)	*12679*	*1.95%*
Peak area of phase H (Niobium thallium oxide hydrate (33/10.5/88.5/1.5))	*13594*	*2.09%*
Peak area of phase I (NIOBIUM THALLIUM OXIDE (3.1/1/8.2))	*5978*	*0.92%*
Peak area of phase J (Rubidium niobium tungsten oxide (12/30/3/90))	*13562*	*2.09%*
*Peak area of phase K (Barium silicate germanate *)*	*2476*	*0.38%*
Peak area of phase L (DICADMIUM TRIARSENIDE BROMIDE)	*4410*	*0.68%*
Peak area of phase M (Rubidium niobium oxide phosphate (1/3/3/3))	*6925*	*1.07%*
Peak area of phase N (Dithallium distrontium copper oxide)	*6658*	*1.03%*
Peak area of phase O (Calcium diphosphate - \b)	*15116*	*2.33%*
*Peak area of phase P (Potassium tecto-phosphatovanadate(III) *)*	*15455*	*2.38%*
Peak area of phase Q (Nonacaesium tecto-trialumononamolybdo(V)undecaphosphate(V))	*10955*	*1.69%*
Peak area of phase R (Cadmium arsenide iodide (2/3/1))	*3898*	*0.60%*
Peak area of phase S (Tetrastrontium nonaoxotriniccolate)	*2719*	*0.42%*
Peak area of phase T (Dibarium oxovanadium(IV) bis(vanadate(V)))	*13783*	*2.12%*
Unidentified peak area	10760	1.66%

Peak Residuals

Peak data	***Counts***	***Amount***
Overall peak intensity	2348	100.00%
Peak intensity belonging to selected phases	2348	100.00%
Unidentified peak intensity	0	0.00%

Diffraction Pattern Graphics

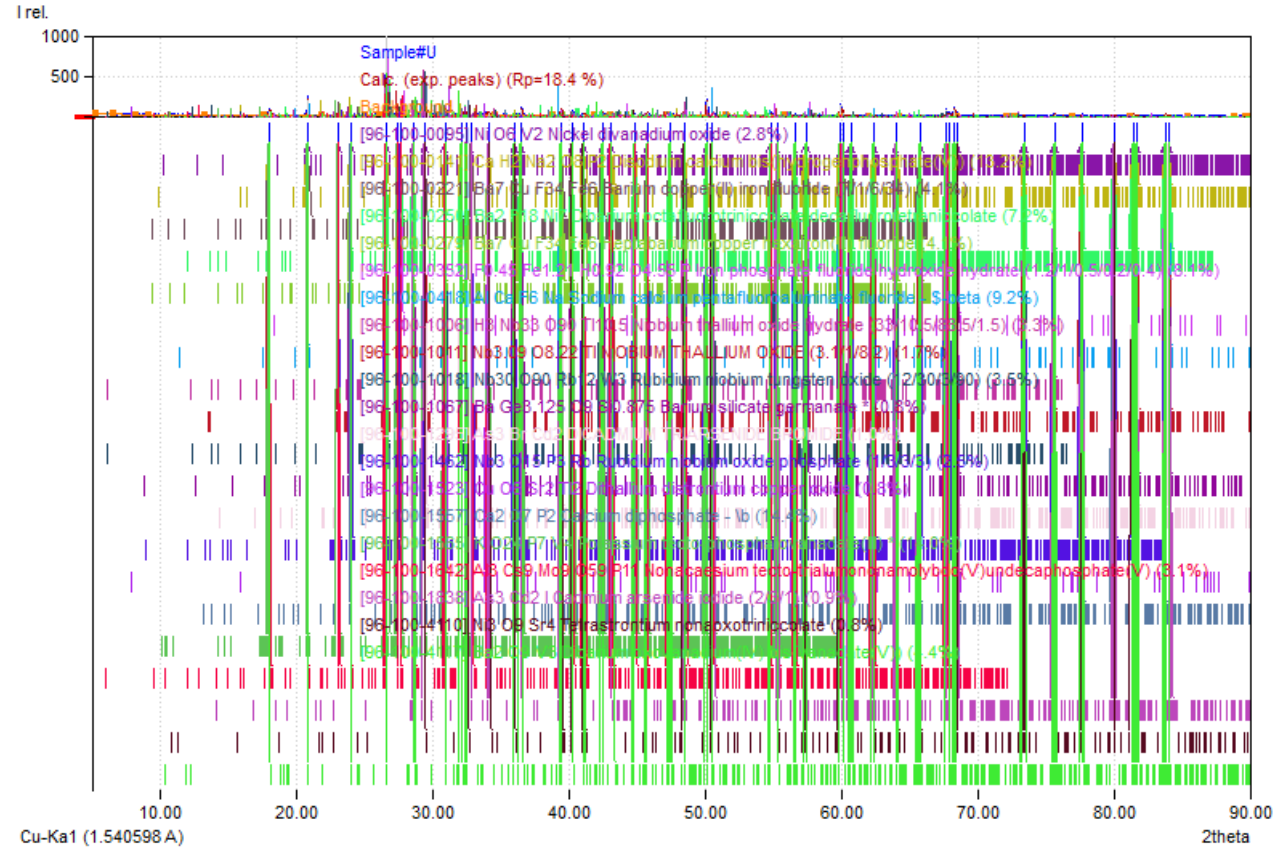

Match! Copyright © 2003-2023 CRYSTAL IMPACT, Bonn, Germany

Amounts of Phases and Elements (Weight %)

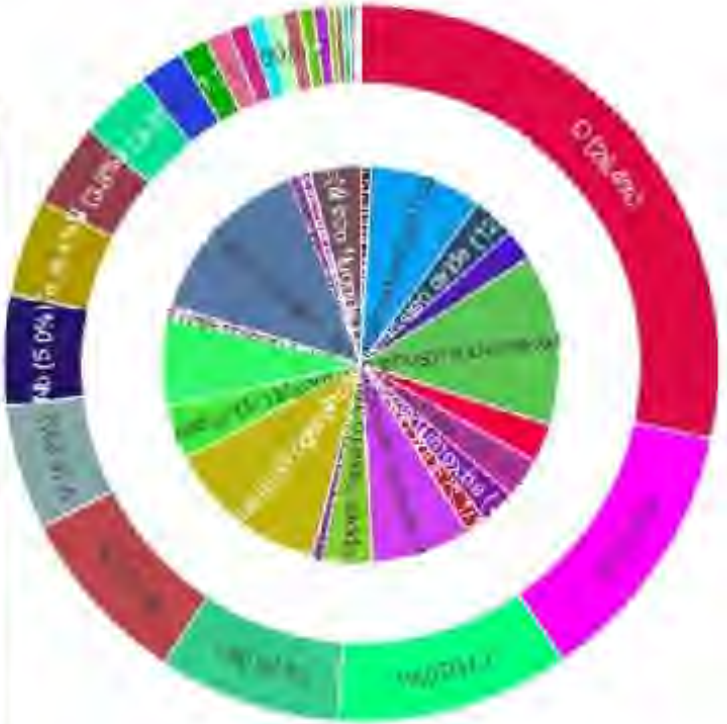

Phase composition:

Calcium diphosphate - \b (14.4%), Potassium tecto-phosphatovanadate(III) * (14.0%), Disodium calcium bis(hydrogenphosphate(V)) (13.2%), Sodium calcium pentafluoroaluminate fluoride - S-beta (9.2%), Iron phosphate fluoride hydroxide hydrate (1.2/1/0.5/0.2/0.4) (8.1%), Dibarium octafluorotriniccolate decafluorotetraniccolate (7.2%), Dibarium oxovanadium(IV) bis(vanadate(V)) (4.4%), Barium copper(II) iron fluoride (7/1/6/34) (4.1%), Heptabarium copper hexairon(III) fluoride (4.1%), Rubidium niobium tungsten oxide (12/30/3/90) (3.5%), Niobium thallium oxide hydrate (33/10.5/88.5/1.5) (3.3%), Nonacaesium tecto-trialumononamolybdo(V)undecaphosphate(V) (3.1%), Nickel divanadium oxide (2.8%), Rubidium niobium oxide phosphate (1/3/3/3) (2.5%), NIOBIUM THALLIUM OXIDE (3.1/1/8.2) (1.7%), DICADMIUM TRIARSENIDE BROMIDE (1.0%), Cadmium arsenide iodide (2/3/1) (0.9%), Tetrastrontium nonaoxotriniccolate (0.8%), Dithallium distrontium copper oxide (0.8%), Barium silicate germanate * (0.8%)

Elemental composition:

O (28.37%), P (12.08%), F (10.58%), Ca (8.25%), Ba (8.19%), V (5.67%), Nb (5.00%), Fe (4.40%), Ni (3.75%), Na (3.22%), Tl (2.07%), Al (1.29%), Cs (1.09%), Rb (0.92%), Mo (0.79%), Cd (0.78%), As (0.78%), K (0.65%), Sr (0.62%), W (0.33%), Cu (0.33%), Ge (0.32%), I (0.21%), Br (0.15%), H (0.14%), Si (0.04%) (LE: 39.08%)

Sample No. 1

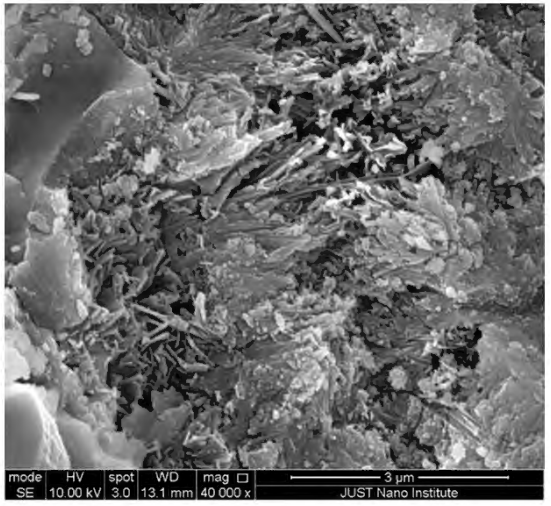
mode HV spot WD mag
SE 10.00 kV 3.0 13.1 mm 40 000 x
3 µm
JUST Nano Institute

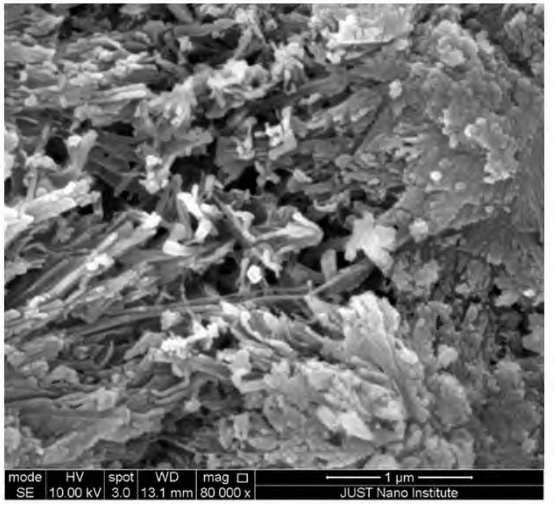
mode HV spot WD mag
SE 10.00 kV 3.0 13.1 mm 80 000 x
1 µm
JUST Nano Institute

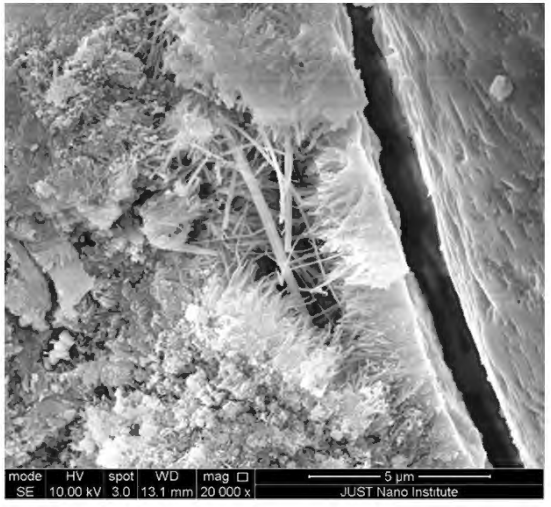
mode HV spot WD mag
SE 10.00 kV 3.0 13.1 mm 20 000 x
5 µm
JUST Nano Institute

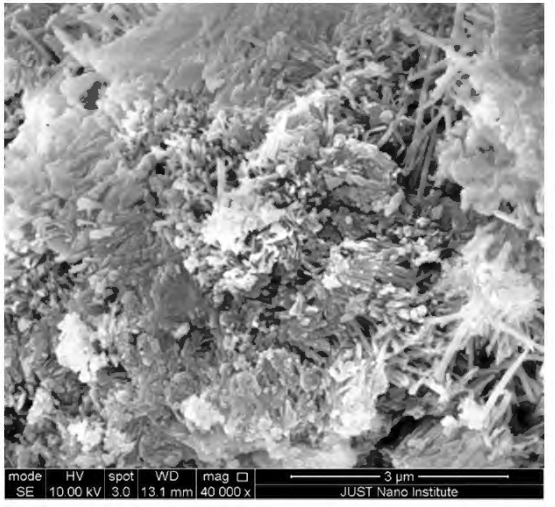
mode HV spot WD mag
SE 10.00 kV 3.0 13.1 mm 40 000 x
3 µm
JUST Nano Institute

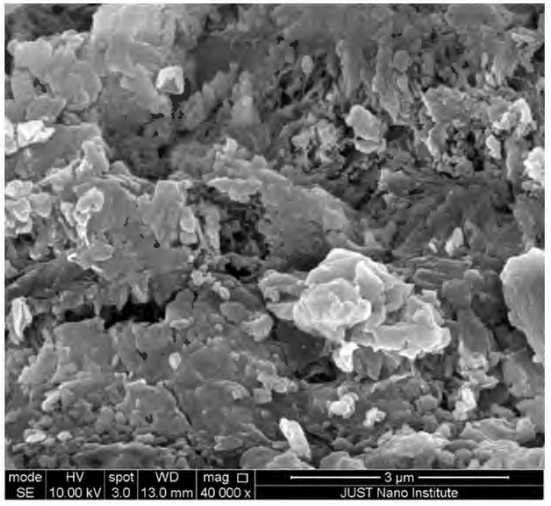
mode HV spot WD mag 3 µm
SE 10.00 kV 3.0 13.0 mm 40 000 x
JUST Nano Institute

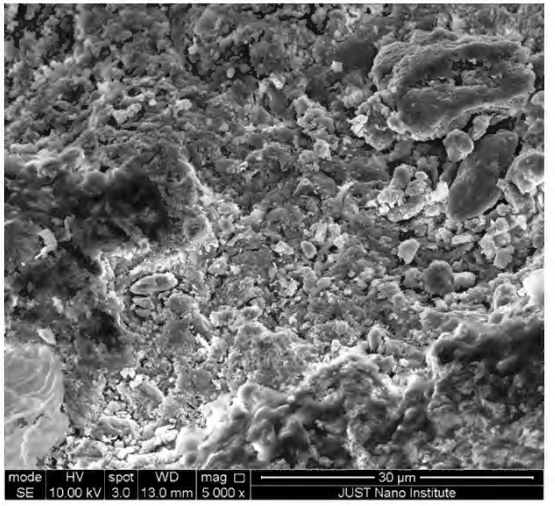
mode HV spot WD mag 30 µm
SE 10.00 kV 3.0 13.0 mm 5 000 x
JUST Nano Institute

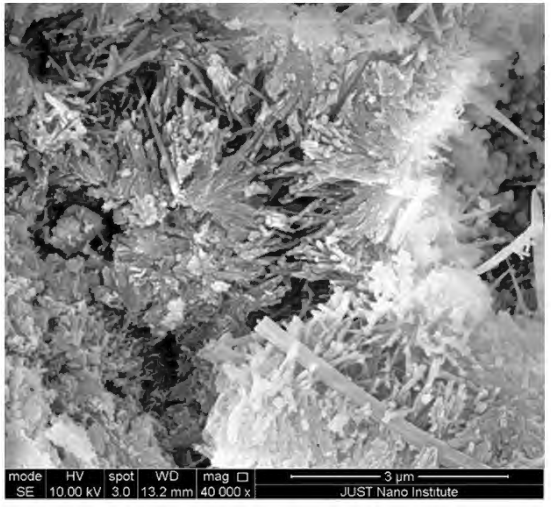
mode HV spot WD mag 3 µm
SE 10.00 kV 3.0 13.2 mm 40 000 x
JUST Nano Institute

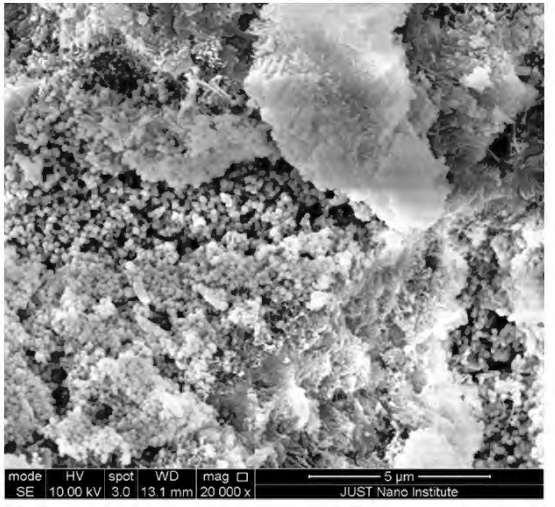
mode HV spot WD mag 5 µm
SE 10.00 kV 3.0 13.1 mm 20 000 x
JUST Nano Institute

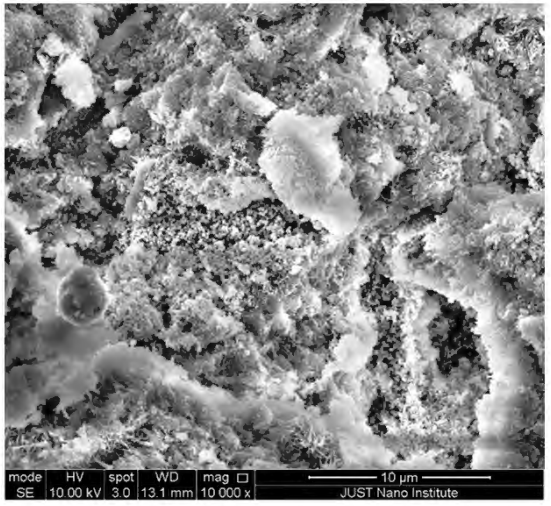
mode
SE
HV
10.00 kV
spot
3.0
WD
13.1 mm
mag
10 000 x
10 µm
JUST Nano Institute

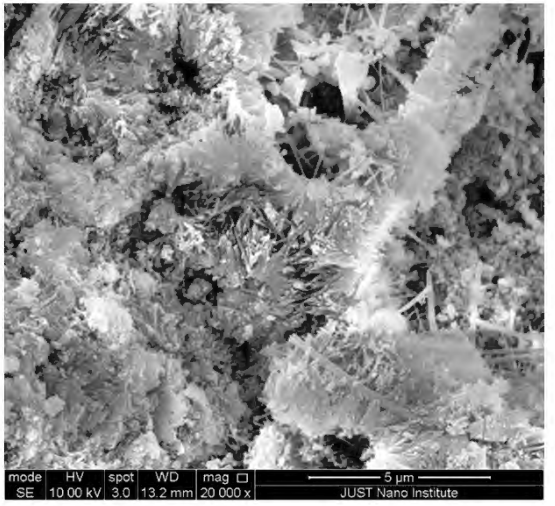
mode
SE
HV
10.00 kV
spot
3.0
WD
13.2 mm
mag
20 000 x
5 µm
JUST Nano Institute

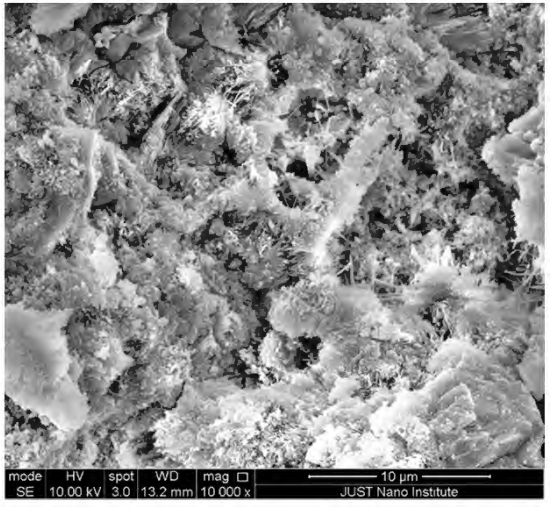
mode
SE
HV
10.00 kV
spot
3.0
WD
13.2 mm
mag
10 000 x
10 µm
JUST Nano Institute

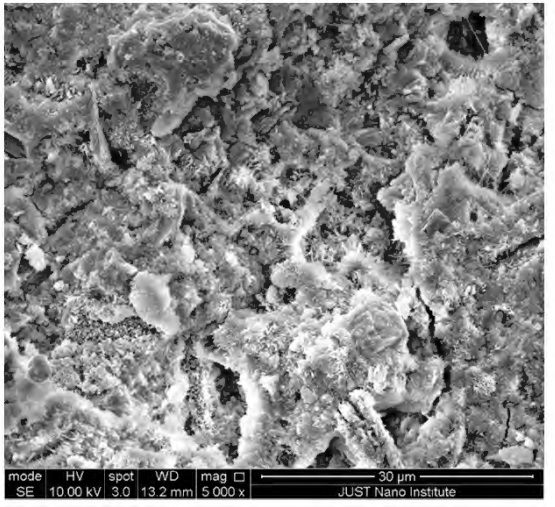
mode
SE
HV
10.00 kV
spot
3.0
WD
13.2 mm
mag
5 000 x
30 µm
JUST Nano Institute

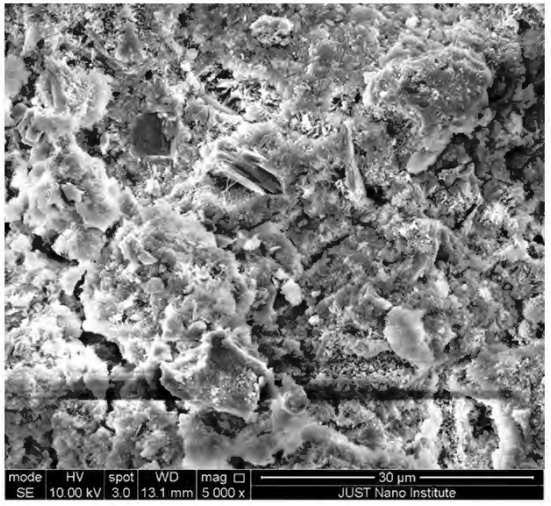
mode
SE
HV
10.00 kV
spot
3.0
WD
13.1 mm
mag
5 000 x
30 µm
JUST Nano Institute

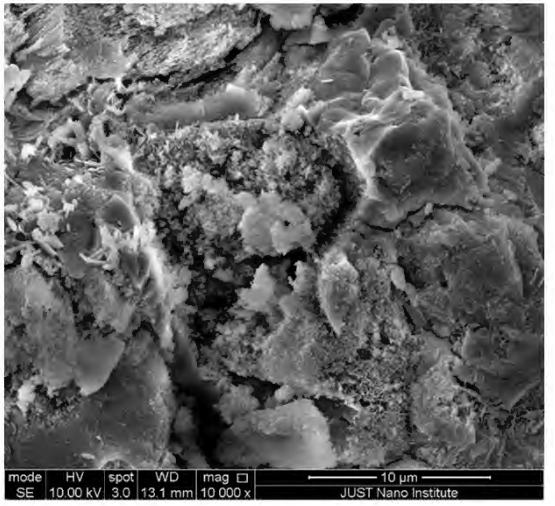
mode
SE
HV
10.00 kV
spot
3.0
WD
13.1 mm
mag
10 000 x
10 µm
JUST Nano Institute

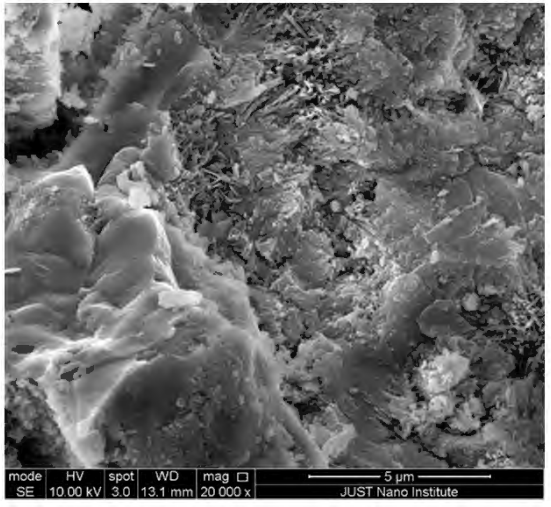
mode
SE
HV
10.00 kV
spot
3.0
WD
13.1 mm
mag
20 000 x
5 µm
JUST Nano Institute

Sample No. 3

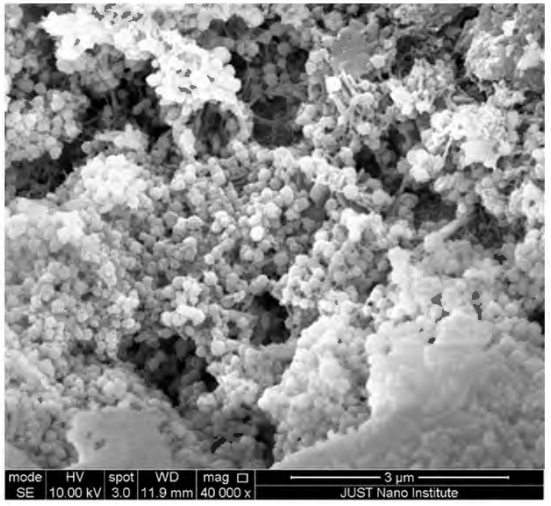
mode SE
HV 10.00 kV
spot 3.0
WD 11.9 mm
mag 40 000 x
3 µm
JUST Nano Institute

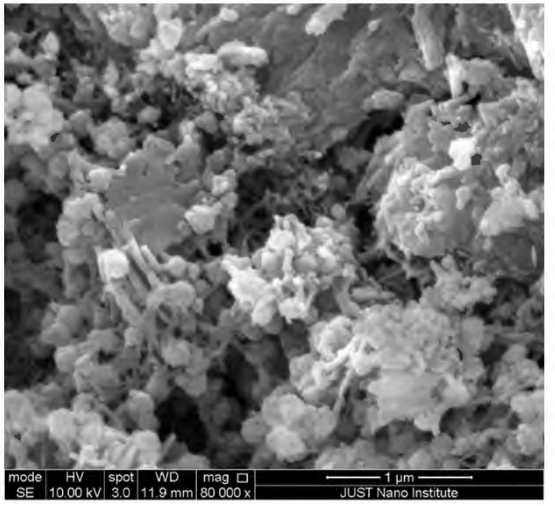
mode SE
HV 10.00 kV
spot 3.0
WD 11.9 mm
mag 80 000 x
1 µm
JUST Nano Institute

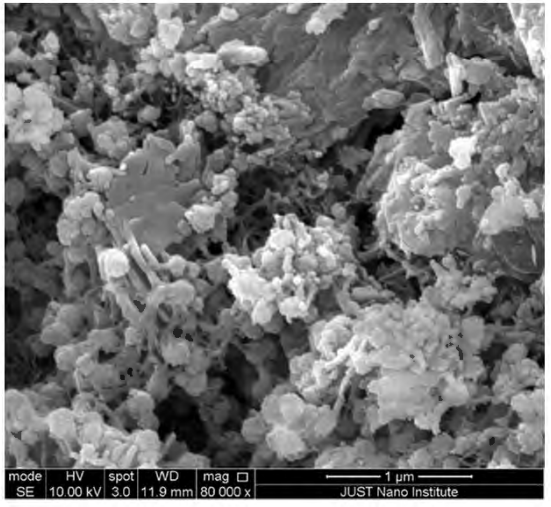
mode SE
HV 10.00 kV
spot 3.0
WD 11.9 mm
mag 80 000 x
1 µm
JUST Nano Institute

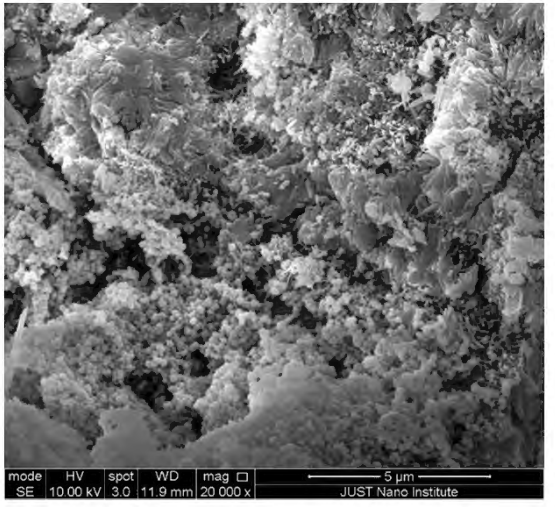
mode SE
HV 10.00 kV
spot 3.0
WD 11.9 mm
mag 20 000 x
5 µm
JUST Nano Institute

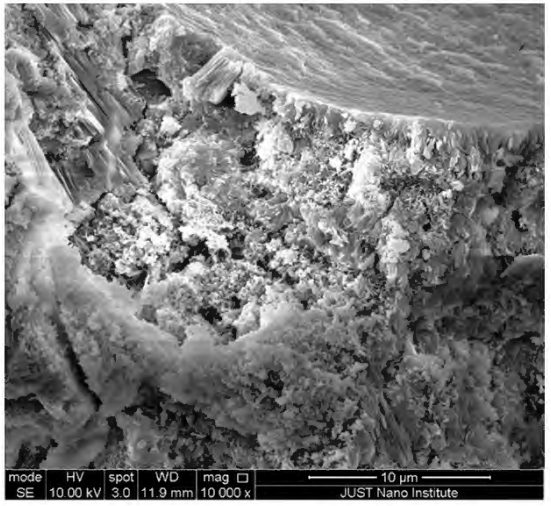
mode SE
HV 10.00 kV
spot 3.0
WD 11.9 mm
mag 10 000 x
10 µm
JUST Nano Institute

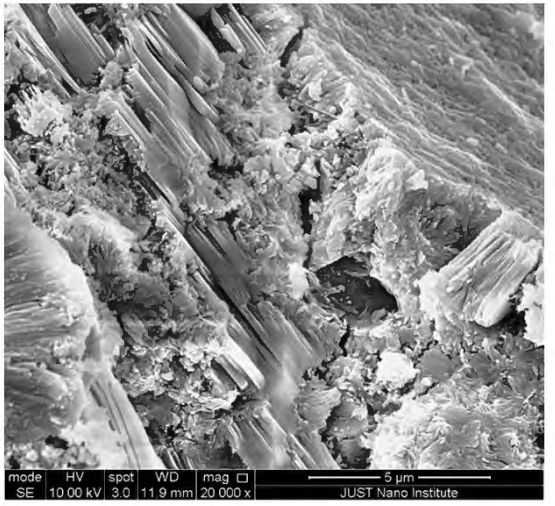
mode SE
HV 10.00 kV
spot 3.0
WD 11.9 mm
mag 20 000 x
5 µm
JUST Nano Institute

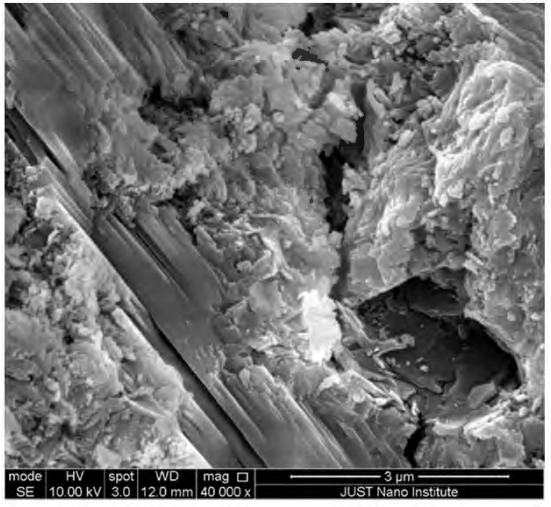
mode SE
HV 10.00 kV
spot 3.0
WD 12.0 mm
mag 40 000 x
3 µm
JUST Nano Institute

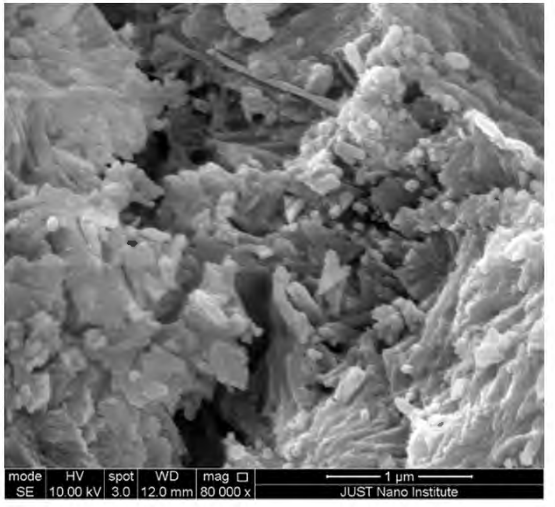
mode SE
HV 10.00 kV
spot 3.0
WD 12.0 mm
mag 80 000 x
1 µm
JUST Nano Institute

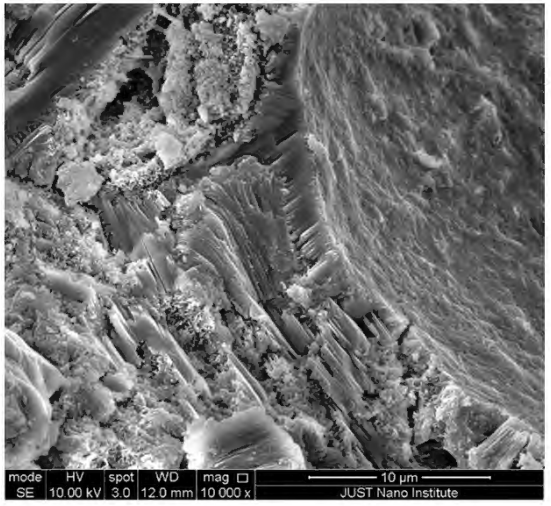
mode
SE
HV
10.00 kV
spot
3.0
WD
12.0 mm
mag
10 000 x
10 µm
JUST Nano Institute

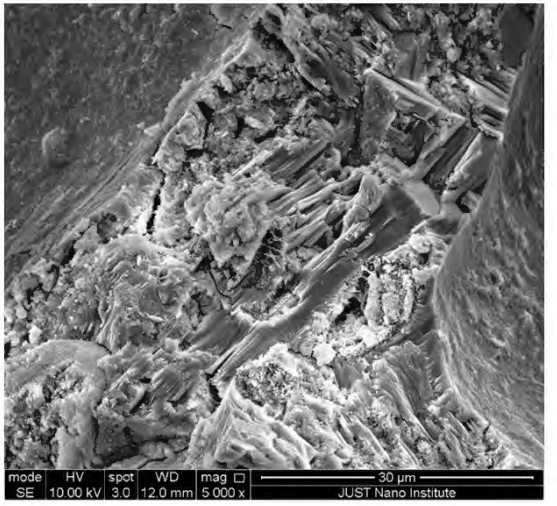
mode
SE
HV
10.00 kV
spot
3.0
WD
12.0 mm
mag
5 000 x
30 µm
JUST Nano Institute

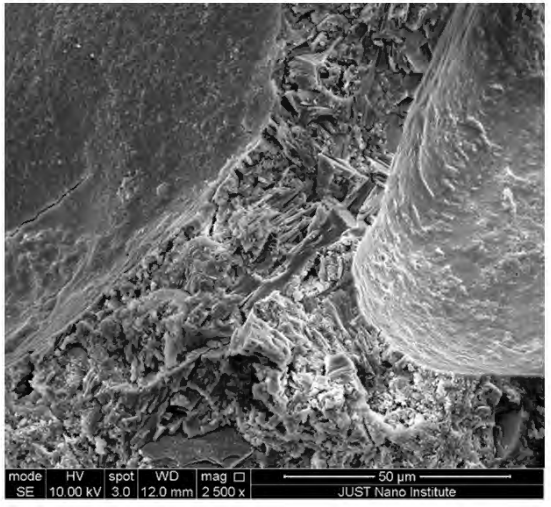
mode
SE
HV
10.00 kV
spot
3.0
WD
12.0 mm
mag
2 500 x
50 µm
JUST Nano Institute

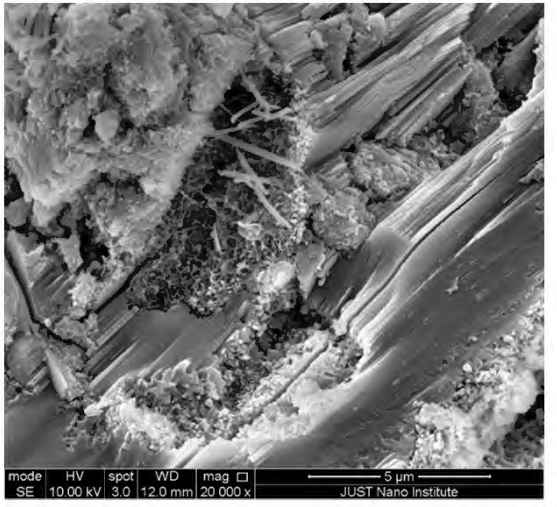
mode
SE
HV
10.00 kV
spot
3.0
WD
12.0 mm
mag
20 000 x
5 µm
JUST Nano Institute

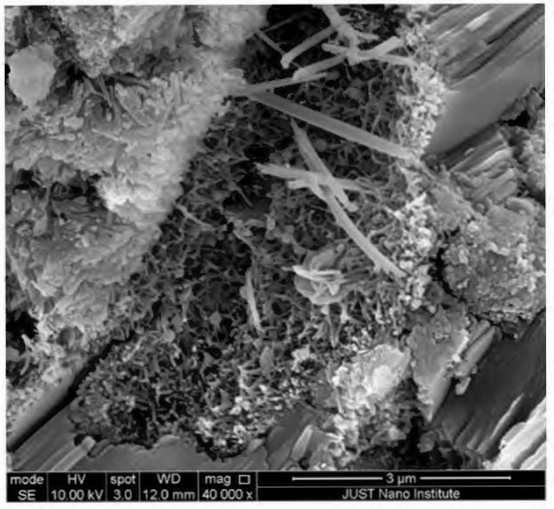
mode SE
HV 10.00 kV
spot 3.0
WD 12.0 mm
mag 40 000 x
3 µm
JUST Nano Institute

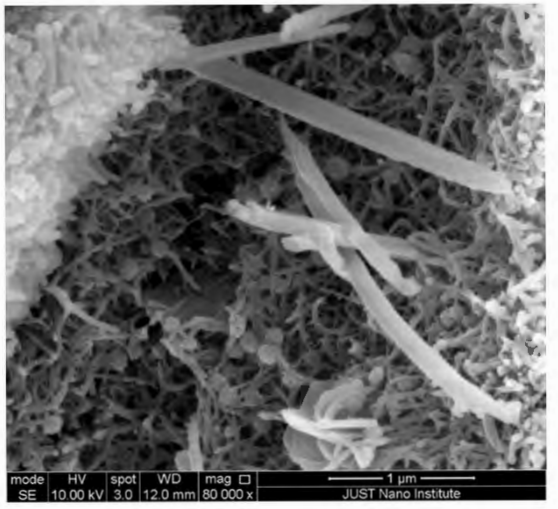
mode SE
HV 10.00 kV
spot 3.0
WD 12.0 mm
mag 80 000 x
1 µm
JUST Nano Institute

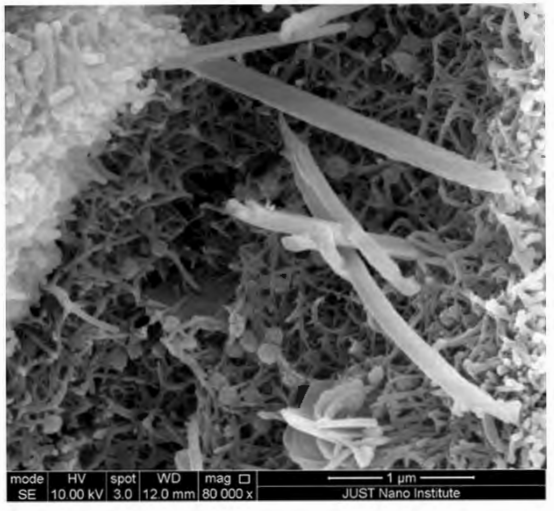
mode SE
HV 10.00 kV
spot 3.0
WD 12.0 mm
mag 80 000 x
1 µm
JUST Nano Institute

mode SE
HV 10.00 kV
spot 3.0
WD 12.0 mm
mag 20 000 x
5 µm
JUST Nano Institute

mode HV spot WD mag 5 µm
SE 10.00 kV 3.0 12.0 mm 20 000 x
JUST Nano Institute

mode HV spot WD mag 100 µm
SE 10.00 kV 3.0 12.0 mm 1 300 x
JUST Nano Institute

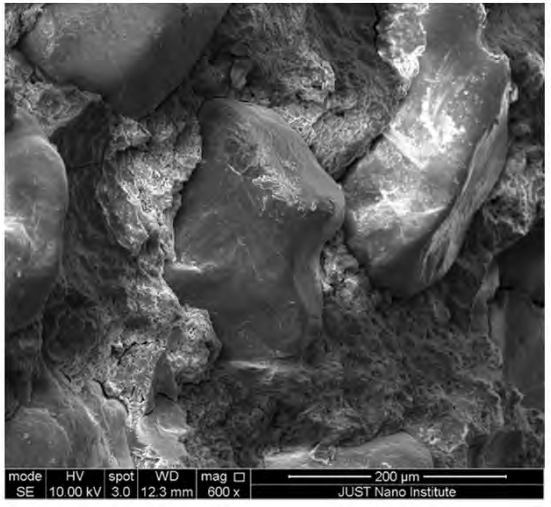
mode HV spot WD mag 200 µm
SE 10.00 kV 3.0 12.3 mm 600 x
JUST Nano Institute

mode HV spot WD mag 100 µm
SE 10.00 kV 3.0 12.4 mm 1 200 x
JUST Nano Institute

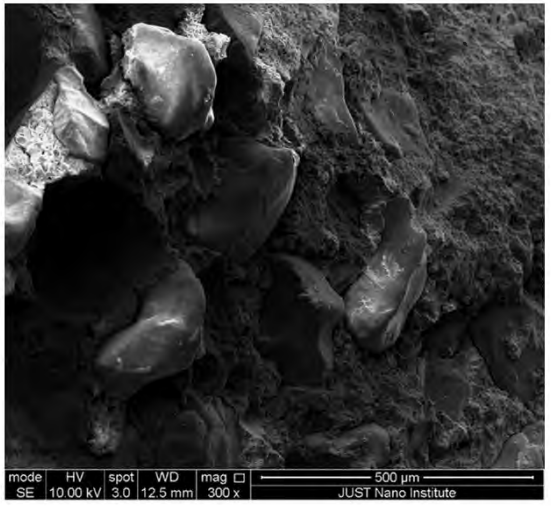
mode SE
HV 10.00 kV
spot 3.0
WD 12.5 mm
mag 300 x
500 µm
JUST Nano Institute

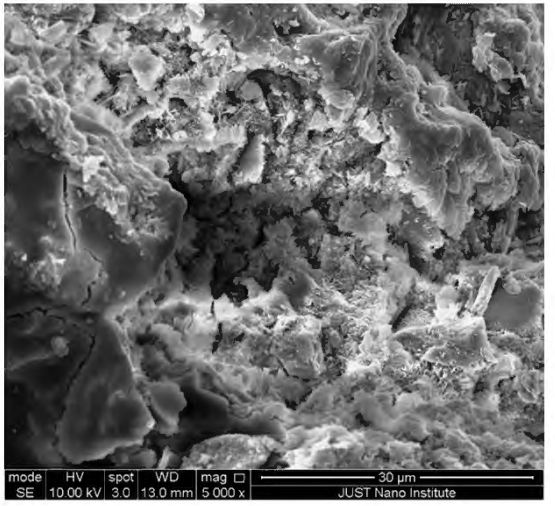
mode SE
HV 10.00 kV
spot 3.0
WD 13.0 mm
mag 5 000 x
30 µm
JUST Nano Institute

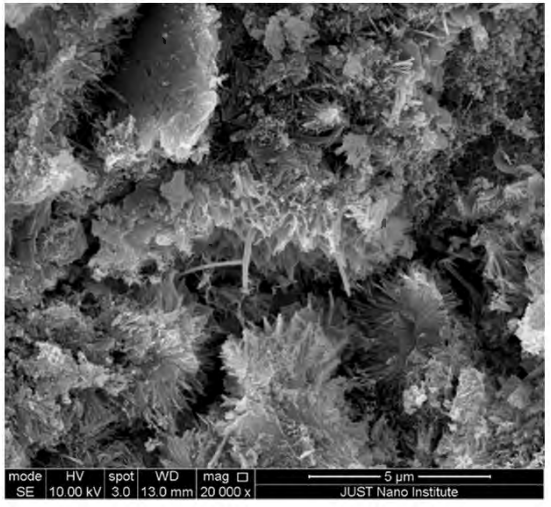
mode SE
HV 10.00 kV
spot 3.0
WD 13.0 mm
mag 20 000 x
5 µm
JUST Nano Institute

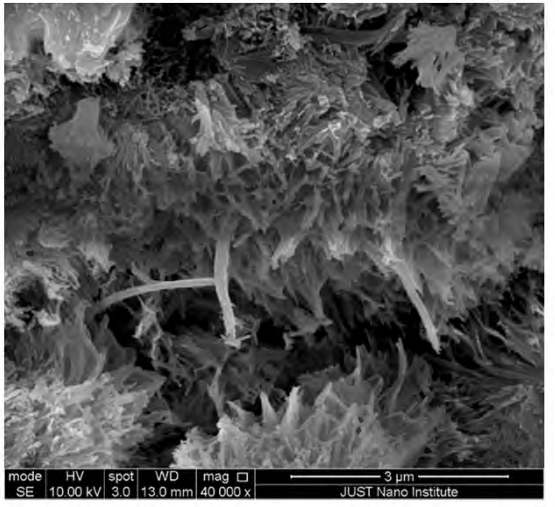
mode SE
HV 10.00 kV
spot 3.0
WD 13.0 mm
mag 40 000 x
3 µm
JUST Nano Institute

Sample No. 7

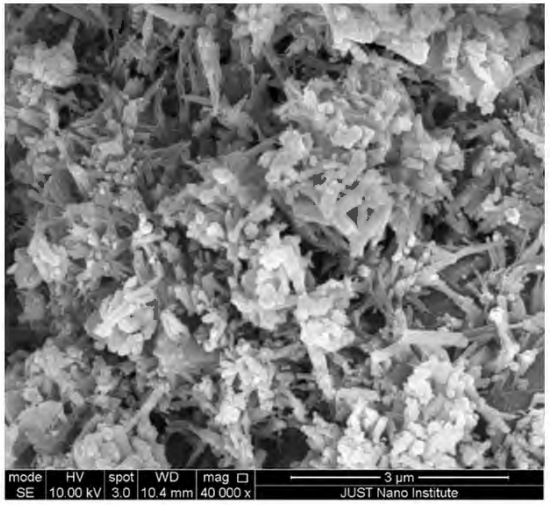
mode HV spot WD mag 3 µm
SE 10.00 kV 3.0 10.4 mm 40 000 x
JUST Nano Institute

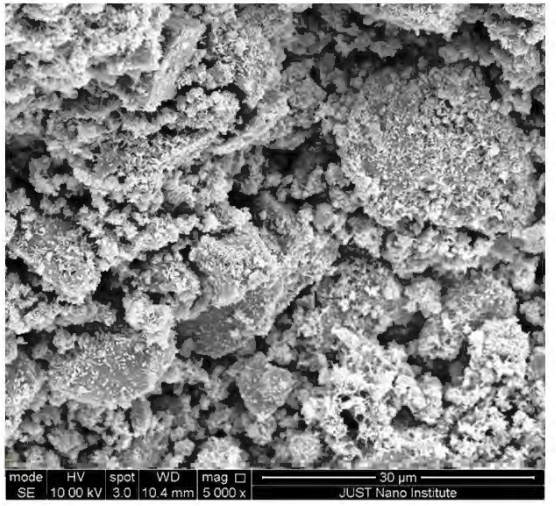
mode HV spot WD mag 30 µm
SE 10.00 kV 3.0 10.4 mm 5 000 x
JUST Nano Institute

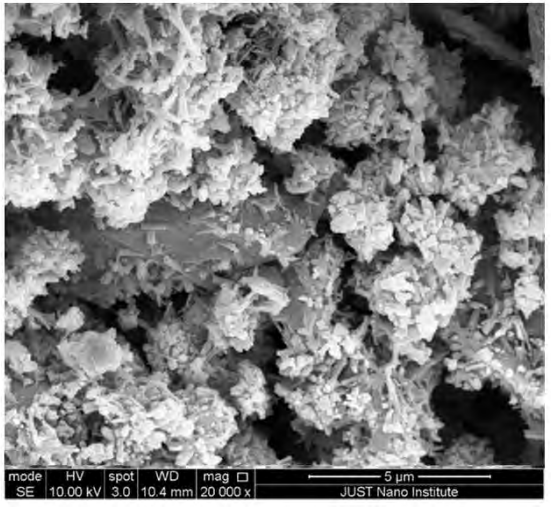
mode HV spot WD mag 5 µm
SE 10.00 kV 3.0 10.4 mm 20 000 x
JUST Nano Institute

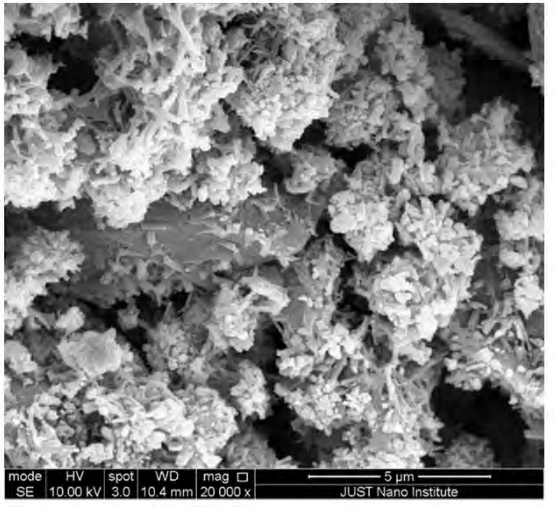
mode HV spot WD mag 5 µm
SE 10.00 kV 3.0 10.4 mm 20 000 x
JUST Nano Institute

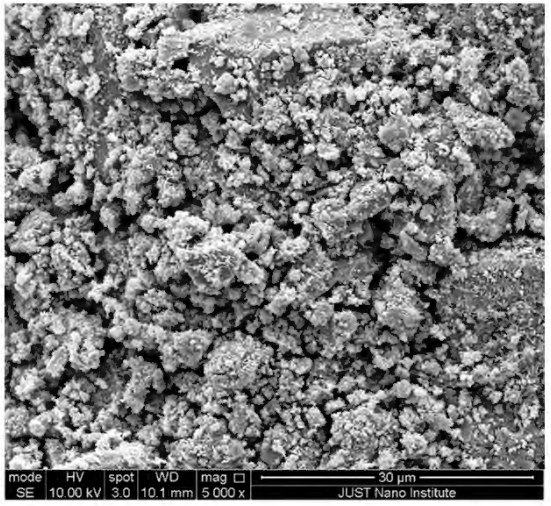
mode
SE
HV
10.00 kV
spot
3.0
WD
10.1 mm
mag
5 000 x
30 µm
JUST Nano Institute

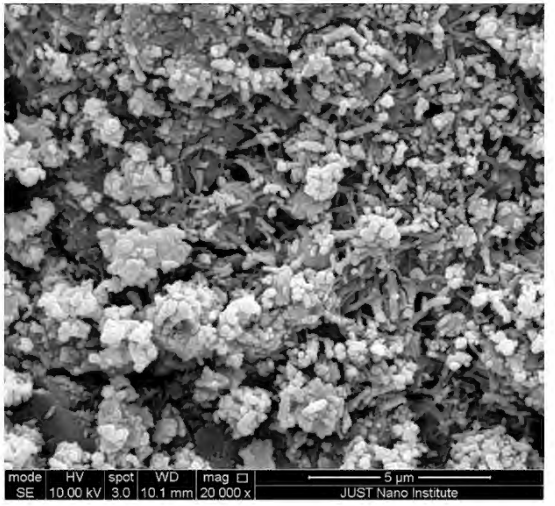
mode
SE
HV
10.00 kV
spot
3.0
WD
10.1 mm
mag
20 000 x
5 µm
JUST Nano Institute

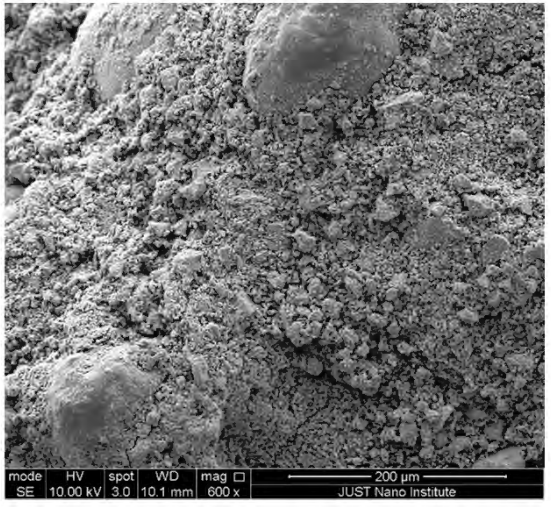
mode
SE
HV
10.00 kV
spot
3.0
WD
10.1 mm
mag
600 x
200 µm
JUST Nano Institute

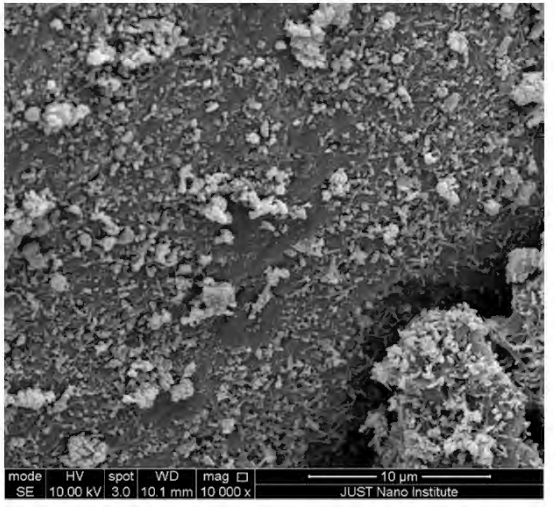
mode
SE
HV
10.00 kV
spot
3.0
WD
10.1 mm
mag
10 000 x
10 µm
JUST Nano Institute

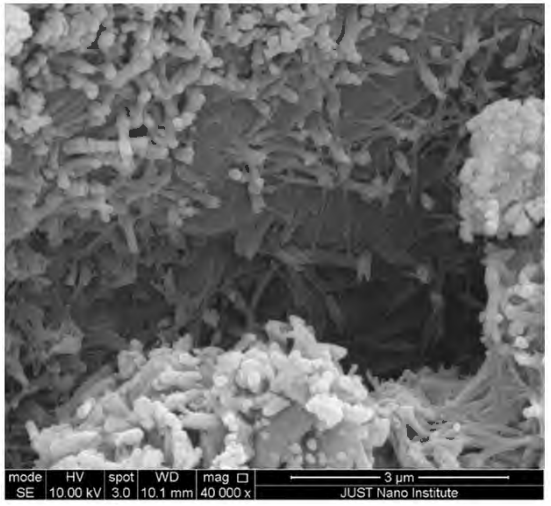
mode HV spot WD mag
SE 10.00 kV 3.0 10.1 mm 40 000 x
3 µm
JUST Nano Institute

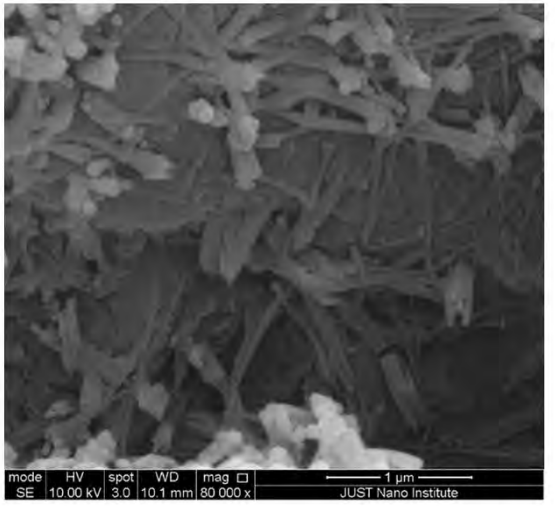
mode HV spot WD mag
SE 10.00 kV 3.0 10.1 mm 80 000 x
1 µm
JUST Nano Institute

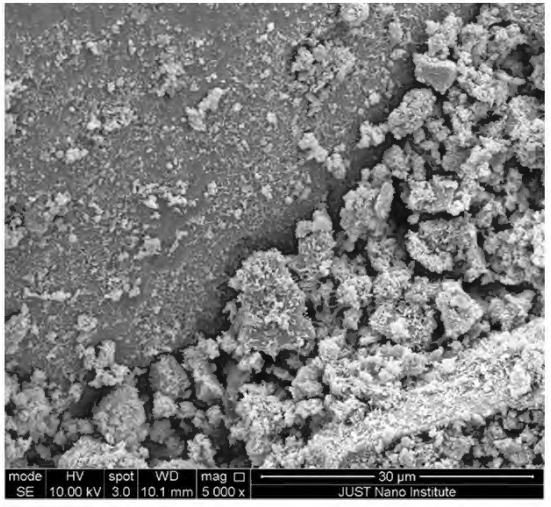
mode HV spot WD mag
SE 10.00 kV 3.0 10.1 mm 5 000 x
30 µm
JUST Nano Institute

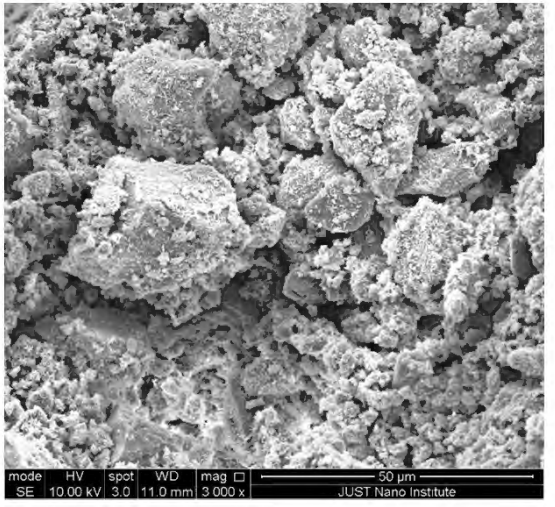
mode HV spot WD mag
SE 10.00 kV 3.0 11.0 mm 3 000 x
50 µm
JUST Nano Institute

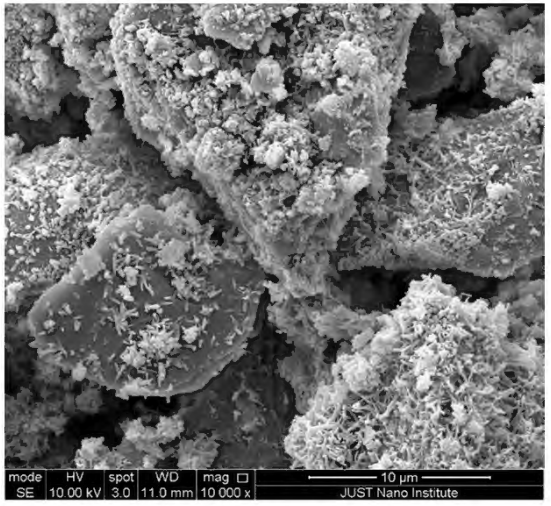
mode HV spot WD mag
SE 10.00 kV 3.0 11.0 mm 10 000 x
10 µm
JUST Nano Institute

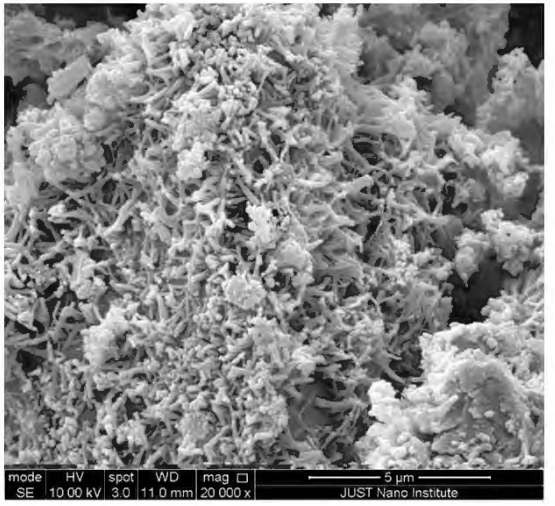
mode HV spot WD mag
SE 10.00 kV 3.0 11.0 mm 20 000 x
5 µm
JUST Nano Institute

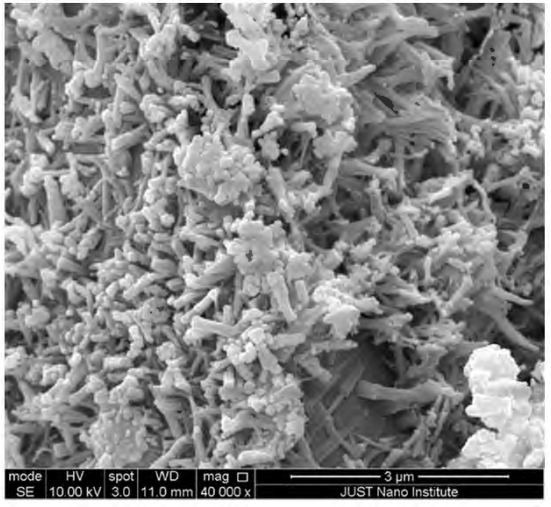
mode HV spot WD mag
SE 10.00 kV 3.0 11.0 mm 40 000 x
3 µm
JUST Nano Institute

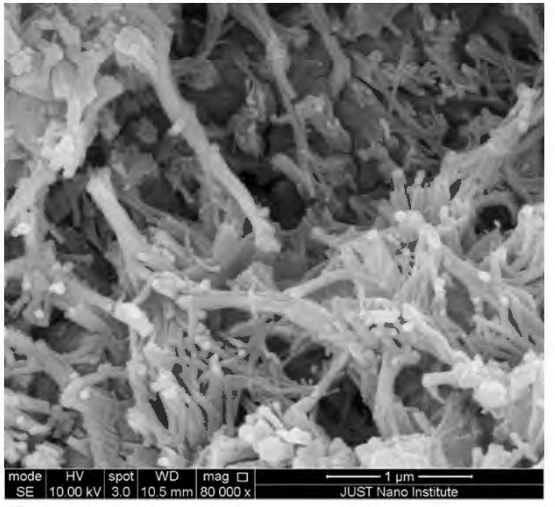
mode HV spot WD mag
SE 10.00 kV 3.0 10.5 mm 80 000 x
1 µm
JUST Nano Institute

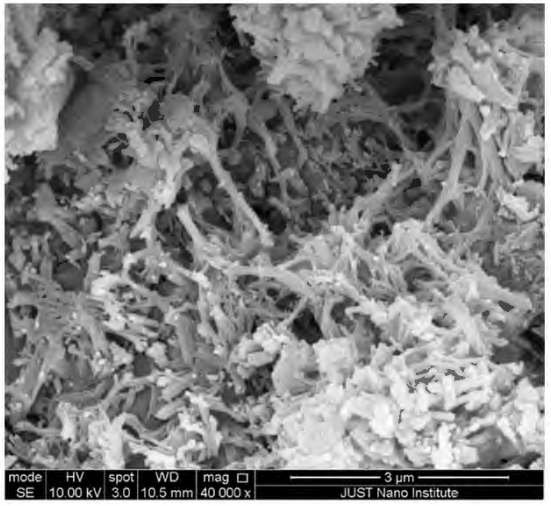
mode HV spot WD mag
SE 10.00 kV 3.0 10.5 mm 40 000 x
3 µm
JUST Nano Institute

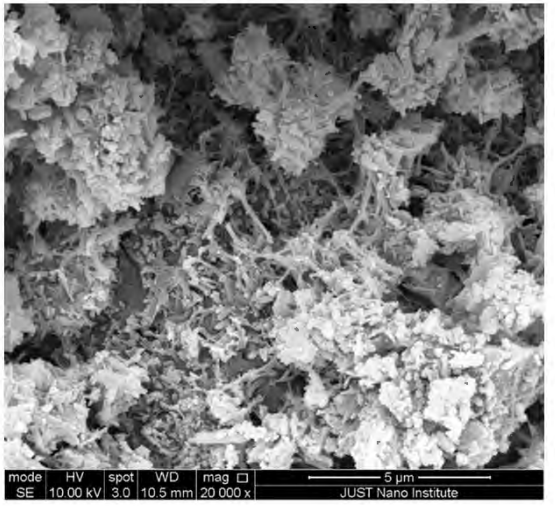
mode HV spot WD mag
SE 10.00 kV 3.0 10.5 mm 20 000 x
5 µm
JUST Nano Institute

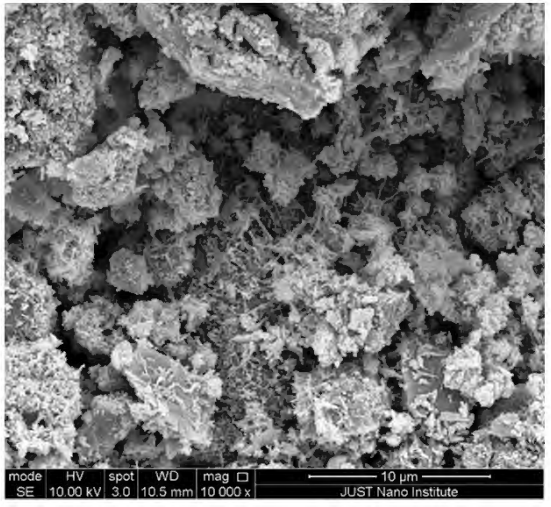
mode HV spot WD mag
SE 10.00 kV 3.0 10.5 mm 10 000 x
10 µm
JUST Nano Institute

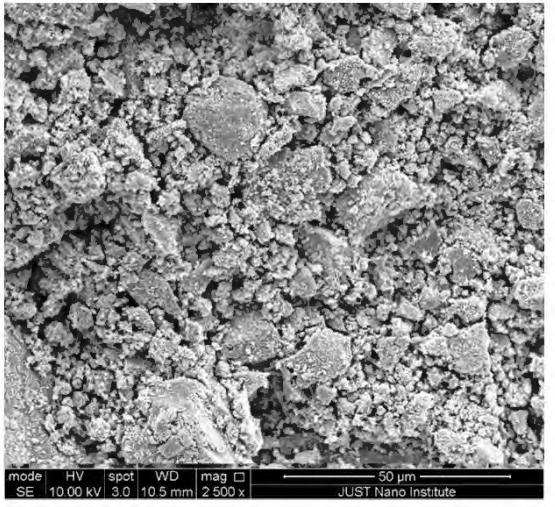
mode HV spot WD mag
SE 10.00 kV 3.0 10.5 mm 2 500 x
50 µm
JUST Nano Institute

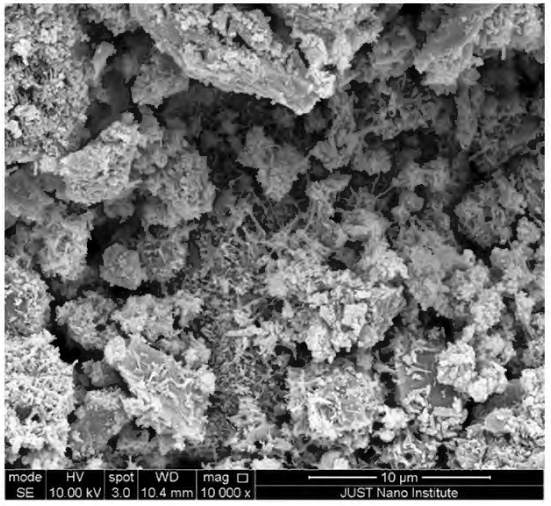
mode
SE
HV
10.00 kV
spot
3.0
WD
10.4 mm
mag
10 000 x
10 µm
JUST Nano Institute

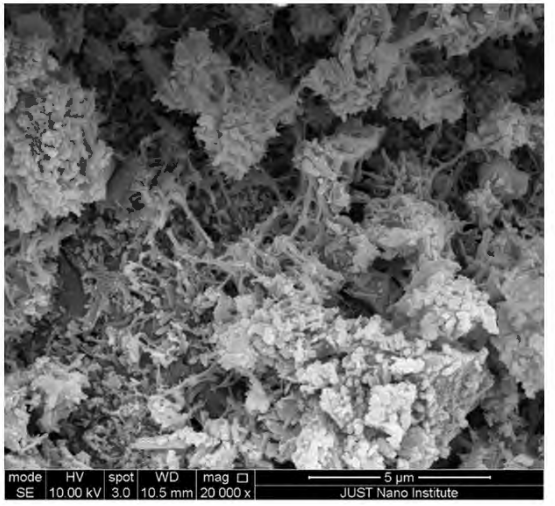
mode
SE
HV
10.00 kV
spot
3.0
WD
10.5 mm
mag
20 000 x
5 µm
JUST Nano Institute

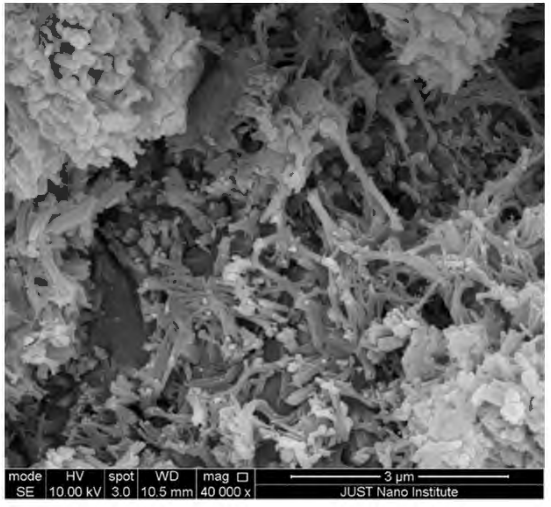
mode
SE
HV
10.00 kV
spot
3.0
WD
10.5 mm
mag
40 000 x
3 µm
JUST Nano Institute

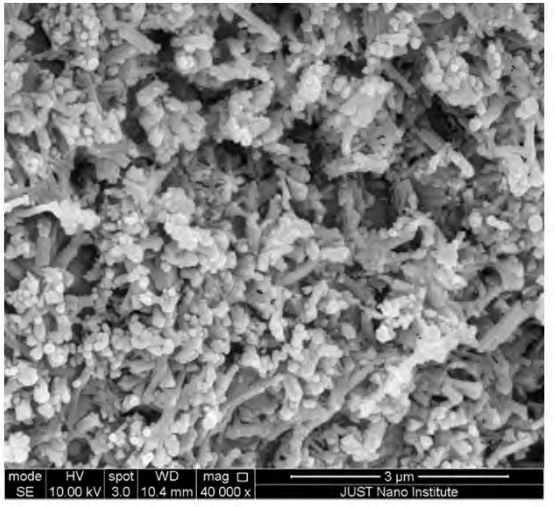
mode
SE
HV
10.00 kV
spot
3.0
WD
10.4 mm
mag
40 000 x
3 µm
JUST Nano Institute

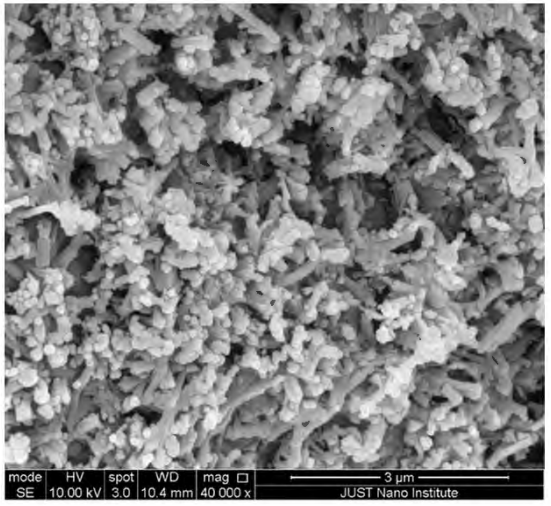
mode
SE
HV
10.00 kV
spot
3.0
WD
10.4 mm
mag
40 000 x
3 µm
JUST Nano Institute

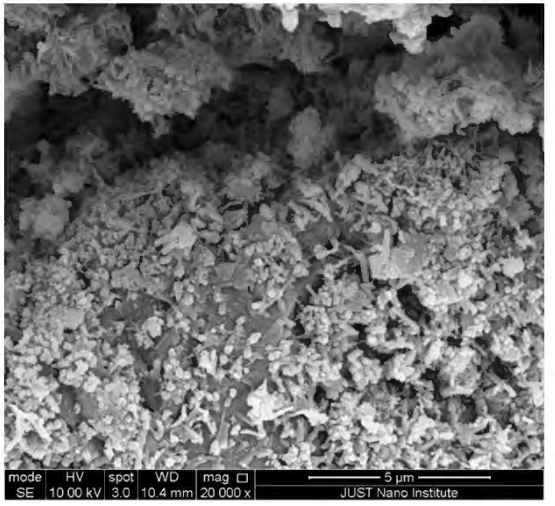
mode
SE
HV
10.00 kV
spot
3.0
WD
10.4 mm
mag
20 000 x
5 µm
JUST Nano Institute

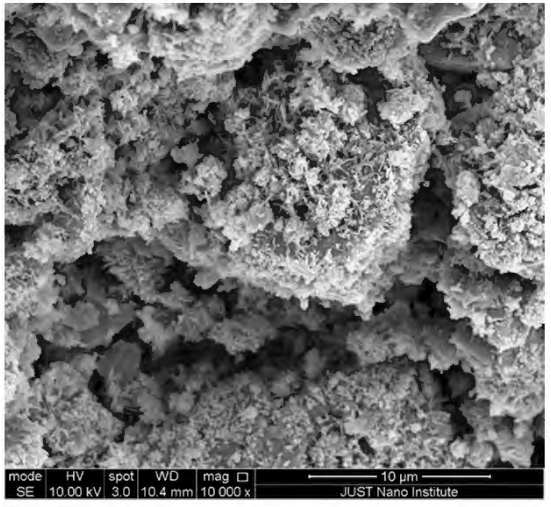
mode
SE
HV
10.00 kV
spot
3.0
WD
10.4 mm
mag
10 000 x
10 µm
JUST Nano Institute

Sample No. B

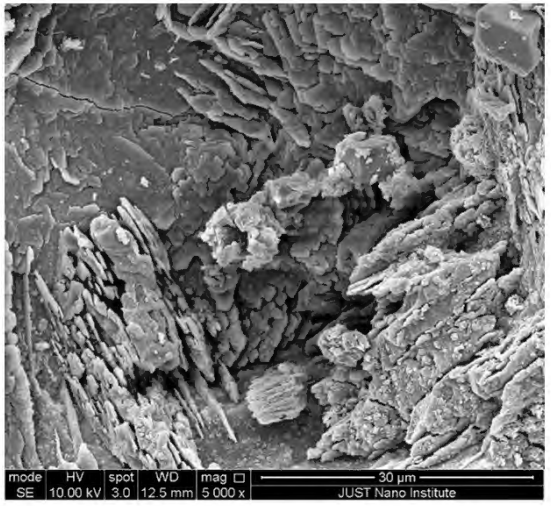
mode HV spot WD mag 30 µm
SE 10.00 kV 3.0 12.5 mm 5 000 x JUST Nano Institute

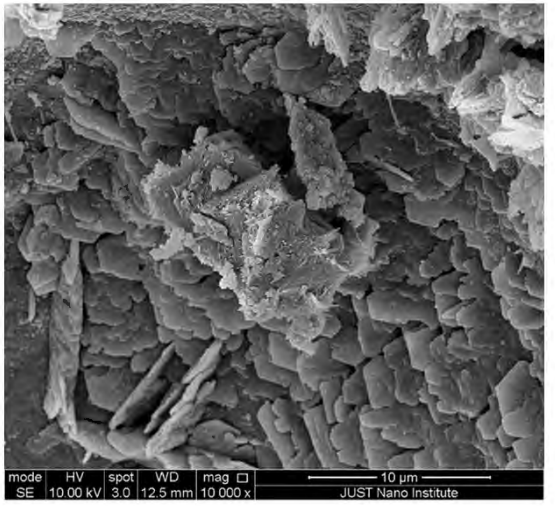
mode HV spot WD mag 10 µm
SE 10.00 kV 3.0 12.5 mm 10 000 x JUST Nano Institute

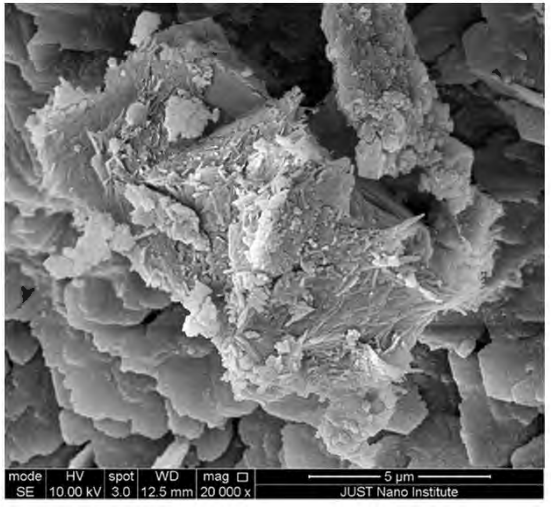
mode HV spot WD mag 5 µm
SE 10.00 kV 3.0 12.5 mm 20 000 x JUST Nano Institute

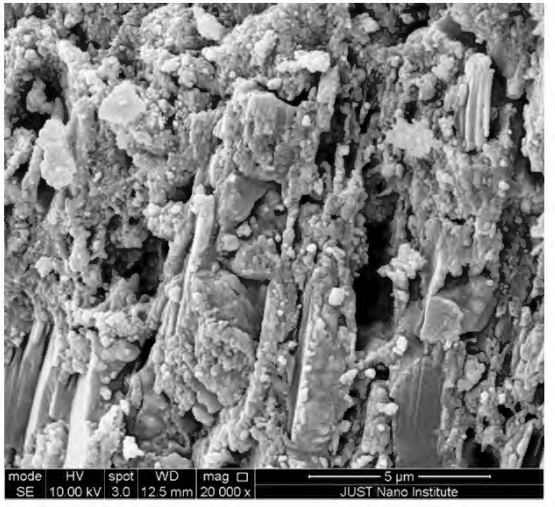
mode HV spot WD mag 5 µm
SE 10.00 kV 3.0 12.5 mm 20 000 x JUST Nano Institute

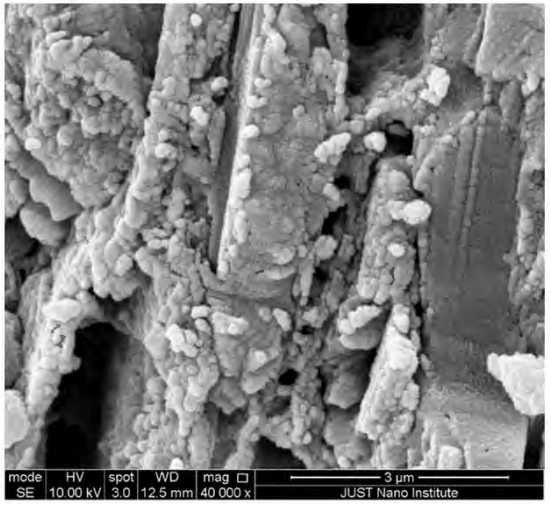
mode
SE
HV
10.00 kV
spot
3.0
WD
12.5 mm
mag
40 000 x
3 µm
JUST Nano Institute

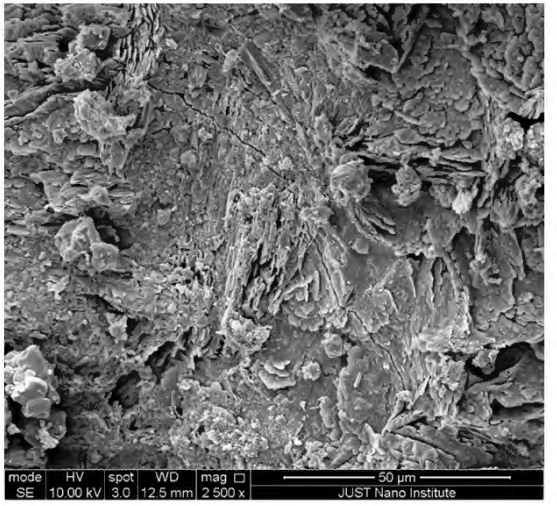
mode
SE
HV
10.00 kV
spot
3.0
WD
12.5 mm
mag
2 500 x
50 µm
JUST Nano Institute

mode
SE
HV
10.00 kV
spot
3.0
WD
12.5 mm
mag
20 000 x
5 µm
JUST Nano Institute

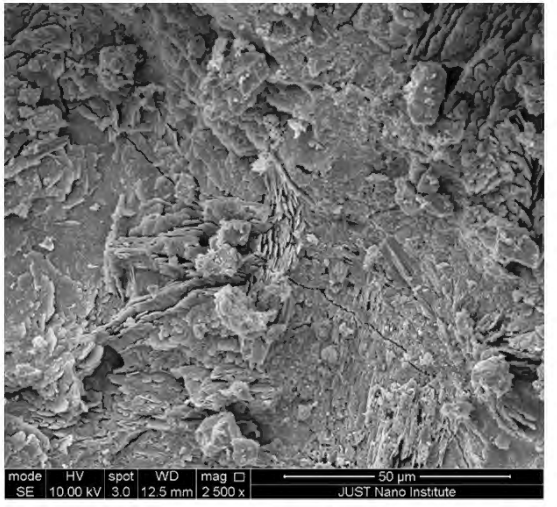
mode
SE
HV
10.00 kV
spot
3.0
WD
12.5 mm
mag
2 500 x
50 µm
JUST Nano Institute

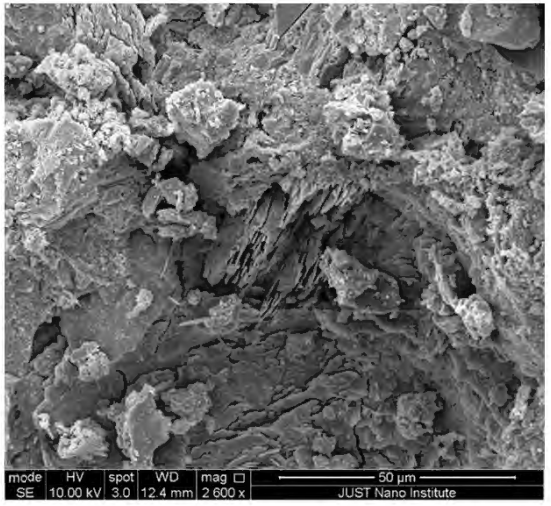
mode HV spot WD mag 50 µm
SE 10.00 kV 3.0 12.4 mm 2 600 x
JUST Nano Institute

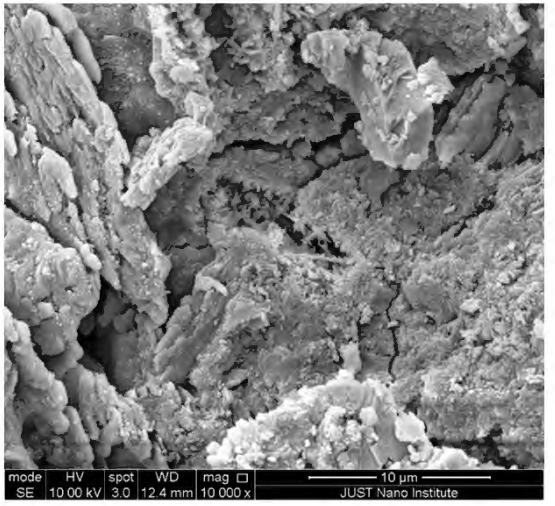
mode HV spot WD mag 10 µm
SE 10.00 kV 3.0 12.4 mm 10 000 x
JUST Nano Institute

mode HV spot WD mag 3 µm
SE 10.00 kV 3.0 12.4 mm 40 000 x
JUST Nano Institute

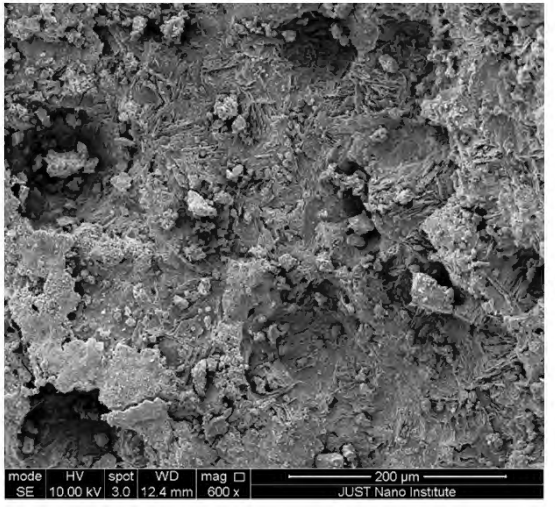
mode HV spot WD mag 200 µm
SE 10.00 kV 3.0 12.4 mm 600 x
JUST Nano Institute

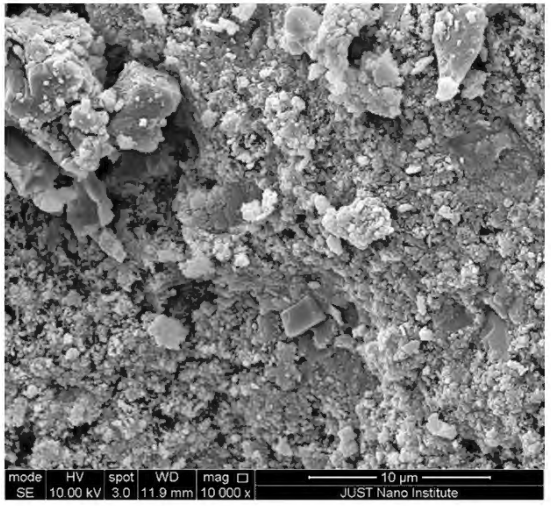
mode HV spot WD mag
SE 10.00 kV 3.0 11.9 mm 10 000 x
10 µm
JUST Nano Institute

mode HV spot WD mag
SE 10.00 kV 3.0 11.9 mm 20 000 x
5 µm
JUST Nano Institute

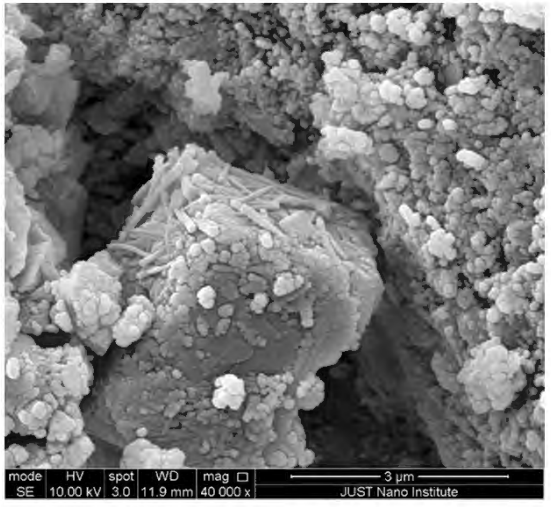
mode HV spot WD mag
SE 10.00 kV 3.0 11.9 mm 40 000 x
3 µm
JUST Nano Institute

mode HV spot WD mag
SE 10.00 kV 3.0 11.9 mm 80 000 x
1 µm
JUST Nano Institute

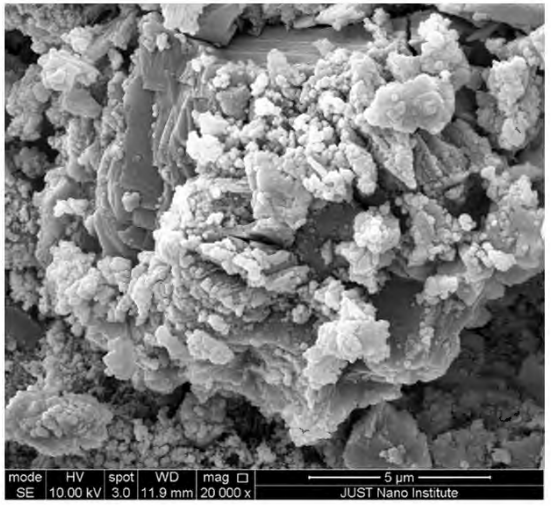
mode SE
HV 10.00 kV
spot 3.0
WD 11.9 mm
mag 20 000 x
5 µm
JUST Nano Institute

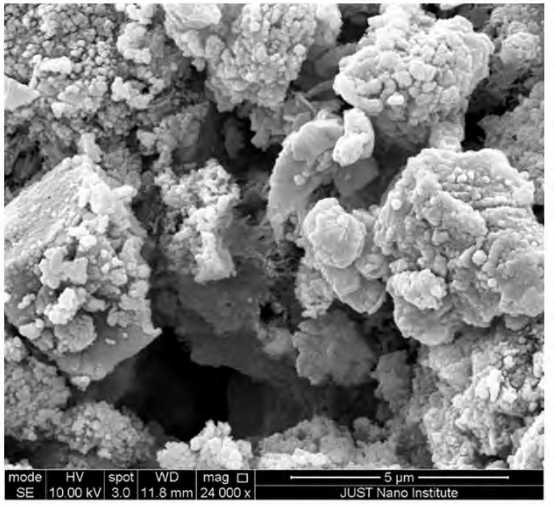
mode SE
HV 10.00 kV
spot 3.0
WD 11.8 mm
mag 24 000 x
5 µm
JUST Nano Institute

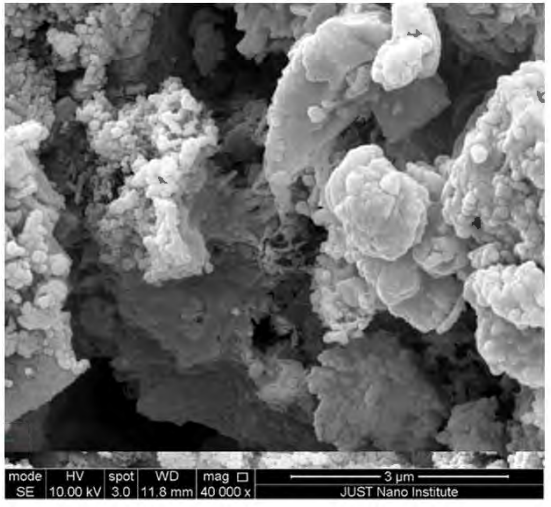
mode SE
HV 10.00 kV
spot 3.0
WD 11.8 mm
mag 40 000 x
3 µm
JUST Nano Institute

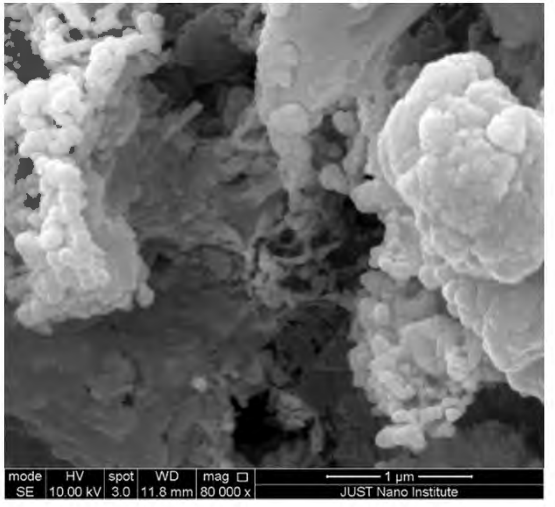
mode SE
HV 10.00 kV
spot 3.0
WD 11.8 mm
mag 80 000 x
1 µm
JUST Nano Institute

mode
SE
HV
10.00 kV
spot
3.0
WD
11.9 mm
mag
5 000 x
30 µm
JUST Nano Institute

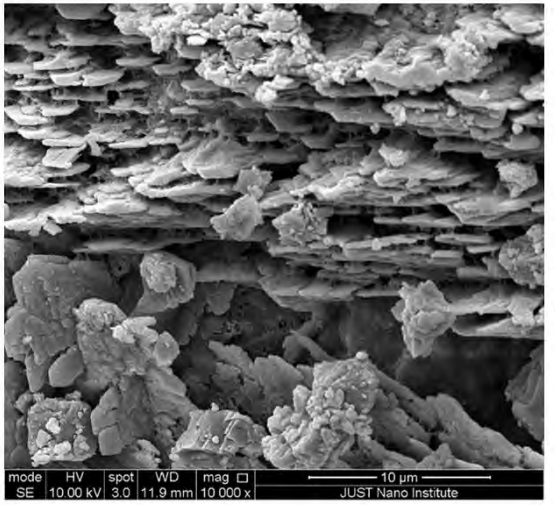
mode
SE
HV
10.00 kV
spot
3.0
WD
11.9 mm
mag
10 000 x
10 µm
JUST Nano Institute

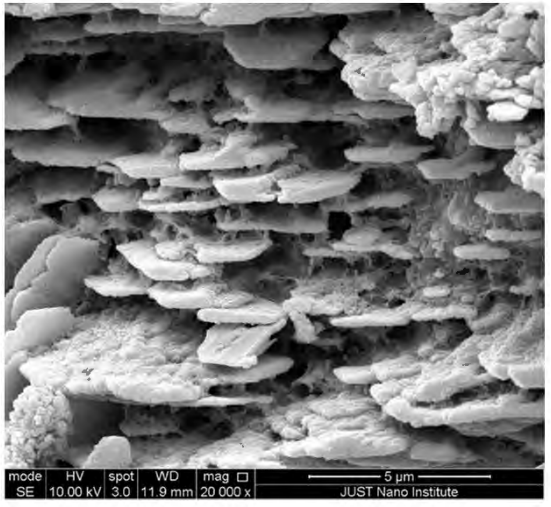
mode
SE
HV
10.00 kV
spot
3.0
WD
11.9 mm
mag
20 000 x
5 µm
JUST Nano Institute

Sample No. G

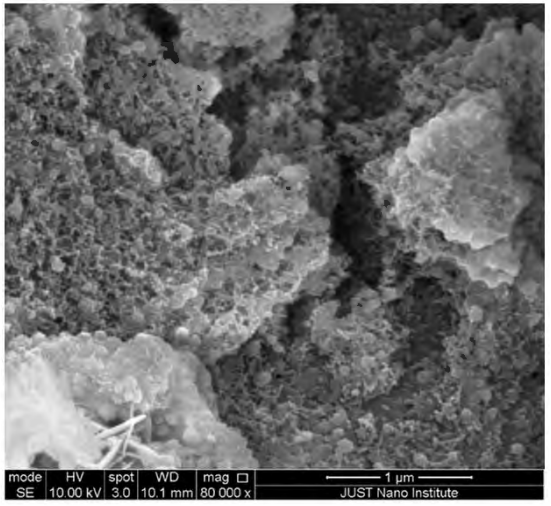
mode HV spot WD mag
SE 10.00 kV 3.0 10.1 mm 80 000 x
1 µm
JUST Nano Institute

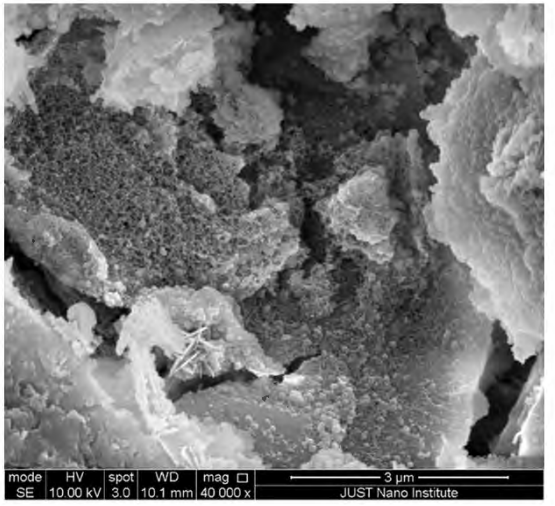
mode HV spot WD mag
SE 10.00 kV 3.0 10.1 mm 40 000 x
3 µm
JUST Nano Institute

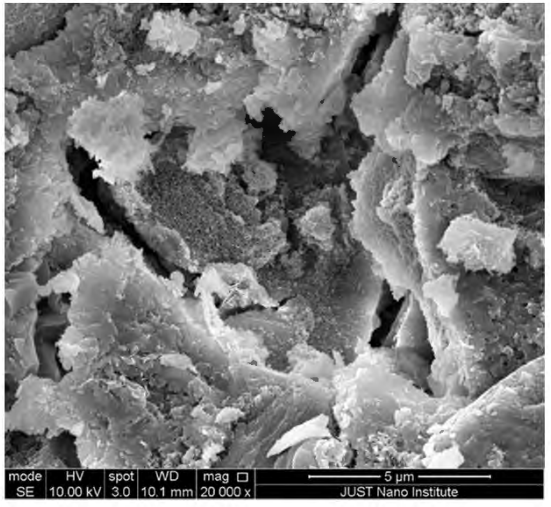
mode HV spot WD mag
SE 10.00 kV 3.0 10.1 mm 20 000 x
5 µm
JUST Nano Institute

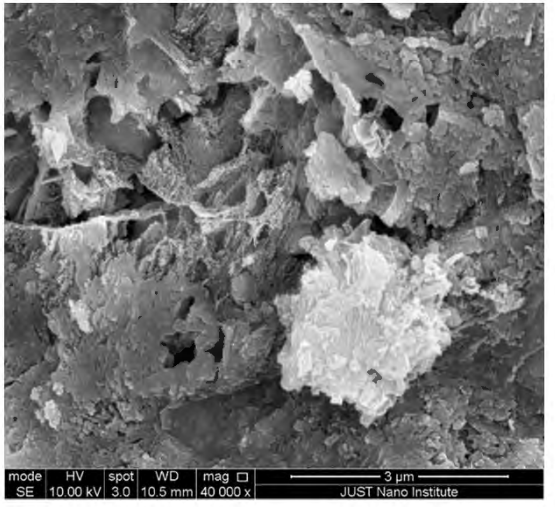
mode HV spot WD mag
SE 10.00 kV 3.0 10.5 mm 40 000 x
3 µm
JUST Nano Institute

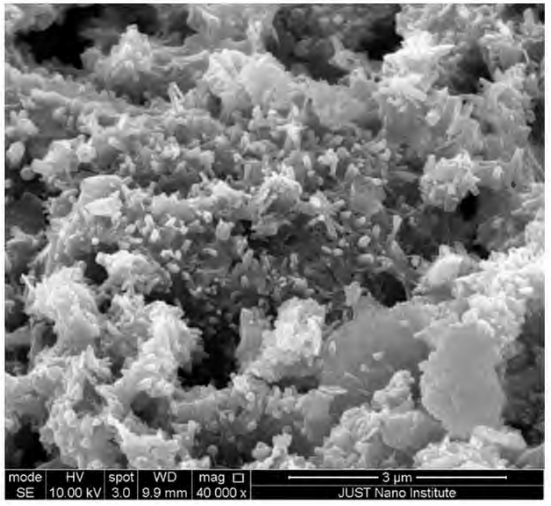
mode HV spot WD mag
SE 10.00 kV 3.0 9.9 mm 40 000 x
3 µm
JUST Nano Institute

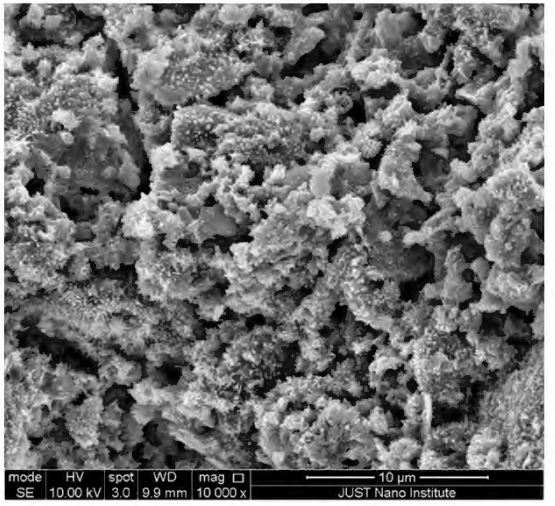
mode HV spot WD mag
SE 10.00 kV 3.0 9.9 mm 10 000 x
10 µm
JUST Nano Institute

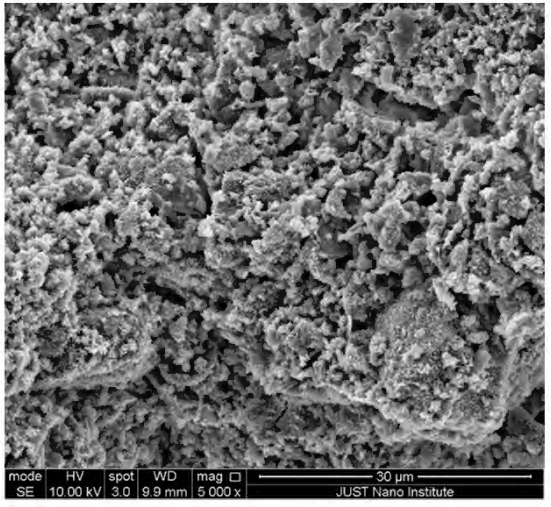
mode HV spot WD mag
SE 10.00 kV 3.0 9.9 mm 5 000 x
30 µm
JUST Nano Institute

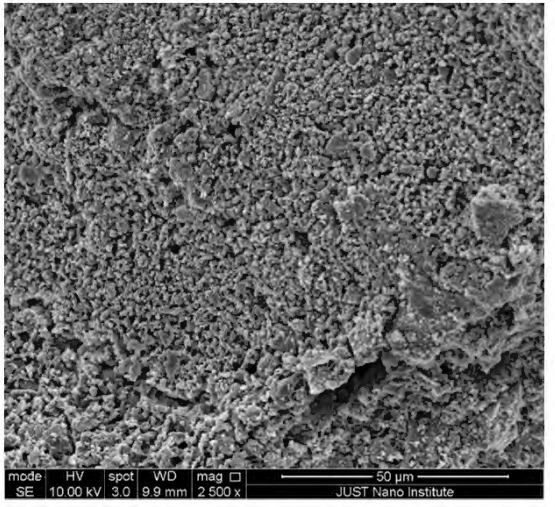
mode HV spot WD mag
SE 10.00 kV 3.0 9.9 mm 2 500 x
50 µm
JUST Nano Institute

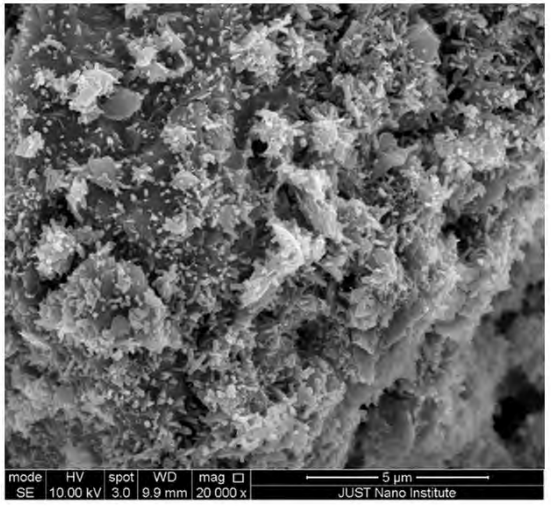
mode HV spot WD mag
SE 10.00 kV 3.0 9.9 mm 20 000 x
5 µm
JUST Nano Institute

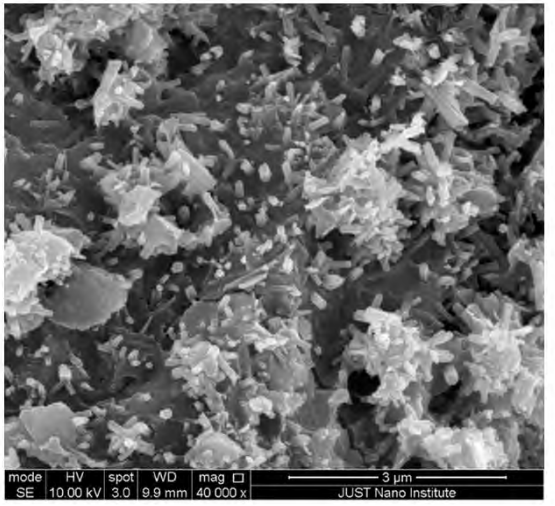
mode HV spot WD mag
SE 10.00 kV 3.0 9.9 mm 40 000 x
3 µm
JUST Nano Institute

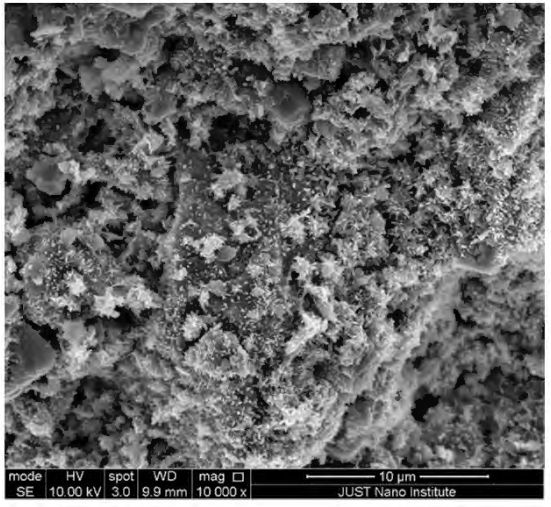
mode HV spot WD mag
SE 10.00 kV 3.0 9.9 mm 10 000 x
10 µm
JUST Nano Institute

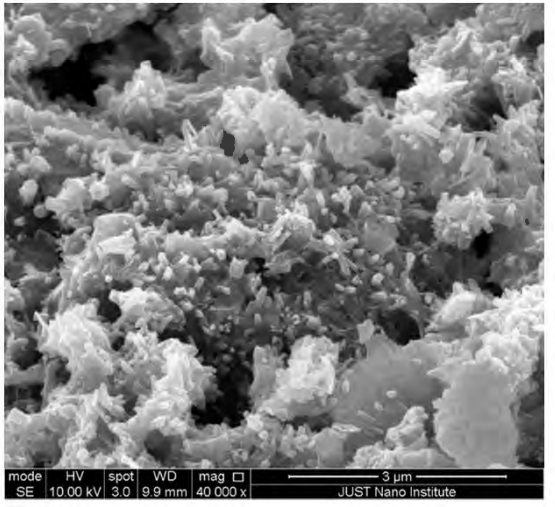
mode HV spot WD mag
SE 10.00 kV 3.0 9.9 mm 40 000 x
3 µm
JUST Nano Institute

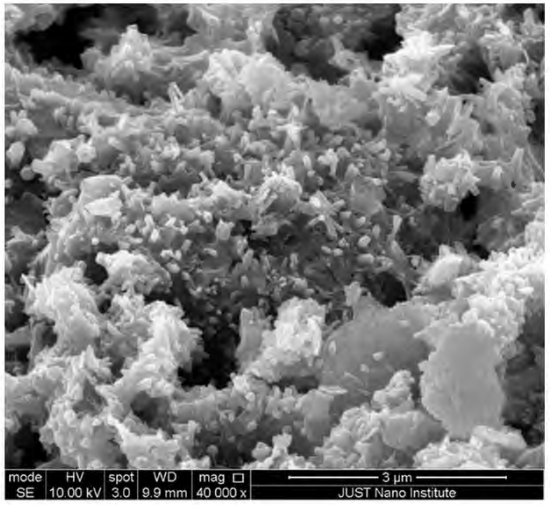
mode HV spot WD mag
SE 10.00 kV 3.0 9.9 mm 40 000 x
3 µm
JUST Nano Institute

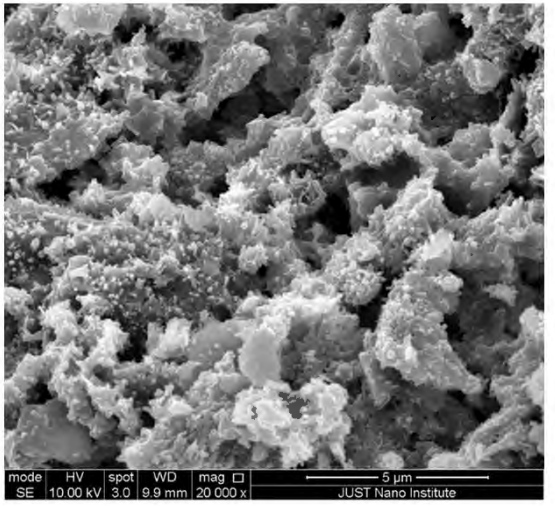
mode HV spot WD mag
SE 10.00 kV 3.0 9.9 mm 20 000 x
5 µm
JUST Nano Institute

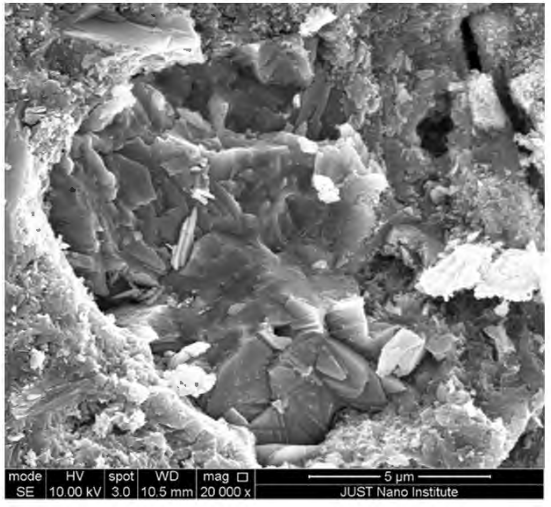
mode HV spot WD mag
SE 10.00 kV 3.0 10.5 mm 20 000 x
5 µm
JUST Nano Institute

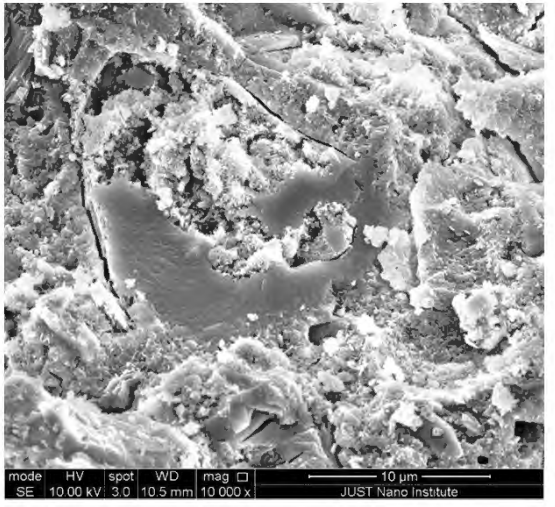
mode HV spot WD mag
SE 10.00 kV 3.0 10.5 mm 10 000 x
10 µm
JUST Nano Institute

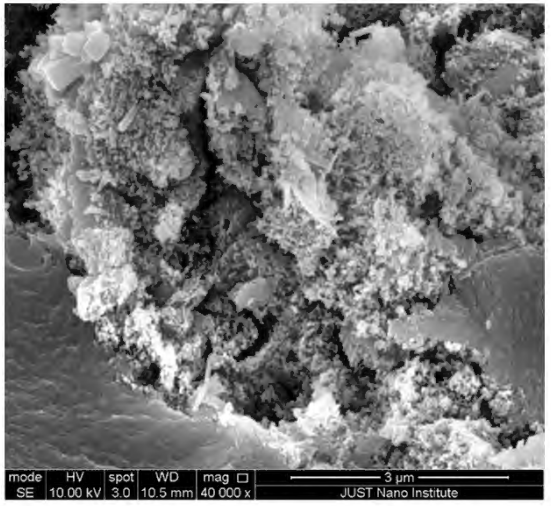
mode HV spot WD mag 3 µm
SE 10.00 kV 3.0 10.5 mm 40 000 x JUST Nano Institute

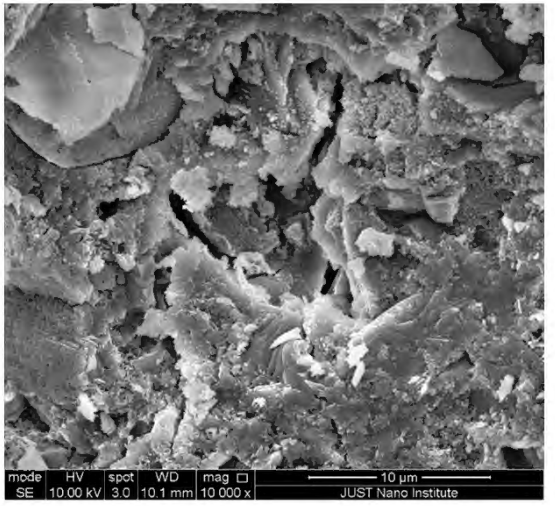
mode HV spot WD mag 10 µm
SE 10.00 kV 3.0 10.1 mm 10 000 x JUST Nano Institute

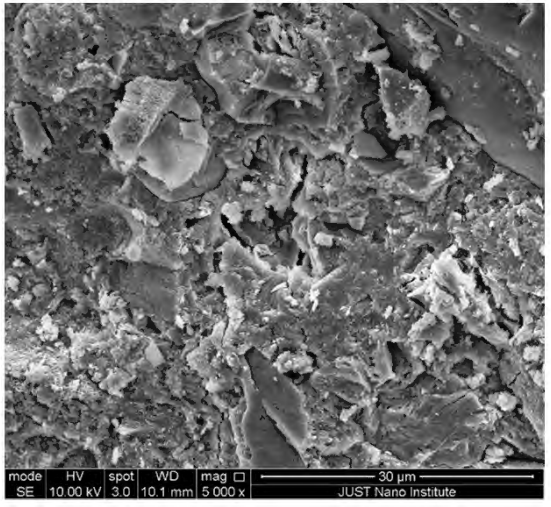
mode HV spot WD mag 30 µm
SE 10.00 kV 3.0 10.1 mm 5 000 x JUST Nano Institute

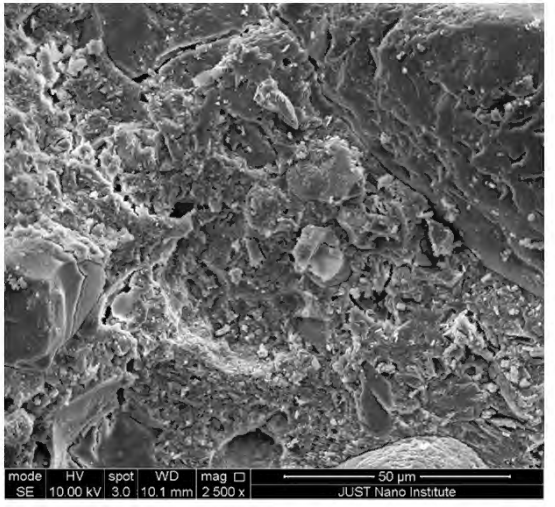
mode HV spot WD mag 50 µm
SE 10.00 kV 3.0 10.1 mm 2 500 x JUST Nano Institute

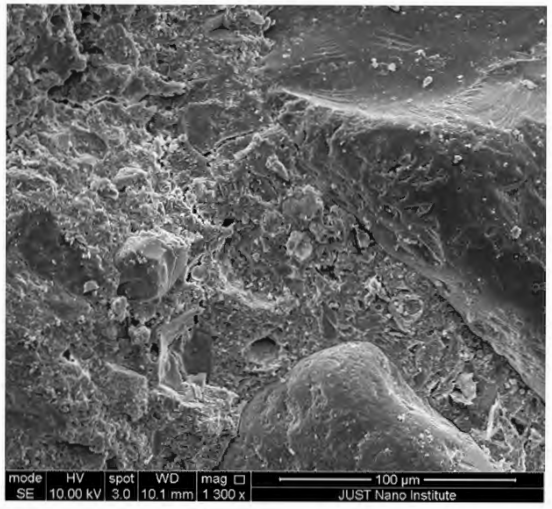
mode SE
HV 10.00 kV
spot 3.0
WD 10.1 mm
mag 1 300 x
100 µm
JUST Nano Institute

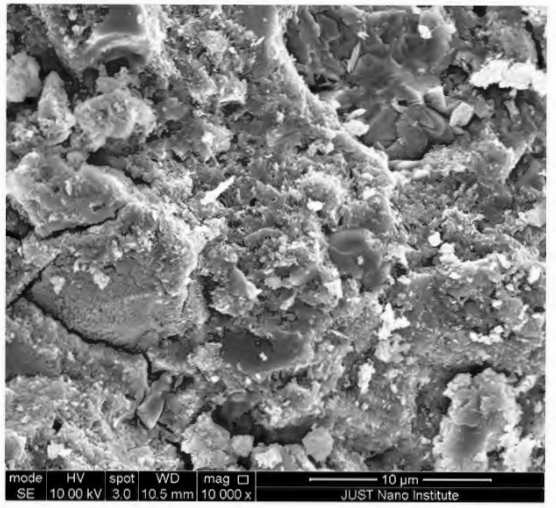
mode SE
HV 10.00 kV
spot 3.0
WD 10.5 mm
mag 10 000 x
10 µm
JUST Nano Institute

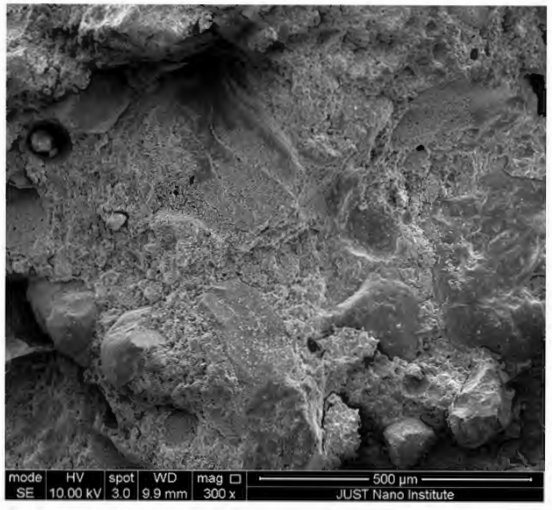
mode SE
HV 10.00 kV
spot 3.0
WD 9.9 mm
mag 300 x
500 µm
JUST Nano Institute

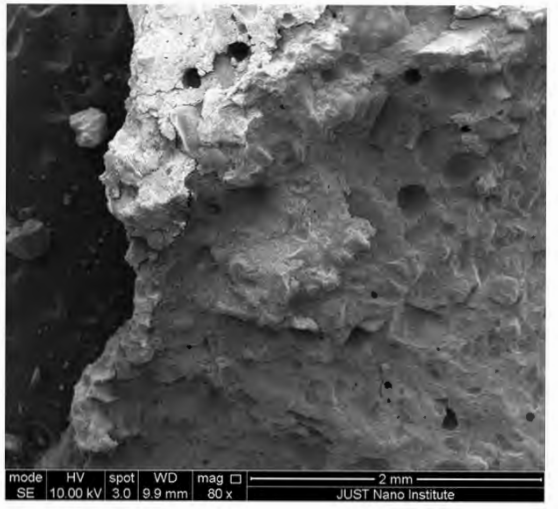
mode SE
HV 10.00 kV
spot 3.0
WD 9.9 mm
mag 80 x
2 mm
JUST Nano Institute

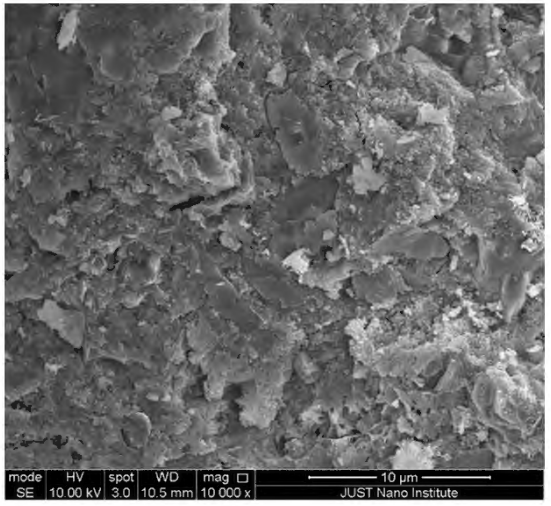
mode
SE
HV
10.00 kV
spot
3.0
WD
10.5 mm
mag
10 000 x
10 µm
JUST Nano Institute

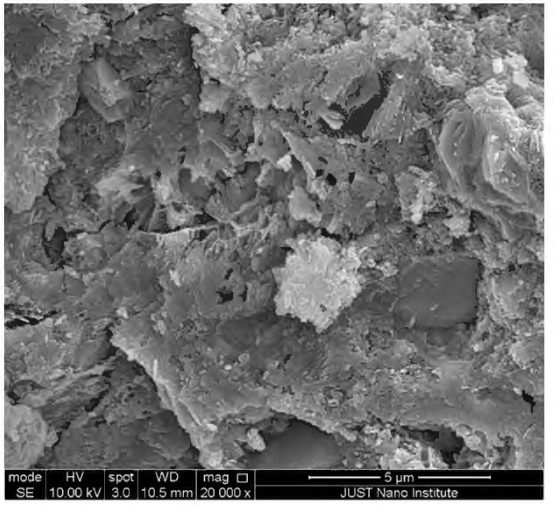
mode
SE
HV
10.00 kV
spot
3.0
WD
10.5 mm
mag
20 000 x
5 µm
JUST Nano Institute

Sample No. H

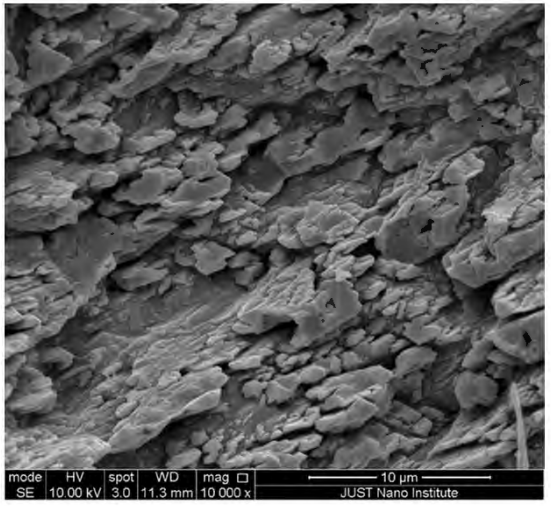
mode
SE
HV
10.00 kV
spot
3.0
WD
11.3 mm
mag
10 000 x
10 µm
JUST Nano Institute

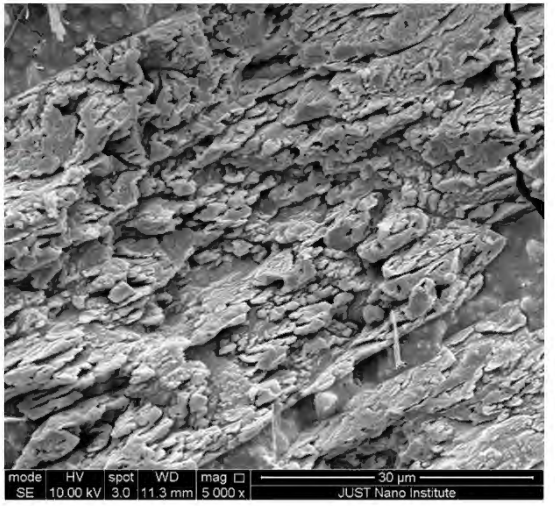
mode
SE
HV
10.00 kV
spot
3.0
WD
11.3 mm
mag
5 000 x
30 µm
JUST Nano Institute

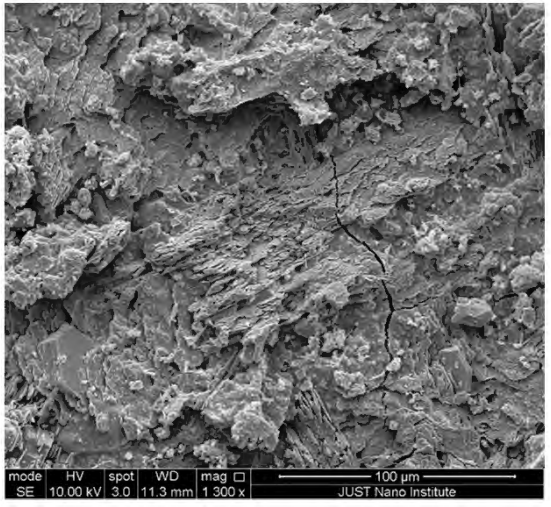
mode
SE
HV
10.00 kV
spot
3.0
WD
11.3 mm
mag
1 300 x
100 µm
JUST Nano Institute

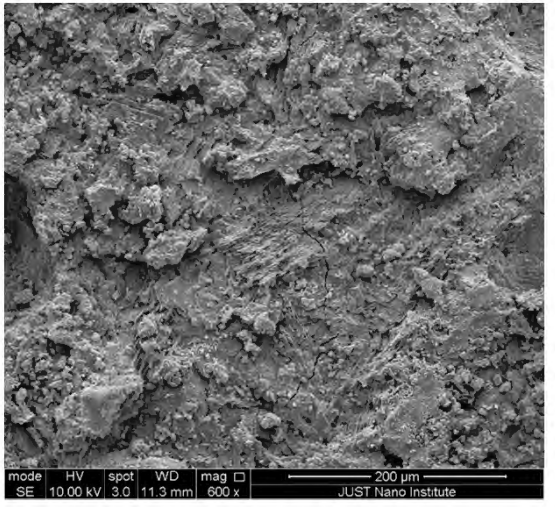
mode
SE
HV
10.00 kV
spot
3.0
WD
11.3 mm
mag
600 x
200 µm
JUST Nano Institute

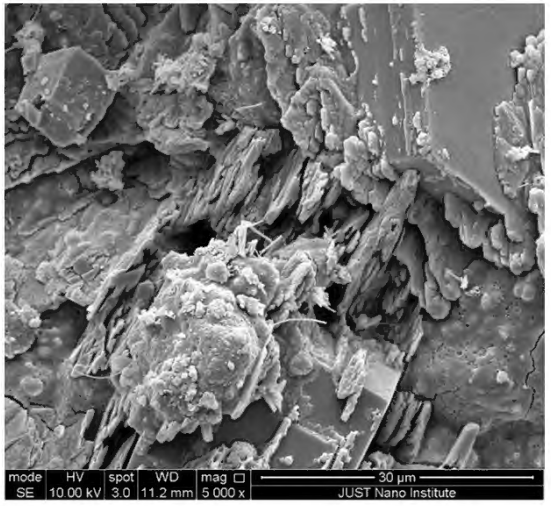
mode SE
HV 10.00 kV
spot 3.0
WD 11.2 mm
mag 5 000 x
30 µm
JUST Nano Institute

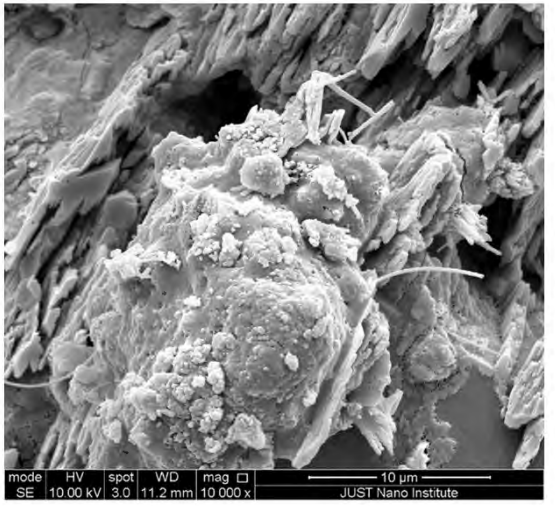
mode SE
HV 10.00 kV
spot 3.0
WD 11.2 mm
mag 10 000 x
10 µm
JUST Nano Institute

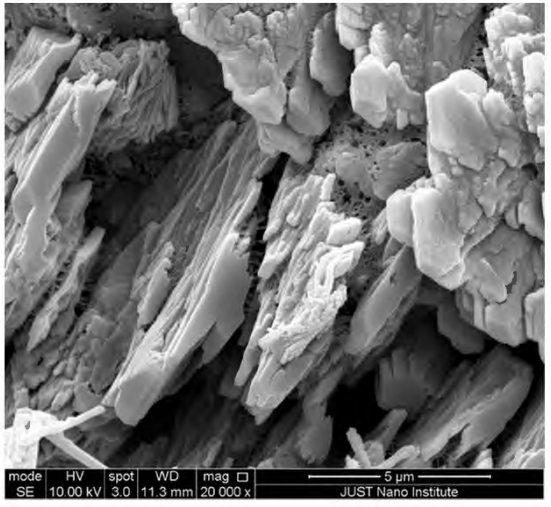
mode SE
HV 10.00 kV
spot 3.0
WD 11.3 mm
mag 20 000 x
5 µm
JUST Nano Institute

mode SE
HV 10.00 kV
spot 3.0
WD 11.2 mm
mag 40 000 x
3 µm
JUST Nano Institute

mode HV spot WD mag
SE 10.00 kV 3.0 11.3 mm 80 000 x
1 µm
JUST Nano Institute

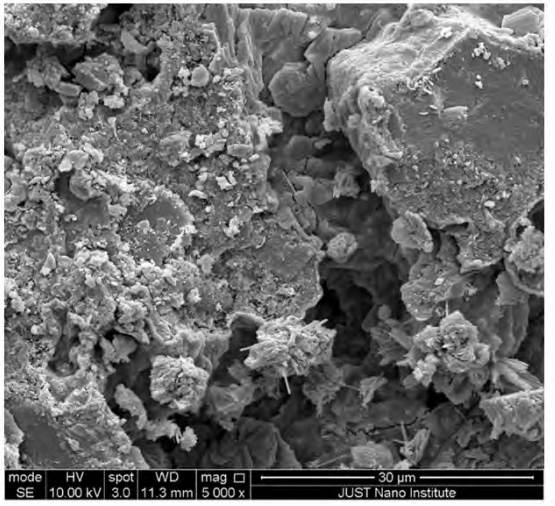
mode HV spot WD mag
SE 10.00 kV 3.0 11.3 mm 5 000 x
30 µm
JUST Nano Institute

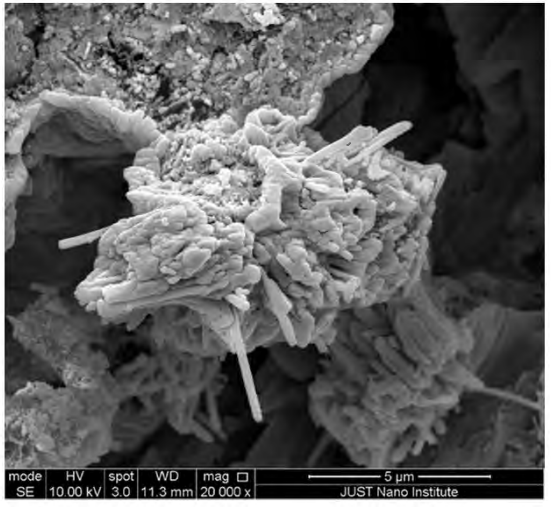
mode HV spot WD mag
SE 10.00 kV 3.0 11.3 mm 20 000 x
5 µm
JUST Nano Institute

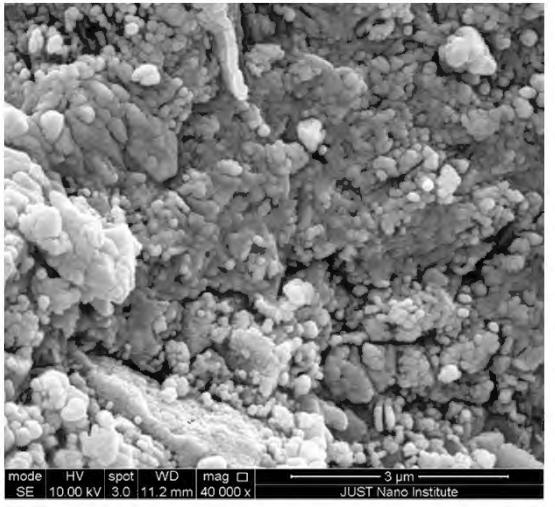
mode HV spot WD mag
SE 10.00 kV 3.0 11.2 mm 40 000 x
3 µm
JUST Nano Institute

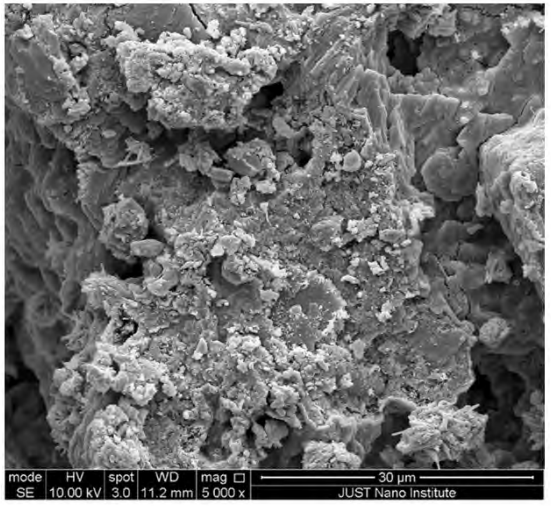
mode HV spot WD mag 30 µm
SE 10.00 kV 3.0 11.2 mm 5 000 x JUST Nano Institute

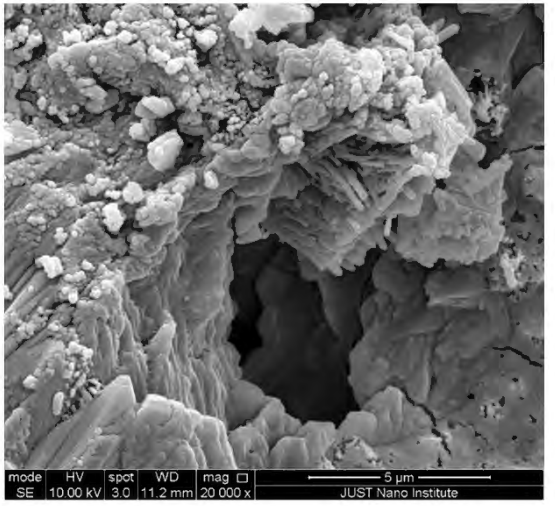
mode HV spot WD mag 5 µm
SE 10.00 kV 3.0 11.2 mm 20 000 x JUST Nano Institute

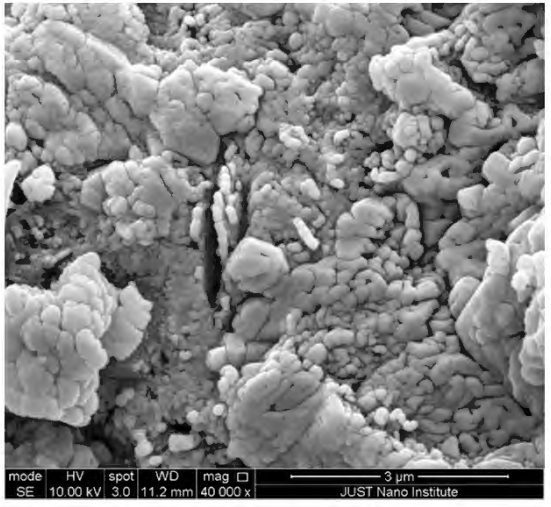
mode HV spot WD mag 3 µm
SE 10.00 kV 3.0 11.2 mm 40 000 x JUST Nano Institute

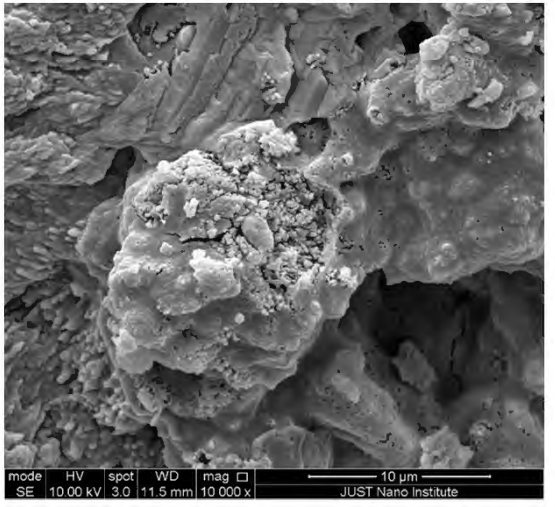
mode HV spot WD mag 10 µm
SE 10.00 kV 3.0 11.5 mm 10 000 x JUST Nano Institute

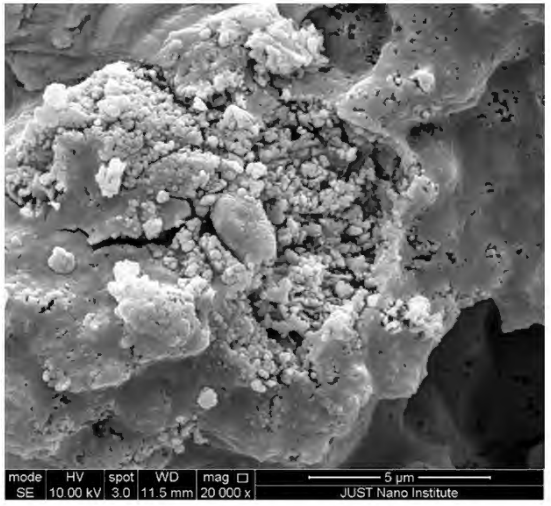
mode HV spot WD mag 5 µm
SE 10.00 kV 3.0 11.5 mm 20 000 x
JUST Nano Institute

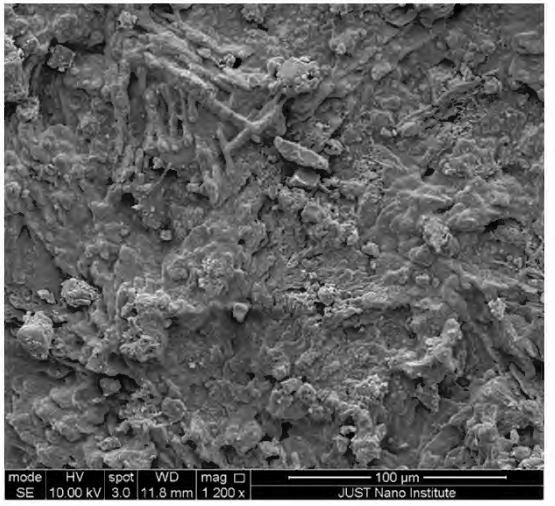
mode HV spot WD mag 100 µm
SE 10.00 kV 3.0 11.8 mm 1 200 x
JUST Nano Institute

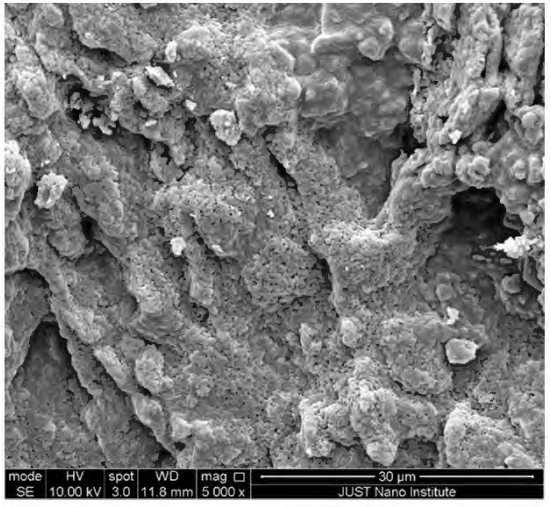
mode HV spot WD mag 30 µm
SE 10.00 kV 3.0 11.8 mm 5 000 x
JUST Nano Institute

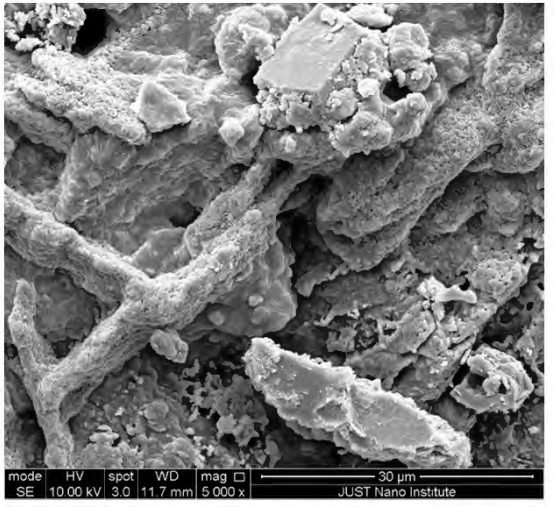
mode HV spot WD mag 30 µm
SE 10.00 kV 3.0 11.7 mm 5 000 x
JUST Nano Institute

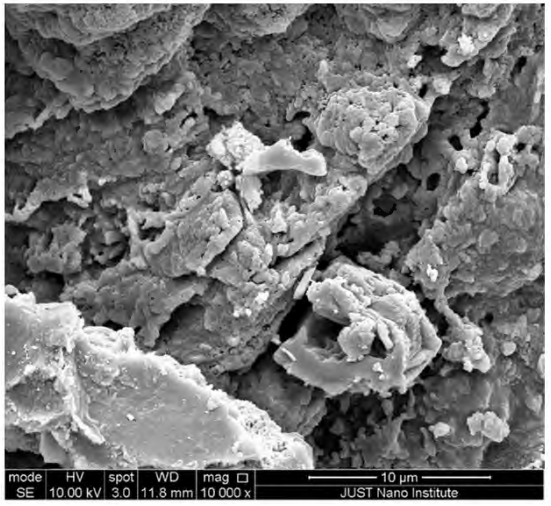
mode HV spot WD mag
SE 10.00 kV 3.0 11.8 mm 10 000 x
10 µm
JUST Nano Institute

mode HV spot WD mag
SE 10.00 kV 3.0 11.8 mm 20 000 x
5 µm
JUST Nano Institute

mode HV spot WD mag
SE 10.00 kV 3.0 11.8 mm 40 000 x
3 µm
JUST Nano Institute

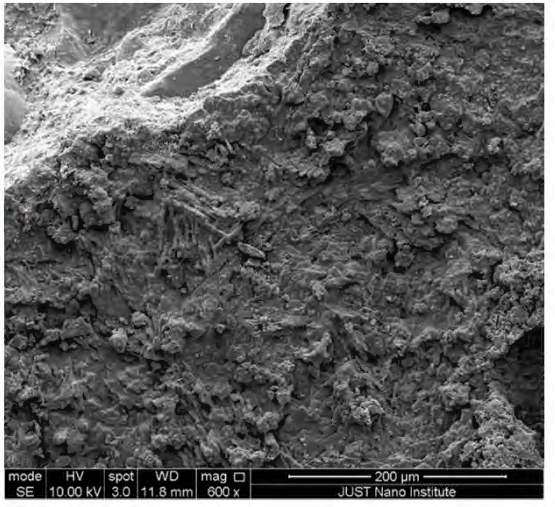
mode HV spot WD mag
SE 10.00 kV 3.0 11.8 mm 600 x
200 µm
JUST Nano Institute

Sample No. J

mode HV spot WD mag 3 µm
SE 10.00 kV 3.0 11.9 mm 40 000 x
JUST Nano Institute

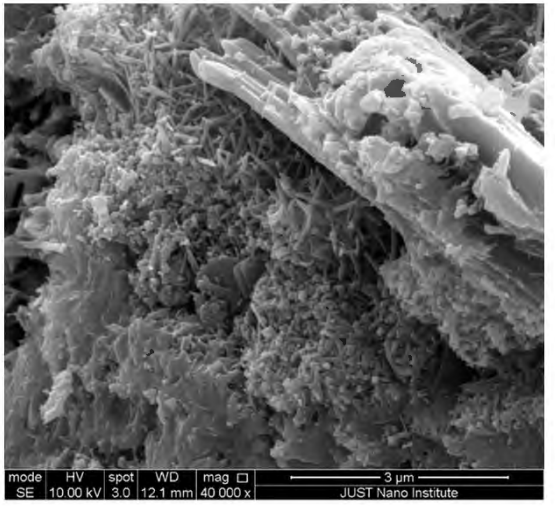
mode HV spot WD mag 3 µm
SE 10.00 kV 3.0 12.1 mm 40 000 x
JUST Nano Institute

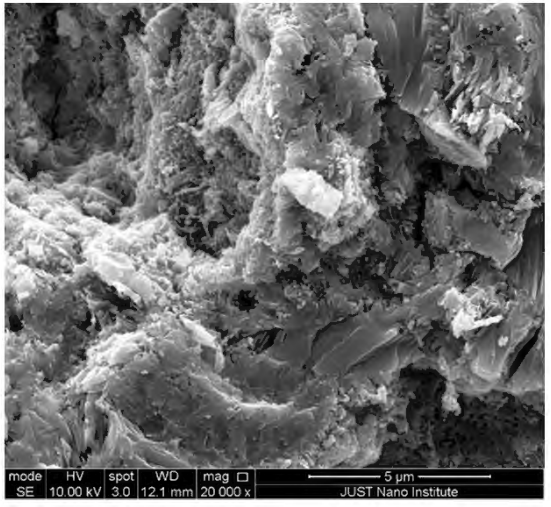
mode HV spot WD mag 5 µm
SE 10.00 kV 3.0 12.1 mm 20 000 x
JUST Nano Institute

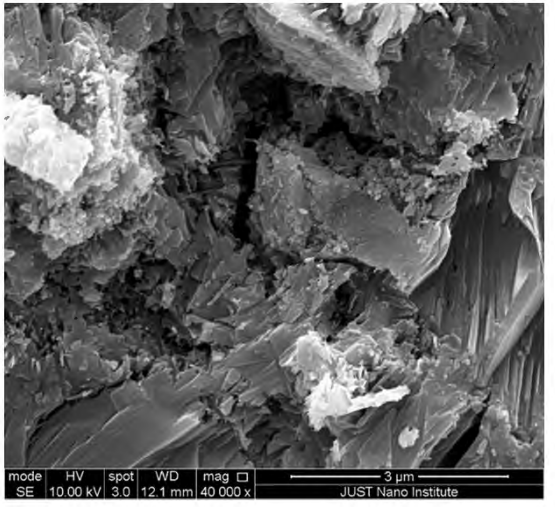
mode HV spot WD mag 3 µm
SE 10.00 kV 3.0 12.1 mm 40 000 x
JUST Nano Institute

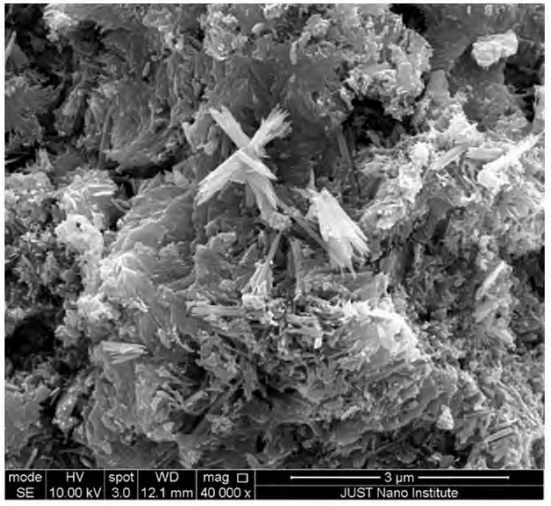
mode
SE
HV
10.00 kV
spot
3.0
WD
12.1 mm
mag
40 000 x
3 µm
JUST Nano Institute

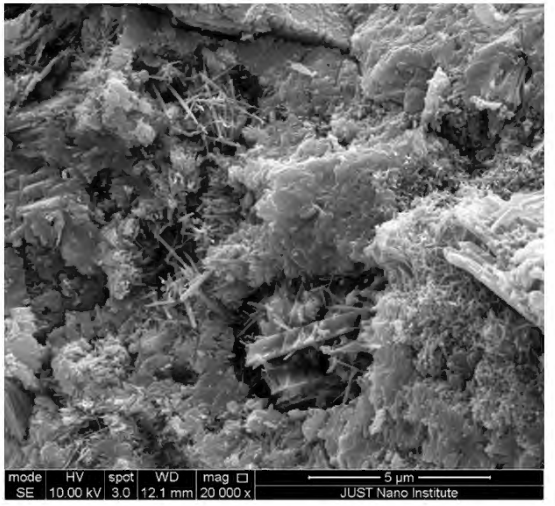
mode
SE
HV
10.00 kV
spot
3.0
WD
12.1 mm
mag
20 000 x
5 µm
JUST Nano Institute

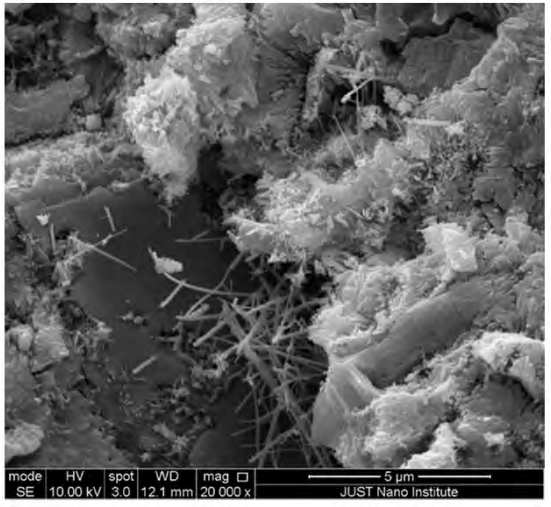
mode
SE
HV
10.00 kV
spot
3.0
WD
12.1 mm
mag
20 000 x
5 µm
JUST Nano Institute

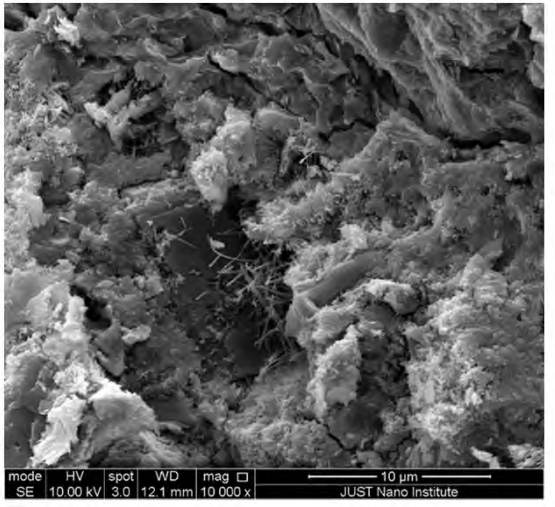
mode
SE
HV
10.00 kV
spot
3.0
WD
12.1 mm
mag
10 000 x
10 µm
JUST Nano Institute

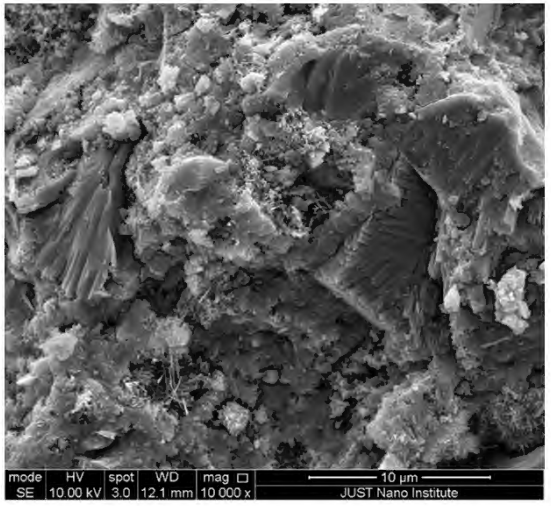
mode
SE
HV
10.00 kV
spot
3.0
WD
12.1 mm
mag
10 000 x
10 µm
JUST Nano Institute

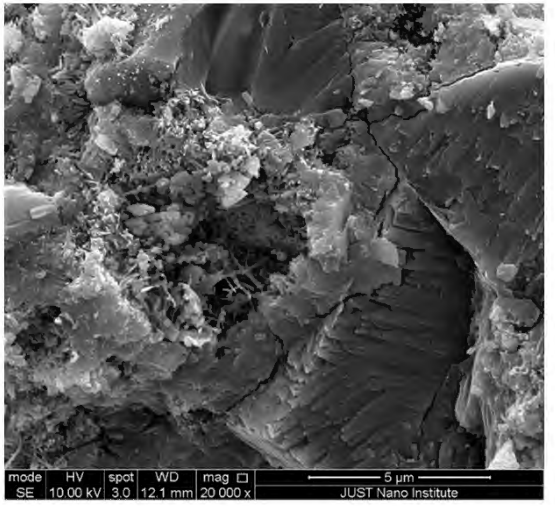
mode
SE
HV
10.00 kV
spot
3.0
WD
12.1 mm
mag
20 000 x
5 µm
JUST Nano Institute

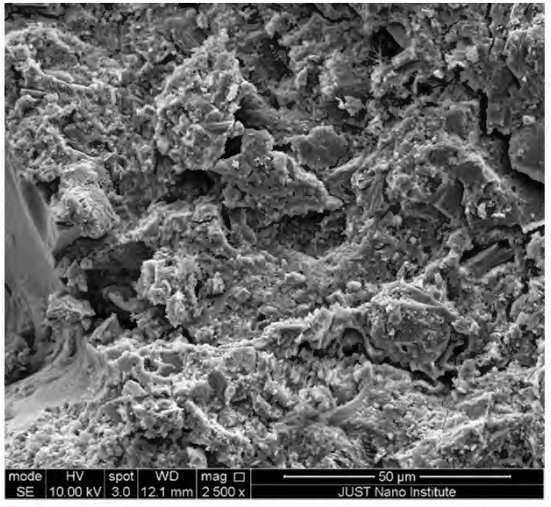
mode
SE
HV
10.00 kV
spot
3.0
WD
12.1 mm
mag
2 500 x
50 µm
JUST Nano Institute

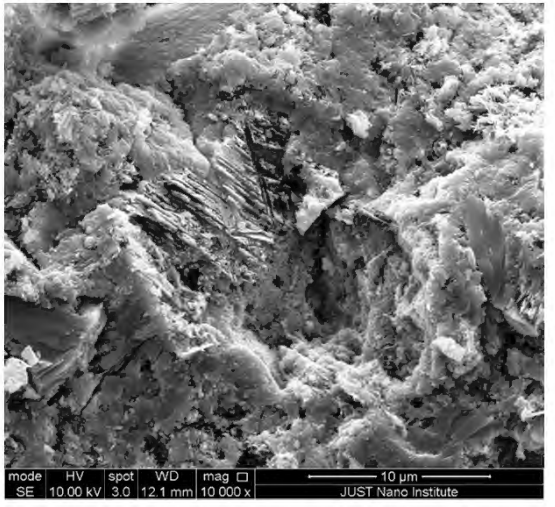
mode
SE
HV
10.00 kV
spot
3.0
WD
12.1 mm
mag
10 000 x
10 µm
JUST Nano Institute

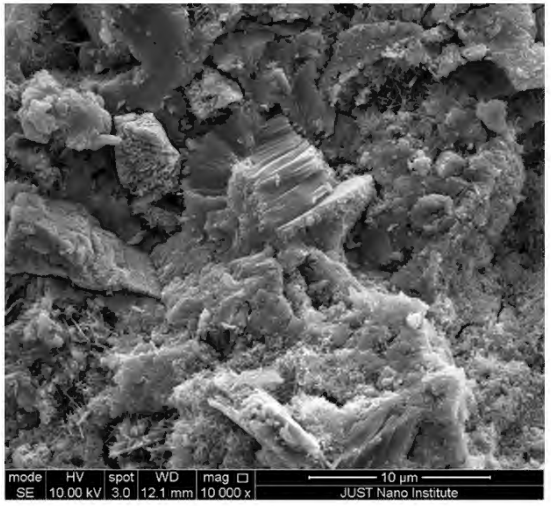
mode HV spot WD mag 10 µm
SE 10.00 kV 3.0 12.1 mm 10 000 x JUST Nano Institute

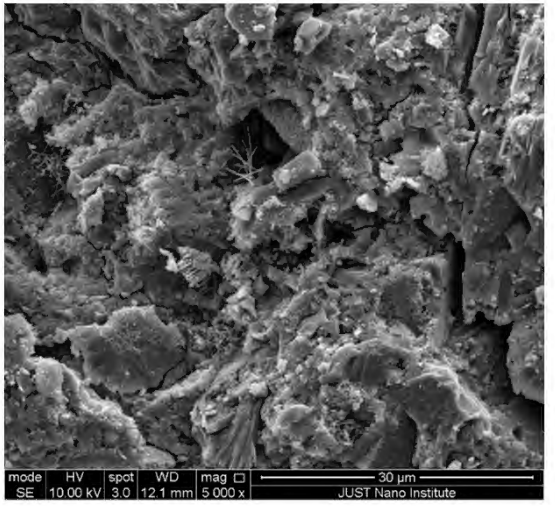
mode HV spot WD mag 30 µm
SE 10.00 kV 3.0 12.1 mm 5 000 x JUST Nano Institute

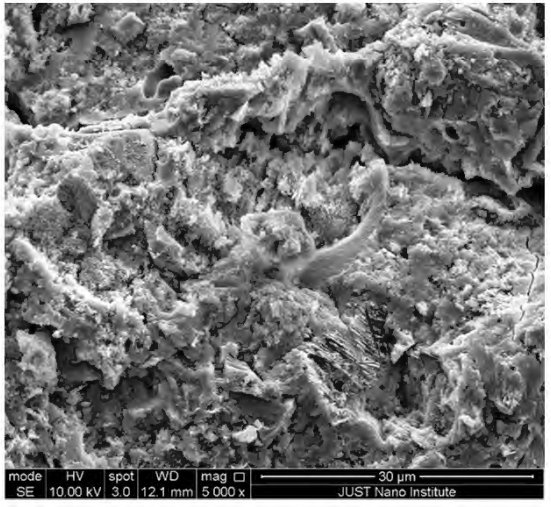
mode HV spot WD mag 30 µm
SE 10.00 kV 3.0 12.1 mm 5 000 x JUST Nano Institute

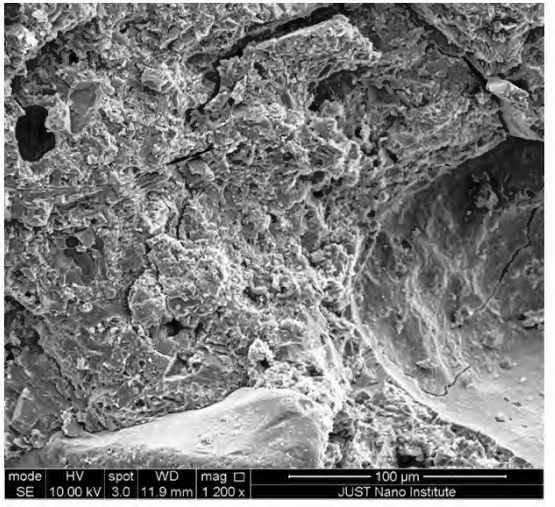
mode HV spot WD mag 100 µm
SE 10.00 kV 3.0 11.9 mm 1 200 x JUST Nano Institute

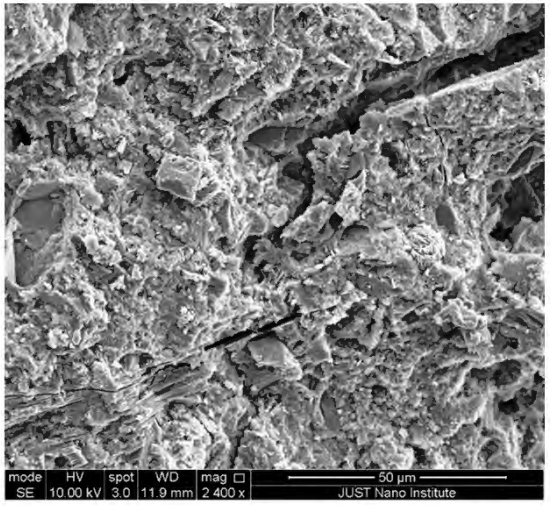
mode HV spot WD mag 50 µm
SE 10.00 kV 3.0 11.9 mm 2 400 x JUST Nano Institute

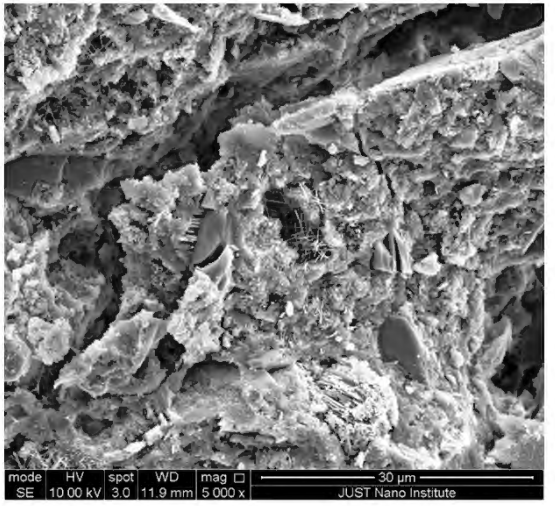
mode HV spot WD mag 30 µm
SE 10.00 kV 3.0 11.9 mm 5 000 x JUST Nano Institute

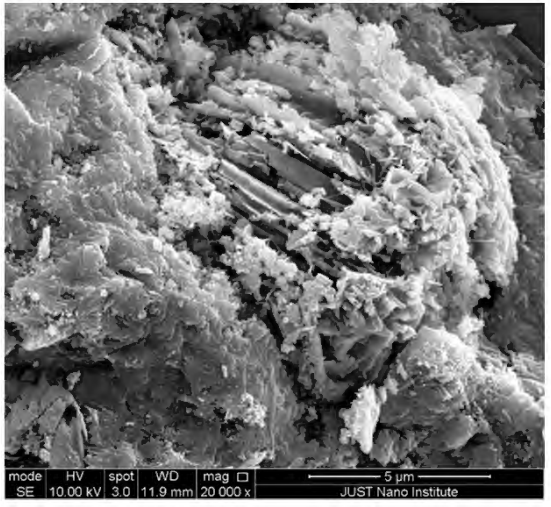
mode HV spot WD mag 5 µm
SE 10.00 kV 3.0 11.9 mm 20 000 x JUST Nano Institute

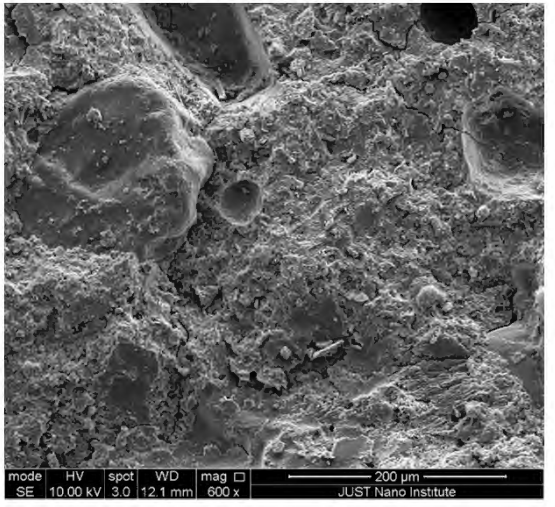
mode HV spot WD mag 200 µm
SE 10.00 kV 3.0 12.1 mm 600 x JUST Nano Institute

Sample No. N

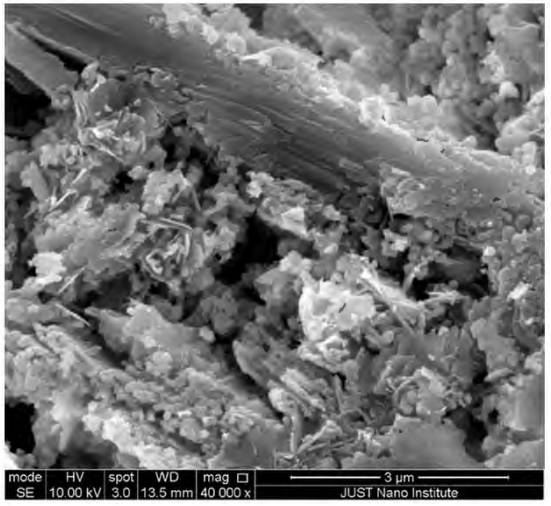
mode HV spot WD mag
SE 10.00 kV 3.0 13.5 mm 40 000 x
3 µm
JUST Nano Institute

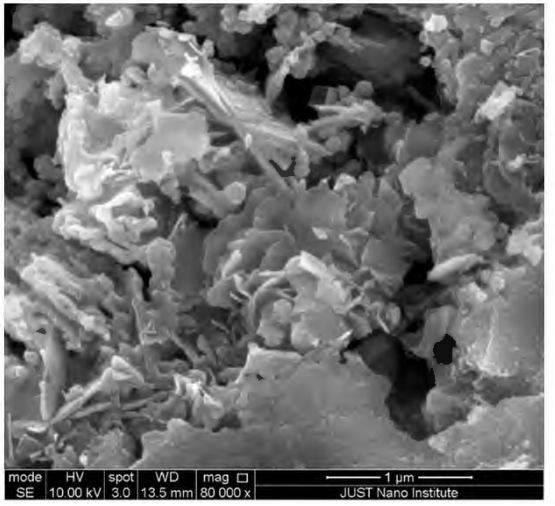
mode HV spot WD mag
SE 10.00 kV 3.0 13.5 mm 80 000 x
1 µm
JUST Nano Institute

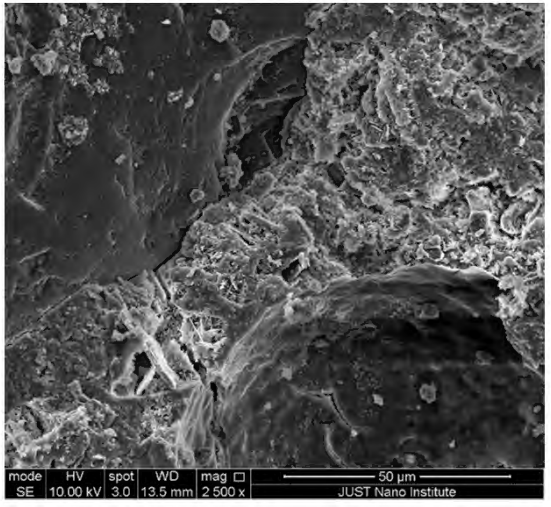
mode HV spot WD mag
SE 10.00 kV 3.0 13.5 mm 2 500 x
50 µm
JUST Nano Institute

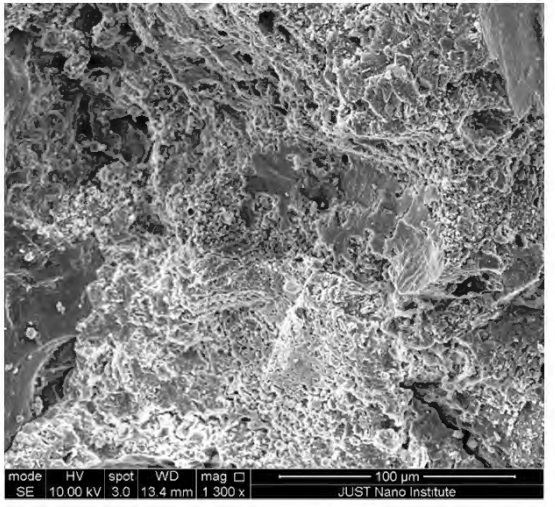
mode HV spot WD mag
SE 10.00 kV 3.0 13.4 mm 1 300 x
100 µm
JUST Nano Institute

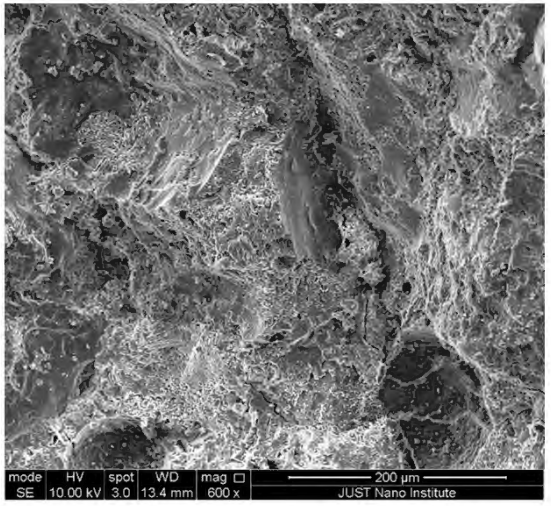
mode HV spot WD mag
SE 10.00 kV 3.0 13.4 mm 600 x
200 µm
JUST Nano Institute

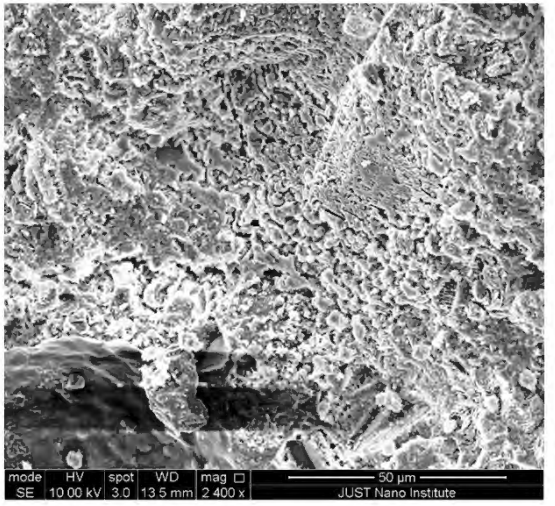
mode HV spot WD mag
SE 10.00 kV 3.0 13.5 mm 2 400 x
50 µm
JUST Nano Institute

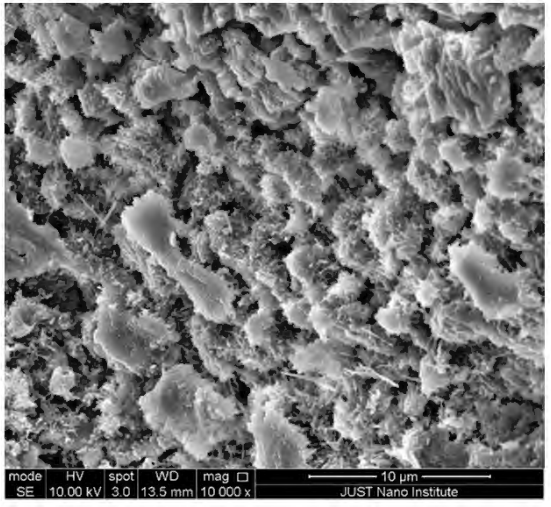
mode HV spot WD mag
SE 10.00 kV 3.0 13.5 mm 10 000 x
10 µm
JUST Nano Institute

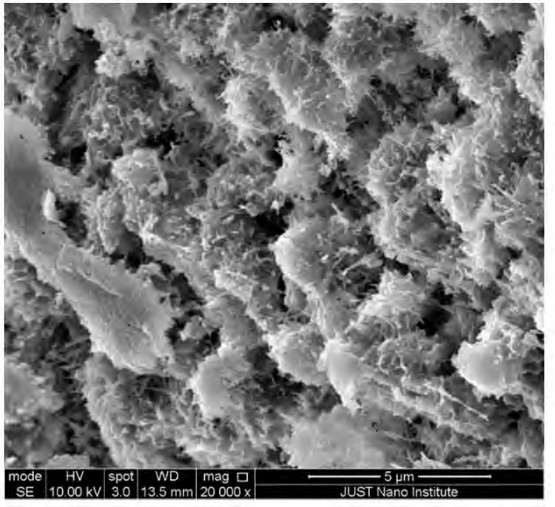
mode HV spot WD mag
SE 10.00 kV 3.0 13.5 mm 20 000 x
5 µm
JUST Nano Institute

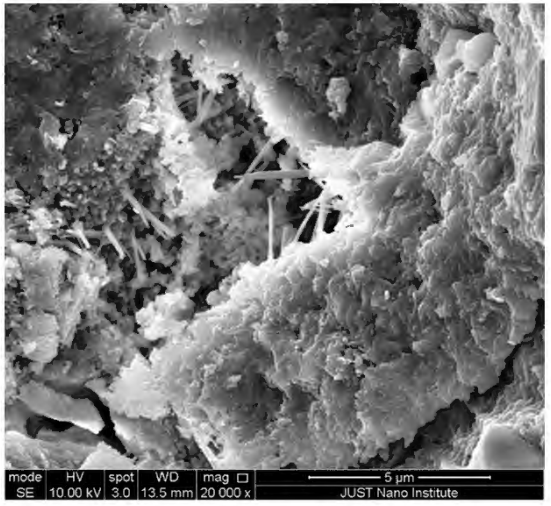
mode HV spot WD mag
SE 10.00 kV 3.0 13.5 mm 20 000 x
5 µm
JUST Nano Institute

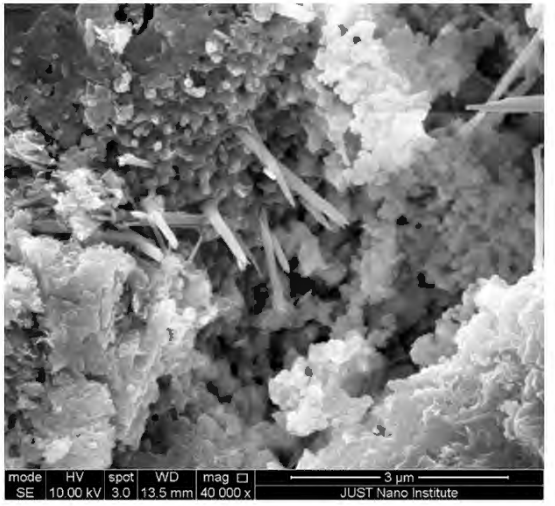
mode HV spot WD mag
SE 10.00 kV 3.0 13.5 mm 40 000 x
3 µm
JUST Nano Institute

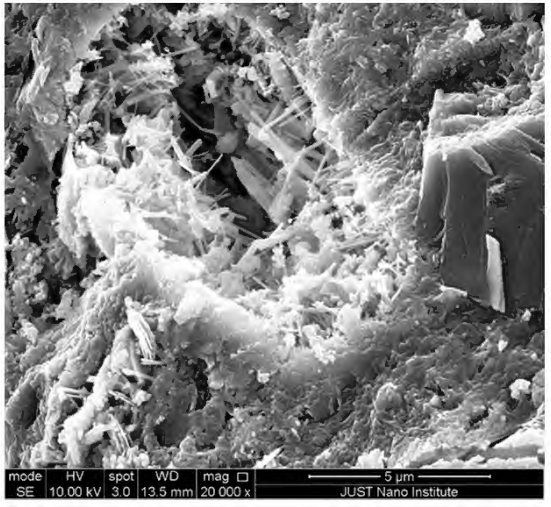
mode HV spot WD mag
SE 10.00 kV 3.0 13.5 mm 20 000 x
5 µm
JUST Nano Institute

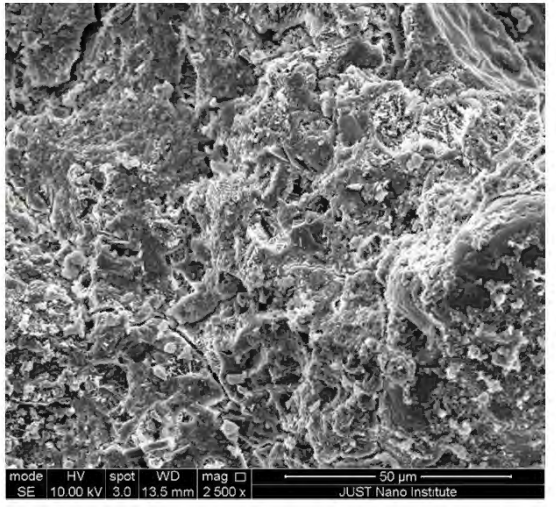
mode HV spot WD mag
SE 10.00 kV 3.0 13.5 mm 2 500 x
50 µm
JUST Nano Institute

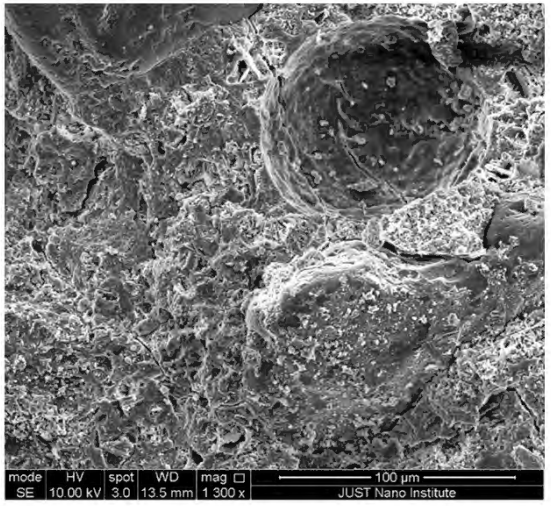
mode HV spot WD mag 100 µm
SE 10.00 kV 3.0 13.5 mm 1 300 x JUST Nano Institute

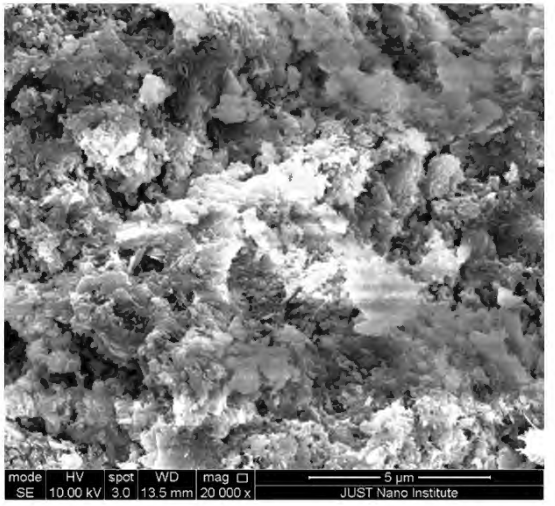
mode HV spot WD mag 5 µm
SE 10.00 kV 3.0 13.5 mm 20 000 x JUST Nano Institute

mode HV spot WD mag 30 µm
SE 10.00 kV 3.0 13.5 mm 5 000 x JUST Nano Institute

mode HV spot WD mag 10 µm
SE 10.00 kV 3.0 13.5 mm 10 000 x JUST Nano Institute

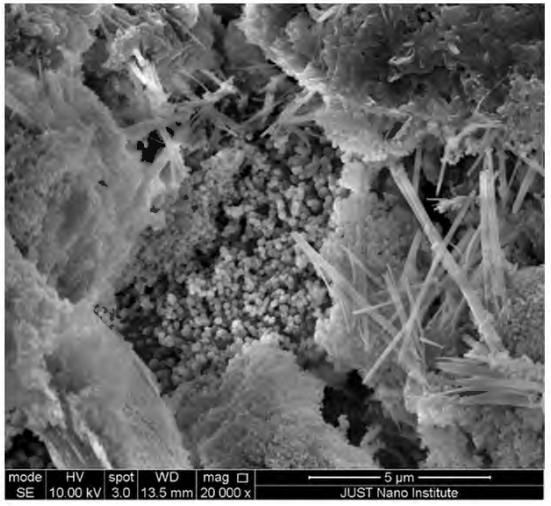
mode
SE
HV
10.00 kV
spot
3.0
WD
13.5 mm
mag
20 000 x
5 µm
JUST Nano Institute

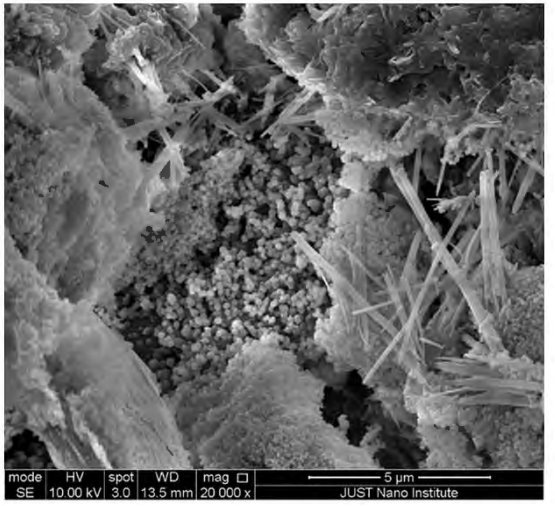
mode
SE
HV
10.00 kV
spot
3.0
WD
13.5 mm
mag
20 000 x
5 µm
JUST Nano Institute

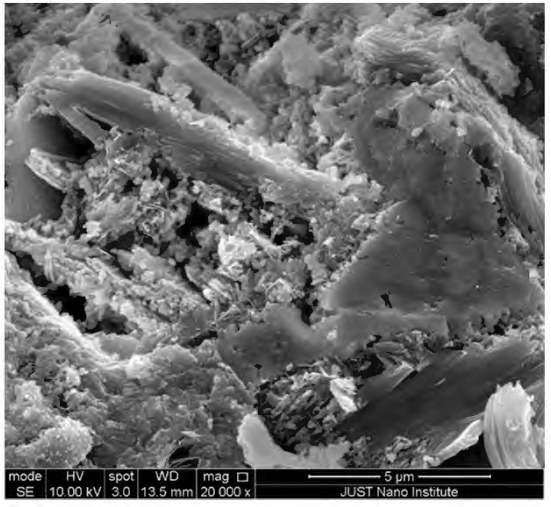
mode
SE
HV
10.00 kV
spot
3.0
WD
13.5 mm
mag
20 000 x
5 µm
JUST Nano Institute

mode
SE
HV
10.00 kV
spot
3.0
WD
13.7 mm
mag
20 000 x
5 µm
JUST Nano Institute

mode
SE
HV
10.00 kV
spot
3.0
WD
13.7 mm
mag
40 000 x
3 µm
JUST Nano Institute

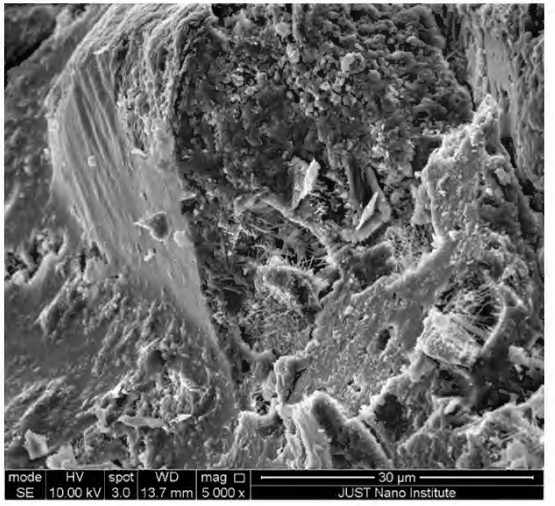
mode
SE
HV
10.00 kV
spot
3.0
WD
13.7 mm
mag
5 000 x
30 µm
JUST Nano Institute

mode
SE
HV
10.00 kV
spot
3.0
WD
13.7 mm
mag
10 000 x
10 µm
JUST Nano Institute

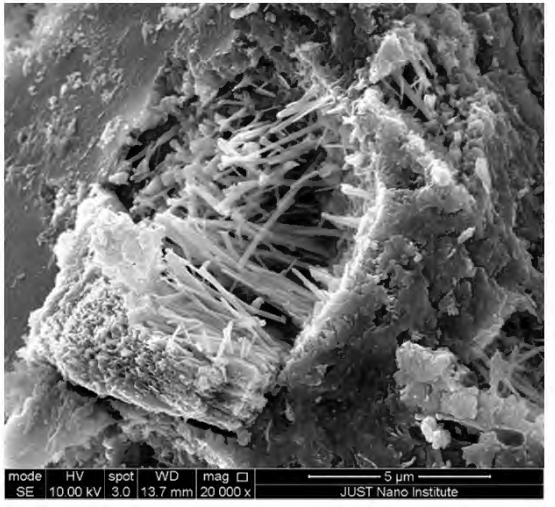
mode
SE
HV
10.00 kV
spot
3.0
WD
13.7 mm
mag
20 000 x
5 µm
JUST Nano Institute

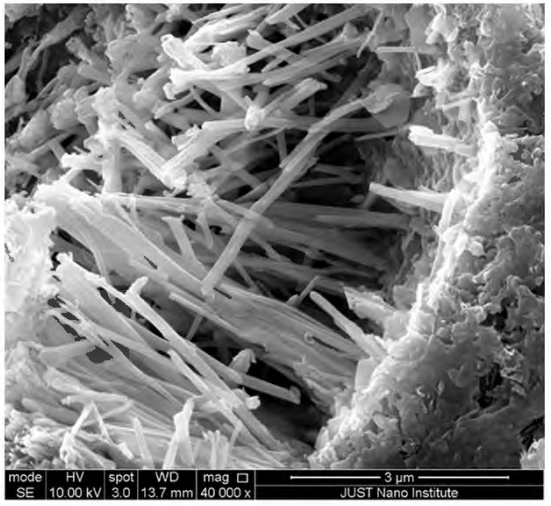
mode SE
HV 10.00 kV
spot 3.0
WD 13.7 mm
mag 40 000 x
3 µm
JUST Nano Institute

mode SE
HV 10.00 kV
spot 3.0
WD 13.7 mm
mag 80 000 x
1 µm
JUST Nano Institute

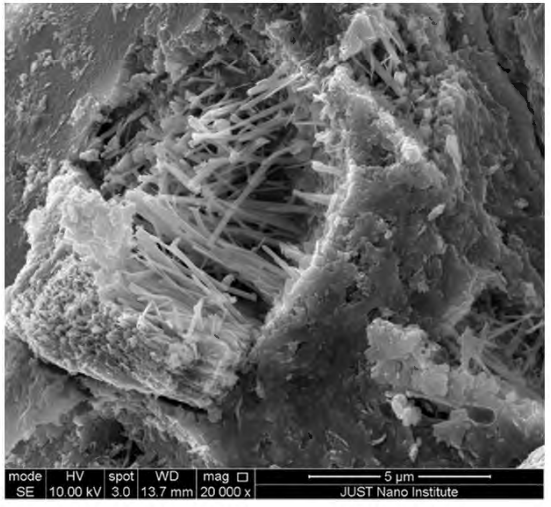
mode SE
HV 10.00 kV
spot 3.0
WD 13.7 mm
mag 20 000 x
5 µm
JUST Nano Institute

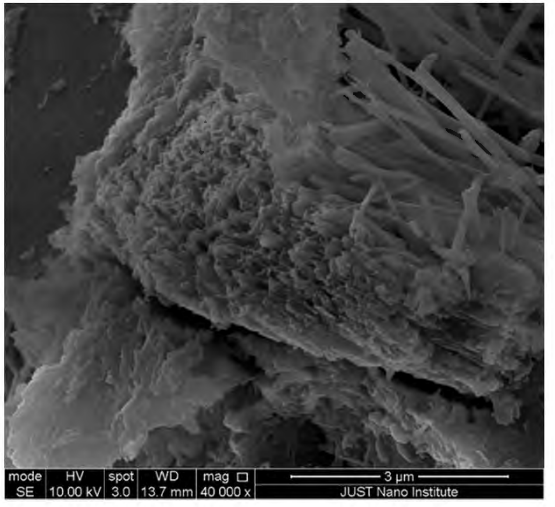
mode SE
HV 10.00 kV
spot 3.0
WD 13.7 mm
mag 40 000 x
3 µm
JUST Nano Institute

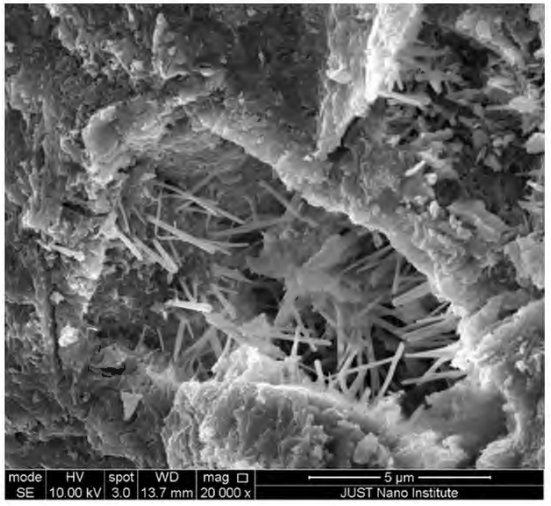
mode SE
HV 10.00 kV
spot 3.0
WD 13.7 mm
mag 20 000 x
5 µm
JUST Nano Institute

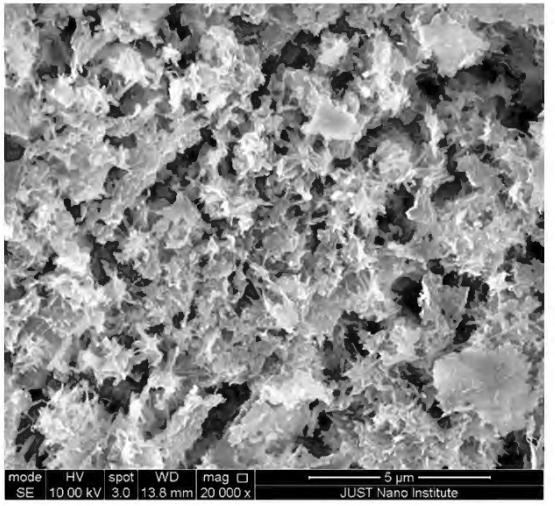
mode SE
HV 10.00 kV
spot 3.0
WD 13.8 mm
mag 20 000 x
5 µm
JUST Nano Institute

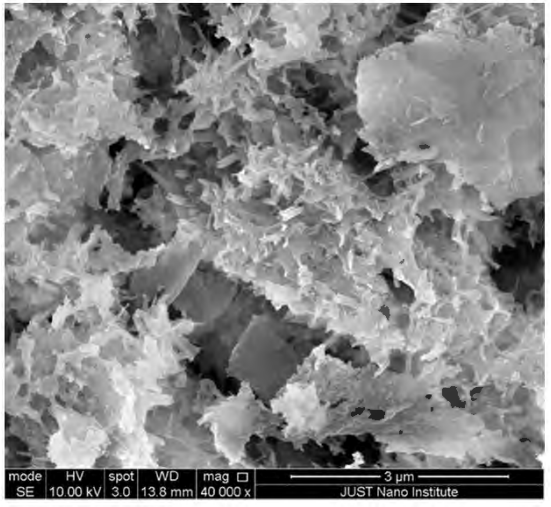
mode SE
HV 10.00 kV
spot 3.0
WD 13.8 mm
mag 40 000 x
3 µm
JUST Nano Institute

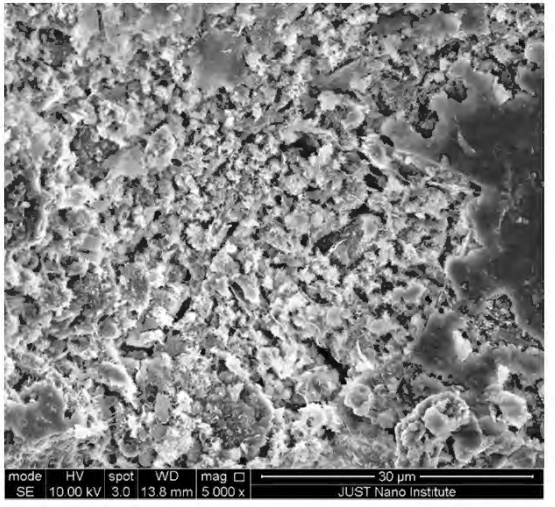
mode SE
HV 10.00 kV
spot 3.0
WD 13.8 mm
mag 5 000 x
30 µm
JUST Nano Institute

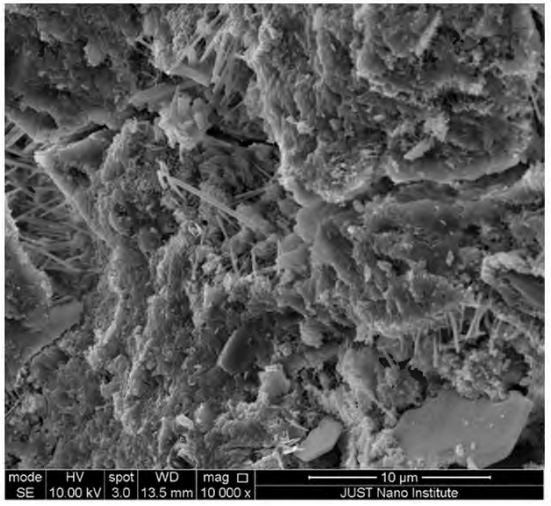
mode SE
HV 10.00 kV
spot 3.0
WD 13.5 mm
mag 10 000 x
10 µm
JUST Nano Institute

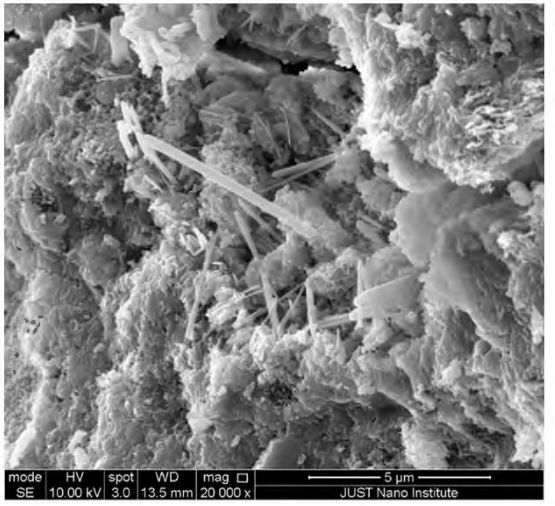
mode SE
HV 10.00 kV
spot 3.0
WD 13.5 mm
mag 20 000 x
5 µm
JUST Nano Institute

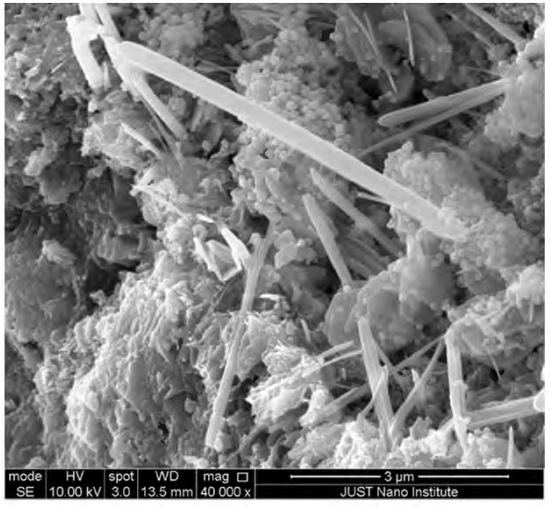
mode SE
HV 10.00 kV
spot 3.0
WD 13.5 mm
mag 40 000 x
3 µm
JUST Nano Institute

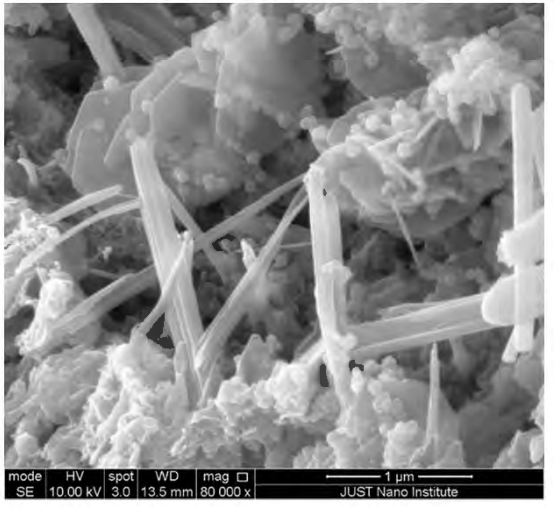
mode SE
HV 10.00 kV
spot 3.0
WD 13.5 mm
mag 80 000 x
1 µm
JUST Nano Institute

Sample No. O

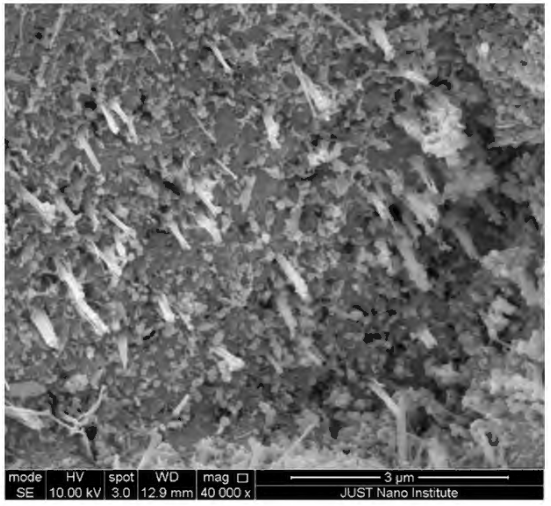
mode
SE
HV
10.00 kV
spot
3.0
WD
12.9 mm
mag
40 000 x
3 µm
JUST Nano Institute

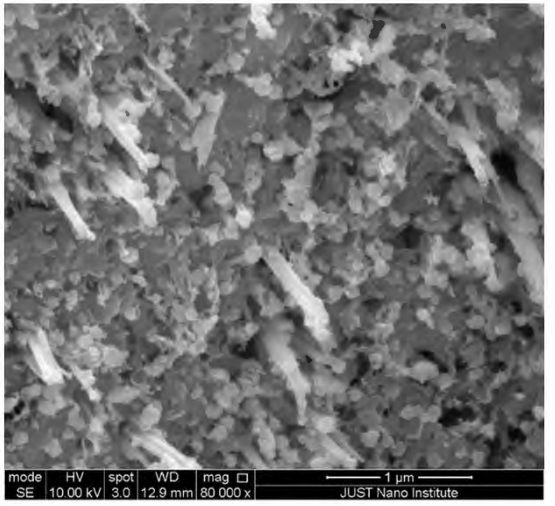
mode
SE
HV
10.00 kV
spot
3.0
WD
12.9 mm
mag
80 000 x
1 µm
JUST Nano Institute

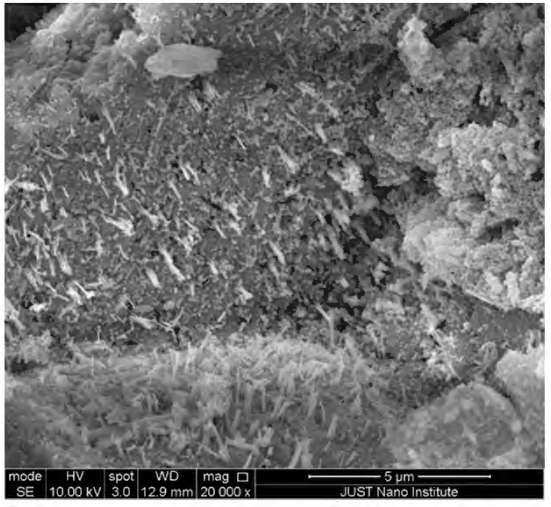
mode
SE
HV
10.00 kV
spot
3.0
WD
12.9 mm
mag
20 000 x
5 µm
JUST Nano Institute

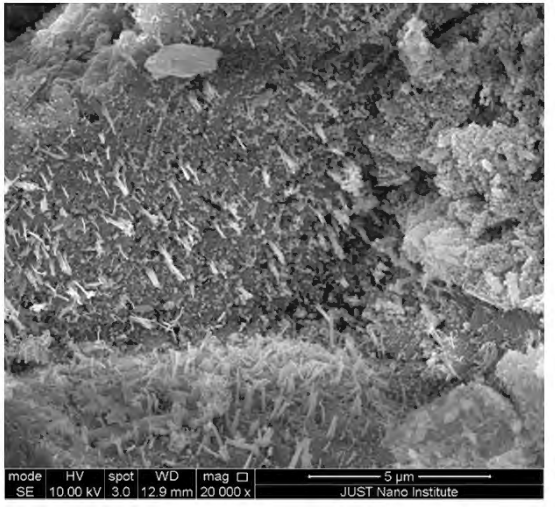
mode
SE
HV
10.00 kV
spot
3.0
WD
12.9 mm
mag
20 000 x
5 µm
JUST Nano Institute

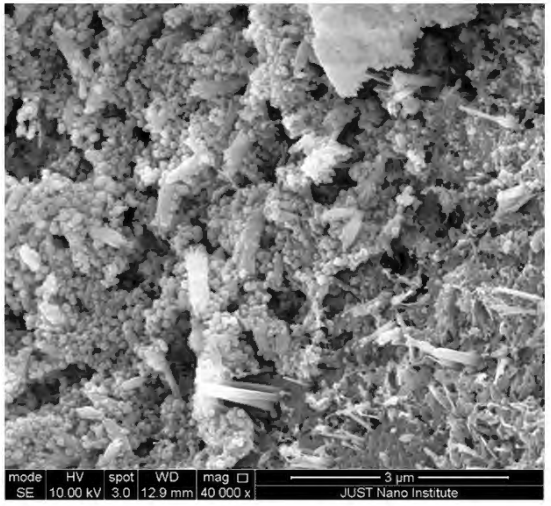
mode
SE
HV
10.00 kV
spot
3.0
WD
12.9 mm
mag
40 000 x
3 µm
JUST Nano Institute

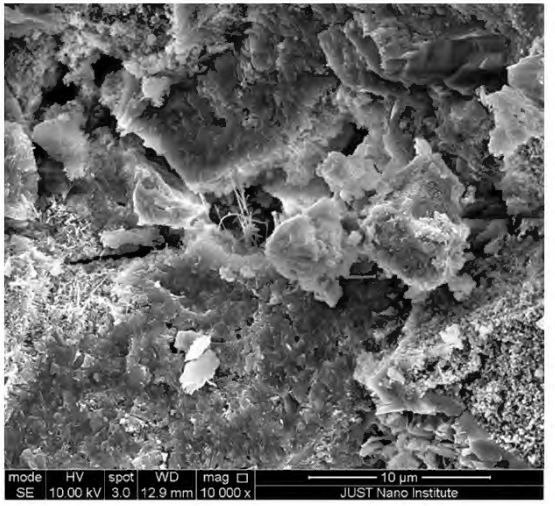
mode
SE
HV
10.00 kV
spot
3.0
WD
12.9 mm
mag
10 000 x
10 µm
JUST Nano Institute

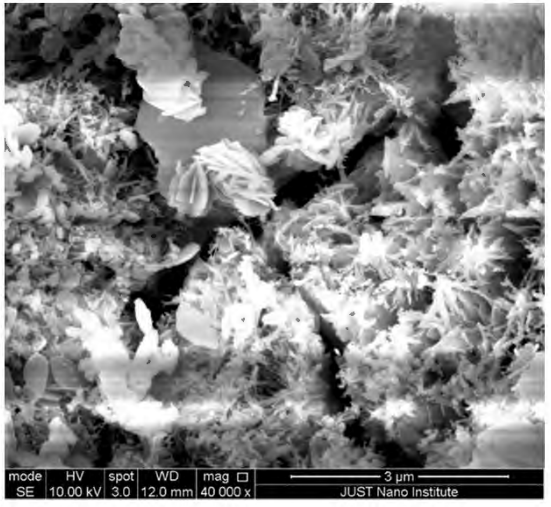
mode
SE
HV
10.00 kV
spot
3.0
WD
12.0 mm
mag
40 000 x
3 µm
JUST Nano Institute

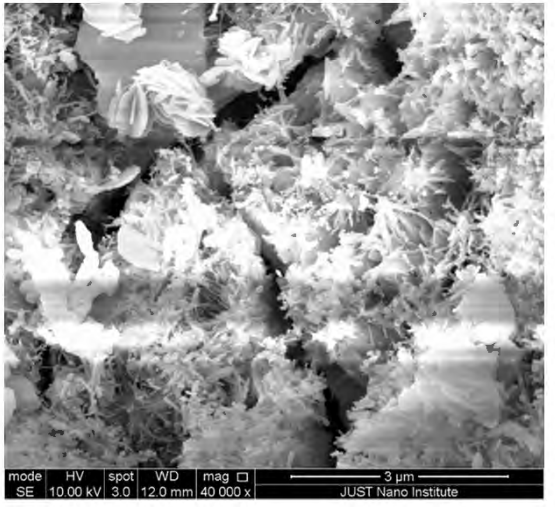
mode
SE
HV
10.00 kV
spot
3.0
WD
12.0 mm
mag
40 000 x
3 µm
JUST Nano Institute

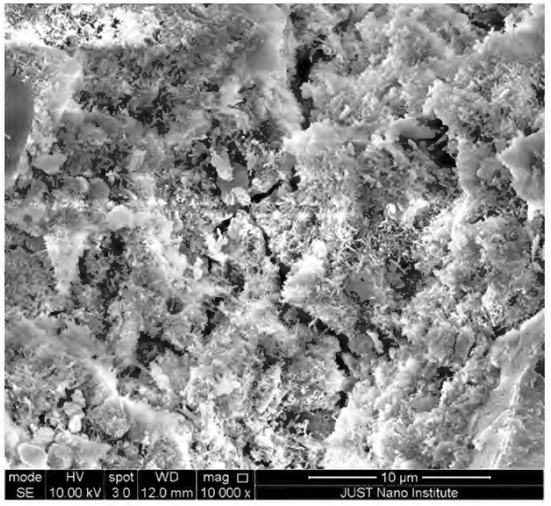
mode HV spot WD mag
SE 10.00 kV 3.0 12.0 mm 10 000 x
10 µm
JUST Nano Institute

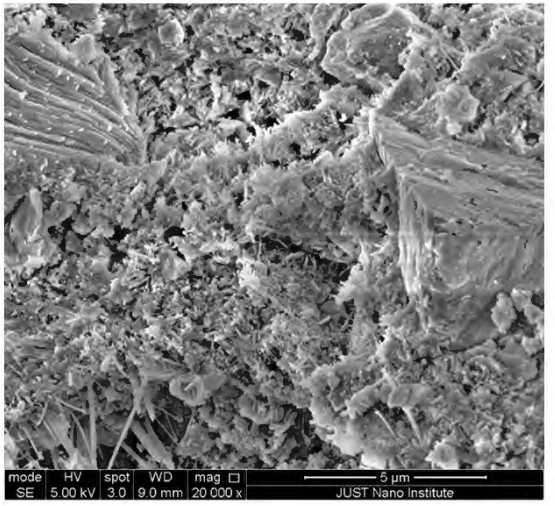
mode HV spot WD mag
SE 5.00 kV 3.0 9.0 mm 20 000 x
5 µm
JUST Nano Institute

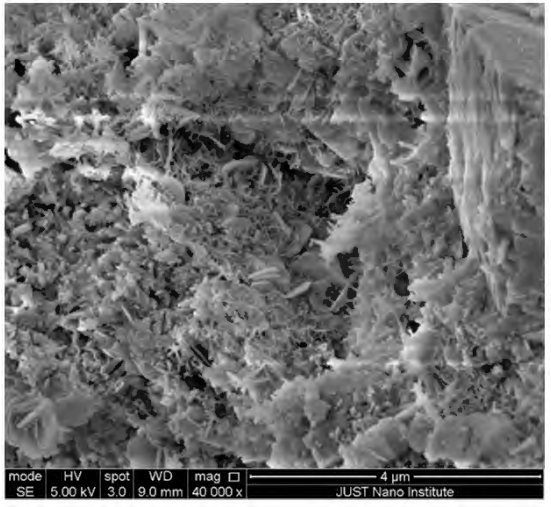
mode HV spot WD mag
SE 5.00 kV 3.0 9.0 mm 40 000 x
4 µm
JUST Nano Institute

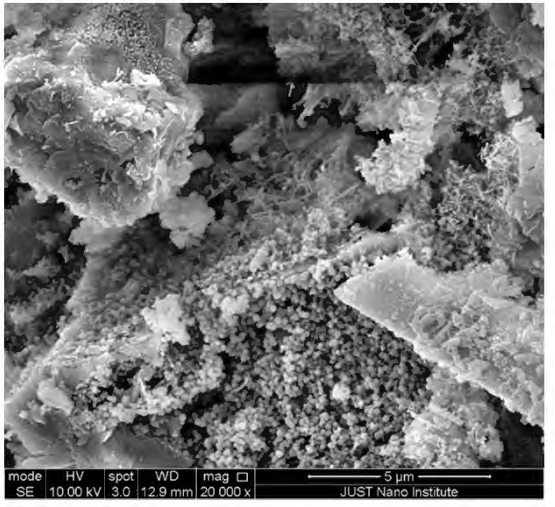
mode HV spot WD mag
SE 10.00 kV 3.0 12.9 mm 20 000 x
5 µm
JUST Nano Institute

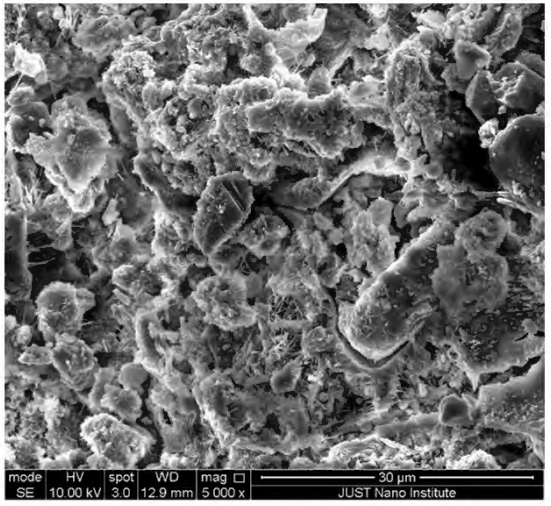
mode
SE
HV
10.00 kV
spot
3.0
WD
12.9 mm
mag
5 000 x
30 µm
JUST Nano Institute

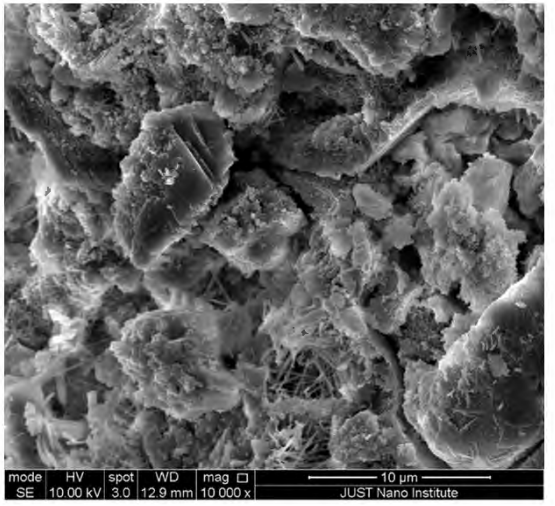
mode
SE
HV
10.00 kV
spot
3.0
WD
12.9 mm
mag
10 000 x
10 µm
JUST Nano Institute

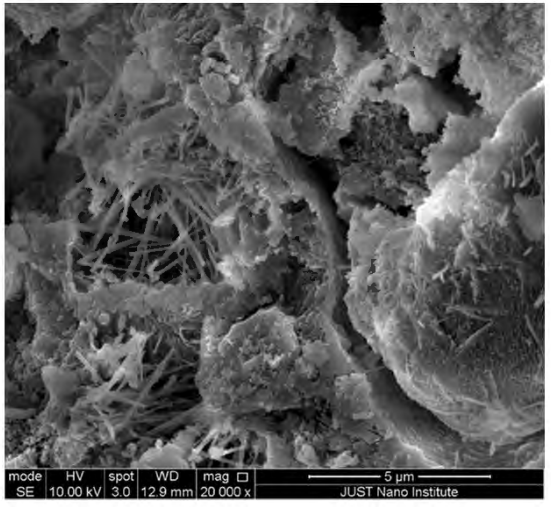
mode
SE
HV
10.00 kV
spot
3.0
WD
12.9 mm
mag
20 000 x
5 µm
JUST Nano Institute

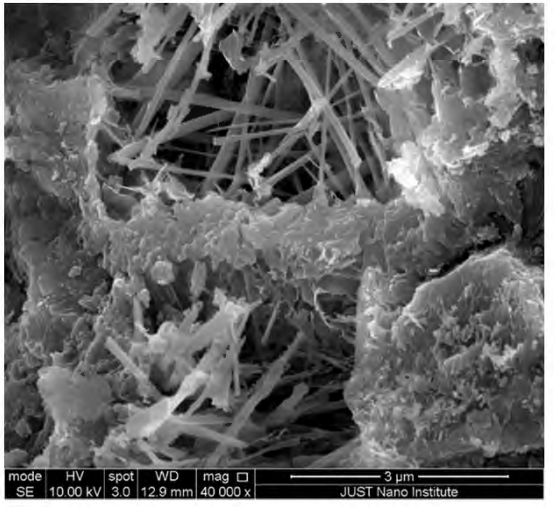
mode
SE
HV
10.00 kV
spot
3.0
WD
12.9 mm
mag
40 000 x
3 µm
JUST Nano Institute

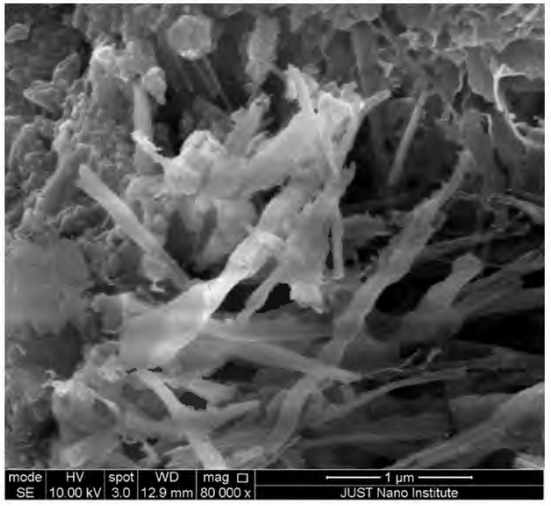
mode HV spot WD mag
SE 10.00 kV 3.0 12.9 mm 80 000 x
1 µm
JUST Nano Institute

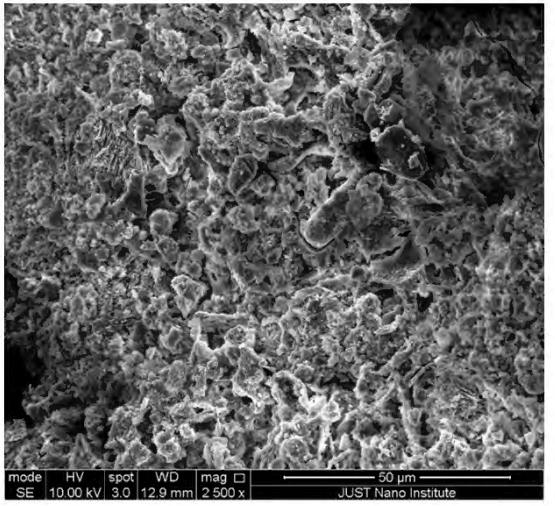
mode HV spot WD mag
SE 10.00 kV 3.0 12.9 mm 2 500 x
50 µm
JUST Nano Institute

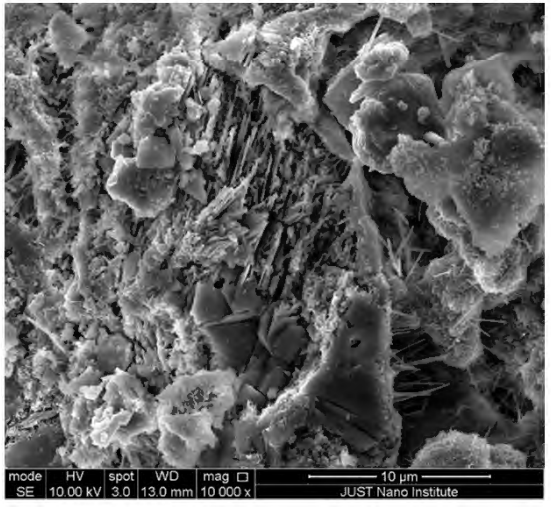
mode HV spot WD mag
SE 10.00 kV 3.0 13.0 mm 10 000 x
10 µm
JUST Nano Institute

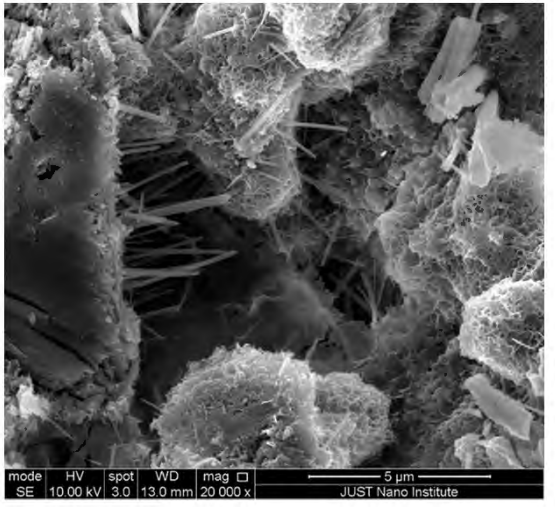
mode HV spot WD mag
SE 10.00 kV 3.0 13.0 mm 20 000 x
5 µm
JUST Nano Institute

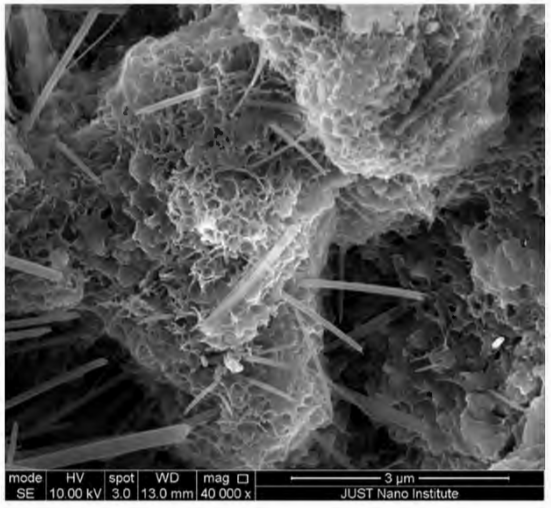
mode SE
HV 10.00 kV
spot 3.0
WD 13.0 mm
mag 40 000 x
3 µm
JUST Nano Institute

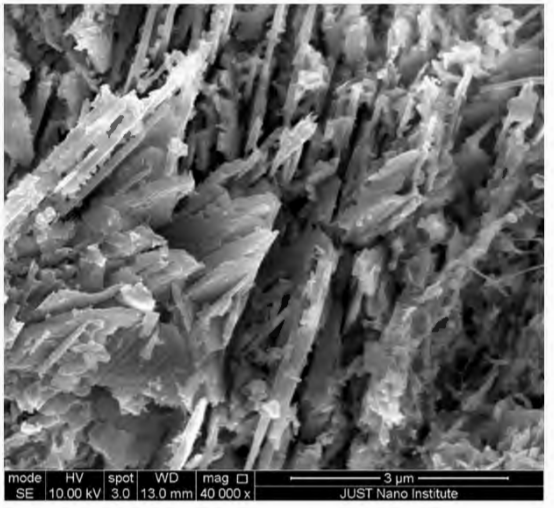
mode SE
HV 10.00 kV
spot 3.0
WD 13.0 mm
mag 40 000 x
3 µm
JUST Nano Institute

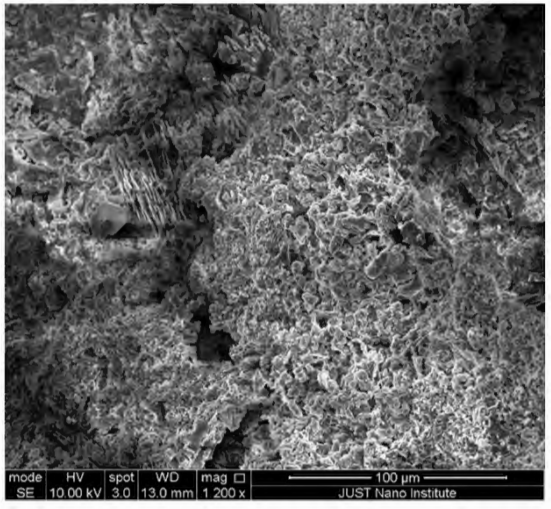
mode SE
HV 10.00 kV
spot 3.0
WD 13.0 mm
mag 1 200 x
100 µm
JUST Nano Institute

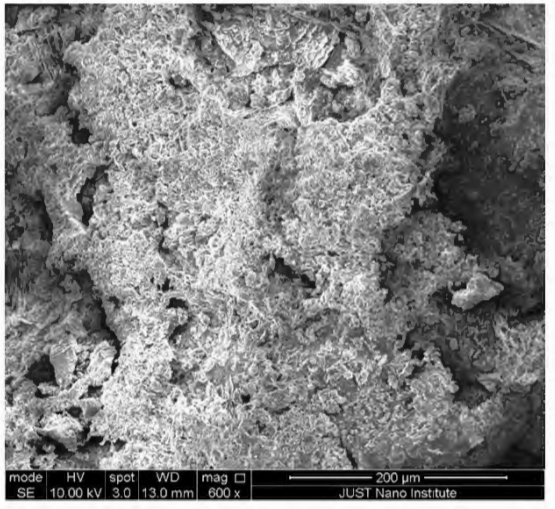
mode SE
HV 10.00 kV
spot 3.0
WD 13.0 mm
mag 600 x
200 µm
JUST Nano Institute

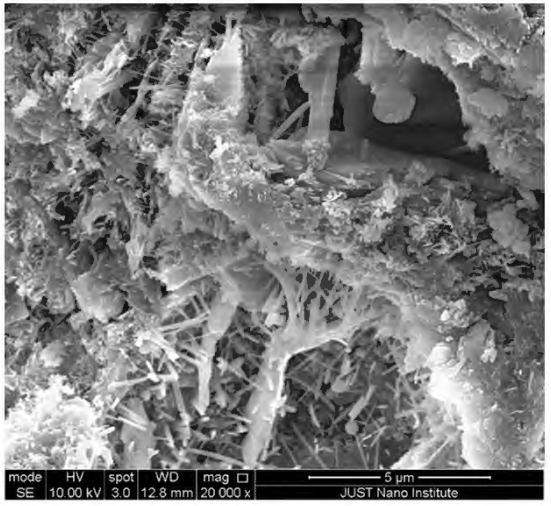
mode HV spot WD mag 5 µm
SE 10.00 kV 3.0 12.8 mm 20 000 x JUST Nano Institute

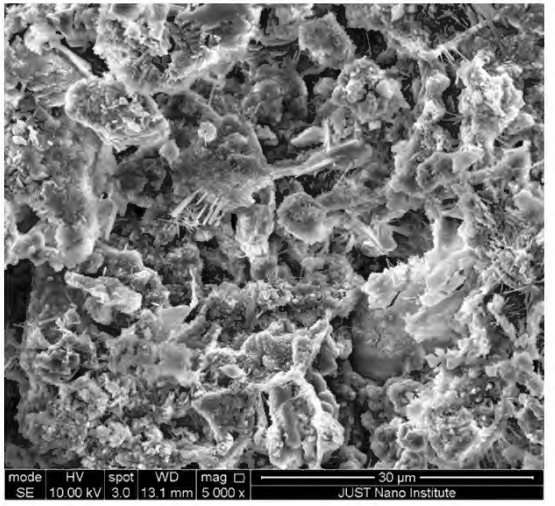
mode HV spot WD mag 30 µm
SE 10.00 kV 3.0 13.1 mm 5 000 x JUST Nano Institute

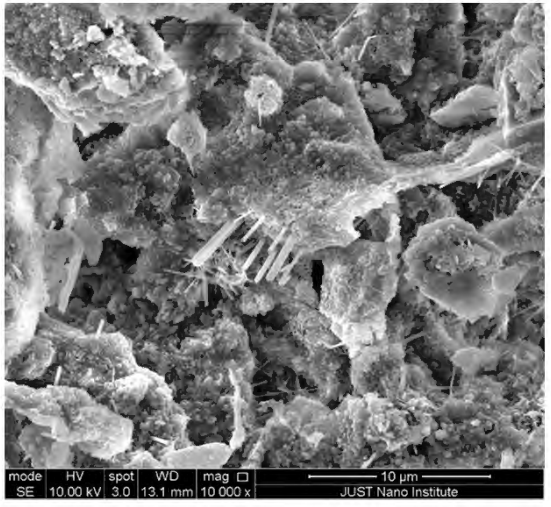
mode HV spot WD mag 10 µm
SE 10.00 kV 3.0 13.1 mm 10 000 x JUST Nano Institute

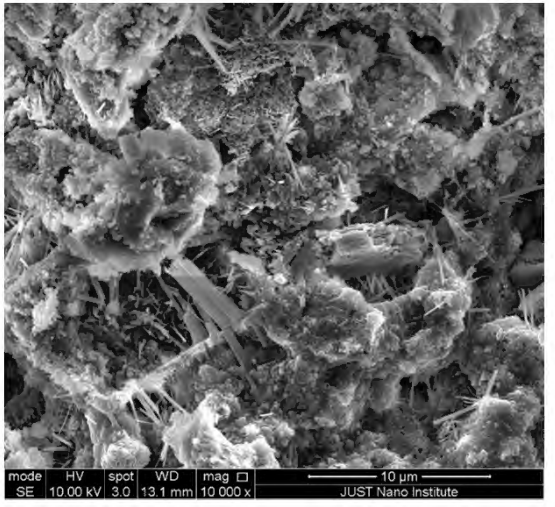
mode HV spot WD mag 10 µm
SE 10.00 kV 3.0 13.1 mm 10 000 x JUST Nano Institute

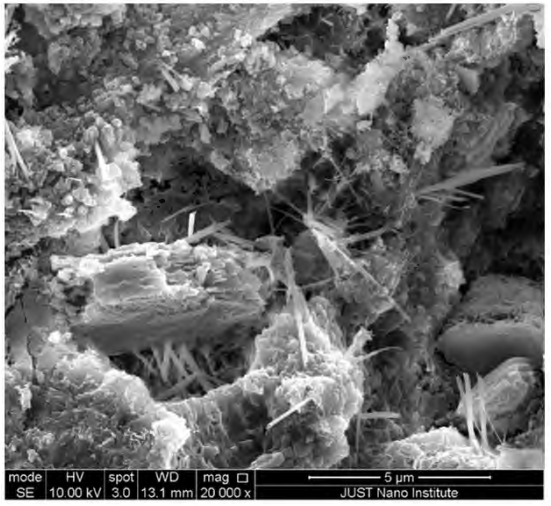
mode HV spot WD mag
SE 10.00 kV 3.0 13.1 mm 20 000 x
5 µm
JUST Nano Institute

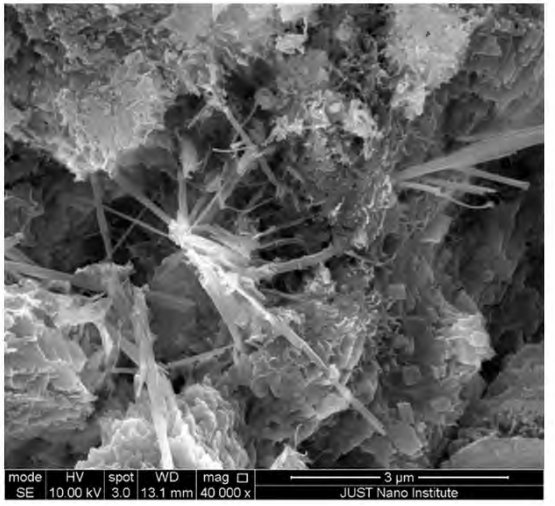
mode HV spot WD mag
SE 10.00 kV 3.0 13.1 mm 40 000 x
3 µm
JUST Nano Institute

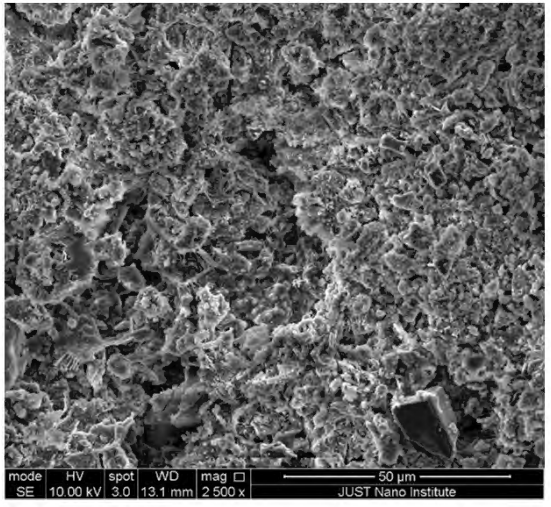
mode HV spot WD mag
SE 10.00 kV 3.0 13.1 mm 2 500 x
50 µm
JUST Nano Institute

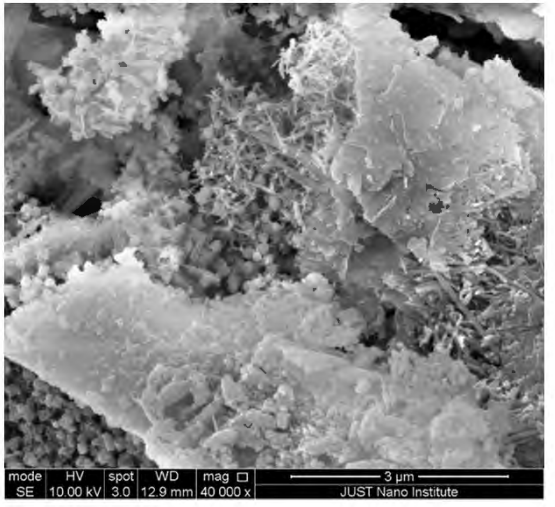
mode HV spot WD mag
SE 10.00 kV 3.0 12.9 mm 40 000 x
3 µm
JUST Nano Institute

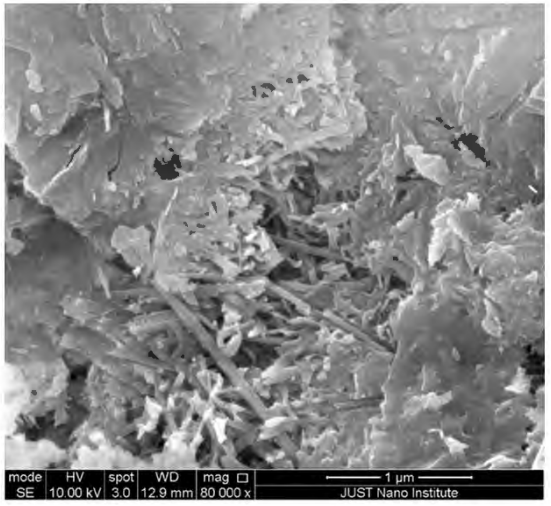
mode HV spot WD mag
SE 10.00 kV 3.0 12.9 mm 80 000 x
1 µm
JUST Nano Institute

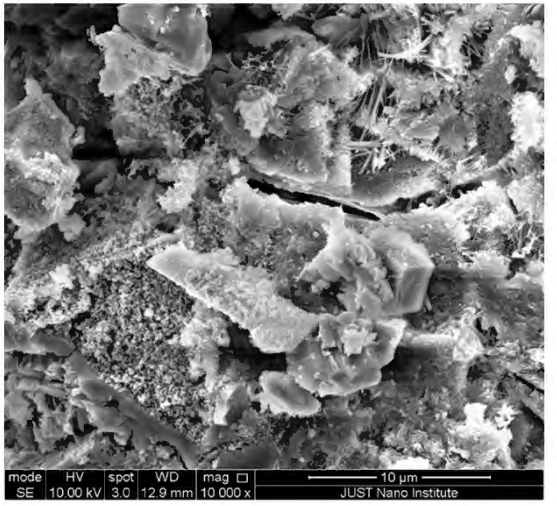
mode HV spot WD mag
SE 10.00 kV 3.0 12.9 mm 10 000 x
10 µm
JUST Nano Institute

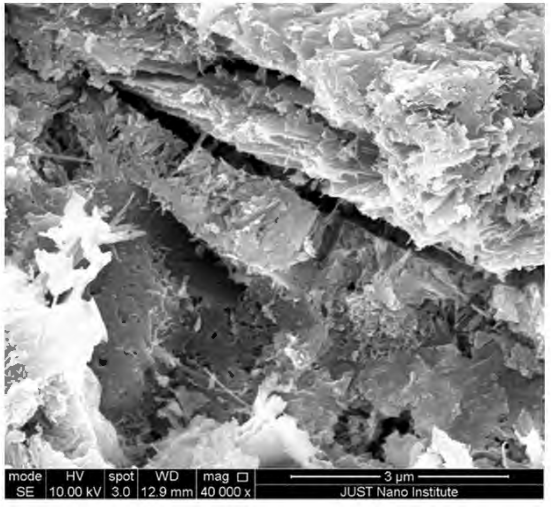
mode HV spot WD mag
SE 10.00 kV 3.0 12.9 mm 40 000 x
3 µm
JUST Nano Institute

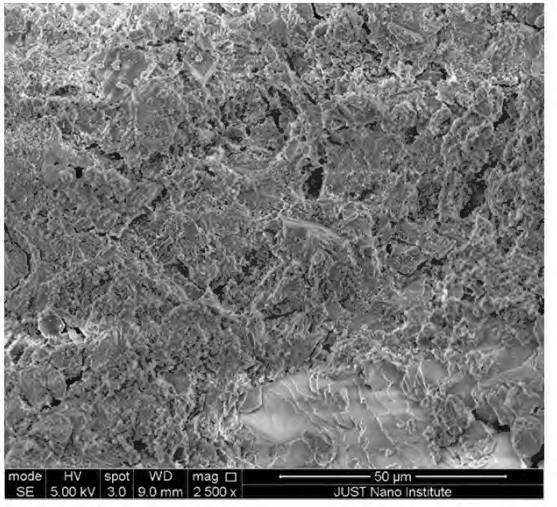
mode HV spot WD mag
SE 5.00 kV 3.0 9.0 mm 2 500 x
50 µm
JUST Nano Institute

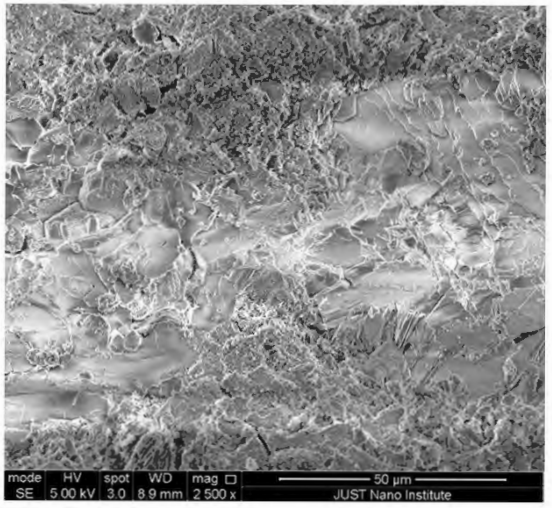
mode HV spot WD mag
SE 5.00 kV 3.0 8.9 mm 2 500 x
50 µm
JUST Nano Institute

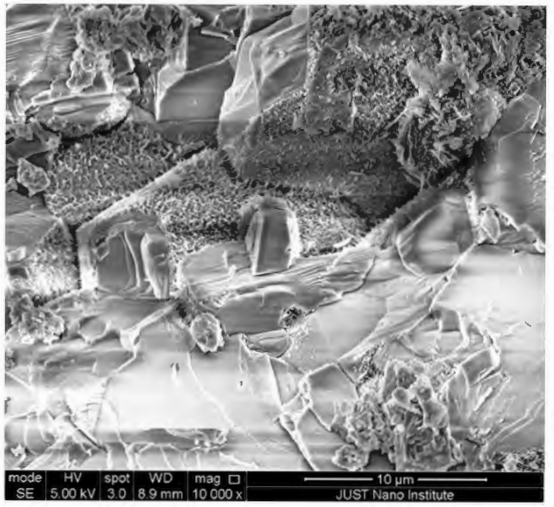
mode HV spot WD mag
SE 5.00 kV 3.0 8.9 mm 10 000 x
10 µm
JUST Nano Institute

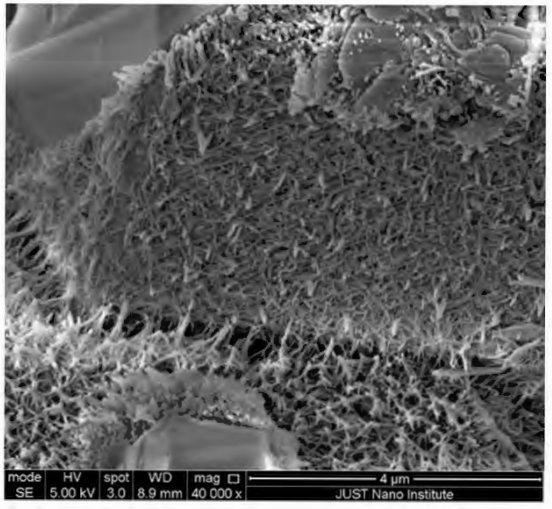
mode HV spot WD mag
SE 5.00 kV 3.0 8.9 mm 40 000 x
4 µm
JUST Nano Institute

Sample No. R

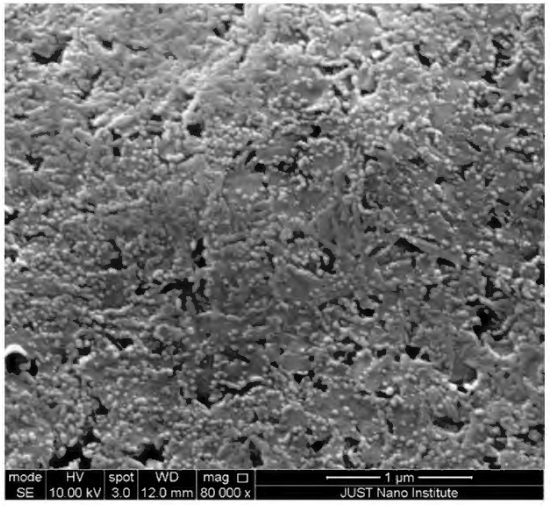
mode SE
HV 10.00 kV
spot 3.0
WD 12.0 mm
mag 80 000 x
1 µm
JUST Nano Institute

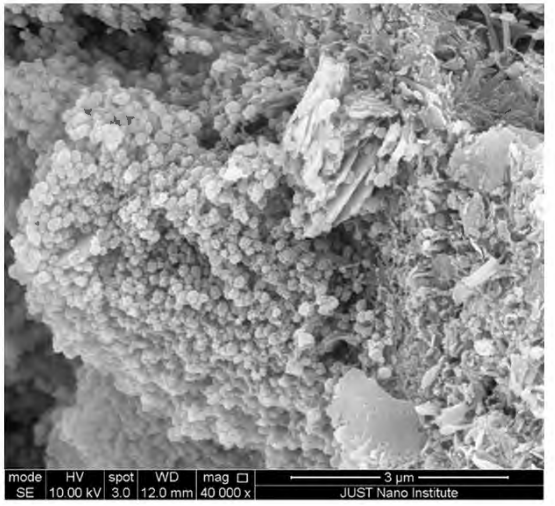
mode SE
HV 10.00 kV
spot 3.0
WD 12.0 mm
mag 40 000 x
3 µm
JUST Nano Institute

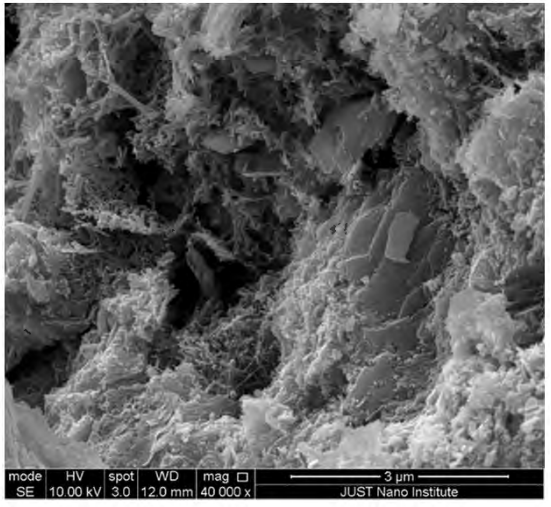
mode SE
HV 10.00 kV
spot 3.0
WD 12.0 mm
mag 40 000 x
3 µm
JUST Nano Institute

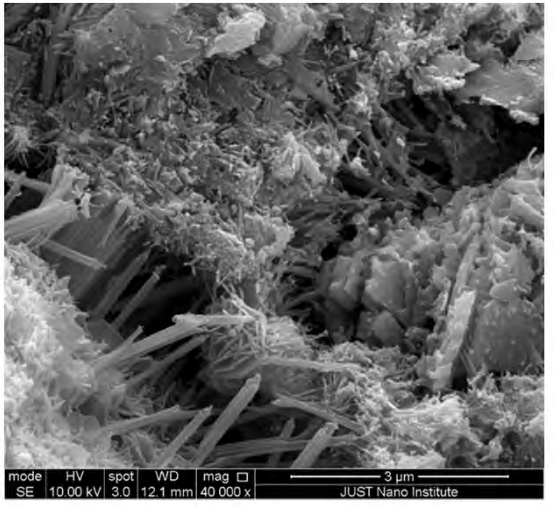
mode SE
HV 10.00 kV
spot 3.0
WD 12.1 mm
mag 40 000 x
3 µm
JUST Nano Institute

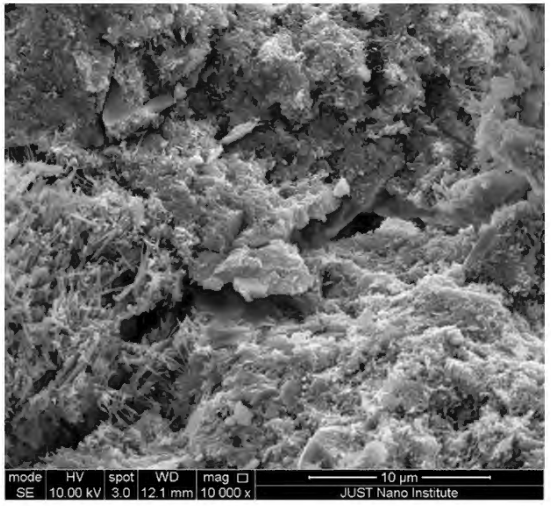
mode HV spot WD mag
SE 10.00 kV 3.0 12.1 mm 10 000 x
10 µm
JUST Nano Institute

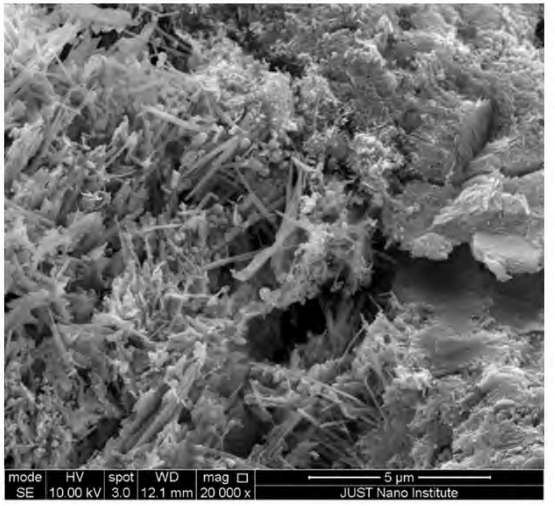
mode HV spot WD mag
SE 10.00 kV 3.0 12.1 mm 20 000 x
5 µm
JUST Nano Institute

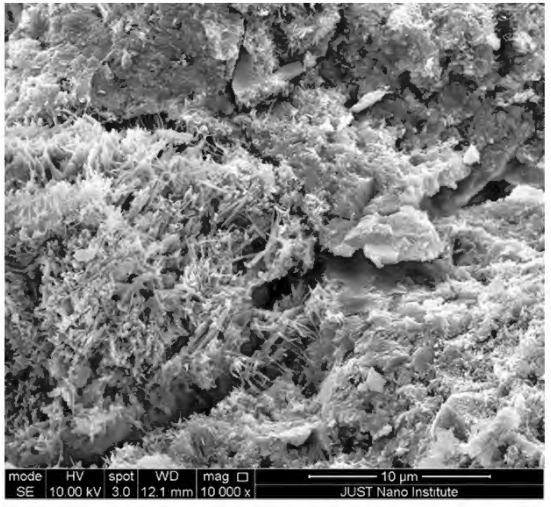
mode HV spot WD mag
SE 10.00 kV 3.0 12.1 mm 10 000 x
10 µm
JUST Nano Institute

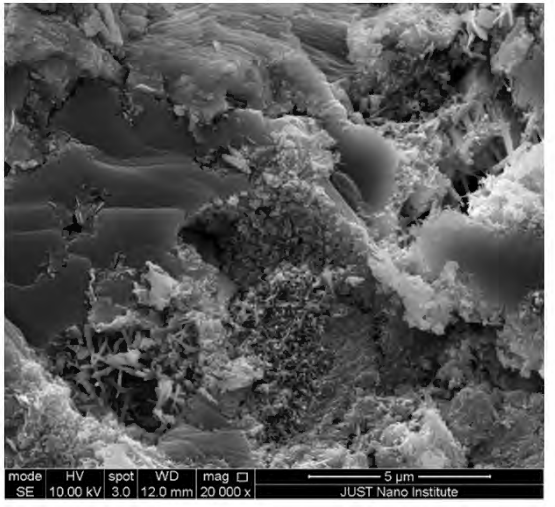
mode HV spot WD mag
SE 10.00 kV 3.0 12.0 mm 20 000 x
5 µm
JUST Nano Institute

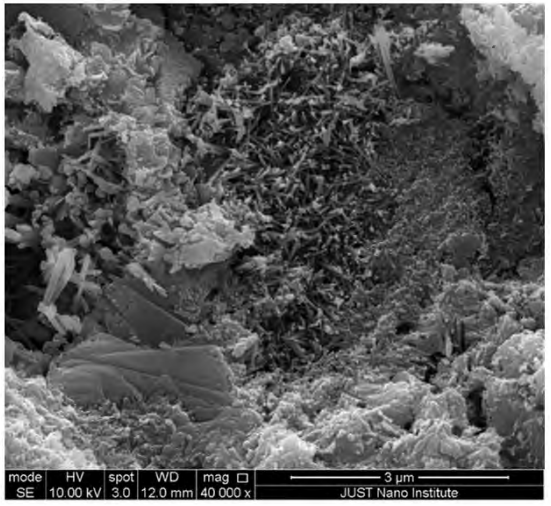
mode
SE
HV
10.00 kV
spot
3.0
WD
12.0 mm
mag
40 000 x
3 µm
JUST Nano Institute

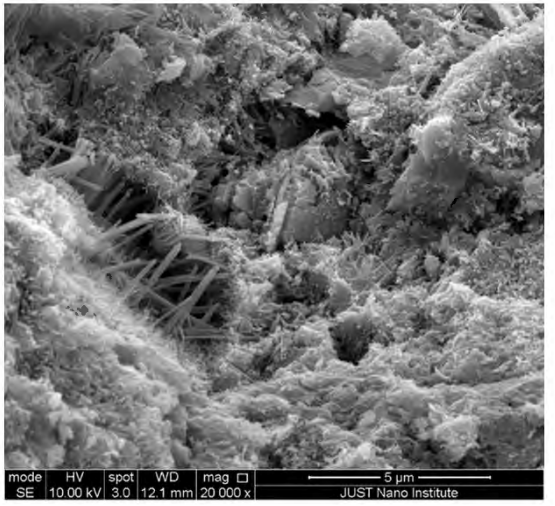
mode
SE
HV
10.00 kV
spot
3.0
WD
12.1 mm
mag
20 000 x
5 µm
JUST Nano Institute

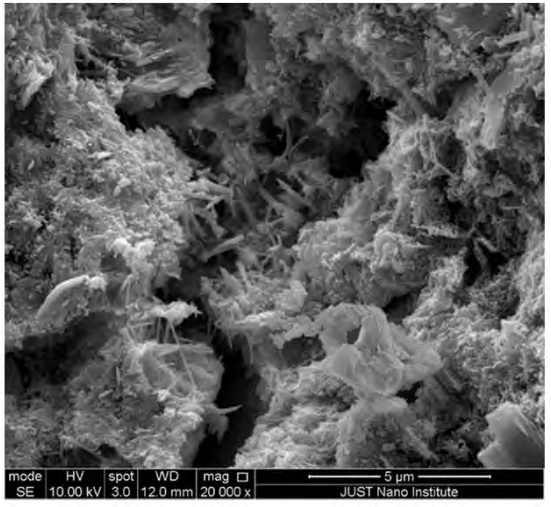
mode
SE
HV
10.00 kV
spot
3.0
WD
12.0 mm
mag
20 000 x
5 µm
JUST Nano Institute

mode
SE
HV
10.00 kV
spot
3.0
WD
12.0 mm
mag
20 000 x
5 µm
JUST Nano Institute

mode HV spot WD mag 10 µm
SE 10.00 kV 3.0 12.0 mm 10 000 x
JUST Nano Institute

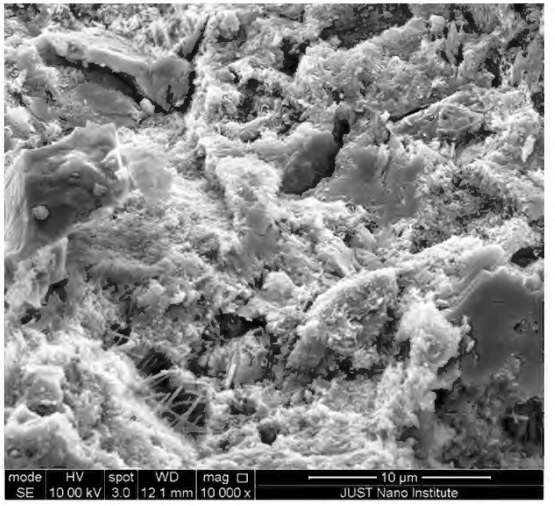
mode HV spot WD mag 10 µm
SE 10.00 kV 3.0 12.1 mm 10 000 x
JUST Nano Institute

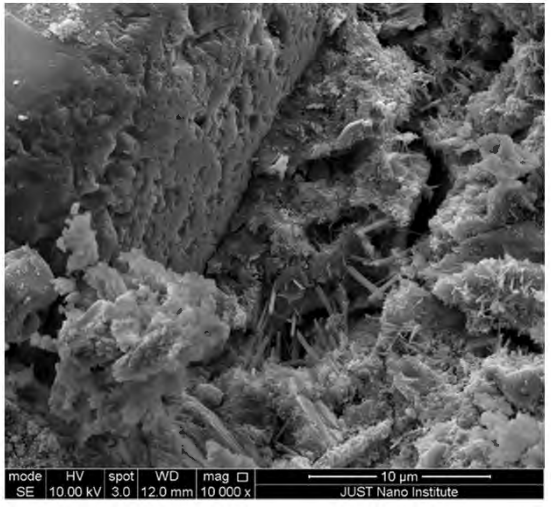
mode HV spot WD mag 10 µm
SE 10.00 kV 3.0 12.0 mm 10 000 x
JUST Nano Institute

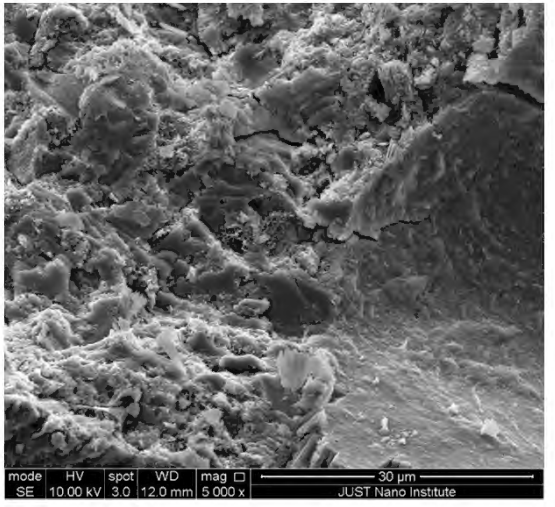
mode HV spot WD mag 30 µm
SE 10.00 kV 3.0 12.0 mm 5 000 x
JUST Nano Institute

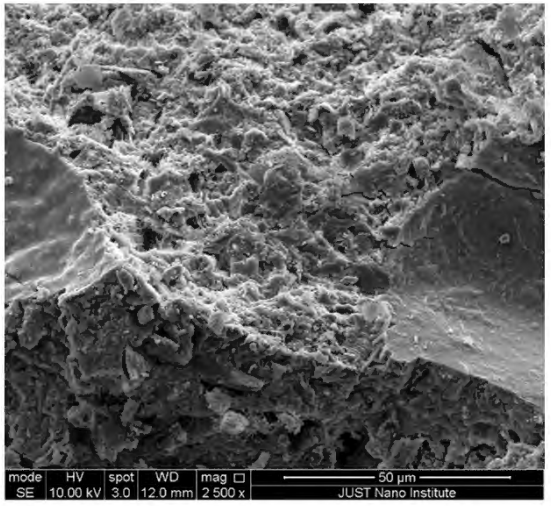
mode SE
HV 10.00 kV
spot 3.0
WD 12.0 mm
mag 2 500 x
50 µm
JUST Nano Institute

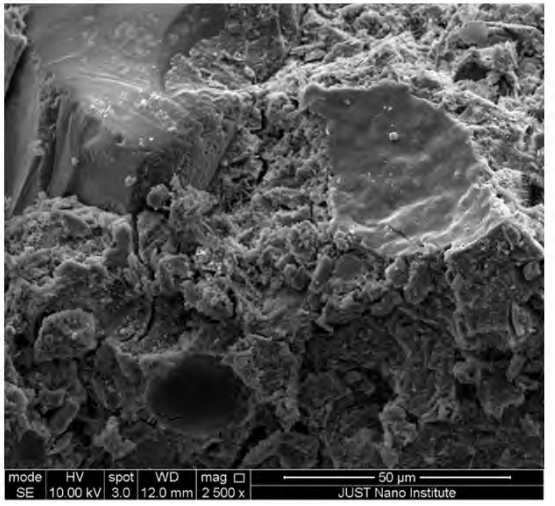
mode SE
HV 10.00 kV
spot 3.0
WD 12.0 mm
mag 2 500 x
50 µm
JUST Nano Institute

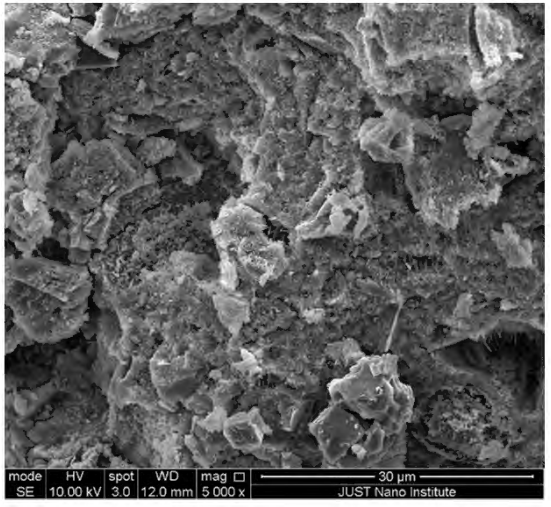
mode SE
HV 10.00 kV
spot 3.0
WD 12.0 mm
mag 5 000 x
30 µm
JUST Nano Institute

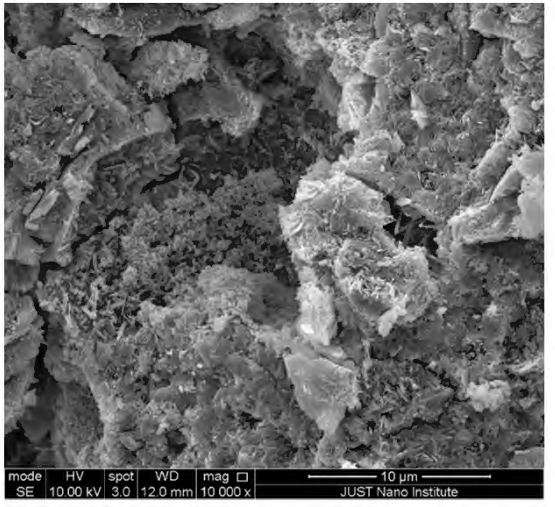
mode SE
HV 10.00 kV
spot 3.0
WD 12.0 mm
mag 10 000 x
10 µm
JUST Nano Institute

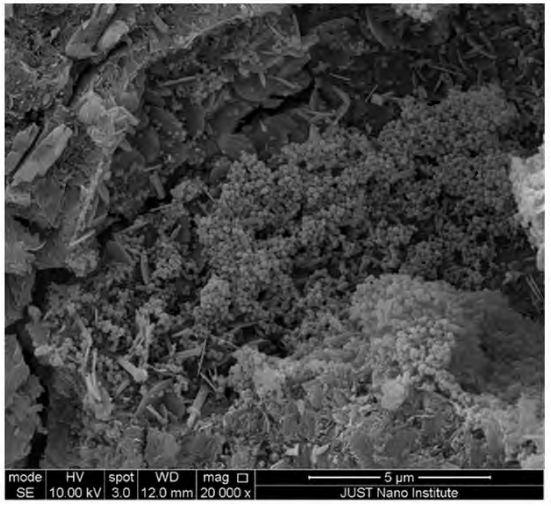
mode
SE
HV
10.00 kV
spot
3.0
WD
12.0 mm
mag
20 000 x
5 µm
JUST Nano Institute

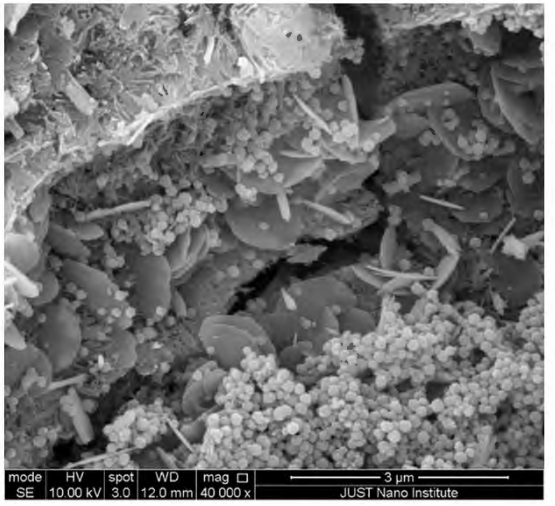
mode
SE
HV
10.00 kV
spot
3.0
WD
12.0 mm
mag
40 000 x
3 µm
JUST Nano Institute

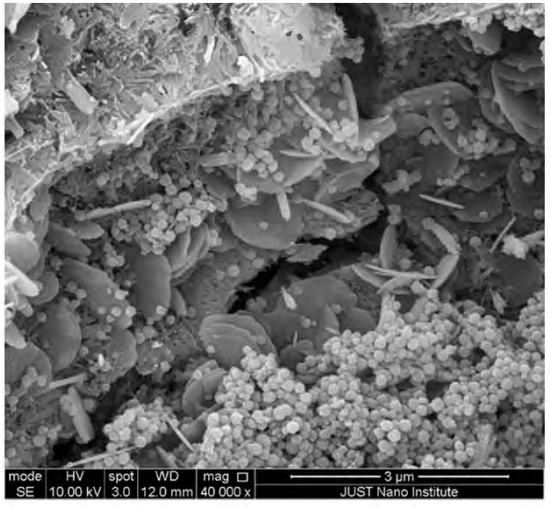
mode
SE
HV
10.00 kV
spot
3.0
WD
12.0 mm
mag
40 000 x
3 µm
JUST Nano Institute

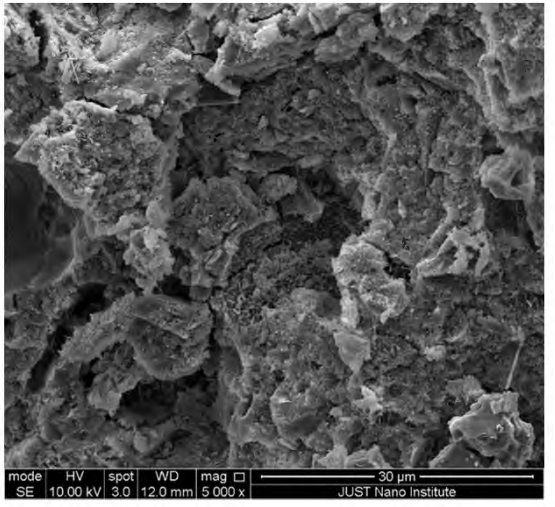
mode
SE
HV
10.00 kV
spot
3.0
WD
12.0 mm
mag
5 000 x
30 µm
JUST Nano Institute

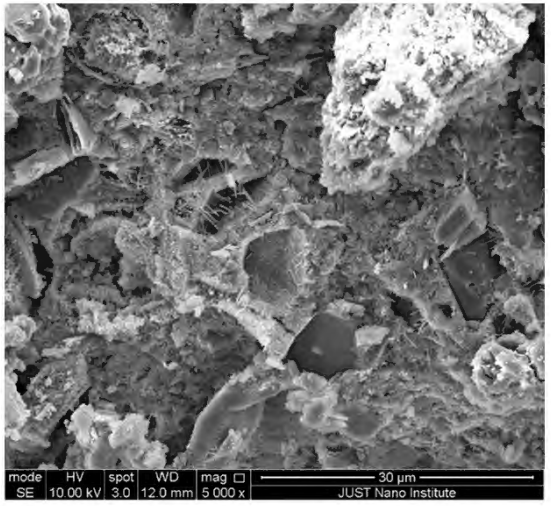
mode
SE
HV
10.00 kV
spot
3.0
WD
12.0 mm
mag
5 000 x
30 µm
JUST Nano Institute

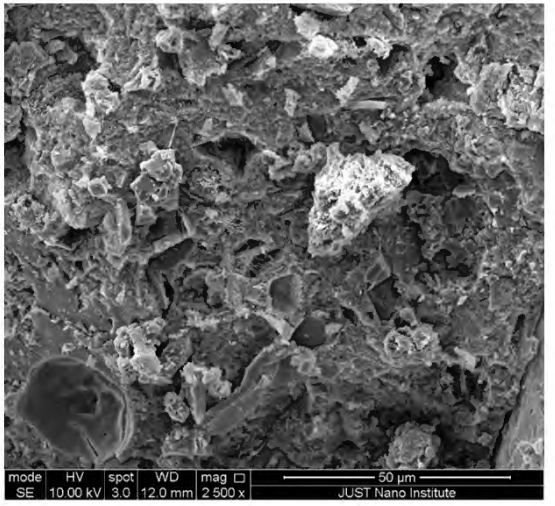
mode
SE
HV
10.00 kV
spot
3.0
WD
12.0 mm
mag
2 500 x
50 µm
JUST Nano Institute

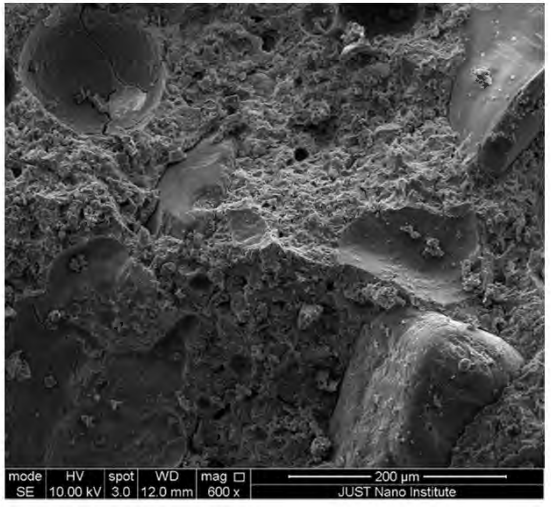
mode
SE
HV
10.00 kV
spot
3.0
WD
12.0 mm
mag
600 x
200 µm
JUST Nano Institute

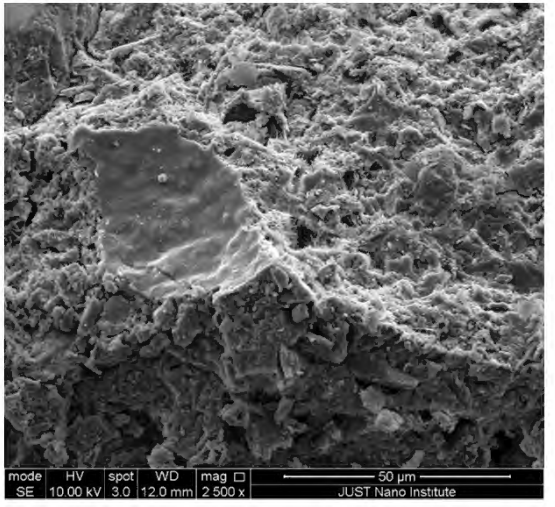
mode
SE
HV
10.00 kV
spot
3.0
WD
12.0 mm
mag
2 500 x
50 µm
JUST Nano Institute

Sample No. U

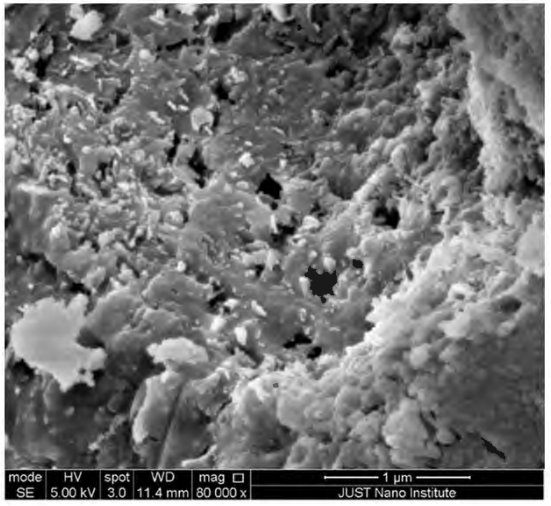
mode HV spot WD mag
SE 5.00 kV 3.0 11.4 mm 80 000 x
1 µm
JUST Nano Institute

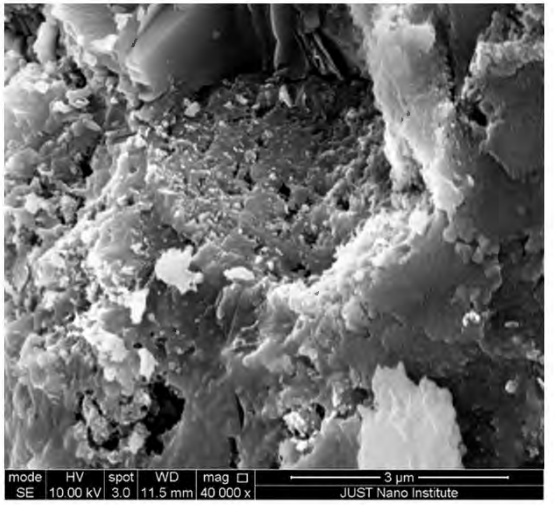
mode HV spot WD mag
SE 10.00 kV 3.0 11.5 mm 40 000 x
3 µm
JUST Nano Institute

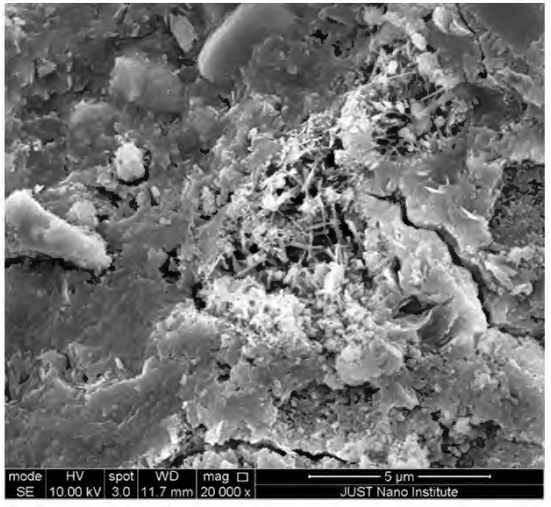
mode HV spot WD mag
SE 10.00 kV 3.0 11.7 mm 20 000 x
5 µm
JUST Nano Institute

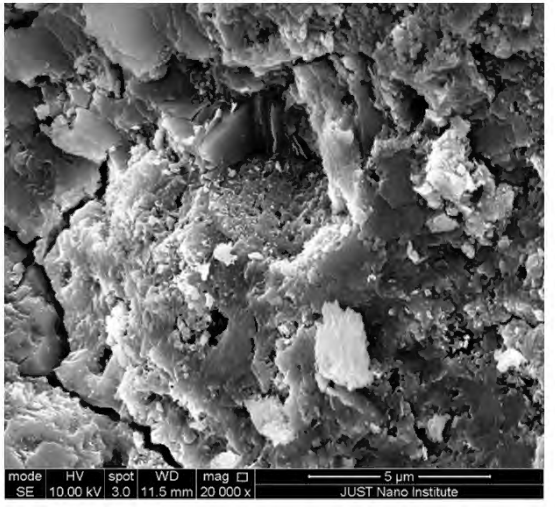
mode HV spot WD mag
SE 10.00 kV 3.0 11.5 mm 20 000 x
5 µm
JUST Nano Institute

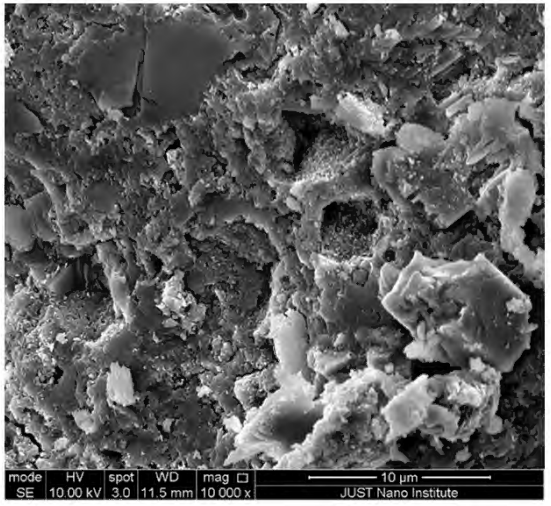
mode HV spot WD mag 10 µm
SE 10.00 kV 3.0 11.5 mm 10 000 x JUST Nano Institute

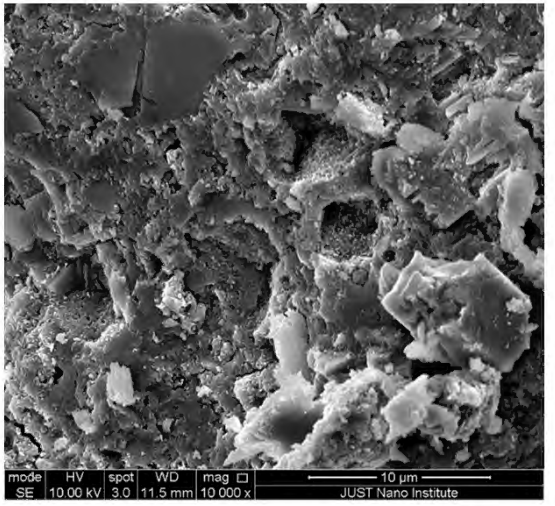
mode HV spot WD mag 10 µm
SE 10.00 kV 3.0 11.5 mm 10 000 x JUST Nano Institute

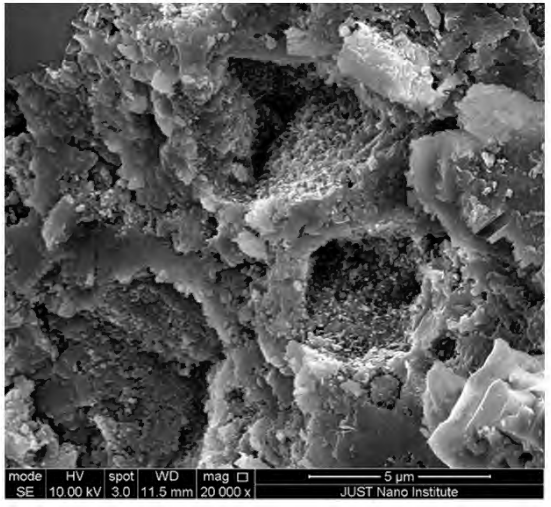
mode HV spot WD mag 5 µm
SE 10.00 kV 3.0 11.5 mm 20 000 x JUST Nano Institute

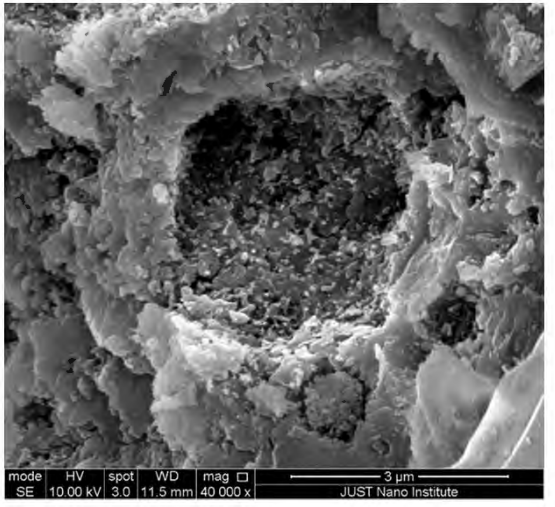
mode HV spot WD mag 3 µm
SE 10.00 kV 3.0 11.5 mm 40 000 x JUST Nano Institute

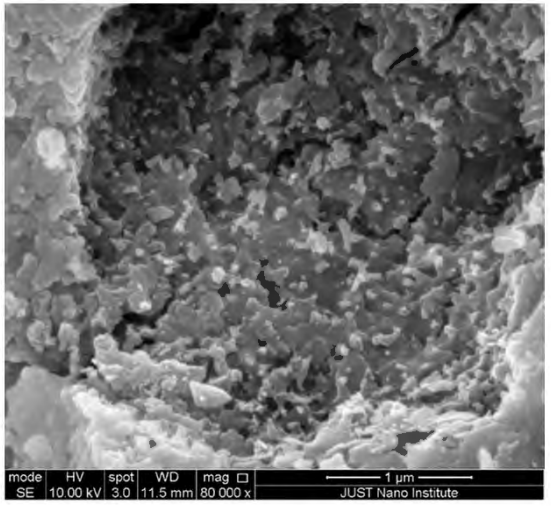
mode
SE
HV
10.00 kV
spot
3.0
WD
11.5 mm
mag
80 000 x
1 µm
JUST Nano Institute

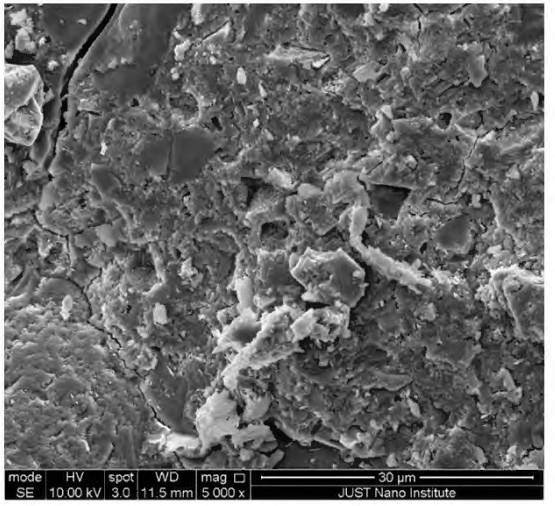
mode
SE
HV
10.00 kV
spot
3.0
WD
11.5 mm
mag
5 000 x
30 µm
JUST Nano Institute

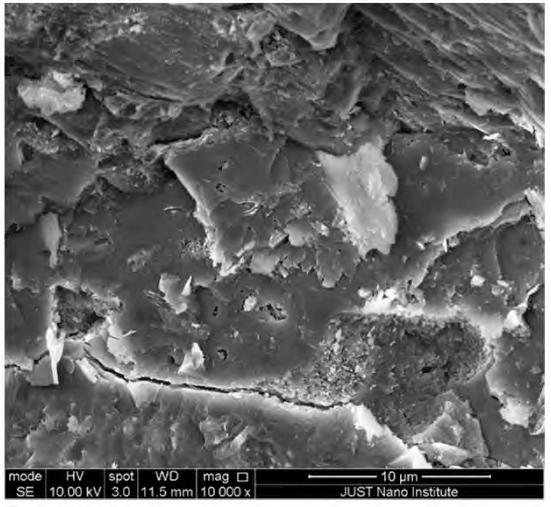
mode
SE
HV
10.00 kV
spot
3.0
WD
11.5 mm
mag
10 000 x
10 µm
JUST Nano Institute

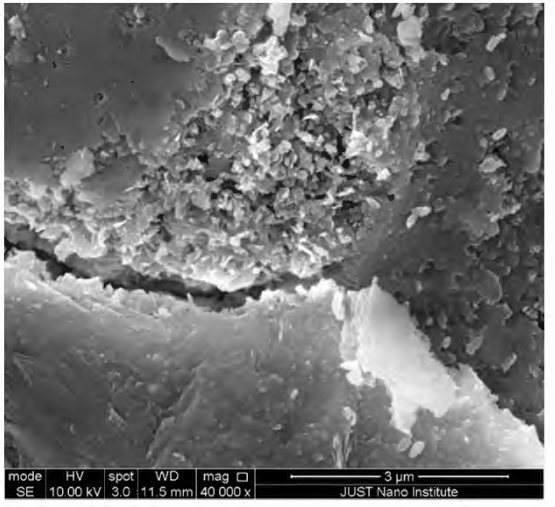
mode
SE
HV
10.00 kV
spot
3.0
WD
11.5 mm
mag
40 000 x
3 µm
JUST Nano Institute

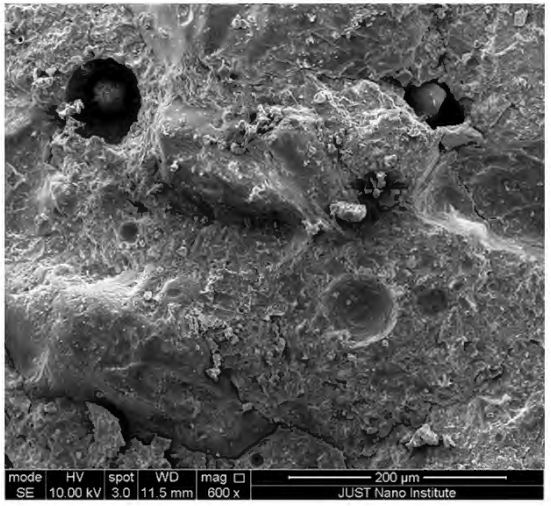
mode
SE
HV
10.00 kV
spot
3.0
WD
11.5 mm
mag
600 x
200 µm
JUST Nano Institute

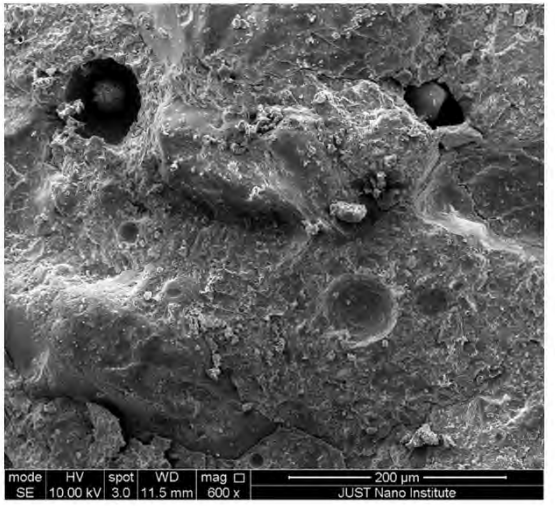
mode
SE
HV
10.00 kV
spot
3.0
WD
11.5 mm
mag
600 x
200 µm
JUST Nano Institute

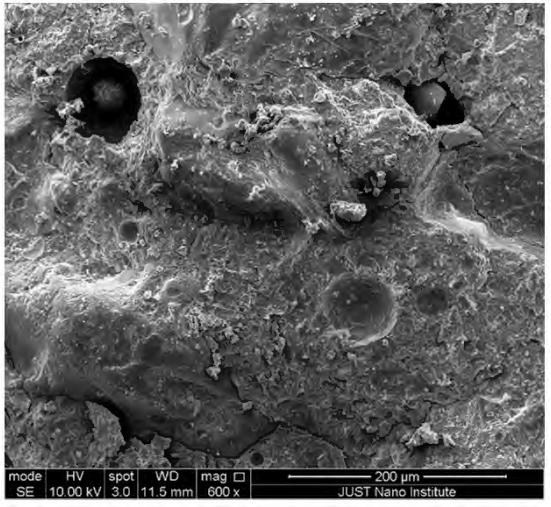
mode
SE
HV
10.00 kV
spot
3.0
WD
11.5 mm
mag
600 x
200 µm
JUST Nano Institute

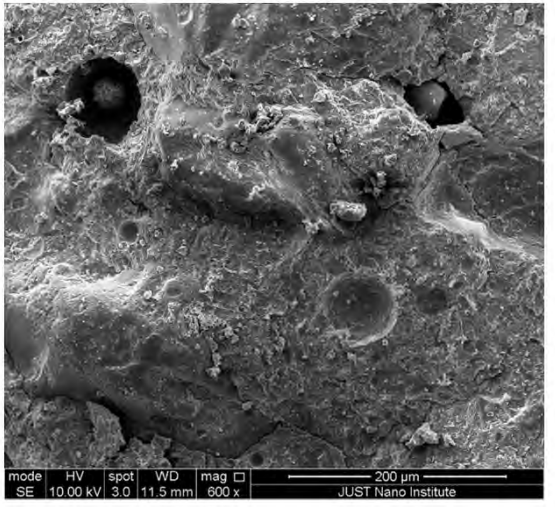
mode
SE
HV
10.00 kV
spot
3.0
WD
11.5 mm
mag
600 x
200 µm
JUST Nano Institute

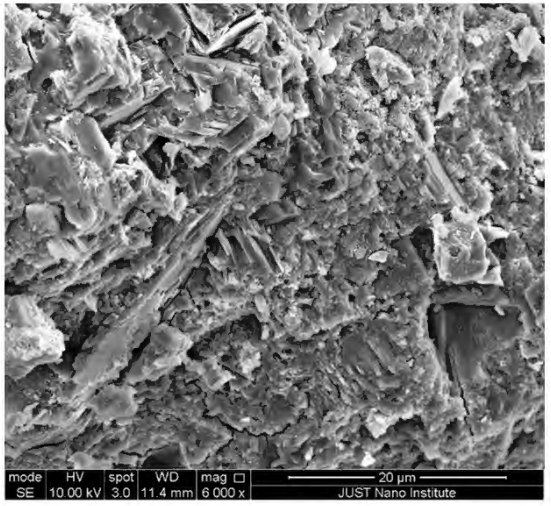
mode HV spot WD mag 20 µm
SE 10.00 kV 3.0 11.4 mm 6 000 x JUST Nano Institute

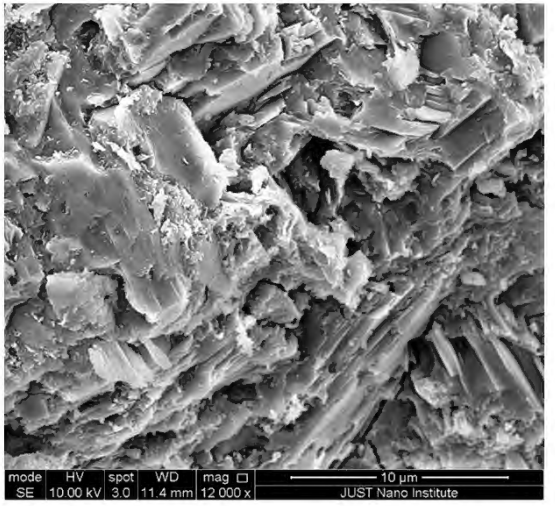
mode HV spot WD mag 10 µm
SE 10.00 kV 3.0 11.4 mm 12 000 x JUST Nano Institute

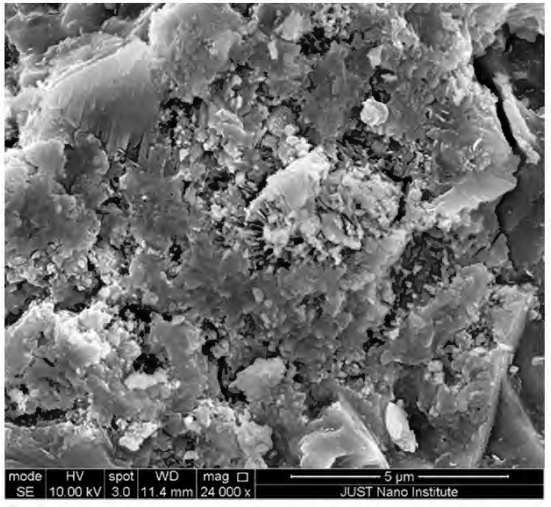
mode HV spot WD mag 5 µm
SE 10.00 kV 3.0 11.4 mm 24 000 x JUST Nano Institute

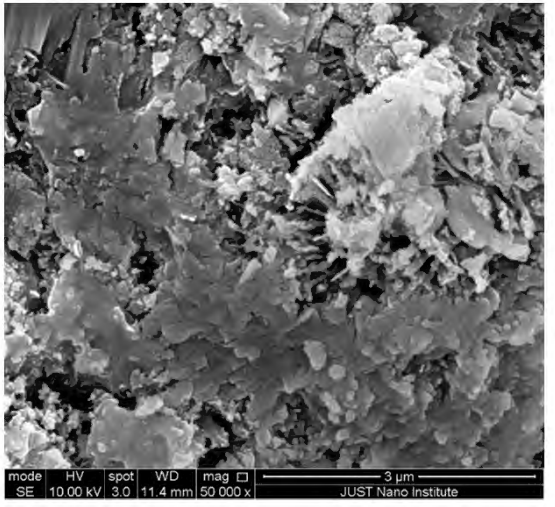
mode HV spot WD mag 3 µm
SE 10.00 kV 3.0 11.4 mm 50 000 x JUST Nano Institute

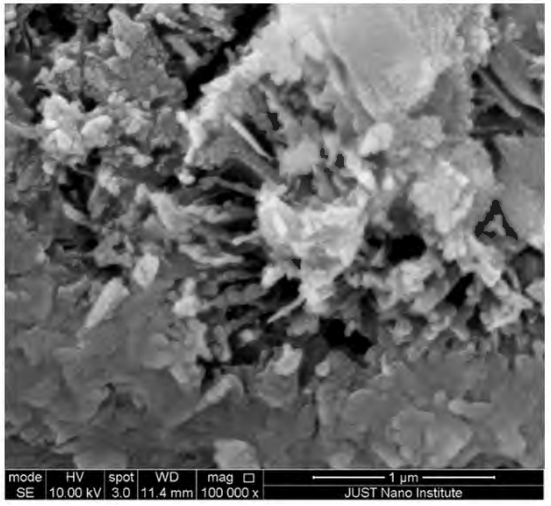
mode HV spot WD mag
SE 10.00 kV 3.0 11.4 mm 100 000 x
1 µm
JUST Nano Institute

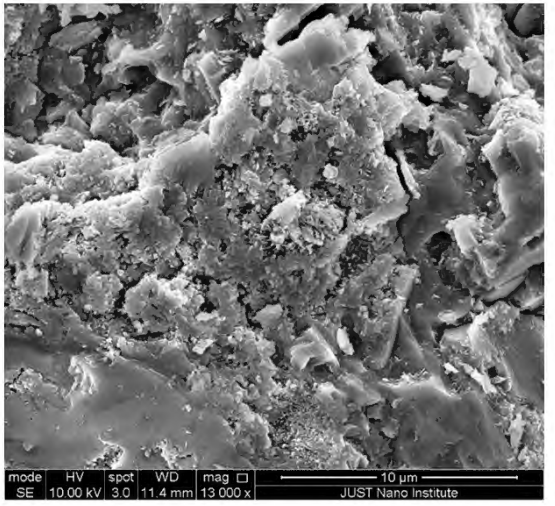
mode HV spot WD mag
SE 10.00 kV 3.0 11.4 mm 13 000 x
10 µm
JUST Nano Institute

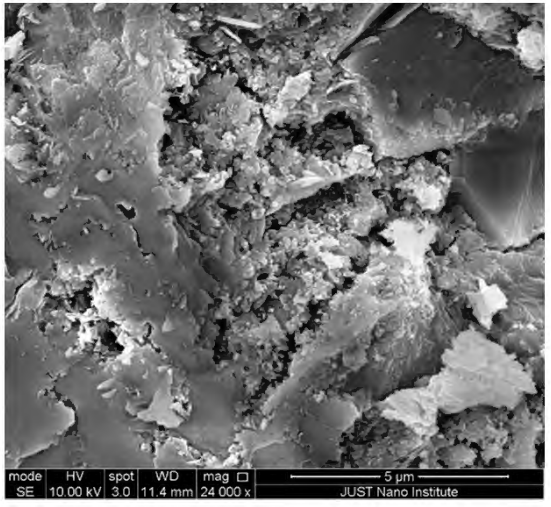
mode HV spot WD mag
SE 10.00 kV 3.0 11.4 mm 24 000 x
5 µm
JUST Nano Institute

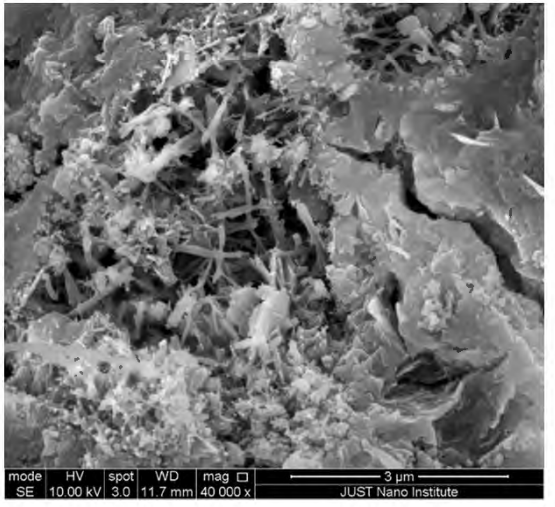
mode HV spot WD mag
SE 10.00 kV 3.0 11.7 mm 40 000 x
3 µm
JUST Nano Institute

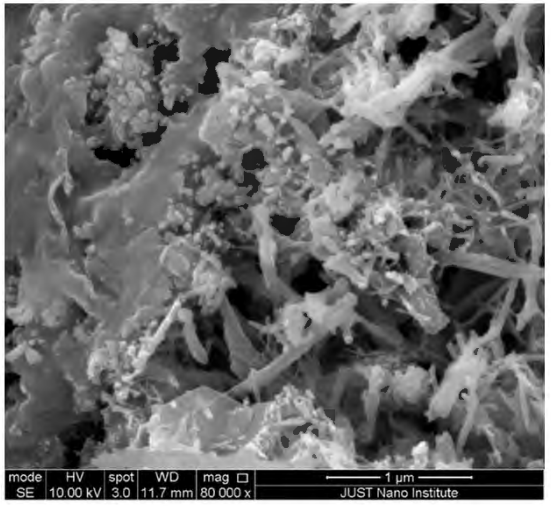
mode HV spot WD mag
SE 10.00 kV 3.0 11.7 mm 80 000 x
1 µm
JUST Nano Institute

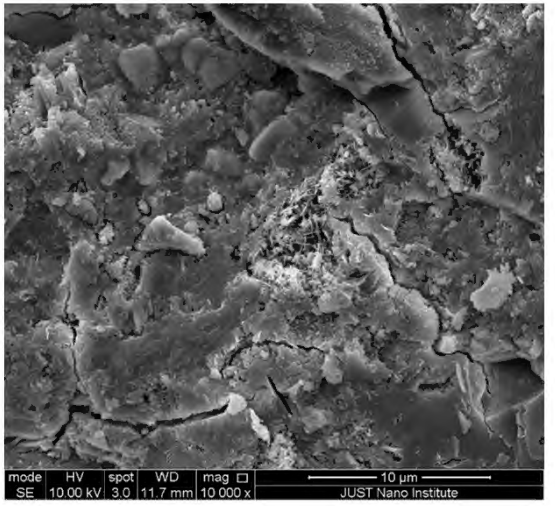
mode HV spot WD mag
SE 10.00 kV 3.0 11.7 mm 10 000 x
10 µm
JUST Nano Institute

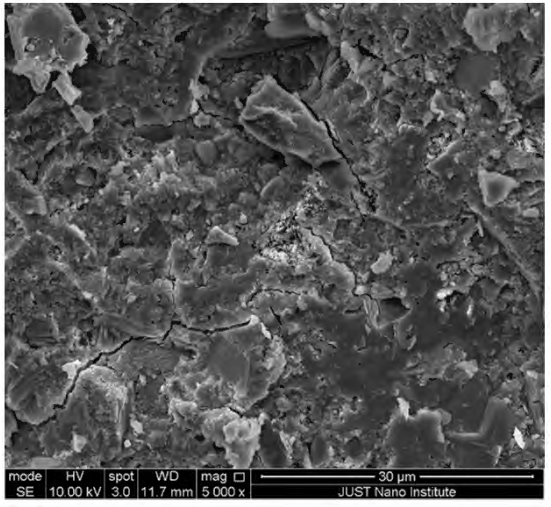
mode HV spot WD mag
SE 10.00 kV 3.0 11.7 mm 5 000 x
30 µm
JUST Nano Institute

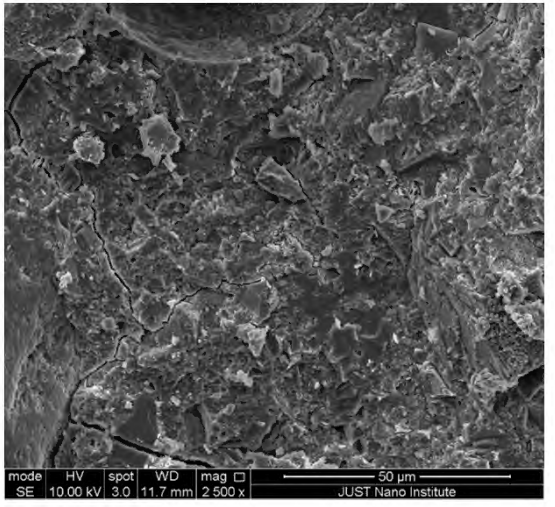
mode HV spot WD mag
SE 10.00 kV 3.0 11.7 mm 2 500 x
50 µm
JUST Nano Institute

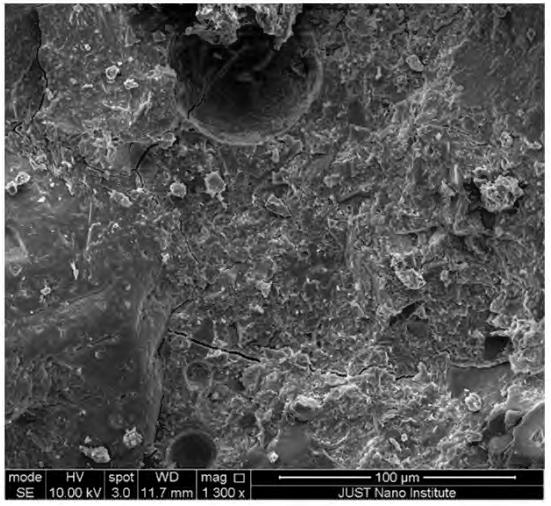
mode HV spot WD mag
SE 10.00 kV 3.0 11.7 mm 1 300 x
100 µm
JUST Nano Institute

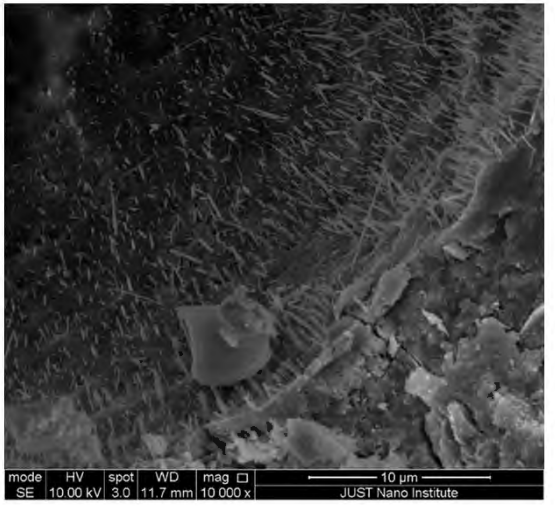
mode HV spot WD mag
SE 10.00 kV 3.0 11.7 mm 10 000 x
10 µm
JUST Nano Institute

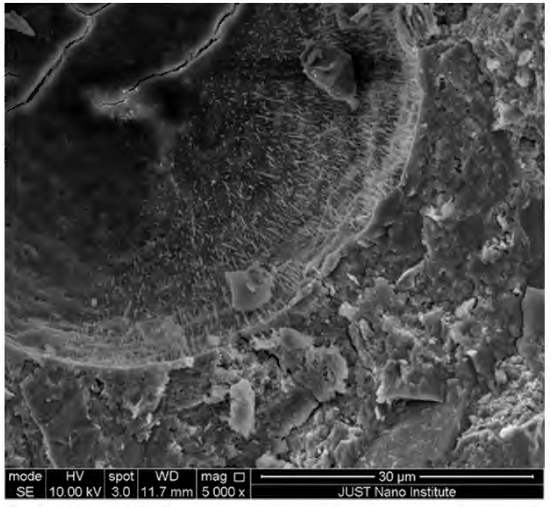
mode HV spot WD mag
SE 10.00 kV 3.0 11.7 mm 5 000 x
30 µm
JUST Nano Institute

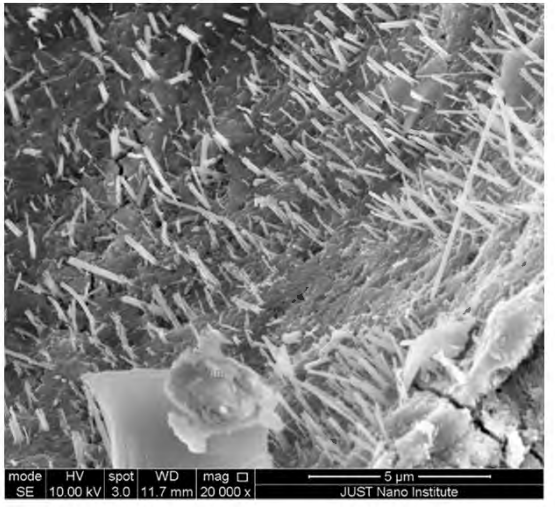
mode HV spot WD mag
SE 10.00 kV 3.0 11.7 mm 20 000 x
5 µm
JUST Nano Institute

Sample No. X

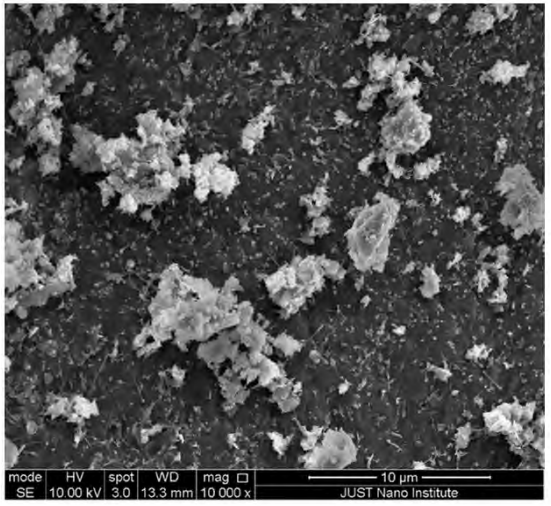
mode SE
HV 10.00 kV
spot 3.0
WD 13.3 mm
mag 10 000 x
10 µm
JUST Nano Institute

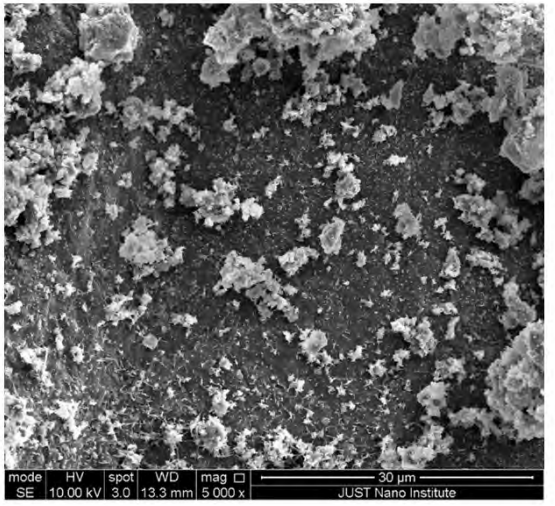
mode SE
HV 10.00 kV
spot 3.0
WD 13.3 mm
mag 5 000 x
30 µm
JUST Nano Institute

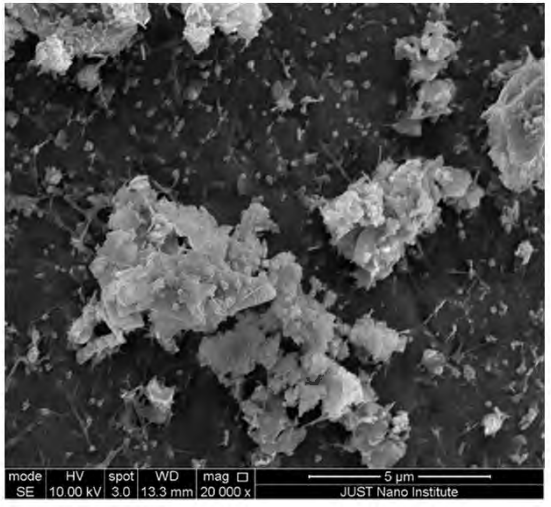
mode SE
HV 10.00 kV
spot 3.0
WD 13.3 mm
mag 20 000 x
5 µm
JUST Nano Institute

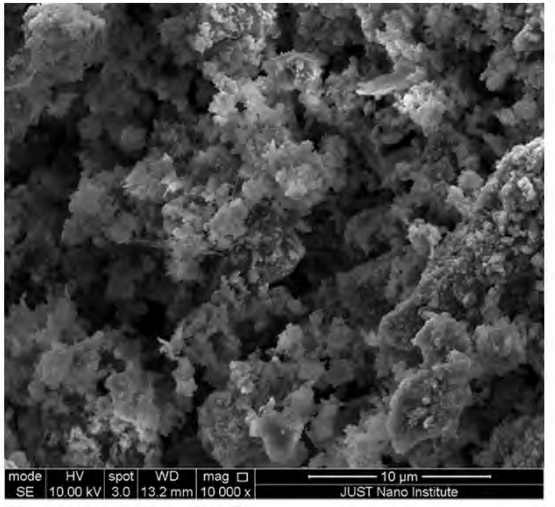
mode SE
HV 10.00 kV
spot 3.0
WD 13.2 mm
mag 10 000 x
10 µm
JUST Nano Institute

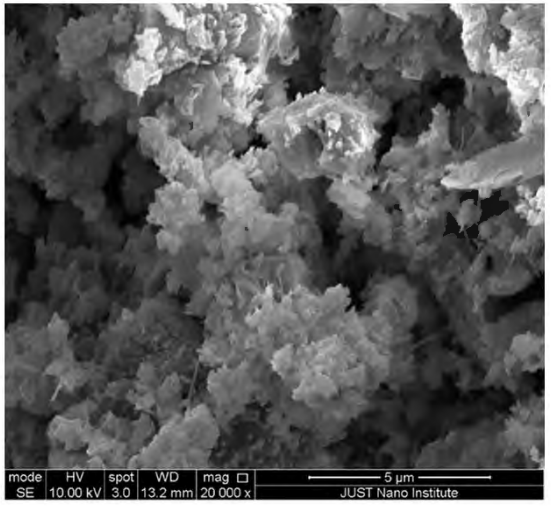
mode
SE
HV
10.00 kV
spot
3.0
WD
13.2 mm
mag
20 000 x
5 µm
JUST Nano Institute

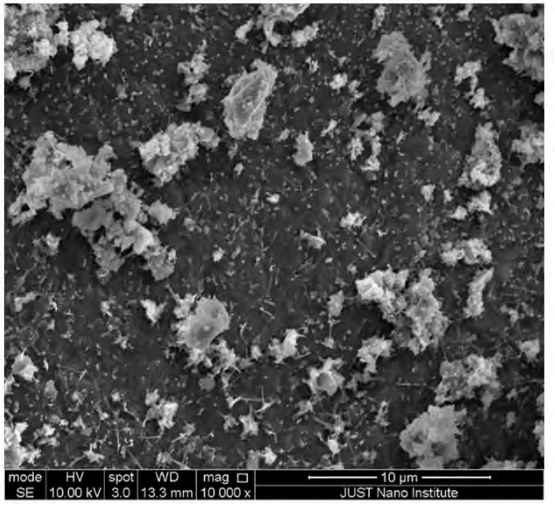
mode
SE
HV
10.00 kV
spot
3.0
WD
13.3 mm
mag
10 000 x
10 µm
JUST Nano Institute

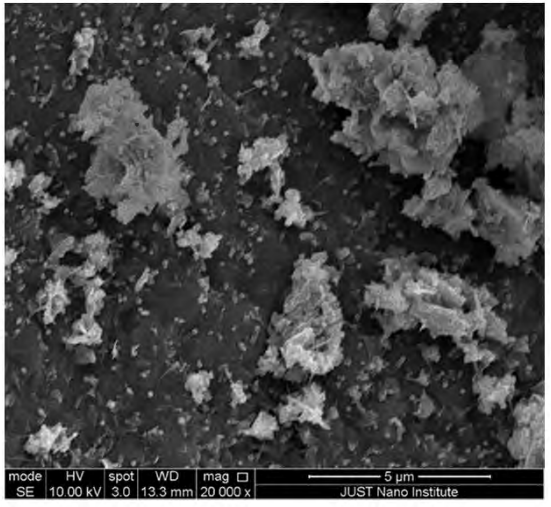
mode
SE
HV
10.00 kV
spot
3.0
WD
13.3 mm
mag
20 000 x
5 µm
JUST Nano Institute

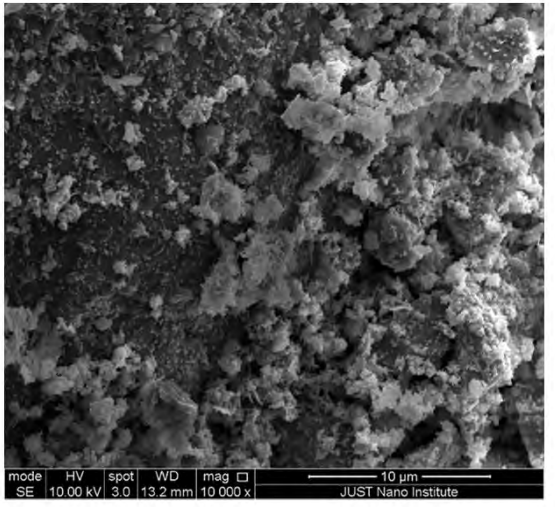
mode
SE
HV
10.00 kV
spot
3.0
WD
13.2 mm
mag
10 000 x
10 µm
JUST Nano Institute

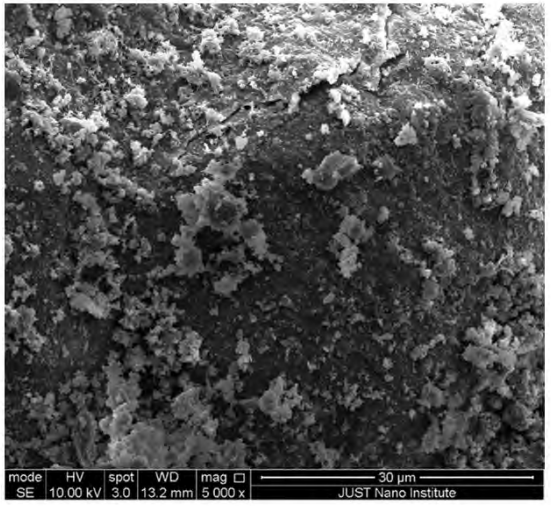
mode SE
HV 10.00 kV
spot 3.0
WD 13.2 mm
mag 5 000 x
30 µm
JUST Nano Institute

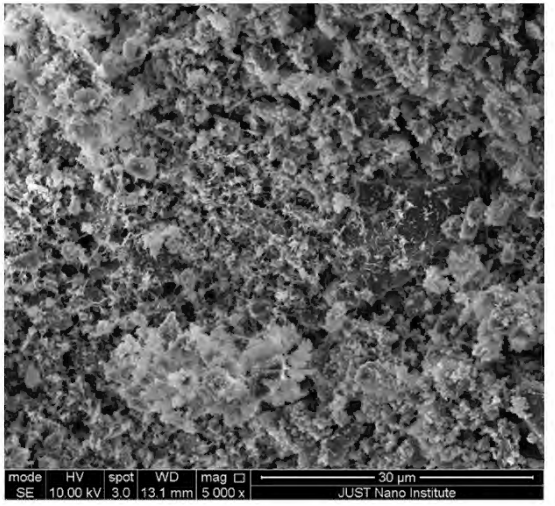
mode SE
HV 10.00 kV
spot 3.0
WD 13.1 mm
mag 5 000 x
30 µm
JUST Nano Institute

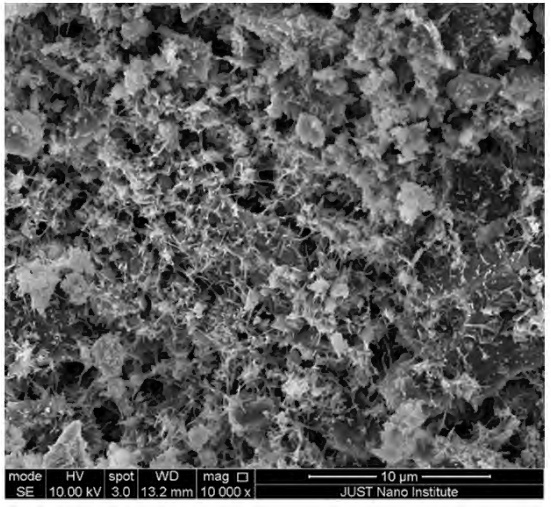
mode SE
HV 10.00 kV
spot 3.0
WD 13.2 mm
mag 10 000 x
10 µm
JUST Nano Institute

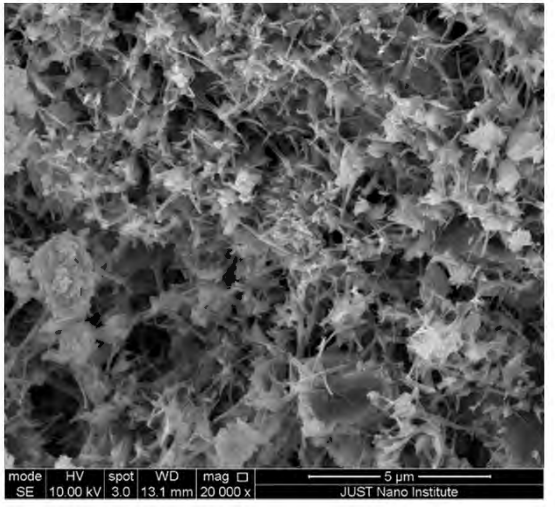
mode SE
HV 10.00 kV
spot 3.0
WD 13.1 mm
mag 20 000 x
5 µm
JUST Nano Institute

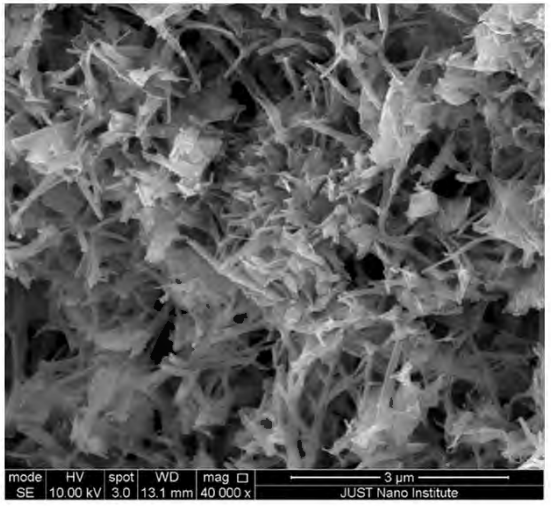
mode HV spot WD mag
SE 10.00 kV 3.0 13.1 mm 40 000 x
3 µm
JUST Nano Institute

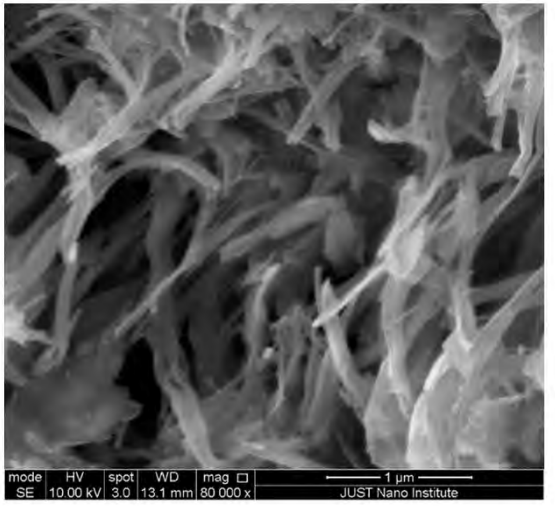
mode HV spot WD mag
SE 10.00 kV 3.0 13.1 mm 80 000 x
1 µm
JUST Nano Institute

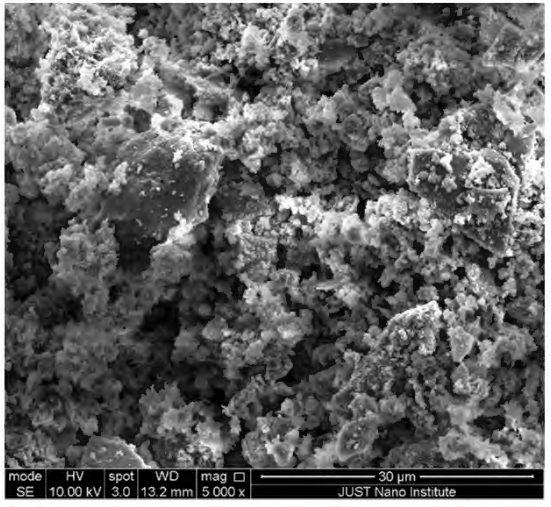
mode HV spot WD mag
SE 10.00 kV 3.0 13.2 mm 5 000 x
30 µm
JUST Nano Institute

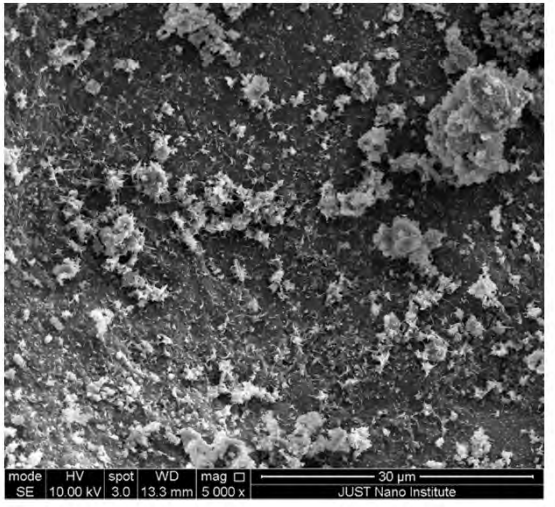
mode HV spot WD mag
SE 10.00 kV 3.0 13.3 mm 5 000 x
30 µm
JUST Nano Institute

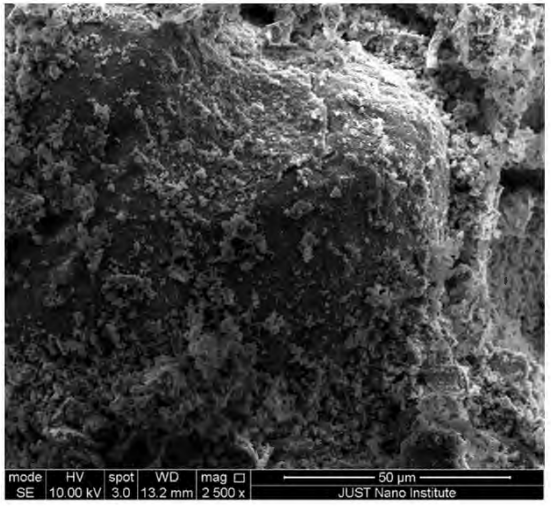
mode HV spot WD mag
SE 10.00 kV 3.0 13.2 mm 2 500 x
50 µm
JUST Nano Institute

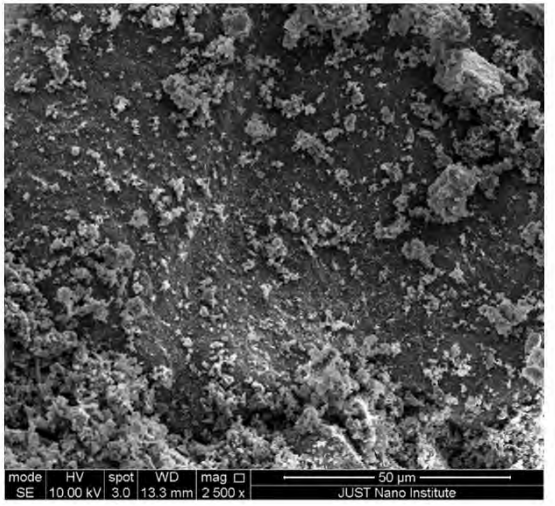
mode HV spot WD mag
SE 10.00 kV 3.0 13.3 mm 2 500 x
50 µm
JUST Nano Institute

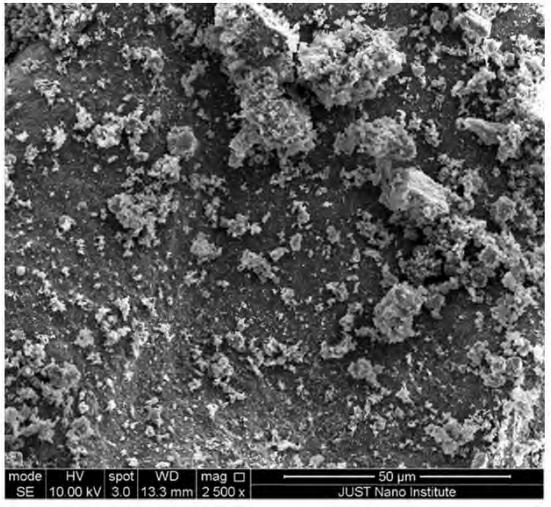
mode HV spot WD mag
SE 10.00 kV 3.0 13.3 mm 2 500 x
50 µm
JUST Nano Institute

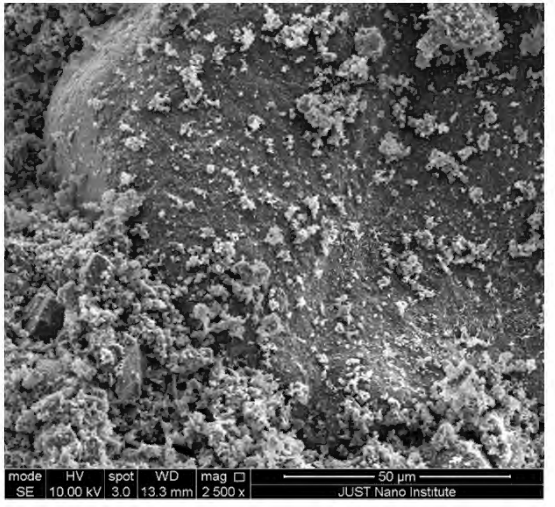
mode HV spot WD mag
SE 10.00 kV 3.0 13.3 mm 2 500 x
50 µm
JUST Nano Institute

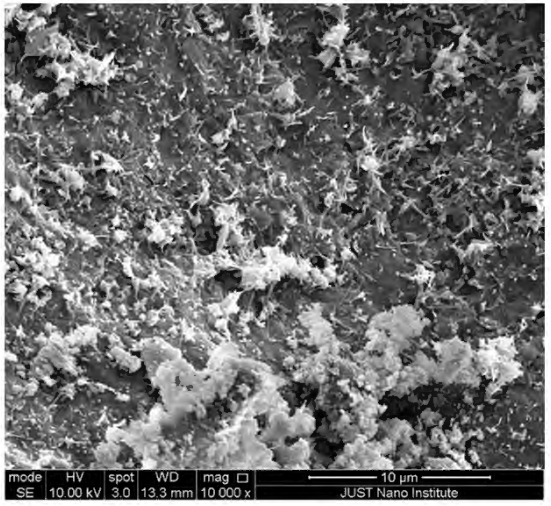
mode HV spot WD mag
SE 10.00 kV 3.0 13.3 mm 10 000 x
10 µm
JUST Nano Institute

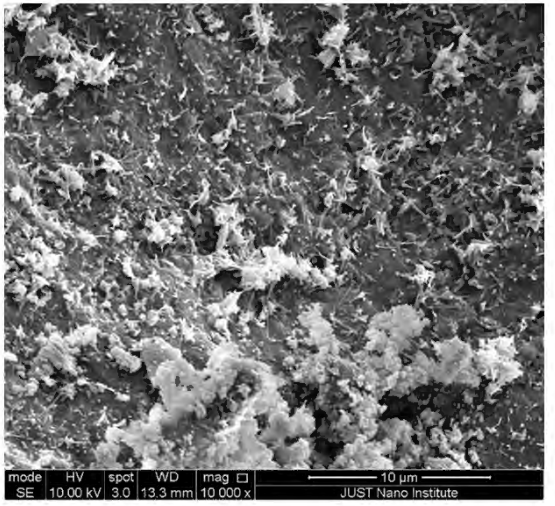
mode HV spot WD mag
SE 10.00 kV 3.0 13.3 mm 10 000 x
10 µm
JUST Nano Institute

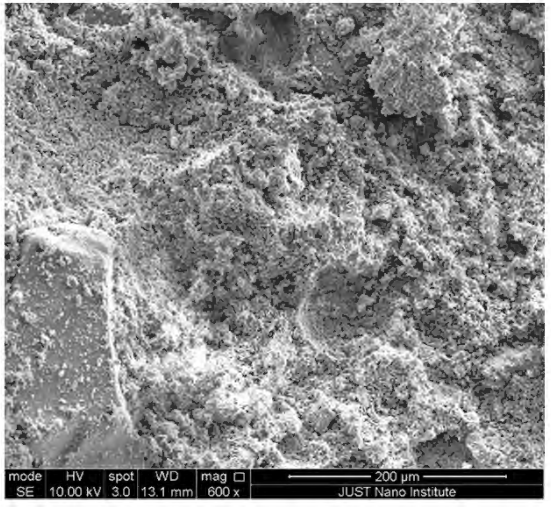
mode HV spot WD mag
SE 10.00 kV 3.0 13.1 mm 600 x
200 µm
JUST Nano Institute

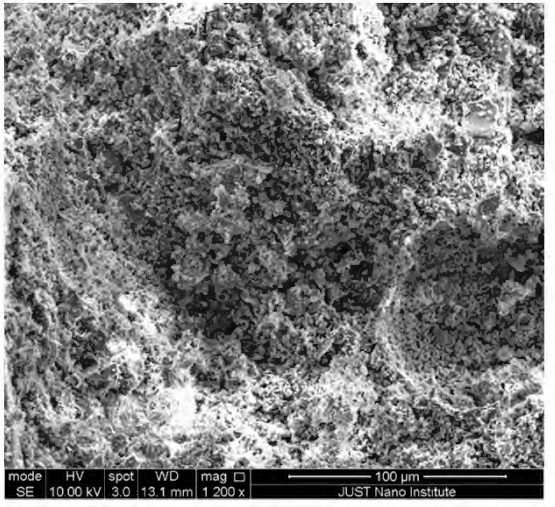
mode HV spot WD mag
SE 10.00 kV 3.0 13.1 mm 1 200 x
100 µm
JUST Nano Institute

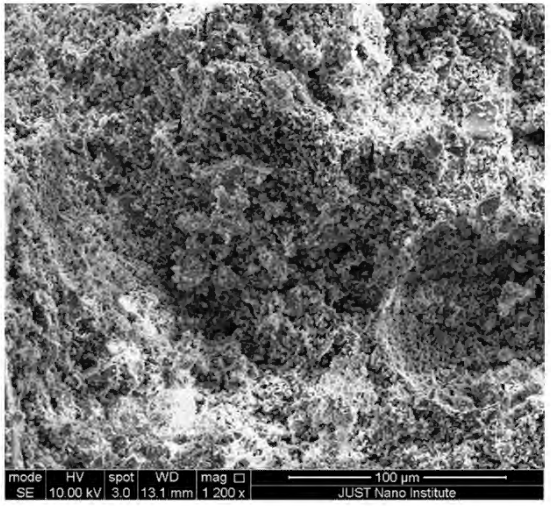
mode
SE
HV
10.00 kV
spot
3.0
WD
13.1 mm
mag
1 200 x
100 µm
JUST Nano Institute

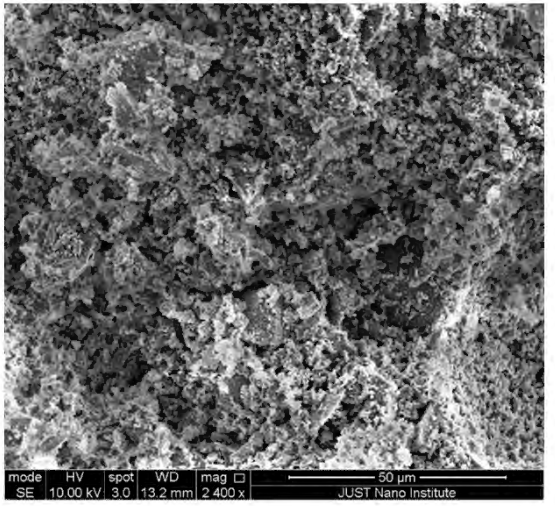
mode
SE
HV
10.00 kV
spot
3.0
WD
13.2 mm
mag
2 400 x
50 µm
JUST Nano Institute

Appendix C: MATLAB output images

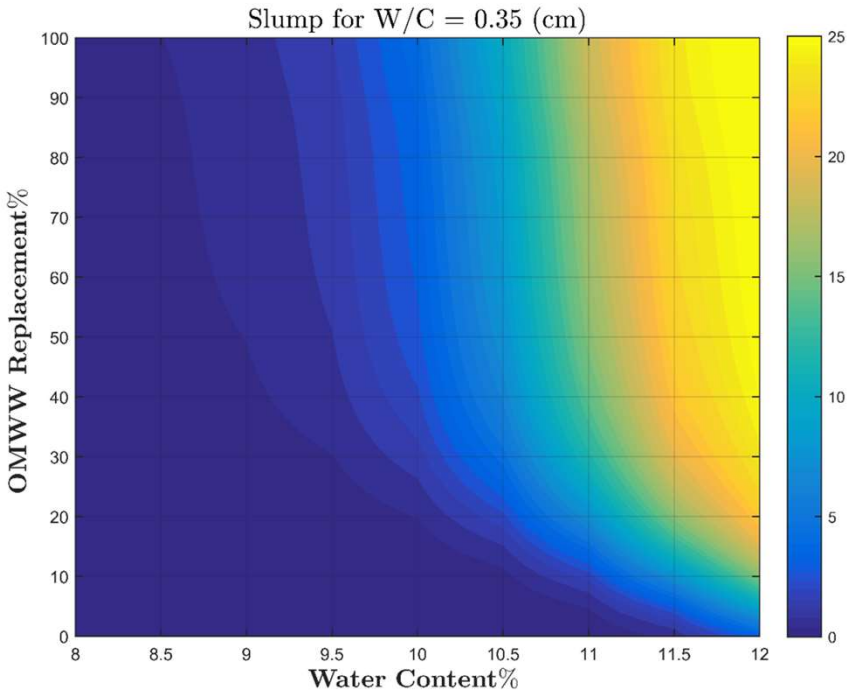
Slump for W/C = 0.35 (cm)
OMWW Replacement%
Water Content%
100
90
80
70
60
50
40
30
20
10
0
8
8.5
9
9.5
10
10.5
11
11.5
12
25
20
15
10
5
0

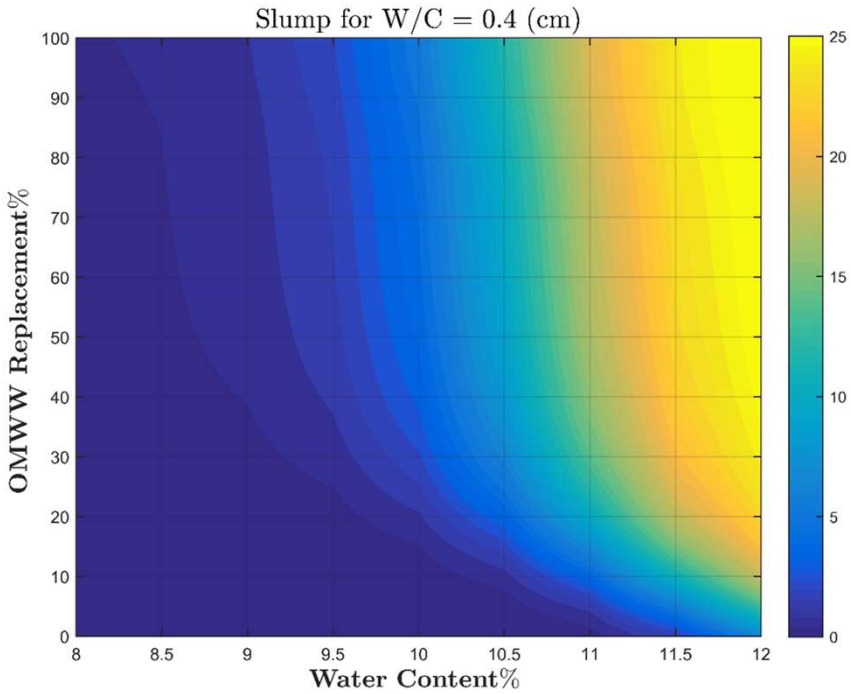
Slump for W/C = 0.4 (cm)
OMWW Replacement%
Water Content%
100
90
80
70
60
50
40
30
20
10
0
8
8.5
9
9.5
10
10.5
11
11.5
12
25
20
15
10
5
0

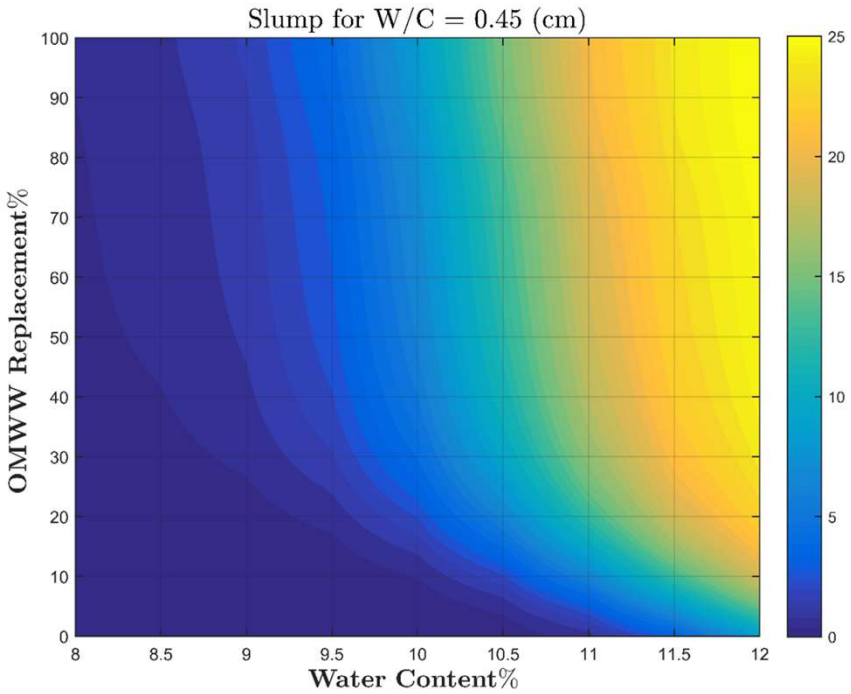
Slump for W/C = 0.45 (cm)
OMWW Replacement%
Water Content%
100
90
80
70
60
50
40
30
20
10
0
8
8.5
9
9.5
10
10.5
11
11.5
12
25
20
15
10
5
0

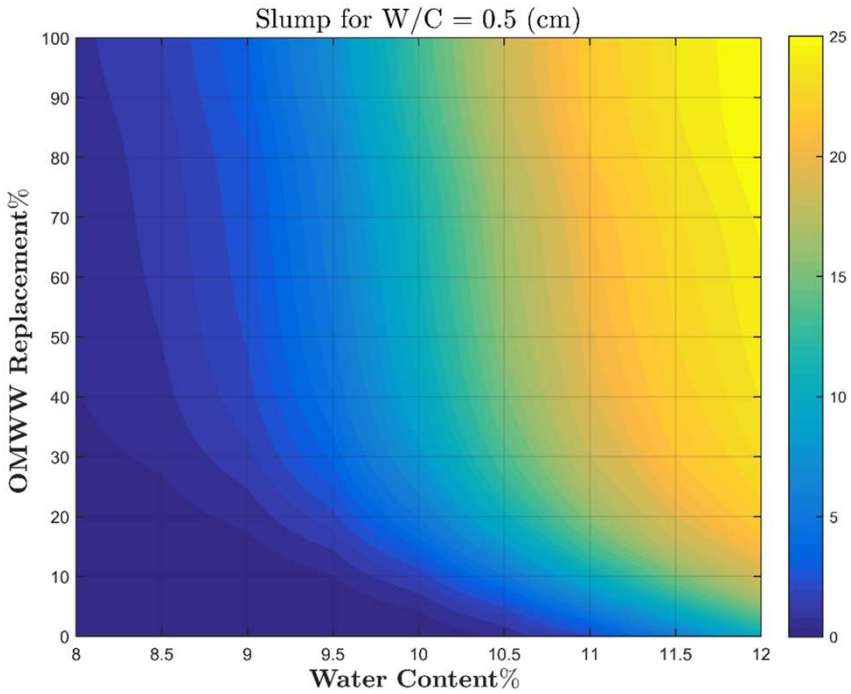
Slump for W/C = 0.5 (cm)
OMWW Replacement%
Water Content%
100
90
80
70
60
50
40
30
20
10
0
8
8.5
9
9.5
10
10.5
11
11.5
12
25
20
15
10
5
0

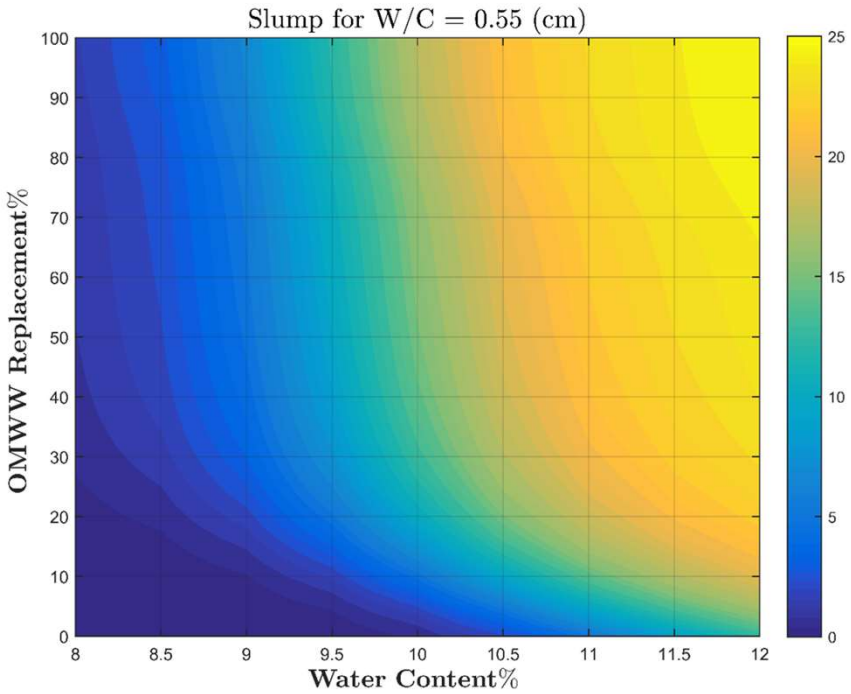
Slump for W/C = 0.55 (cm)
OMWW Replacement%
Water Content%
100
90
80
70
60
50
40
30
20
10
0
8
8.5
9
9.5
10
10.5
11
11.5
12
25
20
15
10
5
0

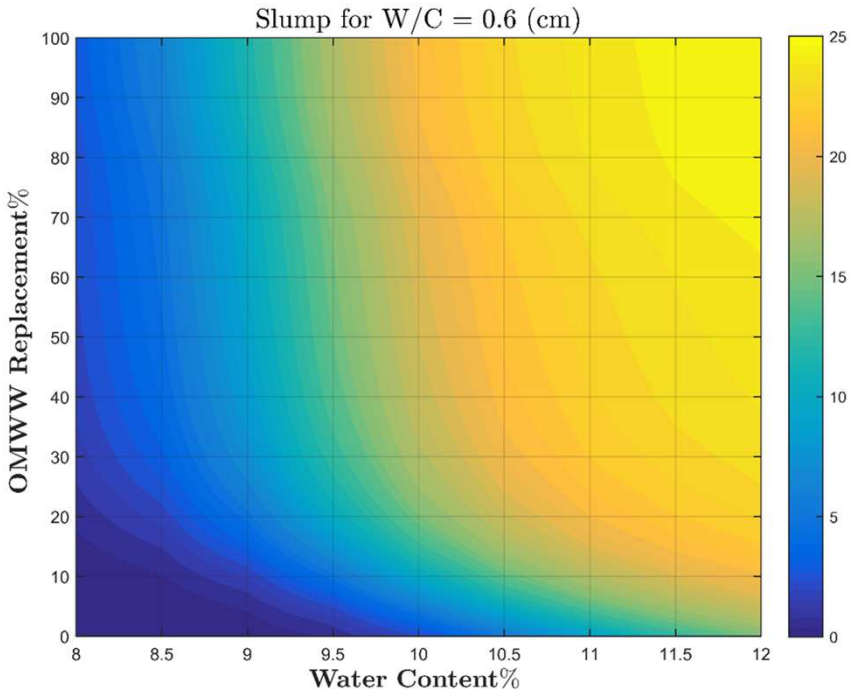
Slump for W/C = 0.6 (cm)
OMWW Replacement%
Water Content%
100
90
80
70
60
50
40
30
20
10
0
8
8.5
9
9.5
10
10.5
11
11.5
12
25
20
15
10
5
0

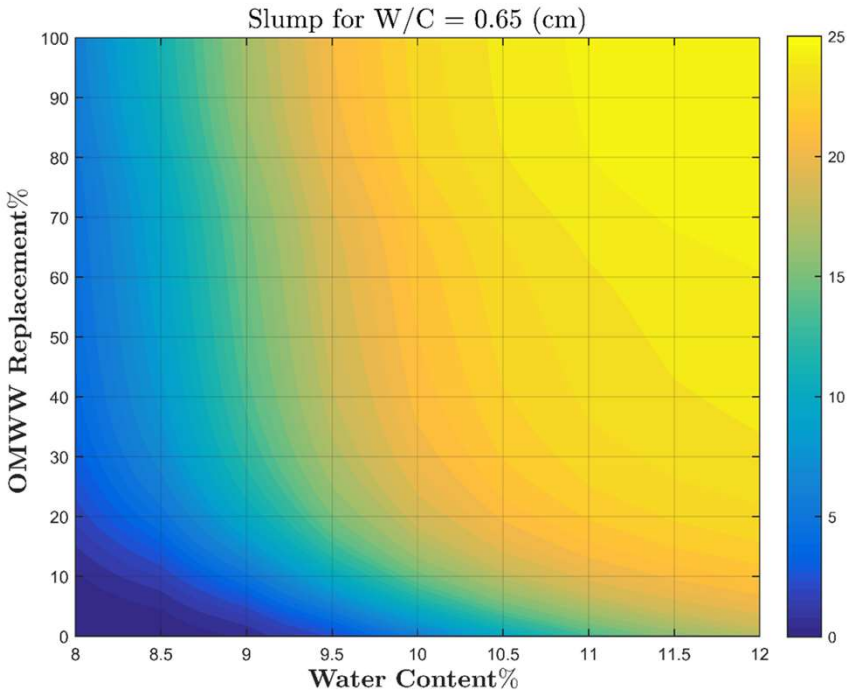
Slump for W/C = 0.65 (cm)
OMWW Replacement%
Water Content%
100
90
80
70
60
50
40
30
20
10
0
8
8.5
9
9.5
10
10.5
11
11.5
12
25
20
15
10
5
0

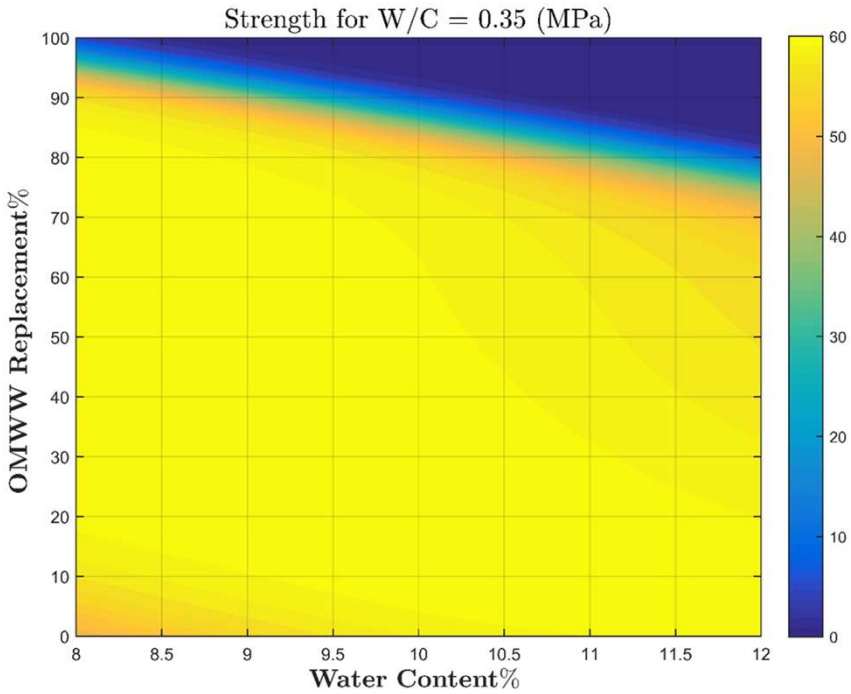
Strength for W/C = 0.35 (MPa)
OMWW Replacement%
Water Content%
100
90
80
70
60
50
40
30
20
10
0
8
8.5
9
9.5
10
10.5
11
11.5
12
60
50
40
30
20
10
0

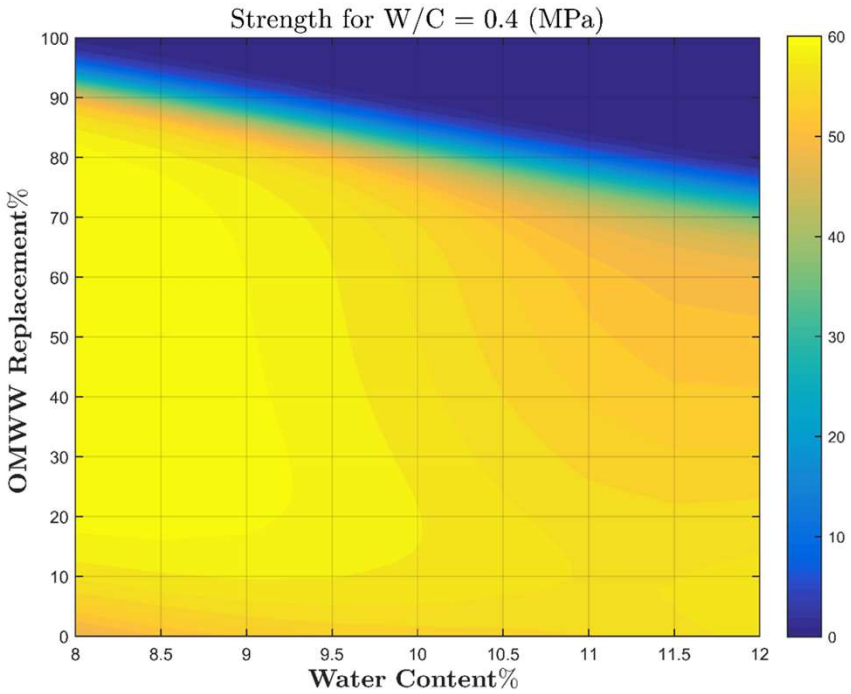
Strength for W/C = 0.4 (MPa)
OMWW Replacement%
Water Content%
100
90
80
70
60
50
40
30
20
10
0
8
8.5
9
9.5
10
10.5
11
11.5
12
60
50
40
30
20
10
0

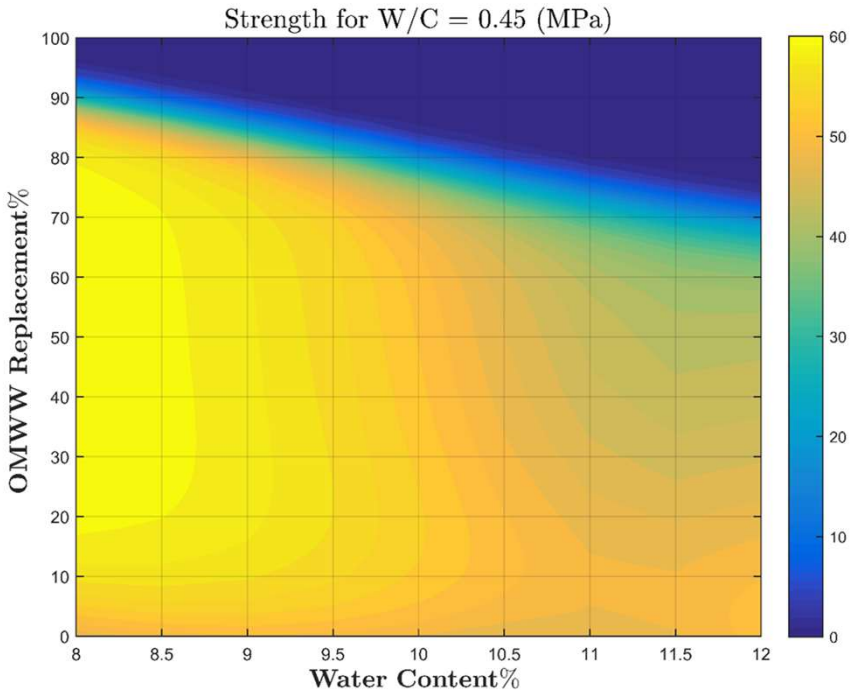
Strength for W/C = 0.45 (MPa)
OMWW Replacement%
Water Content%
100
90
80
70
60
50
40
30
20
10
0
8
8.5
9
9.5
10
10.5
11
11.5
12
60
50
40
30
20
10
0

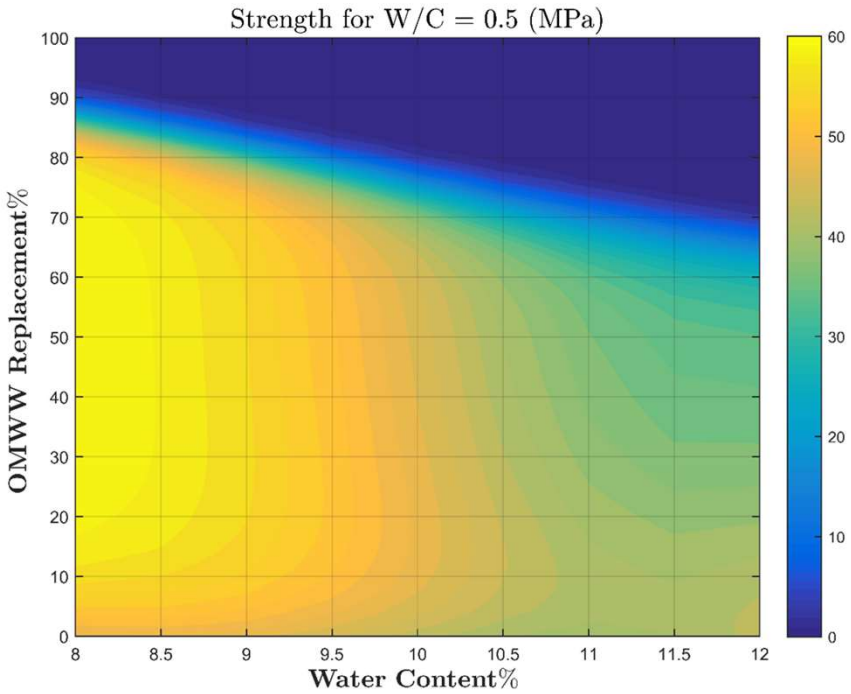
Strength for W/C = 0.5 (MPa)
OMWW Replacement%
Water Content%
100
90
80
70
60
50
40
30
20
10
0
8
8.5
9
9.5
10
10.5
11
11.5
12
60
50
40
30
20
10
0

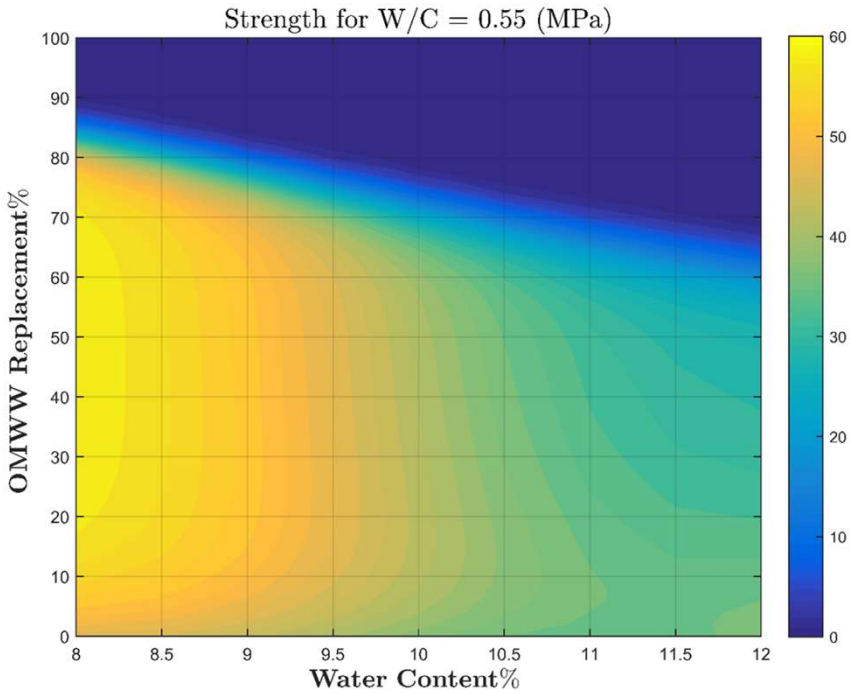
Strength for W/C = 0.55 (MPa)
OMWW Replacement%
Water Content%
100
90
80
70
60
50
40
30
20
10
0
8
8.5
9
9.5
10
10.5
11
11.5
12
60
50
40
30
20
10
0

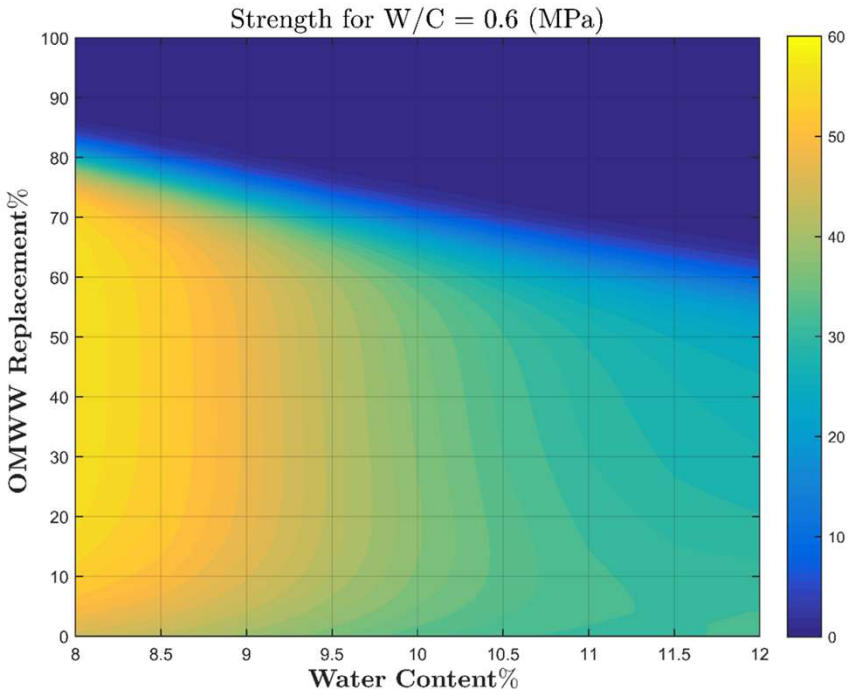
Strength for W/C = 0.6 (MPa)
OMWW Replacement%
Water Content%
100
90
80
70
60
50
40
30
20
10
0
8
8.5
9
9.5
10
10.5
11
11.5
12
60
50
40
30
20
10
0

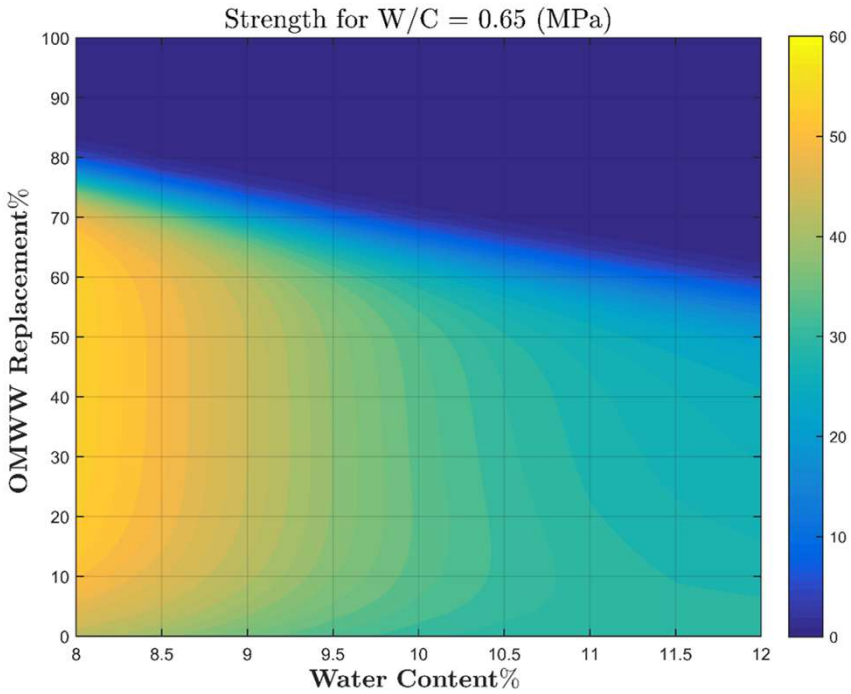
Strength for W/C = 0.65 (MPa)
OMWW Replacement%
Water Content%
100
90
80
70
60
50
40
30
20
10
0
8
8.5
9
9.5
10
10.5
11
11.5
12
60
50
40
30
20
10
0